A Study of Douglas-Fir Anatomical and Mechanical Properties and their Interactions

Bawcombe, Jonathan

Award date:
2012

Awarding institution:
University of Bath

A study of Douglas-fir anatomical and mechanical properties and their interactions

by

Jonathan Mark Bawcombe

A thesis submitted for the degree of

Doctor of Philosophy

University of Bath

Department of Architecture and Civil Engineering

August 2012

The best friend on earth of man is the tree.
When we use the tree respectfully and economically,
we have one of the greatest resources on earth.

Frank Lloyd Wright

Acknowledgements

The research presented within this thesis was funded through collaboration between The Silvanus Trust, Great Western Research and the University of Bath. Additional funding was also gratefully received from Forest Research through the Centre for Forest Resources and Management, led by Barry Gardiner, in order to conduct SilviScan-3 testing.

The journey from forest to thesis has been one that would not have been possible without the valuable contributions of many people. Richard Harris, Pete Walker and Martin Ansell have been fantastic supervisors. Their guidance, support and passion has made the experience enjoyable and been a constant source of motivation. I am also immensely grateful to Jez Ralph, not only for his hard work in instigating the project, but also for sharing his knowledge of the intricacies of forestry in the South West of England and for providing direction and assistance throughout. I would like to thank Jim Sauter and Nick Salter from the Forestry Commission, Geriant Richards from the Duchy of Cornwall and Bryan Elliott from Pryor and Rickett Silviculture, who were instrumental in providing the test material for this work. Without the skill and ingenuity, both in tree felling and the use of 4 x 4 vehicles of Ron Jones, David Harper, David Jenkins, Andrew Davis, Owen Meredith and Blair Warner many of the research samples would never have left the forest. My thanks also goes to Peter Burnet of the Forestry Commission, for providing access to, and tuition in the use of, a vast database of forest maps and information, without which I may have never found my way into, or out of, many forest sites. The warm welcome and careful supervision I received during my two visits to the Innventia Wood and Fibre Measurement Centre in Stockholm from Sven-Olof Lundgvist, Åke Hannson and Lars Olsson made my time their extremely enjoyable and productive. The many contributions to the project from Nick Hoare are greatly appreciated, particularly the numerous hours spent operating the mobile saw mill and the production of several hundred perfectly cut specimens.

I would also like to thank the lab technicians in the Department of Architecture of Civil Engineering, Sophie, Will, Neil and Brian for all of their help, and my office mates, who ensured that no two days were the same and made the whole experience so enjoyable. Particular thanks go to Sarah, Katy and Francis for their support, encouragement and friendship.

I would finally like to thank my parents, for always striving to provide the best for me and for their constant love and support through my many endeavours, the value of which cannot be measured.

Thank you.

Abstract

Low embodied energy, ability to act as a carbon store and ease of recycling gives forest products an important role within a low carbon built environment. Almost 25 % of the coniferous resource within the South West of England is Douglas-fir, a species reputed for producing high quality timber. Despite this, the region is facing challenges in delivering the resources full potential, a contributing factor to which is a loss of knowledge regarding its quality. The aim of the work presented is to gain an improved understanding of the quality of Douglas-fir grown within the region, from the perspective of uses in structural applications, the factors which influence material quality and their interrelationships.

Flexural modulus of elasticity, flexural and compressive strength were determined utilising small clear specimens derived from 1.3 and 8 m heights within 27 trees from six sites across the South West. Results showed a rise in the magnitude of properties with increasing cambial age, particularly so at younger ages. Differences in values were also recorded between stem heights and with rate of growth. These were however less than age related variations. Results compared favourably to those reported in other studies conducted on the species. Utilising SilviScan-3, anatomical properties including density, microfibril angle and cellular dimensions were measured. Significant variations were recorded with cambial age, and in some instances sampling height. The influence of growth rate on anatomical properties was small.

Through statistical and composite modelling, microfibril angle was found to be strongly associated with changes in modulus of elasticity within juvenile wood. Within mature wood and for strength properties, density was the controlling factor. It was shown that a moderate proportion of variations in mechanical properties can be accounted for utilising visually identifiable wood characteristics. The new understanding that has been gained through this work presents opportunities for improved utilisation, the implementation of effective management practices and the development of more efficient visual grading techniques.

Contents

List of figures

List of tables

List of symbols

A	scaling factor for modulus of elasticity prediction utilising SilviScan-3
A_{ij}	stiffness coefficient
A_{11}	longitudinal modulus of elasticity of cell wall system
a_{11}	longitudinal component of extensional compliance matrix
a_i	fixed effect of i^{th} treatment on dependent variable in analysis of variance
B	exponent to allow for curvature of the azimuthal intensity profile
b	small clear specimen radial width
$b_{0 \ldots i}$	regression coefficients
C	tracheid coarseness (mass per unit length)
D	x-ray densitometry derived density
d	small clear specimen depth / tangential width
E_{Cell}	tracheid cell longitudinal modulus of elasticity
E_{CW}	longitudinal tracheid cell wall modulus of elasticity
E_f and E_m	fibre and matrix modulus of elasticity
E_x and E_y	longitudinal and transverse composite modulus of elasticity
E_1	global longitudinal modulus of elasticity
F	specimen ultimate imposed load
G	shear modulus
G_{xy} , G_f , G_m	composite, fibre and matrix shear modulus
h	total composite thickness
h_k	cell wall layer volume proportion
I	x-ray densitometry transmitted radiation intensity
Icv	coefficient of variation of x-ray densitometry azimuthal intensity profile
I_0	x-ray densitometry radiation intensity incident on detector
k	juvenile / mature wood transition age
L	small clear specimen span
m	slope of elastic region of load deflection plot

MOE	SilviScan-3 predicted flexural modulus of elasticity
N_i	extensional stress resultant
n	sample size
P	external perimeter of tracheid cross section
R	radial tracheid dimension
s	standard deviation
s^2	pooled sample variances in t-tests
s_j	random effect of j^{th} site in analysis of variance
T	tangential tracheid diameter
t	specimen thickness or t values
$t_{(k)j}$	random effect of k^{th} tree at the j^{th} site in analysis of variance
V_f and V_m	fibre and matrix volume fractions
Wt	radial tracheid cell wall thickness
$x_{1\ldots i}$	regression coefficients
$\bar{x}_1$	sample 1 mean
$\bar{x}_2$	sample 2 mean
y	original value in log transformation
y'	transformed value in log transformation
y_i	dependent variable
$\bar{y}$	dependent variable sample mean
β	standardised regression coefficient
ε	error term
ε_i^0	mid-plane strain
θ	microfibril angle
μ	mass attenuation coefficient or sample population mean
v	Poisson's ratio
v_{xy} , v_f , v_m	composite, fibre and matrix Poisson's ratio
ρ	density
ρ_{Wall}	tracheid cell wall density
σ_{add}	additive component of microfibril angle dispersion about mean
σ_c	compressive failure initiation stress
$\bar{\sigma}_1$	average in-plane laminate stress
τ_y	shear yield strength of cell wall

Chapter 1 - Introduction

1.1 Introduction

In this chapter an introduction is given to the vital role played by forests and the products derived from them within modern society, and within the built environment in particular. Some of the key issues surrounding the under utilisation and lack of understanding of material quality relevant to the standing timber resource within the South West of England, which form the impetus for this work, are also highlighted. This short contextual précis is then followed by a description of the subject areas covered and the issues to be addressed in this thesis.

1.2 Timber utilisation in the United Kingdom

Throughout history, forests and the products derived from them have played a vital role in the development of communities globally, with a detailed narrative of the modern historical evolution in our relationships with woodlands given by James (1990). Factors which have made forest products a valuable resource historically, such as the ability to source material locally, flexibility of end use and the relative ease of processing are still relevant today. However, it is also the case that, as the need for environmental responsibility and the sustainable use of materials increases, wood based products also offer the benefits of low embodied energy, the ability to act as a carbon store and ease of recycling (BRE, 2006). All of these qualities give timber many advantages as a material for use in construction over steel and concrete.

According to the latest figures produced by the Timber Trade Federation (2011), by both volume (57 %) and value (47 %), sawn softwood is the most highly consumed wood based product within the United Kingdom, with an annual consumption of 8.1 million m^3, of which approximately 36 % was obtained from home grown sources. The three largest markets for sawn softwood material are construction (65 %), pallets and packaging (20 %) and fencing and

outdoor use (10 %) (Moore, 2006). When combined with the high proportion of imported panel and pulp products, the United Kingdom is the third largest net importer of wood based material globally (Forestry Commission, 2010).

Alongside the limited capacity for the production of manufactured wood products, the large quantities of material imported into the United Kingdom can be related to the fact that at 12 %, the forest cover as a proportion of land area is comparatively very low, compared to figures at both European (37 %) and global (30 %) levels (Forestry Commission, 2007). For reasons of both efficiency and economics it is therefore essential that the best end use is made of the timber resources that are available within the United Kingdom.

1.3 Forestry in South West England

The area of focus in this study is the South West of England. A region which is commonly defined from the perspective of forestry as containing the counties of Cornwall, Devon, Dorset, Gloucestershire, Somerset, Wiltshire and the former county of Avon, as shown in Figure 1-1 below.

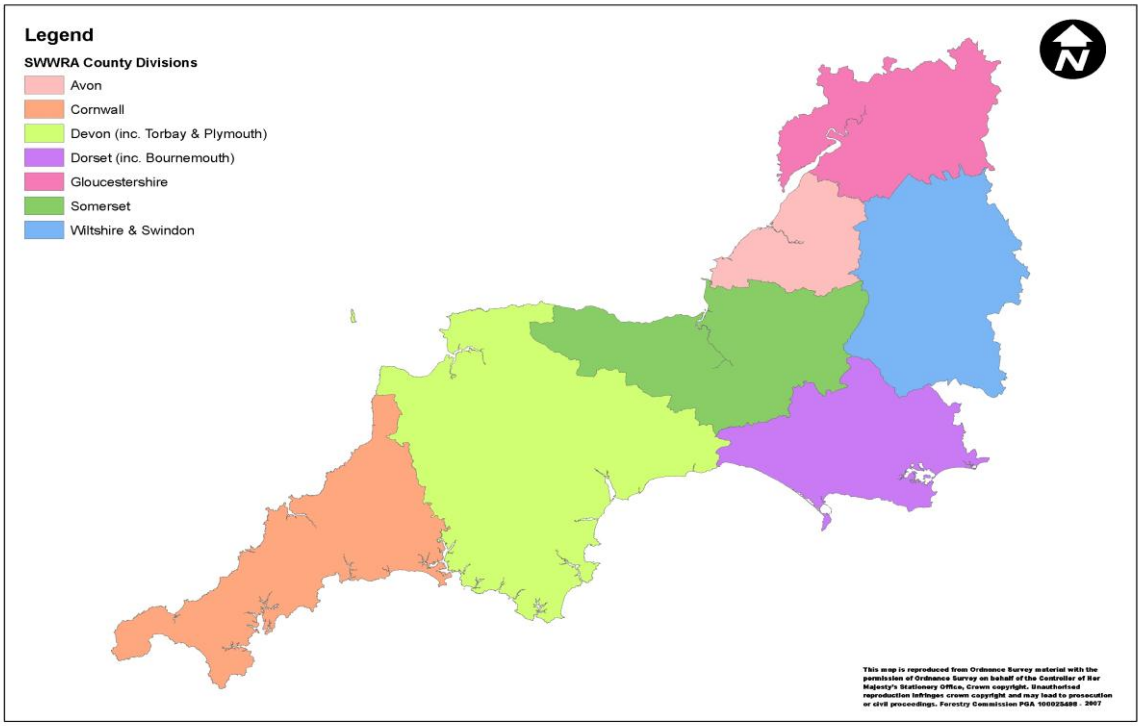

Figure 1-1: Counties within the South West region from Forest Research (2009)

The region accounts for approximately 10 % of the land area of the United Kingdom at 2.4 million hectares, of which 250000 ha are wooded, with 61000 ha of this resource classified as containing solely or predominately coniferous species (Forest Research, 2009), a value which places the South West as one of the top English regions for the availability of softwood material. Accounting for almost 25 % of all softwoods, Douglas-fir is the most abundant coniferous species to be found within the region (Forestry Commission, 2002) and as such forms the basis of this work. As a species, Douglas-fir is well established on international timber markets, where its reputation as a material possessing high values of flexural modulus of elasticity (herein referred to as modulus of elasticity) and flexural strength sees it utilised in a range of structural applications (Barbour and Kellogg, 1990).

Timber production is of economic importance to the South West of England; with it conservatively estimated in a recent study (Ekogen, 2009) that contributions are in the region of £20 million per annum, while through a combination of direct market and indirect non-market benefits, forestry is estimated to generate £375 million for the local economy annually. Despite this, the region is facing many challenges in delivering the full potential of its standing forest resource, as detailed by Ekogen (2009). A contributing factor leading to this under utilisation is a loss of local knowledge on the part of timber growers and processors regarding the quality of the timber produced in the region, compounded by the highly fragmented nature of the resource. There is also a common assumption that the faster growth rate generally found as a result of the mild wet oceanic climate within the Western United Kingdom (Gardiner et al., 2011), results in timber of an inferior quality. Despite this, in two recent reports published by Ekogen (2009) and Forest Research (2009), it was identified that the quality of the forest resource within the South West is believed to be one of its key strengths, and that an increased dissemination of information relating to quality will aid in attracting investment in the region's forest products industry, whilst also providing data of use to timber growers and processors.

1.4 Timber quality

The term 'timber quality' is one which is not easily quantifiable, due to the varied perceptions of quality that commonly exist at different stages in the supply chain for wood based products. From the perspective of the forester or grower, good quality may be related to tree volume, bole form, growth rate, the existence of defects and at a larger scale, the number of incidences of weather or disease related mortalities. For the processor producing sawn products, good quality may be related to size, straightness and the quantity of clear wood, while customer

expectations for quality can vary widely dependent upon the desired end use. The definition of timber quality that perhaps best captures this multifaceted composition is that given by Mitchell (1961), who stated 'wood quality is the resultant of physical and chemical characteristics possessed by a tree or part of a tree that enable it to meet the property requirements for different end products'.

The wood produced by the Douglas-fir trees which form the focus of this work is likely to be suited for use in a wide range of applications. However, given the international reputation of the species for producing highly valued solid sawn sections, it is this end use that will form the basis of the interpretation of the property requirements desirable when assessing material quality. When producing sawn sections for uses such as structural members in the built environment, the quality criteria desirable for good performance and safety in service are the available section size, dimensional stability and the mechanical properties, of which modulus of elasticity and flexural strength are often key parameters (Macdonald and Hubert, 2002). It is the cellular features of the wood at the anatomical level that are responsible for the mechanical properties of timber sections. As such, these cellular features form a further measure by which quality may be classified for the end use that has been prescribed.

1.5 Aims and objectives of PhD study

Within this chapter an introductory overview has been given of the forestry resource found within the South West of England. Some of the challenges facing the forest products industry within the region were discussed and the implications that an improved understanding of timber quality may have on the utilisation of the available material were highlighted. An improvement in the understanding of the quality of the abundant Douglas-fir resource found within the region, from the perspective of its use in structural applications, the factors influencing quality and their interrelationships therefore form the overall aim of the PhD study. The objectives stated below were identified to be addressed in order to fulfil this aim:

- The design of a sampling and testing programme to allow for the within stem assessment of variations in both anatomical and mechanical properties of a representative sample of Douglas-fir trees obtained from the South West region of England.
- The measurement of wood anatomical properties at micro and macroscopic scales and a quantification of variability with age, longitudinal position in the stem and rate of growth.

- The measurement of mechanical properties relevant for uses in structural applications and a quantification of variability with age, longitudinal position in the stem and rate of growth.
- The quantification of the ages of demarcation from juvenile to mature wood production, and an assessment of the influence of rate of growth on demarcation age.
- The development of statistical and micromechanical composite models to enable a better understanding to be gained of the ways in which wood anatomical properties determine timber mechanical characteristics.
- The use of the models developed for the prediction of the assessed mechanical properties based on the values of the assessed anatomical properties within a section, from which suggestions will be made regarding the best visually identifiable features to be used in the determination of wood quality for structural applications.

1.6 Layout of thesis

This thesis is formed of ten chapters, with an additional four chapters of appendices. Following this introductory chapter a review of the literature identifies previous research in the field of wood material property characterisation, including methodologies and the interrelationships between properties. Chapter 3 details the sampling, experimental and theoretical methods employed in the collection and analysis of results. Chapter 4 describes the radial and longitudinal trends observed in the anatomical characteristics studied, while Chapter 5 presents results detailing the impact of growth rate on the anatomical properties and the quantification of the age of demarcation from juvenile to mature wood. An analysis of the variations in mechanical properties is given in Chapter 6, alongside a quantification of the potential impact of these variations on the suitability of material for use in structural applications. Chapters 7 and 8 deal with the prediction of the assessed mechanical properties from anatomical characteristics and a study of the relationships between parameters, firstly utilising statistical methods in Chapter 7 and micromechanical composite modelling in Chapter 8. Finally, a discussion of the findings, their potential implications and recommendations for future work are given in Chapter 9, followed by the key conclusions arising from the study in Chapter 10.

Chapter 2 - Literature review

2.1 Introduction

Given the large number of softwood species and sub-species found globally, the multiple levels at which their properties can be observed, the variability that exists at both the intra- and inter-tree levels and the wide array of measurement techniques that can be utilised, the quantity of literature regarding the anatomical and mechanical properties of softwoods is, not surprisingly, extensive. In this chapter, previously published literature relating to the aims and objectives of this thesis given in Chapter 1 is reviewed.

The chapter begins with an overview of the Douglas-fir species and its history within the United Kingdom, followed by a presentation of the current understanding of the structure of softwoods at a number of hierarchal levels. A review is then given of the known variability of several anatomical and mechanical properties, the current understanding of the interrelationships between them and the techniques available for their assessment. Finally, the methodologies that have been adopted in the development of micromechanical models for the prediction of the modulus of elasticity of softwoods are discussed.

2.2 Douglas-fir

Douglas-fir is one of 20 members of the *Pseudotsuga* genus of trees, native to Europe prior to the Pleistocene glaciations (Hermann and Lavender, 1999). It is now found natively in Western North America (Mitchell, 1972). The first documented discovery of the species was on Vancouver Island in 1792 by Archibald Menzies, with introduction to the British Isles by David Douglas in 1827 (Fletcher and Samuel, 2010). The scientific name for the species is *Pseudotsuga menziesii* and a summary of historical nomenclature is given by Hermann (1982). The current native range of the species extends south for 3400 km from central British Columbia and east from the Pacific coast for 1600 km into the Rocky Mountains (Fletcher

and Samuel, 2010). Two sub-species of Douglas-fir are noted by Hermann (1982), the coastal variety (*Pseudotsuga menziesii* var. *menziesii*) and the inland or Rocky Mountain Douglas-fir (*Pseudotsuga menziesii* var. *glauca*). Coastal Douglas-fir is typically found from central British Columbia south along the Pacific Coast to California, with the habitat of the inland variety extending from the Rocky Mountains south into the mountains of central Mexico (Elias, 1980). The inland variety of Douglas-fir has generally been found to be unsuited for cultivation in the United Kingdom (Fletcher and Samuel, 2010). However, the large native range of the coastal sub-species, which covers a variety of climatic conditions, has enabled it to be successfully grown within the United Kingdom with careful seed source selection, despite mean rainfalls typically being well below the values observed in the native range (Fletcher and Samuel, 2010).

In the United Kingdom Douglas-fir has not been as widely adopted as elsewhere in Europe, and accounts for only a 3 % share of the coniferous growing stock, compared with 50 % and 16 % for Sitka spruce and Scots pine respectively (Smith and Gilbert, 2003). This can primarily be attributed to the intensive regeneration that took place utilising these species in order to develop a strategic timber reserve following the world wars, with Sitka spruce selected primarily because of its fast growth and ability to grow on poor quality upland sites (Stirling-Maxwell, 1931).

2.3 The anatomy of Douglas-fir

2.3.1 Outline

In order to fully understand the variable nature of timber mechanical properties, it is first necessary to gain an understanding of the constituent components of the wood from which it is formed. In this review, previously reported characteristics and variations in the anatomical properties of Douglas-fir trees, and more broadly for softwoods, are presented. This is done following a similar hierarchal approach to that used by Booker and Sell (1998), first looking at molecular features of wood, followed by the features at nano, micro and macroscopic scales.

2.3.2 Molecular structure - the chemistry of wood

2.3.2.1 Chemical constituent characteristics

Wood is formed of three primary chemical constituents, namely cellulose, hemicellulose and lignin which interact in such a way so as to form a natural composite (Bergander and Salmén, 2002). Cellulose, a long chain polymer of β-D-glucose molecules formed from carbon dioxide

and water utilising energy from the process of photosynthesis, is regarded as the fibre within the composite (e.g. Dinwoodie, 2000). Cellulose chains have been estimated to be up to 5000 nm in length (Barnett and Jeronimidis, 2003), with adjacent chains bonded to one another through a combination of hydrogen bonds and van der Waals' forces. This theoretically forms units of infinite length passing through crystalline and non-crystalline regions, creating a cellulose core to the composite measuring approximately 5 nm x 5 nm (Desch and Dinwoodie, 1981). It is these long thin filaments that are commonly termed microfibrils. Like cellulose, hemicellulos is a carbohydrate polymer, however it differs from cellulose in many aspects, notably that it is non-crystalline and that its degree of polymerization is much lower (Siau, 1984). Lignin, the final component of the composite, is an aromatic polymer (Pérez et al., 2002) and along with hemicelluloses can be thought of as forming the matrix of the composite, creating, as described by Dinwoodie (2000), a sheath surrounding the cellulose core. Lignin is found surrounding the hemicellulose within this sheath, where its lower affinity to water improves the integrity of the composite by reducing cell wall water absorption. However lignin is unable to form bonds directly with cellulose and so it is the hemicellulose that maintains the cohesion between the two elements (Sarkanen and Ludwig, 1971). While variation can be large, the dimension of a single composite unit combining the three components typically measures 10 - 30 nm across (Dinwoodie, 2000). A representation of the arrangement of the chemical constituents within the cell walls of tracheids is shown in Figure 2-1.

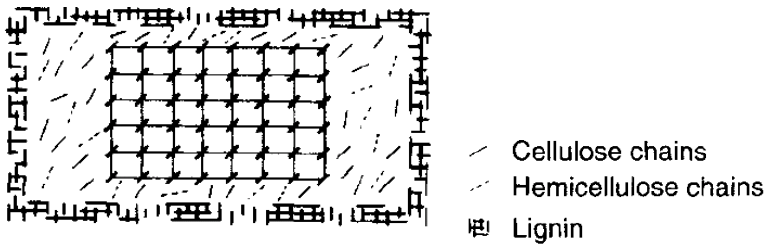

Figure 2-1: Chemical constituent tracheid cell wall arrangement from Dinwoodie (2000)

The fourth component of wood, extractives, are non-structural substances soluble in organic solvents and water found in the cell lumina, cellular voids and channels (Taylor et al., 2007). They have little direct impact on the mechanical properties of wood, although their ability to influence equilibrium moisture contents can result in them having indirect effects on properties (Bodig and Jayne, 1982). They are also responsible for the odour, colour and in part density of wood, and give natural durability against attacks from fungus and insects (Hillis, 1987).

2.3.2.2 Chemical constituents mechanical properties

Numerous studies regarding the mechanical properties of the three primary chemical constituents of wood have been conducted, with typically a large range of results presented in all cases. Variability in results occurs for a number of reasons, including inaccuracies within molecular models due to neglecting to account for the thermal motion of molecules (Persson, 2000) and the difficulties associated with isolating the chemical constituents in the same form found within the cell walls (Salmén, 2004). It is also the case that the mechanical properties of hemicellulose and lignin are sensitive to changes in moisture content, as demonstrated by Cousins (1976, 1978). In Table 2-1, a summary of the key elastic mechanical properties of the three chemical constituents derived through experimental tests, molecular modelling and estimations are shown. In the case of hemicellulose and lignin, mechanical properties are presented at a moisture content of 12 % where a range of values was available. The x axis corresponds to properties in the longitudinal direction of the tracheids, and the y axis the transverse as the constituents are arranged compositely within the cell wall.

2.3.3 Nano structure - wood cells

Studies of the cellular structure of different softwood species have shown that there are large similarities between them, which are likely to have arisen early in the evolution of woody plants and are clearly so important to their survival that they have changed little since (Barnett and Bonham, 2004). Within the stem, wood cells exist to carry out two primary functions; provide a passage for water and nutrient transportation from roots to crown, and to support the large static and dynamic forces induced by the biomass above (Booker and Sell, 1998). In order to fulfil these functions, softwoods are made up of tracheids and rays. Tracheids are aligned vertically and account for approximately 90 % of the cells present, they allow the vertical transportation of materials up the stem and carry the imposed loads (Dinwoodie, 2000). Ray tracheids are found in the horizontal plane and allow for the movement of water and minerals radially, with ray parenchyma cells acting as a material store (Romberger et al., 1993, Walker, 2006). The flow of nutrients between tracheids occurs through openings between them known as bordered pits, as described by Walker (2006).

Table 2-1: Documented values for wood chemical constituent mechanical properties

	Experimental	**Modelled/Estimated**
Cellulose		
E_x (N/mm^2)	137000[1], 138000[2], 120000 - 135000[3]	168000[4], 246000[5]
E_y (N/mm^2)		17700[4], 18000[6], 27700[7]
G_{xy} (N/mm^2)		3000[8], 4500[7], 5100[4]
ν_{xy}		0.1[7]
Hemicellulose		
E_x (N/mm^2)	8000[8]	2000[9]
E_y (N/mm^2)		800[9], 3400[6]
G_{xy} (N/mm^2)		1000[9], 1800[10]
ν_{xy}		0.2[9]
Lignin		
E_x (N/mm^2)	3100[11]	2000[10]
E_y (N/mm^2)		1000 - 2000[10]
G_{xy} (N/mm^2)	1200[11]	600[9],800[7]
ν_{xy}		0.33[12]

1) (Sakurada et al., 1962), 2) (Nishino et al., 1995), 3) (Matsuo et al., 1990), 4) (Tashiro and Kobayashi, 1991), 5) (Mark, 1980), 6) (Cave, 1978), 7) (Mark, 1967), 8) (Cousins, 1978), 9) (Salmén, 2004), 10) (Bergander and Salmén, 2002), 11) (Cousins, 1976), 12) (Bodig and Jayne, 1982)

where: E_x longitudinal modulus of elasticity
E_y transverse modulus of elasticity
G_{xy} shear modulus
ν Poisson's ratio

The now commonly accepted softwood cellular structure is that shown in Figure 2-2, in which the tracheid is divided into an amorphous middle lamella, a thin primary wall and a three-ply secondary wall comprising the S_1, S_2 and S_3 layers. This model was first proposed by Bailey and Kerr (1935), who used polarization microscopy to show the presence of a three-ply structure in which the layers were characterised by different predominating orientations of the cellulose. This was in disagreement to earlier proposal by Preston (1934) that the angle of cellulose fibrils was constant throughout the thickness of the cell wall. Bailey and Kerr's model was found to be correct and understanding was deepened with the early application of

transmission electron microscopy (Wardrop, 1954, 1957, 1958, Harada et al., 1958), and more recently field emission scanning electron microscopy (Abe and Funada, 2005). Within the secondary wall layers the cellulose microfibrils are highly aligned, as discussed below. The deviation of the helical winding of the microfibrils from the tracheid cell longitudinal axis is termed the microfibril angle, as depicted in Figure 2-2. A summary of the functions believed to be carried out by each cell wall layer and their characteristics is given in the sub-sections that follow.

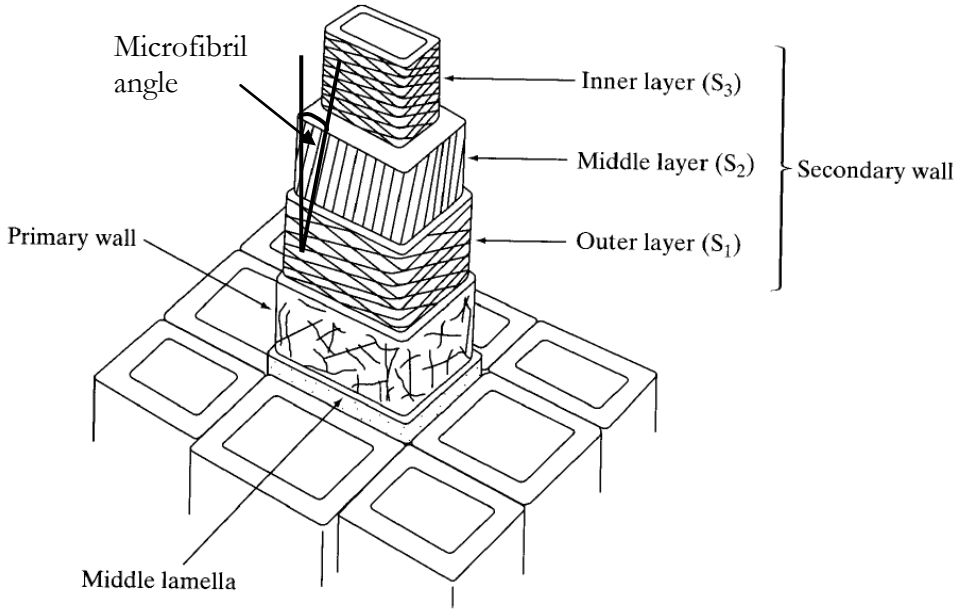

Figure 2-2: Softwood cell wall structure from Dinwoodie (2000)

2.3.3.1 Middle lamella and primary wall

The middle lamella is situated between the cells, acting as a binding material (Walker, 2006). The primary cell wall contains a loose network of microfibrils that were proposed in the model of Harada and Côté Jr (1985) to be orientated approximately longitudinally on the outer face and transversely on the inner, a fact that was confirmed by Abe et al. (1995) with the use of scanning electron microscopy. The transverse orientation on the inner face is thought to restrain lateral cell expansion at the end of the first tracheid developmental phase (Taiz, 1984). It is often difficult to distinguish the middle lamella from the primary cell wall, resulting in the two commonly referred to as the compound middle lamella (Jyske, 2008). The thickness of the compound middle lamella is typically within the range of 0.25 - 0.35 μm, with no significant differences between early and latewood. Typical values of the proportions of chemical constituents at 12 % moisture content are 5 %, 40 % and 55 % for cellulose, hemicellulose and lignin respectively (Persson, 2000, Bergander and Salmén, 2002, Qing and Mishnaevsky Jr, 2009).

2.3.3.2 S_1 layer

In early studies investigating the arrangement of microfibrils within the S_1 layer of the cell wall, such as those conducted with the use of transmission electron microscopy by Wardrop (1954, 1957, 1958) and Harada and Côté Jr (1985), it was thought that the microfibrils were organised in an alternating structure of crossed S and Z helices[1] within the cell wall. It has however been shown more recently with the use of field emission scanning electron microscopy (Abe et al., 1991) and a combination of polarised light and transmission electron microscopy (Donaldson and Xu, 2005), that the arrangement of microfibrils is not crossed, but instead gradually changes from an S helix on the outer face to a Z helix on the inner surface nearest the lumen, with microfibril angles varying from approximately 45° to 70° in the respective orientations, with no systematic variation with age evident. No documented results were found regarding variations in the S_1 layer microfibril angle in Douglas-fir. It was postulated by Donaldson (2008) that due to the thin nature of the S_1 layer, the outer surface of the S_2 layer may have also been observed in early studies, leading to the conclusion of a crossed arrangement. It is thought that this microfibril arrangement aids in limiting excessive radial expansion of the S_2 layer under compressive loads by forming a protective sheath, while also preventing the transformation of intra-wall fracture along the boundary between the compound middle lamella and S_1 layer into transwall fracture across the entire cell wall (Booker and Sell, 1998). The thickness of the S_1 layer has previously been reported as increasing from 0.2 μm within the earlywood to 0.3 μm in the latewood, with typical values of the chemical constituents at 12 % moisture content of 30 %, 30 % and 40 % for cellulose, hemicellulose and lignin respectively (Fengel and Stoll, 1973, Bergander and Salmén, 2002, Qing and Mishnaevsky Jr, 2009).

2.3.3.3 S_2 layer

The microfibrils within the S_2 layer are arranged in a highly ordered Z helix (Barnett and Bonham, 2004). Variation in the microfibril angle is large both within and between trees, typically ranging from 40° to 5° (Donaldson, 2008). The trends of, and factors responsible for these variations are discussed further in Section 2.5.2. The thickness of the S_2 layer has previously been reported as increasing from 1.4 μm within the earlywood to 4 μm in the latewood, with typical values of the chemical constituents at 12 % moisture content of 50 %, 30 % and 20 % for cellulose, hemicellulose and lignin respectively (Fengel and Stoll, 1973, Bergander and Salmén, 2002, Qing and Mishnaevsky Jr, 2009). Given the large thickness

[1] The helix, when observed from the outer face of the cells, is designated an S-helix when it is a left handed helix and a Z-helix when it is a right handed helix relative to the longitudinal axis of the cell.

relative to other cell wall components, it is the S_2 layer that is predominately responsible for carrying loads imposed by the mass of the tree, as well as tension and compression forces generated by imposed loads which may cause the stem to flex, such as wind and passing animals in younger stems (Booker and Sell, 1998).

2.3.3.4 S_3 layer

Data regarding the orientation of microfibrils within the S_3 layer is comparatively limited compared with the other secondary wall layers. This is largely due to difficulties associated with its measurement, with incorrect measurement of the inner S_2 layer possible (Donaldson and Xu, 2005). The results presented by Wardrop (1964), Tang (1973) and Donaldson and Xu (2005) are in general agreement, and show that the microfibril orientations range from an S to Z helix on moving towards the lumen, with microfibril angles typically varying by ± 50° or less from the tracheid longitudinal axis. The differences between the fibril angles reported in the above studies is likely due to a combination of factors, including the limited number of tracheids assessed, differences between trees and species and also variations in measurement techniques. No documented data was found regarding the orientation of microfibrils within the S_3 layer of Douglas-fir trees. This fibril arrangement within the S_3 layer is thought to help greatly in the stiffening of the tracheids against the hydrostatic collapse forces imposed on to the faces of the lumen, generated by the conduction of materials up the stem. Booker (1993) demonstrated that the stiffness of the cell walls to sideways deflection is increased by a factor of approximately 2.5 by the presence of the S_3 layers acting as cross-banding on the inner lumen face. Having the lowest proportion within the cell wall, the thickness of the S_3 layer has previously been reported as increasing from 0.03 μm within the earlywood to 0.04 μm in the latewood, with typical values of the chemical constituents at 12 % moisture content of 48 %, 36 % and 16 % for cellulose, hemicellulose and lignin respectively (Fengel and Stoll, 1973, Bergander and Salmén, 2002, Qing and Mishnaevsky Jr, 2009).

2.3.3.5 Helical thickening

A further cell wall feature specific to Douglas-fir and a limited number of other softwoods are helical or spiral thickenings, ridges of cell wall material, deposited on the lumen side of the tracheid. Helical thickenings are usually found in an S helix (Wardrop, 1964) and have been observed to be an extension of the S_3 layer (Jute and Levy, 1973). The helix angle of the thickenings is thought to be related to tracheid size, with longer and thinner cells having a helix angled nearer to perpendicular to the longitudinal axis of the tracheids (Meylan and Butterfield, 1972). The role that helical thickenings play within the cell is still not fully

understood, it is however thought that they increase cell wall strength, preventing collapse arising due to hydrostatic forces (Yang, 2006), similar to the role of the S_3 layer microfibrils. Images of helical thickenings in the tracheids of Douglas-fir are shown in Figure 2-3.

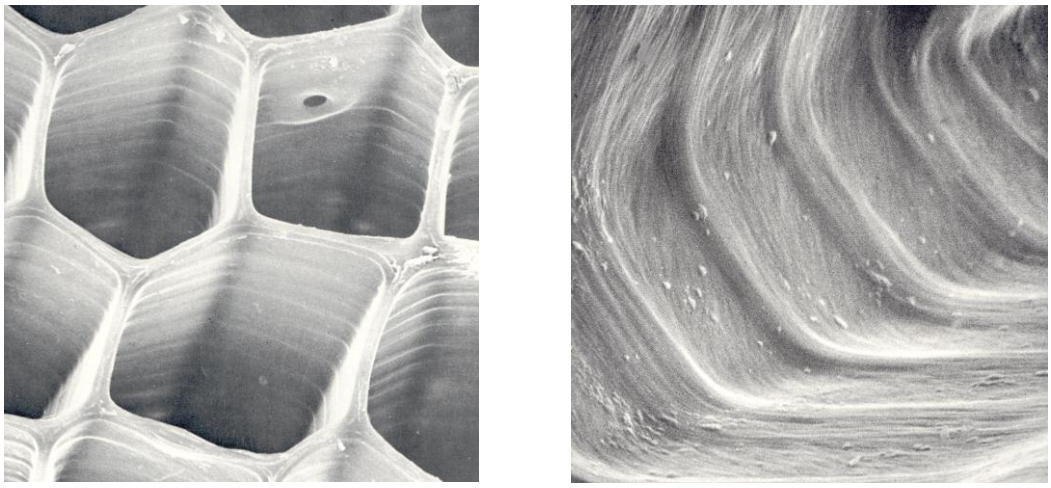

(a) (b)

Figure 2-3: Helical thickenings in Douglas-fir tracheids (a) 1750x magnification (b) 10000x magnification from Meylan and Butterfield (1972)

2.3.4 Micro structure - growth rings

When grown in temperate climates, softwoods produce growth rings that reflect the annual spring onset and autumn cessation of cellular growth activity (Barnett and Jeronimidis, 2003). When grown in stands with a relatively uniform age structure the width of the growth rings produced by Douglas-fir has been shown to exhibit an overall trend of decreasing with age, following peak values attained in the rings immediately adjacent to the pith (Jozsa and Brix, 1989, Abdel-Gadir, 1991, Fabris, 2000, Gartner et al., 2002). Mean peak values in the range 5 - 7 mm, decreasing to widths of 2 - 3 mm by approximately 30 years of age are typical. This reduction in ring width with age is sometimes associated with reduced productivity in the stem. This is not the case however, as rings nearer the pith represent substantially less biomass accumulation than rings of the same width or less at greater ages (Ridley-Ellis et al., 2009). The utilisation of silvicultural practise such as continuous cover forestry described by Macdonald et al. (2010) with a mixed age stand structure, may result in different ring width patterns dependent upon the position of the tree within the stand structure.

The wood produced at the start of the growing season is often referred to as earlywood and that later in the season latewood. On moving from the production of early to latewood transitional tracheids are produced, which possess intermediate characteristics (Larson, 1969a).

The nature of the tracheids produced reflects their different roles within the stem, with the large diameter thin walled earlywood tracheids primarily responsible for water conduction when it is in greatest demand and availability during the spring, while thicker walled smaller diameter latewood tracheids provide a greater degree of structural support (Dinwoodie, 2000). This is reflected in the fact that Douglas-fir earlywood tracheids have been shown to have 11 times the water conductivity of latewood (Domec and Gartner, 2002). It is also the case that the smaller lumens in latewood prevent the occurrence of cavitation as a result of the reduced water availability (Jacobsen et al., 2005).

Data regarding the intra- and inter-growth ring variations in tracheid dimensions in Douglas-fir is limited, due to difficulties in obtaining latewood specimens by use of a microtome and the desire to obtain dimension in the sap conducting earlywood for hydraulic modelling (e.g. Spicer and Gartner, 2001). In a limited study of one Douglas-fir tree, Rathgeber et al. (2006) identified a decrease in tracheid diameter on moving from early to latewood of 45 μm to 24 μm in the radial direction and 38 μm to 32 μm tangentially, while wall thicknesses increased from 3.2 μm to 6.8 μm and 3.8 μm to 8.8 μm in the radial and tangential directions respectively. A differential in wall thicknesses in the two directions was also identified by Ollinmaa (1961). In the measurements of 'late early wood' tracheids, Erickson and Harrison (1974) found sharp increases in both the radial and tangential diameters of 15 μm and 10 μm, from starting values of 25 μm and 23 μm in each of the respective directions during the first 15 years of growth. However, the continuation of trends beyond this age cannot be verified in the study, due to a period of stimulated growth influencing the results. No literature regarding the change in dimensions longitudinally in the stem was found for Douglas-fir, however Spicer and Gartner (2001) did identify an increase in specific conductivity of approximately 40 % with height within the earlywood of Douglas-fir stems due to increased lumen size, indicating potential increases in tracheid diameter and decreases in wall thickness longitudinally. Similar trends to those reported in the limited number of Douglas-fir studies have also been shown for Loblolly and Radiata pine (Burdon et al., 2004), Norway spruce (Brandstrom, 2001, Molteberg and Høibø, 2006, 2007) and Sitka spruce (Denne, 1973).

The method developed by Mork (1928) has long been used to define the boundary between early and latewood tracheids within a growth ring. In Mork's method, the boundary point is defined when the double cell wall thickness becomes greater than or equal to the width of the tracheid lumens. While easily implemented through optical examination of a specimen, this method does not lend itself to use with more recent x-ray densitometry techniques. As such it

has now been largely replaced by the threshold method, in which a set density value is used to differentiate early and latewood (e.g. Parker, 1976), or the maximum derivative method, in which the transition point is defined by the maximum of the derivative of the function describing the intra-ring density profile (Koubaa et al., 2002). While comparable results have been obtained when the three methods have been evaluated (Barbour et al., 1997), a limitation of all three is the lack of consideration of transitional tracheids or transition-wood in the intra-ring developmental profiles. This is likely a result of a continuation in the use of the early definitions adopted by Mork, at a time when the measurement of properties was time intensive.

As a result of the commonly used methods for determining the demarcation from early to latewood, no literature demonstrating variations in the proportions of transition-wood within growth rings with age was found for Douglas-fir, although the presence of transitional tracheids has been acknowledged (e.g. Fabris, 2000). In Douglas-fir an overall trend of increasing latewood proportion with cambial age has been reported, with values rising from approximately 20 % in the growth rings adjacent to the pith, to 40 % by 20 years of age (Erickson and Harrison, 1974, Fabris, 2000, Gartner et al., 2002, Lachenbruch et al., 2010). For equivalent ages at increasing heights, a lower proportion of latewood has also been identified (Gartner et al., 2002). These overall trends are in line with those reported for Balsam-fir (Koga and Zhang, 2004) and Jack pine (Park et al., 2009). The influence of a changing rate of growth on the proportion of latewood present within a growth ring in Douglas-fir has shown mixed results. Erickson and Harrison (1974) demonstrated a reduction in the proportion of latewood of 5 % when ring width increased by 25 % compared to control stems, while Fabris (2000) showed negative linear correlations typically greater than 0.5 between ring width and latewood proportion at every cambial age up to 33 years. Abdel-Gadir and Krahmer (1993) however found only weak negative correlations with ring width in Douglas-fir mature wood, while those in the juvenile wood were positive. The differences in the strength of correlations may arise due to the utilisation of different methods to assess the point of transition from early to latewood, or the fact that correlations calculated by Abdel-Gadir and Krahmer were based on ring width variations grouped by simply juvenile or mature wood, and as such the developmental decline in ring width with age may have influenced the relationships observed. Moderate to strong negative correlations have also been observed between ring width and latewood proportion in Balsam-fir (Koga and Zhang, 2004) and Western hemlock and Western red cedar (Fabris, 2000).

2.3.5 Macro structure - the stem

The image in Figure 2-4 shows a number of macroscopic features commonly found in a Douglas-fir stem.

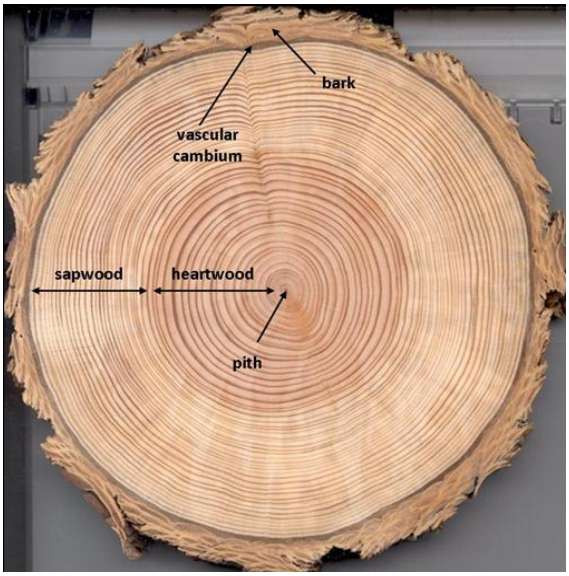

Figure 2-4: Section through Douglas fir stem, http://web.utk.edu/~grissino/

At the centre of the stem is the pith, the zone where initial growth takes place (McLean, 2008). Surrounding the pith is a red band of wood known as heartwood. Heartwood is a region of inactive tissue in which the xylem no longer fulfils the tasks of conduction or storage of water and minerals (Dinwoodie, 2000). Douglas-fir is termed a heartwood species, due to the typically high proportions of this wood type present. Cown (1992) states that even in fast grown trees that the width of the sapwood band rarely exceeds 75 mm. Heartwood is formed through the deposition of extractives such as phenols and terpenes within the lumens of tracheids, which as well as being responsible for the wide variation in heartwood colours, give natural resistance to fungal decay and insect attack (Taylor et al., 2007). It is believed that new increments of heartwood are formed each year at the boundary between heartwood and sapwood (Magel et al., 1994), although the mechanisms are still not fully understood (Taylor et al., 2007). Sapwood surrounds the heartwood and is identified by its lighter colour. It is responsible for the conduction of water and minerals through the stem. This is evidenced in the fact that on felling, Douglas-fir heartwood typically has a moisture content in the range 45 - 50 %, whilst sapwood moisture content ranges from 100 - 180 % (Cown, 1992). Surrounding the sapwood is the vascular cambium, in which the processes through which wood is formed occur (Barnett and Jeronimidis, 2003). This in turn is surrounded by the bark, which plays a protective role and in Douglas-fir is characterised by its thick corky nature on the lower parts of the stem, which gives a high resistance to forest fires (Fontes, 2002).

2.3.6 Wood formation

As the understanding of the wood cell structure has developed, the theory of the mechanisms by which trees produce new cells and grow has changed. A comprehensive summary is given by Larson (1994). Wood is formed within the vascular cambium. In temperate regions, the annual course of cambial activity is induced by increases in temperature and the photoperiod (Uggla et al., 2001), giving rise to the growth rings which signify the start and end of growth periods. Due to difficulty in identifying the exact cells responsible for growth, the cambium is often referred to as the cambial zone or region (Larson, 1994). The cambial zone comprises two cell types, namely fusiform initials responsible for the production of longitudinal tracheid cells and ray initials from which ray parenchyma and ray tracheids are produced (Romberger et al., 1993). The first stage in the initiation of growth is the rehydration of the initials within the cambial zone (Zimmermann and Brown, 1971). Following this, both periclinal and anticlinal cell divisions take place, which allow for tangential and radial expansion of the stem, with both cell types producing radial files of daughter cells, which when created inwardly form xylem cells, and outwardly phloem (Plomion et al., 2001). Following cell division and daughter cell growth, expansion and deposition of the radial cell wall occurs, just prior to the cessation of this expansion, the secondary wall deposition begins on the inner surface of the primary wall followed by a period of lignification (Wardrop and Harada, 1965, Samuels et al., 2006). The production of either early or latewood tracheids is a function of the quantity of photosynthate available for cell wall thickening, and the concentration of growth inducing hormones which play a predominant role in regulating cell expansion (Jozsa and Oliveira, 1992).

2.3.7 Juvenile and mature wood

The terms juvenile and mature wood are often used when referring to timber quality. The concept of two wood zones was developed for practical rather than biological use (Gartner et al., 2002), and as such a strict definition of the characteristics of each does not exist. Broadly, juvenile wood can be defined as 'a zone of wood extending outward from the pith where wood characteristics undergo rapid and progressive changes in successively older growth rings' (Larson, 2001), with the wood beyond this zone referred to as mature wood. Due to the presence of high concentrations of hormonal signals produced by crown foliage controlling factors relating to cell development (Gartner et al., 2002), it is often stated that juvenile wood is produced within the live crown and mature wood below (Maguire et al., 1991, Jozsa, 1995). However, in a detailed study of Douglas-fir by Gartner et al. (2002), it was proposed that a location of two-thirds its length was a better representation of the functional crown from the perspective of juvenile wood production. The relationship between crown recession and stem

growth results in a near cylindrical core of juvenile wood within softwoods, surrounded by a tapered mature wood zone (Macdonald and Hubert, 2002), as displayed in Figure 2-5.

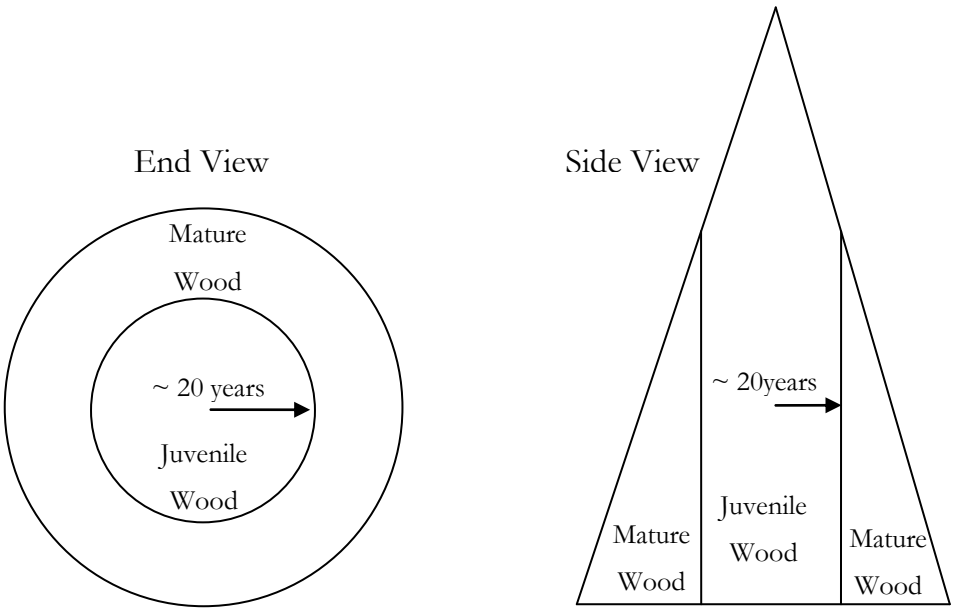

Figure 2-5: Juvenile - mature wood profiles adapted from Macdonald and Hubert (2002)

In comparison to mature wood, the juvenile wood of Douglas-fir has been shown to have increased ring width, a lower whole ring mean density and a lower proportion of latewood (Jozsa and Brix, 1989, Fabris, 2000). It has also been reported for softwoods in general that juvenile wood has shorter tracheids and higher S_2 layer microfibril angles (Zobel and Sprague, 1998, Larson, 2001). These characteristics result in a reduced modulus of elasticity, flexural strength and dimensional stability within juvenile wood (Zobel and Van Buijtenen, 1989, Zobel and Sprague, 1998), and it is therefore seen as undesirable. Defining the boundary between juvenile and mature wood production is complicated by the gradual transition between the two wood types that can occur. The most commonly used method for defining the age of demarcation is by use of both linear and non-linear segmented regression models (Abdel-Gadir and Krahmer, 1993, Sauter et al., 1999, Fabris, 2000, Alteyrac et al., 2006), in which demarcation age is determined based on the intersection point of two regression equations fitted so as to minimise residuals. The threshold method, whereby a value is selected for the property being assessed to define when mature wood production has commenced, was utilised by Clark et al. (2006). While this method allows for a defined property value for mature wood to be set, it does not account for the rate at which properties are changing, a significant factor which makes juvenile wood an undesirable characteristic, and as such it has not been widely adopted.

A large range of demarcation ages have been established for Douglas-fir at breast height, including a mean of 15 years (Wellwood and Smith, 1962 cited in Fabris 2000, Senft et al., 1986), 15 - 34 years (Di Lucca, 1989), 11 - 37 years (Abdel-Gadir and Krahmer, 1993) and a mean of 21 years (Fabris, 2000). The results presented by Fabris also displayed a general trend of decreasing demarcation age with increasing height within the stem. All demarcation ages in these studies were calculated utilising the whole ring mean density, the lack of results for microfibril angle is most likely due to the difficulty associated with obtaining sufficient measurements to perform calculations. The differences in the age of demarcation measured between and within studies has been shown to be due to silvicultural practices and site location (Fabris, 2000, Macdonald and Hubert, 2002), genotypic variability (Abdel-Gadir and Krahmer, 1993) and may also arise due to differences in the implementation of the segmented regression method.

2.3.8 Compression wood

Compression wood forms on the compression side of a stem in response to an external force acting to disrupt the vertical pattern of growth. This can occur through wind forces, growth taking place on a slope or in branches, where compression wood is a means for continually orientating branching angles (Kwon et al., 2001). There is also some evidence that rapid growth may result in the formation of compression wood around the entire stem (Walker, 1993). An excellent review of many factors regarding the occurrence of compression wood in softwoods is given by Timell (1986). Compression wood can be identified due to its wide growth rings compared to those of normal wood growing on the opposite side of the stem, an off-centred pith and a darker colour due to the increased lignin content (Bowyer et al., 2007). In Douglas-fir, compression wood contains shorter tracheids with a rounded outline with large intercellular spaces in the cell corner regions (Kwon et al., 2001). While little literature exists pertaining to the particular anatomical characteristics of compression wood in Douglas-fir, it has been shown more generally for softwood species that compression wood is typified by a highly lignified S_2 layer, the absence of the S_3 layer and a higher mean microfibril angle (Dinwoodie, 1961, Donaldson et al., 2004, Bowyer et al., 2007). The implications of these characteristics on utilisation are a higher compressive strength arising from the increased lignin content and a reduced modulus of elasticity and tendency to distort on drying as a result of the increased microfibril angle (Timell, 1986, Dhubhain et al., 1988, Walker, 2006). As a result of these factors, the presence of compression wood is often seen as negative from the perspective of timber quality in sawn structural members.

2.4 Wood density

2.4.1 Measurement of wood density

The methods available for the determination of wood density have developed significantly in the past half century, with a comprehensive list of methods given by Zobel and Jett (1995). The most commonly employed early technique was the oven dry method, in which the volume of a specimen at the desired moisture content was calculated, typically by the water displacement method, after which the oven dry weight was determined and used to calculate specimen density, as described by Simpson (1993). While this method is simplistic in its execution, it has been used to determine the density of specimens with volumes as low as 7.5 mm^3 (Olesen and Roulund, 1971 in Barnett and Jeronimidis, 2003). However, the method is better suited for use on larger specimens and as such its greatest disadvantage is the inability to obtain easily, detailed profiles of density variations both within, and in slow grown trees between growth rings.

In order to enable the generation of continuous profiles of radial variations in wood density, a technique known as x-ray densitometry was developed and is now widely used. The method involves passing an electromagnetic wave through a wood specimen and detecting the level of transmitted radiation that passes through, from which density is calculated. The use of such methods was developed in the 1960's with the use of Beta-rays by Philips (1960) and x-rays by Polge (1963). Early methods involved the placement of test specimens over photographic film, with the different levels of transmitted radiation, and hence density, identifiable by the different levels of exposure on the film (Polge, 1978). The density values were obtained by comparison to a calibration strip scanned with each specimen containing wood blocks of known density, as described by Parker et al. (1980). Disadvantages applicable to many early systems are described by Cown and Clement (1983) and include slow scanning speeds, the laborious interpretation of analogue outputs and the relatively limited levels of data resolution that can be obtained. The development of x-ray detectors which allowed the direct measurement of the intensity of the radiation transmitted through a specimen enabled the disadvantages of early systems to be overcome. With knowledge of specimen thickness, the interactions of x-rays with matter inside the wood and the intensity of the transmitted and received radiation, Beer's Law shown in Equation 2-1 can be used for the calculation of density by use of x-ray densitometry.

$$I = I_0 e^{-\mu \rho t} \quad 2\text{-}1$$

where: I intensity of transmitted radiation

I_0 intensity of radiation incident on detector

μ mass attenuation coefficient

ρ density

t thickness

Systems utilising x-ray detectors such as SilviScan and Itrax have been successfully employed for the study of density variations in softwoods at intervals as low as 25 μm (Evans, 1994, Bergsten et al., 2001, McLean, 2008). One disadvantage of such systems is the determination of the mass attenuation coefficient of a specimen, which often has to be estimated and results calibrated to the volumetrically derived density of the specimen.

2.4.2 Within tree density variations

Density variations in softwoods occur within a growth ring, radially with age and longitudinally in the stem. The density of oven dry cell wall material has been shown to be approximately 1500 kg/m^3 regardless of species (Huang et al., 2003), and as such density variations are caused due to changes in the proportion of solids in the fibre wall, the size of voids in the lumen (Jozsa and Oliveira, 1992) and changes in moisture content (Simpson, 1993). Variations in density have been most widely studied with increasing cambial age. Early attempts to measure radial density variations in Douglas-fir by Chalk (1953) and Erickson and Harrison (1974) allowed for general trends to be identified. However, the calculation of the density of specimens encompassing more than one growth ring based on oven dry weight and green volume gave a poor level of resolution. It was not therefore until x-ray densitometry analysis was adopted (Di Lucca, 1987, Jozsa and Brix, 1989, Fabris, 2000, Gartner et al., 2002), that a detailed understanding of the intra- and inter-ring density variations in Douglas-fir was gained. Radial variations in dry whole ring mean density at breast height for Douglas-fir and several other softwood species presented by Jozsa and Middleton (1994) are shown in Figure 2-6. In the 60 second-growth Douglas-fir trees sampled, an average relative density[1] value of 0.47 was reported in the first formed growth rings, decreasing to approximately 0.4 at ring 10, after which time the density increased steadily until 30 years of age, at which point the rate of change of increases reduced significantly. It was however shown in a single 500 year old Douglas-fir by Wellwood et al. (1974) that it may take several hundreds of years for density

[1] Relative density is the density of a material relative to the density of water at 4 °C

values to stabilise fully. The radial trends and values recorded by Di Luca (1987), Fabris (2000) and Gartner et al. (2002) in Douglas-fir correspond well to those shown in Figure 2-6.

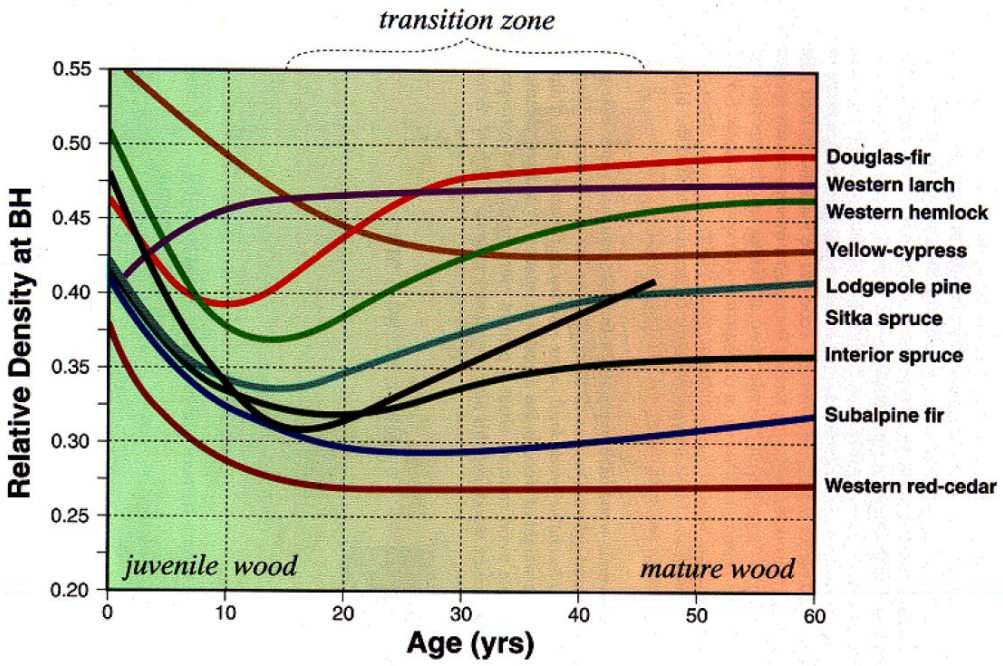

Figure 2-6: Change in relative density with age at breast height for several softwood species from Jozsa and Middleton (1994)

The high densities recorded near the pith in Douglas-fir and a large number of other species are attributed to the morphology of the tracheids within early growth rings which tend to be short with a small diameter, causing an increased number of cell walls for a unit volume, and due to the increased likelihood of compression wood being formed due to high wind stresses on young stems (Kennedy, 1995 in McLean 2008). Longitudinally, Spicer and Gartner (2001) and Gartner et al. (2002) found that wood density patterns exhibited similar trends and values to those found at breast height in Douglas-fir, with similar results also reported in Balsam-fir (Koga and Zhang, 2004), Jack pine (Park et al., 2009) and Norway spruce (Jyske et al., 2008). With the use of x-ray densitometry, Jozsa and Middleton (1994) showed intra-ring density profiles in Douglas-fir juvenile wood with minimum relative density values of 0.25 in earlywood, rising to 0.8 in latewood. In more mature growth rings maximum values in latewood reached 0.85. Equivalent ranges and developmental characteristics with age at the intra-ring level were found in Douglas-fir by Fabris (2000), Gartner et al. (2002) and Lachenbruch et al. (2010).

2.4.3 Influence of growth rate on wood density

The relationship between wood density and growth rate is one that has been studied extensively, due to the high level of importance that has been placed on density in the past as a predictor of wood quality traits. Zobel and Van Buijtenen (1989) and Zobel and Jett (1995) reviewed the results of over 100 studies investigating links between growth rate and density in several softwood species. While there were many conflicting results, Zobel and Jett grouped findings according to species and noted that within hard pines an increased rate of growth had a reduced negative influence on wood density in comparison to the results observed in some spruces and firs, a similar observation was made by Zhang (1995). It was however acknowledged by Zobel and Jett that several contradictory results had been reported for Douglas-fir specifically.

In an early study of the influence of an increased rate of growth on density in Douglas-fir, Erickson and Harrison (1974) identified a decrease in density of 10 % compared to control trees, following the application of fertiliser at 20 years of age resulting in a 50 % increase in ring width. In a study of 12 year old Douglas-fir stems by King et al. (1988), a moderate negative linear correlation of -0.53 was identified between an increasing stem diameter and density. The study was however limited by the fact that the gravimetrically determined density was only evaluated on the outer four growth rings of each tree. A more in depth analysis of intra-tree density on 360 Douglas-fir stems was conducted by Abdel-Gadir (1991), in which x-ray densitometry was used to determine values in juvenile and mature wood, with 10 growth rings from each region assessed per tree. The results showed that there was no relationship between the rate of growth and whole ring density in either juvenile or mature wood. It was however noted that an increasing ring width was moderately negatively correlated with earlywood density in the juvenile region, with an equal and opposite result observed in the latewood. Loo-Dinkins et al. (1991) found a relationship of decreasing density with the increasing volume of 16 year old Douglas-fir discs. While the results give only a broad overview, an increase in volume can be directly related to increasing growth rate, assuming the variable thickness of discs was accounted for. Moderate negative correlations between increasing bole volume and density were also reported by Vargas-Hernandez and Adams (1991).

Perhaps the most extensive study to date regarding the influence of an increased growth rate on density in Douglas-fir was conducted by Fabris (2000), with differences in the rate of growth being primarily induced as a result of variations in the initial spacings of sample trees.

By investigating relationships within individual growth rings, Fabris was able to conduct analysis at a greater resolution than seen previously. It was noted at all cambial ages assessed, that a negative relationship between increasing ring width and whole ring mean density existed. The strength of the relationship did however vary, from weak statistically non-significant linear correlations, to correlation coefficients in excess of -0.5. The majority of the non-significant results were found within the mature wood. Earlywood density was found to exhibit some moderate positive correlations within the juvenile wood, with moderate negative relationships present within the mature wood. The reverse was true of the latewood density, however no explanation was given for these differences in behaviour. While a number of other anatomical features were studied by Fabris, those relating to tracheid dimensions and their changes with growth rate, with the exception of tracheid length, were not assessed. As such it is not possible to fully interpret the causes of the behaviour observed.

2.5 Wood microfibril angle

2.5.1 Measurement of wood microfibril angle

Techniques for measuring the angle of cellulose microfibrils with respect to the longitudinal orientation of tracheids are numerous, with comprehensive reviews given by Barnett and Jeronimidis (2003), Barnett and Bonham (2004) and Donaldson (2008). Methods can broadly be grouped into two types, those which rely on polarised light techniques to study the optical properties of crystalline cellulose, and those which directly or indirectly visualise the orientations of microfibrils (Donaldson, 2008). The polarisation technique was among the first to be used to assess microfibril angle in softwoods, being employed in the pioneering work of Preston (1934) and several subsequent studies (e.g. Page, 1969, Leney, 1981, Donaldson, 1991). The technique utilises the birefringent[1] nature of crystalline cellulose. By illuminating a single cell wall with polarised light and subsequently viewing it through a microscope with a polarising filter crossed to the polarisation direction of the incident light, it is possible to calculate the angle of the microfibrils. This is done by rotating the fibre until the cell wall becomes dark, at which point the microfibril angle is that which exists between that of the fibre and the incident light polarising filter. A limitation of the method is that the polarised light must only be passed through single cell walls. To overcome this, several preparation techniques have been developed, such as the cutting of slide mounted tracheids with a fine blade (Preston, 1934) or reflecting the incident light using mercury forced into tracheid lumens (Page, 1969).

[1] A birefringent material is one which refracts an incident light wave in two distinct directions

While it is not possible to directly visualise cellulose microfibrils with the use of a light microscope, there are several physical and chemical treatments that can be applied to wood tracheids to allow for indirect visualisation. A commonly used indirect method is iodine staining. Originally utilised by Bailey and Vestal (1937) and developed by Senft and Bendtsen (1985) to allow for easier application to a large number of specimens. The method involves placement of thin microtomed sections into an iodine-potassium-iodide solution, which are then removed and nitric acid added which results in the formation of iodine crystals. These crystals have been shown to form within cavities in the cell wall of the S_2 layer at the boundary with the S_1 layer (Donaldson and Frankland, 2004) following the orientation of cellulose microfibrils. When viewed through a light microscope the angle of crystals can be used to infer the orientation of the microfibrils. Chemical treatments, including the placement of specimens in Congo Red (Huang, 1995) and various transition metal salt solutions (Wang et al., 2001), have also been used to aid the visualisation of checks formed in the cell wall induced by ultrasonic treatment, which follow the angle of S_2 layer microfibrils. While good results in detecting the microfibril angle were reported in all studies using chemical treatments, the methods have also been noted to be time consuming in the preparatory stages and the production of results is inconsistent.

The angle of tracheid pit apertures are regarded as being closely aligned with the angle of cellulose microfibrils (Donaldson, 2008), so their orientation with respect to that of the longitudinal tracheid orientation has been used as a measure of microfibril angle (e.g. Cockrell, 1974). After the preparation of microtomed timber sections from which measurements are to be taken, the recording of results is relatively simple and can be conducted with a normal light microscope. Typically, the pit aperture method is only reliable for estimating the fibril angle in latewood tracheids (Huang 1997), due to pit apertures having a greater elongation in this region and therefore being easier to measure (Donaldson, 2008). This can lead to results which are not fully representative, due to the variation in angle that occurs within a growth ring from early to latewood. A further potential difficulty related to the use of this method is that in some tracheids, pit apertures may not be found in sufficient quantities to allow reliable results to be gained (Senft and Bendtsen, 1985).

In work conducted by Donaldson and Xu (2005) and Lacrosse (2010) it was demonstrated that with the use of transmission electron microscopy that cellulose microfibrils within the cell wall could be directly visualised and their angle measured. The methodology used offered the advantage that microfibrils could be assessed in all three secondary cell wall layers, however

the oblique sectioning of tracheids required in order for measurements to be made was time intensive.

Techniques to measure microfibril angle by use of small angle x-ray scattering developed by Wardrop (1952) and wide angle x-ray scattering pioneered by Cave (1966) and Meylan (1967), are increasingly being adopted in wood property studies. The microfibril angle is calculated based on the diffraction patterns generated by reflections of incident x-rays from the various crystalline planes found within cellulose, with a good agreement between the results generated by the two methods typically observed (Lichtenegger et al., 1998, Andersson et al., 2000). Several techniques to interpret the microfibril angle have been developed, including the use of Meylan's angle, T, obtained from the tangents to the outer edges of the diffraction profiles (Meylan, 1967 in Evans, 1999) and the method based on the variance of the diffraction profiles developed by Evans (1999). An advantage of the method developed by Evans is that it does not require calibration against results derived from other methods, however at high angles typically found within the juvenile wood and in the event of excessive fibre tilt the precision of results may fall (Verrill et al., 2011). Studies in which x-ray based methods have been compared to some of the traditional techniques for determining microfibril angle described previously have shown that good correlations exist overall between the methods (Andersson et al., 2000, Long et al., 2000, Donaldson, 2008). X-ray diffractometry has been utilised in a number of studies, some of which are listed by Barnett and Bonham (2004).

A comparison of the accuracy and ease of use of many of the techniques described here was made by Huang et al. (1998). The key disadvantages associated with many of the optical techniques are the specimen preparation time, the difficulty that can occur in measuring results and the large number of observations that are necessary to collect sufficient quantities of data. An advantage of the methods however, is that they allow properties to be assessed within individual tracheids, something that is not possible with x-ray techniques in which an average value is obtained for several tracheids. X-ray techniques also require a large quantity of specialist equipment, though they do offer the advantage of autonomy and enable large quantities of data to be collected.

2.5.2 Within tree microfibril angle variations

An excellent review of the current understanding of the role played by cellulose microfibrils, and their variations within the cell wall is given by Donaldson (2008). In comparison to studies evaluating changes in wood density, those relating to the radial and longitudinal

variation of the cellulose microfibril angle are limited in Douglas-fir. This can be attributed to the difficulty in measurement and the long perceived notion that density was the prime determinant of wood quality. Of the studies that have been conducted, all focus on variations in the S_2 layer, due to its high proportion within the cell wall. Utilising a polarizing microscope, Erickson and Arima (1974) observed a trend of decreasing microfibril angle in the S_2 layer within the tangential walls of latewood Douglas-fir tracheids, with average values of 32° near the pith, falling to 7° by the 30th growth ring. Fabris (2000) documented a similar decrease over the first 33 growth rings in Douglas-fir earlywood tracheids, measuring the angle of induced checking on the radial cell wall. While providing insightful data, both of these studies were limited by the restrictions of the measurement techniques used. The differences between the microfibril angle within Douglas-fir early and latewood have been shown by Ifju and Kennedy (1962), Lofty et al. (1973) and Lachenbruch et al. (2010), with the microfibril angle in latewood found to be lower in all cases. In the study of 183 mature specimens with a mean age of 29 years conducted by Lachenbruch et al., microfibril angles of 16.3° and 11.8° were recorded in the earlywood and latewood respectively. However no documented results were found regarding the developmental profiles with age of intra-ring microfibril angles. The trend of a decreasing microfibril angle with increasing cambial age, and from early to latewood within growth rings, has also been documented for other softwood species including Loblolly pine (Bendtsen and Senft, 1986), Norway spruce (Lundgren, 2004, Saren et al., 2004), Radiata pine (Donaldson, 1992), and Sitka spruce (McLean, 2008). This pattern of a decreasing microfibril angle with age has been attributed to the need of young shoots to have a greater flexibility and therefore lower stiffness, to enable them to better survive forces due to wind and passing animals (Barnett and Jeronimidis, 2003). No documented data was found regarding changes in microfibril angle with increasing longitudinal position within Douglas-fir trees, however in other species including Loblolly pine (Jordan et al., 2005) and Radiata pine (Donaldson, 1992), it was found that for growth rings of an equivalent cambial age a decrease in microfibril angle took place with increasing height in the stem.

Due to the limited proportions found within the cell wall and the difficulty in measuring properties, fewer studies have been conducted evaluating the angles of microfibrils within the S_1 and S_3 layers. Unlike the systematic variation from pith to bark seen in the S_2 layer microfibril angle, no such trend is thought to exist within the S_1 and S_3 layers aside from that which occurs within each cell wall in moving from an S to a Z helix (Donaldson, 2008). A large range of values for microfibril orientation have been reported in the layers, with potential differences due to methodology and species likely. From the values presented a range of

orientations from S to Z helix of 45° to 70° and ± 50° within the S_1 and S_3 layers provides a reasonable indication of the changes which take place (Abe et al., 1991, Booker and Sell, 1998, Donaldson and Xu, 2005). However, further research is required to identify values for Douglas-fir.

2.5.3 Influence of growth rate on microfibril angle

Given the limited number of studies conducted assessing the microfibril angle in softwood tracheids, it is not surprising that documented data regarding the influence of a changing rate of growth on the fibril angle is also scarce. In Douglas-fir, Erickson and Arima (1974) studied the effect of stimulated growth following fertilisation on fibril angle. It was found that a slight positive relationship existed, with microfibril angle displaying an increase of approximately 10 % compared to a near 100 % increase in ring width. Fabris (2000) also identified a positive relationship between ring width and microfibril angle in Douglas-fir when all growth rings of a given cambial age were compared. Linear correlation coefficients were typically moderate at around 0.5. The results presented in both of these studies were limited by the number of growth rings that could be evaluated, due to constraints arising from the methodologies used. A positive relationship between the S_2 layer microfibril angle and the rate of growth has also been demonstrated in Norway spruce (Herman et al., 1999, Lundgren, 2004), Red pine (Deresse et al., 2003) and in the juvenile wood of Sitka spruce (Cameron et al., 2005). However it is also the case that in some studies, limited or no changes in the fibril angle were found with increasing growth rate, such as that conducted on Ponderosa pine (Shuler et al., 1989) and Radiata pine (Donaldson, 1996). While it appears that a rise in microfibril angle is linked to an increased rate of growth, the limited nature of the studies available, both in regards to the methodologies used and the lack of repeat studies within a species, results in difficulty in assessing the scale of the influence of growth rate on microfibril angle.

2.6 Mechanical properties relevant to structural applications

2.6.1 Modulus of elasticity

The modulus of elasticity of a material is the gradient of the linear region of the stress-strain profile in either flexure or tension, with a higher value representing a lower deformation for a given load (Barnett and Jeronimidis, 2003). The modulus of elasticity most commonly of interest when utilising timber in structural applications is the flexural value, which is of primary importance in the determination of the structural grade achieved by a section in accordance with BS EN 338: 2003 'Structural timber: Strength classes' (BSI, 2003). As such, all

references to modulus of elasticity in this work refer to flexural values, unless noted otherwise. The modulus of elasticity is influenced by moisture content, with a decrease noted up to the fibre saturation point (Dinwoodie, 2000), the presence of knots (Vikram et al., 2011) a sloping grain (Pope et al., 2005) and due to variations in anatomical properties, as discussed in Section 2.7. Due to the fibrous nature of wood, timber is an orthotropic material, meaning that it has unique and independent mechanical properties in the longitudinal, radial and tangential directions (FPL, 1999), with the longitudinal modulus of elasticity of fibres being that which is most closely associated with flexural values, due to the fact that tracheids are typically aligned near to parallel with the longitudinal dimension in sawn sections (Barnett and Jeronimidis, 2003).

No documented data regarding the change in modulus of elasticity with increasing cambial age or height was found for Douglas-fir. The results for several other softwood species obtained with the use of defect free small clear specimens including Black spruce (Alteyrac et al., 2006), Loblolly pine (Bendtsen and Senft, 1986), Maritime pine (Machado and Cruz, 2005), Radiata pine (Cown et al., 1999, Tsehaye et al., 2000, Xu and Walker, 2004) and Sitka spruce (McLean, 2008) have shown that large increases, typically of up to 100 % of values obtained nearest the pith, are common within the juvenile wood. Rates of change were noted to reduce significantly with greater cambial age into the mature wood. It was found by Barrett and Kellogg (1991) in Douglas-fir that as the proportion of juvenile wood in structural sized sections increased, the modulus of elasticity decreased. Both Tsehaye et al. (2000) and Xu and Walker (2004) studying mechanical properties in Radiata pine identified little change in modulus of elasticity with height in the stem. Mean values of modulus of elasticity for Douglas-fir trees, determined utilising clear wood specimens, have been published, as summarised in Table 2-2.

From the data presented it can be observed that the mean modulus of elasticity values for Douglas-fir grown within the United Kingdom are lower than many of the values documented in studies conducted on material from other sources. While insightful, the work conducted by Lavers (1983) on timber derived from the United Kingdom is limited, in that it does not allow for an in-depth understanding of mean property variations with age, and there is no indication from where in the stem material was obtained. This limitation also extends to data presented for material from other geographic locations, so direct comparisons between locations are not possible.

Table 2-2: Mean modulus of elasticity of Douglas-fir specimens

Origin	Age (Years)	Modulus of elasticity (N/mm^2)	Source
Australia (New South Wales)	45-55	13000	(Cown, 1992)
Australia (Victoria)	45-55	10900	(Cown, 1992)
Canada	Not given	12700	(Lavers, 1983)
New Zealand	Not given	10000	(Cown, 1992)
United Kingdom	Not given	10500	(Lavers, 1983)
United States (Oregon and Washington)	Not given	12500	(FPL, 1999)
United States (North West Oregon)	28.8 (Mean)	11500	(Lachenbruch et al., 2010)

2.6.2 Flexural and compressive strength

In addition to the modulus of elasticity, flexural and compressive strength parallel to the grain are key parameters when utilising timber in structural applications such as beams and columns. Strength is a measure of the maximum load carrying capacity of a section, whether it is loaded in bending in the case of a beam or compression for a column (FPL, 1999). As with modulus of elasticity, strength properties are also influenced by moisture content (Barnett and Jeronimidis, 2003) and particularly by the presence of defects such as knots which act as stress raisers and reduce the available section size over which stresses can be carried. This is clearly shown in the experimentally derived reduction factors to be applied to clear wood specimens due to the presence of defects given in ASTM D 245: 'Standard practice for establishing structural grades and related allowable properties for visually graded lumber' (ASTM, 2000).

No documented data regarding the change in strength properties with increasing cambial age or height in the stem was found for Douglas-fir. However, as for the modulus of elasticity, the results for several other softwood species obtained with the use of defect free small clear specimens including Black spruce (Alteyrac et al., 2006), Loblolly pine (Bendtsen and Senft, 1986), Maritime pine (Machado and Cruz, 2005), Radiata pine (Cown et al., 1999, Tsehaye et al., 2000, Xu and Walker, 2004) and Sitka spruce (McLean, 2008) have shown large increases, typically of the order of 50 - 100 %, on moving from pith to bark. The majority of these increases were observed to occur within the juvenile wood. In the work conducted by

Bendtsen and Senft and Machado, an increase in the compressive strength of a similar magnitude to that seen in flexural properties was observed. Mean values of flexural and compressive strength for Douglas-fir trees, determined utilising clear wood specimens, have been published, as summarised in Table 2-3.

Table 2-3: Mean flexural and compressive strengths of Douglas-fir specimens

Origin	**Age (Years)**	**Flexural / Compressive strength (N/mm^2)**	**Source**
Australia (New South Wales)	45-55	90/55	(Cown, 1992)
Australia (Victoria)	45-55	76/42	(Cown, 1992)
Canada	Not given	93/52	(Lavers, 1983)
New Zealand	Not given	88/43	(Cown, 1992)
United Kingdom	Not given	91/48	(Lavers, 1983)
United States (Oregon and Washington)	Not given	85/50	(FPL, 1999)
United States (North West Oregon)	28.8 (Mean)	107/Not given	(Lachenbruch et al., 2010)

The values of both strength parameters determined from timber sourced within the United Kingdom are comparable with those from other locations, unlike the modulus of elasticity values. Property variations with age cannot be gained from this information.

2.6.3 Influence of growth rate on mechanical properties

With the increased utilisation of fast grown plantation softwoods, there is a need to identify potential detrimental effects of increased growth rates on mechanical characteristics that may influence end use performance. While studies relating to the influence of growth rate on density, a characteristic long thought to be a prime determinant of mechanical properties, are extensive, those relating directly to mechanical properties are more limited. A wide-ranging study of the influences of growth rate on mechanical properties in eight softwood species was conduced by Zhang (1995). In the large majority of species, moderate to strong negative linear correlations between both modulus of elasticity, flexural and compressive strength were found with an increased rate of growth, assessed through ring width. While Douglas-fir was not assessed in the study, Masson's and Yunnan pine were, both being classified by Zhang as

having abrupt transitions from early to latewood. This characteristic is also commonly observed in Douglas-fir as well as hard pines (Spicer et al., 2000), and formed the basis of the grouping when studying the influence of growth rate on density by Zobel and Jett (1995), as described in Section 2.4.3. As such similar results may be expected in Douglas-fir. The extent to which mechanical properties changed with ring width was not shown by Zhang and therefore a quantification of the impact of the results is not available. In the comparison of slower and faster grown stems of Norway spruce, Kliger et al. (1998) identified a relatively consistent reduction in both modulus of elasticity and flexural strength of 25 % within juvenile and mature wood, with a 50 % difference in ring width between growth rates. Significant reductions in the value of modulus of elasticity, flexural and compressive strengths, in some instances greater in percentage terms than the rise in ring width, were also identified in Scots pine by Eriksson et al. (2006).

2.7 Relationships between anatomical and mechanical properties

Interactions between the anatomical properties of wood and the mechanical properties of the timber derived from it are of interest to silviculturists, tree growers and log processors in maximising quality and value (Lachenbruch et al., 2010). The relationship between density, modulus of elasticity, flexural and compressive strength has been extensively studied, due to the relative ease with which density can be assessed. In their book, Barnett and Jeronimidis (2003) refer to density as 'most likely the best single predictor of mechanical properties of clear, straight grain defect free wood'. This statement has been shown to be true in a large number of previous studies of softwood, in which strong correlations were observed between increases in the magnitude of mechanical properties and a rise in density within both juvenile and mature wood (Armstrong et al., 1984, Zobel and Jett, 1995, Rozenberg et al., 1999, Burdon et al., 2001). While it had been shown theoretically since the 1960's that a decreasing microfibril angle within the S_2 layer of the cell wall was also an important factor in the prediction of the modulus of elasticity (Cave, 1968, Cave, 1976), difficulties in assessing the microfibril angle of large numbers of specimens resulted in limited experimental validation of these predictions. It was only with the advent of x-ray diffractometry techniques for the assessment of fibril angle, that sufficient numbers of specimens could be assessed for it to be clearly shown that the microfibril angle is also an important controlling factor of modulus of elasticity (e.g. Evans and Ilic, 2001). In studies considering the influence of both density and microfibril angle on mechanical properties within defect free specimens, it has been shown

within juvenile wood (Ivkovi et al., 2009) and mature wood (Lachenbruch et al., 2010) that density is more strongly associated with increases in flexural strength than microfibril angle. It was shown for the modulus of elasticity however that, within the juvenile wood, a decreasing microfibril angle is a key determinant of rising modulus (Baltunis et al., 2007, Ivkovi et al., 2009, Via et al., 2009) while in mature wood, density was more strongly associated with any continuing increases in the modulus of elasticity (Lachenbruch et al., 2010). Results relating compressive strength and anatomical characteristics are scarce. While insightful, these previously documented results are of limited use with regard to understanding the interactions occurring across the entire stem, due to the fact that in all but the work conducted by Via et al. (2009), relationships were only assessed within the juvenile or mature wood. As a result of this, it was clearly stated by Lachenbruch et al. (2010) in a study of Douglas-fir mature wood, that further research is needed to learn whether the relationships of anatomy to the modulus of elasticity and flexural strength differ in juvenile wood from those in the mature wood of Douglas-fir.

2.8 Factors influencing variability in wood properties within and between sites

While the focus of this study is the investigation of within tree variations and interactions between Douglas-fir properties, an understanding of the factors within and between sites that may induce variability in results may aid in their interpretation. Macdonald and Hubert (2002) reviewed several factors influencing timber quality in Sitka spruce, which can be separated into three categories; silvicultural practices, site factors and differences relating to genetics. Silvicultural practices include initial spacing, thinning and pruning. In studies investigating the influence of tree spacing conducted on Douglas-fir grown in Germany (Hein et al., 2008) and North America (Fabris, 2000, Briggs et al., 2007) wider spacing had a positive relationship with breast height diameter, the diameter of the thickest branch, live crown ratio and crown diameter as a result of reduced competition with adjacent trees and hence increased availability of light and nutrients. Thinning interventions, in which trees are selectively removed from a site, also reduces inter-tree competition. Thinning prior to crown closure has effects similar to those seen for wider initial spacings, while post closure thinning, when lower stem branch mortality and the transition from juvenile to mature wood production may have already occurred, allows for the production of knot free wood in the lower region of the stem (Macdonald and Hubert, 2002). The silvicultural intervention of branch removal, known as pruning, and its resulting implications on wood quality has also been studied in Douglas-fir.

One benefit of the practice is reduced knottiness. It was also demonstrated by O'Hara (1991) and Gartner et al. (2005) that removal of up to a third of lower branches, even within the live crown, has only limited impact on diameter growth and the magnitude of anatomical characteristics such as density. As discussed in Section 2.3.7, it has been shown that juvenile wood is produced within the live crown, and as such pruning is thought to accelerate the transition from juvenile to mature wood production (Briggs and Smith, 1986 in Macdonald and Hubert, 2002).

Several studies have documented the site factors that have the greatest impact on the growth productivity of Douglas-fir. Those which have commonly been shown to be most strongly associated with increased productivity are the presence of well drained soils derived from shale or granite, an aspect other than north, sites with increased rainfall, good fertility and a low exposure (Dixon, 1971, Tyler et al., 1995, Corona et al., 1998, Dunbar et al., 2002). A low exposure, or good shelter, results in increased growth productivity due to the reduced likelihood of wind damage to newly produced crown foliage. The relative importance of these factors varies between studies, most likely as a result of the variation in the parameters included in each, and the diverse range of the parameters within the studied sites. The variance in wood properties between trees and sites not apportioned to silvicultural and environmental factors is likely due to heritable genetic traits. It has been shown in several studies of Douglas-fir that many factors relating to wood quality have moderate to high heritabilities (Johnson and Gartner, 2006, Cherry et al., 2008, Vikram et al., 2011). Given the large native range of Douglas-fir, genetic differences between seeds sourced from different locations within this range result in a varied suitability for the species to be grown exotically elsewhere. Fletcher and Samuel (2010) developed a seed origin suitability map for Great Britain to aid in selecting the most suitable source region for particular locations. It was identified for the South West that seeds sourced from the Washington coast were best suited for growth within the region. In comparing the climatic details for the various potential seed collection areas and locations within the United Kingdom, Fletcher and Samuel showed that conditions within the South West of England are typically drier than the native range, with a narrower band of temperature variations and a significantly greater number of frost free days annually.

2.9 Micromechanical models of wood structure

It was shown within Section 2.3 that at several levels wood can be considered a natural composite material. In a quest for a greater understanding of the origins of both physical and mechanical properties, several theoretical composite models, based on anatomical

characteristics, have been developed for their prediction. In one of the earliest documented studies modelling the behaviour of wood, Price (1929) represented the cellular structure as a series of hollow cylinders to explain anisotropic behaviour. The study identified many of the features responsible for the variability in behaviour, however as a result of the limited knowledge of the fine structure and its properties at the time, no numerical predictions were made. One of the first models to adopt the concept of modelling wood cells as a composite structure, with microfibrils embedded in a reinforcing matrix, was produced by Barber and Meylan (1964). While used for the prediction of anisotropic shrinkage rather than elastic properties, and only considering the S_2 layer as a flat sided slab, the concepts employed form the basis for many of the more advanced models that have been developed since. It was with the use of a similar two phase composite model that Cave (1968) demonstrated the importance of the cellulose microfibril angle as a controlling factor of cell wall elasticity. Early models taking into account the multi layered laminated structure of the cell wall were developed by Schniewind (1966) and Mark (1967). Improvements in the availability of computational processing, and a greater understanding of the properties of the chemical constituents and varying characteristics of each of the cell wall laminates, allowed Salmén and De Ruvo (1985) to show the influence of fibril angle variations within the S_1 and S_3 layers on cell wall longitudinal modulus, as well as variations within the S_2 layer. This has lead to the development of advanced cell wall models, such as that produced by Bergander and Salmén (2002), in which the double cell wall of the native wood structure was modelled as a nine layered laminate, accounting for differences in thickness, fibril angle and the proportions and properties of the chemical constituents for the prediction of elastic behaviour.

One limitation of the models described above when modelling the elastic properties of softwoods, is that they do not allow for consideration to be given to other important factors which influence these properties in real specimens. These include cell wall thickness, cell dimension and the proportions of early, transition and latewood bands. As a result of this, multi-scale models that allow these factors to be accounted for have been developed. A good example of such a model is that created by Astley et al. (1998), in which composite laminate theory and finite element analysis was used to model each cell wall, while cellular geometries were generated from transverse micrographs of real cells. A similar multi-scale modelling approach was adopted by Persson (2000), utilising both real cell micrographs and a model based on hexagonally shaped tracheids, with comparable results achieved between the two approaches. A hexagonal honeycomb structure was also adopted by Qing and Mishnaevsky Jr (2009). In an alternative approach, Guitard and Gachet (2004) utilised a rectangular structure

to represent the tracheid cells for the calculation of elastic properties. In their work Decoux et al. (2004) compared both hexagonal and rectangular structures for modelling cellular geometries, and found that the results achieved were comparable. In reality, the adoption of one specific cell organisational structure is unlikely to be able to fully replicate that which is found within a real wood specimen. For this reason the taking of wood micrographs represents the best way to truly capture the variable nature of the cellular structure, however this also has the disadvantage of the time intensive nature of analysis and replication for each individual specimen.

The results generated in many of the models described above have been shown to compare favourably to those obtained through testing the elastic properties of single fibres (e.g. Salmén and De Ruvo, 1985) and those determined through the testing of larger specimens (e.g. Astley et al., 1998). However, in most cases a comprehensive validation of the effectiveness of the models in predicting properties was not possible, due to either a lack of data pertaining to the exact cellular structure and microstructure of a specimen, or the mechanical properties of specimens relating to the assessed anatomical properties.

2.10 Concluding remarks

In this review of literature it has been shown that an extensive range of research has been conducted into many factors relating to the anatomical and mechanical properties of softwoods. For Douglas-fir, the intra- and inter-growth ring variability of some parameters, such as density, is relatively well understood. However, limitations in measurement techniques have resulted in a poor understanding of the ways in which properties such as microfibril angle vary within the stem. It is also the case that while typical means and ranges for mechanical properties are widely reported, knowledge of their variability within the stem and the potential implications that this may have for utilisation is relatively limited. Few studies were found in the literature documenting the properties of Douglas-fir grown within the British Isles. Given that the climatic conditions found within the area of focus of this work, the South West of England, are typically much drier with a smaller range of annual temperatures, it is wrong to assume that the properties reported from locations where the species is grown natively will be comparable to those within the study region.

While density has been widely reported to be the best single indicator of wood mechanical properties, many of these conclusions were drawn without assessment of microfibril angle. The microfibril angle has theoretically been shown to also be an important determinant of the

mechanical behaviour of wood, but there is limited experimental data to verify cell wall models and show property variations between juvenile and mature wood. Gaining a deeper understanding of the interactions that exist between these anatomical and mechanical wood properties, and their variations within the stem, therefore presents numerous opportunities for improvements in both efficient processing and utilisation of timber.

Chapter 3 - Materials and methods

3.1 Introduction

In this chapter descriptions of the methodologies used in the collection and analysis of experimental data are given. The techniques employed to select and sample test trees are first presented. This is followed by an account of the steps taken in the preparation and analysis of specimens utilising the SilviScan-3 system to evaluate anatomical properties, and the flexural and compression tests employed to determine mechanical properties. Finally, the various statistical techniques employed in the analysis of the experimental data are described.

3.2 Selection of sample trees

3.2.1 Sample site selection and characteristics

In order that the results obtained from this study were relevant to the Douglas-fir resource found within the South West of the United Kingdom, sample sites from which to extract test trees were split into two categories. The first was those containing trees in the age range of 40 - 50 years and the second those containing trees > 50 years of age. These age ranges were established based on the findings of an assessment of the conifer resource within the South West (Forest Research, 2009), which showed that selecting trees within the 40 - 50 year age range would capture the current peaks in the Douglas-fir age distributions in both public and private estates. An age of 50 - 55 years is also commonly regarded as an optimal felling age for Douglas-fir (e.g. Coed Cymru, 2007) when calculated from the perspective of mean annual volume increment[1]. However, as forest management practices develop towards those which utilise a mixed age stand structure, as discussed by Macdonald et al. (2010), a greater number of trees that have exceeded the optimal felling age calculated using the mean annual increment

[1] The mean annual volume increment is the average volume production per year for a forest area, the maximum value being a measure of greatest productivity.

method will be found. For this reason, a number of trees greater than 50 years of age were included within the sample set.

The review of literature presented in Chapter 2 showed that the large majority of the variations seen in anatomical and mechanical properties were found to occur within the juvenile region of the stem, typically at cambial ages less than 30 years. Trees in the 40 - 50 year age range would therefore capture these changes and were selected to form the basis of the experimental sample set, with a limited number of older trees used to establish if the trends observed continued with increasing age. The large number of variables that can influence the characteristics of the wood produced by trees within and between sites, made the selection of sample sites reflecting typical growing conditions within realistic logistical constraints difficult. It was therefore decided to select sites containing trees within the 40 - 50 year age range randomly from a list of those available and assessed for suitability according to the criteria described below. Younger trees were to be selected from five sites with six trees sampled per site, allowing for a good geographical range to be obtained within the region and also for trees to be selected from the range of growth rates present within each site. Four trees with ages > 50 years from two sites were to be tested to verify the continuation of trends in the results observed in older stems.

The selection of sample sites from those available was conducted according to the following criteria:

- Regional distribution: A sample site distribution reflecting the geographic range of Douglas-fir in the region was desirable.
- Site condition: An assessment was made of the overall condition of the trees within each site, noting any factors which could hinder the implementation of a consistent sampling strategy such as excess numbers of dead trees, storm damage, animal damage and a large number of stems with excessive bow[1].
- Availability of site management history: The availability of information detailing previous silvicultural interventions such as thinning, pruning and fertiliser applications was assessed.
- Even age: In order to allow the variations in growth rate between standing trees within a site to be assessed it was necessary that all trees within 40 - 50 year old sample sites were of an equal age.

[1] The existence of bow in a region of the stem typically indicates the presence of compression wood

- Site access: The ease with which individual trees could be marked, felled and removed was evaluated.

Due to unforeseen circumstances, it was not possible to obtain sample trees in the 40 - 50 year age range from one of the selected sites in the region of Dartmoor National Park. As a result of this only four sites were used. All trees within the 40 - 50 year age range were obtained from the publicly owned forest estate managed by the Forestry Commission, while older trees were obtained from privately owned estates. The location of the sites selected in the context of forestry within the South Western region of England, and the characteristics of each site is shown in Figure 3-2 and Table 3-1.

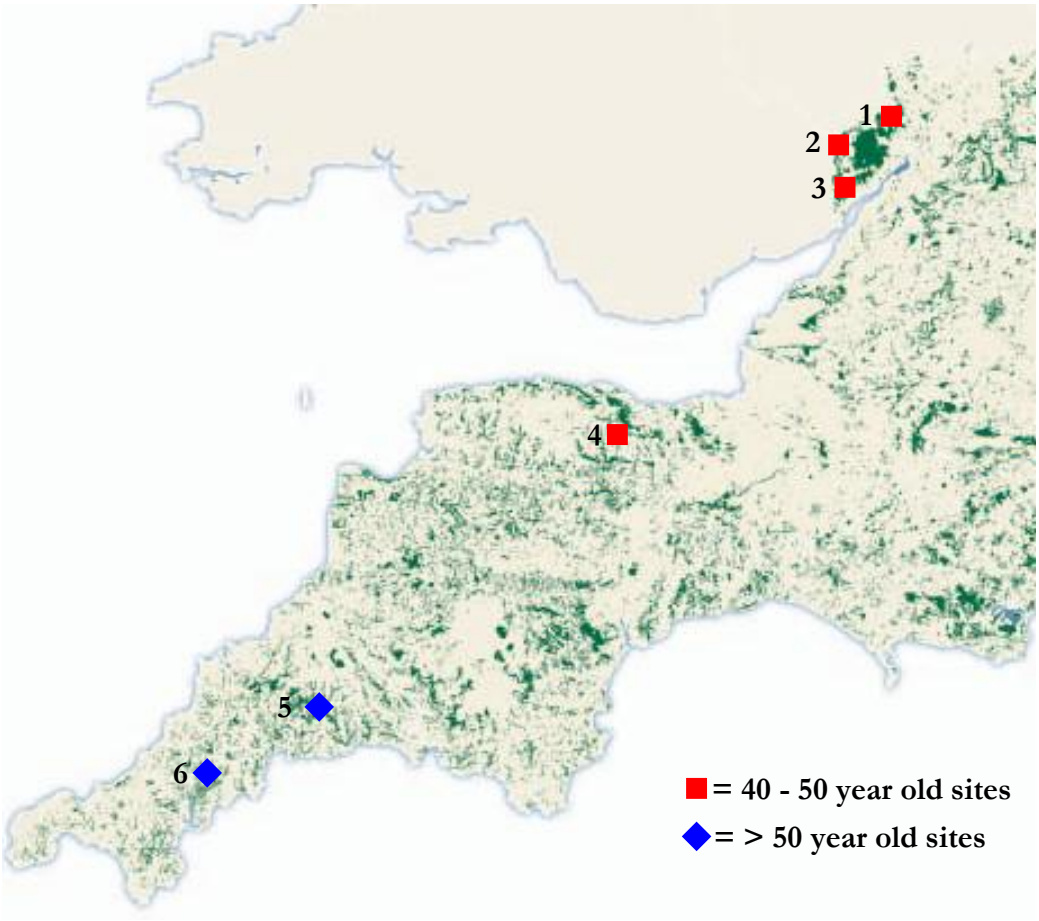

Figure 3-1: Sample site locations within the context of forestry in the South West of England from Forestry Commission (2002)

Table 3-1: Sample felling site characteristics

Site name	Map number	Latitude	Longitude	Elevation (m) AOD	Age (yr)	Stems/ha
Nagshead	1	51º 38'	2º 34'	100	42	200
Highmeadow	2	51° 49'	2° 40'	75	50	250
Tidenham	3	51º 42'	2º 38'	210	48	200
Over Stowey	4	51º 07'	3º 11'	220	46	300
Quethiock	5	50º 27'	4º 20'	50	75	N/A
Lostwithiel	6	50º 25'	4º 39'	80	78	N/A

The site latitude, longitude and elevation were determined by use of a GPS receiver and Ordinance Survey mapping. The number of stems per hectare was determined during the site surveys described in the following section. Data relating to the stems per hectare within the sites from which trees > 50 years of age were obtained was not available due to the different sampling methodology used.

3.2.2 Sample tree selection and characteristics

In order to allow the influence of a changing growth rate on the anatomical and mechanical properties of the sample trees in the 40 - 50 year age range to be evaluated, it was necessary to sample trees from the range of growth rates present within each of the even aged sites. To ensure that this criterion was fulfilled whilst also ensuring that as far as possible trees were selected at random, the methodology described in this section was adopted. The geographic information system 'Forester', a database driven package that gives a visual representation of sub-compartments[1], boundaries and planting details within the publicly owned forestry estate, was used to divide each site into a series of circular survey plots. Each plot had an area of 300 m^2, drawn such that its boundaries met with, but did not overlap, those which were adjacent to it. The plots were positioned within each site in order that a perimeter of 10 m was left around the site boundary, reducing the probability of selecting trees influenced by wind through effects which may have caused damage to the stem.

Each plot was assigned a unique number and a random number generator in Microsoft Excel was used to select four plots from each site to be used for the surveying of potential sample trees. The sole limitation placed on the selection of survey plots within a site was that they could not share a boundary. This restriction was imposed in order to avoid the formation of large openings within the canopy if several adjacent trees were felled. This occurred in one

[1] A sub-compartment is a unit of measure in forestry, typically differentiated from surrounding sub-compartments by changes in species, age or management practices. In this work each sub-compartment is identified by the term 'site'.

instance, and as a result the next randomly generated plot was selected as a replacement. Once four survey plots per site had been selected, the longitude and latitude positions of the plot centres were identified with the use of the Forester software.

The centre of each plot was located with a hand held GPS receiver. Prior to carrying out the survey, an inspection was made in which the conditions of the trees within a plot and the presence of any anomalies not representative of the site were evaluated. The two principle anomalies encountered were the presence of significant bow in the stem at the breast height sampling location and damage to the crown, with the latter typically occurring during extreme weather events. While trees exhibiting these features were included within the survey data for a plot, they were not included in the list of potential trees for sampling. The reason for this exclusion was to avoid the potential creation of large quantities of anomalous results within the data. These may have arisen due to excessive compression wood or unusual growth patterns in trees exhibiting the stated anomalies. The impact of these selection criteria on the intended random sampling methodology is discussed in Section 9.3.2. At one site, Nagshead, one of the survey plots initially selected was moved due to the presence of a footpath through its centre, resulting in only a limited number of trees, as shown in Figure 3-2. In this case the next randomly generated plot was selected as a replacement.

Once the condition of the plots was verified, each was measured out accurately by use of a 9.75 m length of cord attached to a wooden stake located at the centre. Any tree found to be located on the boundary of the plot was included if it was deemed that a proportion of the stem ≥ 50 % fell within the plot area. Each tree within a plot was tagged with a metallic tree marker for future identification. The diameter at breast height of each tree was measured and recorded with use of a diameter tape at 1.3 m above ground level, also referred to as breast height. An attempt to estimate the standing height of each tree was made by using a simple clinometer. However due to the dense nature of the canopy above many of the survey plots, the measurement was only successfully conducted on 18 trees. In total, a survey of 124 trees was conducted.

Figure 3-2: Rejected survey plot at Nagshead sampling site

Upon completion of the surveys the results from each site were collated and trees ranked according to their recorded breast height diameter. Given that all trees within a site were assumed to be of an even age, breast height diameter provided the best indication of the range of growth rates without taking increment core samples from each tree. In order to fulfil one of the key objectives of the study, to quantify the impact of rate of growth on anatomical and mechanical properties, trees were selected from within each site such that a broad spectrum of the growth rates present was sampled. This was done by selecting six trees for felling at regular intervals from the ranked diameter data, including the trees with both the lowest and highest diameters. Once trees for felling had been selected, an assessment was made to ensure that they were evenly distributed amongst the survey plots. This was done to avoid the creation of large openings within the canopy after felling and to guarantee a representative sample from across each site. As a result of this process it was necessary to reselect a number of trees; however this did not have a detrimental affect on the distributions of growth rates obtained from any sites. The characteristics of the trees selected for felling in the 40 - 50 year range are given in Table 3-2.

Table 3-2: Characteristics of sample trees in the 40 - 50 year age range

Site name	Number of trees selected	DBH range (mm)	Mean DBH (mm)
Nagshead	6	330 - 600	480
Tidenham	6	280 - 570	450
Highmeadow	6	260 - 510	400
Over Stowey	6	300 - 590	475

Following the selection of sample trees, each was marked with a unique number along with indicators to allow the cardinal compass directions of each tree to be identified once it had been felled. This was done with tree marking paint, with a single pink line used to designate the northern radius and pink and yellow the eastern, as shown in Figure 3-3.

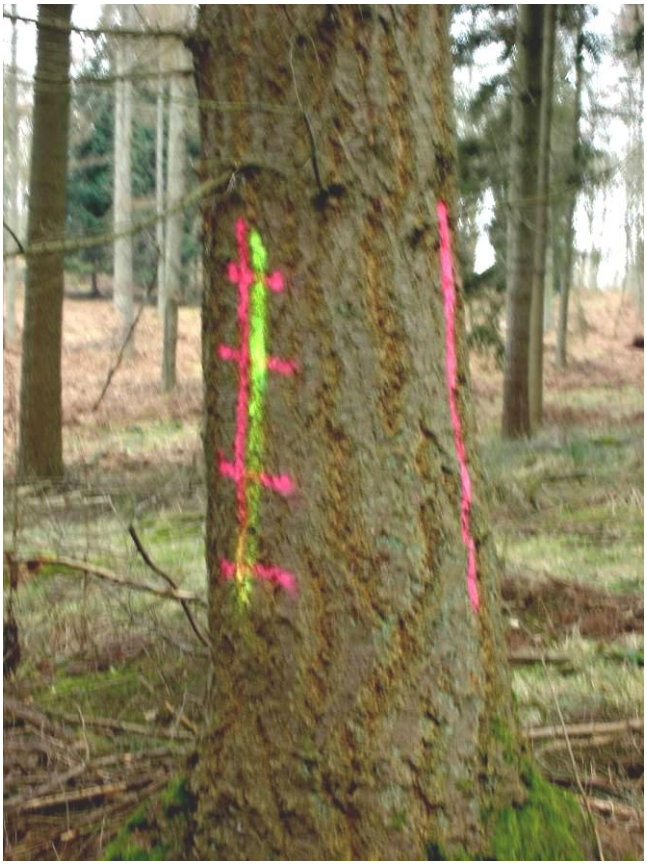

Figure 3-3: Tree markings designating northern and eastern radii

Due to the limited number of sample trees with ages > 50 years to be felled, the methodology described above for their selection within sites was not employed. Instead, sample trees were randomly selected, with the cardinal compass directions again noted for each tree prior to felling. In total it was only possible to select three older trees for felling, rather than the target four. The total number of sample trees was therefore 27.

3.3 Sample tree felling methodology

In order to allow for the determination of variations in anatomical and mechanical properties both radially and vertically within the sampled Douglas-fir trees, test material was collected from two locations within each stem. The two sampling heights used were 1.3 m and 8 m above ground level. The selection of these sampling locations allowed for the characterisation of properties in what is often regarded as the most valuable length of timber, due to its large diameter and typically branch free nature. Within the 40 - 50 year old trees one log and disc were removed from each sampling height. Logs were 400 mm in length and were used for the preparation of small clear mechanical test specimens. Discs measured 100 mm in length and were removed from the crown end of each log. Discs were used for the preparation of radial specimens for studies of variations in anatomical properties utilising the SilviScan-3 system. Each log was sampled centred on the respective sampling height. A flow chart outlining the test material sampling methodology is shown in Figure 3-4.

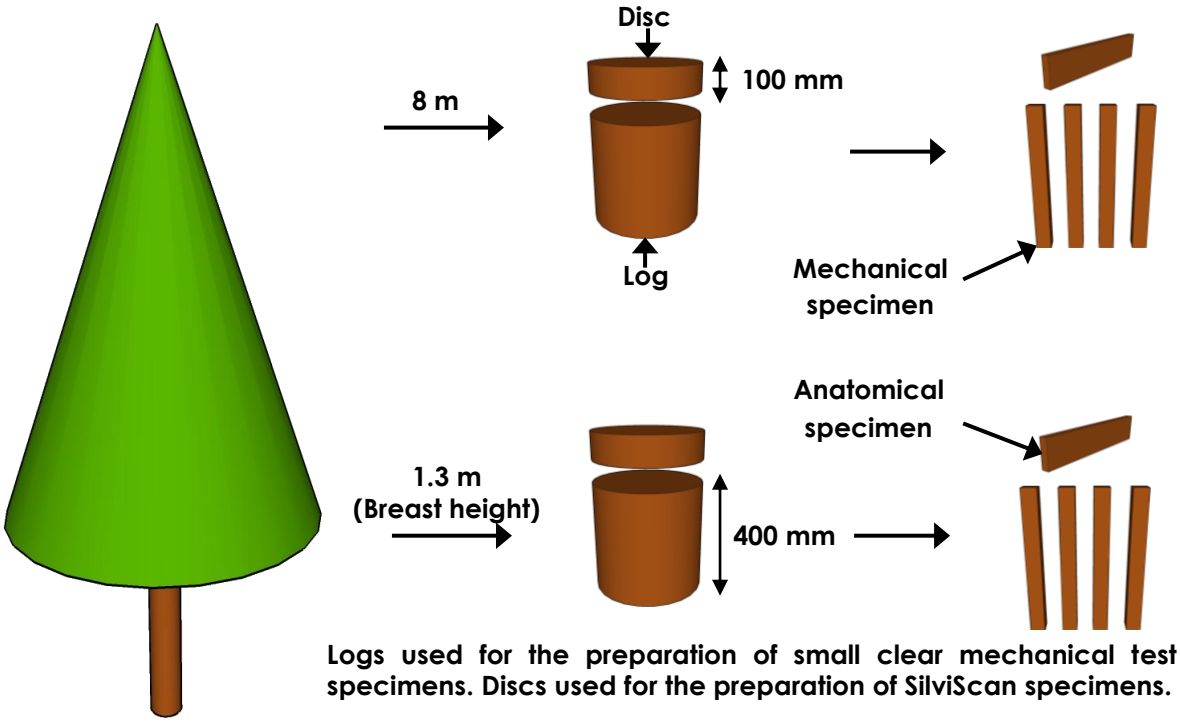

Figure 3-4: Test material sampling methodology

After the felling of a sample tree, but prior to the removal of logs and discs, the tree identification marker and marks on the stem, designating the cardinal compass directions of north and east, were transferred to the log and discs at 8 m. A record was also taken of the total height of the tree and the length of the live crown, defined as the lowest whorl with less than three live branches, as used by Gartner et al. (2002). Sample material was then removed

with a chainsaw. A felled sample tree in the 40 - 50 year age range following the removal of logs and discs is shown in Figure 3-5.

Due to logistical constraints, the methodology used to collect sample material from trees with ages > 50 years was altered from that described for younger trees. Rather than dividing the sample material into logs and discs at each stem height, a log 500 mm in length was removed from the stem at each sampling height. From this log three longitudinal sections 100 mm in width were cut with the main section oriented to contain the northern and southern radii and the second and third sections containing the remainder of the eastern and western radii. Cuts were made onsite by a chainsaw. Although this methodology resulted in a discontinuation of the eastern and western sections, the losses in test material entailed for the preparation of small clear specimens was minimal, as described in Section 3.6.

Figure 3-5: Sample tree in 40 - 50 year age range following removal of logs and discs

3.4 Sample disc scanning

In order to aid in the determination of any future anomalous results generated by the SiliviScan-3 system, and for the determination of tree growth rates as described in Section 3.7, a surface scan of all sample discs was taken. This was done in the days following the felling of sample trees, such that the occurrence of splits formed by the drying of the discs was minimised. Prior to scanning, all discs were sanded by means of a handheld belt sander to remove any marks that were present as a result of the felling process. Scanning was carried out

using an A3 flat bed scanner. A thin acrylic sheet was placed on the scanning surface to protect it and a scale rule was attached. The unique identification code for the disc and markers designating the direction of north and east on the disc were also included in the scan. It was found that if a sponge was used to wet the scanning surface prior to scanning, the colours within the image could be enhanced. When the disc was too large to be scanned in one piece, a mark was made on the bark designating the position of the pith and two scans were conducted, ensuring that the pith was present in each. A black sheet was placed over the scanning equipment to prevent light intrusion. An example of the results achieved through the scanning process can be seen in Figure 3-6.

Figure 3-6: Sample disc surface scan

Following scanning, the software package 'CDendro' was used for the determination of mean ring widths in the four cardinal compass directions. This was done utilising the features of the programme to automatically determine the boundaries between adjacent growth rings in each of the four directions and to give a measure of ring width following calibration to the scale rule included in the image.

3.5 SilviScan-3 method

3.5.1 Outline

In order to meet the objectives specified in Section 1.5, the collection of data showing the magnitude and variations of the following properties within the sample trees was necessary:

- S_2 layer microfibril
- Density
- Tracheid radial and tangential dimensions and wall thicknesses
- Proportions of tracheid types within growth rings
- Ring width

In the literature presented in Chapter 2, several potential methods were identified for use in the collection of specimen microfibril angle and density data. Some time was spent developing the iodine staining method described by Senft and Bendtsen (1985) to visualise the S_2 layer microfibril within Douglas-fir tracheids. While this was successful, it was too slow to be suitable for the collection of the quantity of data that was required. This was also the case for the gravimetric method trialled for the determination of specimen density. Hence, the SilviScan-3 system was used for the analysis of variations in wood anatomical properties of radial pith to bark specimens. Testing was conducted at the Innventia Wood and Fibre Measurement Centre in Stockholm. In this section, the methods used to prepare specimens and conduct analysis using the SilviScan-3 system are described. In total 54 specimens, one from each height in all sample trees, were analysed. Testing was conducted in two rounds, with 36 specimens analysed in April 2010 and the remaining 18 in January 2011.

3.5.2 Specimen preparation

Pith to bark specimens for analysis utilising the SilviScan-3 system were obtained from the northern radius within each sample disc. A fixed sampling axis was used across all sites in order to remove a potential source of variability within the dataset. In order to obtain specimens from sample discs taken from the 40 - 50 year old trees, each was first cut into three sections, an approximately 50 mm wide section along the north - south axis containing the pith, and two off cut sections containing the remainder of the east and west axis. A further cut was then made to divide the north - south section about the pith, ensuring that the pith was maintained within the northern half, as shown in Figure 3-7. Subsequently all but the northern section were marked such that growth ring numbers within them could be identified

and were stored for potential future use. Further cuts were made on the northern section to extract a specimen measuring approximately 15 x 15 mm longitudinally and tangentially, spanning from the pith to the bark. The offcuts from these specimens were kept to aid in the investigation of any anomalous results that may have been generated during the analysis. The 36 pith to bark specimens prepared for the first round of analysis are shown in Figure 3-8. Preliminary specimens from trees with ages > 50 years were removed from the upper end of each northern radius of the longitudinal sections extracted from the sample trees.

Following removal from the sample discs, all specimens were immersed in acetone for two 24 hour cycles. The primary objective of this was to ensure a rapid and even drying of all specimens which still had relatively high moisture contents. A secondary benefit of placing the specimens in acetone was the removal of any resins or extractives, although all specimens were subject to soxhlet extraction prior to analysis as described later in this section, to ensure the complete removal of any such material. Following the removal from acetone, all specimens were stored in an environmentally controlled room at 65 % relative humidity and 20 ºC prior to transportation to the Innventia Wood and Fibre Measurement Centre, where the remainder of the preparation was conducted.

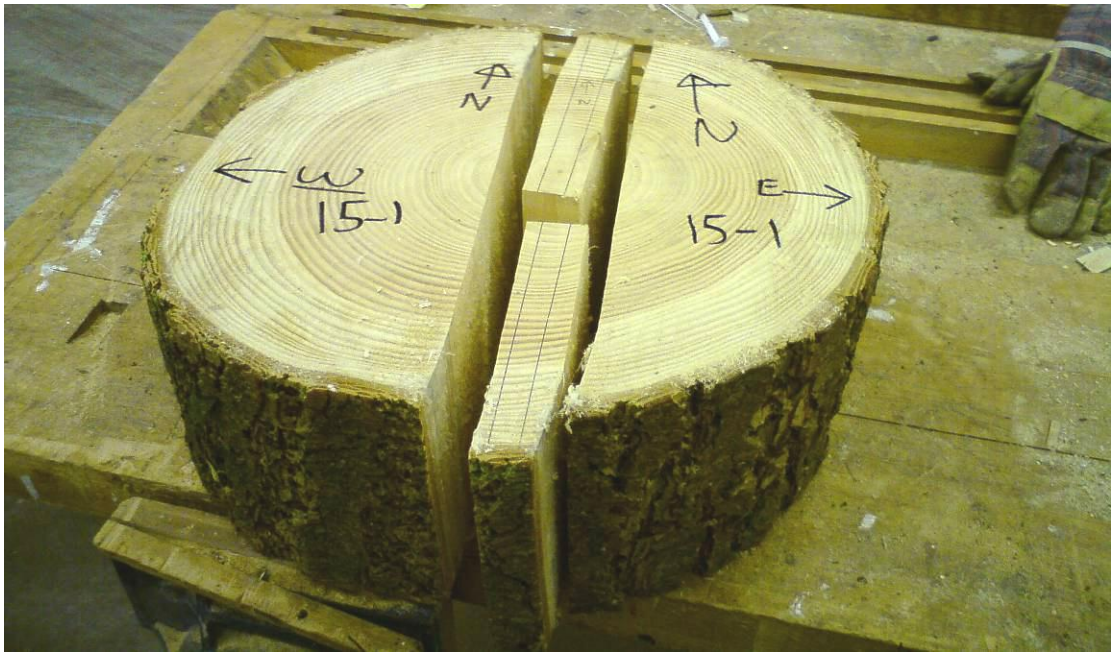

Figure 3-7: Disc cut for extraction of SilviScan-3 test specimens

Figure 3-8: 15 x 15 mm preliminary SilviScan-3 specimens

The final specimen size for testing using the SilviScan-3 system is 2 mm in the tangential direction and 7 mm in the longitudinal direction. In preparation for final sawing to these dimensions, all specimens were glued to a specimen holder along one of its radial-tangential edges with the use of a polyvinyl acetate based glue. Gluing was conducted ensuring that the pith was centrally located on the specimen holder and all specimens were left for a period of eight hours after gluing. An example of a specimen attached to a holder is shown in Figure 3-9.

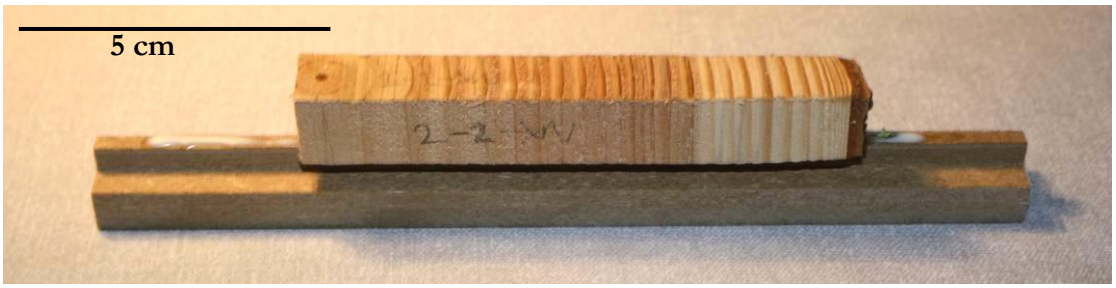

Figure 3-9: Specimen glued to a specimen holder

The cutting of specimens to the final test dimensions was conducted in two stages utilising two custom built circular saws. Each saw contained a set of twin circular blades, with the first set to make a 2 mm cut and the second 7 mm. Prior to commencing sawing, the specimen on its holder was placed onto a metal sledge containing two pneumatic clamps to hold it securely in position. Upon activation of the saw, the metal sledge moved beneath the saw blades at a constant speed, stopping at the end of the process to allow for the removal of the specimen before resetting to the original position. Following the completion of the first stage of sawing, a pith to bark specimen measuring 15 mm longitudinally and 2 mm in the tangential direction was obtained. Prior to commencing the second stage of sawing, each specimen was broken

away from its holder and had any remaining pith and bark removed, before being placed laterally in a metal clamp designed to pass between the second set of circular saw blades. Each specimen was placed into the clamp between two pieces of thin birch wood, so as to reduce the risk of damage to the specimen as a result of pressure applied by the clamp. The specimen was then cut utilising the second saw, after which the final test dimensions of 2 mm tangentially and 7 mm longitudinally were achieved. All specimens were then marked and placed in a specially designed holder. The specimen cutting process is displayed in Figure 3-10.

Following the cutting of specimens to final test dimensions, all were subject to soxhlet extraction for a period of 12 hours. This was conducted in order to remove any naturally occurring extractives found within the cell lumens which may have had an effect on the results obtained. The soxhlet extractor used is shown in Figure 3-11 and consists of a pot at its base containing acetone with a chamber above into which the specimens were placed. During the extraction process the acetone was heated to reflux, allowing the vapour to travel into the chamber above causing the extractives to dissolve. Once the chamber was full of solvent it was siphoned off back into the lower pot and the process repeated.

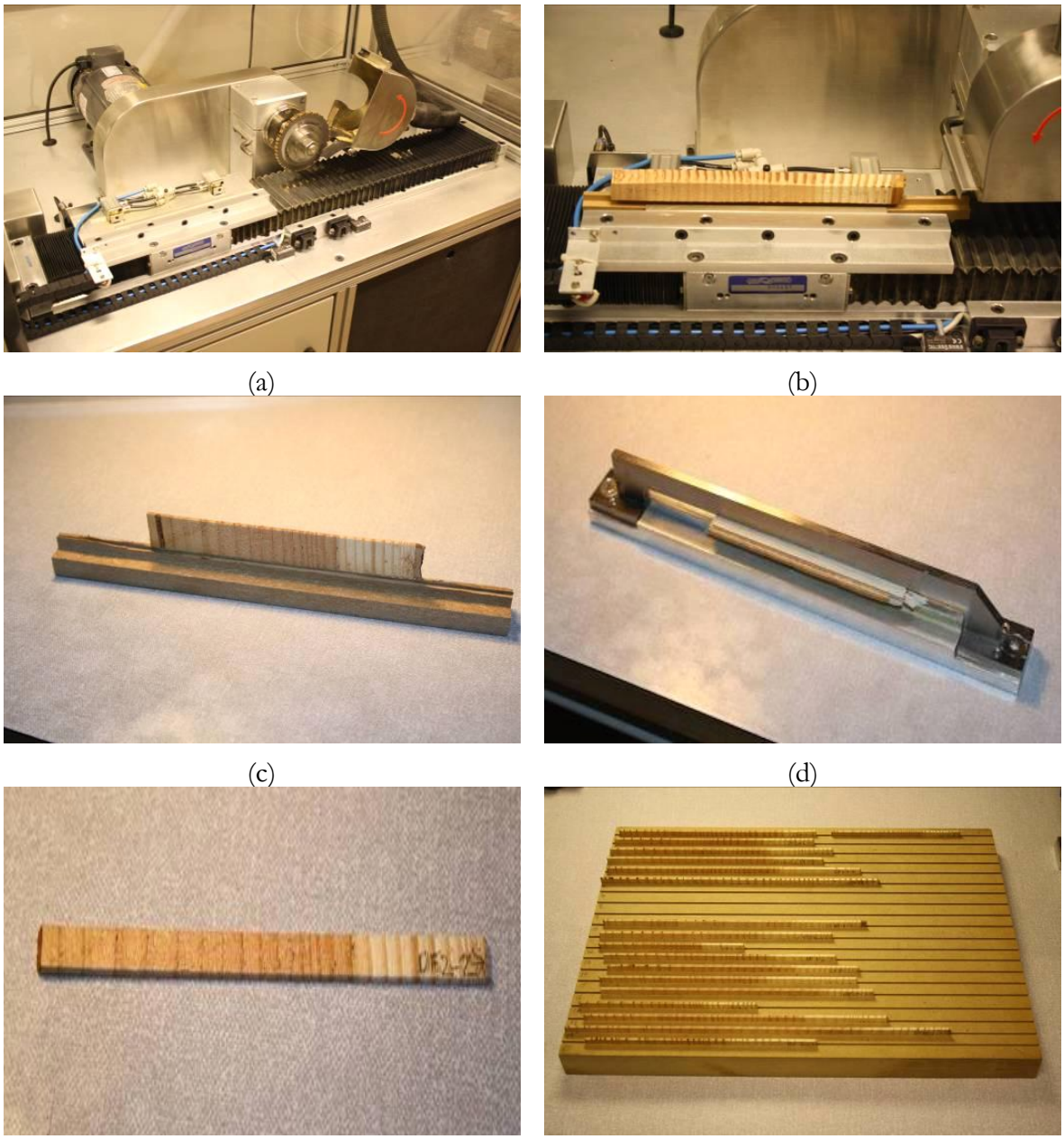

(a) (b)

(c) (d)

(e) (f)

Figure 3-10: Specimen sawing process (a) Saw system (b) Specimen clamped to sledge (c) 2 x 15 mm specimen (d) Metal specimen clamp (e) Final 2 x 7 mm specimen (f) Finished specimens in holder

Figure 3-11: Soxhlet extraction process

The final stage in preparing specimens for analysis was the polishing of one of the radial-tangential surfaces of each. This was conducted to ensure accurate and reliable results during the first stage of the SilviScan-3 analysis, which involves the measurement of tracheid dimensions and growth ring characteristics with the use of a digital optical microscope, as described in Section 3.5.3.1. The presence of any marks or debris on the surface from the sawing process may have therefore had a detrimental impact on the accuracy of the results achieved. Polishing was undertaken using a specially constructed system that allowed each specimen to be clamped into position and passed over abrasive sheets for a preset number of passes, typically 100 - 250. During the process the abrasive sheets were continually moved to prevent any of the grit stones becoming lodged within the cell lumens. A series of finer sheets, typically from 1200 to 4000 grit, were used to produce the desired surface finish. The specimen holder and polishing system are shown in Figure 3-12.

(a) (b)

Figure 3-12: (a) Specimen in holder for polishing (b) Polishing system

To ensure that that the individual tracheid cell walls would be visible during the first stage of the SilviScan-3 analysis, each specimen was checked for signs of debris or damage using a digital optical microscope at the end of a complete polishing cycle. On occasions where it was necessary to repeat the polishing process, the cycle was restarted from the coarsest abrasive sheet. Images showing a comparison of the surface finish before and after polishing are shown in Figure 3-13.

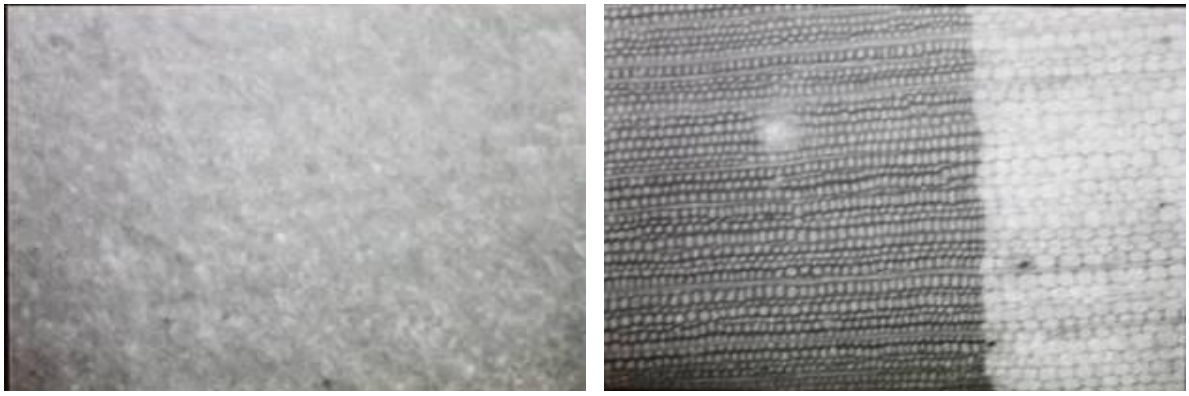

(a) (b)

Figure 3-13: (a) Specimen surface prior to polishing (b) Specimen surface following polishing

Following the completion of all preparatory steps, specimens were allowed to equalise to the laboratory environmental conditions of 23 °C and 43 % relative humidity, giving a moisture content of approximately 8.5 %. During the preparation of the specimens two were damaged in the process of removing the bark, resulting in the loss of some growth rings. One of these specimens was obtained from site one, which had an age of 42 years, as a result of the damage the maximum cambial age that could be assessed across all younger specimens at breast height was 40 years. The second was from site five and had an age of 75 years, as a result of the

damage the maximum cambial age that could be assessed across all older specimens at breast height was 65 years.

3.5.3 SilviScan-3 anatomical property analysis

The SilviScan system was developed at the Commonwealth Scientific and Industrial Research Organisation for the assessment of wood anatomical properties (Evans, 1994). The third generation of the system, SilviScan-3, combines three non-destructive analytical techniques, these are:

- Optical imaging
- X-ray densitometry
- X-ray diffractometry

The analysis of the data generated by these three methods allows for several anatomical and mechanical properties to be determined or predicted, these are summarised in Table 3-3.

Table 3-3: SilviScan-3 property measurement methods

Method	**Optical imaging**	**X-ray densitometry**	**X-ray diffractometry**
Primary results	Tracheid diameter	Wood density	Microfibril angle
Secondary results	Tracheid wall thickness	Modulus of elasticity	

The methodologies and principles applied in the analysis and calculation of each of these properties is described in the following sub-sections.

3.5.3.1 Optical imaging

The first stage in the SilviScan-3 analysis process was the use of a high resolution digital microscope to determine the diameter of tracheids in the radial and tangential directions. This was done utilising the experimental equipment shown in Figure 3-14.

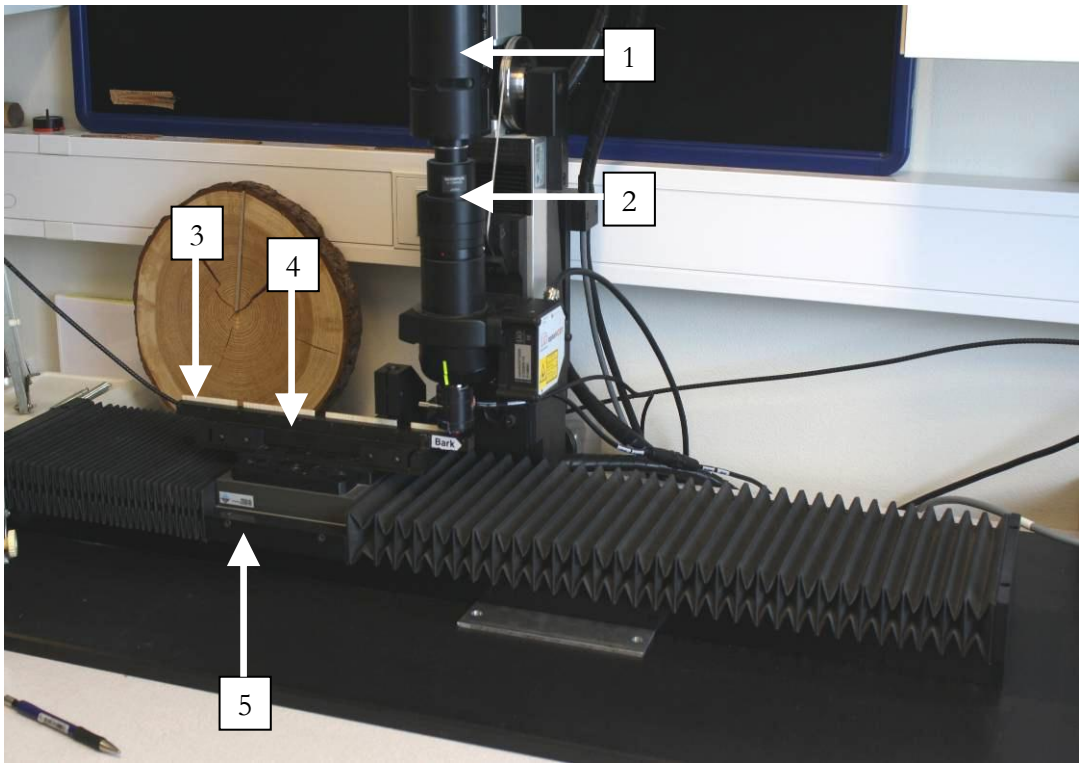

Figure 3-14: SilviScan-3 optical imaging 1. Digital camera 2. Optical microscope 3. Specimens 4. Specimen holder 5. Motorised stage

Prior to the analysis, each of the specimens was placed into a holder such that the previously polished surface was visible through the microscope, with the bark end positioned on the right hand side. Each specimen holder was then located on a motor driven stage and the analysis commenced. During the analysis process, the stage moved in a linear direction, from left to right in the image above, stopping at 1.8 mm intervals. As it moved each specimen was passed beneath an auto-focusing light microscope with 5x magnification. Fitted to the top of the microscope was a digital camera which recorded images with a pixel size of 1.29 μm at each interval. This process was continued until all specimens within a holder had been analysed.

Following the acquisition of all surface images from a specimen, they were binarized and processed to identify the radial and tangential cell wall boundaries. Further automated image analysis was then conducted in order to determine the radial and tangential tracheid diameters, as well as the cell perimeter, area and population within an image. All data were calculated as mean values at 25 μm intervals, so as to correspond with the results obtained for specimen density. As each of the specimens measured 2 mm in the tangential direction, each interval represented 25 - 50 tracheids. The angles of each growth ring with respect to the radial edge of each specimen were also determined during the image analysis process for use in the subsequent x-ray densitometry and diffractometry scans.

3.5.3.2 X-ray densitometry

The second stage in the SilviScan-3 analysis process was the use of an x-ray densitometer, the output from which was used to determine radial profiles of specimen density and wall thickness. The experimental setup used is shown in Figure 3-15.

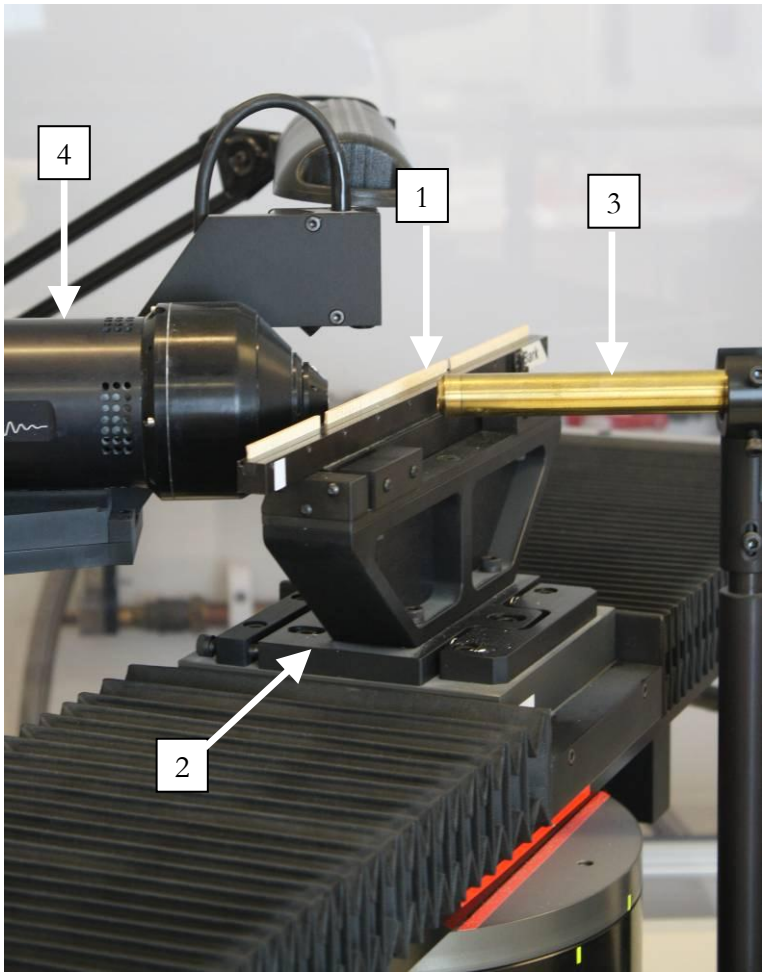

Figure 3-15: SilviScan-3 x-ray densitometry 1. Specimens 2. Motorised stage 3. X-ray collimator 4. X-ray detector

Prior to commencing the x-ray densitometry analysis, specimens in the same holder used previously during the collection of optical images were located onto a motor driven goniometric stage. At the start of the analysis, the stage was positioned automatically utilising location data gathered from the optical images, such that the start of the first specimen was located between the x-ray collimator and detector. During the course of the analysis, an x-ray beam exited the collimator and passed through the specimen, the level of incident radiation falling on the x-ray detector, which had a pixel size of 6 μm and was located directly opposite the collimator, was then recorded. Throughout the analysis, the stage progressed forward such

that the level of incident radiation could be recorded at 25 μm intervals. In order to ensure that the x-ray beam falling on the specimen was perpendicular to the radial-longitudinal surface, data gathered from the optical images was used to calculate the orientation of each growth ring, from which the rotation of the stage was constantly varied to change the angle of the specimens with respect to the incident rays. This allowed for a sharper definition of the annual ring boundaries to be obtained and therefore a greater level of accuracy in the density values calculated. The x-ray absorption of the specimen was related to its density using a rearrangement of Beer's law, as shown in Equation 3-1.

$$\rho = \frac{1}{\mu t} \ln \frac{I_0}{I} \qquad 3\text{-}1$$

where: ρ specimen density

μ mass attenuation coefficient

t specimen thickness

I transmitted x-ray intensity

I_0 incident x-ray intensity

The mass attenuation coefficient used in the above equation is estimated from calibration conducted with wood specimens of a known density. As the coefficient is only estimated, small differences between the measured and actual density profile within each specimen may have existed. In order to take account of this, the average density of each specimen was calculated gravimetrically from its volume, determined with the use of a stage mounted micrometer, and weight. Each density profile was then normalised, such that average density values calculated by the two methods corresponded. As the volumetric density was determined on specimens at a moisture content of 8.5 %, this was therefore also the equivalent moisture content of the SilviScan-3 derived density profiles.

In order to calculate the thickness of the single radial tracheid cell walls, results obtained during the optical imaging and x-ray densitometry analysis were combined. This was done utilising Equations 3-2 to 3-4 from Evans (1994).

$$P = 2(R + T) \quad 3\text{-}2$$

$$C = RTD \quad 3\text{-}3$$

$$Wt = \frac{P}{8} - \frac{1}{2}\sqrt{\frac{P^2}{16} - \frac{C}{\rho_{Wall}}} \quad 3\text{-}4$$

where: P external perimeter of tracheid cross section

R radial tracheid dimension

T tangential tracheid dimension

C tracheid coarseness (mass per unit length)

D x-ray densitometry derived density

Wt radial tracheid cell wall thickness

ρ_{Wall} tracheid wall density ($\approx$ 1500 kg/m^3)

This method for the determination of wall thickness has been shown to offer a high degree of precision, with repeated measurements carried out on the same specimen giving results with differences much less than 1 μm. However, the accuracy of the results is extremely difficult to measure as a perfect reference specimen is required. Due to the large number of sample types and variations in sample preparation that can occur no such reference specimen exists, as such the accuracy of the system cannot be completely defined (Pers. com. Olsson, 2010).

Radial density profiles were also used for the determination of ring widths, by identifying the sudden drop in density values that occurs between the late and earlywood in adjacent growth rings. The widths of the early, transition and latewood regions and the proportions of each within a growth ring were calculated following the determination of the position of the boundaries between them, as described in Section 3.8.

3.5.3.3 X-ray diffractometry

The final stage in the SilviScan-3 analysis process was the use of an x-ray diffractometer, the output from which was used to determine radial profiles of specimen S_2 layer microfibril angle. The experimental setup used is shown in Figure 3-16.

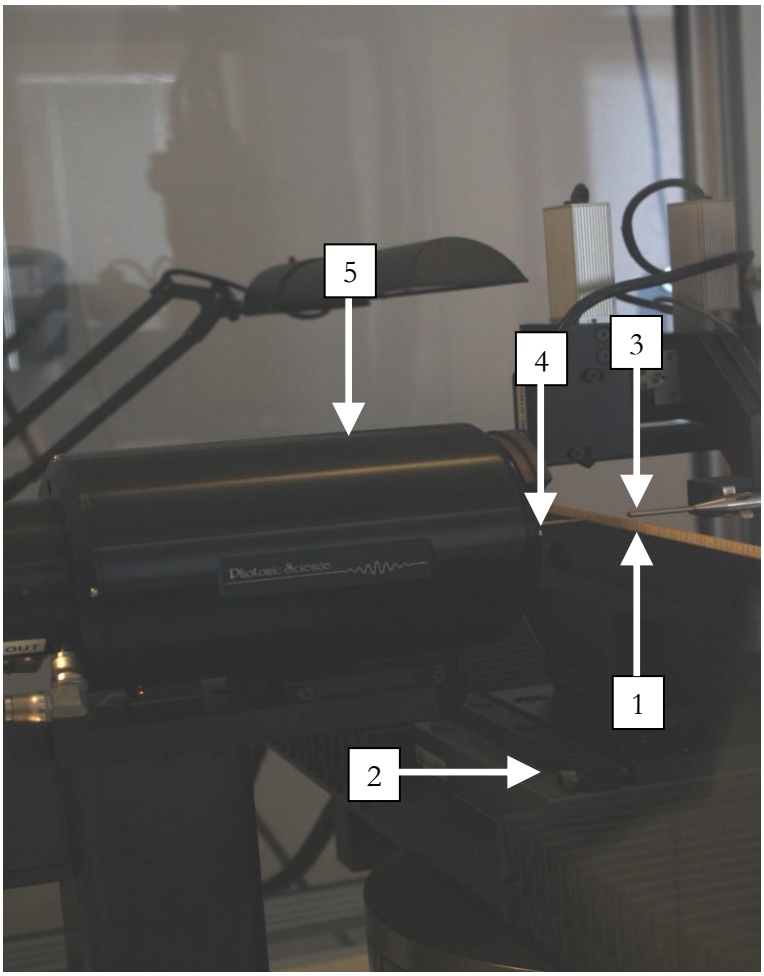

Figure 3-16: SilviScan-3 x-ray diffractometry 1. Specimens 2. Motorised stage 3. X-ray emitter 4. Beam stop 5. Wide angle x-ray detector

Prior to commencing the x-ray diffractometry analysis, specimens in the same holder used in the previous analysis steps were located onto a motor driven goniometric stage. At the start of the analysis, the stage was positioned automatically utilising location data gathered from the optical images, as detailed for x-ray densitometry. During the course of the analysis, an x-ray beam was passed through the specimen, with the resulting diffraction patterns recorded using a two-dimensional wide angle x-ray detector. As a result of the time required to record a single diffraction pattern, two scanning intervals were used. The low resolution scans were conducted at 2 mm intervals along the radial length of the specimen. These scans were conducted on 36 specimens from the 18 trees obtained from sites one, two and three in Table 3-1. The remaining specimens were scanned at a higher resolution, with diffraction patterns recorded at 25 μm intervals, corresponding with the results obtained through the x-ray densitometry analysis. The rotation of the stage was constantly varied throughout the testing, as discussed in the previous section.

A typical x-ray diffraction pattern returned during the SilviScan-3 analysis is shown in Figure 3-17. On the diffraction pattern the crystal planes which produce the main cellulose I reflections are also shown. The reflections produced are predominately due to the S_2 layer, as a result of its greater thickness in comparison to the other cell wall layers. The strongest reflections are obtained from the 002 planes, whose normals are perpendicular to the microfibril axis. It is these 002 reflections that form the basis of calculating the microfibril angle through the SilviScan-3 system.

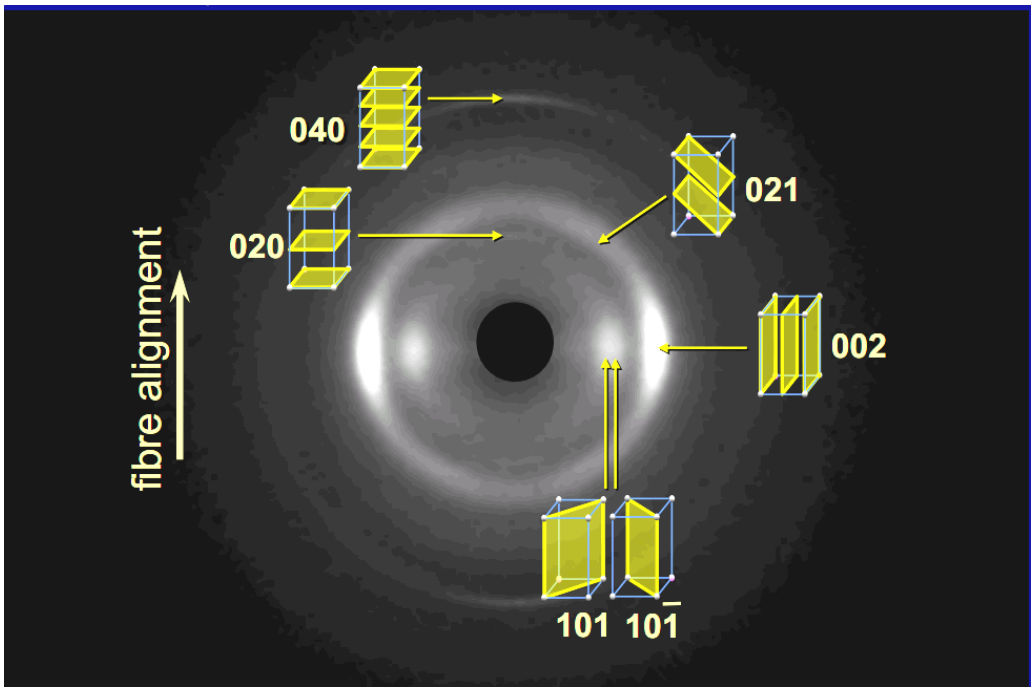

Figure 3-17: X-ray diffraction pattern and major Cellulose I crystal planes from Evans (2001) in McLean (2008)

It was demonstrated by Evans (1999), that in converting the intensity of the diffraction pattern into a linear scale as shown in Figure 3-18 and by integrating around the circle representative of the Bragg angle for the 002 plane, the microfibril angle can be calculated (McLean, 2008). While the diffraction pattern appears to show only two peaks, there are actually four, corresponding to reflections returned from the radial and tangential walls, which have opposing fibril angles on opposite faces.

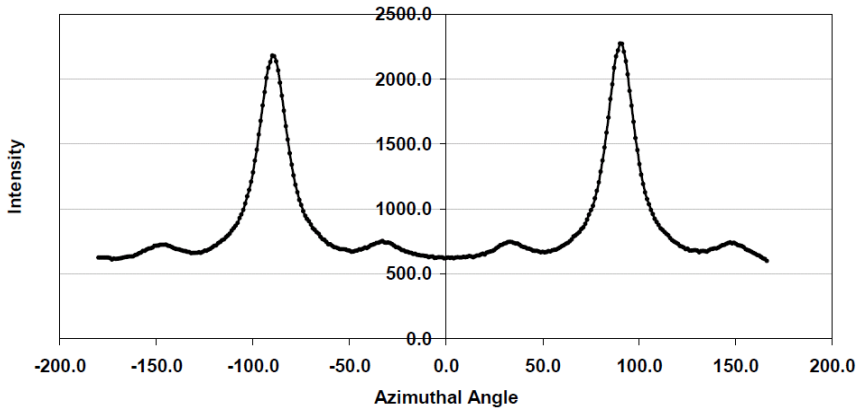

Figure 3-18: Diffraction pattern intensity profile from McLean (2008)

The detailed derivation of the methodology for microfibril angle calculation is described by Evans (1999). In summary, Evans showed that the variance of the azimuthal 002 diffraction profile is related to the mean microfibril angle by the expression shown in Equation 3-5.

$$\bar{\theta} \approx \sqrt{\frac{18}{11}\left(s^2 - \sigma_{add}^2\right)} \qquad 3\text{-}5$$

where: $\bar{\theta}$ mean microfibril angle

s standard deviation of 002 azimuthal reflection profile

σ_{add} additive component of microfibril angle dispersion about mean

The additive variance component is required within Equation 3-5 to account for the fact that while the microfibril angle can be zero within a tracheid wall, it is unlikely that the total variance of the microfibril orientation is zero. The value of σ_{add} was determined empirically by Evans (1999) to be 6°.

3.5.3.4 Modulus of elasticity prediction

As well as providing data regarding the anatomical properties of specimens, the SilviScan-3 system also provides a prediction at each 25 μm scanning interval of modulus of elasticity, based upon the assessed anatomical properties. This is done utilising Equation 3-6, a description of the derivation of which is given in Evans (2006).

$$MOE = A(Icv \cdot D)^{B} \quad (3\text{-}6)$$

where: MOE predicted flexural modulus of elasticity

A scaling factor

B exponent to allow for curvature of the azimuthal intensity profile

Icv coefficient of variation of the azimuthal intensity profile

D density

The scaling factor A and exponent to allow for curvature B have been shown to be insensitive to wood species, however they do vary according to the method used to determine modulus of elasticity, against which the equation is calibrated (Evans, 2006). This is in response to the fact that modulus of elasticity obtained using dynamic methods has been shown to be in the order of 30 % higher than that found using static flexural testing (Evans and Ilic, 2001). The standard results obtained from SilviScan-3 analysis predict dynamic modulus utilising values of $A = 0.165$ and $B = 0.85$ (Evans et al., 2000). When compared to the experimentally derived dynamic modulus of elasticity, linear correlations with $r > 0.9$ have been achieved (Evans, 2006).

3.6 Mechanical property testing

3.6.1 Outline

In order to allow the radial and longitudinal variations in modulus of elasticity, flexural strength and compressive strength within the sampled Douglas-fir trees to be determined, small clear specimens were tested in accordance with the methods described in BS 373: 1957 'Methods of testing small clear specimens of timber' (BSI, 1957). The lack of defects such as knots, compression wood and a sloping grain within small clear specimens allows for a greater degree of consistency between tests, and hence for material properties to be more easily compared. While the testing methods detailed in BS 373: 1957 have been superseded by more recent standards, they are still widely used in wood property evaluations, due to the large quantities of published literature in which they are adopted and the speed and ease of measurement the methodologies present. In this section the methods utilised in the extraction and preparation of specimens for testing, as well as the procedures used in the collection of results are described.

3.6.2 Flexural specimen preparation

Flexural test specimens were prepared from the two log sections obtained from each of the sample trees in the 40 - 50 year age range and from the longitudinal sections obtained from trees with ages > 50 years. The size of final test specimen detailed in BS 373: 1957 is 300 x 20 x 20 mm. In order to allow for a detailed understanding of the variations in mechanical properties to be determined with age, specimens were taken radiating outwards from the pith in four directions corresponding to north, east, south and west, with minimal spacing between the successive specimens. The cutting pattern used to extract specimens from the sample logs is shown Figure 3-19.

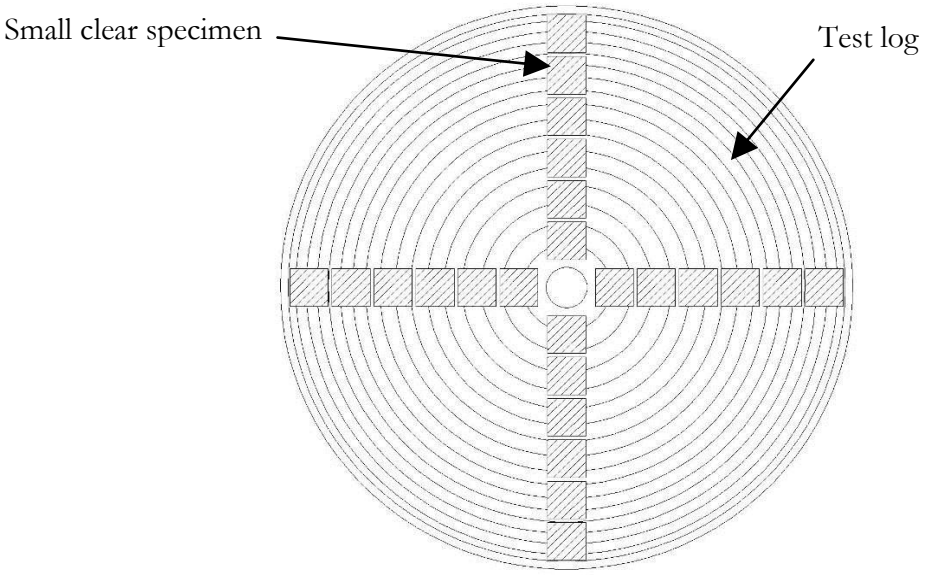

Figure 3-19: Small clear specimen cutting pattern

Specimen preparation in the 40 - 50 year old trees was conducted in two stages, the first involved the removal of three boards from each log, one containing the north - south radius and the remaining two the east and west radii. In the second stage small clear specimens were removed from each of these boards. The first stage was conducted with use of a Lucas portable saw mill at the Stourhead estate, each board was cut to a thickness of 25 mm to allow for potential shrinkage upon drying and clearly marked with tree, log and orientation identifiers. Following this each board was placed in an environmentally controlled room at 65 % relative humidity and 20 °C for a period of two weeks, to allow time for potential shrinkage to occur prior to preparation to final test dimensions. Each of the boards was then reduced to a dimension of 20 mm in the tangential dimension with the use of a thicknesser, and the number of each growth ring counted outwards from the pith marked.

In the second preparation stage each of the small clear specimens was removed from the boards with the use of a band saw. Prior to cutting an assessment was made of the best position within the length of each board to be used to ensure that all specimens produced were devoid of defects. It was also ensured that specimens to be removed from the north - south board were cut in such a way to avoid the presence of the pith, whilst maintaining as much of the first growth ring as possible. Longitudinal cuts were made at 22 mm intervals to allow for the thickness of the blade, with specimens then finished to a length of 300 mm. Where specimens contained any defects within the central third, or significant defects at any location, they were rejected. The presence of minor defects outside of the central region was recorded prior to testing, as described in the following section. Following cutting, each specimen was marked with a unique identifier based on a Cartesian co-ordinate system, in which the east - west radius was represented by the x axis and north - south the y. The key stages in the preparation of small clear specimens within younger trees are shown in Figure 3-20.

Small clear specimens were removed from the longitudinal sections taken from trees with ages > 50 years with the use of a band saw. A similar cutting pattern was employed as for younger trees, with a cut made at 22 mm intervals along the centreline of each section. As the longitudinal sections measured 100 mm tangentially, the first specimen in the east and west directions was obtained adjacent to the pith in the north - south section. Specimens were then finished to their final dimensions and marked as described for younger trees. All specimens were then placed back into the environmentally controlled room and allowed to equilibrate to a moisture content of 12 %.

(a)

(b)

(c)

(d)

Figure 3-20: Specimen sawing process (a) Marked log (b) Lucas mobile saw radial board cutting (c) Radial boards obtained from log (d) Small clear specimens removed from radial boards

3.6.3 Flexural specimen testing

Prior to testing the small clear specimens, the moisture content of each was checked with a moisture meter to ensure that the test moisture content of 12 % specified in BS 373: 1957 was attained. The accuracy of the moisture meter was verified by oven drying a sample of 25 specimens and recording their mass. The specimens were subsequently placed back into the environmentally controlled room until no measurable change in moisture content was detected by assessing the change in mass. The moisture content was then calculated with use of the oven dry method and compared to that shown by the moisture meter. It was found that the moisture meter had an accuracy of ± 0.5 %, hence values within the range 11.5 - 12.5 % were deemed acceptable when checking specimens prior to testing. Specimens were removed in batches of 20 for mechanical testing.

Flexural mechanical testing was conducted utilising an Instron 3369 testing system fitted with a 50 kN load cell. In accordance with BS 373: 1957 all specimens were tested in three point bending, with each specimen spanning 280 mm and the load applied at the centre of the span. The rate of loading was 6.6 mm/min in accordance with the standard and specimen deflection during testing was recorded by means of the loading head displacement. During testing data was logged utilising Instron Bluehill software, with the extension and applied load recorded 100 times per second. Prior to commencing testing all specimens had their mass recorded on a balance, accurate to ± 0.1 g and their radial and tangential thickness measured with a set of digital callipers accurate to ± 0.1 mm. The dimensions were taken as the mean of four readings at regular intervals along the specimen length, and were inputted into the Bluehill software for use in the calculation of mechanical properties. A record was also made of the age of the growth rings contained in each specimen and the presence of any defects in order to help explain potential anomalous results.

Within BS 373: 1957 it is stated that the orientation of the growth rings within test specimens should be 'parallel to the direction of loading'. This was taken to mean loading on to the radial-longitudinal face, such that growth rings were aligned vertically, as shown in Figure 3-21.

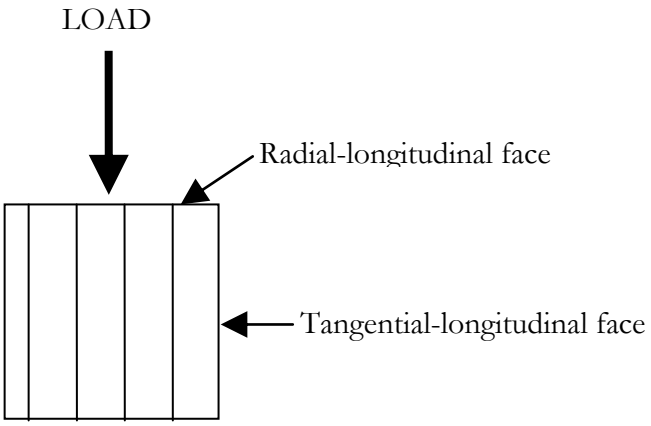

Figure 3-21: Small clear specimen flexural testing orientation. View of end face (cross-section) showing annual rings with longitudinal axis into the sheet

The orientation in which sections are tested was discussed by McLean (2008). It is an important factor to consider, as the different anatomical properties of wood in the different directions can play a large role in determining the consistency of results (Beery et al., 1983). In a study looking into the effect of growth ring orientation on small Douglas-fir beams, Grotta, Leichti et al. (2005) found that both the modulus of elasticity and flexural strength were influenced by orientation, agreeing with results obtained by Biblis (1971) conducting similar work on Yellow pine. The difference in values occurs as a result of either early, transition or latewood being present on the surface of beams if loaded on the tangential-longitudinal face, with latewood on the surface increasing mechanical properties compared to the presence of either early or transition-wood (Grotta et al., 2005). A greater degree of consistency in results should be expected by orientating the sections as shown in Figure 3-21, such that the load is applied to the radial-longitudinal face and the results obtained are a function of the properties of the complete cross-section.

Having commenced loading, each test progressed until specimen failure occurred, evident by the significant decline in the load required for continued displacement, at which point the test was terminated. The experimental test setup is shown in Figure 3-22.

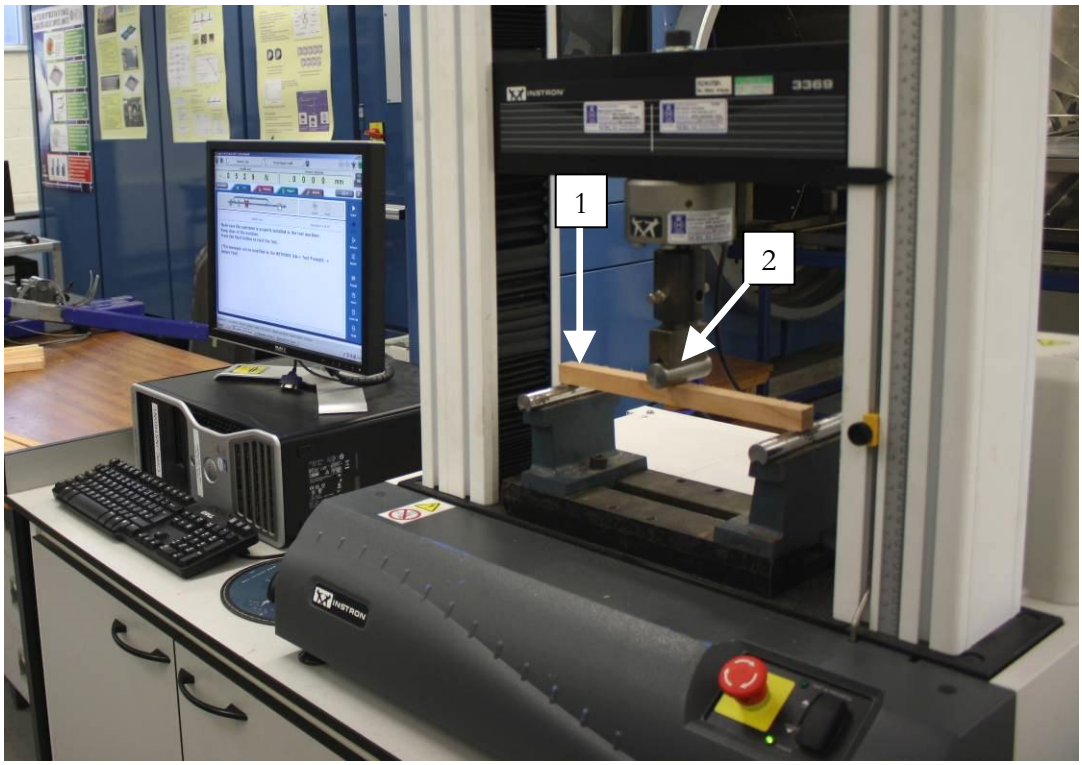

Figure 3-22: Small clear specimen flexural test setup 1. Flexural specimen 2. Loading head

The modulus of elasticity and bending strength of each small clear specimen were calculated by the Bluehill software utilising Equations 3-7 and 3-8 below.

$$\text{Modulus of elasticity} = \frac{L^3 m}{4bd^3} \qquad 3\text{-}7$$

$$\text{Flexural strength} = \frac{3FL}{2bd^2} \qquad 3\text{-}8$$

where: L specimen span

m slope of elastic region of load deflection plot

b specimen width

d specimen depth

F specimen ultimate load

The results calculated by the Bluehill software were checked for a random selection of 25 specimens to ensure that the slope of the elastic region used to obtain the modulus of elasticity was accurate. In all cases the results were found to be acceptable. In total 1446 small clear flexural specimens were tested using this method.

3.6.4 Compression specimen preparation

The size of specimens required for the evaluation of compressive strength parallel to the grain detailed in BS 373: 1957 is 60 x 20 x 20 mm. The evaluation of compressive strength was conducted on the northern radius only due to time constraints. This axis was selected so as to allow comparisons to be made with data collected utilising the SilviScan-3 system. All specimens were obtained from the excess material at the end of each flexural small clear specimen during the preparation stage. This was done by removing a 70 mm long section from the end of each flexural specimen following the cutting to the final test dimensions of 20 mm in the radial and tangential directions, ensuring that the growth ring numbers and specimen identification markings were transferred to the lengths removed.

When conducting compression tests, a key factor in obtaining accurate results is that the ends of the specimen to which loading is applied are parallel to each other. It was found that it was not possible to achieve such a finish utilising a saw alone. Therefore, a simple jig was developed as shown in Figure 3-23. After being passed through the thicknesser prior to removal from flexural specimens, each of the unfinished compressive specimens had radial-longitudinal faces which showed divergences along their length of less than 0.5 mm when assessed with digital callipers, and as such were assumed parallel. In order to achieve a similar finish on the adjacent tangential-longitudinal faces, the specimens were passed through a small circular table saw set to give a 20 mm cut. Specimens were then placed inside the jig, which itself was placed within a 90° guide positioned on a disc sander. The jig was designed such that when its end met the yellow guard shown in Figure 3-23 the length of the specimen within it was 60 mm, as required by BS 373: 1957. Whilst sanding, each specimen in the jig was rotated about all its axes to ensure both ends were parallel, and sanding continued until the required length was achieved. Following preparation, all specimens were stored in an environmentally controlled room at 65 % relative humidity and 20 °C.

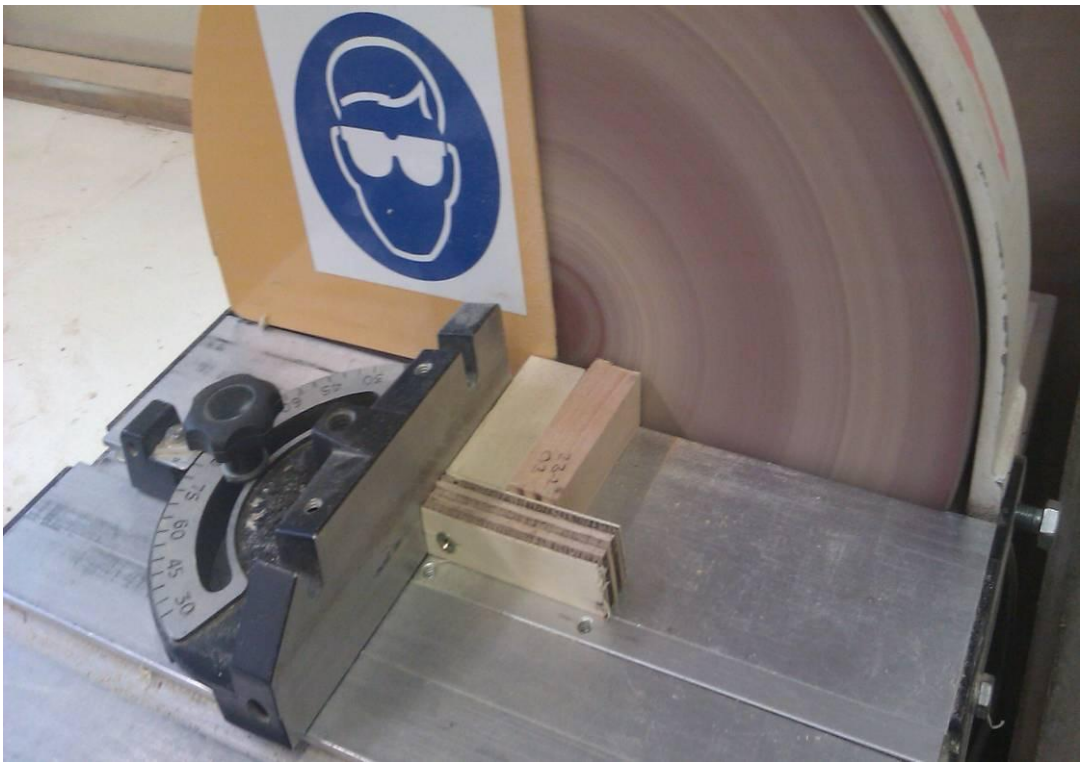

Figure 3-23: Small clear compressive specimen preparation

3.6.5 Compression specimen testing

Prior to conducting tests to determine compressive strength parallel to the grain, each specimen was checked with a moisture meter to ensure that the 12 % moisture content stipulated in BS 373: 1957 was achieved. Given the findings discussed in Section 3.6.3, a moisture content range of 11.5 - 12.5 % was deemed acceptable. Compression testing was conducted utilising an Instron 3369 testing system fitted with a 50 kN load cell. Prior to commencing testing, all specimens had their mass recorded on a balance and their radial and tangential thickness measured with a set of digital callipers. The dimensions were taken as the mean of two readings along the specimen length and were inputted into the Bluehill software for use in the calculation of compressive strength. A record was also made of the age of the growth rings contained in each specimen. In accordance with the standard, specimens were placed into the test machine such that the load was applied in a direction parallel to the grain, through plates that remained parallel to each other for the duration of the test. During the test, the top loading plate was set to move downwards at a rate of 0.6 mm/min. During testing data was logged utilising Instron Bluehill software, with the applied load recorded 100 times per second. The testing was continued until a noticeable decline in the load required for continued downward motion of the loading head was recorded, indicating that compressive failure had occurred, at which point the test was reset. The experimental setup is shown in Figure 3-24.

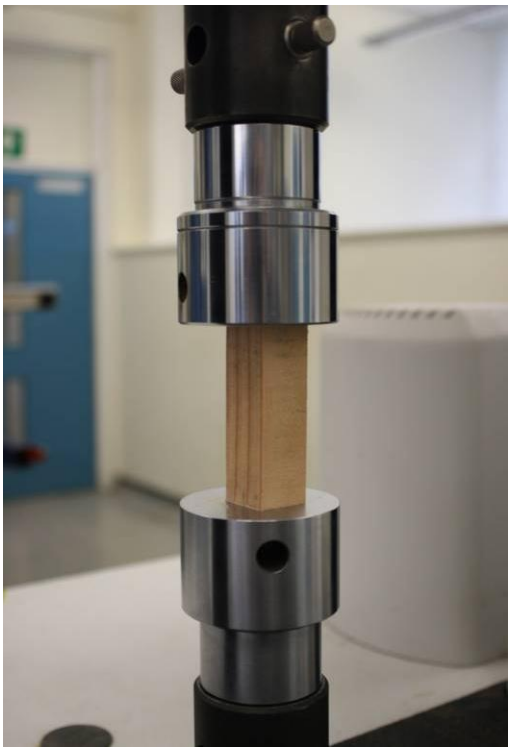

Figure 3-24: Small clear specimen compression parallel to grain test setup

The compressive strength of each specimen was calculated with the Bluehill software utilising Equation 3-9 below. In total 363 small clear compression specimens were tested using the method described here.

$$\text{Compressive strength} = \frac{F}{bd} \qquad 3\text{-}9$$

where: F specimen ultimate load

b specimen radial width

d specimen tangential width

Although care was taken to ensure that the load bearing ends of each specimen were parallel to each other, slight divergences were present in several specimens. While this did not have a detrimental impact on strength results, the uneven nature of initial strains across the specimen ends, that may have arisen during initial loading, meant that compressive modulus could not be reliably calculated utilising the deflection of the loading head. Due to this compressive modulus results are not presented.

3.7 Categorisation of trees as slower and faster growing

In order to allow the influence of different growth rates on anatomical and mechanical properties across the sample trees in the 40 - 50 year age range to be evaluated, each was categorised as being either slower or faster growing. The categories were developed for comparison within the sample set, and bore no reference to any wider interpretation of what may constitute slow or fast growth within Douglas-fir trees. In order to split trees into the two categories, each was ranked from lowest to highest by the mean ring width over the first 40 years of growth at breast height. This was determined utilising the scanned images of each disc in the north, east, south and west directions as described in Section 3.4. The 12 trees with the lowest mean ring width were then classified as slower growing and the remaining 12 faster growing. The same method was used in order to separate the six trees felled within each site into slower or faster growing categories for the comparison of growth rate effects within a site, with three trees being placed within each of the slower and faster growing categories.

Disc scans were used to obtain values rather than measurements derived from SilviScan-3 data, to ensure that the judgment of growth rate was made considering the whole stem cross-section. On inspection of the results it was found that the categorisation would have remained the same if the SilviScan-3 data alone were used. The results were also checked at 10 yearly intervals from the pith to ensure that all trees classified as slower or faster growing had been so over the course of their life. An inspection was also made of the discs at the 8 m sampling location, where it was found that the growth rate categorisation within each tree matched that determined at breast height in all cases. The mean ring width values used in all analysis of the data relevant to growth rate were determined from the SilviScan-3 results.

3.8 Determination of early, transition and latewood boundaries

In Section 2.3.4, previously used methods to determine the boundaries between the different stages of tracheid development within a growth ring were reviewed. The lack of consideration of transitional tracheids was a disadvantage associated with previous methods when evaluating the developmental processes taking place within and between successive growth rings. As a result of this, a boundary demarcation method that allowed for the identification of transition-wood tracheids, alongside early and latewood, in the analysis of anatomical property data was utilised. The boundaries between early, transition and latewood were determined with the use of the intra-ring density profiles, which represent changes occurring in both tracheid dimensions and wall thicknesses using Equation 3-10. The method calculates the density at the

boundary between the respective zones, from which the dimensions of each could be calculated.

$$EW - TW = \min + 0.2(\max - \min)$$
$$TW - LW = \min + 0.8(\max - \min) \quad \text{3-10}$$

where: $EW - TW$ earlywood to transition-wood boundary density

$TW - LW$ transition-wood to latewood boundary density

$\min$ minimum density within growth ring

$\max$ maximum density within growth ring

Implementation of the methodology is depicted for a single growth ring in Figure 3-25.

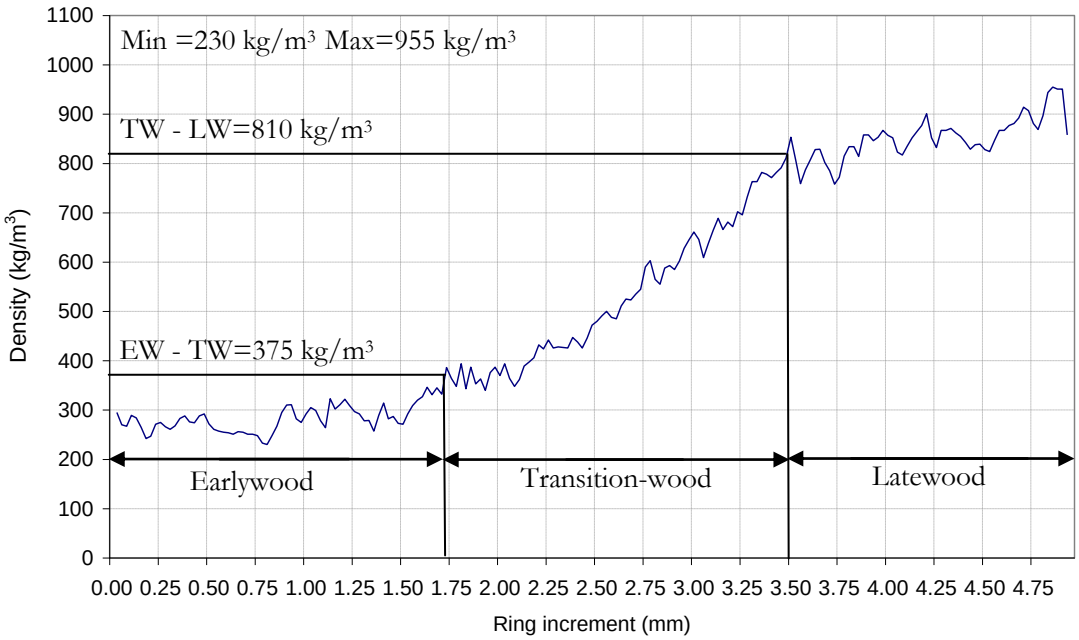

Figure 3-25: Intra-growth ring developmental zone demarcation

The values of 0.2 and 0.8 used in the determination of the demarcation points were derived empirically through the testing of several species (Olsson, 2010). The values were checked visually on a sub-sample of 100 randomly selected growth rings from the dataset, and it was found that they provided the best overall estimation for the transition zone.

Alternative methods to that used here would have been either a threshold, derivative or segmented regression method. The disadvantages of using the threshold method is that it is insensitive to individual variations within a growth ring, so it is possible to obtain rings with no early or latewood and therefore does not provide an accurate representation of the

developmental changes taking place. The maximum derivative method described in Section 2.3.4 was not suitable for application in identifying a transition zone, due to the need to identify two boundaries on the density profile, rather than the one obtained by finding the maximum derivative. A segmented regression model, similar to that used to determine the demarcation between juvenile and mature wood to be described in Section 3.10.6, was seen as a viable alternative to that employed here. However, the processing time for the 2040 individual growth rings was significant, while any improvement in accuracy would have been marginal. Having determined the boundaries, the mean values of anatomical properties within the early, transition and latewood were calculated, as well as those for the complete growth ring.

3.9 Anatomical and mechanical specimen matching

In order to allow the results from the SilviScan-3 analysis to be matched with those of the mechanical properties of small clear specimens for the purpose of analysis, a method utilised by McLean (2008) was adopted. In this method, each of the profiles of anatomical properties obtained from SilviScan-3 was broken down by growth ring, and within each growth ring regions of early, transition and latewood. In knowing the growth rings present within each of the small clear specimens, it was then possible to match the corresponding mechanical and anatomical datasets. Having matched the data, the mean anatomical characteristics of each small clear specimen could be calculated.

This method of matching the corresponding datasets meant that there was the potential for anatomical data used to not be fully representative of the anatomical characteristics of the mechanical test specimens. This arose from the fact that there was a separation of typically 200 mm from the region in the sample logs from which small clear mechanical specimens were obtained and that in sample discs from which SilviScan-3 specimens were taken. An alternative method would have involved taking SilviScan-3 specimens directly from the end of mechanical test specimens. This method was however ruled out due to the fact that it would not have allowed for continuous profiles of anatomical characteristics to be recorded. When matching the mechanical and anatomical specimens very good fits were achieved. It was therefore assumed that little change in the wood characteristics had taken place in the small region between the specimens.

3.10 Statistical methods

3.10.1 Outline

Within this section the statistical methods utilised in the analysis of results presented in the subsequent chapters is detailed. In all statistical tests, results were deemed significant if the probability of them occurring by chance was 5 % or less, referred to as $P \leq 0.05$. Statistical analysis was conducted in SPSS 18 and Minitab 16.

3.10.2 Assumptions and transformations

When conducting many of the statistical tests described in the sections below, the following conditions must be met:

- Random sampling
- Approximately normal distribution of property values within a sample
- Equal variances between samples being compared

In selecting a sample randomly it is assumed that every potential item, in this case trees, within a population has an equal chance of being selected. If the population in this study is considered as all trees within the selected sites, then given the methodologies described previously in Section 3.2.2, the sampling process can be considered random and the criteria satisfied. The condition of normality for all distributions was evaluated visually with the use of frequency histograms, and also by means of a Shapiro - Wilk test. In order to check the final assumption, that samples being compared had homogenous variance, an F-test was used, in which the ratio of the larger to smaller sample variance was calculated, and the critical F value for unequal variances found within F-tables for the stated significance level.

In situations where the results of tests showed that a particular dataset was not normally distributed, or variances were not equal, a log transformation was applied to all values within the particular dataset. A log transformation works by reducing the influence of any atypical values and also correcting distributions displaying a right-sided skew, which was found to be the case in all situations where distributions were found not to be normal. Log transformations were applied to entire datasets utilising Equation 3-11, and the conditions of normality and equal variance revaluated. In all cases, it was found that the application of log transformations allowed all datasets to conform to the previously stated conditions.

$$y' = \log_{10}(y + 1) \qquad 3\text{-}11$$

where: y' transformed value

y original value

3.10.3 Linear correlation and regression analysis

Linear correlation and regression analysis were used throughout the study to evaluate the presence of linear relationships between variables and for the generation of equations for the prediction of a given dependent variable through varying combinations of independent variables. The correlation coefficient, r, is a measure of how well points fit to a straight line, varying between -1 and 1. The coefficient of determination, R^2 gives a measure of the proportion of variation in the dependent variable that can be predicted by knowing the values of independent variables, varying between 0 and 1 (Townend, 2002). In calculating the coefficient of determination, the line of best fit through the points when plotted on a scatter graph was found by minimising the sum of squares of the residuals, with the resulting equation for the line as shown in Equation 3-12.

$$y_i = b_0 + b_1 x_1 + \varepsilon \qquad 3\text{-}12$$

where: y_i dependent variable

b_0 y intercept

b_1 slope coefficient

x_1 independent variable

ε error term

In cases where the relationships between a dependent variable and multiple independent variables were evaluated, the equation describing the fitting of a plane, or in the case of more than two dependent variables a hyperplane, is shown in Equation 3-13.

$$y_i = b_0 + b_1 x_1 + b_2 x_2 + ... \varepsilon \qquad 3\text{-}13$$

where: y_i dependent variable

b_0 y intercept

b_1 slope coefficient for first independent variable

x_1 first independent variable

b_2 slope coefficient for second independent variable

x_2 second independent variable

ε error term

3.10.4 Univariate analysis of variance

In order to test for the existence of statistically significant differences in the mean values of the assessed anatomical and mechanical properties with cambial age and also between growth orientations within the stem, a univariate repeated measures analysis of variance was conducted. It was necessary to utilise a repeated measures approach to the analysis, as the likely relationship between the properties of a growth ring, and those of the neighbouring growth rings, means that the condition of independent measurements cannot be assumed. In order to ensure that a balanced analysis across sites and trees was conducted when assessing variations with cambial age, means were compared utilising results from the four sampling sites in the 40 - 50 year age range only. Changes in mean values with cambial age were assessed within age ranges of 2 - 10 (3 - 10 for mechanical properties), 11 - 20, 21 - 30 and 31 - 40 years at breast height, and in all but the 31 - 40 year range at the 8 m sampling location. This ensured that differences at the various developmental stages over the life of the tree could be assessed. Assessment started from the second or third growth ring due to potentially unreliable results in the first growth ring from SilviScan-3 tests, and the inability to calculate mean specimen mechanical properties at younger ages. Tests for variations in mechanical properties with orientation considered the means of all values in the 3 - 40 year range. In conducting the analysis, the fixed effects model shown in Equation 3-14 was used, in which the treatment was either cambial age (e.g. 2nd, 3rd, 4th growth ring) or cardinal orientation (e.g. north, east, south, west).

$$y_i = \mu + a_i + \varepsilon \qquad 3\text{-}14$$

where: y_i dependent variable

μ sample population mean

a_i fixed effect of the ith treatment on the dependent variable

ε variance due to error

An F-test was used to determine if a statistically significant difference existed between the mean values of different treatments within a sample population utilising the methodology shown in Equation 3-15.

$$F = \frac{msg}{mse} \qquad 3\text{-}15$$

where: msg mean squares of the deviation of the treatment means from the sample population mean

mse mean squares of the deviation of data around treatment means

The repeated measures are accounted for by apportioning the deviation of data around the treatment means to that which is consistent between subjects and that which is the unaccounted, or error, variability. It is this error that is used in the calculation of the F value. As the F value increases, it indicates an increased likelihood of the presence of a difference between the mean values of the various treatments levels. Statistical significance was determined by use of F-tables. In the case of assessing variations in anatomical and mechanical properties with cambial age, a second analysis was conducted to evaluate the variance associated with differences between the sample sites and trees within these sites. A hierarchal approach was adopted in this analysis, with the treatment effect 'tree' nested within the 'site' treatment effect, with both effects classified as random. The model is shown in Equation 3-16

$$y_{jk} = \mu + s_j + t_{(k)j} + \varepsilon \qquad 3\text{-}16$$

where: y_{jk} dependent variable

μ sample population mean

s_j random effect of j^{th} site

$t_{(k)j}$ random effect of k^{th} tree at the j^{th} site

ε variance due to error

The variance components of the random effects of site and tree were expressed in percentage terms, along with the variance due to error.

3.10.5 t-tests

In order to assess if there was a statistically significant difference between the mean values of two populations within the sample dataset, unpaired t-tests were used. The mean values of populations compared included those for properties at the two stem heights, slower and faster growing trees and the demarcation age from juvenile to mature wood between density and microfibril angle. A t-test determines if a statistically significant difference is present by comparing the mean and variance of each sample using Equation 3-17.

$$t = \frac{\bar{x}_1 - \bar{x}_2}{\sqrt{s^2\left(\frac{1}{n_1} + \frac{1}{n_2}\right)}} \qquad 3\text{-}17$$

where: t t value

$\bar{x}_1$ sample 1 mean

$\bar{x}_2$ sample 2 mean

s^2 pooled sample variances

n_1 sample 1 size

n_2 sample 2 size

The pooled sample variances are calculated using Equation 3-18.

$$s^2 = \frac{\sum_{i=1}^{n} (x_i - \bar{x}_1)^2 + \sum_{j=1}^{n} (x_j - \bar{x}_2)^2}{n_1 + n_2 - 2} \qquad 3\text{-}18$$

The t value attained will be large if the difference between the sample means is large and the variance small; the opposite is true of small t values. The difference between two mean values is deemed statistically significant when the value is above that specified for the sample size and required probability level, in this case $P \leq 0.05$, within t distribution tables.

3.10.6 Determination of juvenile to mature wood demarcation age

Within softwoods, juvenile wood is a region in which a high degree of variability exists in the anatomical and mechanical properties, while mature wood properties generally exhibit a more gradual change with increasing cambial age. In order to determine the point of demarcation from juvenile to mature wood production, a segmented regression model was used. This methodology was selected over the threshold method discussed in Section 2.3.7, because simply stipulating the threshold at which mature wood production commenced did not reflect the nature of the transition taking place. When using a segmented regression model two regression equations, or segments, are fitted to the data points such that the total residual sums of squares are minimised. The intersection point between the two segments represents the age of demarcation from juvenile to mature wood production.

In the development of the segmented regression method, several combinations of linear and non-linear regression equations were used to form the two segments when modelling

demarcation age for both microfibril angle and density. In both cases, the best fits were found when a quadratic equation was fitted to data points within the juvenile wood region, and a linear equation with a non-constant value in the mature wood. Equation 3-19 was used within the juvenile regions, while Equation 3-20 was used in mature wood.

$$y_i = b_0 + b_1 x_i + b_2 x_i^2 + \varepsilon \quad \text{for } x_i < k \qquad 3\text{-}19$$

$$y_i = b_0 + k(b_1 - b_3) + b_2 k^2 + b_3 x_i + \varepsilon \quad \text{for } x_i \geq k \qquad 3\text{-}20$$

where: y_i dependent variable

$b_{0\ldots i}$ regression coefficients

x_i cambial age

k juvenile/mature wood transition age

ε error term

Each of the equations was fitted and the demarcation age found with use of the non-linear regression function in SPSS 18. All results were also verified for their fit visually. An example of measured values and the fitted regression equations are shown for microfibril angle and density in Figures 3-26 and 3-27.

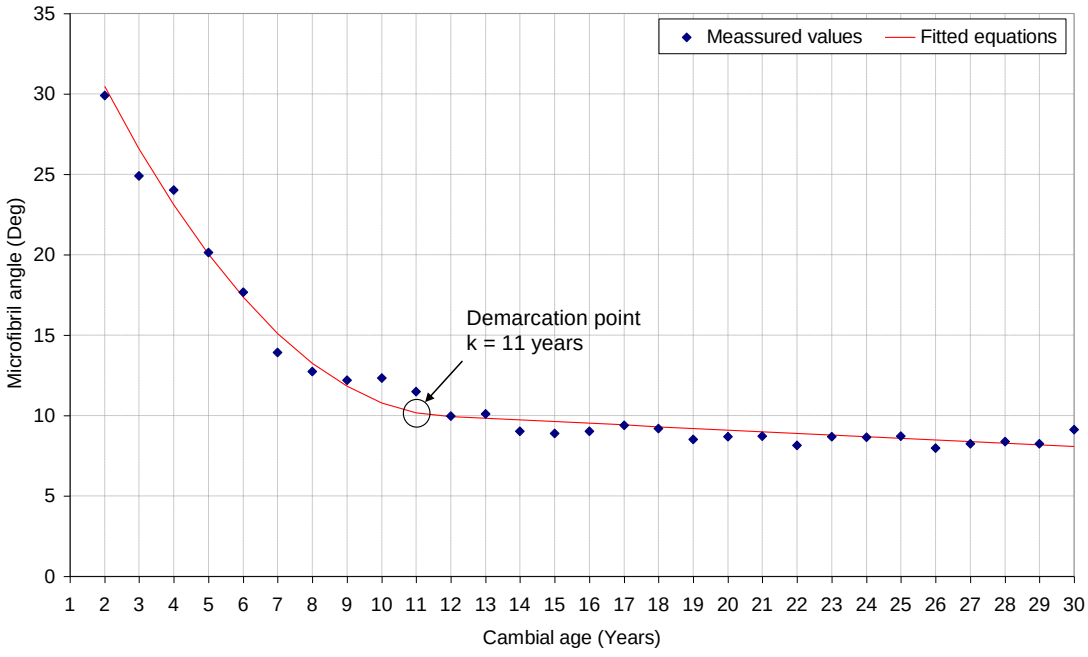

Figure 3-26: Determination of juvenile / mature wood demarcation age for microfibril angle

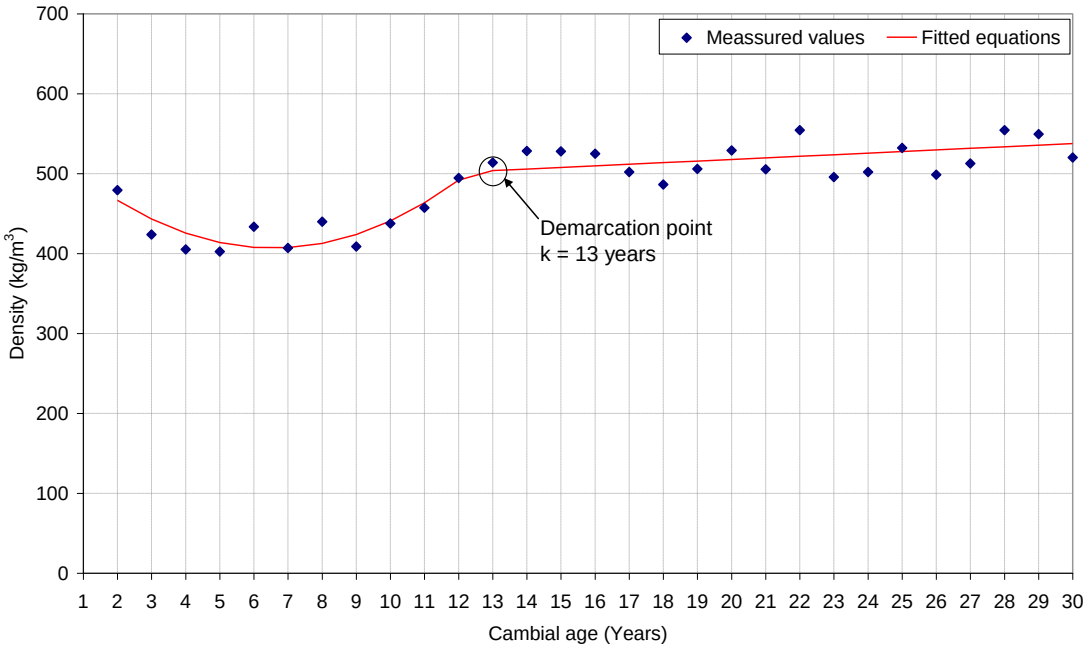

Figure 3-27: Determination of juvenile / mature wood demarcation age for density

The use of a transitional zone between the juvenile and mature wood, similar to that seen between early and latewood, was considered when estimating the demarcation age. Such a methodology was not used however, due to the fact that, unlike earlywood, large degrees of variability are seen in the inter-growth ring properties for both microfibril angle and density at all locations within the juvenile wood. As such, a clear definition of the characteristics of a transitional zone could not be formulated.

3.10.7 Path analysis

In order to allow for a greater degree of understanding to be gained into the relationships that exist between dependent and independent variables in multiple regression analysis, a statistical technique known as path analysis was used. An example of a simple path diagram is shown in Figure 3-28.

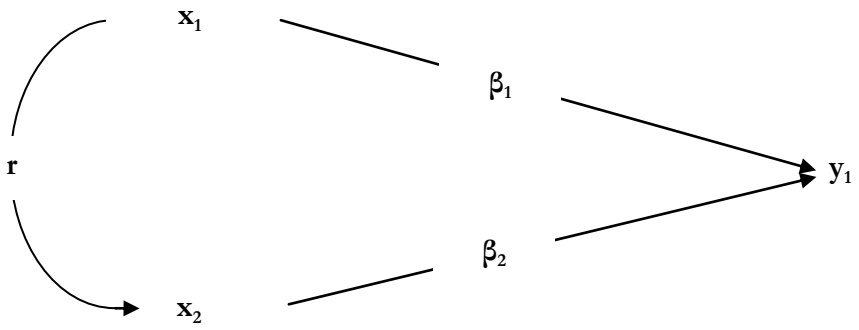

Figure 3-28: Example path diagram

In path analysis, the effect of the independent variables, x_1 and x_2, on the dependent variable, y_1, is apportioned into direct effects, β, and indirect effects, r. The value of r is the simple linear correlation that exists between the variables x_1 and x_2, while the values β_1 and β_2 are standardised regression coefficients. The reason for using standardised coefficients is that due to different units and variances, unstandardised coefficients for each of the x variables cannot be compared. Standardisation results in all variables having a mean of zero and a standard deviation of one, this is achieved by subtracting the sample mean from a variable and dividing by the standard deviation. An example of a multiple regression analysis conducted with the use of standardised coefficients is shown in Equation 3-21.

$$\frac{\sum_{i=1}^{n}(y_i - \bar{y})}{s_y} = \frac{b_1 s_1}{s_y}\left(\frac{\sum_{j=1}^{n}(x_j - \bar{x}_1)}{s_1}\right) + \frac{b_2 s_2}{s_y}\left(\frac{\sum_{k=1}^{n}(x_k - \bar{x}_2)}{s_2}\right) \qquad 3\text{-}21$$

where: n sample size

y_i dependent variable

$\bar{y}$ dependent variable sample mean

s_y dependent variable sample standard deviation

$b_{1,2}$ independent variable 1 or 2 unstandardised coefficient

$s_{1,2}$ independent variable 1 or 2 sample standard deviation

$x_{j,k}$ independent variable within sample 1 or 2

$\frac{b_1 s_1}{s_y}$ β_1

$\frac{b_2 s_2}{s_y}$ β_2

In utilising this method, the standardised regression coefficients represent the change in terms of standard deviation of the dependent variable, arising from a one standard deviation change in the given independent variable. By comparison of the magnitude of β values, it is then possible to ascertain which of the independent variables is most strongly associated with the dependent variable. From path diagrams it is possible to calculate the simple correlation between an independent and dependent variable, e.g. x_1 - y_1, by summing the standardised regression coefficient on the direct path, β_1, with the multiples of each of the individual indirect paths, $r\beta_2$.

Chapter 4 - Anatomical properties part 1: variations with cambial age and height

4.1 Introduction

The anatomical properties of wood and their variations within a tree are directly related to many of the factors by which wood quality and suitability for different end uses are judged. As such, gaining an understanding not only of the way in which these properties change with age and height, but also the ways in which they are related to one another is important, if the best end use is to be made of the available material.

In this chapter, the development of anatomical properties with increasing cambial age and longitudinal variations within the Douglas-fir sample trees are evaluated. Results are reported first for the 24 younger trees in the 40 - 50 year age range, with the continuation of any trends observed then verified in a separate assessment of the three older sample trees with ages > 50 years. Two statistical tests were employed in the analysis of the results, firstly a repeated measures univariate analysis of variance, assessing the statistical significance of differences in the studied properties due to cambial age, tree and site and secondly t-tests, comparing the mean values at the two sampling heights. The results from both were deemed significant when $P \leq 0.05$. Detailed descriptions of the methods used to obtain the results presented, and the statistical techniques employed to interpret them are given in Chapter 3. In order to allow statistical techniques to be conducted at common intervals, radially and longitudinally, results were grouped by cambial age into the growth periods; 2 - 10, 11 - 20, 21 - 30 and 31 - 40

years[1]. The results of each test can be found with the descriptive statistics in Appendix A, as indicated at the start of each sub-section.

In analysing the results of the statistical tests within each of the growth periods, two hypotheses were tested, the null hypothesis of which were:

> $H_{4\text{-}1}$: No change in the magnitude of the studied property takes place with increasing cambial age.
>
> $H_{4\text{-}2}$: No difference exists in the magnitude of the studied property with increasing longitudinal position in the stem.

The results obtained from the analysis are grouped by anatomical property and presented in this chapter in the following order:

- Ring widths
- Proportions of wood types
- Radial and tangential tracheid diameters
- Radial tracheid wall thickness
- Density
- Microfibril angle

The presentation of results is followed by a discussion, relating the changes observed to developmental processes taking place within the living tree.

[1] The 31-40 year growth period was only present at the 1.3 m sampling location.

4.2 Ring width - variations with cambial age and height

4.2.1 Outline

Ring width and its early, transition and latewood components were determined utilising the optical imaging and x-ray densitometry functions of the SilviScan-3 system, as described in Section 3.5.3. In the following sub-sections, the radial profiles of mean values at the two assessed stem heights for whole ring, early, transition and latewood width in 40 - 50 year old trees, and whole ring mean values in trees with ages > 50 years are presented, and the results discussed.

4.2.2 Variations in younger trees

4.2.2.1 Whole ring widths

Figure 4-1 shows mean values and the 95th percentile range for whole ring width at the two assessed stem heights, descriptive statistics alongside the results of the analysis of variance and t-tests can be found in Tables A-1 and A-2. At both stem heights assessed, mean ring width development was subject to an initial increase in values upon moving away from the pith, followed by a period of decreasing width from a cambial age of 4 - 5 years onwards. Peak widths and the subsequent rate at which they decreased were greatest at the 8 m sampling location and a decline in width continued for all growth periods following the peak. The rate of decrease in ring width following the peak values seen at 1.3 m quickly reduced, and from the age of approximately 15 years onwards the inter-ring rate of decline was relatively small. The results of the analysis of variance showed that in all growth periods assessed, with the exception of 21 - 30 years at 1.3 m, variation in mean whole ring width with cambial age was statistically significant, which is in agreement with the observations made above. The non-significant result appears to have been caused by a period of accelerated growth, potentially due to silvicultural interventions. The results of a t-test showed that the mean of whole ring width was statistically significantly different in all growth periods between the two stem heights. Negative t values were observed within the first two growth periods, indicating higher mean widths at 8 m, with positive results between 21 - 30 years, over which time the mean widths higher in the stem were lower. These results reflect the sharp decrease in ring width seen at the 8 m position within the stem.

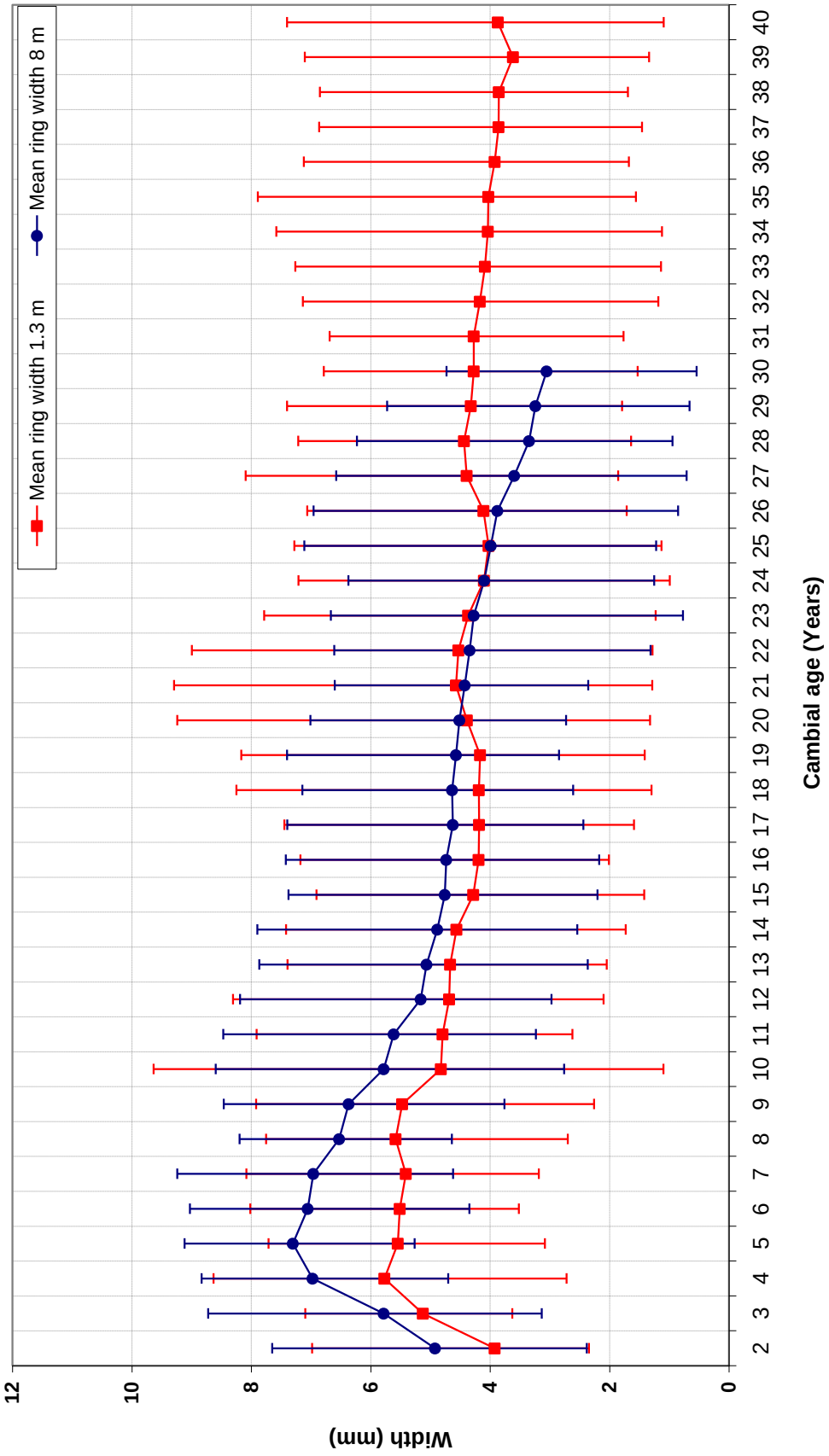

Figure 4-1: Mean whole ring width and 95th percentile range as a function of cambial age at stem heights of 1.3 m and 8 m within younger sample trees

4.2.2.2 Earlywood widths

Figure 4-2 shows mean values for earlywood ring width at the two assessed stem heights, descriptive statistics alongside the results of the analysis of variance and t-tests can be found in Tables A-3 and A-4. Trends in the development of earlywood widths closely followed those seen for whole ring values at both stem heights. An initial increase, peaking at growth ring 5 - 7 was followed by a continual decline at 8 m, with a more gradual decrease in values at breast height, relatively stable beyond 15 years of age. Trends in the values and significance of the analysis of variance and t-tests were as described previously for whole ring widths.

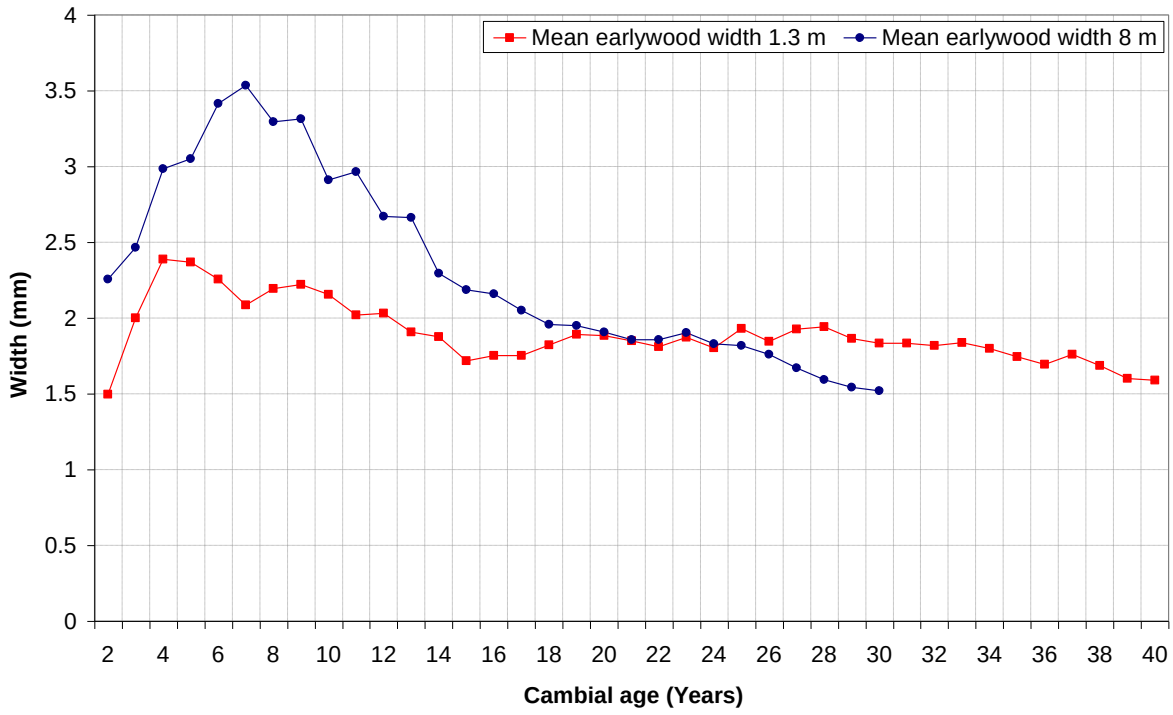

Figure 4-2: Mean earlywood width as a function of cambial age at stem heights of 1.3 m and 8 m within younger sample trees

4.2.2.3 Transition-wood widths

Figure 4-3 shows mean values for transition-wood ring width at the two assessed stem heights, descriptive statistics alongside the results of the analysis of variance and t-tests can be found in Tables A-5 and A-6. Transition-wood width was also found to show an increase to a peak value in the growth rings immediately adjacent to the pith, reaching a maximum at a cambial age of 4 years at both stem heights, with mean widths at 8 m 0.5 mm greater than those seen in equivalent rings lower in the stem. Following this, large declines in values were observed, resulting in the peaks of approximately 3 mm reducing by half over the subsequent 10 years of growth. Beyond this, transition-wood widths at breast height exhibited inter-ring fluctuations

around a mean of 1.2 mm, however no overall trend of decreasing values was observed. This was confirmed by the analysis of variance results, which showed that beyond the 11 - 20 year growth period, no statistically significant differences in mean transition-wood widths due to cambial age were present. An overall decline in transition-wood width at 8 m was observed, and confirmed by the fact that cambial age was a significant factor in the analysis of variance in all growth periods. The results of a t-test comparing the mean values at the two heights were found to be significant in the first and last growth periods, being negative and positive respectively as a result of the continual decline in transition-wood width seen higher in the stem.

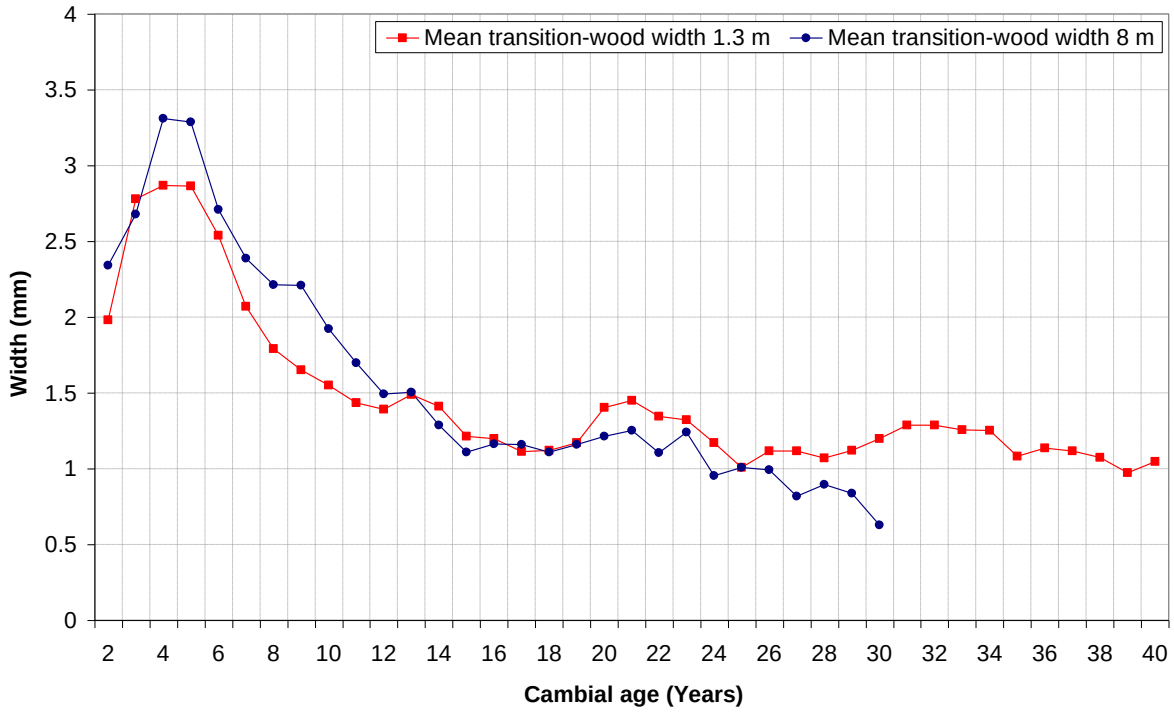

Figure 4-3: Mean transition-wood width as a function of cambial age at stem heights of 1.3 m and 8 m within younger sample trees

4.2.2.4 Latewood widths

Figure 4-4 shows mean values for latewood ring width at the two assessed stem heights, descriptive statistics alongside the results of the analysis of variance and t-tests can be found in Table A-7 and A-8. Latewood width development, as with all cases described previously, displayed a marked increase upon moving outwards from the pith at both positions in the stem. The magnitude of the increase was similar at both 1.3 m and 8 m, reducing at growth ring 8 - 9. Beyond this, unlike early and transition-wood, values of mean latewood width remained relatively stable, although some inter-ring fluctuations were observed. This resulted

in the output of the analysis of variance showing no significant difference in latewood width at either height with respect to cambial age beyond the 2 - 10 year growth period. Latewood widths displayed similar values at both stem heights across the timescale over which they were assessed, with mean stable values of approximately 1.1 mm in the later years of growth. As a result of this, t-tests to evaluate the difference between the mean values recorded at the two heights showed that there was no statistically significant difference at any age.

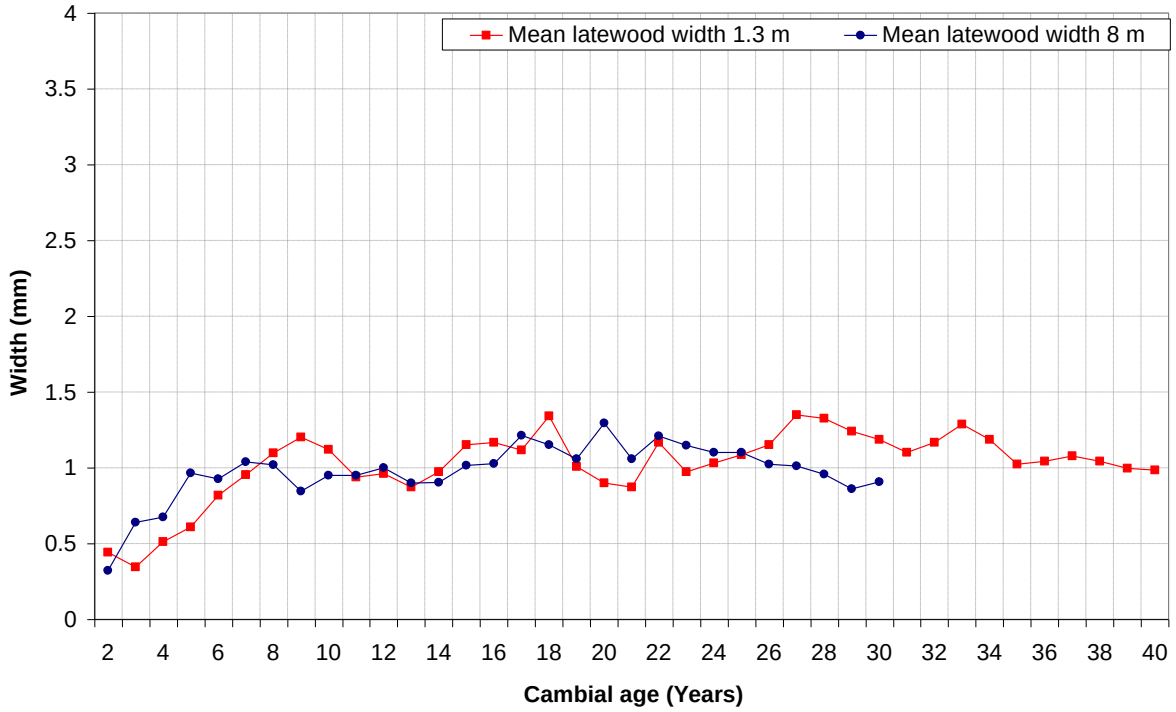

Figure 4-4: Mean latewood width as a function of cambial age at stem heights of 1.3 m and 8 m within younger sample trees

4.2.3 Variations in older trees

Figure 4-5 shows the profile of mean ring width development within the older sample trees. The purpose of testing older trees was to evaluate the continuation of any trends observed in the younger stems. As only three sample trees were felled for this purpose, the mean profiles generated were more susceptible to variations occurring in the properties of individual trees due to changes in the growing environment. This fact is clearly evident in the graph of mean ring widths, particularly so in the first 25 - 30 years of growth. At breast height the initial increase to a peak value followed by a decline observed in younger trees is evident, however the rate of decline is much greater and the final mean ring widths observed are much lower than those seen in younger trees. No initial increase to a peak is evident at the 8 m sampling location. On inspection of the individual tree profiles, this difference in behaviour appears to

be due to the close initial spacing at one of the sampling sites for older trees. This close spacing most likely resulted in early crown closure, coupled with the suppressed nature of the tree, resulting in a rapid decline in productivity in the xylem and hence narrow growth rings. It then appears that between 15 - 20 years of age thinning took place at the site, resulting in the opening up of the crown and a subsequent increase in ring widths due to reduced competition. Given the limited number of sample trees and the large variations seen in the early growth periods, firm conclusions regarding ring width development in older Douglas-fir stems cannot be made. However, from the results presented it does appear that in the later years of growth, during which time minimal silvicultural interventions were made, a gentle decline in values similar to that observed in younger stems existed within the sampled tress.

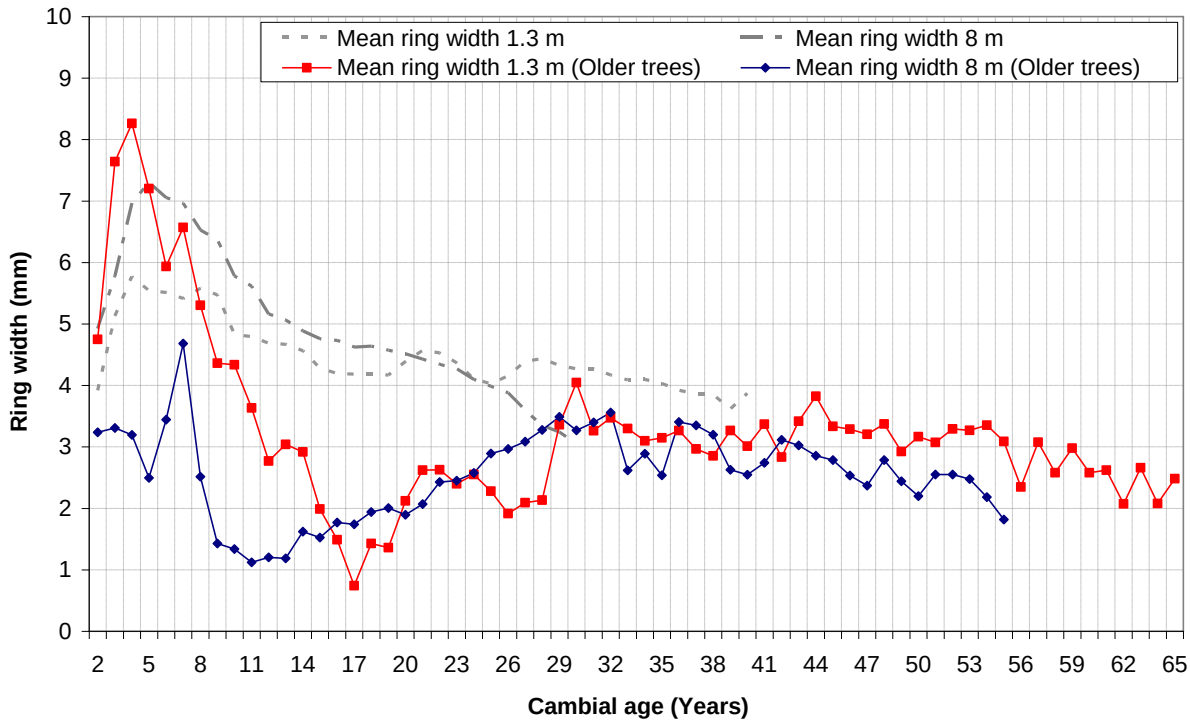

Figure 4-5: Mean whole ring width as a function of cambial age at stem heights of 1.3 m and 8 m within older sample trees

4.2.4 Discussion of variations in ring width results

The coefficient of variation for all ring width components was found to be large, with mean whole ring values across the entire stem at both sampling heights of approximately 40 %, with similar values observed for each of the wood types. This is a result of the high variation in ring widths seen within a stem, as well as the selection method used to sample trees, in which a large range of growth rates, and hence ring widths, were obtained between trees. Mean ring widths and coefficients of variation across all sites were in a similar range, as shown in

Table A-9, consequently the site factor accounted for only a small percentage of the variation in the analysis of variance, typically lower than 5 %. Differences between trees within sites typically accounted for between 10 - 50 % of the variation, with the magnitude of the value increasing in successive growth periods.

The patterns of radial and longitudinal whole ring width development and its components shown here are in line with the findings of previous Douglas-fir studies (Jozsa and Brix, 1989, Abdel-Gadir, 1991, Fabris, 2000, Gartner et al., 2002). Making a direct quantitive comparison between the ring widths obtained in different studies is complicated by the large number of external factors known to influence productivity and the relatively small dataset available for comparison. However, on inspection of the results presented here, the mean ring widths attained in both the early and later years of growth were higher than those reported in previous studies on North American grown Douglas-fir. Differences in mean widths at breast height at 30 years of age were of the order of 1 mm, equivalent to 25 % of the width reported here. A potential reason for this may be the different climatic conditions found within the study region, compared to those in North America from which test material for the previously documented results was obtained. The Western United Kingdom is described as having a mild wet oceanic climate (Gardiner et al., 2011), with it shown by Fletcher and Samuel (2010) that the South West of England has a much reduced temperature range and a significantly greater number of frost free days than much of the North American native range of Douglas-fir. The impact of this faster rate of growth on the comparability of other anatomical characteristics with those obtained in previous Douglas-fir studies is evaluated in the following sections.

4.3 Proportions of wood types - variations with cambial age and height

4.3.1 Outline

The classification of early, transition and latewood regions within a growth ring was determined utilising the SilviScan-3 system as described in Section 3.8. In the following sub-sections, the radial profiles of mean values at the two assessed stem heights for early, transition and latewood proportions within 40 - 50 year old trees, and in trees with ages > 50 years are presented, and the results discussed.

4.3.2 Variations in younger trees

4.3.2.1 Earlywood proportions

Figure 4-6 shows the mean values of earlywood proportions within a growth ring at the two assessed stem heights, descriptive statistics alongside the results of the analysis of variance and t-tests can be found in Tables A-10 and A-11. The proportion of earlywood found within a growth ring showed a markedly different behaviour in the first 15 years of growth between samples taken at breast height and 8 m. At breast height, earlywood proportion was found to vary little with cambial age within the 2 - 10 year growth period from the initial 40 % value observed adjacent to the pith. This was confirmed by the non-significant impact of cambial age seen in the analysis of variance during this time. Beyond this, an increase with cambial age occurred within the 11 - 20 year growth period, with the analysis of variance results also showing statistically significant differences in proportions with cambial age. This was followed by a gradual non-significant decline, with mean values of 45 % found between 31 - 40 years of age. At the 8 m sampling location the increase in earlywood proportion upon moving away from the pith occurred at a much greater rate, with a statistically significant increase with cambial age of almost 10 % occurring within the first growth period. Beyond this, a slight but statistically significant decline in values was observed, before relatively large fluctuations around a mean earlywood proportion of 50 %. As a result of the difference in the developmental profiles at the two stem heights, t-tests showed that mean values were statistically significantly different during all growth periods assessed, with the mean earlywood proportions at 1.3 m being lower than those at 8 m.

4.3.2.2 Transition-wood proportions

Figure 4-7 shows the mean values of transition-wood proportions within a growth ring at the two assessed stem heights, descriptive statistics alongside the results of the analysis of variance and t-tests can be found in Tables A-12 and A-13. Radial profiles of transition-wood proportion exhibited similar trends at both assessed stem heights. Large declines were observed with respect to cambial age in the 2 - 10 year growth period, continuing until approximately 15 years of age. These were found to be statistically significant. During this time, mean values at both heights fell by over 20 %, from starting values of 51 % and 47 % in the second growth ring at 1.3 m and 8 m respectively.

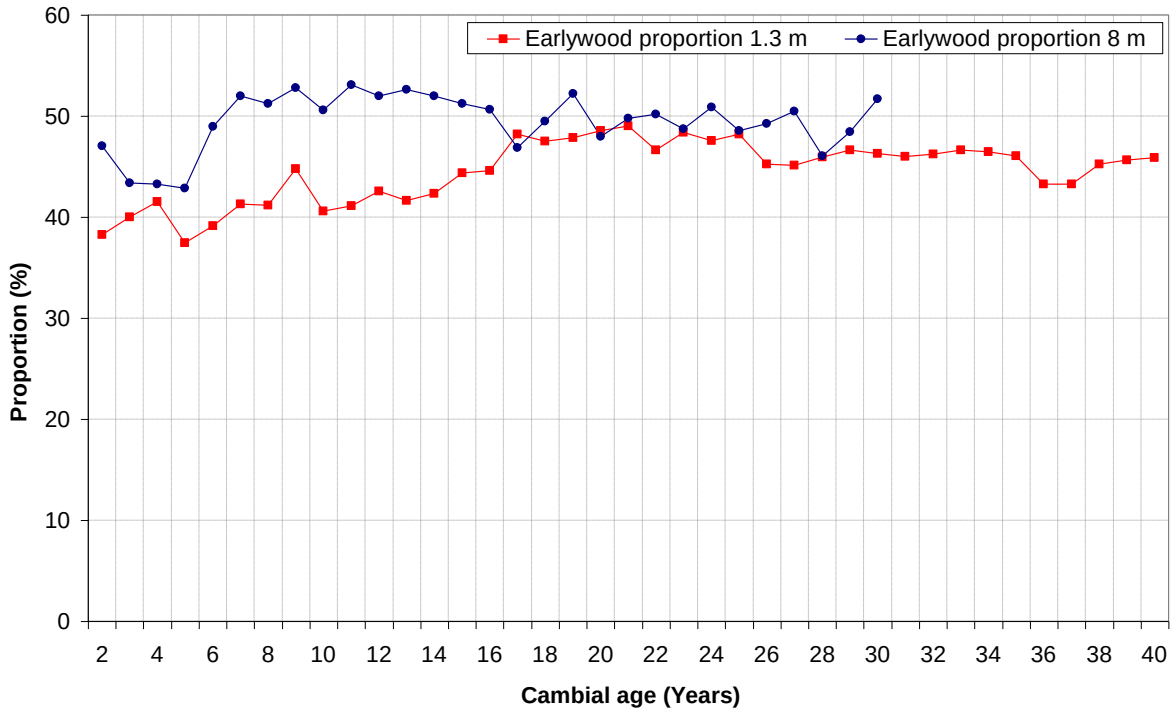

Figure 4-6: Mean earlywood proportion as a function of cambial age at stem heights of 1.3 m and 8 m within younger sample trees

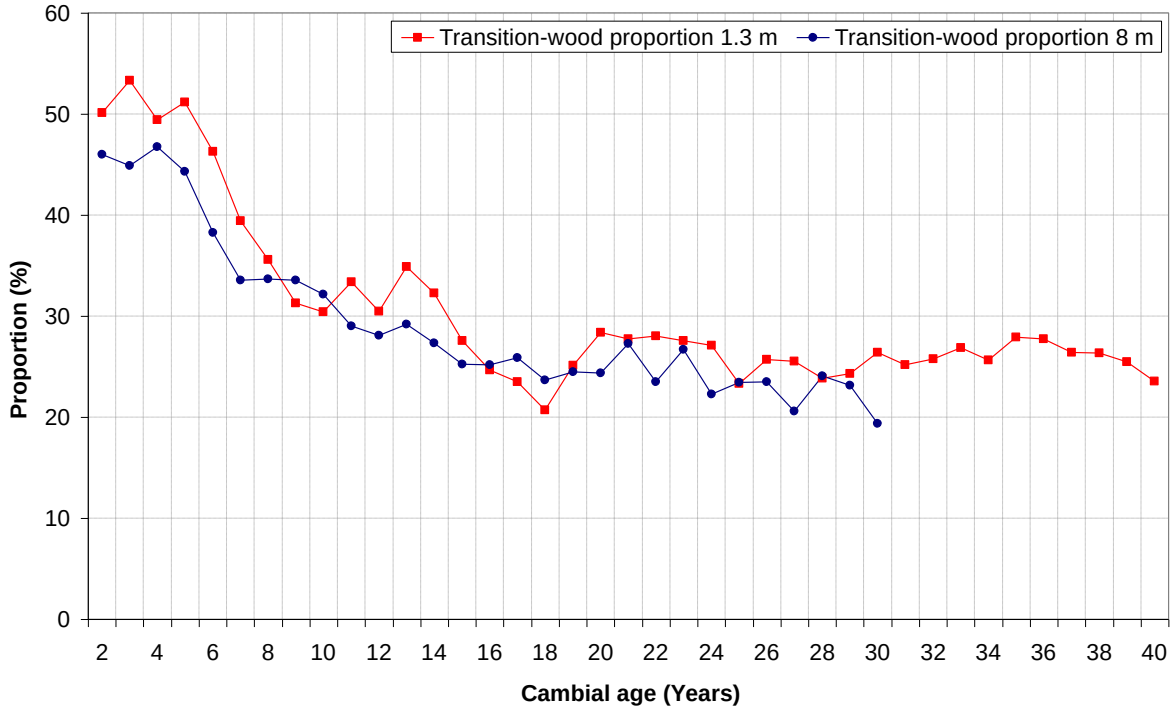

Figure 4-7: Mean transition-wood proportion as a function of cambial age at stem heights of 1.3 m and 8 m within younger sample trees

Following this, fluctuations in transition-wood proportion were observed at 1.3 m; however no significant change with respect to cambial age was found in the analysis of variance results in either of the last two growth periods, and mean transition wood proportions of 26 % were observed across all subsequent growth rings. At the 8 m sampling location a small, but statistically significant decrease in proportions with respect to cambial age was observed in the final growth period, with a mean of 23 %. The results of a t-test showed that the slight difference in mean proportions between heights, typically less than 5 %, was statistically significant in all growth periods.

4.3.2.3 Latewood proportions

Figure 4-8 shows the mean values of latewood proportions within a growth ring at the two assessed stem heights, descriptive statistics alongside the results of the analysis of variance and t-tests can be found in Tables A-14 and A-15. Latewood proportion showed large statistically significant increases on moving outward from the pith at both stem heights, with increases at 1.3 m occurring at a greater rate than those seen higher in the stem. Beyond a cambial age of about 10 years at breast height proportions of latewood were observed to begin to stabilise, fluctuating about a mean of 27 % and with no further significant increase or decrease with respect to cambial age seen in the analysis of variance. Higher in the stem, the proportion of latewood found within a growth ring continued to increase and was significant with respect to cambial age in the two remaining growth periods. The continued increase in values at the 8 m sampling location resulted in the final mean values being similar to those recorded lower in the stem. As a result of this, the statistically significant differences between mean values at the two stem heights shown in the results of the t-test in the first two growth periods were not repeated between cambial ages of 21 - 30 years. As the proportion of tracheids with transitional properties was observed to be relatively similar at both stem heights, the increased proportion of earlywood found at younger cambial ages higher in the stem was accompanied by lower proportions of latewood tracheids in the same region. This can be related to developmental processes taking place as new xylem material is formed and is discussed in section 4.8.

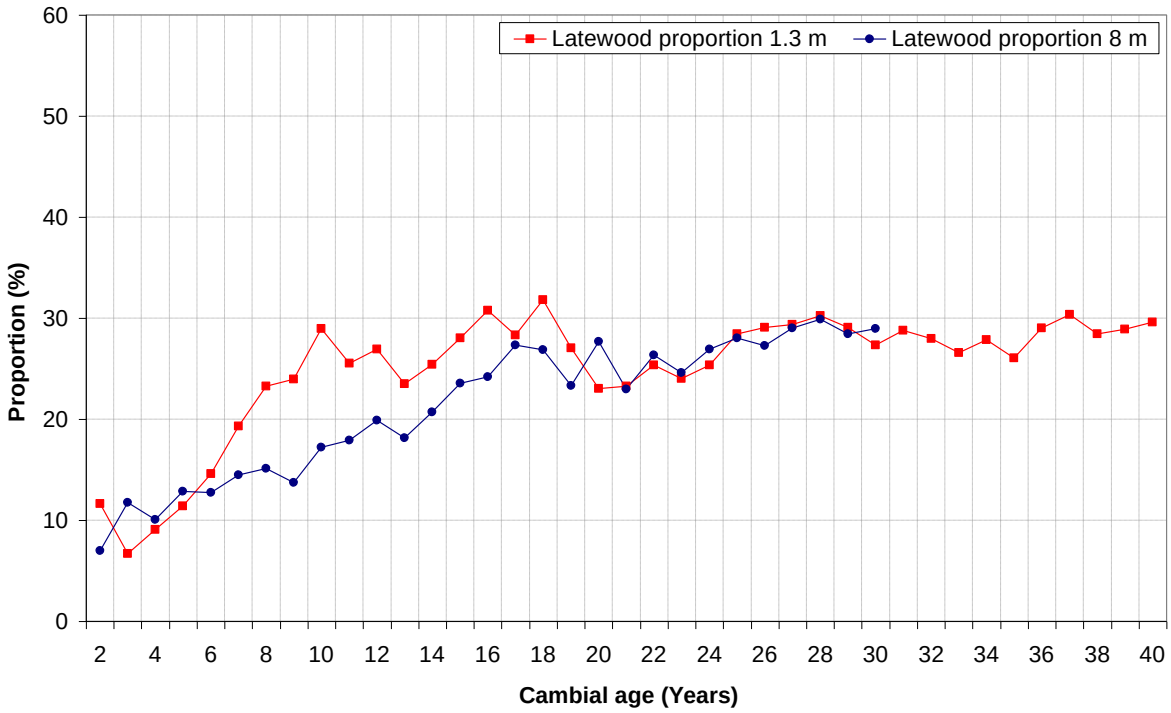

Figure 4-8: Mean latewood proportion as a function of cambial age at stem heights of 1.3 m and 8 m within younger sample trees

4.3.3 Variations in older trees

Figures 4-9 to 4-11 show the changes in mean early, transition and latewood proportions within growth rings at both stem heights in older sample trees. Despite the large variations in ring widths observed for older trees in Figure 4-5, many of the trends described previously in the larger sample of younger trees are repeated. The proportions of latewood seen in the older stems are initially much higher than the mean values for younger trees, the most likely explanation for which is the low growth rate seen in this region. The relationship between growth rate and proportions of wood types is presented in Section 5.2.3. As ring widths increase, a corresponding drop in latewood proportion is observed and while some relatively large inter-ring variations in proportions in all regions of the growth ring are evident, the proportions do show signs of stabilisation in the later years of growth, as noted within the younger trees.

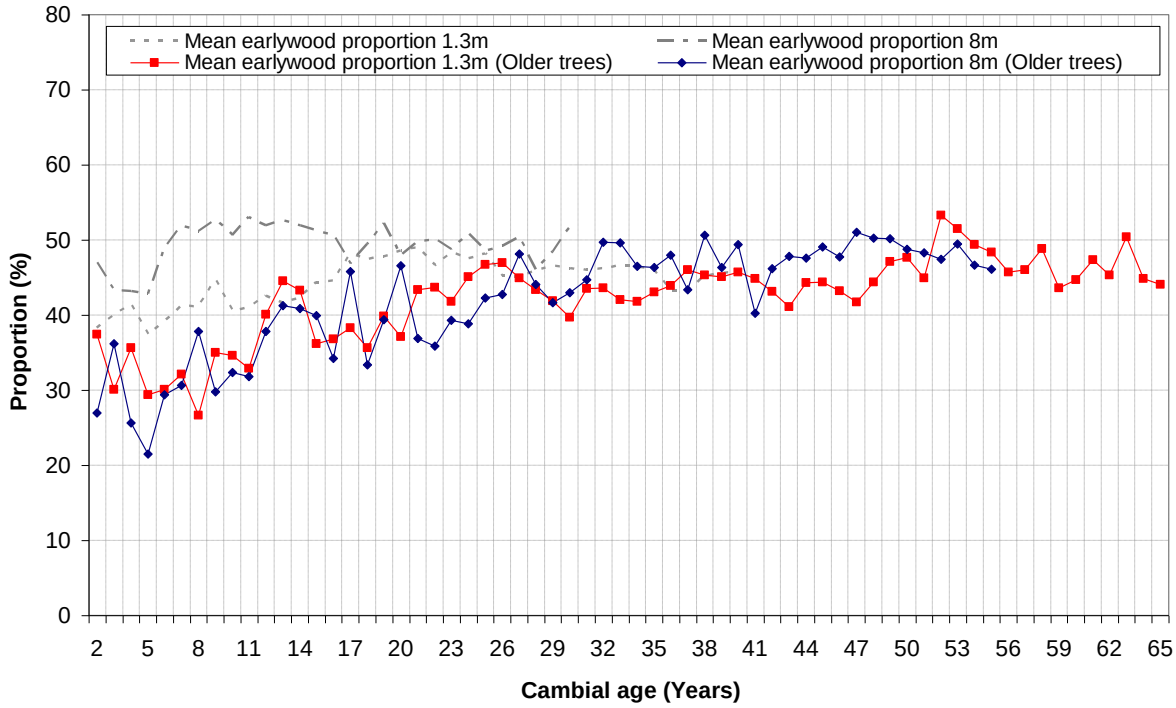

Figure 4-9: Mean earlywood proportion as a function of cambial age at stem heights of 1.3 m and 8 m within older sample trees

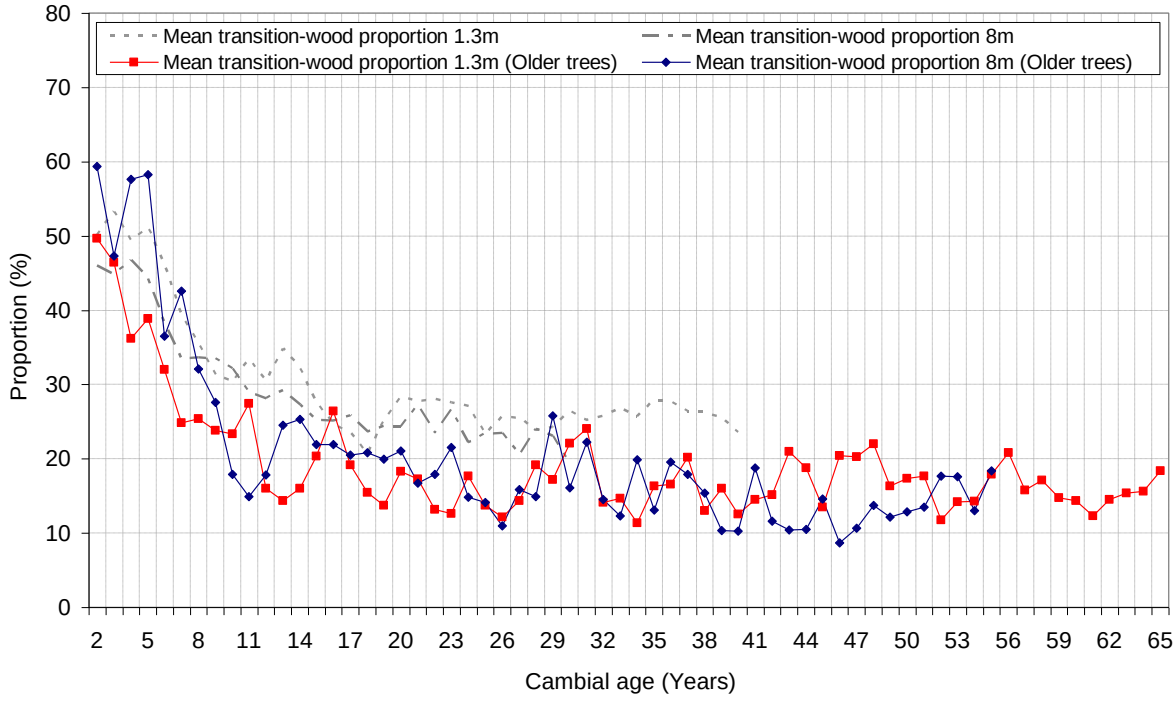

Figure 4-10: Mean transition-wood proportion as a function of cambial age at stem heights of 1.3 m and 8 m within older sample trees

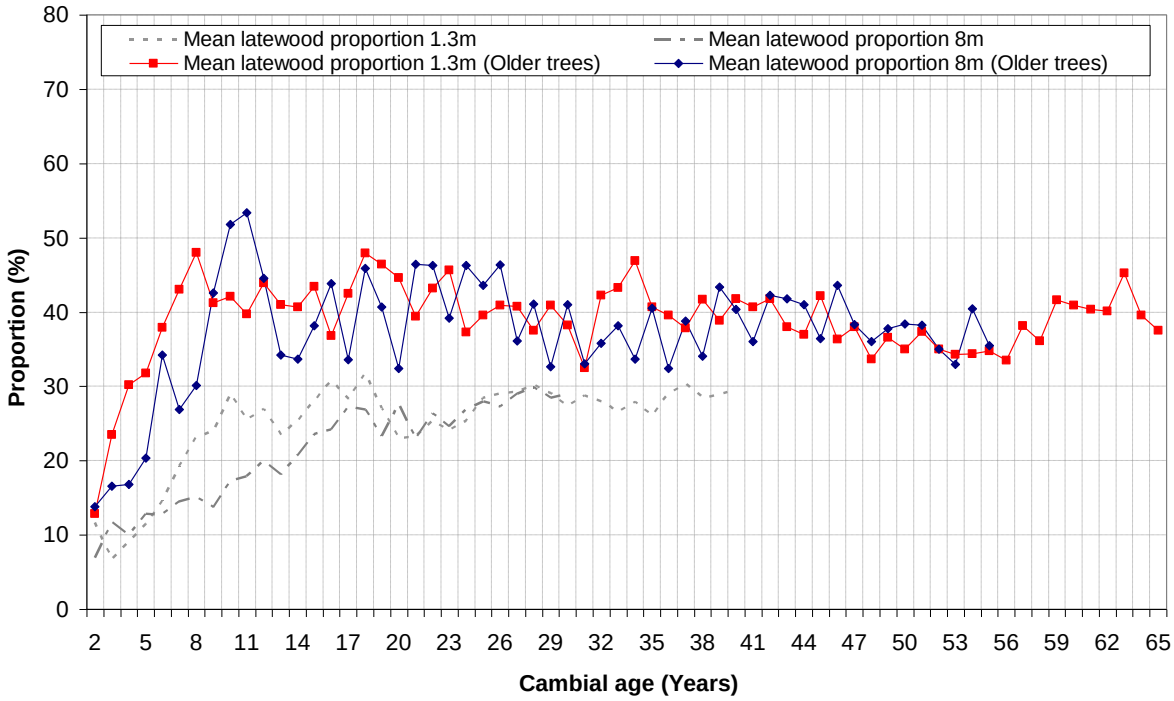

Figure 4-11: Mean latewood proportion as a function of cambial age at stem heights of 1.3 m and 8 m within older sample trees

4.3.4 Discussion of variations in proportions results

Coefficients of variation for the proportion of wood types within a growth ring varied, from approximately 25 % in earlywood to 50 % in transition and latewood. This reflects the different magnitudes of intra-tree variations observed in the three properties. The relationship between growth rate and proportions, that may also account for some of the variation seen due to differences between trees, is investigated further in Section 5.2.3. Mean values and coefficients of variation across all sites were within a similar range for all proportion components, as shown in Tables A-16 to A-18. Consequently the site factor accounted for only a small percentage of the variation in the analysis of variance, lower than 10 % in all cases. Differences due to trees within a site ranged from approximately 5 - 70 %, with the value generally observed to increase in successive growth periods.

It is widely accepted that regardless of methodology used for its determination, the proportion of latewood within a growth ring increases with cambial age, with the largest gains typically observed in the juvenile region of the stem (e.g. Gartner et al., 2002). Although the presence of tracheids with transitional properties is often acknowledged (e.g. Fabris, 2000), they are typically not quantified, despite their use in helping to understand the processes taking place in wood formation and tree development. The profiles presented here show a sharp decrease in

transition-wood and a corresponding increase in latewood proportion on moving away from the pith. This is in disagreement with other Douglas-fir studies (Erickson and Harrison, 1974, Fabris, 2000, Gartner et al., 2002), which showed either a relatively constant increase in latewood proportion from the pith outwards in the juvenile zone, or an initial decrease followed by an increase, both of which slowed upon reaching mature wood. The latewood proportions reported in the mature wood of Douglas-fir are also often higher than those recorded here, typically in the region of 40 % (Fabris, 2000, Gartner et al., 2002, Lachenbruch et al., 2010). The differences in both of these observations can be attributed to the alternative method used here to define the different regions of tracheid development within a growth ring, by inclusion of transition-wood as a separate parameter.

4.4 Radial and tangential tracheid diameter - variations with cambial age and height

4.4.1 Outline

Radial and tangential tracheid diameters were determined utilising the optical imaging functions of the SilviScan-3 system as described in Section 3.5.3.1. In the following sub-sections, the radial profiles of mean values at the two assessed stem heights for whole ring, early, transition and latewood radial and tangential tracheid diameter in 40 - 50 year old trees, and whole ring mean values in trees with ages > 50 years are presented, and the results discussed.

4.4.2 Variations in younger trees

4.4.2.1 Radial diameters

Descriptive statistics for radial tracheid diameter results, alongside the results of the analysis of variance and t-tests can be found in Tables A-19 to A-26. Whole ring radial tracheid diameters shown in Figure 4-12, displayed large increases in the growth rings immediately adjacent to the pith at both sample heights, increasing from initial mean values of 25 μm, reaching a maximum of approximately 31 μm and 33 μm at 1.3 m and 8 m respectively. Thereafter, year to year variations in mean diameters were observed, however values remained relatively stable with increasing cambial age. These observations were confirmed by the analysis of variance results, which showed that at both stem heights there was no statistically significant difference in the whole ring radial diameter within any growth period, beyond 2 - 10 years of age. Results of the t-tests also showed that the greater radial diameters seen at 8 m in the stem were statistically significant in all three growth periods compared. The sharp increase in whole ring mean radial diameter observed in the 2 - 10 year growth period appears to be largely due to an increase in the radial diameter of tracheids in the earlywood region of the growth ring shown in Figure 4-13. During the same period, transition-wood (Figure 4-14) exhibited a similar but reduced increase, whilst only small changes in latewood (Figure 4-15) radial diameter were observed.

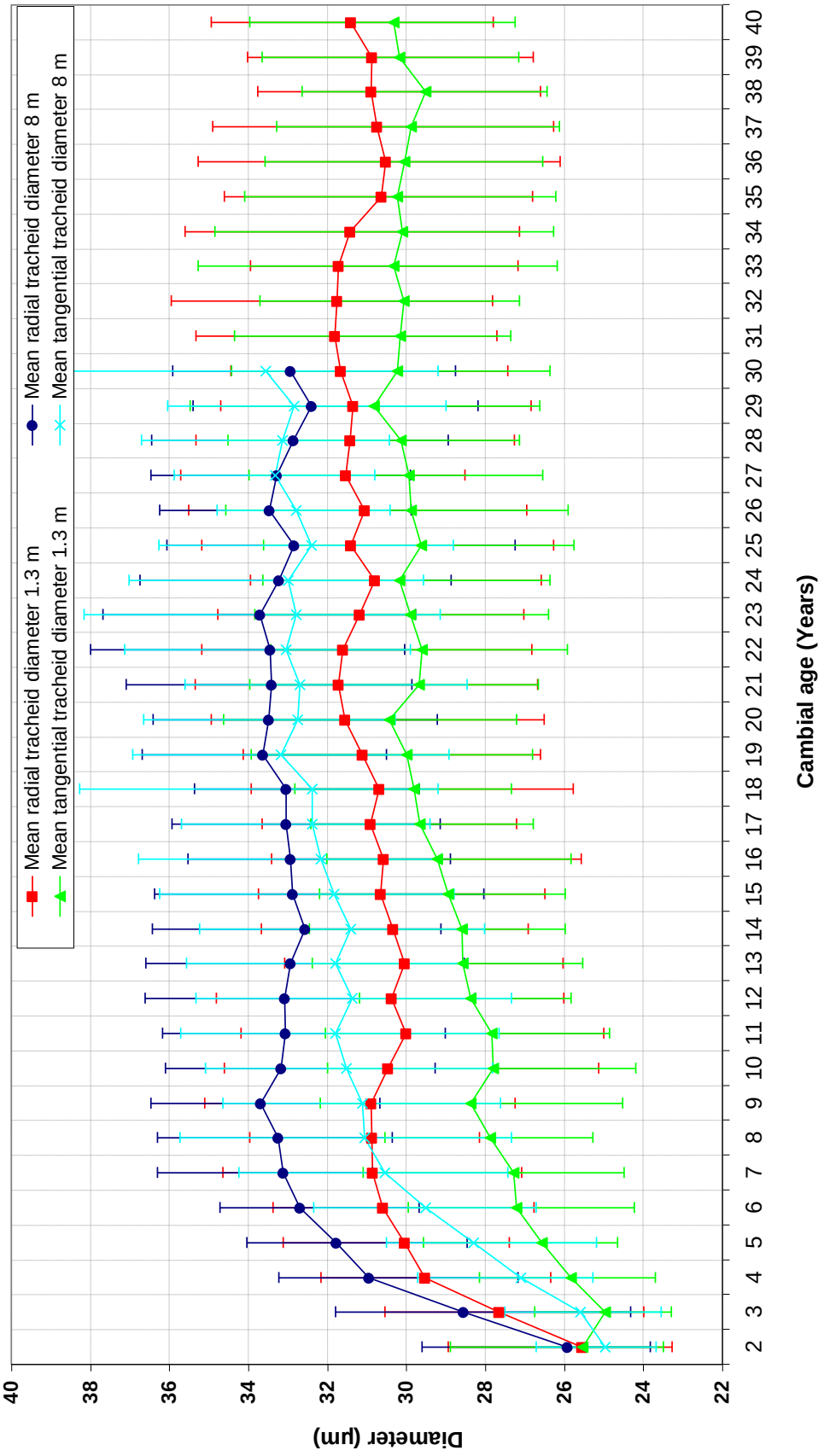

Figure 4-12: Mean whole ring radial and tangential tracheid diameters and 95th percentile range as a function of cambial age at stem heights of 1.3 m and 8 m in younger trees

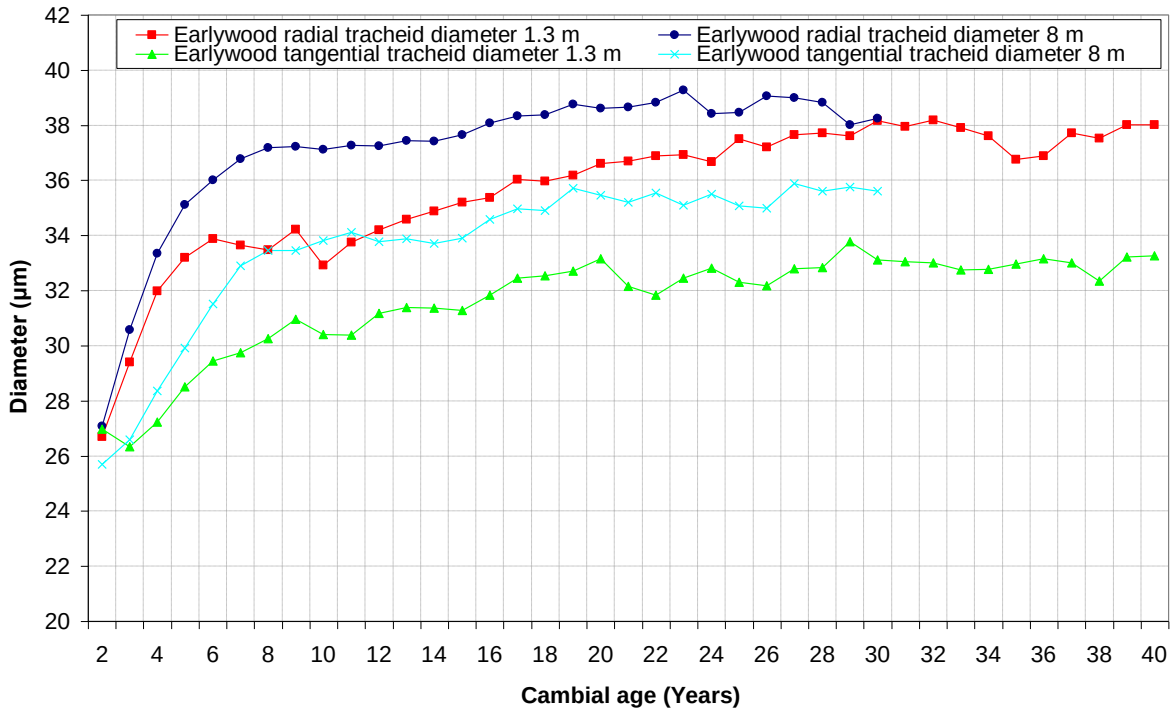

Figure 4-13: Mean earlywood radial and tangential tracheid diameters as a function of cambial age at stem heights of 1.3 m and 8 m in younger trees

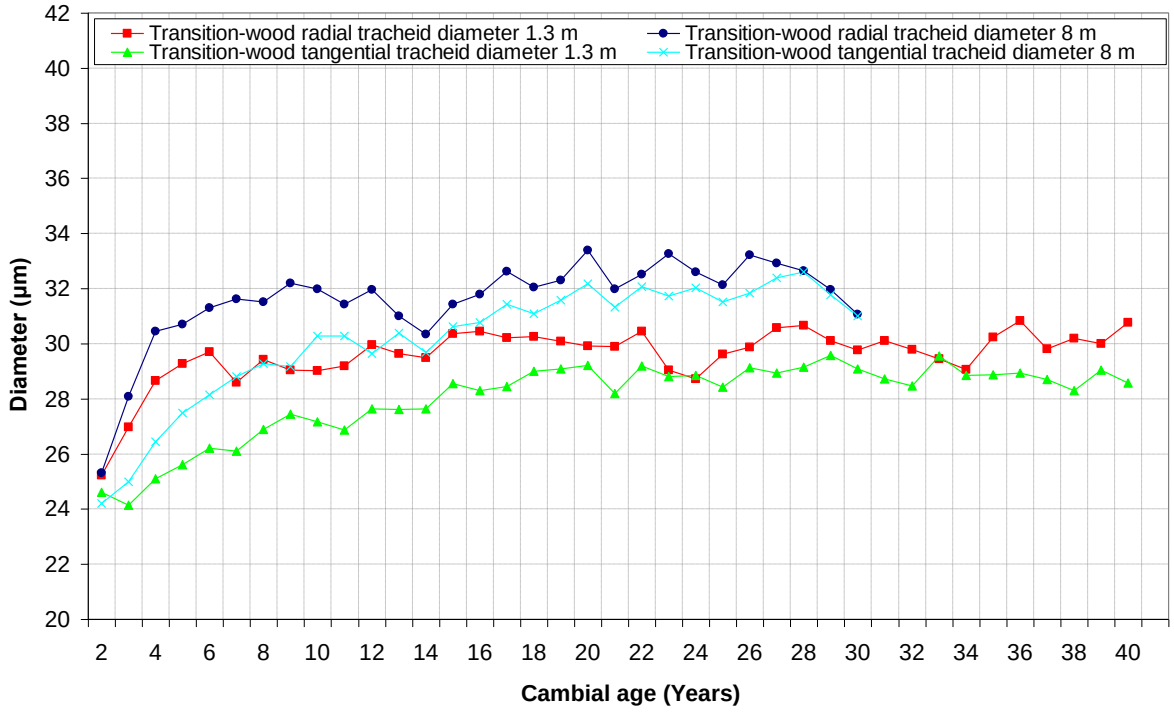

Figure 4-14: Mean transition-wood radial and tangential tracheid diameters as a function of cambial age at stem heights of 1.3 m and 8 m in younger trees

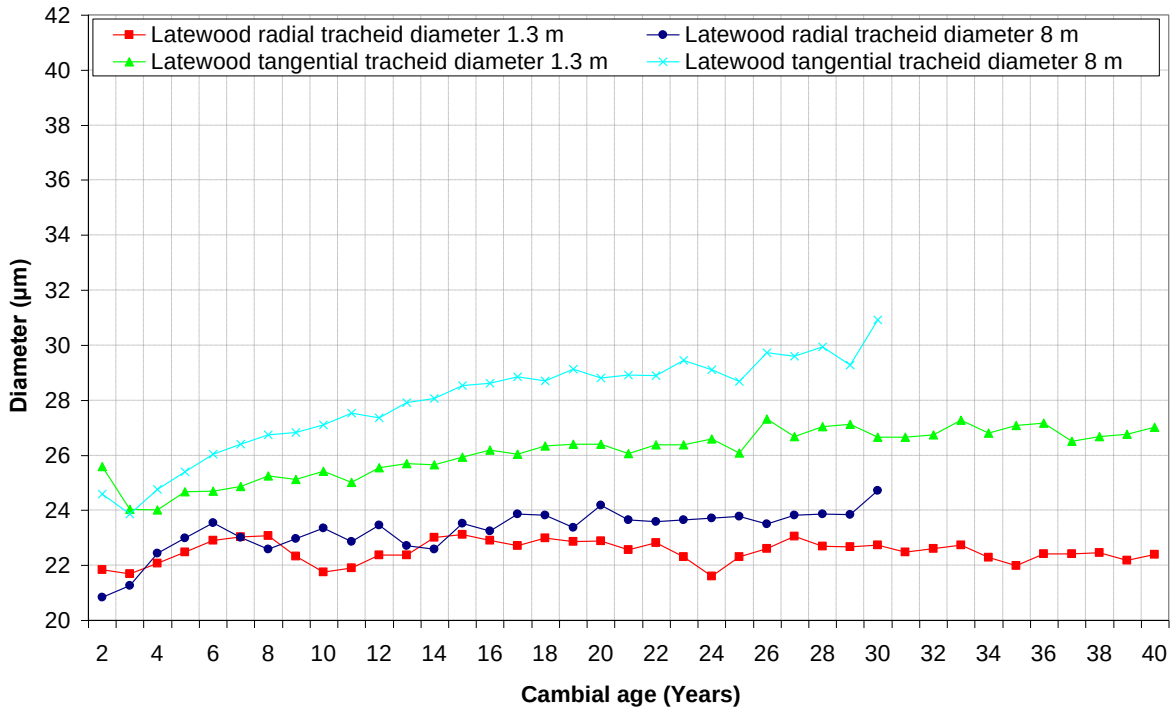

Figure 4-15: Mean latewood radial and tangential tracheid diameters as a function of cambial age at stem heights of 1.3 m and 8 m in younger trees

During the first growth period, the analysis of variance showed decreasing F values with cambial age on moving from early to latewood, as the diameter variation across the growth period remained similar on moving from early to latewood the decreasing F values are a sign of less distinction between the means for each cambial age, in agreement with the observed results. Values were statistically significant within early and transition wood. Beyond the first 10 years of growth similar trends continued, with statistically significant increases in the radial diameter of earlywood tracheids occurring at both stem heights, whilst transition and latewood tracheids were found to show only limited, and in many cases non-significant changes in diameter with cambial age. By the time the final growth period was reached at each stem height, the analysis of variance showed no significant change in tracheid radial diameters with cambial age in any part of the growth ring. In virtually all cases the results of the t-test confirmed that mean diameters higher in the stem were statistically significantly greater than those observed at breast height. It appears that the continued increase observed in the radial diameter of earlywood tracheids was in part offset by increases in the proportion of latewood tracheids shown in Section 4.3 over a similar time period. As a result of this no corresponding increase in whole ring mean diameters was seen.

4.4.2.2 Tangential diameters

Descriptive statistics for tangential tracheid diameter results, alongside the results of the analysis of variance and t-tests can be found in Tables A-28 to A-35. The mean whole ring tangential tracheid diameter (Figure 4-12) was found to exhibit similar trends to those seen in the radial direction. A sharp initial rise in diameter upon moving away from the pith at both heights was followed by a more gradual increase in values beyond a cambial age of eight until approximately 20 years of age, after which time the increase in diameters stabilised. The findings of the analysis of variance confirm this, with statistically significant differences in diameter with cambial age during the first two growth periods at each stem height, and non-significant results thereafter. As with radial results, increases in the tangential diameter near the pith were largest in earlywood tracheids (Figure 4-13), with transition-wood (Figure 4-14) and latewood (Figure 4-15) undergoing statistically significant but reduced increases, in most cases continuing until the penultimate growth period at each height, at which point values appear to stabilise. On transitioning from early to latewood, mean radial diameter displayed a decrease of approximately 40 %, with changes of about half this amount observed in the tangential direction. As a result of this, the ratio between tangential and radial diameters decreased from approximately 1.15 in earlywood, to 0.85 in latewood.

4.4.3 Variations in older trees

Figures 4-16 and 4-17 show the developmental profiles of whole ring mean radial and tangential tracheid diameters in older sample trees. The influence of the unusual ring width patterns identified previously in the early years of growth are apparent, particularly so in the radial direction where the suppressed growth appears to have limited the radial expansion of the tracheids. However, in later years of growth increases in diameter were observed, with values eventually appearing to begin to stabilise, which is in good agreement with the findings presented previously for younger trees.

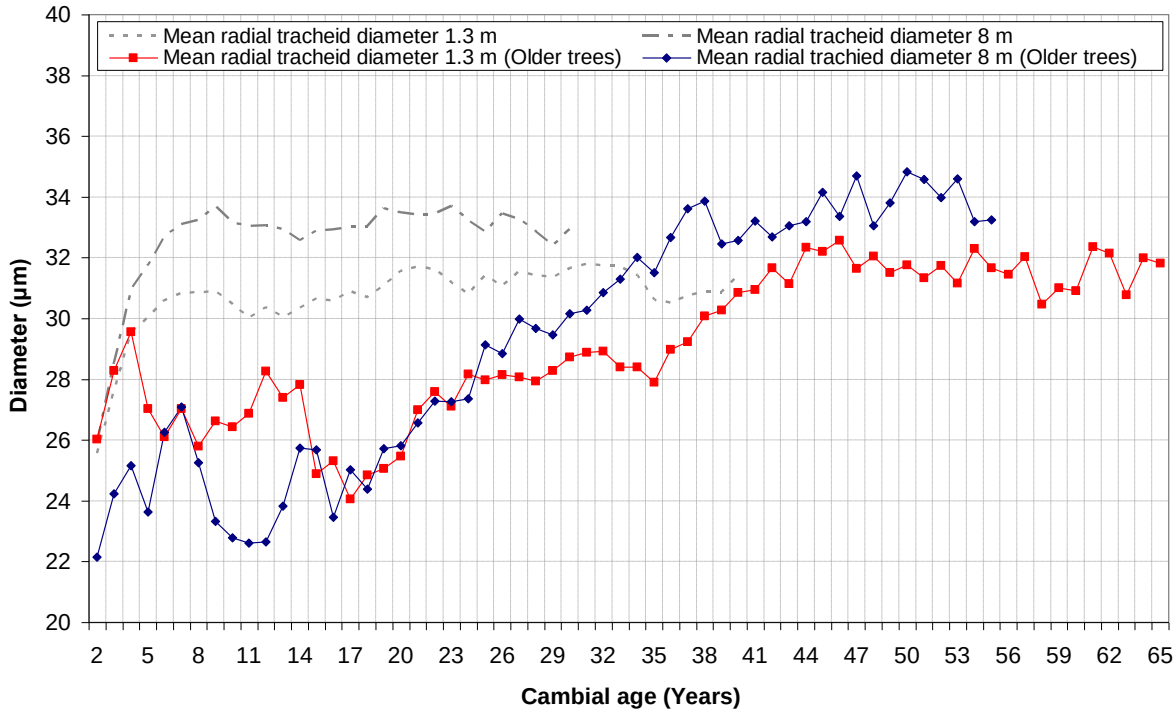

Figure 4-16: Mean whole ring radial tracheid diameters as a function of cambial age at stem heights of 1.3 m and 8 m within older sample trees

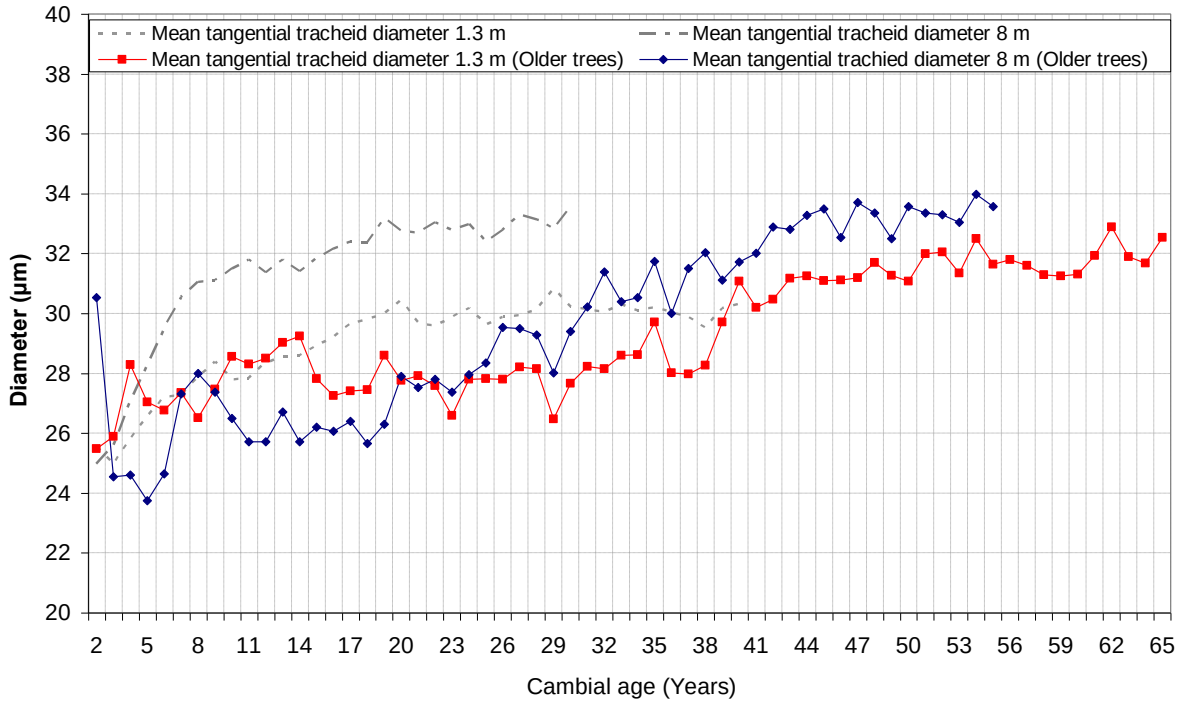

Figure 4-17: Mean whole ring tangential tracheid diameters as a function of cambial age at stem heights of 1.3 m and 8 m within older sample trees

4.4.4 Discussion of variations in tracheid diameter results

Coefficients of variation for radial and tangential tracheid diameter at all positions within the growth ring at the two sampling heights were typically less than 10 %. Values were lower than those seen previously for ring width and proportions, most likely as a result of the limited intra-tree variations observed in tracheid diameters. Mean values and coefficients of variation across all sites were within a similar range at the whole ring level, as shown in Table A-27 and A-36. Consequently, as was observed in the previous sub-sections, the site factor accounted for only a small percentage of the variation in the analysis of variance, with differences due to trees within a site ranging from approximately 10 - 70 %, typically increasing with age.

Difficulties in measuring the dimensions of tracheids in the latewood region of the growth ring using manual optical methods, alongside the often primary desire to obtain dimension in the sap conducting earlywood for hydraulic modelling, have led to relatively little information being available regarding intra- and inter-ring profiles of tracheid dimensions in Douglas-fir. The tracheids investigated in the study undertaken by Erickson and Harrison (1974) were described as 'late early wood' taken from breast height, which would most likely place them within the transition-wood zone in this study. The dimensions recorded adjacent to the pith in both radial and tangential directions by Erickson and Harrison are broadly similar to those reported here, however subsequent increases in size and the values at which dimensions became stable, were far sharper than those found in the transition-wood in the current study and places them at the top end of the variation found amongst the earlywood tracheids. This may be due to different growing conditions of the trees or the point on the tracheid that was measured, with dimensions having been shown to vary along a tracheids length due to tapering at its ends (Smith, 1967). Rathgeber et al (2006) reported intra-growth ring changes in tracheid diameter in Douglas-fir, showing similar findings to those presented here. The change in ratio between tangential and radial diameters on moving from early to latewood reported by Rathgeber was greater than that observed here, however the study was limited to only one tree. A study of earlywood tracheid lumen diameters in Douglas-fir conducted by Spicer and Gartner (2001) showed increasing size with height for the same cambial age, however no further data was found regarding longitudinal variations in Douglas-fir stems. The general trends of increasing tracheid diameters from the pith outwards slowing with increasing age, as well as intra-ring variations and differences observed between radial and tangential directions reported here are in general agreement with results reported in Sitka spruce (Denne, 1973), Radiata and Loblolly pine (Burdon et al., 2004) and Norway spruce (Brandstrom, 2001, Molteberg and Høibø, 2006, 2007).

4.5 Tracheid radial wall thickness - variations with cambial age and height

4.5.1 Outline

The radial wall thicknesses of tracheids (herein referred to as wall thickness), was determined utilising the x-ray densitometry functions of the SilviScan-3 system as described in Section 3.5.3.2. In the following sub-sections, the radial profiles of mean values at the two assessed stem heights for whole ring, early, transition and latewood wall thicknesses in 40 - 50 year old trees, and whole ring mean values in trees with ages > 50 years are presented, and the results discussed.

4.5.2 Variations in younger trees

4.5.2.1 Whole ring tracheid radial wall thickness

Figure 4-18 shows mean values and the 95th percentile range for whole ring wall thickness at the two assessed stem heights, descriptive statistics alongside the results of the analysis of variance and t-tests can be found in Tables A-37 and A-38. On moving outwards from the pith, the mean whole ring wall thickness was found to exhibit an overall trend of rising values with increasing cambial age. Between the first and last growth rings assessed, increases of 35 % and 45 % were observed at 1.3 m and 8 m respectively, following a similar starting value of 2.25 μm adjacent to the pith. Between 2 - 10 years of age at breast height, the limited variability in wall thickness between growth rings resulted in there being no statistically significant impact of cambial age observed in the analysis of variance. During the same growth period, the slight increases at the 8 m sampling location were found to be statistically significant. In all subsequent growth periods, mean wall thickness showed an increase between start and finish at both sample heights and the results returned by the analysis of variance showed a statistically significant difference between mean values with cambial age. The increases observed at the 8 m sampling location occurred at a slightly greater rate than those at breast height; consequently mean values higher in the stem were greater than those seen at 1.3 m. This observation was confirmed by the results of the t-tests, which showed a statistically significant difference between the means at the two heights in all growth periods compared.

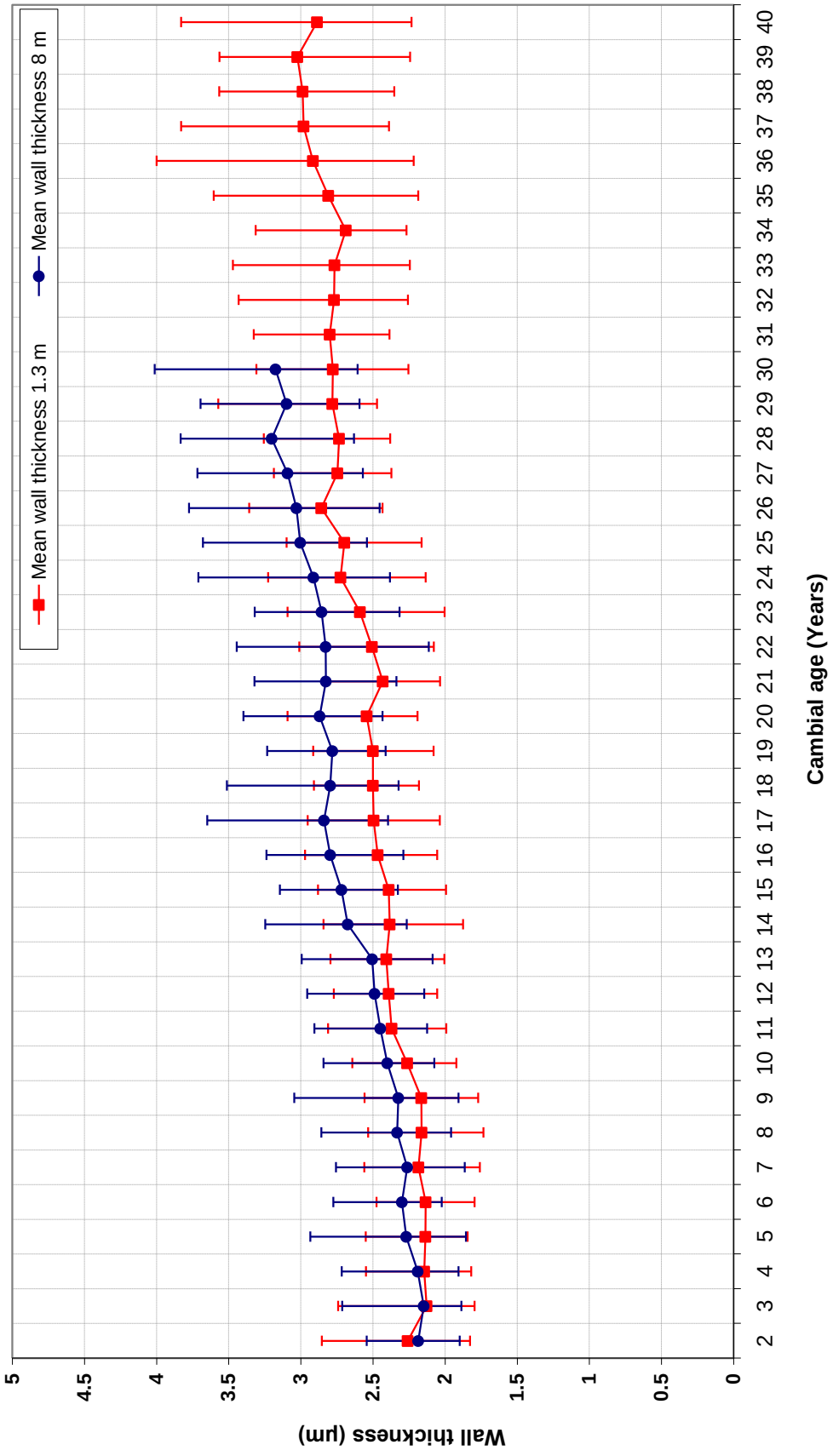

Figure 4-18: Mean whole ring tracheid radial wall thickness and 95th percentile range as a function of cambial age at stem heights of 1.3 m and 8 m within younger sample trees

4.5.2.2 Earlywood tracheid radial wall thickness

Figure 4-19 shows mean values for earlywood wall thickness at the two assessed stem heights, descriptive statistics alongside the results of the analysis of variance and t-tests can be found in Tables A-39 and A-40. From starting values of 1.8 - 1.9 µm adjacent to the pith, earlywood wall thickness exhibited an initial decrease during the 2 - 10 year growth period, greatest at the 1.3 m sampling height, resulting in statistically significant results in the analysis of variance. This was followed by a period of gradual increases in wall thickness, with values appearing to stabilise in the final growth period at each stem height. These observed trends were reflected in the magnitude of F values and their significances achieved in the analysis of variance. The overall increases in mean values between the first and last growth period were however small, at approximately 10 %. The increase occurred at a slightly greater rate at breast height, however the smaller decrease in wall thickness observed in rings of younger cambial ages higher in the stem, resulted in earlywood mean wall thickness being shown to be statistically significantly greater at 8 m than at breast height in the results of the t-tests across all growth periods compared. The differences in mean values were however small.

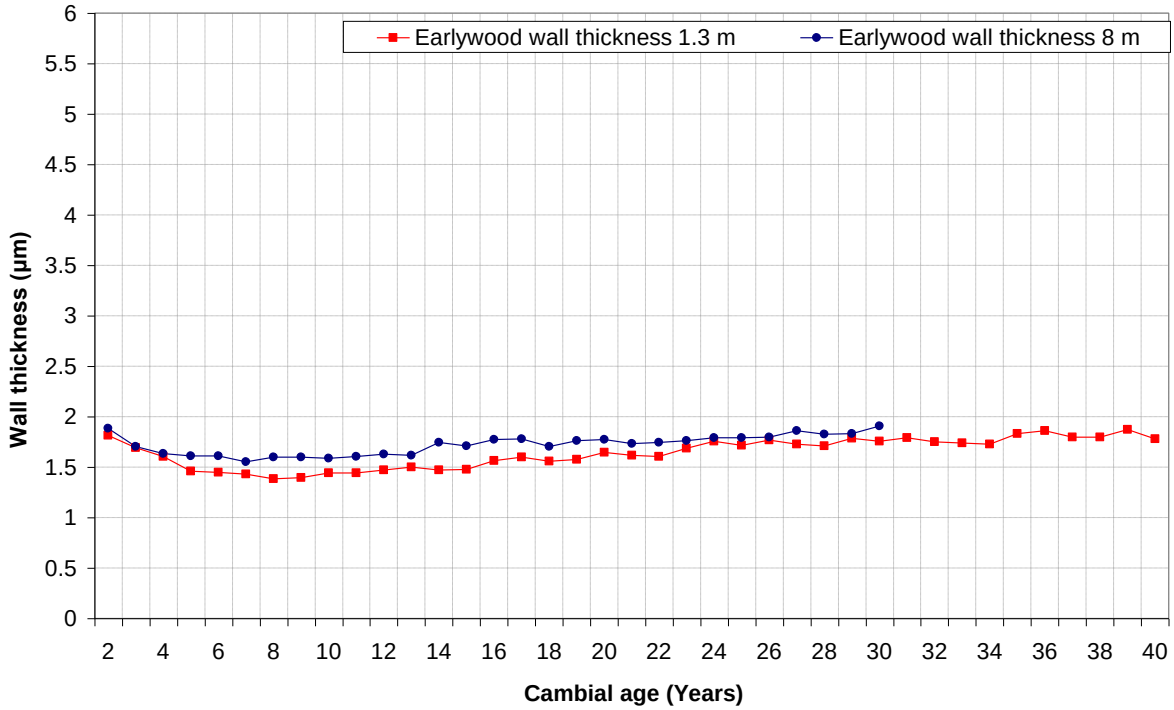

Figure 4-19: Mean earlywood tracheid radial wall thickness as a function of cambial age at stem heights of 1.3 m and 8 m within younger sample trees

4.5.2.3 Transition and latewood tracheid radial wall thickness

Figures 4-20 and 4-21 show mean values for transition and latewood wall thicknesses at the two assessed stem heights, descriptive statistics alongside the results of the analysis of variance and t-tests can be found in Tables A-41 to A-44. The radial profiles of transition and latewood wall thicknesses showed similar trends at both sampling locations within the stem. On moving from the pith to the bark wall thicknesses increased, with all but the first growth period at 1.3 m showing statistically significant differences with cambial age in the results of the analysis of variance. Increases in the mean wall thicknesses between the first and last growth periods assessed at breast height were approximately 30 % in both transition and latewood, with the rates of increase higher in the stem slightly greater. Given the similar wall thicknesses in the growth rings nearest the pith at both stem heights, this resulted in t-tests showing a statistically significant difference in the mean values between 1.3 m and 8 m in all growth periods compared in both transition and latewood.

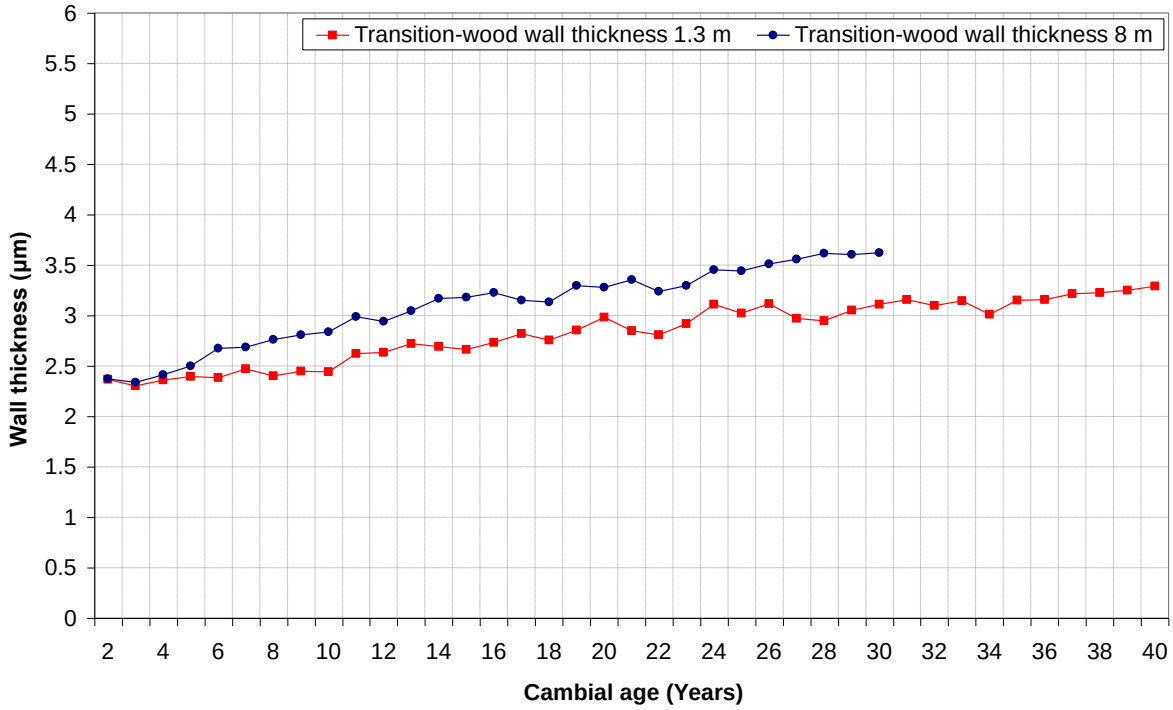

Figure 4-20: Mean transition-wood tracheid radial wall thickness as a function of cambial age at stem heights of 1.3 m and 8 m within younger sample trees

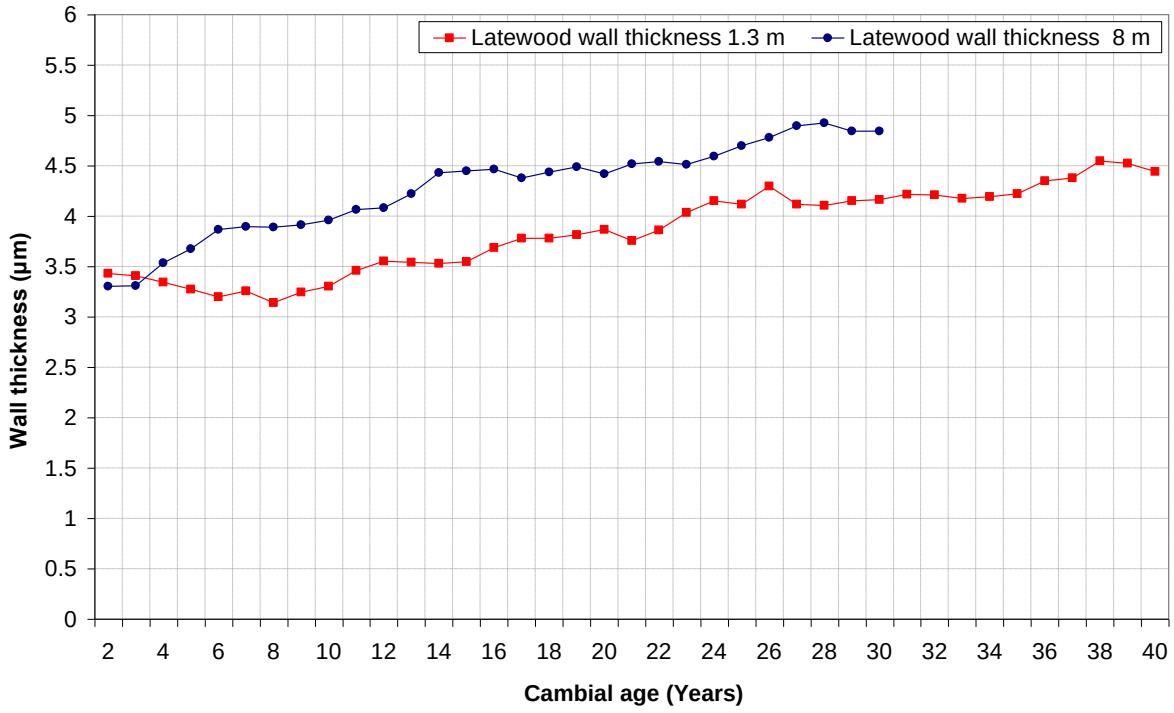

Figure 4-21: Mean latewood tracheid radial wall thickness as a function of cambial age at stem heights of 1.3 m and 8 m within younger sample trees

4.5.3 Variations in older trees

Figure 4-22 shows the developmental profile of mean whole ring tracheid wall thickness in the older sample trees. The suppressed growth identified in Figure 4-5 at young cambial ages appears to have resulted in a sharper increase in mean wall thickness than was observed in the younger stems. However, it also appears that with the exception of inter-ring variations, that tracheid wall thickness stabilises from a cambial age of approximately 20 years at both stem heights, with values remaining relatively constant beyond. The mean wall thicknesses observed were higher than those seen within the sample of younger trees.

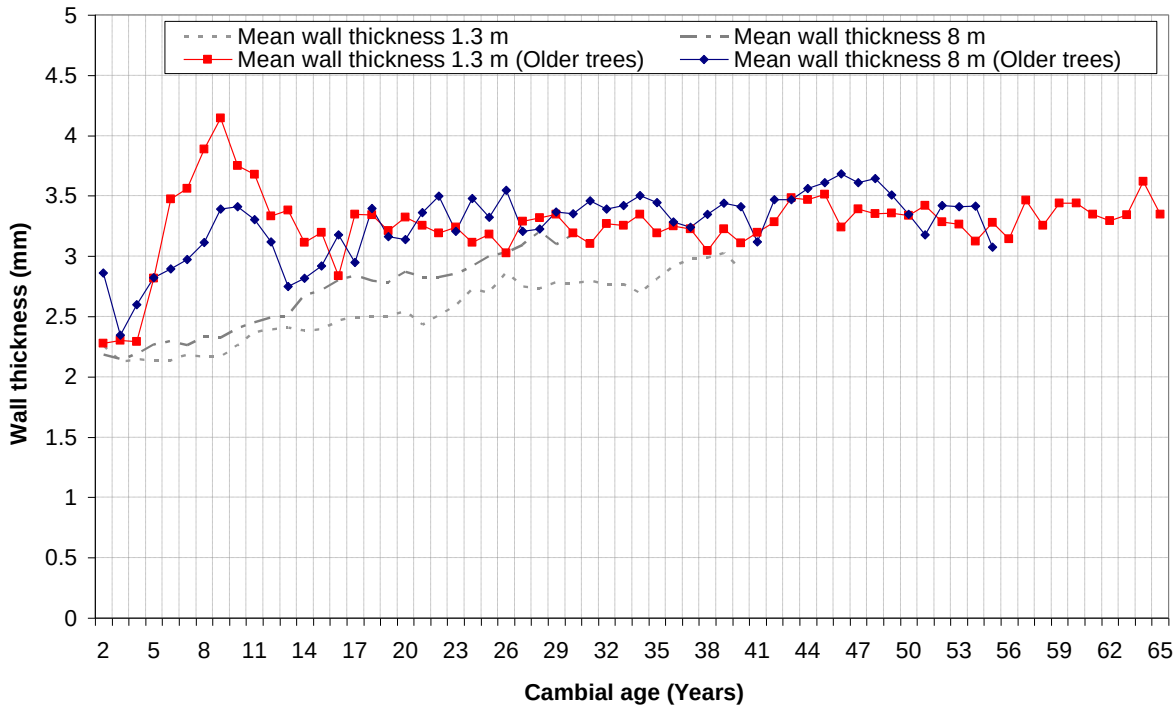

Figure 4-22: Mean whole ring tracheid radial wall thickness as a function of cambial age at stem heights of 1.3 m and 8 m within older sample trees

4.5.4 Discussion of variations in radial wall thickness results

The coefficients of variation for wall thickness were of the order of 15 % at all sampling locations, in line with those seen previously for tracheid diameters and substantially less than the variations found for ring widths and proportions. This is likely due to the comparatively smaller changes seen in wall thickness within each growth period, with relationships to changes in growth rate, to be assessed in Section 5.2.5, also a contributing factor to the low values. Mean values and coefficients of variation across all sites were within a similar range at the whole ring level, as shown in Table A-45. Consequently, as was observed in the previous sub-sections, the site factor accounted for only a small percentage of the variation in the analysis of variance. Differences due to trees within sites typically accounted for between 30 - 60 % of variation, with the values increasing as variation due to cambial age fell.

Difficulties associated with determining the accuracy of the SilviScan-3 system predictions of tracheid cell wall thickness were discussed in Section 3.5.3.2. As such, there is the potential that some of the results presented and compared here where the differences in values are small, such as between the two stem heights within earlywood, may fall within the margin of error of the predictions. However, as the number of specimens tested was relatively high, and

the variations between them low, the overall radial and longitudinal trends can be reported with confidence.

In the results presented here, mean wall thickness was observed to increase by approximately 140 % at the intra-growth ring level at both stem heights, with increases being relatively evenly distributed between early to transition-wood and transition to latewood tracheids. Relatively few studies have been conducted assessing the development of tracheid wall thickness within Douglas-fir stems. Quirk (1984) utilised optical methods to measure the mean wall thickness around a tracheid, with no differentiation of direction. Results were reported in the form of tracheid wall area, however from the equations presented for the derivation of wall area it is possible to obtain wall thickness data. The results found showed that wall thickness and its variation on transitioning from early to latewood fit within the range of results presented here, although neither the age of the tracheids measured nor their position within the stem is stated, meaning direct comparisons are not possible. In the limited study conducted by Rathgeber et al. (2006), variations in both radial and tangential wall thickness determined optically were presented. The results showed that in the radial direction, cell wall thickness increased by 110 % on moving from early to latewood, in good agreement with the values reported here. The thicknesses reported were 3.2 μm in earlywood and 6.8 μm in latewood, higher than those reported here, however the analysis was conducted on only one tree. Similar radial developmental profiles for wall thickness development have been observed in other coniferous species such as Sitka and Norway spruce (Denne, 1973, Brandstrom, 2001).

4.6 Density - variations with cambial age and height

4.6.1 Outline

Specimen density was determined utilising the x-ray densitometry functions of the SilviScan-3 system as described in Section 3.5.3.2. In the following sub-sections, the radial profiles of mean values at the two assessed stem heights for whole ring, early, transition and latewood density in 40 - 50 year old trees, and whole ring mean values in trees with ages > 50 years are presented, and the results discussed.

4.6.2 Variations in younger trees

4.6.2.1 Whole ring density

Figure 4-23 shows mean values and the 95th percentile range for whole ring density at the two assessed stem heights, descriptive statistics alongside the results of the analysis of variance and t-tests can be found in Tables A-46 and A-47. A similar pattern of whole ring mean density development on moving outwards from the pith was displayed at both stem heights. Following mean starting values of approximately 475 kg/m^3 in the second growth ring, a decline in values reaching a minimum in the seventh to eighth rings was observed. An overall trend of increasing values was displayed thereafter at both stem heights. In later growth rings, the rate of increase in density appeared to reduce, particularly at 8 m, however the repeated measures analysis showed significant variations with respect to cambial age in all growth periods. As a result of the observed trends, mean density values showed a 20 % increase between the first and last growth periods, with final values of 536 kg/m^3 and 519 kg/m^3 at 1.3 m and 8 m respectively. Some small differences in mean values with stem height were noted, with t-test results showing statistically significant positive t values during the first growth period, becoming significantly negative in the third.

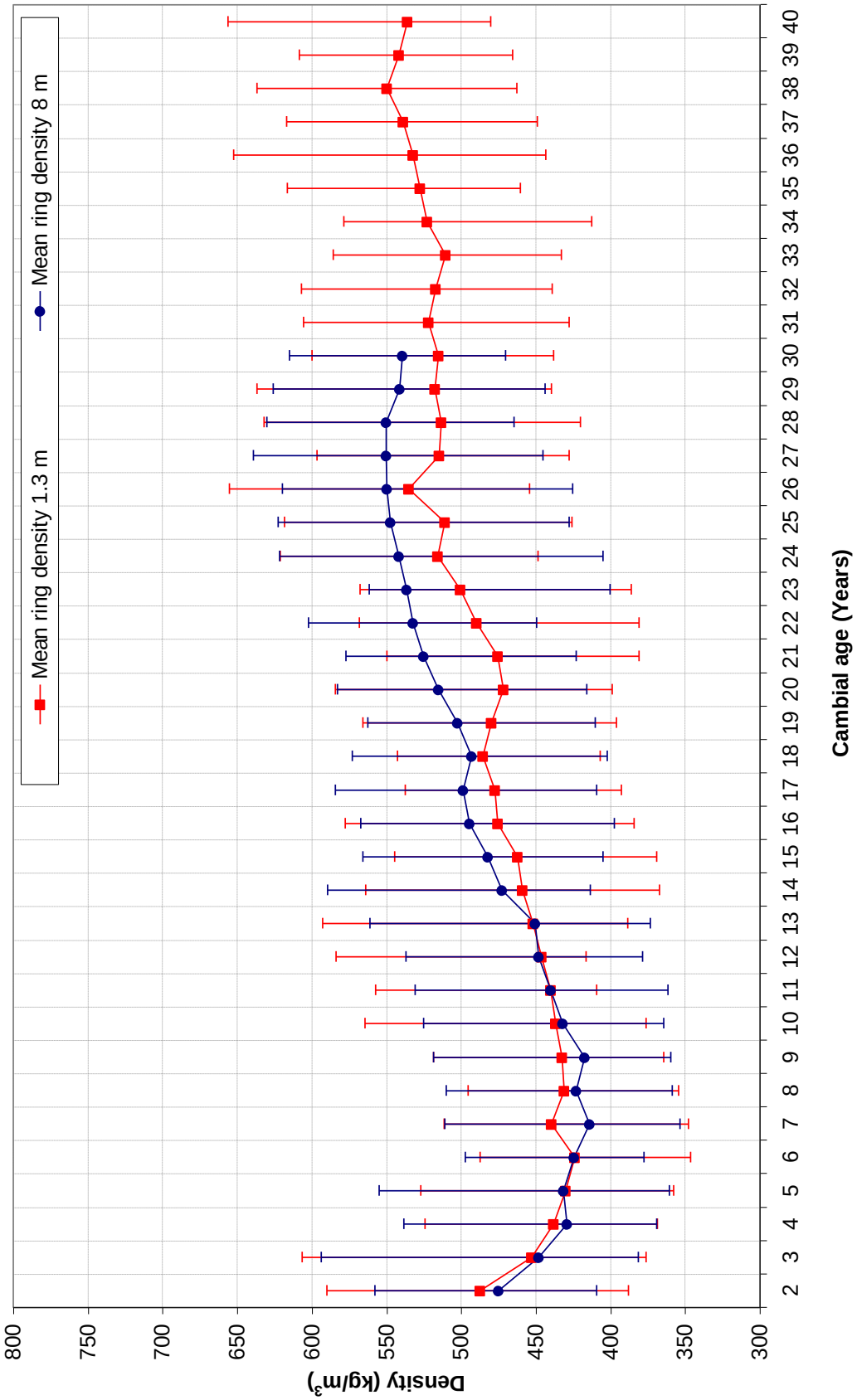

Figure 4-23: Mean whole ring density and 95th percentile range as a function of cambial age at stem heights of 1.3 m and 8 m within younger sample trees

4.6.2.2 Earlywood density

Figure 4-24 shows mean values for earlywood density at the two assessed stem heights, descriptive statistics alongside the results of the analysis of variance and t-tests can be found in Tables A-48 and A-49. The maximum mean earlywood density observed at both stem heights occurred in the second growth ring. With increasing distance from the pith a decline in earlywood density occurred, ceasing in the region of the tenth growth ring. Beyond this, a constant gentle increase continued with time for all remaining growth periods, with low and often non-significant F values for variations with respect to cambial age in the analysis of variance. Earlywood density profiles and values at both stem heights matched well, with no statistically significant difference between means at 1.3 m and 8 m for any growth period compared. The mean earlywood density beyond 10 years of age was in the region of 270 kg/m^3.

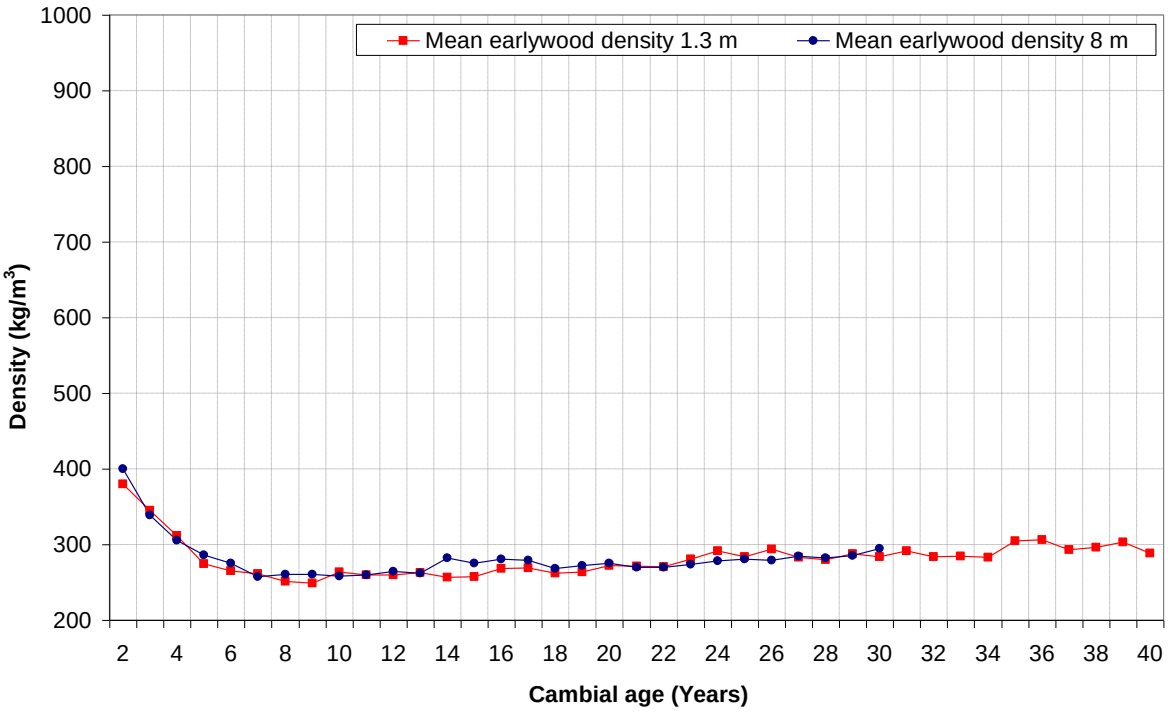

Figure 4-24: Mean earlywood density as a function of cambial age at stem heights of 1.3 m and 8 m within younger sample trees

4.6.2.3 Transition-wood density

Figure 4-25 shows mean values for transition-wood density at the two assessed stem heights, descriptive statistics alongside the results of the analysis of variance and t-tests can be found in Tables A-50 and A-51. As with earlywood, transition-wood mean density displayed a decrease in magnitude in the growth rings immediately adjacent to the pith. The decrease was however

much gentler than that seen for earlywood and ceased by rings six to seven. Following this a steady, moderate, increase was observed in all subsequent growth periods at both stem heights. Due to the moderate rate of the increase and the relatively large within ring variations, the analysis of variance showed several non-significant results with cambial age. Between the first and the last growth period at each stem height the increase in mean density was in the region of 20 %, with mean transition-wood densities of 579 kg/m^3 and 595 kg/m^3 in the final growth period at 1.3 m and 8 m respectively. With the exception of the 2 - 10 year growth period, mean values at 8 m were statistically significantly higher than those at breast height, as shown by the results of the t-tests, the differences in means were however small at approximately 10 kg/m^3.

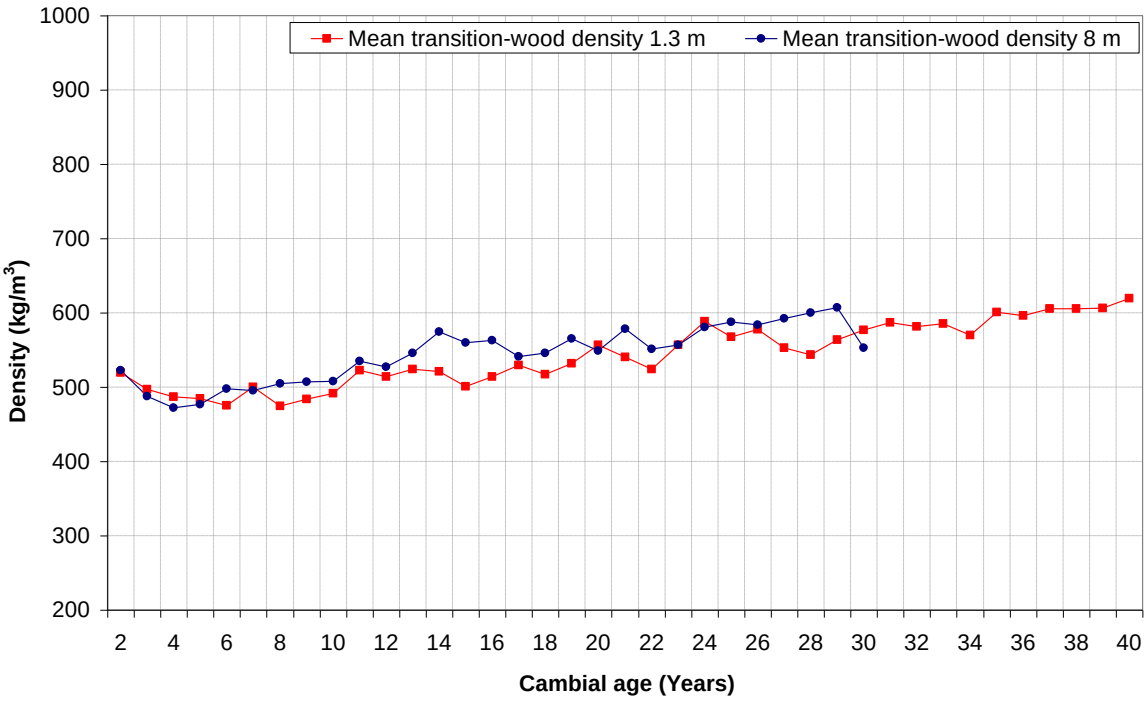

Figure 4-25: Mean transition-wood density as a function of cambial age at stem heights of 1.3 m and 8 m within younger sample trees

4.6.2.4 Latewood density

Figure 4-26 shows mean values for latewood density at the two assessed stem heights, descriptive statistics alongside the results of the analysis of variance and t-tests can be found in Tables A-52 and A-53. Profiles of latewood density development in the growth rings immediately adjacent to the pith were markedly different at the two longitudinal positions. At 8 m latewood density showed a steady increase in magnitude throughout the 2 - 10 year growth period. However, as was observed in both early and to a lesser extent transition-wood, a sharp decline was displayed at 1.3 m, ceasing at a cambial age of eight, after which an

immediate increase in values was displayed. This increase, and that seen at 8 m, was found to continue in all subsequent growth periods. As a result, cambial age appeared as a significant factor in the analysis of variance in all age groups. During the period in which density was seen to increase, rates of change at both stem heights were similar, with approximately 20 % rise in mean latewood density being observed from the first to the last growth period, reaching a mean of 878 kg/m^3 and 888 kg/m^3 at 1.3 m and 8 m respectively. As a result of the sharp decrease in values seen at young cambial ages at 1.3 m, t-test results showed that latewood density was statistically significantly greater at 8 m in all growth periods compared. With reference to the whole ring density profile, it is evident that the initial decrease in values that was observed is largely a result of decreases in earlywood density, with declines in latewood density contributing to a lesser extent due to the lower latewood proportion in this region, as shown in Figure 4-8. Subsequent increases in density are a result of increasing transition and latewood densities and the increase in latewood proportion observed with increasing cambial age.

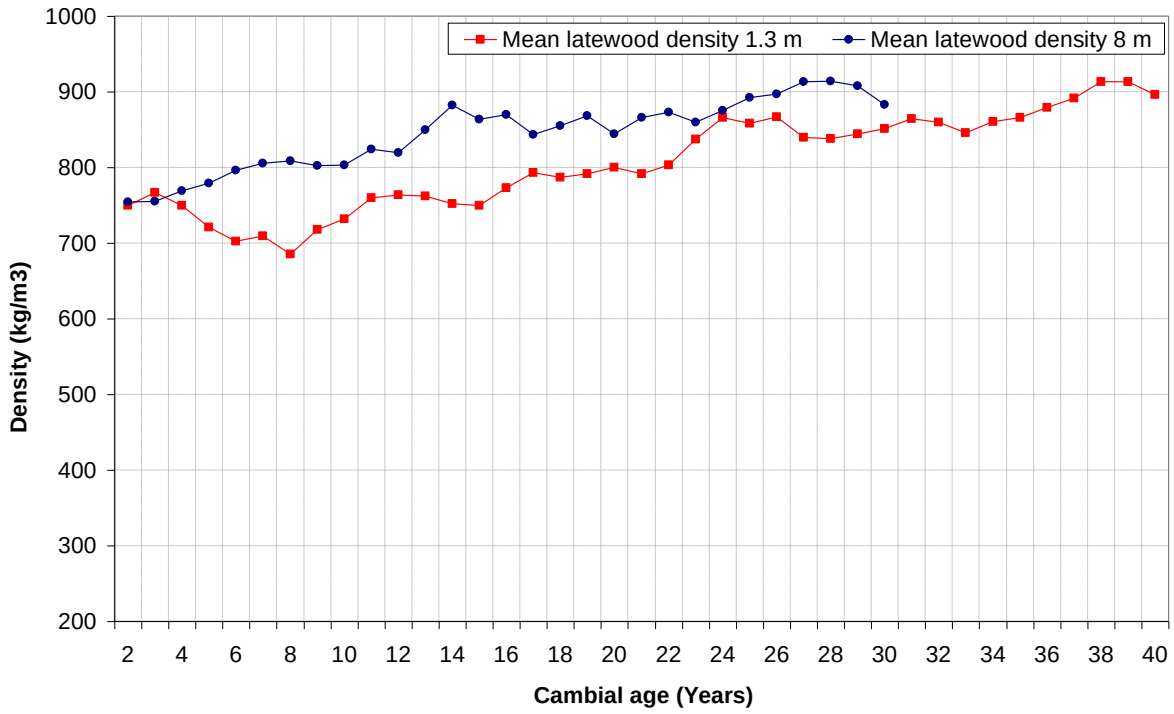

Figure 4-26: Mean latewood density as a function of cambial age at stem heights of 1.3 m and 8 m within younger sample trees

4.6.2.5 Detailed density variation profile

A typical intra-ring variation profile of density recorded at 25 µm intervals is displayed in Figure 4-27. Many of the trends described previously can be seen in the graph, including the decreases in earlywood density on moving outwards from the pith and an overall increase in latewood density during the same period. Following the initial decrease and increase in early and latewood values, it can be seen that the large intra-ring variation in density, which typically in this case averages 800 - 900 kg/m^3, remains relatively constant. The tendency for a sharper transition from early to latewood with increasing cambial age, identified in Section 4.3, is also evident.

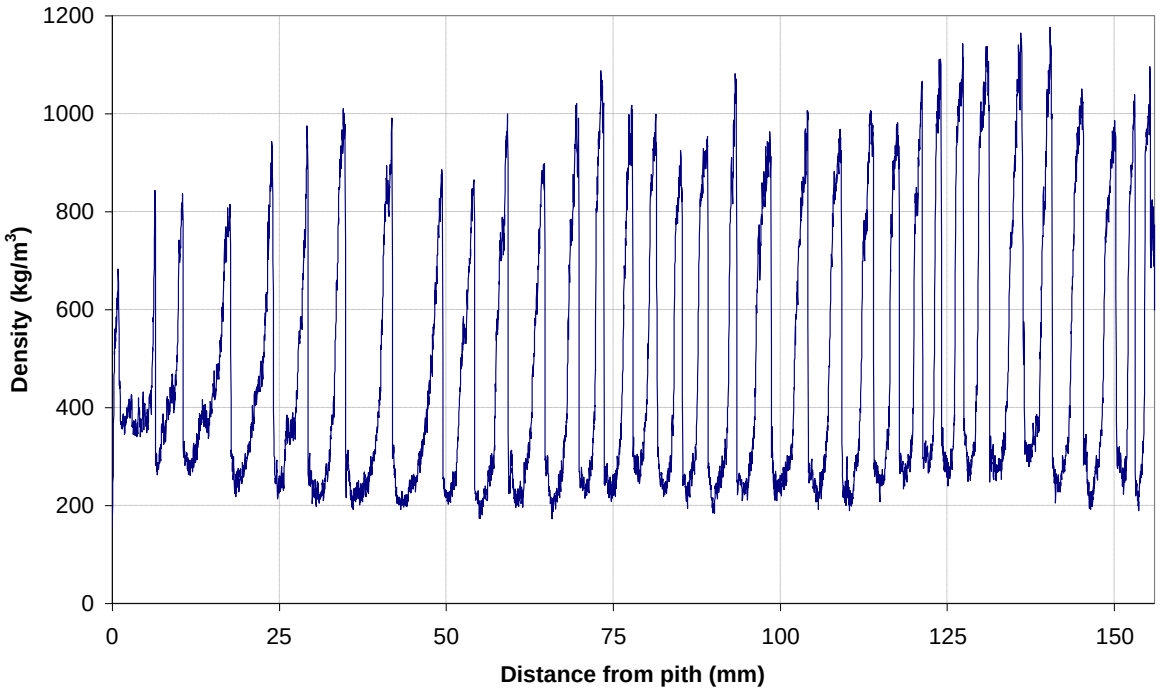

Figure 4-27: Typical intra-ring density profile as a function of distance from the pith

4.6.3 Variations in older trees

The graph in Figure 4-28 shows the developmental profile of mean whole ring density in older sample trees. As a result of the growth patterns discussed previously in Section 4.2.3, the initial decrease in density on moving away from the pith followed by an overall trend of increasing values was not evident. Rather, the highest values were observed in the rings adjacent to the pith, which concurs with the results for wall thickness and tracheid diameters in this region. With increasing cambial age density exhibited a decrease which is in line with the decreasing latewood proportions observed in Figure 4-11, with values appearing to stabilise from approximately 40 years onwards, with densities in the region of 600 kg/m^3 observed.

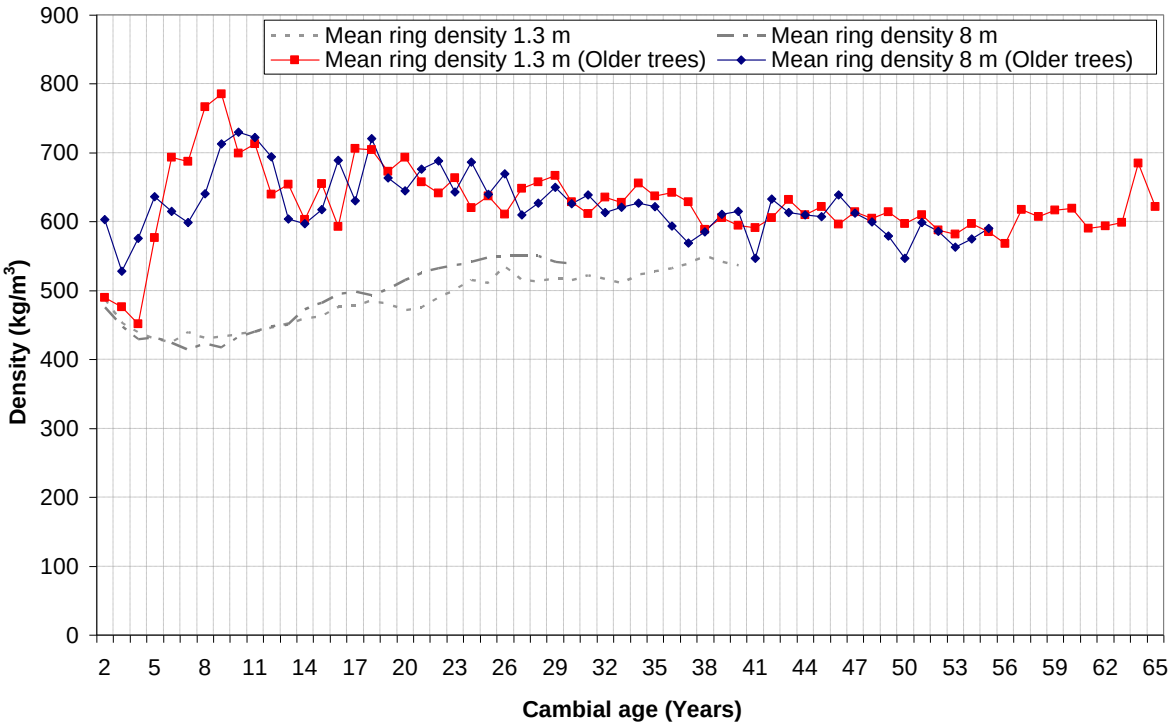

Figure 4-28: Mean whole ring density as a function of cambial age at stem heights of 1.3 m and 8 m within older sample trees

4.6.4 Discussion of variations in density results

The coefficients of variation for all density components were between 10 - 15 %, in line with the values found for cellular dimensions. A result that was expected, given the relationships between cellular dimensions and density to be discussed in Section 4.8. Mean values and coefficients of variation across all sites were within a similar range at the whole ring level, as shown in Table A-54. Consequently, the site factor accounted for only a small percentage of the variation in the analysis of variance, typically lower than 10 %. Differences due to trees within sites typically accounted for between 30 - 60 % of variation. With the exception of earlywood, variation due to error remained relatively high compared to the results seen in previous sub-sections.

The variations of density within tree stems has been relatively widely evaluated in a number of previous studies, due to both its relative ease of measurement compared to some other anatomical features and the good correlations that have been shown to exist between density and wood quality traits. The radial trends for mean, early and latewood density described here are similar to those that have been obtained previously for Douglas-fir by Chalk (1953), Erickson and Harrison (1974), Di Luca (1987), Megraw (1986), Cown (1992), Jozsa and Middleton (1994), Fabris (2000), and Gartner et al. (2002) that were reported and discussed in

Section 2.4.2. Longitudinal variations in density have been less well studied, with most results obtained from samples taken at breast height. The differences with position longitudinally in the stem shown here do however agree with the findings of Spicer and Gartner (2001) and Gartner et al. (2002). The mean whole ring density values presented correspond well with those obtained by work undertaken on material of North American and New Zealand origin mentioned above. It is however the case that for the majority of these studies the mean values stated for early and latewood are typically higher and lower respectively. This is due to transition-wood not being considered, resulting in transitional tracheids being classified as either early or latewood, thereby increasing or decreasing the density recorded. Lachenbruch et al. (2010) utilised the SilviScan system to assess density in the mature wood of North American Douglas-fir. The results attained by Lachenbruch et al. correspond closely to those found in the later growth periods of the breast height samples assessed here.

4.7 Microfibril angle - variations with cambial age and height

4.7.1 Outline

Specimen microfibril angle was determined utilising the x-ray diffractometry functions of the SilviScan-3 system, as described in Section 3.5.3.3. In the following sub-sections, the radial profiles of mean values at the two assessed stem heights for whole ring, early, transition and latewood microfibril angle in 40 - 50 year old trees, and whole ring mean values in trees with ages > 50 years are presented, and the results discussed.

4.7.2 Variations in younger trees

4.7.2.1 Whole ring microfibril angle

Figure 4-29 shows mean values and the 95th percentile range for whole ring microfibril angle at the two assessed stem heights, descriptive statistics alongside the results of the analysis of variance and t-tests can be found in Tables A-55 and A-56. From initial values approaching 30° adjacent to the pith, whole ring mean microfibril angle was observed to show large declines with increasing cambial age within the 2 - 10 year growth period at both stem heights. The rate of decline at 8 m was greater than that seen at breast height, resulting in the t-tests comparing the means at the two heights showing statistically significant differences during this and all subsequent growth periods, typically of 5°. Beyond a cambial age of 10 years, the rate of decline in microfibril angle showed large reductions. While the analysis of variance results showed that differences in mean values due to cambial age were statistically significant in all growth periods, with the exception of 21 - 30 years at breast height, the magnitude of F values exhibited an overall trend of decreasing with age. As the within ring microfibril angle did not reduce significantly between the different growth periods, the reduction in the magnitude of F values is an indication that the tracheid microfibril angle was beginning to stabilise. Mean values in the final growth period were 14° and 11° at 1.3 m and 8 m respectively.

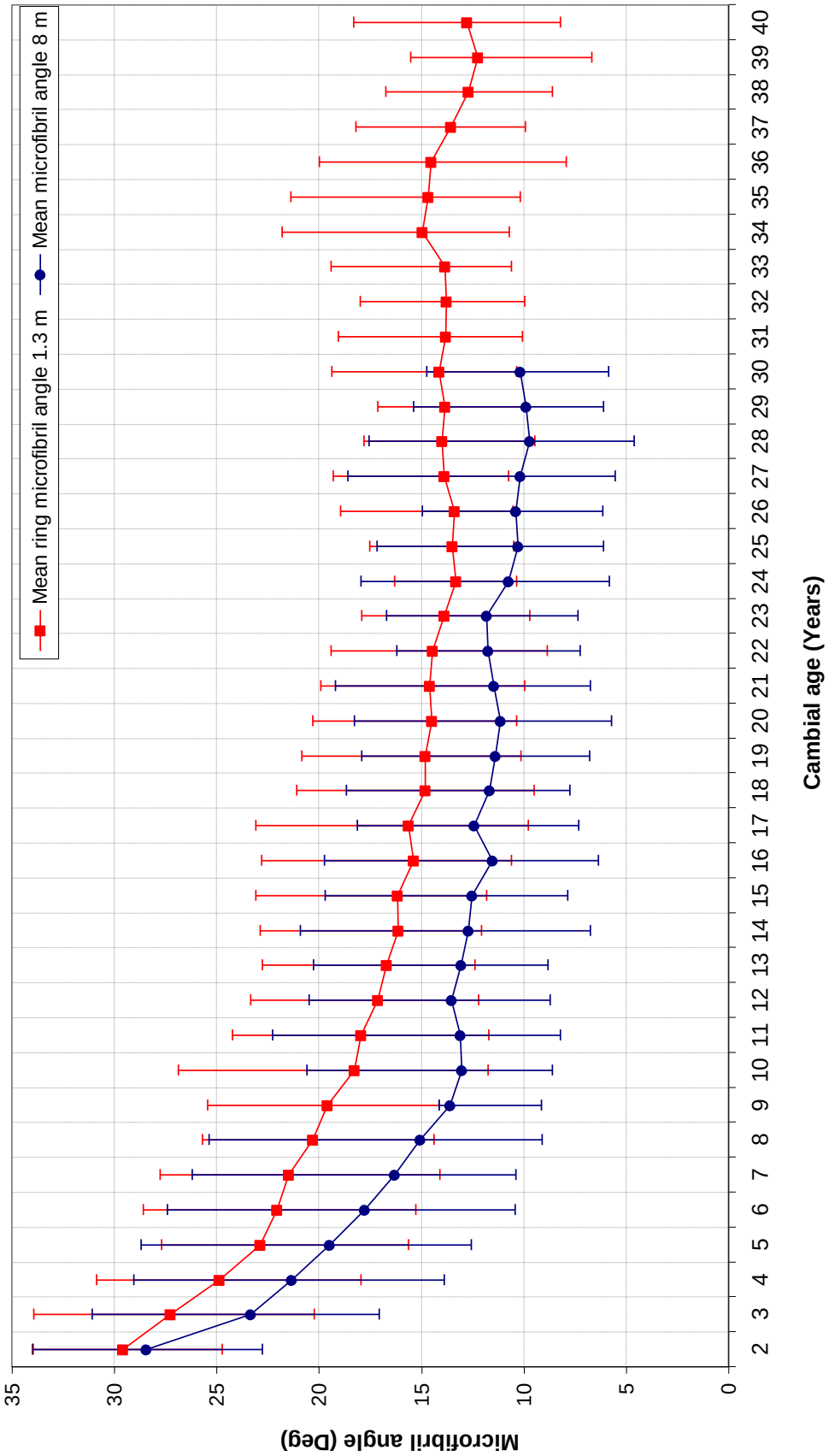

Figure 4-29: Mean whole ring microfibril angle and 95th percentile range as a function of cambial age at stem heights of 1.3 m and 8 m within younger sample trees

4.7.2.2 Early, transition and latewood microfibril angle

Figures 4-30 to 4-32 show mean values for early, transition and latewood microfibril angle at the two assessed stem heights, descriptive statistics can be found in Tables A-57 to A-59. Due to the time intensive nature of obtaining high resolution intra-ring microfibril angle data, these measurements were conducted on a sub-sample of six trees in the 40 - 50 year age range. The development of microfibril angle with age and longitudinally in the stem across early, transition and latewood tracheids closely mirrored that seen for whole ring mean values. The mean microfibril angles of 21° degrees in earlywood at breast height were large compared to those in the latewood, where the mean was 11°. Transition-wood at breast height was found to have a mean microfibril angle of 13°, as such it would appear that the majority of the reduction in the angle of cellulose microfibrils that is seen on transitioning across the growth ring takes place between early and transition-wood. Similar trends were observed at 8 m. Due to the limited number of samples analysed, an analysis of variance and t-tests were not conducted on the high resolution dataset.

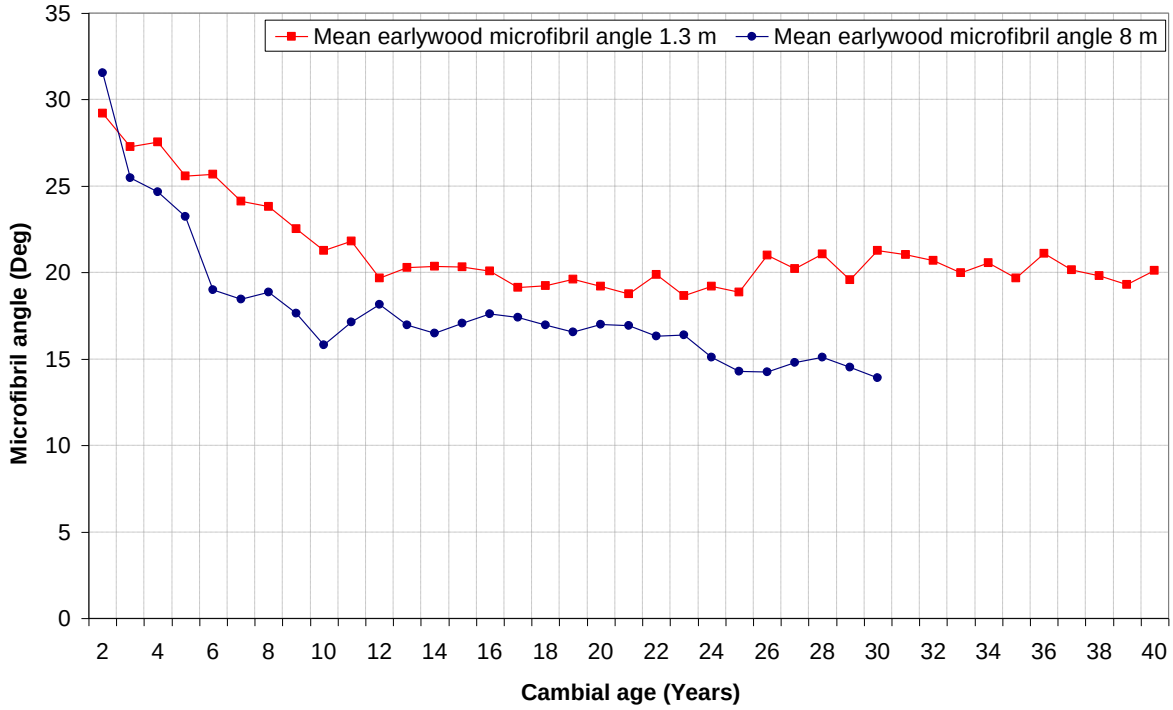

Figure 4-30: Mean earlywood microfibril angle as a function of cambial age at stem heights of 1.3 m and 8 m within a sub-sample of younger trees

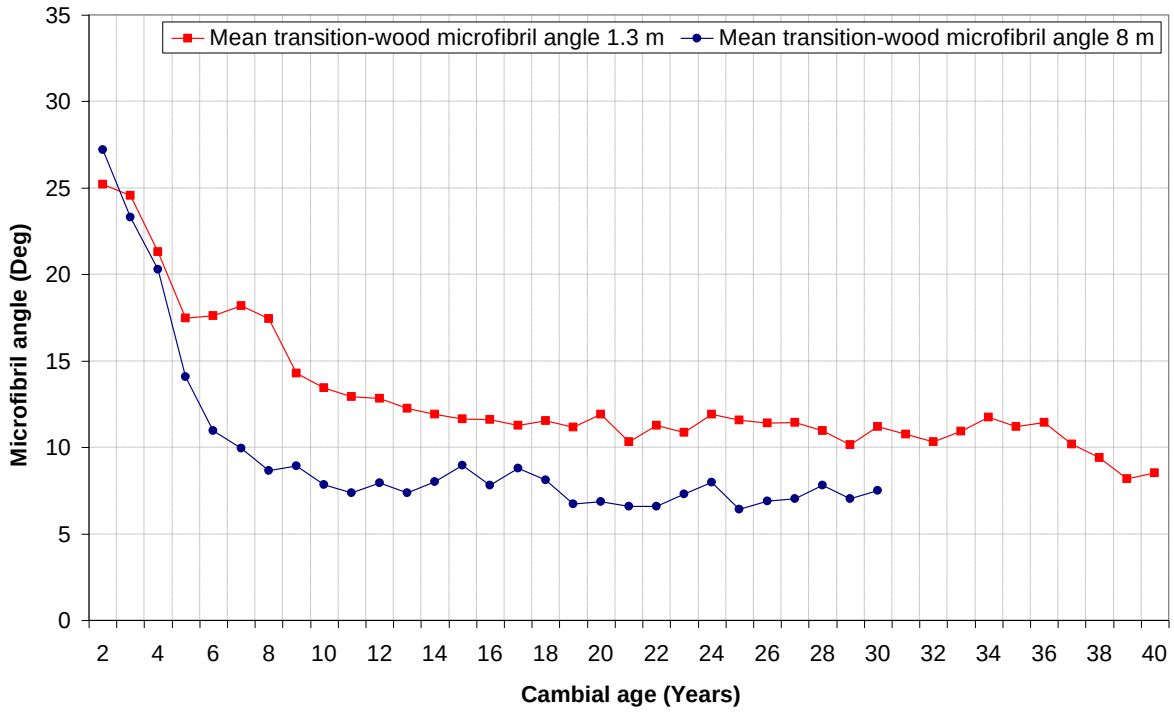

Figure 4-31: Mean transition-wood microfibril angle as a function of cambial age at stem heights of 1.3 m and 8 m within a sub-sample of younger trees

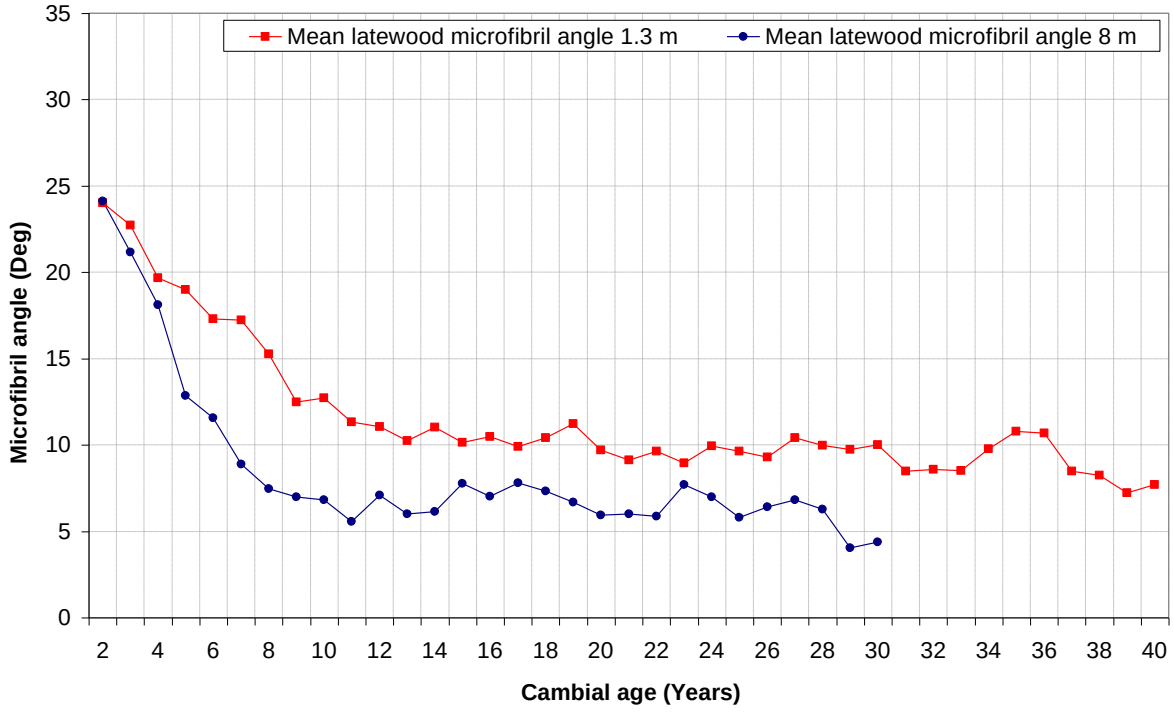

Figure 4-32: Mean latewood microfibril angle as a function of cambial age at stem heights of 1.3 m and 8 m within a sub-sample of younger trees

4.7.2.3 Detailed microfibril angle variation profile

A typical intra-ring microfibril angle profile generated from the raw SilviScan-3 data at 25 µm intervals is shown in Figure 4-33. The profile clearly demonstrates the large within ring variations of microfibril angle observed in the mean values shown previously. Beyond the first formed tracheids, within ring variations were relatively consistent with a range of approximately 15° in this case. As a result of this, fibril angles within mature wood tracheids varied from 15° in the earlywood, to values approaching 0° in the latewood.

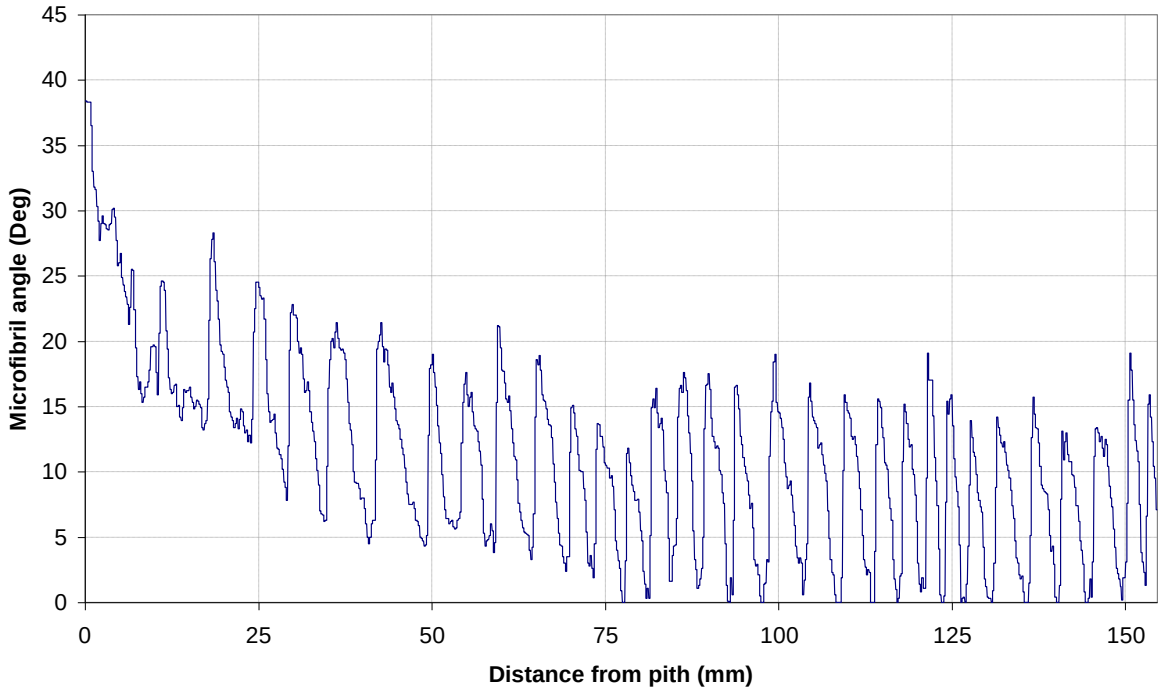

Figure 4-33: Typical intra-ring microfibril angle profile as a function of distance from the pith

4.7.3 Variations in older trees

The graph in Figure 4-34 shows the mean whole ring microfibril angle development profile at both stem heights in the older sample trees. The effects of suppressed growth followed by a period of increased growth rate can be observed when comparing the profiles of the older and younger stems below cambial ages of 25 years. The initial decrease in microfibril angle is interrupted by a period of increasing angle, which corresponds with an increase in ring width seen in Figure 4-5. Beyond this however it appears that microfibril angle values return to those observed in the younger stems and in the later periods of growth, beyond approximately 40 years, values appear to stabilise with a mean of 14° at 1.3 m and 9° at 8 m, with no obvious trends of deviations away from these values. The influence of growth rate on microfibril angle is studied in Section 5.2.7.

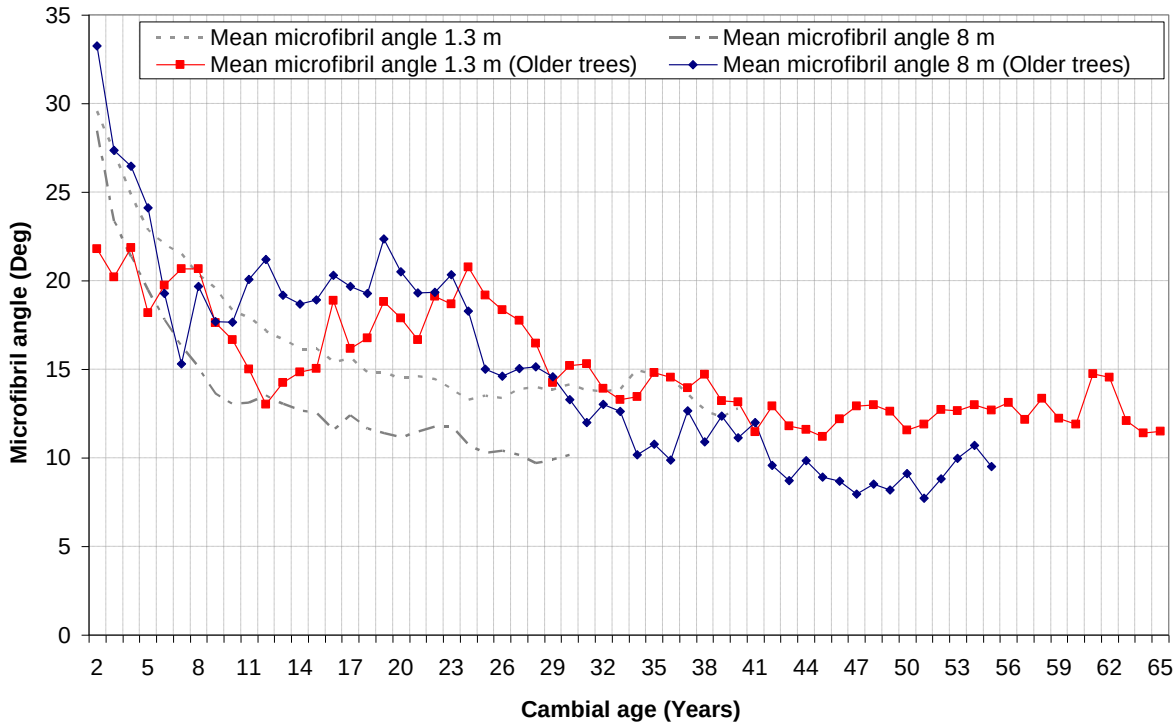

Figure 4-34: Mean whole ring microfibril angle as a function of cambial age at stem heights of 1.3 m and 8 m within older sample trees

4.7.4 Discussion of variations in microfibril angle results

The large intra-tree variations observed in whole ring microfibril angle and its early, transition and latewood components resulted in relatively large coefficients of variation, ranging from 30 - 60 %. The variations observed at 8 m were higher than those at 1.3 m, due to the sharper initial decline from similar starting values, with higher variations also observed in the transition and latewood, where overall decreases in fibril angle were largest. Mean values and coefficients of variation across all sites were within a similar range at the whole ring level, as shown in Table A-60. Consequently, as has been observed in all previous sub-sections, the site factor accounted for only a small percentage of the variation in the analysis of variance. Differences due to trees within sites typically accounted for between 30 - 60 % of variation, with values rising with increasing cambial age.

The pith to bark trends in microfibril angle development observed here are similar to those that have previously been shown to exist in softwoods, as described by Donaldson (2008). The time intensive nature of the measurement techniques available until relatively recently has resulted in a lack of complete datasets showing both intra- and inter-ring variations within Douglas-fir stems. The results presented here are in good agreement with the findings of previous Douglas-fir studies conducted using optical techniques on earlywood tracheids by

Fabris (2000) and latewood tracheids by Erickson and Arima (1974). Results showing the decrease in microfibril angle between early and latewood in Douglas-fir were presented by Ifju and Kennedy (1962) and Lofty et al. (1973). The differences in the values recorded at different locations within a growth ring were not as great as those presented here which, alongside variations due to genetics and growing conditions, may have arisen due to the common practice of classifying transition-wood as either early or latewood as discussed previously. In the case of microfibril angle this could potentially result in lower and higher mean values for early and latewood being reported respectively. The results of a study utilising SilviScan to assess North American Douglas-fir mature wood conducted by Lachenbruch et al. (2010) are in excellent agreement with those presented here if compared over a comparable age period. No data showing the longitudinal variation of microfibril angle in Douglas-fir stems was found, however studies in other softwood species have also demonstrated decreasing microfibril angles for rings of equivalent cambial age with increasing height in the stem (Donaldson, 1992, Jordan et al., 2005).

4.8 Discussion of results

The objectives of this chapter were to identify trends in the developmental profiles of several key anatomical properties in the Douglas-fir sample trees. In doing this two hypotheses were tested, the null hypotheses of which were:

> $H_{4\text{-}1}$: No change in the magnitude of the studied property takes place with increasing cambial age.
>
> $H_{4\text{-}2}$: No difference exists in the magnitude of the studied property with increasing longitudinal position in the stem.

Considering the radial profiles of each anatomical property in their entirety, all showed a change in the magnitude of the assessed values with increasing cambial age, and as such the null hypothesis given in $H_{4\text{-}1}$ can be rejected and the alternative hypothesis, that cambial age does have an effect on anatomical properties, accepted. A similar result was achieved when studying longitudinal variations within the stem, with all properties beside latewood width and earlywood density showing statistically significant differences between the two stem heights. As a result, the null hypothesis stated in $H_{4\text{-}2}$ is rejected and the alternative hypothesis, that a difference exists in the magnitude of studied anatomical properties with increasing longitudinal position in the stem, accepted.

Upon breaking the developmental profiles down into separate growth periods, a rather more mixed outcome regarding the acceptance of either the null or alternative hypothesis emerges. In general for all properties studied, large changes with cambial age were noted early in the growing cycle, with rates of change decreasing and eventually appearing to stabilise with increasing age for many of the properties assessed. Although the results obtained from older sample trees exhibited some unusual growth patterns in the early years of growth, they appeared to confirm the stabilisation of values with increasing cambial age seen in younger trees.

The variations in the results encountered can be better understood when the changes occurring during the life cycle of the living tree are considered. Variations in anatomical properties occur in response to the changing demands of nutrient transportation required by the live crown and the need to support the increasing weight of the tree above (Barnett, 2004). Within an individual growing season, environmental factors such as photoperiod, precipitation, temperature and the availability of nutrients have been shown to have a large influence on the nature of the wood material produced (e.g. Larson, 1960, Lebourgeois, 2000). Wood is produced within the cambial zone or cambium, with new growth in temperate regions triggered by increases in temperature and photoperiod. As observed in Figure 4-1, ring widths were typically greatest in the growth rings immediately adjacent to the pith. As all younger sample trees were grown within even aged stands this factor arises in part due to stand dynamics. At younger cambial ages little or no competition exists between adjacent trees and wide rings are therefore observed. As the crowns of neighbouring trees begin to meet, the competition for light and nutrients increases and as a result ring widths begin to decline. The fall in ring widths does not directly relate to a decrease in the rate of biomass accumulation, due to the fact that as the tree grows in circumference a growth ring of a certain width will contain a greater quantity of material than in trees with a smaller circumference. This factor also accounts for the decline in ring widths seen with increasing cambial age

The ring widths and changing proportions of early, transition and latewood within a growth ring reported in Sections 4.2 and 4.3 are highly dependent on the duration of tracheid maturation experienced following cambial division. Maturation takes place in two phases; radial expansion and secondary cell wall thickening (Dodd and Fox, 1990, Samuels et al., 2006). As seen in Sections 4.4 and 4.5, earlywood tracheids are observed to have larger diameters and thinner cell walls, with the reverse being true of latewood. The type of cell produced is thought to be under the control of hormonal signals and the availability of

materials produced through photosynthesis. The production of the phytohormone indole-3-acetic acid (IAA) during early terminal shoot growth and its basipetal flow through the stem, has been shown to be linked to increases in the production of xylem and phloem within the cambial zone and the promotion of cell expansion (Larson, 1962, Larson, 1969b), resulting in the production of large diameter tracheids. The production of new foliage within the crown at this time is a major metabolic sink of photosynthate, consequently the tracheids produced have thin cell walls which alongside their large diameter typify earlywood. As this newly produced foliage reaches maturity it becomes a net exporter of material to the stem, with the extra carbohydrate available used in the production of tracheid cell wall material. A similarly timed drop in the production of growth hormones sees tracheid expansion reducing and consequently the production of cells with latewood characteristics (Larson, 1964). Renninger (2006) showed that a decline in the production of IAA as a result of cessation of leader growth and an increase in the availability of photosynthate is an independent process in Douglas-fir, possibly correlated with the same environmental cues. The change in tracheid dimensions across the growing season from early to latewood that arises from the processes described above was shown in Sections 4.4 and 4.5.

Section 4.2 shows that whilst earlywood production remains relatively stable at all cambial ages, large changes in the proportions of transition and latewood tracheids take place. Typically, the wood produced within the live crown contains the greatest number of transitional tracheids due to the high concentrations of IAA and material produced through the process of photosynthesis. As cambial age and the distance to the live crown increases at a given sampling location, the concentration of growth hormones declines and as such latewood production usually commences first at the stem base (Larson, 1969a). This accounts for the increase in latewood proportion observed with age in Figure 4-8. Greater nutrient and hormonal concentrations due to the increased quantity of crown foliage at the time of production of wood at the 8 m sampling location, may account for the differences seen in the developmental profiles for early and latewood between the two sample heights at young cambial ages. While many studies of anatomical properties overlook the presence of transitional tracheids, instead apportioning them to either early or latewood, their importance in understanding the physiological changes taking place during the life of the tree have been clearly demonstrated here.

As well as the changes observed to take place within the growing season described above, more gradual changes in the nature of the cell wall material produced were observed at each

sampling location with increasing cambial age. These changes have been shown to be linked to maturation processes occurring within the cambium (Olesen, 1978, Olesen, 1982). The large differences in properties for a given growth ring between the two sampling heights have also been shown to be linked to cambial maturation, with wood produced higher in the stem being ontogenetically older than that produced at the stem base (Schweingruber et al., 2006).

Wood density is a measure of the total amount of cell wall material per unit volume. As such, the profiles of wood density development displayed in Section 4.6 are closely related to the relative proportions of the different cell types described in Section 4.3, as well as the dimensions of the cells and the thicknesses of the cell walls presented in Sections 4.4 and 4.5. The overall trend of increasing density exhibited with age is therefore a result of both increasing latewood proportions and changes to cell wall dimensions due to cambial maturation.

As with density, the decrease in whole ring, early, transition and latewood microfibril angle with cambial age and height observed in Section 4.7 can be attributed to increases in the proportion of latewood within a growth ring, which was observed to have a low microfibril angle, and due to the maturation of the cambium. The exact mechanism by which microfibril orientation is controlled is still uncertain, however it is thought to be associated with the orientation of microtubules within the living cell protoplast during wall formation (Donaldson, 2008). The functional significance of the changes observed in fibril angle within and between growth rings is better understood. The three primary loading conditions imposed upon a stem are lateral forces from wind, bending to a critical angle by animals and gravitational forces from material above (Lichtenegger et al., 1999). The decrease in whole ring mean microfibril angle seen in Figure 4-29 with increasing cambial age is therefore a direct response to these loading conditions, providing the optimal resistance to stem damage as a result of fracture stresses, crack propagation, strains and compressive stress at different times during the life of the tree (Booker and Sell, 1998). The decrease in S_2 microfibril angle observed upon transitioning from early to latewood was shown by Booker and Sell (1998) to be related to the increasing tracheid wall thickness observed over the same period. Thinner cell walls allow for larger lumens in earlywood for the conduction of nutrients through the stem, while vertically aligned microfibrils provide the most efficient vertical load carrying capacity. As such the most efficient orientation of cellulose microfibrils in all parts of a growth ring in older trees, where supporting the weight of the tree above is the primary imposed load, would appear to be vertically aligned. However, thin cell walls and low microfibril angles

would present a large risk of tracheid transwall fracture, hence the relatively high microfibril angles seen in earlywood tracheids at all ages. As the need for sap conduction decreases, the cell wall thickens and cell diameters narrow resulting in a smaller lumen, thicker cell walls are able to sustain lower microfibril angles without increasing the risk of transwall fracture, hence the intra-ring microfibril angle profile seen in Figure 4-33.

Differences between the mean values of the assessed properties due to site were found to be low in the variance components analysis of random effects, generally accounting for less than 10 % and remaining relatively constant in progressive growth periods for each property assessed. A low difference between the mean values for each site was to be expected, given the close geographic spacing, growth taking place over similar timescales and a similar distribution of tree average growth rates within each site. Differences that exist between sites could be accounted for by a number of factors including differences in silvicultural treatments, micro climatic effects at the site, topography, soil conditions and genetic differences. The large variances associated with trees nested within sites were to be expected, given the sampling methodology used to select trees of varying growth rates. It was generally found that in anatomical properties demonstrating a stabilisation of values in later years of growth, that the variance associated with trees increased. This was most likely due to the fall in variance associated with cambial age in successive growth periods, which would have been a component of the variation due to error.

4.9 Concluding remarks

Within this chapter, radial and longitudinal variations of wood anatomical properties known to be of importance in the determination of wood quality attributes have been assessed. All properties showed a change in magnitude upon moving away from the pith, particularly so at younger cambial ages in most cases. Results showing variations in the properties of transition-wood, which have not been widely reported for any softwood species, were of particular interest as they allowed a greater understanding of the developmental processes occurring to be gained. The variations, along with those observed between the two sampling heights, were attributed to the changing roles of the cellular material both within a growing season and as the cambial zone matured. The decline in the rate of change of many anatomical characteristics at older cambial ages was verified in the assessment of a sub-sample of older Douglas-fir trees. As well as providing insightful information on their own, the findings presented here form the basis of the interpretation of many of the results presented in the subsequent chapters.

Chapter 5 - Anatomical properties part 2: variations with growth rate and juvenile to mature wood demarcation age

5.1 Introduction

In the previous chapter, the development of anatomical properties within the Douglas-fir sample trees that have previously been linked to wood quality were presented. A large degree of variability was observed in the properties assessed, both in their development with time and also at a given cambial age. The rate of growth of a tree has often been noted as a key factor in inducing variability in the nature of the wood material produced, and hence quality. In this chapter the influence of a changing rate of growth between test trees is evaluated and quantified. It was also noted in the radial development profiles shown in Chapter 4 that many values assessed displayed signs of stabilising with increasing cambial age. In this chapter the decline in the rate of change of properties is quantified from the perspective of juvenile and mature wood.

The key objectives of the analysis presented here are therefore to:

- Quantify the impact of growth rate on anatomical properties throughout the growing cycle and relate the results found to stand development dynamics.
- Establish ages for the demarcation between juvenile and mature wood production with respect to whole ring density and microfibril angle, and quantify the impact of accelerated growth on demarcation ages and juvenile/mature wood proportions.

Results of the analysis of the influence of growth rate on anatomical properties are first presented in Section 5.2, with those relating to the demarcation age from juvenile to mature wood production in Section 5.3. The presentation of results is followed by a discussion, relating the changes observed to developmental processes taking place within the living tree. A summary of the findings and the conclusions that can be drawn from them is given at the end of the chapter in Section 5.4.

5.2 Influence of growth rate on anatomical properties

5.2.1 Outline

In this section, the influence of changes in growth rate on the anatomical properties presented in Chapter 4 is evaluated. Gaining an understanding of the extent to which changes in the rate of growth can influence anatomical properties is important, as it is often one of the factors by which wood quality is judged and also has implications regarding the use of silvicultural practices. In the following sub-sections the impact of changing growth rates is first evaluated with use of a linear correlation analysis, comparing the magnitude of the studied property to ring width at each cambial age. The methodology used in this analysis is described in Section 3.10.3. This is followed by a comparison of the mean values attained within stems classified as either slower or faster grown, according to the definition given in Section 3.7, by means of t-tests, using the method described in Section 3.10.5. Lower means in slower grown stems compared to those that were faster grown returned negative t values, with positive values returned when the reverse situation occurred. All statistical tests were deemed significant when $P \leq 0.05$. The results of each test can be found alongside the descriptive statistics in Appendix B, as indicated at the start of each sub-section.

In evaluating the impact of growth rate on anatomical properties two hypotheses were tested, the null hypotheses of which were:

> $H_{5\text{-}1}$: There is no statistically significant linear relationship between ring width and the magnitude of the studied property for a given growth ring.
>
> $H_{5\text{-}2}$: There is no statistically significant difference between the mean values of studied properties in slower and faster grown trees.

5.2.2 Ring widths - variation with rate of growth

5.2.2.1 Correlation analysis

Figures 5-1 to 5-3 show the correlation coefficients for ring width and the variables early, transition and latewood width for individual cambial ages at both 1.3 m and 8 m sampling heights. Correlation coefficients are also shown in Tables B-1 to B-3. At all cambial ages greater than 10 years in both early and transition-wood, a relatively strong positive linear relationship with ring width existed, with correlation coefficients typically greater than 0.8. This indicates increasing values with increases in the rate of growth. Below ten years of age in earlywood, correlations were found to be weaker and in some instances non-significant. The linear relationship between ring and latewood width was found to be weaker than that seen earlier in the growth ring, with widths at older cambial ages displaying moderate correlations of 0.6 to 0.8. In growth rings closer to the pith correlations were generally found to be non-significant in the latewood.

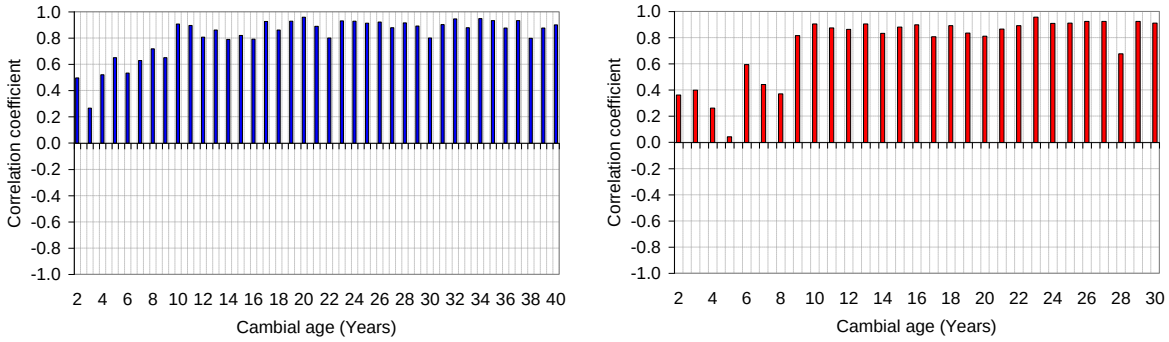

Figure 5-1: Correlation coefficients for earlywood width against ring width for individual growth rings in 40 - 50 year old trees at 1.3 m (L) and 8 m (R)

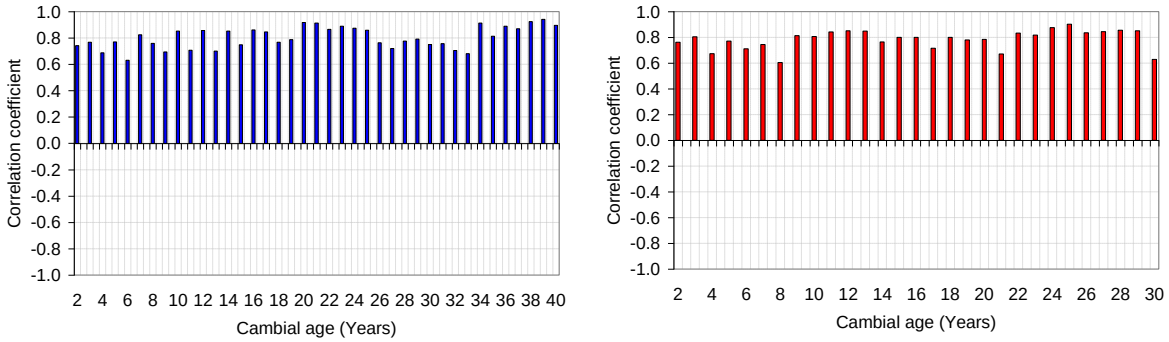

Figure 5-2: Correlation coefficients for transition-wood width against ring width for individual growth rings at 1.3 m (L) and 8 m (R)

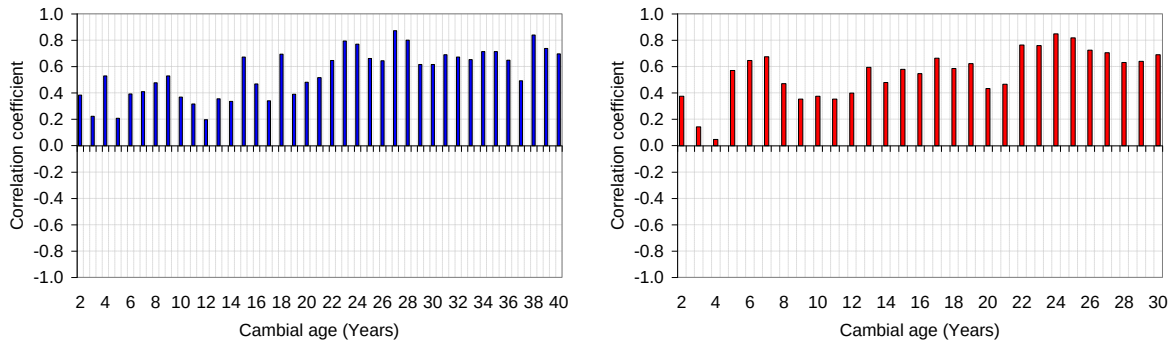

Figure 5-3: Correlation coefficients for latewood width against ring width for individual growth rings at 1.3 m (L) and 8 m (R)

5.2.2.2 Comparison of means

The box and whisker plots shown in Figure 5-4 illustrate the changes in mean ring widths for 40 - 50 year old trees, considering values from both 1.3 m and 8 m in combination within stems classified as either slower or faster growing, compared with the sample mean for all trees. Descriptive statistics alongside the results of t-tests comparing the means can be found in Table B-4. The box and whisker plots show the mean and median, designated by a cross and horizontal line, the interquartile range, designated by the lower and upper limits of the grey box and potential outliers, which are shown with an asterisk. Individual results were deemed outliers by the Minitab 16 software used for the analysis when their values were more than 1.5 times the interquartile range from the upper and lower quartile values.

The mean whole stem ring width across all sample trees was 4.7 mm. The mean values in the slower and faster growing trees were found to be 3.9 mm and 5.4 mm respectively, representing a change of ± 17 %. The percentage difference from the whole sample mean was however found to vary within the different regions of the growth ring. In earlywood, increases in width were found to occur at a similar rate to those taking place at the whole ring level, with changes of ± 17 %. It was however discovered that latewood width increased at a slower rate than whole ring values, whilst the opposite was true of transition-wood, with values of ± 14 % and ± 19 % respectively. In the results of t-tests, the differences between mean values in the slower and faster growing trees was found to be statistically significant in all cases.

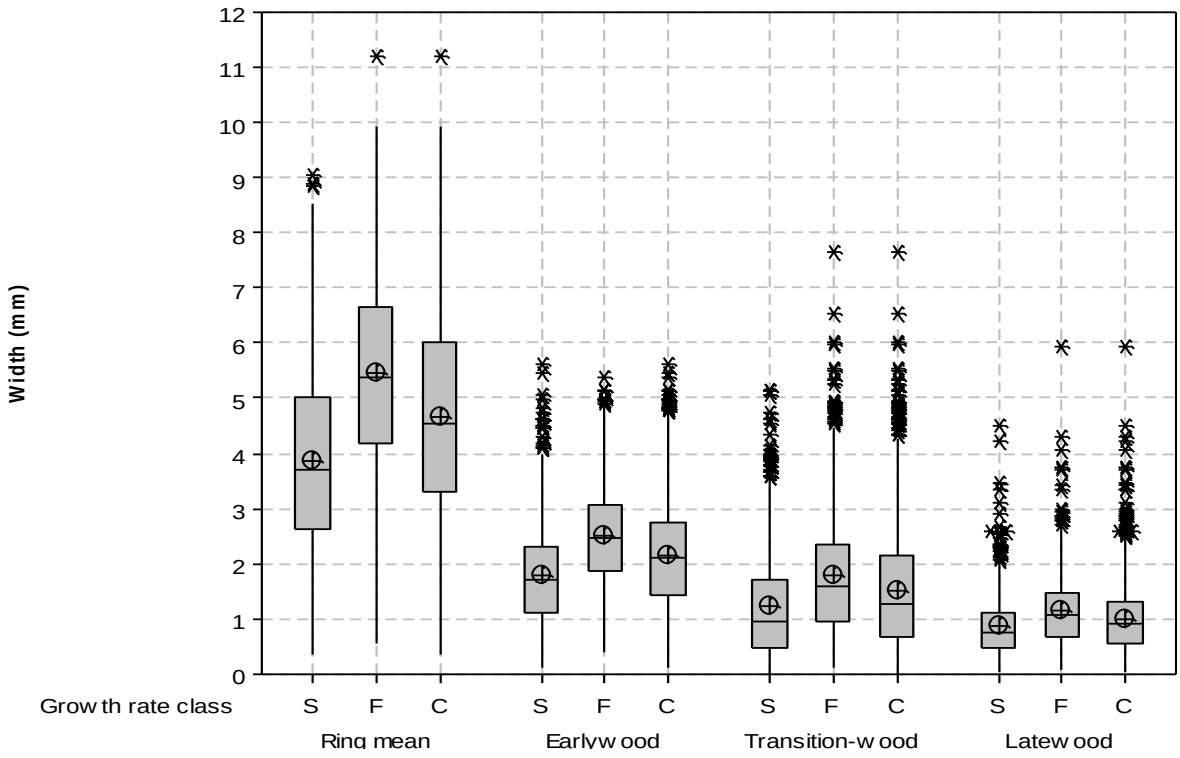

Figure 5-4: Whole stem ring widths in slower (S) and faster (F) growing trees and in combination (C) within 40 - 50 year old sample trees

At the site level, separating the six trees felled at each of the four main sampling sites for 40 - 50 year old trees into either slower or faster growing stems returned similar results to those described above. Statistically significant lower mean widths were observed in t-tests in stems classified as slower growing across all sites and regions of the growth ring, this is shown by the negative values returned by the t-test results in Table B-5.

5.2.3 Proportions of wood types - variation with rate of growth

5.2.3.1 Correlation analysis

Figures 5-5 to 5-7 show the correlation coefficients for ring width and the variables early, transition and latewood proportion for individual cambial ages at both 1.3 m and 8 m sampling heights. Correlation coefficients are also shown in Tables B-6 to B-8. Correlations with ring width showed varying degrees of strength and significance in the three different wood types within a growth ring. The correlation coefficients between ring width and earlywood proportion were negative in virtually all instances, a sign of a decreasing proportion with increasing growth rate, the correlation coefficients were however not found to be statistically significant in any growth rings. The proportion of transition-wood observed within a growth ring displayed a stronger relationship with growth rate. All correlation coefficients

were found to be positive and in most instances significant, with values typically between 0.5 and 0.7, indicating a moderate to strong linear relationship of increasing transition-wood proportion with increases in the rate of growth. The trends observed in the interaction between latewood proportion and ring width typically mirrored those seen in the transition-wood, with correlation coefficients found to be negative and significant in most growth rings with values between 0.5 and 0.6, indicating the existence of a moderate linear relationship. For both transition and latewood proportions the majority of the non-significant correlation coefficients were found to occur in the growth rings nearest the pith, at cambial ages less than 10 years.

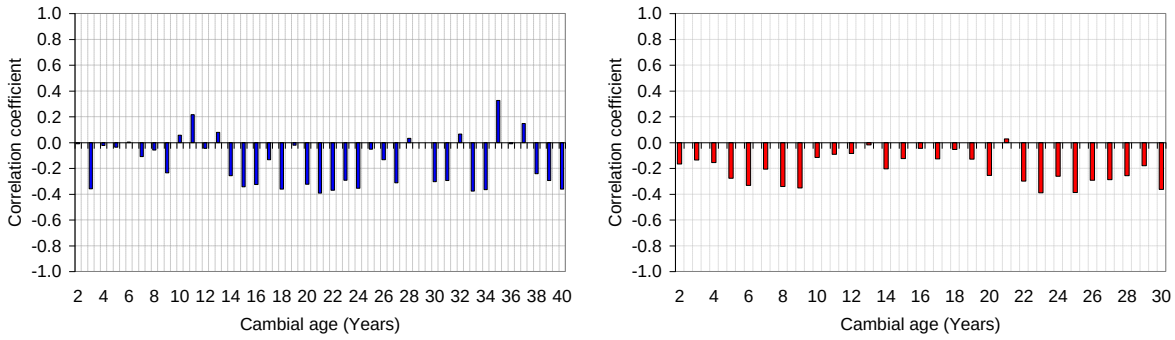

Figure 5-5: Correlation coefficients for earlywood proportion against ring width for individual growth rings in 40 - 50 year old trees at 1.3 m (L) and 8 m (R)

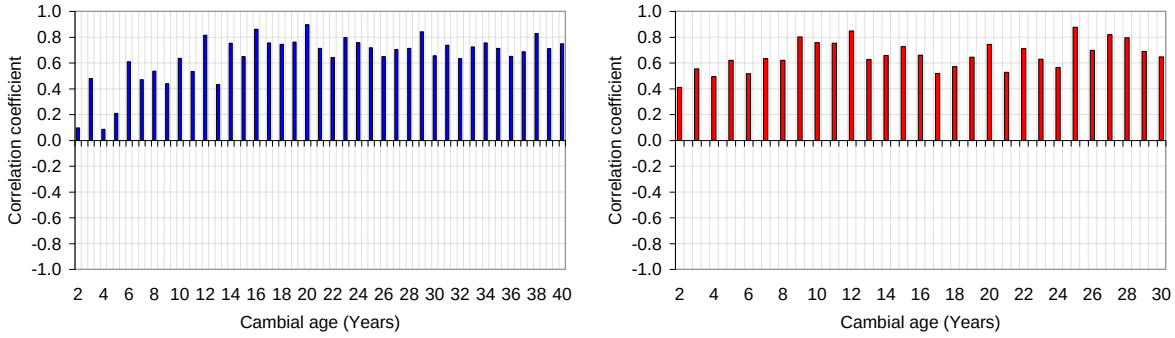

Figure 5-6: Correlation coefficients for transition-wood proportion against ring width for individual growth rings in 40 - 50 year old trees at 1.3 m (L) and 8 m (R)

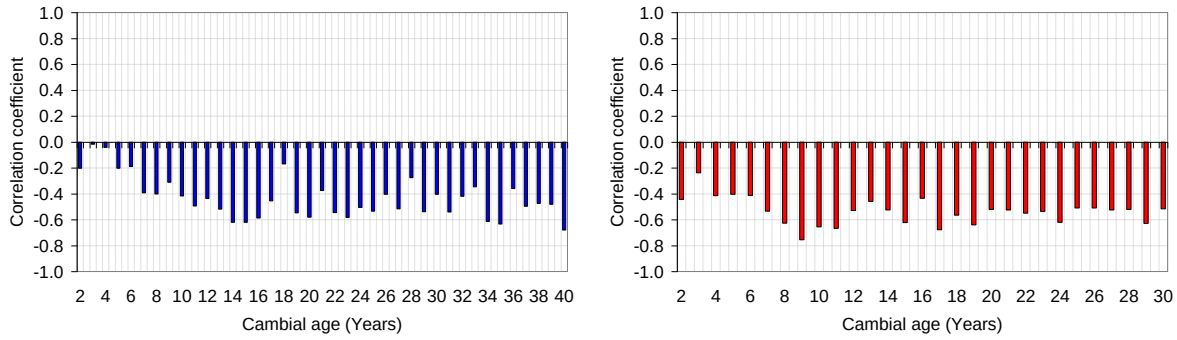

Figure 5-7: Correlation coefficients for latewood proportion against ring width for individual growth rings in 40 - 50 year old trees at 1.3 m (L) and 8 m (R)

5.2.3.2 Comparison of means

The box and whisker plots shown in Figure 5-8 illustrate the changes in mean wood type proportions within a growth ring for 40 - 50 year old trees, considering values from both 1.3 m and 8 m in combination within stems classified as either slower or faster growing, compared with the sample mean for all trees. Descriptive statistics alongside the results of t-tests comparing the means can be found in Table B-9. Earlywood proportion was found to exhibit no difference in mean values between slower and faster growing trees, this was confirmed by the statistically non-significant results of the t-test. This is in agreement with the non-significant results of the correlation analysis shown previously. The changes in the proportions of transition and latewood with slower and faster growth were found to be equal and opposite. Within the faster growing stems, the mean transition-wood proportion was 1.5 % greater than the mean for all trees, which was accompanied by a corresponding decrease in the proportion of latewood. Equal and opposite results were observed with slower growth. Although small, these differences in the mean values were found to be statistically significant in the results of the t-tests. This is in agreement with the results of the correlation analysis shown previously, where positive and negative correlations with increasing ring width were found for transition and latewood respectively.

At the site level, separating the six trees felled at each of the four main sampling sites for 40 - 50 year old trees into either slower or faster growing returned similar results to those described above. Statistically significant higher proportions of mean transition-wood and lower proportions of mean latewood were observed in t-tests within trees classified as faster growing in all but one of the sampling sites. Results are presented in Table B-10.

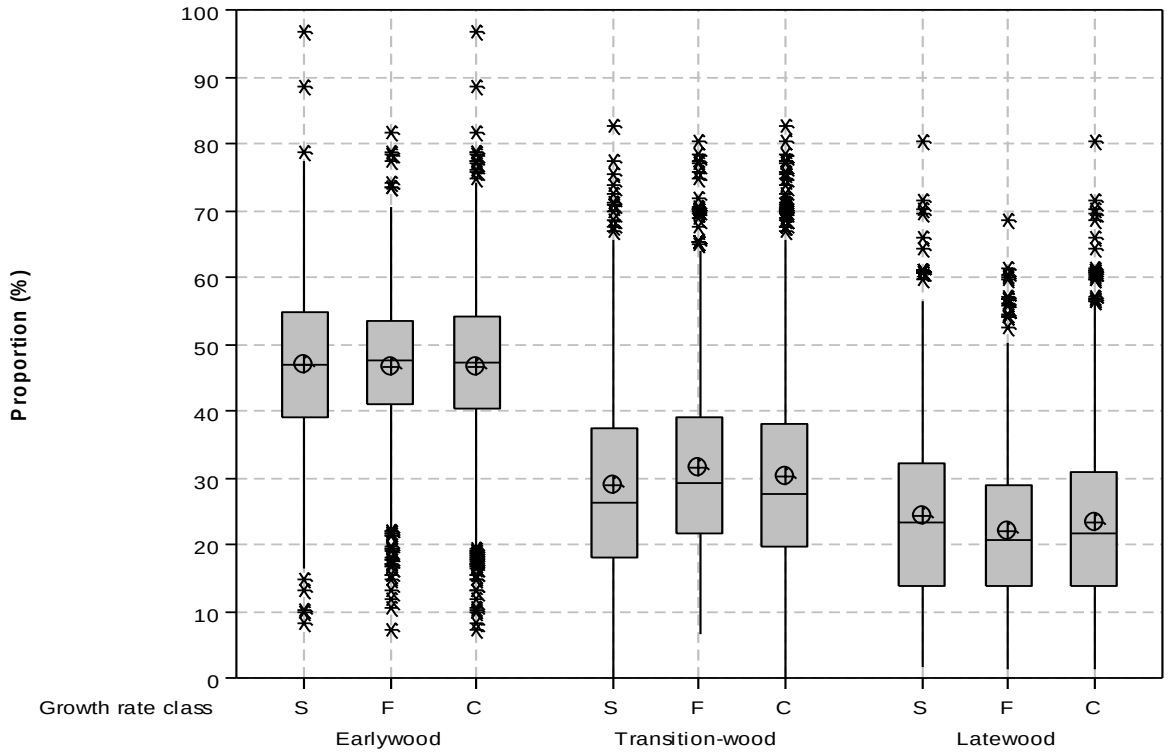

Figure 5-8: Whole stem tracheid type proportions in slower (S) and faster (F) growing trees and in combination (C) within 40 - 50 year old sample trees

A number of previous studies have shown the relationship between rate of growth and latewood proportion in Douglas-fir. The results detailed here are in agreement with the findings of Smith et al. (1956), Drow et al. (1957), Erickson and Harrison (1974) and Fabris (2000) which showed that the percentage of latewood present within a growth ring decreases with an increasing rate of growth. Abdel-Gadir et al. (1993) also found weak negative correlations between ring width and latewood proportion in mature wood, however in the juvenile wood of the same trees the correlations were weak and positive. In other softwood species including Balsam-fir (Koga and Zhang, 2004), Sitka spruce (Livingston et al., 2004), Western hemlock and Western red cedar (Fabris, 2000) negative relationships between latewood proportion and ring width of varying strength have been presented. Data regarding variations in early and transition-wood proportions with growth rate are scarce, due to the common practice of not classifying transitional tracheids. Along with differences in measurement techniques, this may in part explain the results of previous studies that have shown weak and in some cases positive correlations between latewood proportion and growth rate. By classifying a certain number of transitional tracheids as latewood, the positive correlation seen between transition-wood proportion and growth rate may act to reduce the significance of the effect of growth rate on latewood proportion.

The limited impact of growth rate on the proportions of earlywood tracheids compared to transitional and latewood accounts for, at least in part, the lower coefficients of variation observed within the earlywood portion of the growth ring in the data presented in Section 4.3.2.1.

5.2.4 Radial and tangential tracheid diameters - variation with rate of growth

5.2.4.1 Correlation analysis

Figures 5-9 and 5-10 show the correlation coefficients for ring width and the radial and tangential tracheid diameters at the whole ring level for individual cambial ages at both 1.3 m and 8 m sampling heights. Correlation coefficients for early, transition and latewood alongside whole ring values are also shown in Tables B-11 to B-18. Similar results were returned by the correlation analysis for both radial and tangential diameters at the two stem heights. Correlation coefficients were found to be positive, indicating increasing diameters with increasing rates of growth, values were however low, typically below 0.5, with significance achieved at only a limited number of cambial ages, particularly so for radial diameters, indicating a relationship with growth rate that was at best weak. As observed in many results presented previously, correlation coefficients in the growth rings adjacent to the pith approached zero. The results returned for the analysis assessing relationships of radial diameter within the earlywood showed a mix of very weak positive and negative correlations, with significance achieved in only a few instances. Results for all other regions of the growth ring showed similar trends to whole ring values for both radial and tangential diameters.

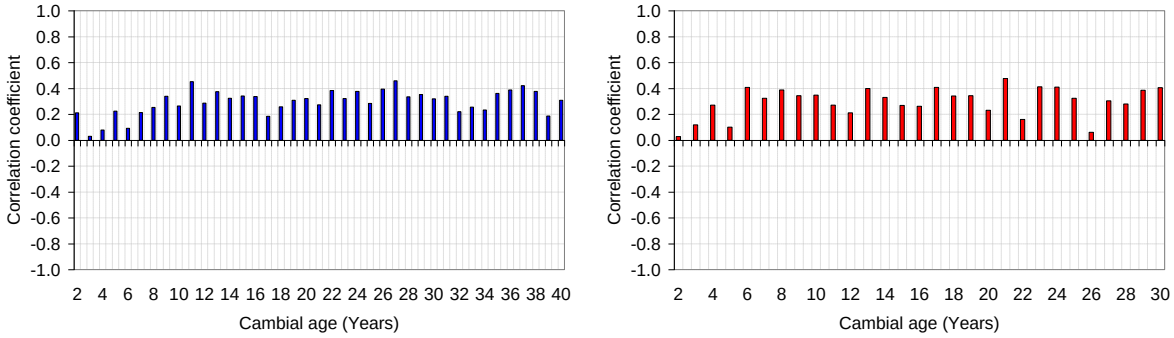

Figure 5-9: Correlation coefficients for whole ring mean radial tracheid diameter against ring width for individual growth rings in 40 - 50 year old trees at 1.3 m (L) and 8 m (R)

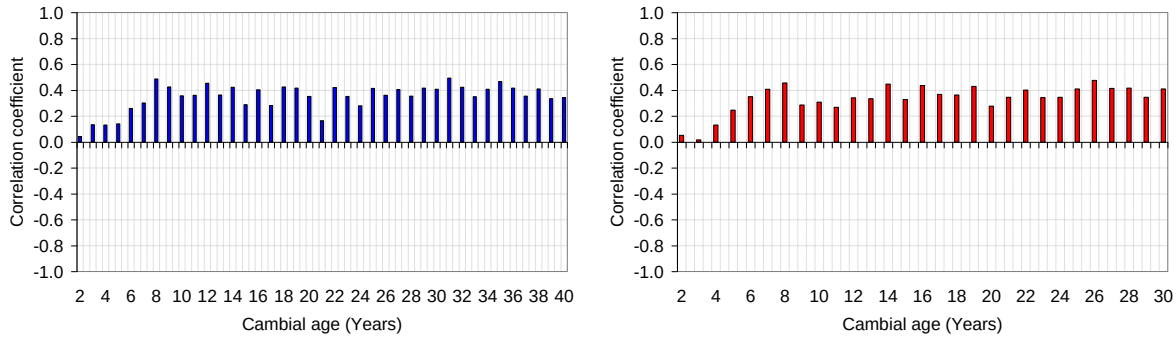

Figure 5-10: Correlation coefficients for whole ring mean tangential tracheid diameter against ring width for individual growth rings in 40 - 50 year old trees at 1.3 m (L) and 8 m (R)

5.2.4.2 Comparison of means

The box and whisker plots shown in Figures 5-11 and 5-12 illustrate the changes in mean radial and tangential tracheid diameters within a growth ring for 40 - 50 year old trees, considering values from both 1.3 m and 8 m in combination within stems classified as either slower or faster growing, compared with the sample mean for all trees. Descriptive statistics alongside the results of t-tests comparing the means can be found in Tables B-19 and B-20. Statistically significant differences in the mean values of radial diameter were observed for whole ring mean and transition-wood only, with faster growth leading to increases in diameter. The variations were however small, with diameter changing by ± 0.2 μm at the whole ring level from the sample mean for all trees, representing a change of ± 0.5 %. Similar changes were observed in the transition-wood. In the tangential direction larger differences between mean values were displayed in stems of different growth rates. All were found to be statistically significant in the results of t-tests and showed an increase in diameter with faster growth. Changes for whole ring values from the sample mean were of the order of ± 2 %, representing a change in diameter of ± 0.5 μm, with similar results observed in all regions of the growth ring. The magnitude of the changes in diameter observed here are small given the 1.29 μm pixel size of the SilviScan-3 system described in Section 3.5.3.1. As such, it is likely that some of the variation in the diameters between slower and faster growing stems lies within the margin of error of the system. However the fact that in a number of cases statistically significant increases in diameter with faster growth was observed indicates that some small differences are likely.

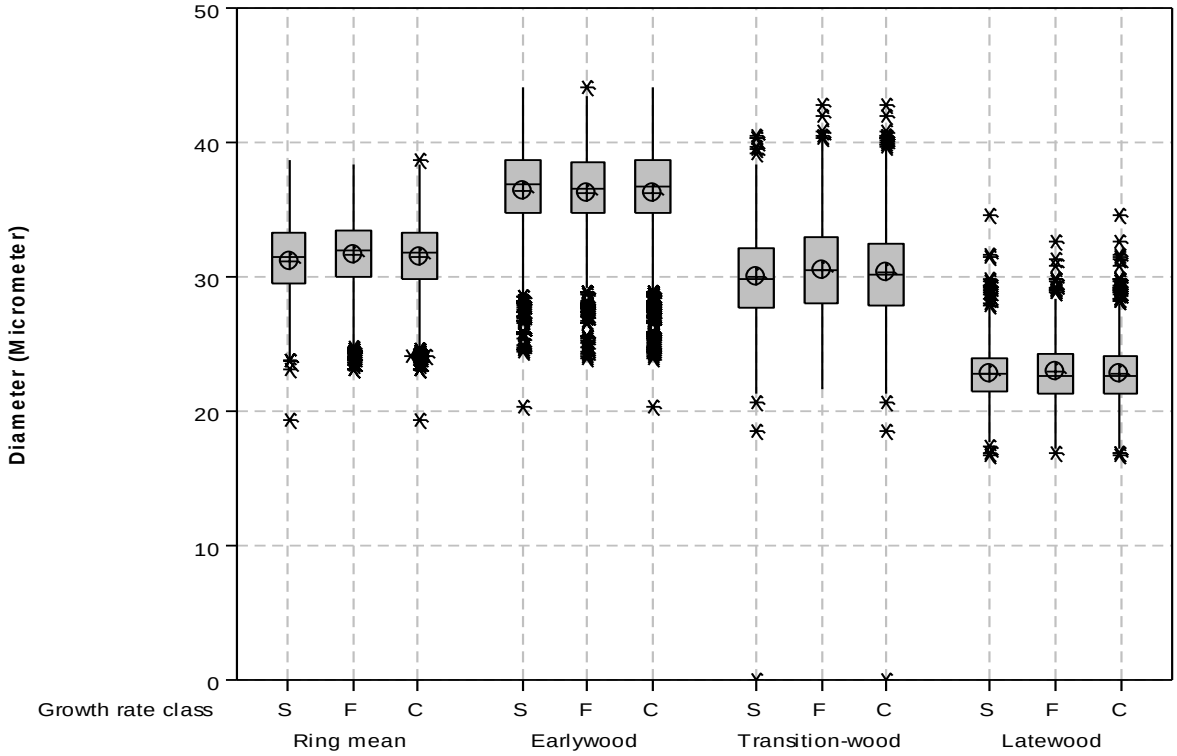

Figure 5-11: Whole stem radial tracheid diameters in slower (S) and faster (F) growing trees and in combination (C) within 40 - 50 year old sample trees

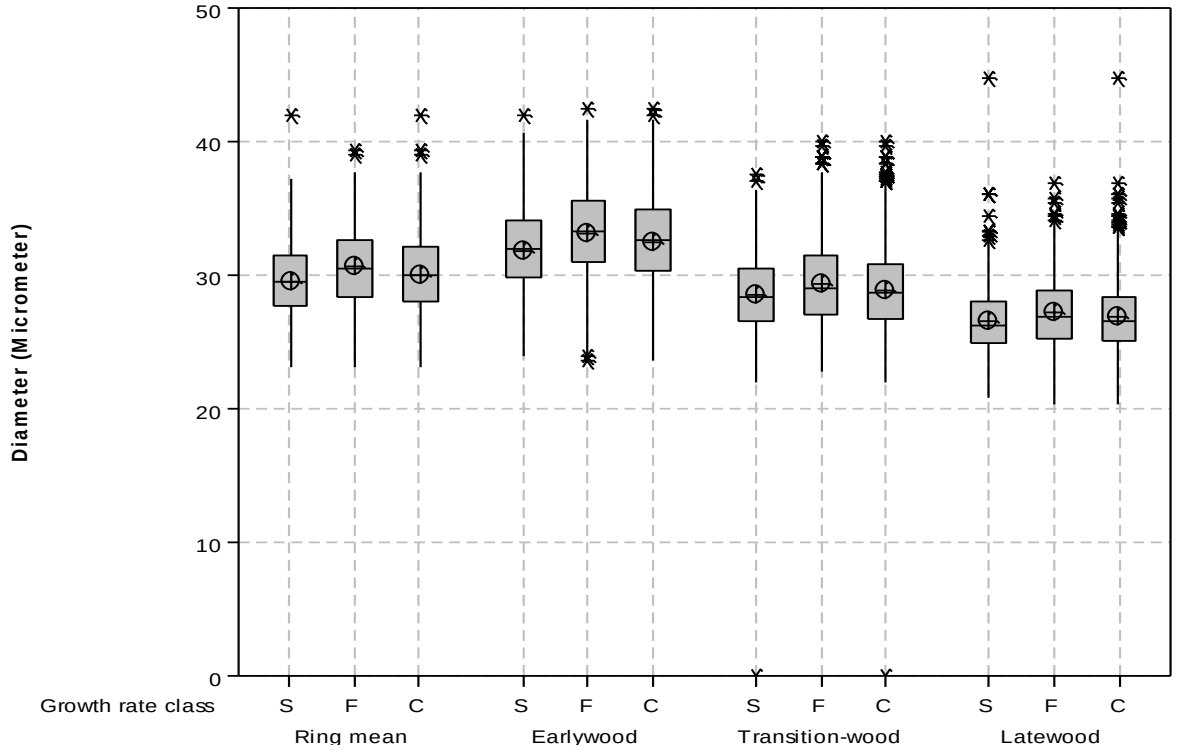

Figure 5-12: Whole stem tangential tracheid diameters in slower (S) and faster (F) growing trees and in combination (C) within 40 - 50 year old sample trees

At the site level, separating the six trees felled at each of the four main sampling sites for 40 - 50 year old trees into either slower or faster growing returned similar results to those described above. For radial diameters, significant differences in comparing means with a t-test was generally observed for only whole ring and transition-wood values, while tangential diameters displayed significant results in all but one case. Results are presented in Tables B-21 and B-22.

The impact of increased growth rate on tracheid dimensions has been reported for numerous softwood species. In Douglas-fir Erickson and Harrison (1974) found that radial diameter showed an increase of approximately 1 μm while tangential diameter demonstrated a slight decrease when ring width doubled as a result of fertilisation. If the 'late earlywood' tracheids tested by Erickson and Harrison are considered equivalent to the transitional tracheid results reported here, then findings in the radial direction are in agreement. Results in the tangential direction are however contrary to those reported here. The much larger changes in radial diameter seen by Erickson and Harrison may be as a result of the near 100 % increase in rate of growth experienced following fertilisation. In Norway spruce Mäkinen et al (2002) reported a 12 % rise in tracheid diameter when ring width more than doubled, Saren (2004) reported similar results. Denne (1973) showed a strong positive correlation between radial diameter and the rate of shoot elongation in Sitka Spruce saplings, tangential dimension were not evaluated. The majority of findings tend to point towards larger tracheid dimensions with increased growth rate. However, due to the different ways in which changes in growth rate are induced, the different measurement techniques used and the time period over which measurements are taken, direct quantitative comparisons between studies is not possible.

5.2.5 Tracheid radial wall thickness - variation with rate of growth

5.2.5.1 Correlation analysis

Figure 5-13 shows the correlation coefficients for ring width and tracheid radial wall thickness at the whole ring level for individual cambial ages at both 1.3 m and 8 m sampling heights. Correlation coefficients for early, transition and latewood alongside whole ring values are also shown in Tables B-23 to B-26. Very little tracheid wall thickness variation was associated with ring width development at either of the two sampling locations. Whole ring mean wall thickness displayed negative correlation coefficients, indicating a decreasing wall thickness with increasing growth rate. In most cases however statistical significance was not achieved and in the few rings where results were found to be significant correlations were typically weak

($r < 0.5$). As has been observed previously, at young cambial ages adjacent to the pith correlation coefficients were found to approach zero. Results in the early, transition and latewood displayed similar relationships to those observed for whole ring mean values.

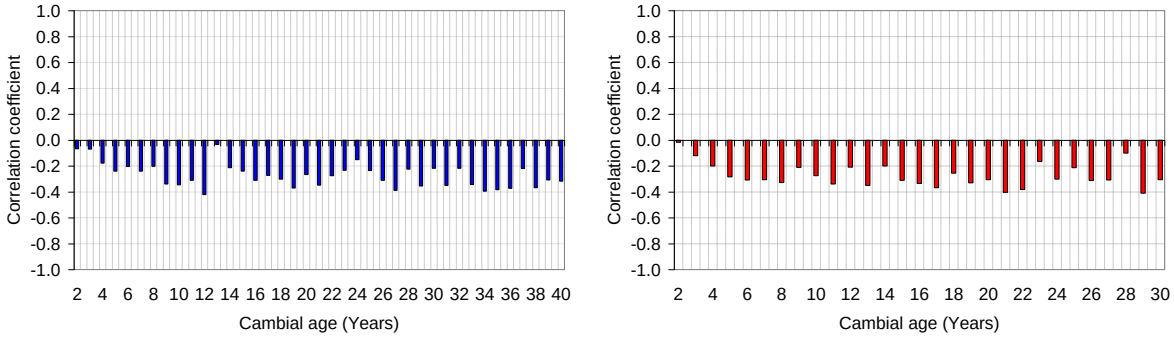

Figure 5-13: Correlation coefficients for whole ring mean tracheid radial wall thickness against ring width for individual growth rings in 40 - 50 year old trees at 1.3 m (L) and 8 m (R)

5.2.5.2 Comparison of means

The box and whisker plots shown in Figure 5-14 illustrate the changes in mean wall thickness within a growth ring for 40 - 50 year old trees, considering values from both 1.3 m and 8 m in combination within stems classified as either slower or faster growing, compared with the sample mean for all trees. Descriptive statistics alongside the results of t-tests comparing the means can be found in Table B-27. At the whole ring level and within early, transition and latewood, t-tests showed that a statistically significant difference existed in wall thicknesses with slower and faster growth. The positive t values indicate a decreasing thickness with increasing growth rate, in agreement with the negative correlation coefficients that were observed previously. However, with changes of less than $\pm$ 0.1 µm from whole sample means, the differences were very small. Given the discussion in Section 3.5.3.2 regarding the accuracy of the wall thickness measurement utilising SilviScan-3 and the small differences observed in values with changing growth rates, firm conclusions regarding the exact magnitude of the changes in wall thickness cannot be made. However from the results presented it can be concluded that no sizeable divergence in values between trees occurs within the range of ring widths presented here.

At the site level, separating the six trees felled at each of the four main sampling sites for 40 - 50 year old trees into either slower or faster growing returned similar results to those described above, with statistically significant positive t-values observed in all but two case. Results are presented in Table B-28.

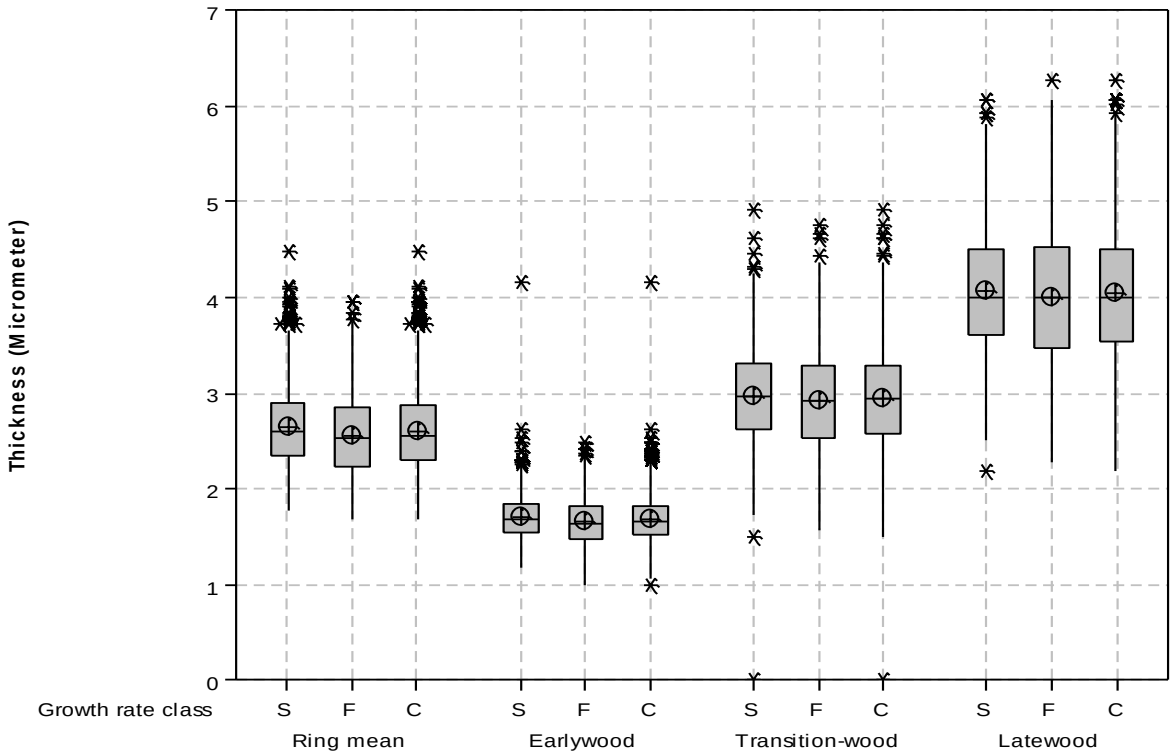

Figure 5-14: Whole stem tracheid radial wall thicknesses in slower (S) and faster (F) growing trees and in combination (C) within 40 - 50 year old sample trees

Previous studies detailing variations in wall thickness with growth rate for Douglas-fir are limited. Brix and Mitchell (1980) found that the cell wall thickness of earlywood increased due to the faster growth rate observed following thinning. This finding is in contradiction to that of most other studies conducted on softwood species which have typically shown either no effect of growth rate on wall thickness, such as the findings in Sitka spruce by Denne (1973), or a decrease in wall thickness being observed for increasing growth rate such as that seen in Norway spruce (Mäkinen et al., 2002, Lundgren, 2004, Saren et al., 2004). As with the radial and tangential tracheid diameter the different ways in which changes in growth rate are induced, the different measurement techniques used and the time period over which measurements are taken make direct comparisons difficult.

5.2.6 Density - variation with rate of growth

5.2.6.1 Correlation analysis

Figure 5-15 shows the correlation coefficients for ring width and mean density at the whole ring level for individual cambial ages at both 1.3 m and 8 m sampling heights. Correlation coefficients for early, transition and latewood alongside whole ring values are also shown in Tables B-29 to B-32. At both locations in the stem the whole ring density was found to

display a negative correlation with respect to ring width, indicating that a higher rate of growth leads to reduced density values. Beyond cambial ages of five years most growth rings displayed statistically significant correlation coefficients in the range 0.4 to 0.6 at both stem heights, signifying the existence of a weak to moderate linear relationship. Below five years of age correlations were found to be weaker and in most instances were non-significant. Negative correlation coefficients were also displayed in the early, transition and latewood. The correlations observed were weaker than those seen at the whole ring level, typically below 0.5, with significance achieved in a limited number of cases.

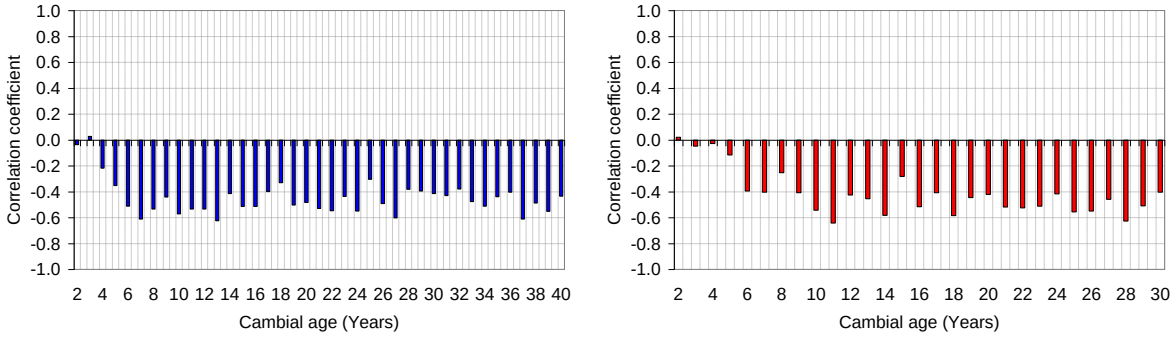

Figure 5-15: Correlation coefficients for whole ring density against ring width for individual growth rings in 40 - 50 year old trees at 1.3 m (L) and 8 m (R)

5.2.6.2 Comparison of means

The box and whisker plots shown in Figure 5-16 illustrate the changes in mean density within a growth ring for 40 - 50 year old trees, considering values from both 1.3 m and 8 m in combination within stems classified as either slower or faster growing, compared with the sample mean for all trees. Descriptive statistics alongside the results of t-tests comparing the means can be found in Table B-33. At the whole ring level and within early, transition and latewood, the results of the t-tests showed that mean values within faster grown trees were statistically significantly lower than those which were slower grown, indicated by the positive values, in agreement with the negative correlation coefficients shown in the previous sub-section. The mean whole ring density was found to show a change of ± 3 % from whole sample mean values with slower and faster growth, equivalent to a change in density of ± 13 kg/m^3. Density variations within individual regions of the growth ring were ± 6 kg/m^3 in the earlywood and ± 8 kg/m^3 within transition and latewood.

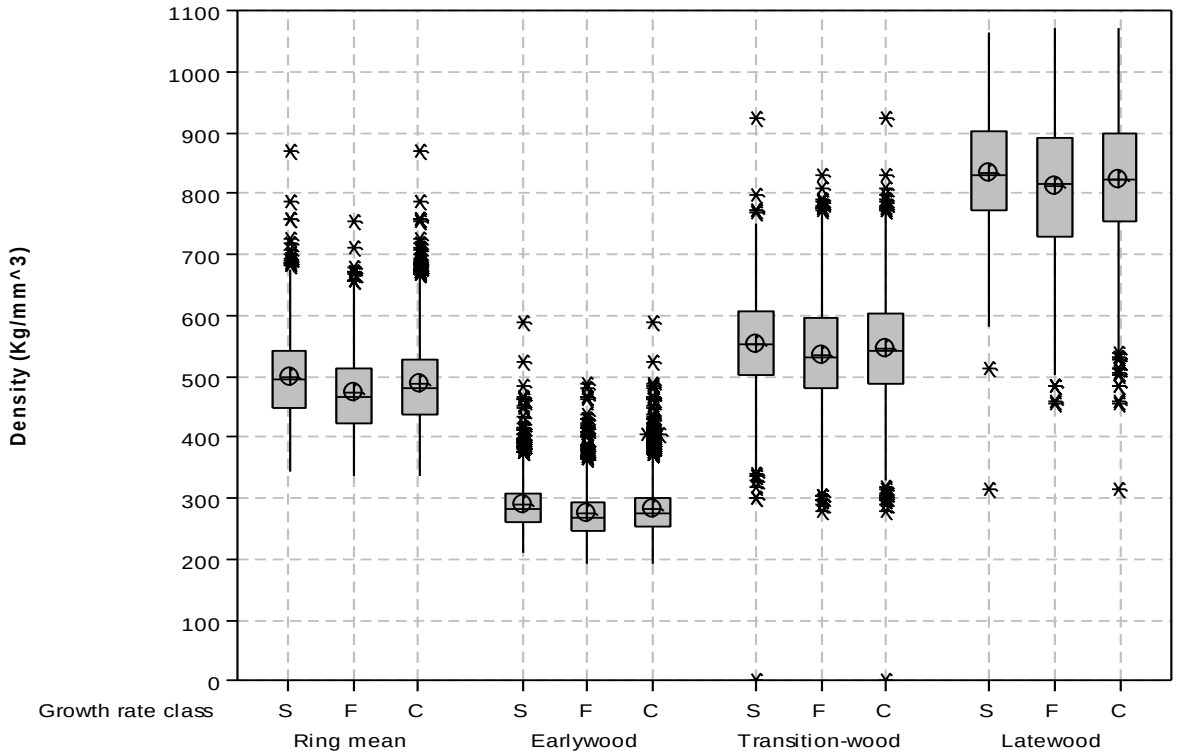

Figure 5-16: Whole stem densities in slower (S) and faster (F) growing trees and in combination (C) within 40 - 50 year old sample trees

At the site level, separating the six trees felled at each of the four main sampling sites for 40 - 50 year old trees into either slower or faster growing returned similar results to those described above, with statistically significant positive t-values observed in all but two cases. Results are presented in Table B-34.

As discussed in Section 2.4.3, the influence of changing rates of growth on wood density has been widely studied. The results presented here, in which a negative relationship with wood density of weak to moderate strength was identified, are in agreement with those found in a number of previous Douglas-fir studies (Erickson and Harrison, 1974, King et al., 1988, Loo-Dinkins et al., 1991, Vargas-Hernandez and Adams, 1991, Fabris, 2000). Abdel-Gadir (1991) reported mixed negative and positive relationships between density and rate of growth within the juvenile and mature wood of Douglas-fir, however as correlations were established across 10 year periods, the natural reduction in ring widths with age, as well as changes in ring width in response to external conditions, may have influenced the results.

5.2.7 Microfibril angle - variation with rate of growth

5.2.7.1 Correlation analysis

Figure 5-17 shows the correlation coefficients for ring width and microfibril angle at the whole ring level for individual cambial ages at both 1.3 m and 8 m sampling heights, including measurements taken utilising both the low and high resolution methods described in Section 3.5.3.3. Correlation coefficients are also shown in Table B-35. In most instances, correlations at both stem heights were positive, indicating an increasing S_2 layer microfibril angle with increasing ring width. However within some growth rings, particularly at younger cambial ages at breast height, a number of negative coefficients were also returned. Overall, coefficients were lower at the 8 m sampling location and statistical significance was achieved in only a limited number of growth rings at either stem height. Due to the limited number of growth rings for which high resolution data was available in early, transition and latewood, a correlation analysis was not conducted for intra-ring variations.

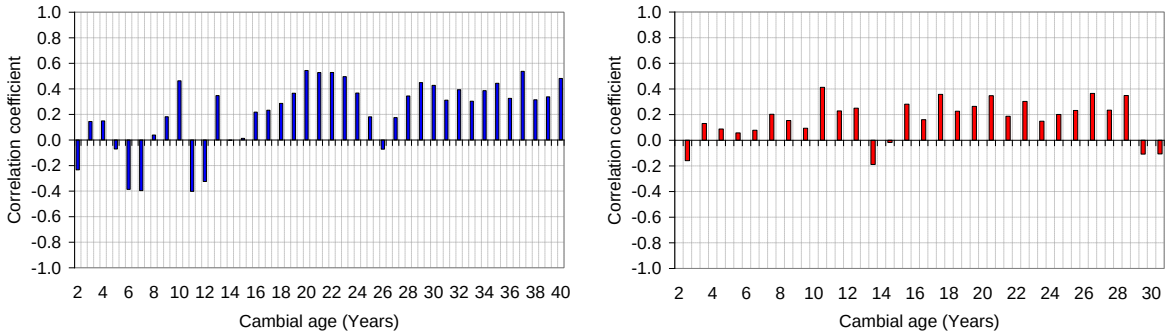

Figure 5-17: Correlation coefficients for whole ring mean microfibril angle against ring width for individual growth rings in 40 - 50 year old trees at 1.3 m (L) and 8 m (R)

5.2.7.2 Comparison of means

The changes in mean microfibril angle values in trees that were slower and faster growing were compared separately for low and high resolution results. The box and whisker plots in Figure 5-18 shows the difference in mean whole ring microfibril angle for 40 - 50 year old trees utilising low resolution data, considering values from both 1.3 m and 8 m in combination. Figure 5-19 shows results at the whole ring level and in the early, transition and latewood utilising high resolution data for 40 - 50 year old trees. Descriptive statistics alongside the results of t-tests comparing the means can be found in Tables B-36 and B-37. Results from low resolution scans showed that mean values in faster grown trees exhibited an increase of approximately 2 % from whole sample values, with equal and opposite results

returned for slower growing stems. This difference was however small, equating to approximately ± 0.5°, with the results of the t-test also showing that it was not statistically significant. Higher resolution results showed a decrease in microfibril angle in the faster growing stems at the whole ring level, with a difference from the sample mean of the six trees assessed of ± 5 %, equating to a change of approximately ± 1°. Declines with faster growth of a similar magnitude were observed at all regions within the growth ring, with all differences in mean values besides those within the transition-wood shown to be statistically significant in the results of the t-tests.

The contradictory results observed between the low and high resolution data may be due to several factors. Firstly, the scanning interval of 2 mm used for the low resolution data, while suitable for the establishment of trends with age, is likely not high enough for use in assessing the influence of growth rate, due to the wide variability in the region of the growth ring assessed at each scanning interval. Secondly, on inspection of the microfibril angle results for each of the individual trees used for the collection of higher resolution data, it was found that one classified as slower growing had microfibril angle values that were uncharacteristically high compared to the other trees within the sample. Due to this and the small number of trees in the sample, the results from the high resolution tests may not be reliable. These factors also apply to the results of the correlation analysis, and as such definitive conclusions cannot be drawn from the results presented.

At the site level, separating the six trees felled at each of the three main sampling sites for 40 - 50 year old trees for which low resolution scans were conducted into either slower or faster growing, showed no statistically significant differences in whole ring mean microfibril angles in the results of the t-tests at any of the sites. Results are presented in Table B-38.

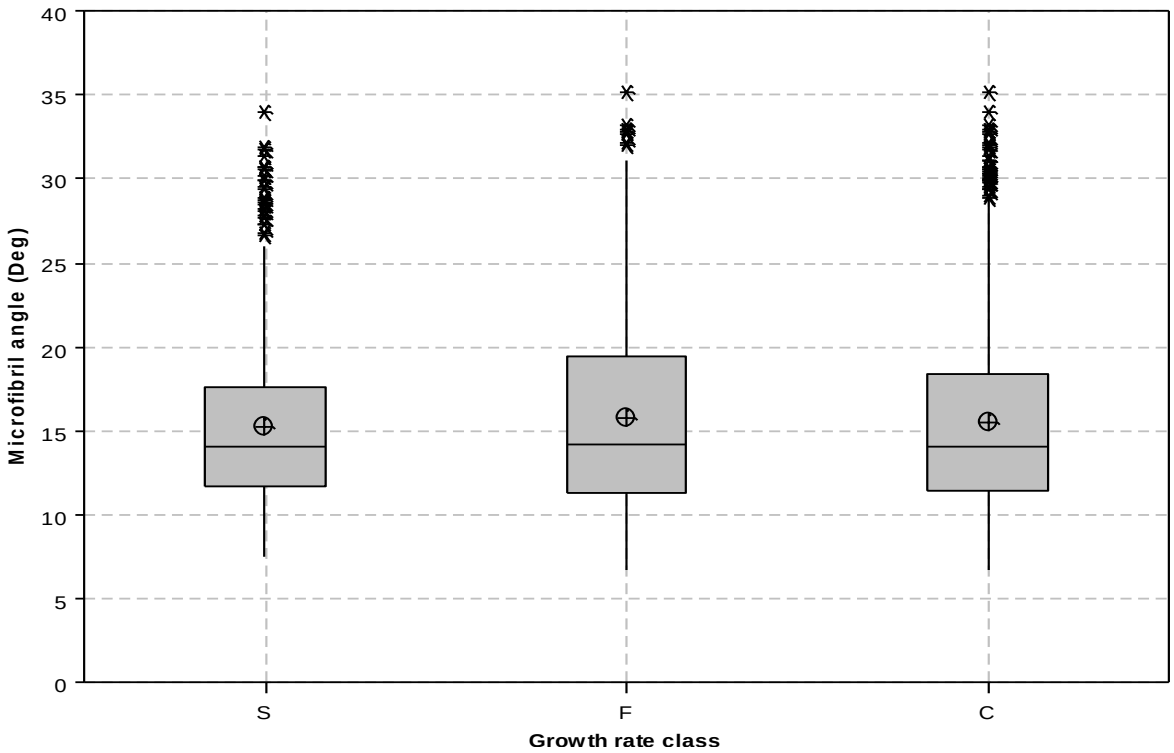

Figure 5-18: Whole stem microfibril angles in slower (S) and faster (F) growing trees and in combination (C) obtained within 40 - 50 year old sample trees using low resolution scanning

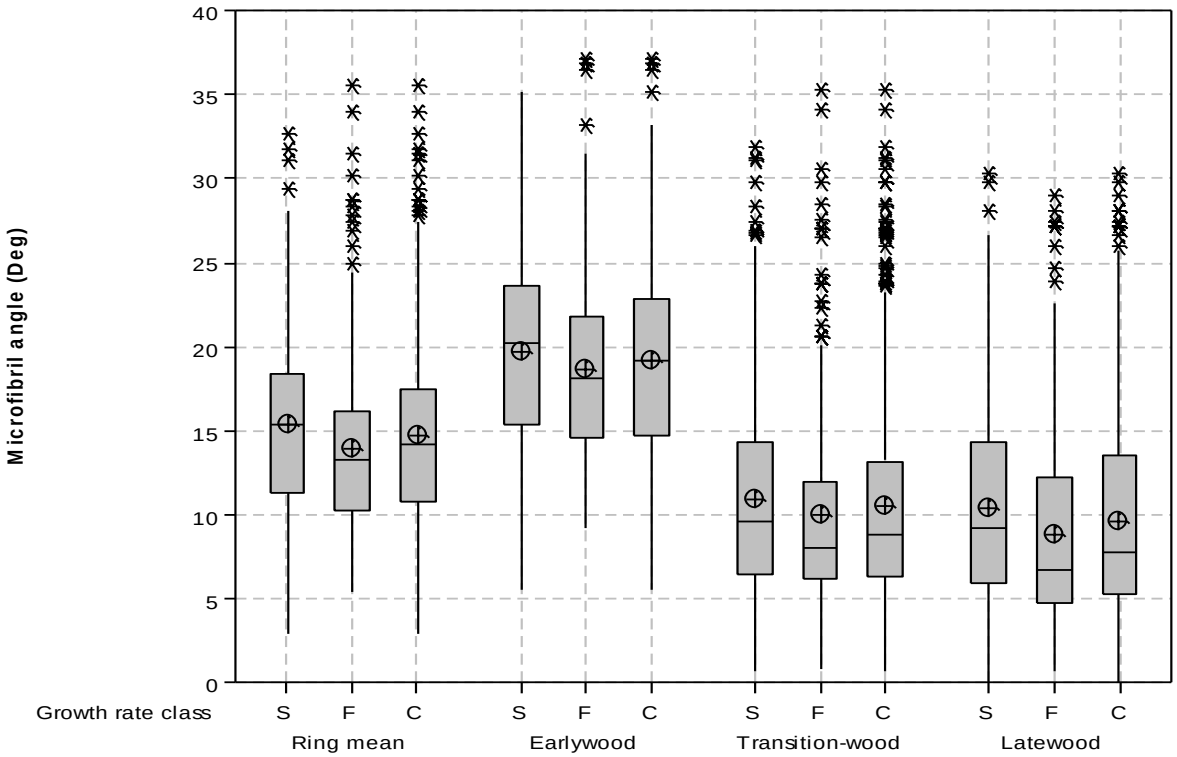

Figure 5-19: Whole stem microfibril angles in slower (S) and faster (F) growing trees and in combination (C) obtained within 40 - 50 year old sample trees using high resolution scanning

Tests conducted by Erickson and Arima (1974) and Fabris (2000) have pointed to the existence of a positive relationship between microfibril angle and growth rate in Douglas-fir. The increase in fibril angle observed by Erickson and Arima was relatively small at approximately 10 %, when compared with the near 100 % increase observed in ring width in the two years following fertilisation. The results presented by Fabris also displayed positive correlation coefficients between microfibril angle and increasing ring width of a similar magnitude to those observed here. The methodologies utilised in both of these past studies were susceptible to some of the limitations in measuring microfibril angle as found in the current study, limiting the ability to exactly quantify the interaction between microfibril angle and growth rate. Positive relationships between microfibril angle and growth rate have also been reported for Norway spruce (Herman et al., 1999), Sitka spruce (Cameron et al., 2005) and Radiata Pine (Downes et al., 2002).

5.2.8 Discussion of results showing the influence of rate of growth on anatomical properties

The objectives of this section of the study were to identify and quantify the impact of changing rates of growth, within and between trees, on wood anatomical properties. In doing this two hypotheses were tested, the null hypotheses of which were:

> $H_{5\text{-}1}$: There is no statistically significant linear relationship between ring width and the magnitude of the studied property for a given growth ring.
>
> $H_{5\text{-}2}$: There is no statistically significant difference between the mean values of studied properties in slower and faster grown trees.

Considering the profiles of correlation coefficients with cambial age displayed for each individual anatomical characteristic, large variations were observed in the levels of significance achieved both between growth rings for a given anatomical property and between the properties themselves. For earlywood proportion, radial tracheid diameters, wall thicknesses and microfibril angle at 8 m, a large number of the growth rings assessed were found to have no statistically significant relationship with ring width, and as such the hypothesis stated above holds for most growth rings. It was also typically found for most properties that this hypothesis was accepted below five to ten years of age, where correlation coefficients were found to be particularly weak. In cases where a statistically significant linear relationship was achieved, the alternative hypothesis, that there is a linear relationship between ring width and the magnitude of the studied property for a given growth ring, is accepted.

The second hypothesis tested looked at the impact of growth rate at a larger scale, by splitting trees into either slower or faster growing categories and comparing the means of the results attained. In the cases of all anatomical properties, aside from earlywood proportion, early and latewood radial tracheid diameters and microfibril angle at the whole ring level for low resolution results and within transition-wood for high resolution, a statistically significant difference was found to exist between the mean values of the two stem growth rate categories. In these cases, the null hypothesis stated in $H_{5\text{-}2}$ is rejected and the alternative hypothesis, that a statistically significant difference between the mean values in slower and faster growing trees exists, accepted.

In order to understand the changes occurring in the anatomical properties of trees growing at different rates, it is first necessary to gain an understanding of the drivers of this differential in growth rate. The development of wood properties is a complex process that is controlled by multiple factors such as genetics, geographic location, silvicultural practices and maturation processes (Macdonald and Hubert, 2002). The anatomical properties of the test stems used here have been shown in Chapter 4 to be relatively consistent between sites, with the differences observed potentially associated with a number of site level factors. The largest variations in ring widths, and hence growth rate, between trees was therefore found within sites, as a consequence of the sampling methodology used. The results in Table B-39 show the mean live crown ratios[1] for all sample trees in the 40 - 50 year age range and then separately for the slower and faster grown categories. It is clear from these results that the crown ratio was greater in the trees classified as faster growing. It is believed that this difference in live crown ratio is the primary cause of the differences in anatomical properties observed between slower and faster grown trees in the results shown previously.

An excellent description of the stand dynamics which lead to this differential in crown ratios is given by Fabris (2000), a summary of which follows. Within even age sites such as those used for the sampling of 40 - 50 year old trees in this study, all trees can initially be classified as being open grown following planting. As the trees within a site grow both radially and longitudinally, the lower branches meet and overlap, with branch death eventually occurring due to a lack of available light. This process continues as the vertical growth of the tree proceeds and complete crown cover is maintained. Where growth continues at the same rate in all trees, crown dimensions across a site are likely to remain broadly similar (Oliver et al., 1997). However in many instances growth does not proceed at an even rate among trees, as a

[1] Crown ratio is calculated by dividing the length of the live crown by tree height.

result of this, different crown classes exist within a stand, with the more dominant trees getting the largest amount of direct sunlight, with these trees therefore typically found to have the greatest crown ratio, whilst suppressed trees get little direct light and consequently have smaller crowns. In the case of severely suppressed trees, mortality can occur. In selecting trees from a wide range of growth rates within even age sites, the sample trees used here are likely to have contained trees tending towards both the suppressed and dominant crown classes, evident from the live crown ratio ranges for each site given in Table B-40.

Consequences of smaller crown ratios are limited ability to photosynthesise due to reduced foliage and reduced concentrations of the phytohormone IAA within the stem, a result of limited bud development. As was described in Section 4.8, IAA is thought to be in part responsible for the promotion of cell expansion. As a result of these two factors, suppressed trees appear to exhibit more abrupt transitions from early to latewood (Larson, 1973) as well as having less active cambiums and consequently narrower growth ring widths. The more abrupt transition from early to latewood was clearly evident in the results shown in Section 5.2.3, in which the latewood proportion in the slower grown trees was shown to increase. Small differences were observed in the tracheid diameters and wall thicknesses between stems of different growth rates, most likely as a result of higher IAA concentrations in faster growing trees promoting a greater degree of cell expansion, and the tracheids in the slower growing trees spending longer in the secondary cell wall development stage. Consequently, the increases in density observed in slower growing stems displayed in Figure 5-16 occurred as a result of increasing density within the individual constituent parts of the growth ring, due increases in the cell wall material per unit area, and also due to the increase in proportions of denser latewood tracheids. This is evident from the greater increase in density that was found at the whole ring level than was observed within the individual regions of the growth ring. The increased proportion of latewood may have also accounted for some of the differences in microfibril angle observed between slower and faster growing stems in the low resolution data, however without more detailed information regarding intra-ring variations, specific quantifications cannot be made. This increase in latewood proportion in slower grown stems also accounts for the reason that the strength of the linear relationship between a studied property and ring width was in most cases greater at the whole ring level than within the individual constituent regions within the growth ring. The correlation analysis also showed that, in the case of most properties studied, there was no statistically significant relationship with ring width in the early years of growth. Similar results were presented for Douglas-fir by Fabris (2000) for several anatomical properties. These results are likely due to the limited

differences between young stems, with the characteristics of the tracheids produced by a young cambium largely heritable and aimed at resisting the potentially damaging forces discussed in Section 4.8.

In the studies discussed previously, following the presentation of results for individual anatomical properties, it was noted that in many cases the response of properties to changes in the rate of growth was more severe than that reported here. The probable reason for this is the fact that in many of these studies, accelerated growth was as a result of the application of fertilisers, which was observed to cause a substantially larger differential between the rates of growth in control and test trees than was seen between the mean values of slower and faster grown trees in this study. This highlights the complexities of quantifying the impact of growth rate on anatomical properties.

5.3 Determination of demarcation age from juvenile to mature wood production

5.3.1 Outline

In this section the age of demarcation between juvenile and mature wood in the Douglas-fir sample trees within the 40 - 50 year age range is evaluated. Juvenile wood is that which is formed within the live crown by a young cambium and is typified in softwoods as having lower density, higher microfibril angle and lower latewood proportion than seen within the mature wood (Panshin and Zeeuw, 1980). As will be demonstrated in Chapter 7, these characteristics are typically associated with inferior mechanical properties. As a result of this, juvenile wood is often regarded as being of inferior quality to mature wood for the production of sawn structural timber. The first objective of the analysis conducted here was to determine the mean and range of demarcation ages from juvenile to mature wood production in the test stems, as a function of both whole ring mean microfibril angle and density. In doing so two hypotheses were tested, the null hypotheses of which were:

> $H_{5\text{-}3}$: There is no statistically significant difference in the age of demarcation from juvenile to mature wood of the studied property between the 1.3 m and 8 m sampling location.
>
> $H_{5\text{-}4}$: There is no statistically significant difference between the ages of demarcation from juvenile to mature wood observed between microfibril angle and density.

Following this, the impact of rate of growth on the demarcation ages for both microfibril angle and density was evaluated. Gaining an understanding of the impact that the rate of growth can have on the duration that juvenile wood is produced is important, as it could have implications regarding the use of certain silvicultural practices. In order to evaluate the effect of growth rate on the demarcation age, sample trees were categorised as either slower or faster growing, as conducted in Section 5.2, utilising the methodology described in Section 3.7.

The following null hypothesis was then tested:

> $H_{5\text{-}5}$: There is no statistically significant difference in the mean values of demarcation age of studied properties in trees categorised as slower or faster growing.

The statistical significance of all results was evaluated using the t-test method outlined in Section 3.10.5, with results classified as significant where $P \leq 0.05$. The results of each test can be found alongside the descriptive statistics in Appendix B, as indicated at the start of each sub-section. The methodology used to identify the age of demarcation between juvenile and mature wood is detailed in Section 3.10.6.

5.3.2 Density demarcation age

The box and whisker plots in Figure 5-20 show the mean and range of transition ages calculated in each sample tree in the 40 - 50 year age range at the two sampling heights, with respect to whole ring density. Descriptive statistics alongside the results of t-tests comparing the means at the two heights can be found in Tables B-41 and B-42.

The segmented regression model used to estimate the demarcation age from juvenile to mature wood with respect to density was found to fit the data well in most instances. In four cases no obvious transition point from juvenile to mature wood could be found and as a result of this no demarcation age was determined. In all specimens this was found to be as a result of a steady increase in whole ring density values from the pith outwards. Confidence intervals were not as narrow as those seen within microfibril angle results to be shown in the following sub-section, with the lower and upper confidence intervals from predicted demarcation ages in the range of 2 - 8 years with a mean of 4 years at both sampling heights. The reason for the higher confidence intervals in the density measurements is most likely due to the more gradual transition from juvenile to mature traits compared to the microfibril angle profiles, together with the large inter-ring differences in whole ring density which were commonly observed between adjacent growth rings.

The mean transition age was found to be greater at the 1.3 m sampling location than at 8 m, with values of 19 and 14 years respectively. The range of transition ages was also found to be broad, with values of 9 - 30 years and 6 - 29 years at 1.3 m and 8 m. The results of the t-test showed that the differences observed in the mean demarcation ages at the two heights were statistically significant.

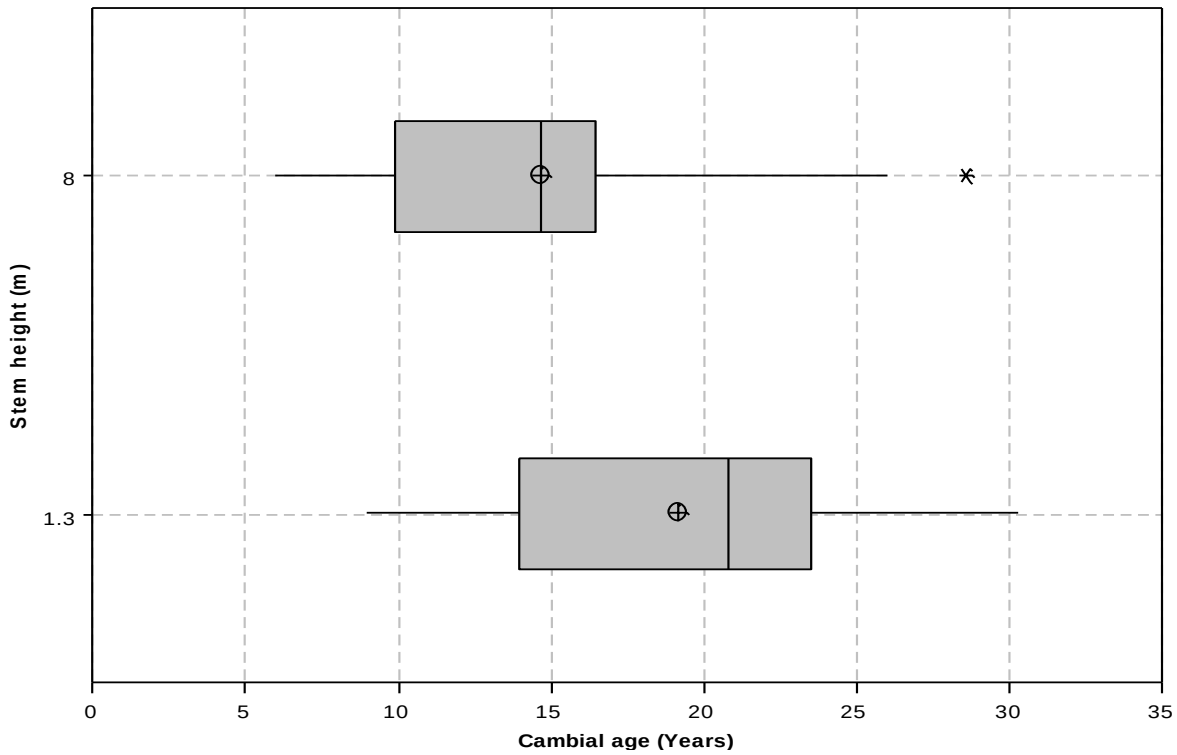

Figure 5-20: Density juvenile to mature wood demarcation age variations in 40 - 50 years old trees

The range of methodologies used to determine the demarcation age between juvenile and mature wood, alongside the fact that assessments may be conducted at different longitudinal locations within the stem, means that a large degree of variability in results would be expected when comparing findings with previous studies, even before phenotypic differences are considered. Despite this, the results presented here are in line with those recorded in studies which have also compared demarcation ages from the perspective of whole ring density in Douglas-fir, conducted by Wellwood and Smith (1962), Di Lucca (1989), Abdel-Gadir and Krahmer (1993) and Fabris (2000). The results presented by Fabris also displayed a general trend of decreasing demarcation age with increasing height within the stem.

5.3.3 Microfibril angle demarcation age

The box and whisker plots in Figure 5-21 show the mean and range of transition ages calculated in each sample tree in the 40 - 50 year age range at the two sampling heights, with respect to whole ring mean microfibril angle. Descriptive statistics alongside the results of t-tests comparing the means at the two heights and the results obtained for density and microfibril angle can be found in Tables B-41 to B-43.

The segmented regression model used to estimate the transition age from juvenile to mature wood with respect to microfibril angle returned strong results. In all but two instances microfibril angle development showed a very clear decrease in its rate of change, indicting a transition from juvenile to mature wood by the definition used here. The decrease in rate of change typically occurred over a period of just a few years, after which time inter-ring variations in microfibril angle were much reduced. The model was therefore able to provide a good fit to the data, with the lower and upper confidence intervals from predicted values ranging between 1 - 4 years with a mean of 2 and 3 years at 1.3 and 8 m respectively. The two cases in which no model fit with the data could be attained were as a result of no apparent demarcation point between juvenile and mature wood existing in the microfibril angle developmental profile, with near constant decreases observed from pith to bark.

The mean transition age for microfibril angle at breast height was found to be 16 years, with a transition age of 12 years recorded at the 8 m sampling location. The range of mean values was 11 - 25 and 6 - 21 years at 1.3 m and 8 m respectively. In virtually all instances the transition age at breast height was observed to be greater than that found at 8 m within the same tree. The results of the t-test showed that the differences observed in the mean values from the two stem heights were statistically significant, as shown in Table B-42. The mean demarcation ages at both stem heights were found to be lower with respect to microfibril angle than density. The results of t-tests shown in Table B-43 showed that these differences were statistically significant at both sampling heights.

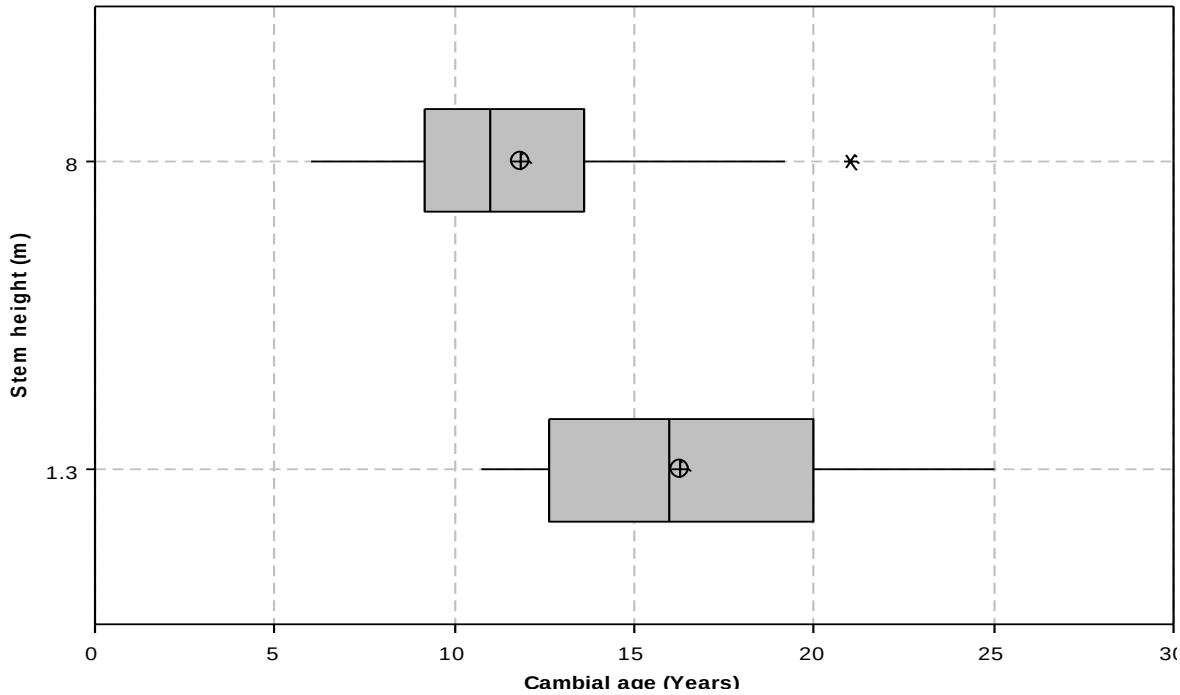

Figure 5-21: Microfibril angle juvenile to mature wood demarcation age variations in 40 - 50 years old trees

Previous studies in the literature evaluating the transition age from juvenile to mature wood with respect to microfibril angle are limited. This is most likely due to the difficulty associated with measuring the microfibril angle compared to other anatomical properties as noted by Fabris (2000), who was unable to assess demarcation age for microfibril angle in Douglas-fir due to an insufficient quantity of measurements. In Loblolly pine (Clark et al., 2006) and Lodgepole pine (Mansfield et al., 2009), the age of transition from juvenile to mature wood with respect to microfibril angle and density was assessed and in both cases the microfibril angle demarcation age was found to be lower, in line with the findings reported here. A more common practice conducted in many evaluations, is to determine the demarcation age between juvenile and mature wood for a more easily assessed property, such as density, and then to report the mean values of microfibril angle within each wood type given the ages determined (e.g. Bao et al., 2001). When assessed in this way microfibril angle is commonly found to fall between juvenile and mature wood, which is to be expected given the findings reported in Section 4.7.

5.3.4 Influence of growth rate on demarcation age

The box and whisker plots in Figures 5-22 and 5-23 show the mean and range of juvenile to mature wood transition ages, assessed on whole ring density and microfibril angle in trees

classified as slower and faster growing at the two sampling heights. Descriptive statistics alongside the results of t-tests are shown in Tables B-44 to B-47.

At both the 1.3 m and 8 m sampling locations the mean demarcation age with respect to density was observed to be lower in the stems of slower grown trees. At 1.3 m the mean transitional age was found to be 17 and 21 years while at 8 m ages were 14 and 16 years in the slower and faster growing trees respectively. The range of demarcation ages observed in all cases was large, however given the findings reported previously in Section 5.3.2 this was to be expected. The results of the t-tests (Table B-45) showed that the differences observed in the mean values between slower and faster growing trees was statistically significant at the 1.3 m sampling location, however at 8 m no significance was achieved.

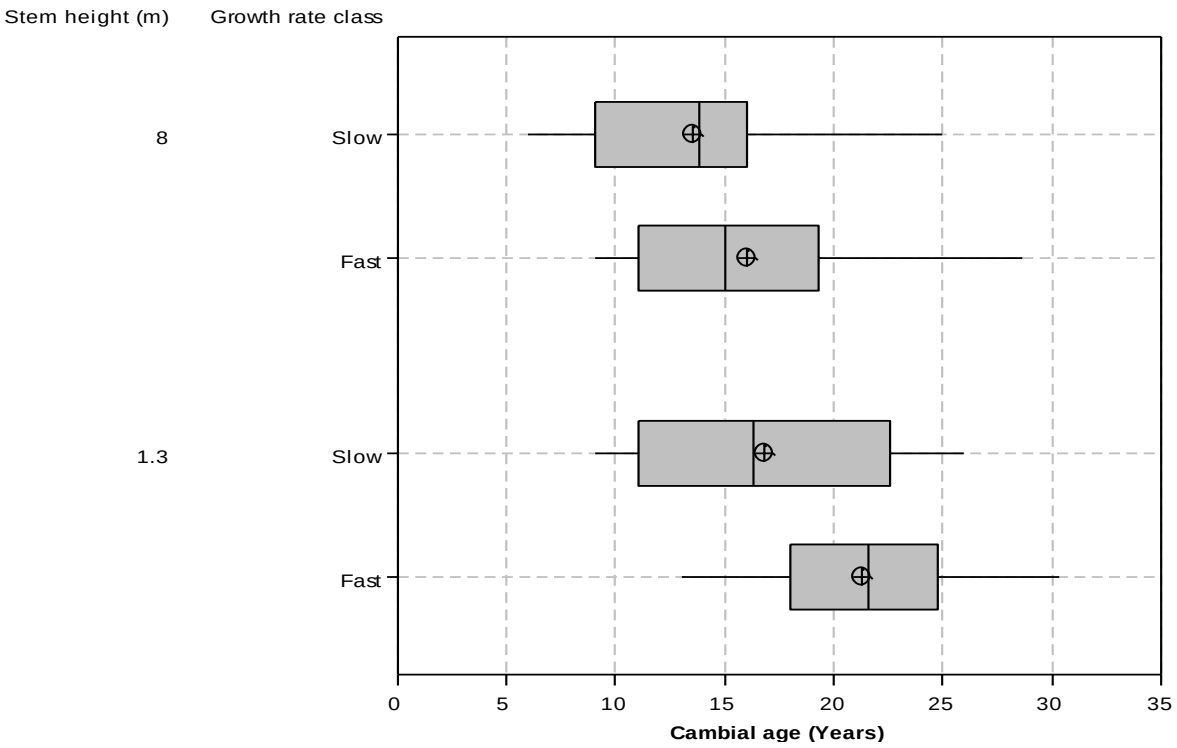

Figure 5-22: Juvenile to mature wood density demarcation age range with slower and faster growth in 40 - 50 year old sample trees

The trends observed in the change of demarcation age with respect to microfibril angle within stems that were classified as being either slower or faster growing followed those seen for density. The mean cambial ages for demarcation at 1.3 m were 15 and 18 years, and at 8 m 10 and 12 years in the slower and faster growing stems respectively. The range of ages at which the transition from juvenile to mature wood was found to occur was large in all cases. At both sampling heights, the results of the t-tests (Table B-47) showed that the mean demarcation

ages found in slower growing trees were statistically significantly lower than those with a greater rate of growth.

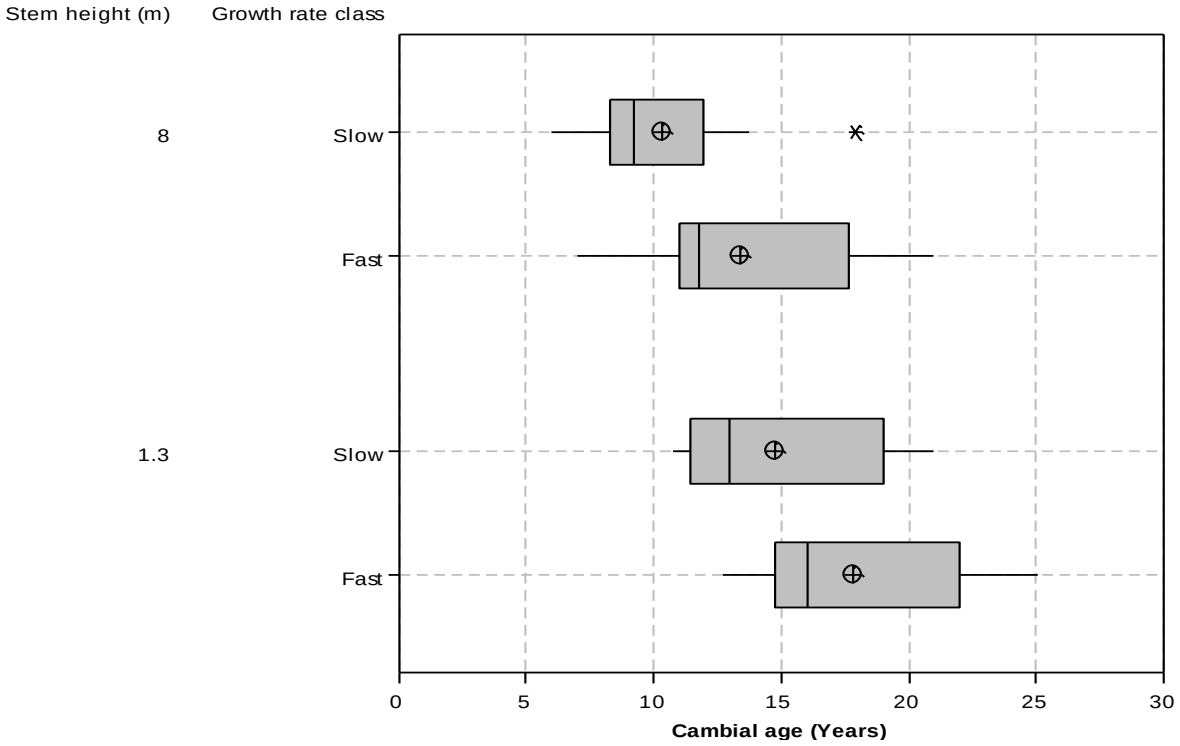

Figure 5-23: Juvenile to mature wood microfibril angle demarcation age range with slower and faster growth in 40 - 50 year old sample trees

5.3.5 Discussion of juvenile to mature wood demarcation age results

The first objective of this section of the study was to determine the means and range of demarcation ages from juvenile to mature wood in sample trees as a function of both whole ring mean density and microfibril angle. In doing this two hypotheses were tested, the null hypotheses of which were:

> $H_{5\text{-}3}$: There is no statistically significant difference in the age of demarcation from juvenile to mature wood of the studied property between the 1.3 m and 8 m sampling location.
>
> $H_{5\text{-}4}$: There is no statistically significant difference between the ages of demarcation from juvenile to mature wood observed between density and microfibril angle.

The results presented in Section 5.3.2 and 5.3.3 showed that in the case of both density and microfibril angle, a statistically significant difference was observed between the values of demarcation age at 1.3 m and 8 m sampling locations. As such, the null hypothesis given in

$H_{5\text{-}3}$ is rejected and the alternative hypothesis, that demarcation ages are statistically significantly different with height is accepted.

In comparing the mean demarcation ages for the two studied properties, it was observed at both stem heights that the mean transition age from juvenile to mature wood was lower for microfibril angle than for density. On carrying out t-tests comparing the mean values, results were statistically significant at both stem heights. Therefore the null hypothesis stated in $H_{5\text{-}4}$ is rejected and the alternative hypothesis, that a statistically significant difference does exist between the ages of demarcation from juvenile to mature wood observed between density and microfibril angle is accepted.

The second objective of this section was to evaluate the impact of changing growth rates within stems on the demarcation ages for the two studied properties. In doing this the following null hypothesis was evaluated:

> $H_{5\text{-}5}$: There is no statistically significant difference in the mean values of demarcation age of studied properties in trees categorised as slower or faster growing.

The results presented in Section 5.3.4 showed that in the case of both density and microfibril angle that mean ages of demarcation were lower in stems that were classified as slower growing in all cases. When these results were evaluated with the use of t-tests, it was found that in all but one case differences observed were statistically significant. As such where no statistical significance was observed the null hypothesis stated in $H_{5\text{-}5}$ is accepted. In all other cases the null hypothesis is rejected and the alternative hypothesis, that there is a statistically significant difference between mean values of demarcation ages of studied properties in trees categorised as slower or faster grown is accepted.

The terms juvenile and mature wood and the existence of an age of demarcation, were developed for practical not biological usage (Gartner et al., 2002). The actual transitional process occurs over a number of years in response to tree and stand growth dynamics. The rate of transition observed with respect to density was found to occur at a slower rate than that for microfibril angle, as such the confidence intervals of models for density were typically higher. Juvenile wood is often thought to be formed within, or in the vicinity of, the live crown. Varying results have been reported regarding the specific position within the stem in relation to the live crown in Douglas-fir by Di Lucca (1989), Fabris (2000) and Gartner et al. (2002). However given the large number of factors which may induce variability between

studies, the lack of an exact quantification is to be expected. A transition from the production of juvenile to mature wood occurs through a combination of a decline in heritable properties such as a large microfibril angle found in early years of growth, as well as the lessening effect of growth inducing hormones, with the distance to the live crown increasing at a specific point as the tree grows in height and crown recession proceeds (Larson, 2001). As described in Section 4.8, this process results in a lessening of the number of transitional tracheids produced and therefore a more definitive boundary between early and latewood. The process of maturation progresses up the stem with each new growth increment. The results presented in Chapter 4 demonstrated that the juvenile wood produced by a younger tree is not the same as that which is produced in the vicinity of the crown of an older tree, due to cambial maturation (Olesen, 1978).

Previous studies in which transitional ages were defined for more than one characteristic have also shown that a common age of demarcation does not exist across different traits (Koubaa et al., 2005, Alteyrac et al., 2006, Clark et al., 2006), in line with the overall findings for density and microfibril angle reported here. Although no consistent difference was observed to occur between the demarcation ages of these two properties within individual trees, values were generally found to lie within a range of five years of each other in the individual sample trees. As such it would appear that the initiation of the move towards the production of tracheids with mature characteristics shares similar environmental cues in the case of both properties. The extensive range of values reported for demarcation ages within each of the anatomical properties studied can be attributed to many factors including the fit of the segmented regression model, variations in the growth rate between trees and phenotypic variability (Abdel-Gadir and Krahmer, 1993).

In the results for both density and microfibril angle presented in Sections 5.3.2 and 5.3.3, statistically significantly lower demarcation ages were observed higher in the stem. From this it can be inferred that the juvenile wood core within the stem is not perfectly cylindrical. As juvenile wood is typically assumed to be formed in the vicinity of the live crown, the same demarcation ages with increasing height in the stem would entail crown recession occurring at the same rate as height growth throughout the life of the tree. In reality, prior to crown closure height growth far exceeds that of crown recession, due to limited shading induced branch mortality. Once crown closure is achieved, crown recession begins at a faster rate and therefore the transition from juvenile to mature wood occurs at a later age lower in the stem (Fabris, 2000).

The early transition to the production of tracheids with mature characteristics from the perspective of both density and microfibril angle in slower grown trees can be related to the crown structure. It was discussed in Section 5.2.8 that trees within the slower growing category, both between and within sites, had a lower live crown ratio than those trees which were faster growing. As a result of competition from surrounding trees and a lower quantity of foliage, it is likely that trees with smaller crown dimensions would experience both reduced hormonal and photosynthetic activity, and consequently the earlier formation of tracheids with mature characteristics. Similar findings to those reported here were also shown in the work of Fabris (2000), where earlier demarcation ages for mean density were observed in trees with suppressed and intermediate crown classes compared to those of dominant trees. It was also observed by Fabris that closely spaced trees had lower demarcation ages due to increased competition. The reduction of the period of juvenile wood production through increased stand density is therefore a viable silvicultural option (Larson, 2001), as is the use of mixed age stand structures in which slow initial growth can be achieved. The potential implication of the results presented on informing management practices is discussed in Section 9.4.2.

In the application of silvicultural practices that may reduce the juvenile to mature wood demarcation age, consideration must also be given to the impact on the quantity of wood produced as a result of decreased productivity of the cambium. The results in Table 5-1 show the mean proportions of juvenile and mature wood within the 40 breast height growth rings common to all younger trees, calculated based on the approximate mean surface areas of each at the 1.3 m sampling locations in the slower and faster grown trees. Juvenile wood areas in each tree were calculated by determining the area of the circle with a radius equivalent to the combined growth ring widths within each juvenile wood zone, with the mean then calculated for the slower and faster growing trees. Mature wood areas were subsequently calculated by determining the area of the circle with a radius equivalent to the combined ring widths for the first 40 growth rings within each tree. The previously calculated juvenile wood areas were then subtracted and the mean mature wood areas calculated for the slower and faster growing trees.

Table 5-1: Proportions and areas of juvenile and mature wood in slower and faster growing trees at the 1.3 m sampling location

Growth rate class	Juvenile/Mature wood proportion (%)	Juvenile wood area (m^2)	Mature wood area (m^2)
Slow	21/79	0.013	0.050
Fast	26/74	0.031	0.089

The results show that the proportion of juvenile wood within slower growing stems was 5 % lower than that observed in those which were faster grown, a result which was expected give the findings presented in Section 5.3.4. The area of juvenile wood in the slower grown stems was also found to be lower. Perhaps the most important finding however is the greater area of mature wood present in the faster growing trees, which was found to be almost double that seen within the slower growing stems. In this case, a consequence of the slower growth that caused a reduction in juvenile wood production is a reduced growth rate in mature growth rings. Consequently, if trees older than 40 - 50 years were assessed it may have been found that the juvenile wood proportion was higher within those that were slower grown. The quantities of material produced, as well as factors relating to the quality of the material, are therefore important considerations when deciding on the implementation of silvicultural practices.

5.4 Concluding remarks

In this chapter the effects of changes in growth rate, primarily induced by stand competition, on several anatomical properties has been shown. Faster growth induced lower latewood proportions, larger tracheids and thinner radial tracheid cell walls when results were analysed within growth rings and at the whole tree level. However, in many instances the changes observed were small. A finding of particular interest that highlights the advantage of separately classifying transition-wood was that which showed that the decreases in latewood proportion observed with faster growth were largely due to increases in transition-wood proportion. A combination of the changes in tracheid proportions and dimensions also resulted in reduced density with faster growth. Due to an insufficient quantity of high resolution data, definitive conclusions regarding the influence of growth rate on microfibril angle cannot be made. It is expected, given the findings of Johansson (1993), Yang and Hazenberg (1994) and Fabris (2000) that the changes in fibre properties reported here are likely to be similar to those observed in response to variations in stand density. As such the results provide an indication of the changes in properties that may be expected under different silvicultural regimes.

The results of a study of demarcation age from juvenile to mature wood led to the conclusions that for both density and microfibril angle lower transitional ages were observed higher in the sample trees, with microfibril angle profiles also exhibiting mature behaviour earlier than those for density. It was also found that trees which were faster grown, largely as a result of stand dynamics, exhibited demarcation ages which were greater than those observed in slower grown trees. A general observation from the study is that the determination of demarcation age utilising segmented regression, or indeed any of the other methods outlined in Section 3.10.6, provide only a theoretical estimate of the transition from the production of juvenile to mature wood. The actual transitional process is rather more gradual and the results presented here therefore provide a practical best estimation of a complex biological process.

Chapter 6 - Mechanical property variations

6.1 Introduction

The large variability observed in wood anatomical properties in Chapter 4 leads to one of the main obstacles associated with the use of timber in structural engineering applications, its lack of consistent and predictable mechanical properties. In this chapter the intra- and inter-tree variations of modulus of elasticity, flexural and compressive strength are evaluated. These three parameters are key to the structural performance of sawn timber and as such the knowledge gained from quantifying their variability improves the potential for more efficient processing and end product utilisation.

The key objectives of the analysis conducted in this chapter are therefore to:

- Quantify the change in mechanical properties with increasing cambial age at the two sampling heights.
- Identify any relationship between mechanical properties and geographic orientation in the stem.
- Determine the impact of rate of growth on mechanical properties.
- Identify the potential implications of the results for the utilisation of Douglas-fir grown in the South West of the United Kingdom as a structural material.

The chapter begins by presenting the failure mechanisms observed in test specimens in Section 6.2, followed by an analysis of the radial and longitudinal variations of properties in Section 6.3. The influence of geographic orientation and growth rate is shown in Sections 6.4 and 6.5, with the relationship between SilviScan-3 predicted modulus of elasticity and the results obtained with use of flexural tests compared in Section 6.6. Finally, the implications of

the results for utilisation are discussed in Section 6.7. A summary of the findings and the conclusions that can be drawn from them is given at the end of the chapter.

6.2 Test specimen failure modes

6.2.1 Flexural specimens

In total 1446 small clear flexural specimens were tested in accordance with the method described in Section 3.6.3 in order to identify variations in modulus of elasticity and flexural strength. Due to the heterogeneous composite nature of timber, it is typical for several different failure modes to be identified when testing multiple specimens utilising the same experimental methodology. The most common types of failure in timber specimens tested in static bending are identified in ASTM standard D 143-94 (ASTM, 2007). As a result of the tensile strength of wood being, on average, greater than the compressive strength (Dinwoodie, 2000), most failure modes commence on the compression side of the specimen due to crushing action, in some instances identifiable by a small fold on the specimen surface. This is followed by ultimate failure occurring in tension. Two primary failure modes were identified during flexural testing, simple tension failure shown in Figures 6-1 and 6-2 and cross grain tension failure shown in Figure 6-3.

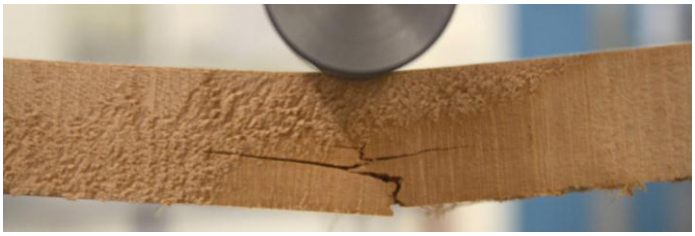

Figure 6-1: Simple tension flexural small clear specimen failure mode

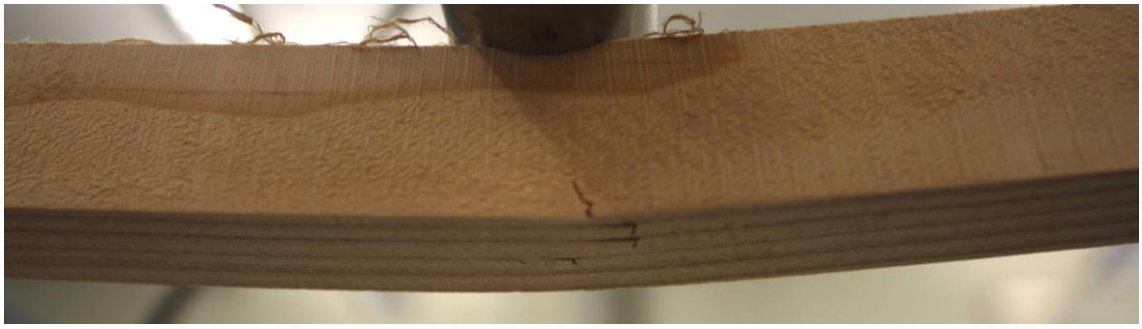

Figure 6-2: Simple tension flexural small clear specimen failure mode underside

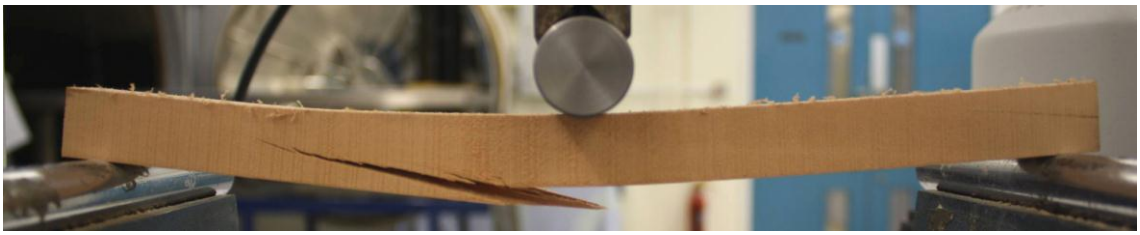

Figure 6-3: Cross grain tension flexural small clear specimen failure mode

The percentage incidence of each failure mode in all flexural test specimens is given in Table 6-1 below. There was no trend evident in the occurrence of a particular failure mode with increasing cambial age or longitudinal position within the stem. There was also no relationship evident with the magnitude of either modulus of elasticity or flexural strength.

Table 6-1: Incidence of failure modes in flexural small clear test specimens

Failure mode	**Percentage incidence (%)**
Simple tension	98 (1419)
Cross grain tension	2 (27)

Note: Number of specimens shown in brackets

The different behaviours exhibited by the two failure modes were as follows. The simple tension failure was characterized by a direct pulling apart of the wood on the underside of the specimen due to tensile stress developing parallel to the grain. When viewed from the underside as shown in Figure 6-2, this typically produced an uneven break, as annual ring density variations acted as crack stoppers. Splits in the wood along the grain then propagated along the length of the specimen from the initial failure site, continuing to grow in length until the test was stopped. The cross grained tension failure shown in Figure 6-3 was caused by a sloping grain resulting in a tensile force acting obliquely to the direction of the grain. In the preparation of test specimens, every effort was made to ensure that the direction of the grain was parallel to the edges of the specimen in order to reduce variation in results that may be caused due to a changing angle. In some cases however it was not possible to visually identify the direction of the grain, as such there were a limited number of specimens that experienced cross grain failure. In these cases the specimens were removed from the analysis in order to preserve the consistency of the dataset.

6.2.2 Compressive specimens

A total of 363 small clear compressive specimens were tested utilising the method described in Section 3.6.5 in order to identify variations in compressive strength parallel to the grain. As discussed previously for flexural specimens, the heterogeneous nature of timber means that, when conducting tests utilising the same experimental setup, it is possible for a range of different failure mechanisms to develop. Opriman and Taranu (2004) describe the most common types of failure occurring when timber specimens are tested in compression parallel to the grain. Of the six failure mechanisms identified by Opriman and Taranu two were encountered whilst conducting the experimental tests, longitudinal splitting and shear failure. The percentage incidence of each type is given in Table 6-2. There was no trend evident in the occurrence of a particular failure mode with increasing cambial age or longitudinal position within the stem. Figure 6-4 shows specimens exhibiting each of the failure modes following testing.

Table 6-2: Incidence of failure modes in compressive small clear specimen tests

Failure mode	Percentage incidence (%)
Shear failure	97 (352)
Longitudinal splitting	3 (11)

Note: Number of specimens shown in brackets

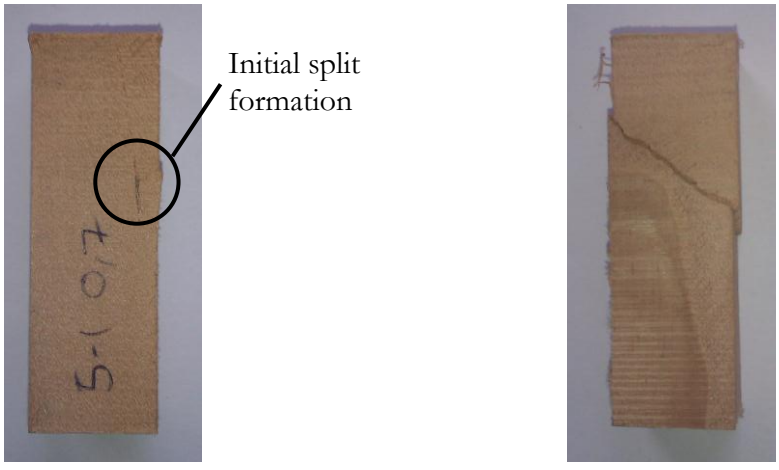

(a) (b)

Figure 6-4: Compressive small clear specimen failure mechanisms (a) Longitudinal splitting (b) Shearing

As can be seen from the percentage incidence of each failure type, virtually all specimens failed as a result of shear failure. The mechanism of failure whereby longitudinal splits formed

in the specimen was considered to occur as a result of a defect within the specimen, such as a high proportion of resin or internal splitting, potentially formed during the initial drying process. It was therefore decided that these specimens did not fulfil the defect free nature of small clear testing and were therefore removed from the results analysis.

When a material is loaded in compression, the greatest shear stress occurs along a plane at an angle of 45° to the direction of loading. As such, a large majority of the small clear compressive specimens were found to have failure planes at, or close to, this angle. At the cellular level a shear failure such as this is initiated when small kinks form within the microfibril structure in the cell wall, typically originating in the fibre wall at the location of rays where the longitudinal cell is displaced vertically to make way for the horizontal running ray. As the strains increase so do the number and magnitude of the kinks, eventually leading to the failure of the specimen (Dinwoodie, 2000). The effect of microstructure and stress state on the behaviour of wood is discussed by Boatright and Garret (1983). The complex composite nature of the material alone can make the prediction of failure modes difficult. This is compounded by the influence that slight changes in orientation of specimen and varying cellular structure both within and between growth rings can have. This explains the wide range of shear plane angles observed alongside the varied location of shear plane development within each specimen.

6.3 Mechanical property variations with age and height

6.3.1 Outline

In the following section, various mechanical properties recorded in tests on small clear specimens are presented. Wood quality is often defined in terms of attributes that make it valuable for a given end use (Jozsa and Middleton, 1994). From a structural engineering perspective, the key attributes are the mechanical properties of the timber produced by a tree. An understanding of the extent to which mechanical properties vary with both age and height in the stem is therefore important in identifying the most appropriate end use and allowing for optimization in processing. Results are reported first for the 24 younger trees in the 40 - 50 year age range, with the continuation of any trends observed then verified in a separate assessment of the older trees with ages > 50 years. Two statistical tests were employed in the analysis of the results, firstly a repeated measures univariate analysis of variance, assessing the statistical significance of differences in the studied properties due to cambial age, tree and site and secondly t-tests, comparing the mean values at the two sampling heights. The results from

both were deemed significant when $P \leq 0.05$. Detailed descriptions of the methods used to obtain the results presented, and the statistical techniques employed to interpret them are given in Chapter 3. In order to allow statistical techniques to be conducted at common intervals, radially and longitudinally, results were grouped by cambial age into the growth periods: 3 - 10, 11 - 20, 21 - 30 and 31 - 40 years[1]. The results of each test can be found with the descriptive statistics in Appendix C, as indicated at the start of each sub-section.

In analysing the results of the statistical tests within each of the growth periods, two hypotheses were tested, the null hypotheses of which were:

> $H_{6\text{-}1}$: No change in the magnitude of the studied property takes place with increasing cambial age.
>
> $H_{6\text{-}2}$: No difference exists in the magnitude of the studied property with increasing longitudinal position in the stem.

6.3.2 Modulus of elasticity - variations with age and height

6.3.2.1 Variations in younger trees

In this sub-section the profiles of mean modulus of elasticity in 40 - 50 year old sample trees are presented. Figure 6-5 shows mean values and the 95th percentile range for specimen modulus of elasticity at the two assessed stem heights, descriptive statistics alongside the results of the analysis of variance and t-tests can be found in Tables C-1 and C-2.

An overall trend of increasing modulus of elasticity with cambial age was observed at both stem heights. The mean values across a growth period were found to increase by 60 % between the first and last assessed at each height, with a mean modulus of elasticity of 11600 - 11800 N/mm^2 recorded in the final growth periods. The developmental profile of modulus of elasticity upon moving away from the pith displayed similar trends at both sampling heights. The lowest results were observed at the youngest cambial ages, with mean values of 5500 - 6000 N/mm^2. Beyond this, the magnitude of results continued to increase at a relatively constant rate until approximately growth ring 15. The analysis of variance showed that a statistically significant difference with cambial age existed in mean modulus of elasticity within the first two growth periods at both 1.3 m and 8 m, confirming the observations made above. Beyond a cambial age of 15, the rate of increase in the modulus was observed to decline. The

[1] The 31-40 year growth period was only present at the 1.3 m sampling location.

results of the analysis of variance showed significant differences between the mean values observed, with cambial age, within the 21 - 30 year growth period, at both stem heights; however the magnitude of the F values was reduced compared with the two previous growth periods. Between cambial ages of 31 - 40 years, at breast height, the rate of increase in values of modulus of elasticity was observed to fall further still, which was in agreement with the analysis of variance results which showed that there was no significant differences in values with cambial age. The mean modulus of elasticity was found to be greater at the 8 m sampling location than at breast height, with differences in growth period means ranging from 500 to 1100 N/mm^2. These differences were found to be statistically significant in the results of the t-tests across all three growth periods.

At each cambial age assessed, results were found to show a relatively large range of modulus of elasticity values. Across the whole dataset, coefficients of variation were in the region of 25 %, showing a decrease with increasing cambial age as the spread of values recorded within a growth period reduced. Mean values and coefficients of variation across all sites were within a similar range, as shown in Table C-3. Consequently, the site factor accounted for less than 10 % of the variation in the analysis of variance, with differences due to trees within a site ranging from approximately 40 - 70 %, with values found to increase in subsequent growth periods as the variation due to error declined.

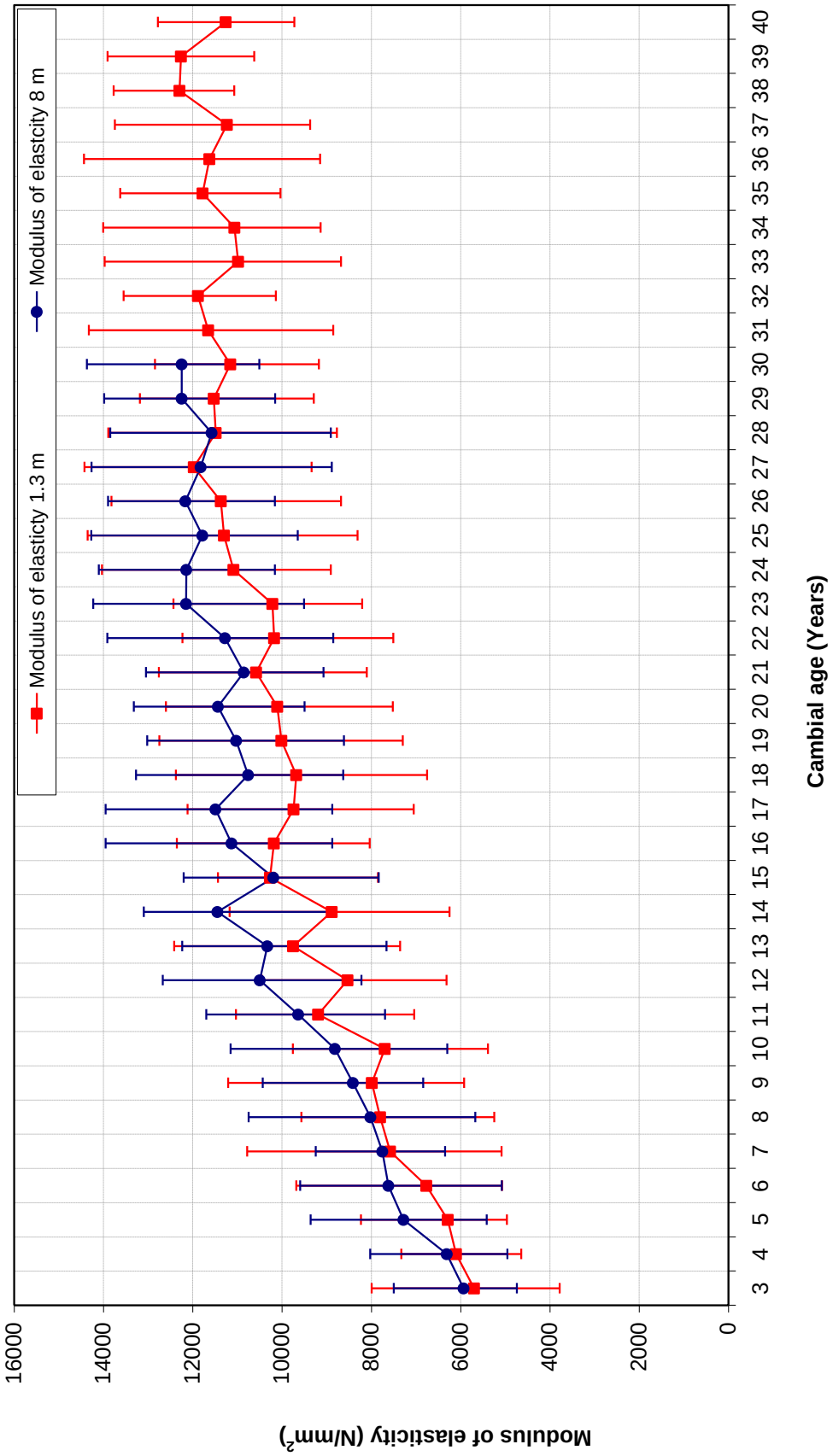

Figure 6-5: Mean modulus of elasticity and 95th percentile range as a function of cambial age at stem heights of 1.3 m and 8 m within younger sample trees

6.3.2.2 Variations in older trees

Figure 6-6 shows the changes in mean modulus of elasticity at both stem heights in older sample trees, up to a cambial age of 72 years. Due to the limited number of older sample trees obtained not all cambial ages were represented in the mean ages calculated for the small clear test specimens. The developmental profile of modulus of elasticity in older trees varied from that seen previously in the larger sample of younger trees, particularly so at breast height, where initial increases in values were found to occur at a significantly greater rate within older stems, before experiencing a decline and further rise. Beyond approximately growth ring 30, results appeared to stabilise, falling in a band with modulus of elasticity values ranging from 11000 - 15000 N/mm^2.

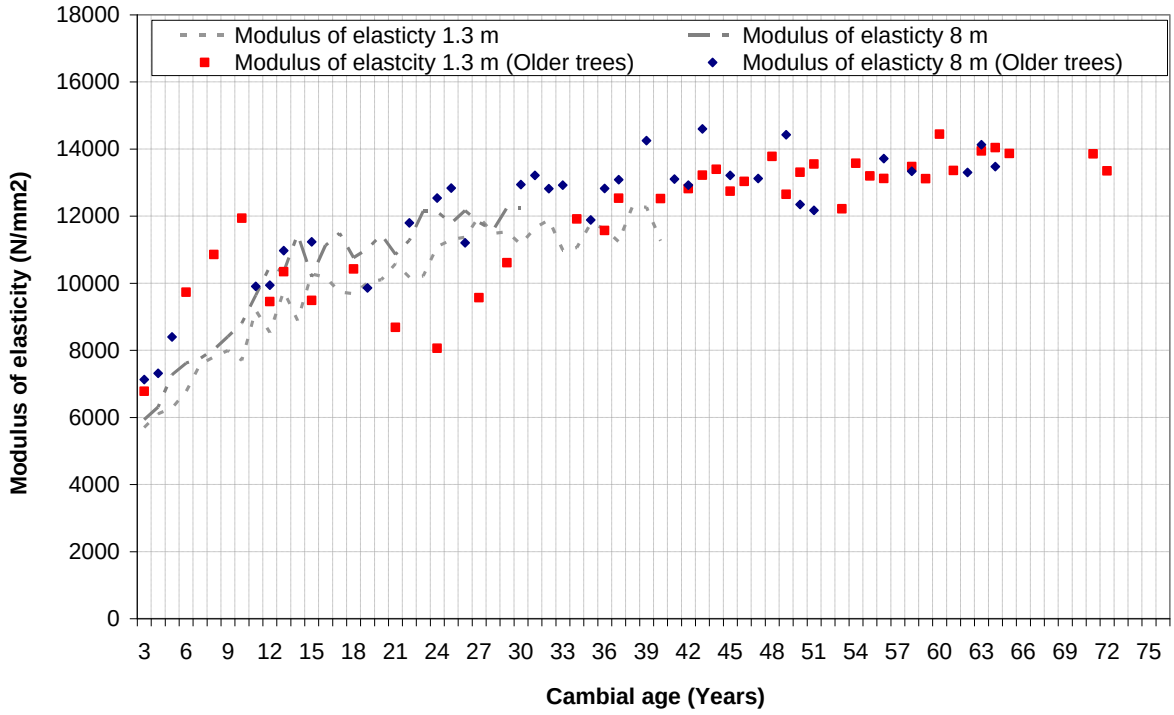

Figure 6-6: Mean modulus of elasticity as a function of cambial age at stem heights of 1.3 m and 8 m within older sample trees

6.3.3 Flexural strength - variations with age and height

6.3.3.1 Variations in younger trees

In this sub-section the profiles of mean flexural strength in 40 - 50 year old sample trees are presented. Figure 6-7 shows mean values and the 95th percentile range for specimen flexural strength at the two assessed stem heights, descriptive statistics alongside the results of the analysis of variance and t-tests can be found in Tables C-4 and C-5.

As observed in the radial development profiles for modulus of elasticity displayed in Figure 6-5, flexural strength exhibited an overall trend of increasing values with time. At approximately 70 %, the change in means for a growth period, from the first to the last assessed at each stem height, was within a similar range to that found for the modulus of elasticity, with flexural strength values in the region of 95 - 100 N/mm^2 in the final growth periods. Upon moving away from the pith, a slight decrease in strength was observed. Consequently, the lowest mean flexural strengths were recorded in the region of growth ring seven, with values of 50 N/mm^2. Beyond this, the magnitude of the results displayed a continuous rise at both stem heights until approximately 20 years of age. Due to the limited difference between the means for different cambial ages within the first growth period, the analysis of variance showed that there was no statistically significant difference in mean flexural strength with cambial age. Within the 11 - 20 year growth period a statistically significant difference was observed at both stems heights. Beyond this, the rate of increase in the flexural strength values of specimens at both sampling heights in the stem reduced. As a result of this, the analysis of variance showed that there was no statistically significant difference in flexural strength with cambial age at 8 m. While F values were statistically significant in the two remaining growth periods at breast height, their magnitudes were lower compared to previous values. This is likely due to a reduction in the deviation of the flexural strength values at each cambial age around the mean for the respective growth periods, in agreement with the observed decline in the rate of increase of flexural strength. Unlike the results seen for modulus of elasticity, t-tests showed that there was no statistically significant difference in the flexural strength with height in any of the three growth periods compared, which agrees with the results that can be observed visually in Figure 6-7.

The mean coefficient of variation for flexural strength was in the region of 20 %, with decreasing values observed as the rate at which strength increased fell. Mean values and coefficients of variation across all sites were within a similar range, as shown in Table C-6. Consequently, the site factor typically accounted for less than 10 % of the variation in the analysis of variance, with differences due to trees within a site ranging from approximately 30 - 60 %.

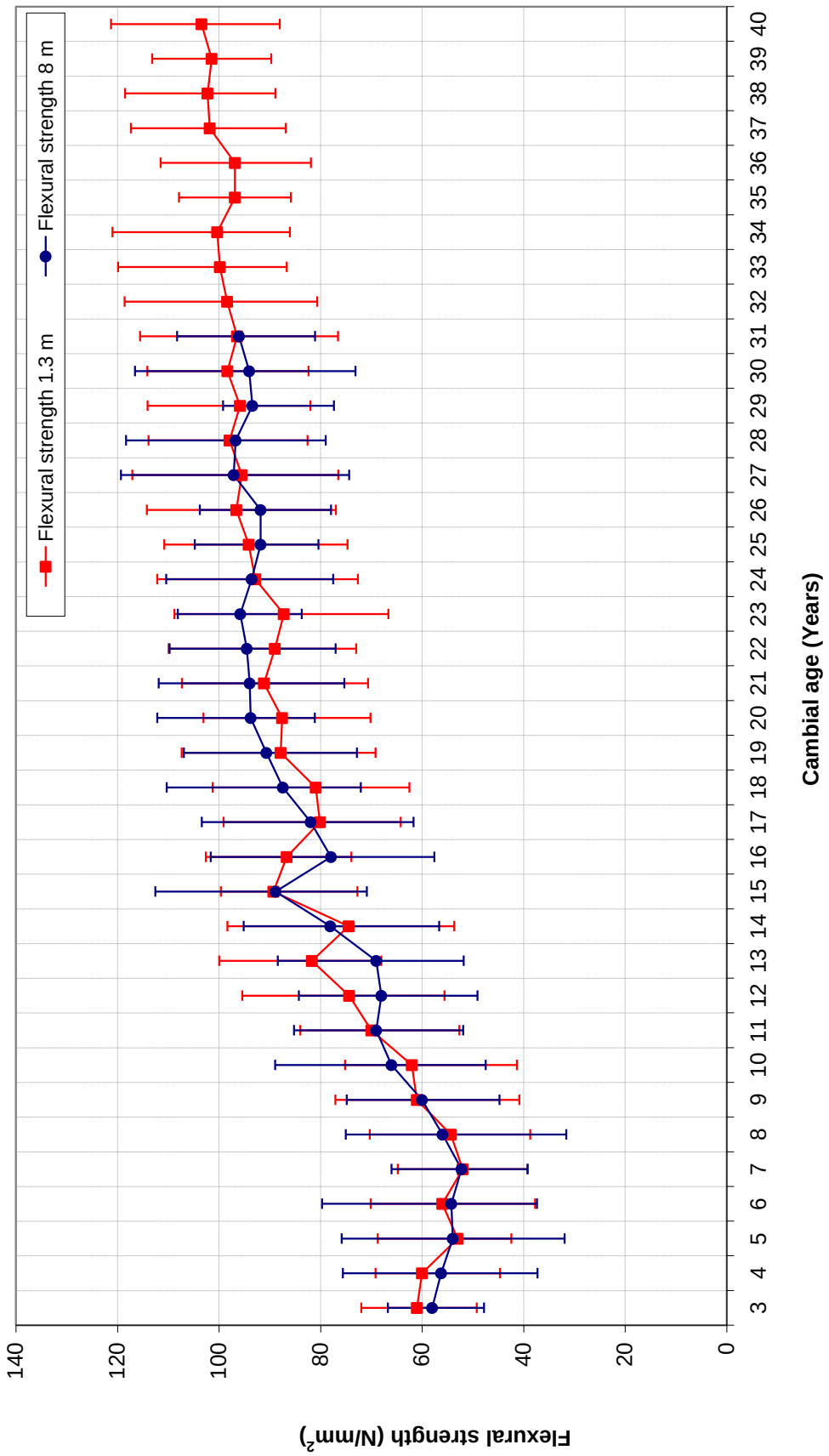

Figure 6-7: Mean flexural strength and 95th percentile range as a function of cambial age at stem heights of 1.3 m and 8 m within younger sample trees

6.3.3.2 Variations in older trees

Figure 6-8 shows the radial profile of flexural strength in the older sample trees, up to an age of 72 years. The developmental profile was found to vary from that seen in the larger sample of younger trees. No decline in values was observed near the pith, and peak strengths were achieved at much lower cambial ages within the older trees, remaining relatively consistent for all growth rings thereafter. Flexural strengths at both stem heights were found to occupy a band with minimum and maximum values of 90 N/mm^2 and 110 N/mm^2 once peak strengths had been achieved.

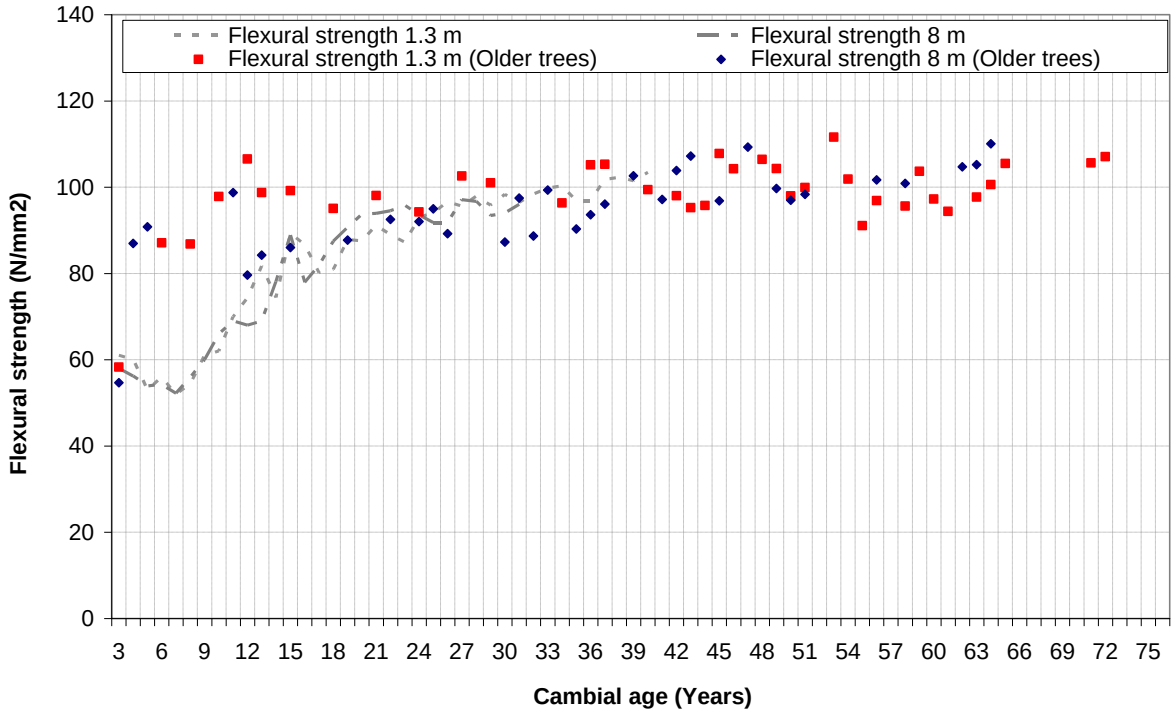

Figure 6-8: Mean flexural strength as a function of cambial age at stem heights of 1.3 m and 8 m within older sample trees

6.3.4 Compressive strength parallel to the grain - variations with age and height

In this sub-section the profiles of mean compressive strength in 40 - 50 year old sample trees are presented. As a result of testing for compressive strength in the northern radius only, it was not possible to conduct a repeated measures analysis due to the limited number of specimens available at each treatment level. For this reason results are also not presented for trees with ages > 50 years. Figure 6-9 shows mean values for compressive strength at the two assessed stem heights, descriptive statistics alongside the results of t-tests can be found in Tables C-7 and C-8.

As observed previously in the radial development profiles of results obtained from flexural tests, an overall trend of increasing compressive strength was seen with increasing cambial age. The mean values across a growth period were found to increase by 30 % between the first and last assessed at each stem height, with mean compressive strengths of approximately 40 N/mm^2 in the final growth periods. The lowest mean results were returned in the growth rings nearest the pith, with values in the region of 30 N/mm^2. Beyond this, the magnitude of the results continued to increase at a relatively constant rate until a cambial age of approximately 20 years. Beyond this it appears that the compressive strength began to stabilise, with the rates of increase reducing significantly and any trend of changing values largely masked by inter-ring variations. The results of the t-tests comparing the mean values obtained at each stem height showed that there was no statistically significant difference between the means in any growth period compared, which is in good agreement with the results shown in Figure 6-9.

Within each of the growth periods assessed, compressive strengths were found to show a relatively large range. Coefficient of variation were in the region of 20 %, and as was found in flexural tests, this decreased in the later growth periods as the rate of change of values began to decrease. The means and coefficients of variation at each of the four sampling sites were found to be of a similar magnitude, as shown in Table C-9.

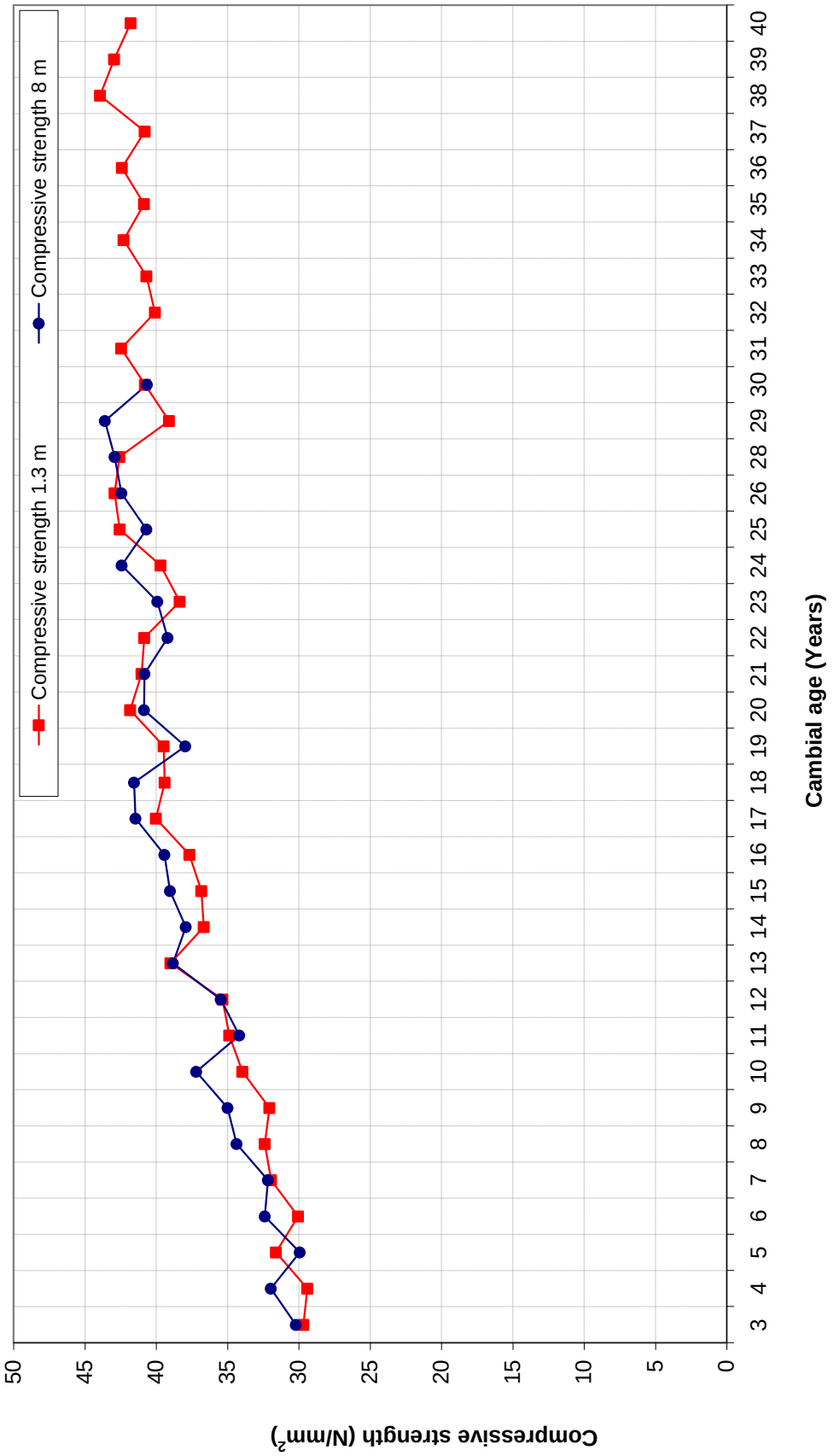

Figure 6-9: Mean compressive strength as a function of cambial age at stem heights of 1.3 m and 8 m within younger sample trees

6.3.5 Discussion of results showing variations in mechanical properties

The results presented in this section have described the within tree variation in a number of mechanical properties important when utilising timber within structural engineering applications. In doing this two hypotheses were tested, the null hypotheses of which were:

> $H_{6\text{-}1}$: No change in the magnitude of the studied property takes place with increasing cambial age.
>
> $H_{6\text{-}2}$: No difference exists in the magnitude of the studied property with increasing longitudinal position in the stem.

Considering the radial profiles of each mechanical property in their entirety, all showed a change in the magnitude of the assessed values with increasing cambial age, and as such the null hypothesis given in $H_{6\text{-}1}$ can be rejected and the alternative hypothesis, that mechanical properties do vary with cambial age, accepted. Upon breaking the developmental profiles down into separate growth periods, a rather more mixed outcome regarding the acceptance of either the null or alternative hypothesis emerges. In general for all mechanical properties studied, large changes with cambial age were noted early in the growing cycle, with rates of change decreasing in the region of 15 - 20 years of age, after which time the magnitude of the results attained for all mechanical properties appeared to begin to stabilise. In some instances no statistically significant difference in properties with cambial age was observed in these later regions and in these cases the null hypothesis given in $H_{6\text{-}1}$ holds.

With regard to the null hypothesis given in $H_{6\text{-}2}$, different results were attained for the three mechanical properties evaluated. Modulus of elasticity values were found to show statistically significant differences between the two stem heights. As such, the null hypothesis is rejected and the alternative hypothesis, that a difference in the magnitude of the studied mechanical property exists with increasing longitudinal positions in the stem, accepted. Both flexural and compressive strength were however found to show no statistically significant differences in values with longitudinal position, as such the null hypothesis stands in these cases.

Results showing the radial and longitudinal development and the magnitudes of changes in mechanical properties for Douglas-fir are limited, the findings presented here are however in good agreement with those of studies conducted on a wide range of softwood species

including Black spruce (Alteyrac et al., 2006), Maritime pine (Machado and Cruz, 2005), Norway spruce (Kliger et al., 1998), Radiata pine (Cown et al., 1999, Tsehaye et al., 2000) and Sitka spruce (McLean, 2008). The continued production of timber with high modulus of elasticity and strength properties in older trees has also been reported for Sitka spruce (Ridley-Ellis et al., 2009).

Tables 2-2 and 2-3 show values of Douglas-fir mechanical properties that have been attained through testing material obtained from a wide range of locations. The magnitude of the results of the various mechanical properties reported varies widely, potentially as a result of the geographic region the material was obtained from, as well as its location within the sample trees. On comparison of the whole sample mean values found here, it is noted that they lie at the lower end of the range of values presented for both modulus of elasticity and strength. However, when mean values of the growth periods at greater distances from the pith are considered, the results compare favourably with those presented and are in excess of those found for Douglas-fir grown within the United Kingdom by Lavers (1983).

Differences between the mean values of the assessed mechanical properties due to different sites were found to be low in the variance components analysis of random effects, typically accounting for less than 10 %. A low difference between the means was expected, given the close geographic spacing, growth taking place over similar timescales and a similar distribution of tree average growth rates within each site. Differences that exist between sites could be accounted for by a number of factors including differences in silvicultural treatments, micro climatic effects at the site, topography, soil conditions and genetic differences. It was generally found that in later years of growth, the variance associated with trees nested within sites increased, as the within group variability due to cambial age, included in the error variance, decreased. The relationship between mechanical properties and rate of growth that may have induced variability into the between trees results is investigated in Section 6.5.

It is clear when comparing the results obtained in Chapter 4 regarding the developmental profiles of anatomical properties in both younger and older sample trees, and those presented here, that links exist between them. A detailed analysis of the relationships between anatomical and mechanical properties will be presented in Chapters 7 and 8. The implications of the findings presented here, with regard to the utilisation of the timber studied within a structural engineering context, are discussed further in Section 6.7.

6.4 Influence of geographic orientation on mechanical properties

6.4.1 Outline

The nature of the wood produced in different radial orientations for the same cambial age within a tree is not necessarily uniform. The most common reason associated with this non-uniformity is the production of compression wood, formed in response to an external force acting to disrupt the vertical pattern of growth in the stem (Kwon et al., 2001). The two primary external forces likely to cause the formation of compression wood are; those due to the direction of the prevailing wind and those caused due to growth on sloping ground. Gaining an understanding of the presence and magnitude of any directional effects on timber properties at a regional and site level is important, as it is common practice when conducting property evaluations to select specimens from one consistent geographic orientation, in order to increase the number of results that can be obtained from separate trees when testing resource are limited. From the point of view of timber quality, identifying large differences in the quality of timber produced depending on orientation could have consequences relating to the optimisation of log cutting patterns.

Specimens for the determination of modulus of elasticity and flexural strength were obtained from the north, east, south and west compass positions within each tree. In the following sub-sections, comparisons between the results obtained from specimens taken in each of the four directions from 40 - 50 year old trees at the two sampling heights are made, with the intention of identifying and quantifying any differences that exist. This was done with the use of a univariate analysis of variance in which the treatment effect was the orientation of the specimen, as described in Section 3.10.4. In analysing the results of the analysis of variance, the following null hypothesis was tested:

> $H_{6\text{-}3}$: No change in the mean of the studied property takes place with changing radial orientation within a stem.

The results obtained from the first specimen nearest the pith in the north and south directions were excluded from the analysis, due to the cutting pattern used to prepare specimens, detailed in Section 3.6.2, making it impossible to obtain equivalent specimens in the east and west orientations. The study of orientation effects on compressive strength was not possible due to specimens only being obtained from the northern radius.

6.4.2 Modulus of elasticity - variation with orientation

The effect of orientation on the modulus of elasticity of small clear specimens in 40 - 50 year old trees at the two sampling heights is shown in the box and whisker plots in Figure 6-10. Results of the analysis of variance, alongside descriptive statistics are given in Tables C-10 and C-11.

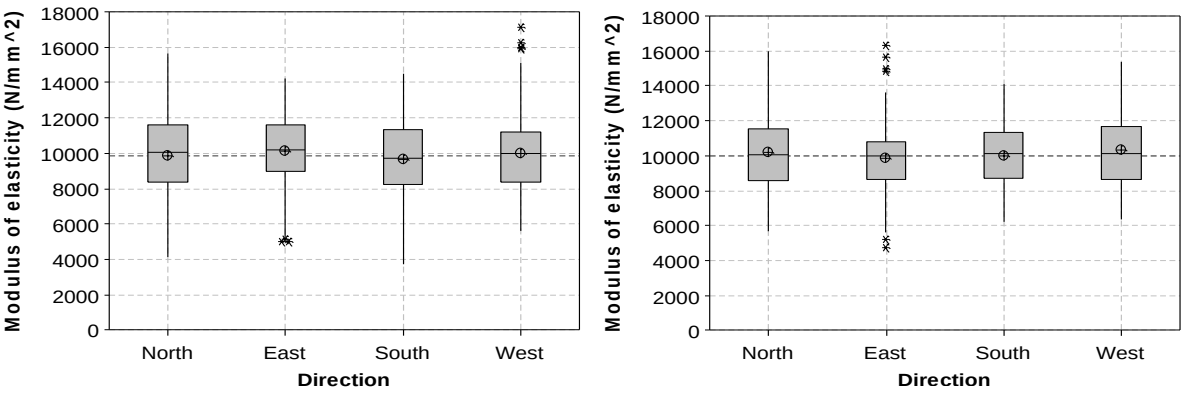

Figure 6-10: Modulus of elasticity variation with geographic orientation at 1.3 m (L) and 8 m (R) in 40 50 year old trees

Results showed some small differences in the mean modulus of elasticity obtained at different orientations in the stem compared to the sample mean as a whole, with a maximum difference of 200 - 300 N/mm^2 at either sampling height. The analysis of variance however showed that these differences were not statistically significant. Given this, the null hypothesis stated in $H_{6\text{-}3}$ can be accepted for modulus of elasticity values in this dataset. The predominant factor expected to have had an impact on properties from all sites was the prevailing wind, which in the British Isles is from a south westerly direction and would therefore result in the formation of compression wood on the north easterly side of the tree. The lack of any apparent influence of the prevailing wind direction on the modulus of elasticity may be explained with consideration of the sampling method used to select trees, which eliminated stand edge trees where wind forces would have been highest. Similar results were reported by Machado and Cruz (2005) and McLean (2008).

The results from the analysis of variance comparing the mean values of each geographic orientation separately across each 40 - 50 year old site are shown in Table C-12. The results also show no statistically significant differences between the mean modulus of elasticity values achieved in any geographic orientation at any sample site. It was expected that results at the local level would have shown some differences between the mean values achieved at each site,

as some sites were steeply sloping which is generally a condition under which compression wood forms. The lack of any significant differences as function of orientation may again be due to the sampling methods used to select trees, which specifically avoided swept butts, typically associated with compression wood formation.

6.4.3 Flexural strength - variation with orientation

The effect of orientation on the flexural strength of small clear specimens in 40 - 50 year old trees at the two sampling heights is shown in the box and whisker plots in Figure 6-11. Results of the analysis of variance, alongside descriptive statistics are given in Tables C-13 and C-14.

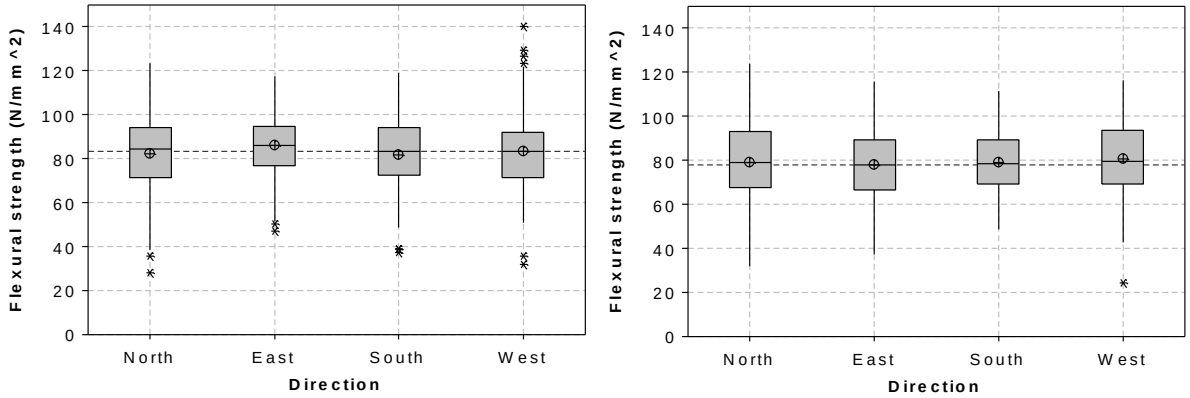

Figure 6-11: Flexural strength variation with geographic orientation at 1.3 m (L) and 8 m (R) in 40 - 50 year old trees

The results for the variation of mean flexural strength values with geographic orientation were similar to those found for modulus of elasticity previously. The small variations in means for different orientations, which were not greater than 3 N/mm^2 from whole sample means at a given stem height, were found to be statistically non-significant in the results of the analysis of variance. As is shown in Table C-15, when the mean values for each geographic orientation were compared separately by site, they were also found to show no statistically significant difference. Given this, the null hypothesis stated in $H_{6\text{-}3}$ can be accepted for flexural strength values in this dataset. The potential reasoning for these results is as described in the previous sub-section. Similar findings were reported by Machado and Cruz (2005), however McLean (2008) observed a small but statistically significant difference in mean values, which appears to be as a result of the prevailing wind direction, with lower values recorded in the northern and eastern orientations.

6.5 Influence of growth rate on mechanical properties

6.5.1 Outline

The results presented in Section 6.3 demonstrated the large variability that exists in the mechanical properties of the Douglas-fir test stems, both within a tree and also between individual trees within a stand. It was shown in Section 5.2 that some of the between tree variability in anatomical properties can be attributed to changes in growth rates. In this section an evaluation of the impact of growth rate on mechanical properties is presented.

The selection of sample trees was conducted in such a way that a wide range of growth rates within even aged stands were obtained. In order to quantify the impact of growth rates on properties, trees were grouped into either slower or faster grown categories, utilising the methodology given in Section 3.7. The mean growth ring width across the 40 - 50 year old sample trees at both stem heights was 4.7 mm. The mean values for slower and faster grown trees were 3.9 mm and 5.4 mm respectively, representing a change of ± 17 % from the sample mean. Details regarding the variation in ring widths within each growth rate class are shown in Section 5.2.2.

In the following sub-sections, the mean mechanical property values for slower and faster grown trees are compared by use of t-tests, utilising the method described in Section 3.10.5. Higher means in slower grown stems compared to those that were faster grown returned positive t values. All statistical tests were deemed significant when $P \leq 0.05$. The results of each test can be found alongside the descriptive statistics in Appendix C, as indicated at the start of each sub-section.

In evaluating the impact of growth rate on anatomical properties the following null hypothesis was tested:

> $H_{6\text{-}4}$: There is no statistically significant difference between the mean values of studied properties in slower and faster grown trees.

6.5.2 Modulus of elasticity - variations with growth rate

The box and whisker plots shown in Figure 6-12 illustrate the changes in modulus of elasticity, considering values from both 1.3 m and 8 m in combination within stems classified as either slower or faster growing, compared with the sample mean for all trees. Descriptive statistics alongside the results of t-tests comparing the means can be found in Table C-16.

Mean modulus of elasticity in specimens derived from slower grown trees was higher than that found in those taken from trees in the faster growing class. The difference observed from sample mean values was ± 4 %, with modulus of elasticity values of 10300 N/mm^2 and 9600 N/mm^2 within slower and faster growing trees respectively. Differences between the means of the two growth rate classes were found to be statistically significant in the results of the t-test.

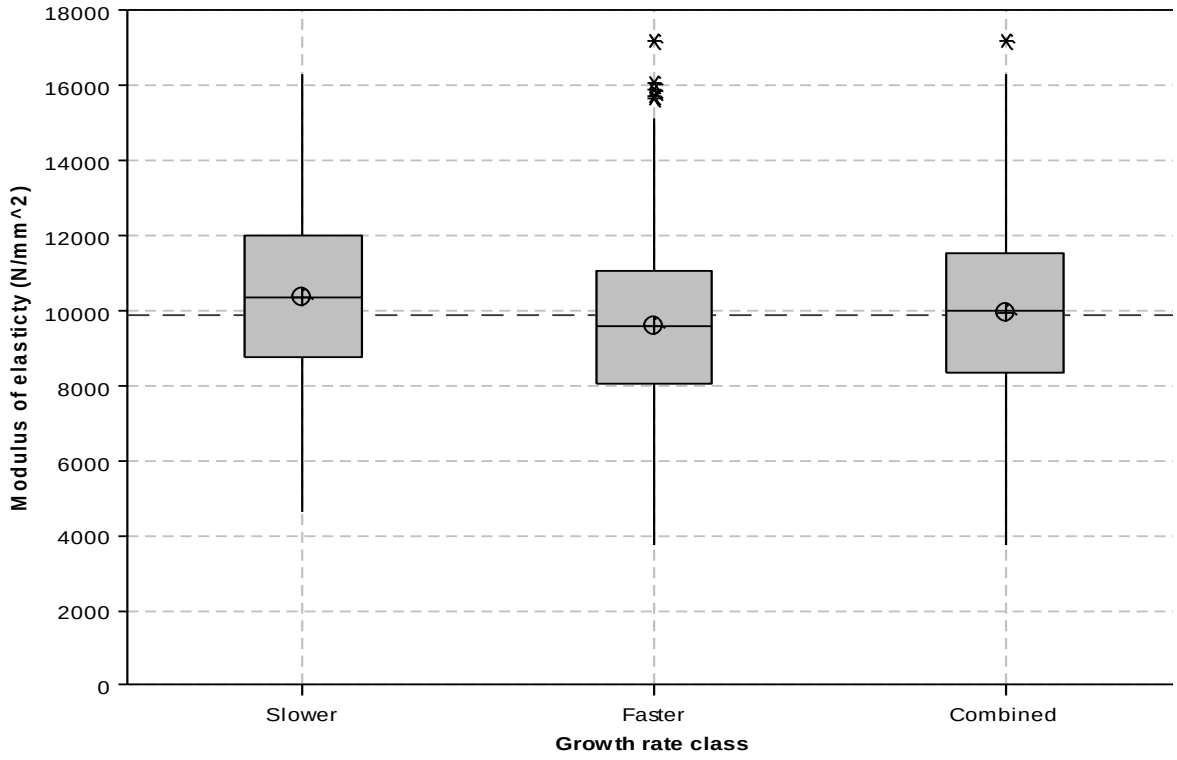

Figure 6-12: Whole stem modulus of elasticity variations with slower and faster growth in 40 - 50 year old sample trees

At the site level, separating the six trees felled at each of the four main sampling sites for 40 - 50 year old trees into either slower or faster growing returned similar results to those described above, with statistically significant differences being observed in the t-tests in three of the four sites. Results are presented in Table C-17.

6.5.3 Flexural strength - variations with growth rate

The box and whisker plots shown in Figure 6-13 illustrate the changes in flexural strength, considering values from both 1.3 m and 8 m in combination within stems classified as either slower or faster growing, compared with the sample mean for all trees. Descriptive statistics alongside the results of t-tests comparing the means can be found in Table C-18.

The relationship between growth rate and flexural strength was found to be similar to that for modulus of elasticity presented previously. Results showed that the mean flexural strength in specimens derived from slower growing trees was greater than that found in trees that were faster growing. The difference observed from sample mean values was ± 4 %, with flexural strengths of 83 N/mm^2 and 77 N/mm^2 in slower and faster growing trees respectively. The t-test results showed that these differences were statistically significant.

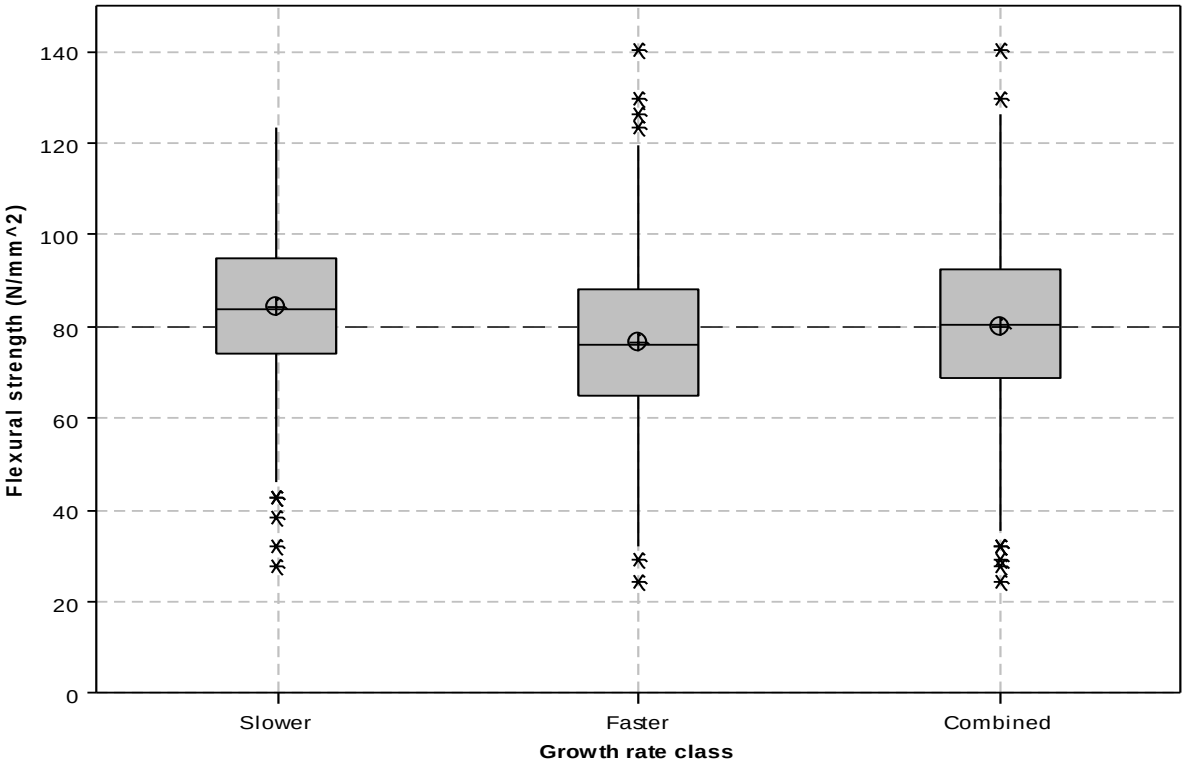

Figure 6-13: Whole stem flexural strength variations with slower and faster growth in 40 - 50 year old sample trees

At the site level, separating the six trees felled at each of the four main sampling sites for 40 - 50 year old trees into either slower or faster growing returned similar results, with statistically significant differences being observed in the t-tests in three of the four sites. Results are presented in Table C-19.

6.5.4 Compressive strength parallel to the grain - variations with growth rate

The box and whisker plots shown in Figure 6-14 illustrate the changes in compressive strength, considering values from both 1.3 m and 8 m in combination within stems classified as either slower or faster growing, compared with the sample mean for all trees. Descriptive statistics alongside the results of t-tests comparing the means can be found in Table C-20.

As observed in flexural test results, the mean compressive strength in specimens classified as slower growing was higher than that for those taken from trees in the faster growing class. The difference observed from the whole sample mean was approximately ± 4 %, with mean compressive strengths of 39 N/mm^2 and 37 N/mm^2 in slower and faster growing trees respectively. The t-test results showed that these differences were statistically significant.

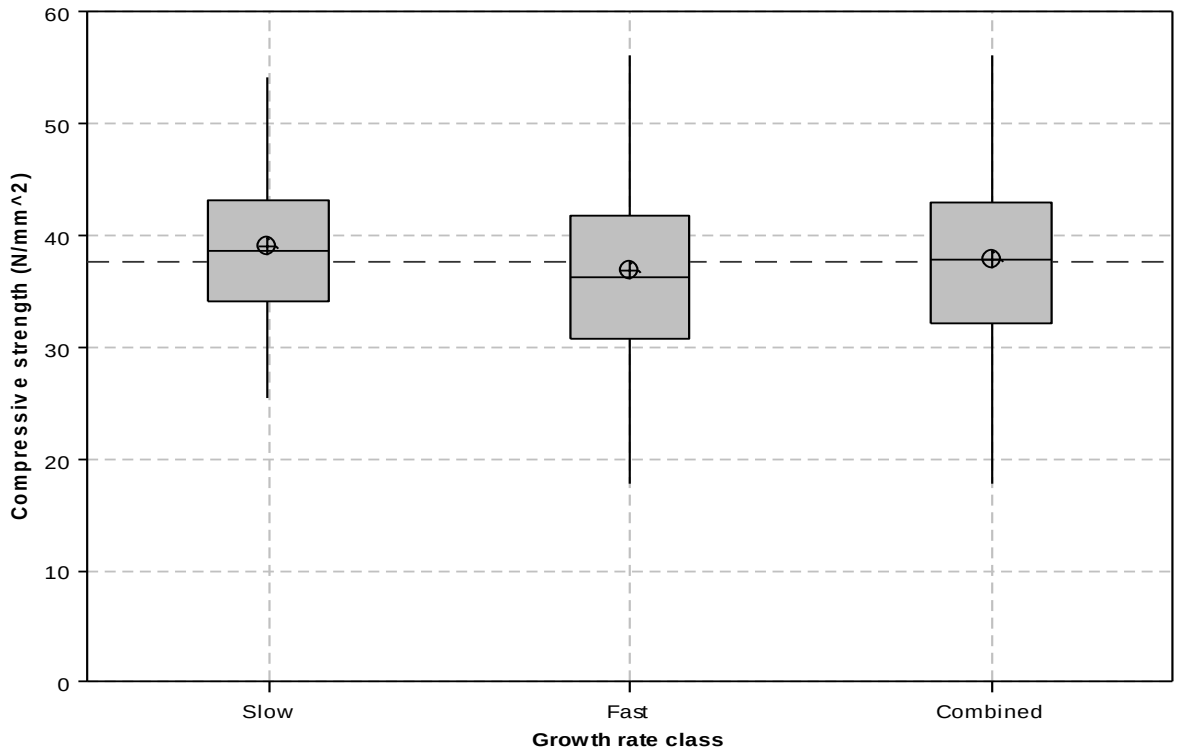

Figure 6-14: Whole stem compressive strength variations with slower and faster growth in 40 - 50 year old sample trees

At the site level, separating the six trees felled at each of the four main sampling sites for 40 - 50 year old trees into either slower or faster growing returned similar results, with statistically significant differences being observed in the t-tests for all but one site. Results are presented in Table C-21.

6.5.5 Discussion of variation in mechanical properties with growth rate

In this section the response of the three mechanical properties evaluated to changing growth rate has been assessed. In doing this the following null hypothesis was tested:

> $H_{6\text{-}4}$: There is no statistically significant difference between the mean values of studied properties in slower and faster grown trees.

When all trees in the 40 - 50 year age range were considered, all mechanical properties assessed displayed a statistically significant difference between slower and faster growth. As such the null hypothesis stated above is rejected and the alternative hypothesis, that growth rate does have a statistically significant impact on mechanical properties, accepted. When evaluated within sites, the null hypothesis was found to hold in three cases.

Growth ring width means were found to show a ± 17 % change from sample means. The corresponding changes observed in all three mechanical properties assessed were significantly lower, at approximately 4 %. The magnitude of the percentage changes observed are however in line with many of those reported for anatomical properties in Section 5.2. The relationship between anatomical and mechanical properties that may have resulted in this similarity in values is explored in Chapters 7 and 8.

The number of previous studies directly quantifying the impact of growth rate on mechanical properties is relatively limited, and as with anatomical properties the large array of analysis techniques makes direct comparisons difficult. In the wide ranging study conducted by Zhang (1995), the results presented appeared to point towards moderate to strong correlations between modulus of elasticity, flexural and compressive strength in Douglas-fir, although this postulation was only made based on the findings for similar species. In Norway spruce, the findings presented by Kliger et al. (1998) are in good agreement with those found here, although differences found between slower and faster growing stems were significantly greater, most likely due to the greater difference in mean ring widths in slower and faster growing trees, and potentially the difference in species. Similar results were also reported by Eriksson et al. (2006) for Scots pine.

6.6 Relationship between SilviScan-3 predicted and small clear specimen modulus of elasticity

The SilviScan-3 system provided a prediction of modulus of elasticity at each scanning interval based on the assessed anatomical properties, as described in Section 3.5.3.4. This was done with the use of Equation 6-1 shown below.

$$MOE = A(Icv \cdot D)^{B} \qquad (6\text{-}1)$$

where: MOE predicted flexural modulus of elasticity

A scaling factor (0.165)

B exponent to allow for curvature (0.85)

Icv coefficient of variation of the azimuthal intensity profile

D density

In order to evaluate the accuracy of these predicted values, their means for theoretical small clear specimens, derived according to the methodology given in Section 3.9, are plotted against static flexural test values for equivalent real specimens as shown in blue in Figure 6-15.

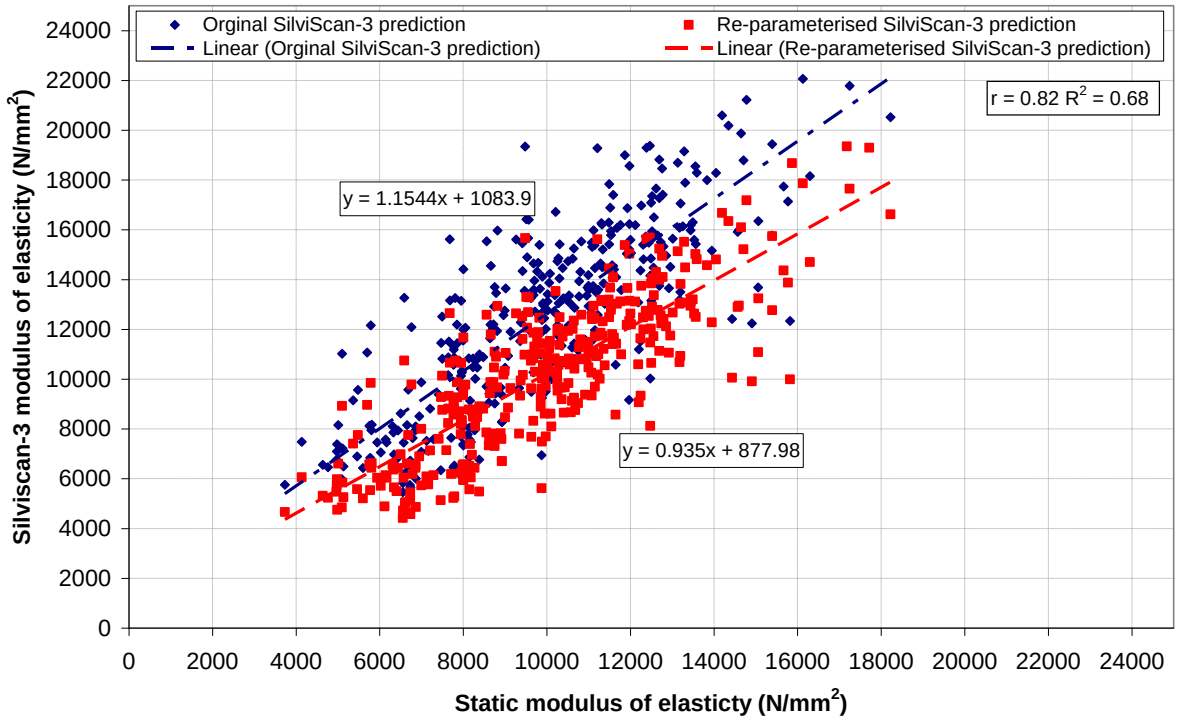

Figure 6-15: SilviScan-3 predicted modulus of elasticity against static flexural test values

It was found that a strong linear relationship existed between the modulus of elasticity values calculated by the two methods, with correlation coefficients of 0.82. This is in line with the findings reported by McLean (2008) in Sitka spruce, but lower than the results with $r > 0.9$ reported by Evans (2006). The lower degree of linearity found in this study may be explained by the method used to match physical small clear specimens to their corresponding predicted values, which may not have accurately encompassed all properties relevant to a particular specimen. Obtaining microfibril angle data at a low resolution in the large majority of cases may have also contributed to the differential in results. The results predicted utilising SilviScan-3 were found to be 20 - 50 % higher than those obtained in static flexural tests, a result that was expected, given that the modulus of elasticity obtained using dynamic methods, which the Silviscan-3 measured results are calibrated with, has been shown to be in the order of 30 % higher than that found using static flexural testing (Evans and Ilic, 2001). In Figure 6-15 a second dataset, in red, is also shown, again comparing predicted and static values. In this second dataset, the scaling factor A was reduced by 24 % to 0.133. As a result of this the overestimation due to predicting the dynamic modulus of elasticity is reduced and a good fit achieved between predicted and actual values. This is evident from the reduction in the constant value in the re-parameterised regression equation compared to original values, alongside a slope coefficient that lies closer to one. While this reduced factor may only be applicable for the dataset used here, it does confirm that the equation in principle can be used to provide a reasonable estimation of static modulus of elasticity.

6.7 Implications of results for utilisation

In the previous sections, the impact of increasing cambial age and changes in the rate of growth on timber mechanical properties were presented. In this section the impact of these changes on the quality of the material produced from the perspective of utilisation in structural engineering applications will be evaluated. As has been demonstrated, large variability exists in the mechanical properties of timber both within and between trees on a single site. In order to take account of this inherent variability, timber for structural applications is graded according to its anticipated performance in service. The historical development of the methodology used to obtain timber grades and design stresses is presented by Dinwoodie (2000).

Early methods to derive working design stresses utilised small clear specimens tested in accordance with BS 373 'Methods of testing small clear specimens of timber' (BSI, 1957), as conducted in this study, the results from which were modified with a series of reduction

factors to take account of imperfections in the timber. In order to allow design values to be derived on sections more representative of the actual service conditions, the standardised testing methodology has changed in recent years, such that structural sized test pieces are now used. Under the current methods employed, sections are tested in accordance with BS EN 408 'Timber structures - Structural timber and glued laminated timber - Determination of some physical and mechanical properties' (BSI, 2010b), from which characteristic values of several key properties can be obtained using the methods given in BS EN 384 'Structural timber - Determination of characteristic values of mechanical properties and density' (BSI, 2010a). These results can then be used to assign softwood timber sections to one of 12 strength classes when machine strength graded. The characteristic values for each strength class can be found in BS EN 338 'Structural timber. Strength classes' (BSI, 2003). A specific population can be assigned to a certain strength class if the characteristic values of 5th percentile density and flexural strength and mean modulus of elasticity match or exceed the values of the desired class. Additional mechanical properties are derived from these basic values by empirical relationships (Steiger and Arnold, 2009). Under visual grading methods, sections are classified as either General Structural (GS) or Special Structural (SS) based on their visually assessed properties, including slope of grain, knot sizes and ring widths. For Douglas-fir grown in the United Kingdom, these classifications are equivalent to C14 and C18 strength classes respectively. The key characteristic values for each strength class are shown in Table 6-3.

Table 6-3: Key characteristic strength class values from BS EN 338:2003

Property	**Strength class**											
	C14	**C16**	**C18**	**C20**	**C22**	**C24**	**C27**	**C30**	**C35**	**C40**	**C45**	**C50**
Bending strength N/mm² (5%)	14	16	18	20	22	24	27	30	35	40	45	50
Modulus of elasticity N/mm²(Mean)	7000	8000	9000	9500	10000	11000	11500	12000	13000	14000	15000	16000
Density kg/m³ (5%)	290	310	320	330	340	350	370	380	400	420	440	460

The use of small clear specimens in this investigation allows the results recorded to be directly compared with those obtained in the numerous studies which employ the same method, and also for intra-tree variations to be understood. A limitation of the methodology is however that it does not allow the direct classification of the sample population strength class to be

calculated, as test pieces are not fully representative of structural sized sections. The results presented in the following are therefore regarded as the upper bound of the wood quality that can be obtained. The impact of imperfections such as knots and sloping grain that may act to reduce the quality is discussed further later in this section.

In order to assign a timber section to a particular strength class it is necessary to grade it by either mechanical or visual methods, explanations of which can be found in the BRE digest 'Guide to machine strength grading of timber' (Benham et al., 2003). Grade settings for machine strength grading and the relationships between visually identified timber characteristics and section properties are determined by tests on large samples of timber sections for each species. Once grade settings have been derived, mechanical grading machines work on the basis of measuring the applied load to achieve a set deflection in a section passed through the machine, or vice versa. These results are then used to calculate section modulus of elasticity, which is used as an indicator for flexural strength. As such, the method relies on a strong relationship between the two parameters.

The graph in Figure 6-16 shows flexural strength plotted against modulus of elasticity for each small clear test specimen derived from 40 - 50 year old sample trees. The two parameters were found to be well related, with linear correlation coefficient of 0.88, higher than the results of 0.6 - 0.8 that have been reported elsewhere (Glos, 1995 in Steiger and Arnold, 2009, Steiger and Arnold, 2009). The stronger correlation observed here may be as a result of there being no defects present in the test specimens which could have introduced a degree of non-linear behaviour within the results. Figure 6-16 also shows the characteristic values of mean modulus of elasticity and 5th percentile flexural strength for the test specimens, alongside the characteristic values required for each strength class to be achieved, as set out in BS EN 338:2003. The mean and 5th percentile values of 9900 N/mm^2 and 50 N/mm^2 for modulus of elasticity and flexural strength satisfy the requirements for the C20 strength class. The characteristic 5th percentile density value for the C20 strength class is 330 kg/m^3, upon calculating the bulk density of all small clear specimens the 5th percentile density was found to be 415 kg/m^3 and therefore more than satisfies the requirements. As stated previously, the strength classes presented here represent the upper bound of theoretical quality that could be achieved in timber sections obtained from the sample trees, due to the lack of defects and the small section size. It can also be seen from Figure 6-16, that in the absence of defects, the mean modulus of elasticity was the limiting factor regarding the maximum strength class requirements that were satisfied.

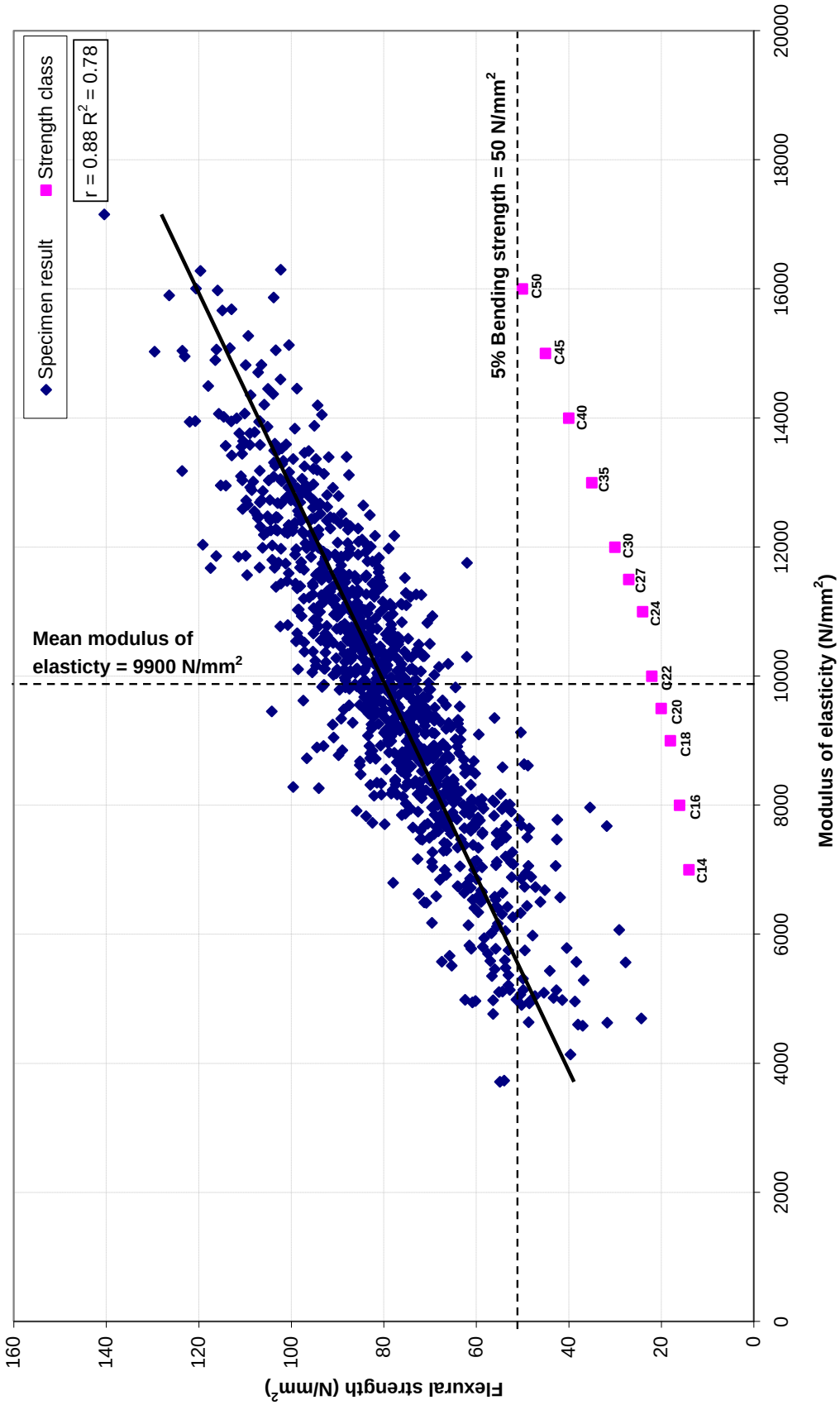

Figure 6-16: Flexural strength plotted against modulus of elasticity for test specimens from 40 - 50 year old trees

The results presented in Section 6.3 showed the large variations that exist in mechanical properties with increasing cambial age. As such, the location within a stem from which a sample population is obtained will potentially have implications for the strength class achieved. Figure 6-17 shows flexural strength plotted against modulus of elasticity for 40 - 50 year old trees, with a differentiation made regarding whether the specimen was obtained from a region classified as either juvenile or mature. The classification of juvenile or mature wood was made on the basis of the results presented in Section 5.3 for each individual tree. The first specimen containing no growth rings evaluated as juvenile from the perspective of both density and microfibril angle was classified as mature. The impact of separating specimens in this way is clear in the distributions of flexural strength and modulus of elasticity, with juvenile specimens skewed towards the lower end of the range of results returned, with the reverse true of the mature wood specimens. Mean modulus of elasticity and 5th percentile flexural strength were both found to be lower in specimens containing juvenile wood, as would be expected given the results presented in Figure 6-5 and 6-7. As a consequence of these results, the sample of juvenile wood specimens satisfied the requirements of the C18 strength class, whilst mature wood specimens satisfied the C24 requirements. In both instances, modulus of elasticity was the limiting factor regarding the maximum strength class requirements that were satisfied in the absence of defects. At 395 kg/m^3 and 450 kg/m^3, the 5th percentile densities within juvenile and mature wood respectively met the requirements for the C18 and C24 strength classes satisfied by the mechanical properties.

As with age, rate of growth was shown in Section 6.5 to have an impact on the magnitude of the mechanical properties recorded. In order to investigate the impact of growth rate on strength class, stems were classified as either slower or faster growing utilising the methodology described in Section 3.7; results are shown in Figure 6-18. The impact of differentiating specimens by growth rate was less than that seen for age, a result that was expected, given the extent of the variations in properties observed with growth rate in Section 6.5. It was however noted that a slight skew towards higher values was evident in slower growing stems, with the reverse true for faster growth rates. As a result of these differences in distribution, slower grown trees satisfied the strength class requirements for the C22 grade, while those that were faster grown satisfied the requirements for the C20 grade only. At 425 kg/m^3 in slower growing trees and 400 kg/m^3 in those that were faster grown, the characteristic values for 5th percentile density were found to satisfy the requirements for each respective strength class, with the mean modulus of elasticity again the limiting factor.

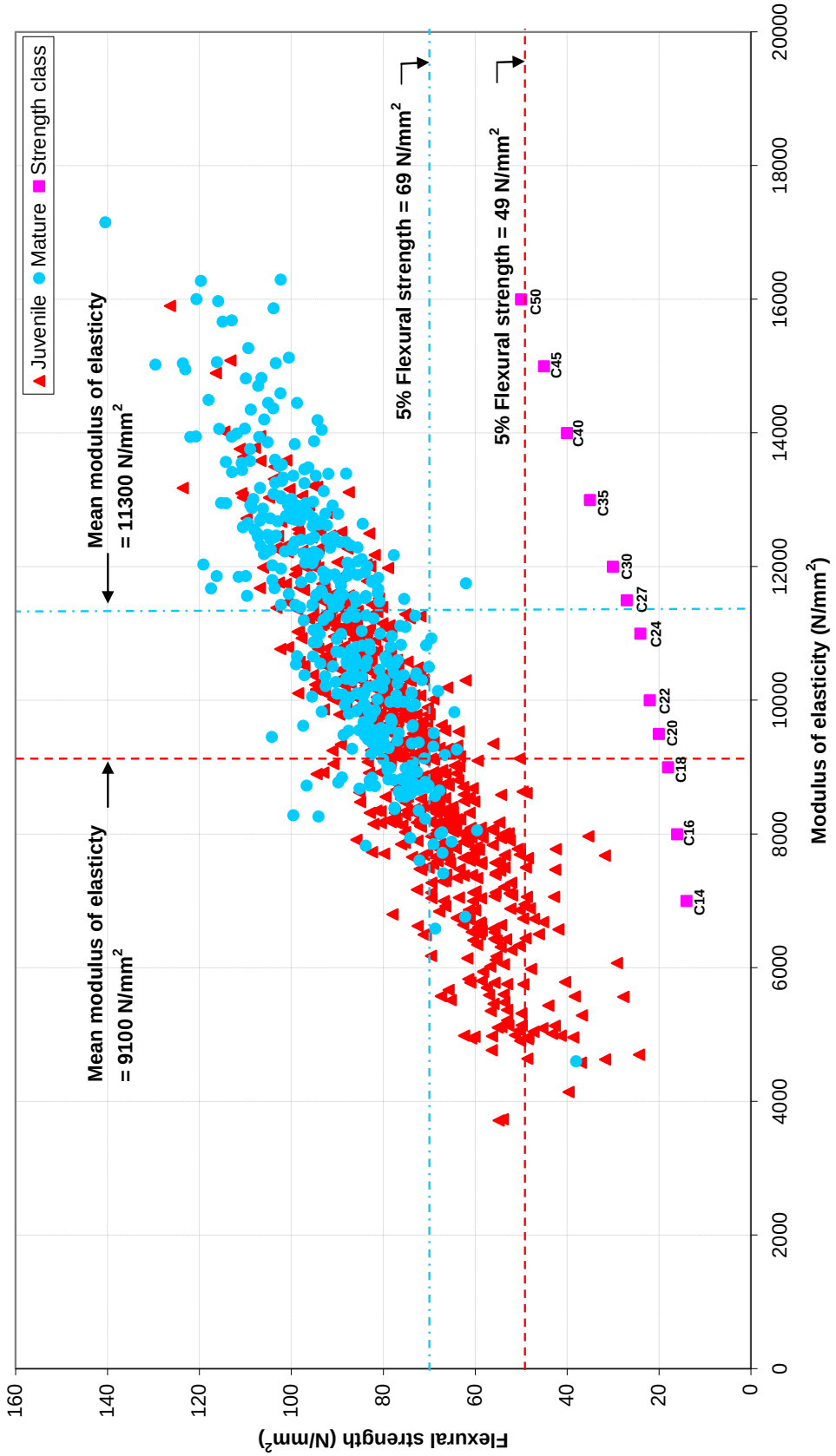

Figure 6-17: Flexural strength plotted against modulus of elasticity for test specimens from 40 - 50 year old trees classified as juvenile or mature

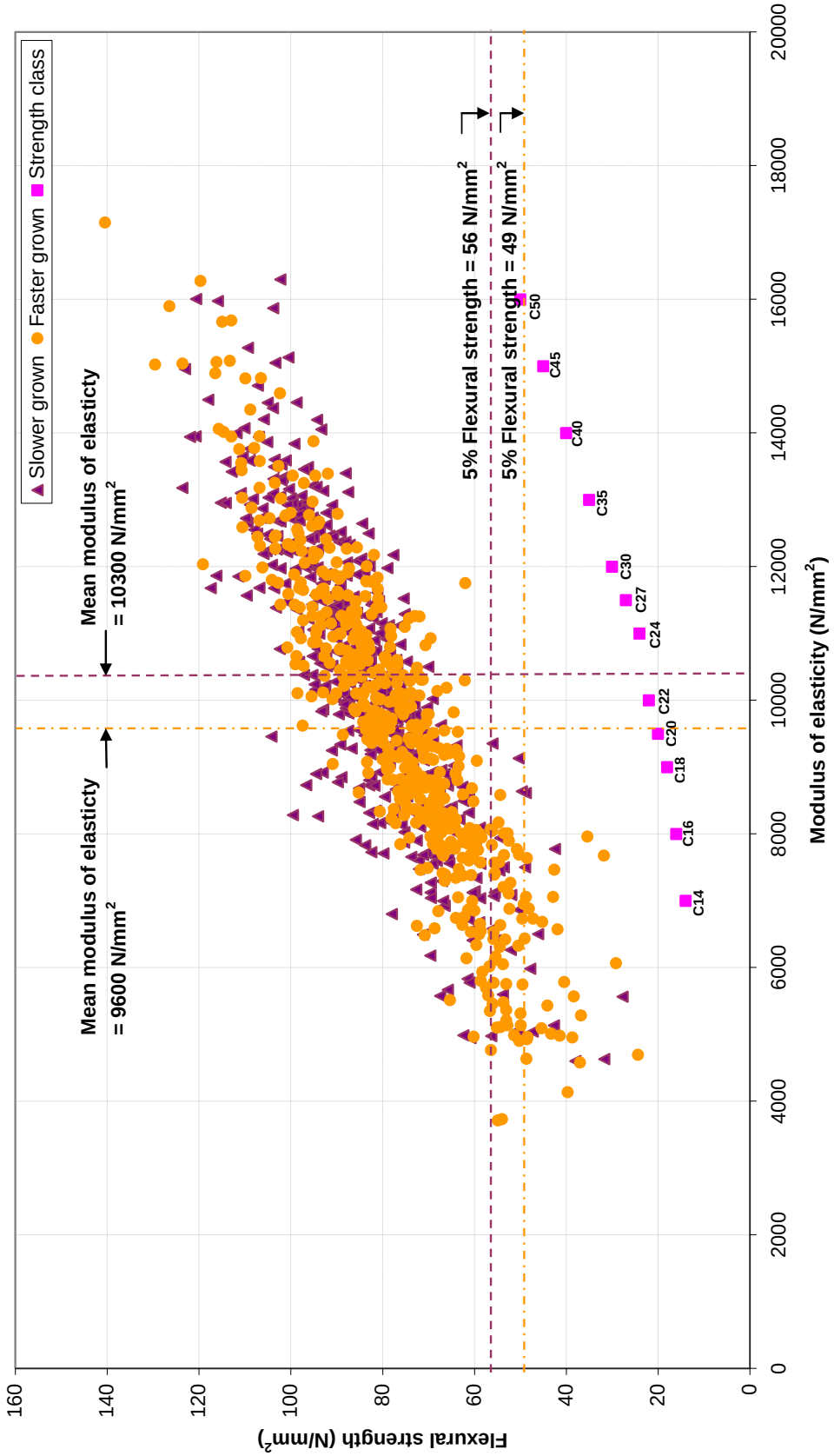

Figure 6-18: Flexural strength plotted against modulus of elasticity for test specimens from 40 - 50 year old trees classified as slower or faster growing

The results shown in Table 6-4 indicate the strength class requirements satisfied when the previously presented findings regarding the impact of age and growth rate are considered in combination. The segregation has a marked effect on the results, and is an indication of the wide quality range of timber that can be achieved between and within trees in a site.

Table 6-4: Strength class classification considering specimen age and growth rate in combination for 40 - 50 year old trees

	Juvenile wood	**Mature wood**
Slower grown	C18	C27
Faster grown	C16	C24

In all results shown previously, modulus of elasticity was found to be the limiting factor with regard to the strength classification achieved. In sections largely devoid of imperfections, such as those used here, this is to be expected, as the magnitude of flexural strength is more commonly related to stress risers such as knots or a sloping grain rather than anatomical characteristics (Lachenbruch et al., 2010). Quantifying the impact that imperfections have on the mechanical properties of timber is complicated by their uneven distribution within specimens. Despite this, several studies have shown negative correlations between knot ratio and flexural strength and to a lesser extent modulus of elasticity (Brazier et al., 1985, Kliger et al., 1995, Vikram, 2008). Knots influence these properties by reducing the effective section dimensions, causing localised grain deviations in their proximity, as well as acting as stress risers (Jozsa and Middleton, 1994). The slope of grain within a section has a similar impact on mechanical properties as discussed by Macdonald and Hubert (2002) and shown by Pope et al. (2005). In order to allow for the impact of defects to be taken into account whilst visually grading timber, ASTM D 245 (ASTM, 2000) was developed based on extensive research covering tests of small clear specimens and of full sized structural members, incorporating the strength and variability of clear wood and the effect on flexural strength and modulus of elasticity of factors such as knots and sloping grain. This is done by providing a series of reduction factors applied to the flexural strength and modulus of elasticity of small clear specimens in order to take account of imperfections. Despite not fully quantifying the impact of imperfections, due to the statistically derived nature of the reduction factors, ASTM D 245 does provide perhaps the best overall indication of the impact of imperfections on mechanical properties within a section. Three knot locations are considered in the standard; on the narrow face, centreline and edge, as shown in Figure 6-19. The slope of grain of a section is measured with reference to its longitudinal axis.

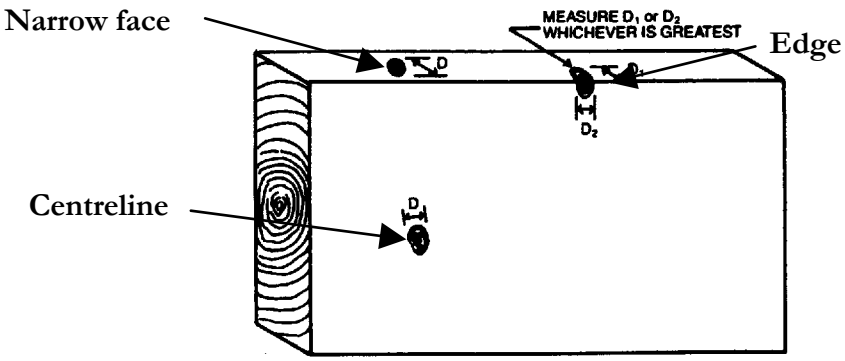

Figure 6-19: Knot locations in timber beams in ASTM (2000)

The graphs displayed in Figures 6-20 and 6-21 indicate the reductions in the values of flexural strength and modulus of elasticity derived from small clear specimens to take account of increasing knot area and slope of grain. The results show the increasing reduction factors, with increasing knot size and slope of grain, derived for a theoretical beam of dimensions 225 mm x 75 mm, a section size at the upper end of that which would commonly be sawn from a tree (Pirie, 2009). When utilising the standard the worst case reduction factor is considered.

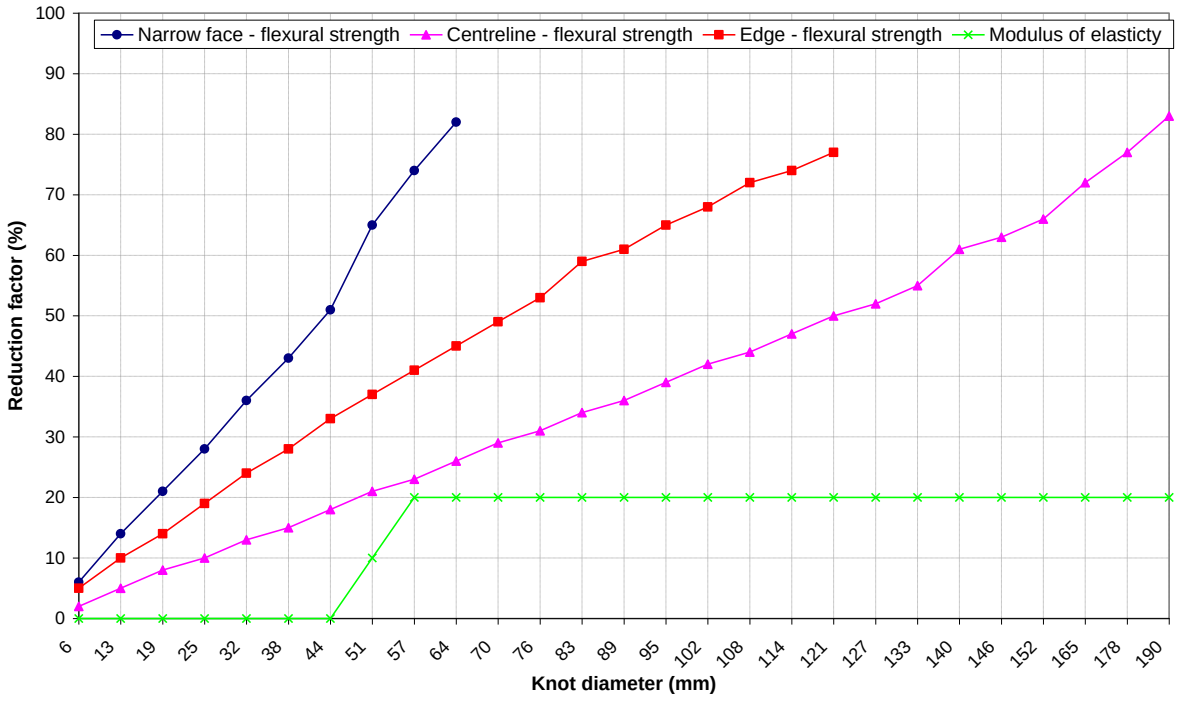

Figure 6-20: Reductions of small clear specimen mechanical properties for increasing knot size in a theoretical 225 mm x 75 mm section derived from ASTM D 245

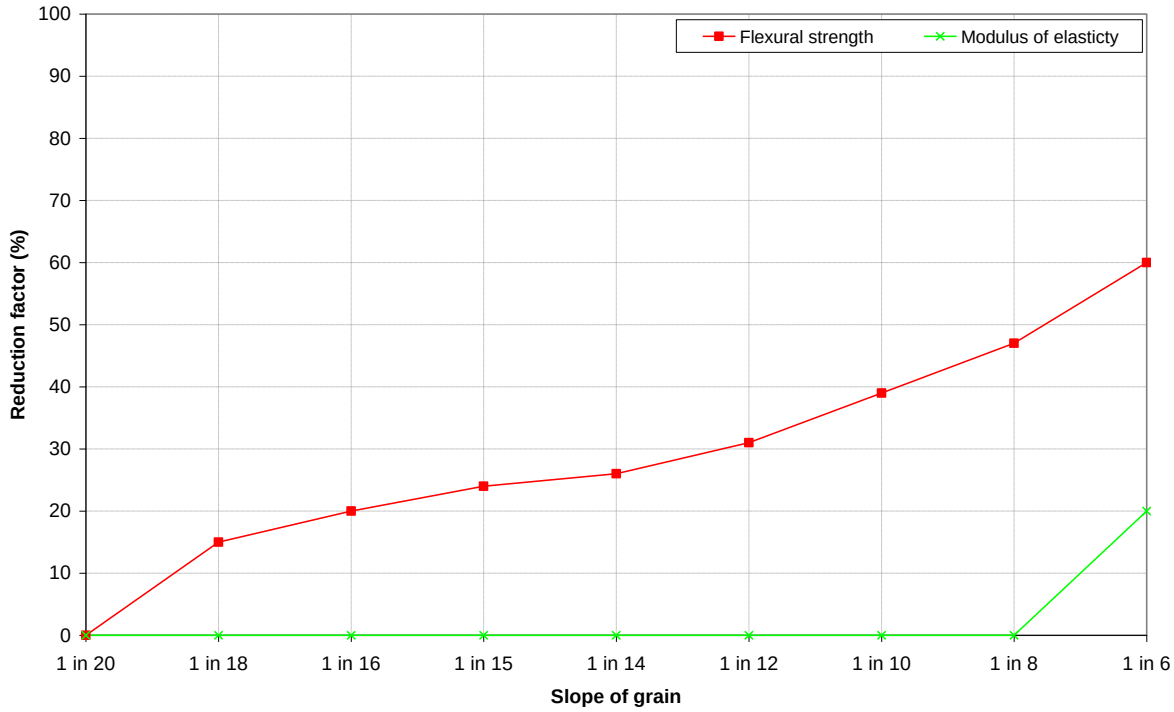

Figure 6-21: Reductions of small clear specimen mechanical properties for increasing slope of grain in a theoretical 225 mm x 75 mm section derived from ASTM D 245

The reduction factors presented in Figures 6-20 and 6-21 show that the greatest impact on mechanical properties as a result of increasing knot area and slope of grain is the reduction in flexural strength, with changes in the modulus of elasticity being relatively small in comparison. Utilising the methodology detailed in ASTM D 245 it was observed that knots located on the narrow face were associated with the largest reductions in flexural strength, a result that was expected, given the distribution of stresses in a beam under a flexural load.

While timber grades are no longer derived utilising small clear specimens, it is possible to use the results obtained for the specimens tested in this study to gain indicative results of the flexural strength and modulus of elasticity values that may be achieved in full size sections, containing defects similar to those found within sections classified as either GS and SS visual grades, as specified in BS 4978:2007 'The visual strength grading of softwood specification' (BSI, 2007). This is done utilising a method described in Dinwoodie (1981), in which the flexural strength reduction associated with the defects found within GS sections is stated as being approximately 70 % and those in SS sections 40 %. No reduction is applied to modulus of elasticity results using the method. In utilising these reduction factors with the methodology given in CP 112:1971 'The structural use of timber' (BSI, 1971) which utilised small clear specimens for the determination of properties, the grade stresses for the sample can be

calculated. While the method outlined by Dinwoodie was intended to match the criteria for GS and SS sections specified in the 1973 edition of BS 4978 (BSI, 1973), little difference exists in the core requirements regarding acceptable imperfections for GS and SS sections compared with the current 2007 edition. Table 6-5 shows the calculation steps required in CP112:1971 and their application on the results obtained through testing 40 - 50 year old sample trees in this study.

Table 6-5: Calculation of flexural strength for GS and SS visual grades based on CP 112:1971

Calculation steps in CP112:1971	**Application to test results**
Step 1 Calculate the lower 1 percentile value of the flexural strength distributions for the specimens by subtracting 2.33 standard deviations (S) from the mean	**Step 1** Mean = 80 N/mm^2 Standard deviation = 14 N/mm^2 80 - (2.33*14) = 47 N/mm^2
Step 2 Divide results obtained in step one by 2.25 to take account of rate of loading, specimen size and shape	**Step 2** 47/2.25 = 21 N/mm^2
Step 3 Apply reduction factors of 70 % for GS and 40 % for SS	**Step 2** GS: 21 - 70 % = 6.3 N/mm^2 SS: 21 - 40 % = 12.6 N/mm^2

The grade stress for flexural strength that Douglas-fir sections classified as either GS or SS should be able to satisfy, as stated in Dinwoodie (1981), are 6.3 and 9 N/mm^2 respectively. The results calculated here met these requirements in both cases. The requirements for mean modulus of elasticity are 9800 and 10700 N/mm^2 respectively, as such the mean for all 40 - 50 year old specimens, at 9900 N/mm^2, meets the requirement for the GS but not SS grade. The results for repeating the calculations shown in Table 6-5 for the results obtained in juvenile and mature wood separately are shown in Table 6-6.

Table 6-6: Calculation of flexural strength for GS and SS visual grades based on CP 112:1971 for juvenile and mature specimens

Juvenile wood	**Mature wood**
Flexural strength	Flexural strength
GS = 5.6 N/mm^2	GS = 7.7 N/mm^2
SS = 10 N/mm^2	SS = 15.3 N/mm^2
Modulus of elasticity	Modulus of elasticity
Mean = 9100 N/mm^2	Mean = 11300 N/mm^2

The results show that within juvenile wood the requirements for neither GS nor SS grades are achieved, with the values for flexural strength and modulus of elasticity influenced by the low values seen near the pith, while in the mature wood the requirements are satisfied in both cases. It is also noted in the mature wood that some large differences exist between the calculated flexural strengths and required values, particularly in the case of the SS grade. The implications of which are discussed further in Chapter 9. As was stated previously, the statistical nature of the reduction factors used means that the results obtained here are only indicative of those which may be found in structural sized sections. As such, further work is required to fully account for the influence of imperfections on structural sized sections, and to assess the characteristic values of visually graded Douglas-fir sections grown in the South West of the United Kingdom.

6.8 Concluding remarks

Results derived from the testing of defect free specimens of timber presented in this chapter have demonstrated that within and between trees, a large variability exists in the selected mechanical characteristics of importance when utilising timber in structural applications. Both the cambial age of specimens and rate of growth were identified as key drivers of this variability, with large increases observed in the magnitude of selected properties at younger cambial ages. An increased rate of growth was found to have a negative impact on properties, although changes in values were less substantial than those seen with increasing cambial age. No influence of geographic orientation on either flexural strength or modulus of elasticity was identified. The mechanical properties obtained in mature specimens were found to compare favourably with documented results for material obtained from different locations globally.

The potential implications of the results for utilisation in structural applications were assessed through the calculation of strength classes according to British Standard methods. This was

done for various combinations of age and rate of growth, with satisfactory strength classes for general structural applications achieved in most cases. The results for mature timber in particular indicated the potential for the production of high quality material. The modulus of elasticity of test specimens was identified as the limiting factor in all cases considered. However, it was shown that the presence of defects in structural sized specimens may result in significant reductions in material performance, and as such the results presented demonstrate the upper bound of the structural performance that may be achieved with the sample material.

Chapter 7 - Anatomical and mechanical property relationships

7.1 Introduction

In previous chapters the changes in several properties related to wood quality with age, growth rate and sampling location within the Douglas-fir sample trees were evaluated. As a result of the relatively recent development of tools to more readily assess the microscopic characteristics of large numbers of wood specimens, there is still only a limited understanding of the associations that exist between the properties presented previously, at different stages of maturation within the tree. The aim of this chapter is therefore to develop a greater understanding of the relationships between the mechanical performance of timber derived from both juvenile and mature wood, and its physical and anatomical characteristics. This is done firstly by studying the linear correlations between properties in Section 7.2, followed by the splitting of the direct and indirect effects of relationships utilising path analysis in Section 7.3. Finally, a series of statistical models are developed in Section 7.4 for the prediction of the three assessed mechanical properties based on various combinations of micro and macroscopic anatomical characteristics. The key findings of each analysis are presented within each section, with complete results shown within Appendix D, as denoted at the start of each sub-section.

7.2 Correlations between wood properties

7.2.1 Outline

The results presented previously in Chapters 4 and 6, showed that there was a large degree of variability in all of the properties evaluated over at least a part of the time period for which the assessments were conducted. The primary objective of the analysis conducted in this section was to establish the correlations between the dependent variables of modulus of elasticity, flexural and compressive strength and the independent variables of microfibril angle, density and the proportions of early, transition and latewood. The correlations between other growth related factors such as ring widths and cambial age with the mechanical properties were also evaluated. A secondary objective was the investigation of the relationships that exist within different combinations of mechanical and anatomical properties, allowing a further understanding and validation of the results presented in previous chapters to be gained.

The results presented in this section relate to those obtained from 40 - 50 year old sample trees. The values of mechanical properties used in the analysis were obtained utilising the flexural and compressive small clear specimen tests described in Section 3.6. Anatomical properties were evaluated with the use of the SilviScan-3 system following the methodologies given in Section 3.5. In order to allow the results for mechanical and anatomical properties to be compared directly, small clear specimens were matched to the equivalent radial position on the corresponding SilviScan-3 specimen, the process for which is described in Section 3.9. Mean ring widths were determined based on the widths of complete growth rings within each small clear specimen. Whilst assessing the correlations between dependent and independent variables, non-linear as well as linear relationships were evaluated. It was however found in all cases that the strongest results across juvenile and mature wood and at the whole tree level were achieved with the use of linear relationships. As such all references to correlations in the following discussions refer to the linear correlation coefficient, determined utilising the methodology detailed in Section 3.10.3. All correlations were deemed significant when $P \leq 0.05$. The analysis was conducted considering results from both sampling heights in combination. This was done firstly considering all specimens, regardless of cambial age, the results of which are referred to as 'whole tree' results. Following this, the analysis was conducted separately for specimens classified as either juvenile or mature wood. The classification of either type of wood was made on the basis of the results presented in Section 5.3. The first specimen of a radial sample containing no growth rings evaluated as juvenile from the perspective of both density and microfibril angle was classified as mature. The results

of the correlation analysis are presented at the whole tree level and then separately for juvenile and mature wood in Table 7-1.

Table 7-1: Correlation coefficients between studied anatomical and mechanical properties in small clear test specimens

MOE	1 *1,1*												
FS	0.87 *0.81,0.85*	1 *1,1*											
COMP S	0.75 *0.73,0.58*	0.77 *0.72,0.64*	1 *1,1*										
AGE	0.51 *0.56,**0.10***	0.56 *0.50,0.30*	0.59 *0.60,0.25*	1 *1,1*									
RW	-0.46 *-0.33,-0.54*	-0.52 *-0.44,-0.53*	-0.37 *-0.24,-0.39*	-0.21 *-0.31,**0.03***	1 *1,1*								
EWP	**0.09** ***0.12**,**0.10***	**-0.01** ***-0.01**,**-0.04***	0.11 *0.17,**0.10***	**0.09** *0.16,**0.02***	-0.13 ***-0.06**,-0.25*	1 *1,1*							
TWP	-0.58 *-0.53,-0.37*	-0.53 *-0.44,-0.36*	-0.53 *-0.51,-0.28*	-0.53 *-0.62,-0.27*	0.44 *0.35,0.57*	-0.57 *-0.64,-0.50*	1 *1,1*						
LWP	0.60 *0.54,0.39*	0.61 *0.56,0.42*	0.50 *0.45,0.27*	0.54 *0.60,0.26*	-0.39 *-0.37,-0.55*	-0.27 *-0.28,-0.41*	-0.64 *-0.56,-0.59*	1 *1,1*					
BULK DEN	0.68 *0.50,0.71*	0.75 *0.70,0.77*	0.69 *0.65,0.71*	0.51 *0.32,0.31*	-0.44 *-0.45,-0.36*	-0.17 *-0.21,-0.22*	-0.39 *-0.24,-0.34*	0.62 *0.54,0.56*	1 *1,1*				
SS DEN	0.70 *0.54,0.69*	0.76 *0.68,0.70*	0.70 *0.60,0.58*	0.56 *0.33,0.34*	-0.44 *-0.43,-0.38*	-0.23 *-0.30,-0.31*	-0.41 *-0.25,-0.33*	0.70 *0.64,0.63*	0.87 *0.80,0.88*	1 *1,1*			
EW DEN	0.24 ***0.02**,0.55*	0.35 *0.18,0.61*	0.13 ***-0.06**,0.39*	0.13 *-0.35,0.40*	-0.25 *-0.16,-0.34*	**-0.09** ***-0.11**,**-0.09***	**-0.03** ***0.14**,-0.25*	0.13 ***-0.06**,0.34*	0.52 *0.40,0.69*	0.60 *0.55,0.75*	1 *1,1*		
TW DEN	0.64 *0.54,0.53*	0.64 *0.58,0.48*	0.57 *0.56,0.33*	0.56 *0.37,0.37*	-0.48 *-0.40,-0.44*	0.20 *0.23,**0.16***	-0.45 *-0.40,-0.26*	0.35 *0.25,**0.12***	0.63 *0.54,0.55*	0.72 *0.64,0.64*	0.36 *0.28,0.45*	1 *1,1*	
LW DEN	0.66 *0.52,0.61*	0.61 *0.47,0.53*	0.63 *0.57,0.46*	0.57 *0.37,0.41*	-0.34 ***-0.14**,-0.45*	0.36 *0.39,0.37*	-0.55 *-0.45,-0.46*	0.3 ***0.13**,**0.15***	0.62 *0.43,0.63*	0.67 *0.49,0.70*	0.34 *0.19,0.56*	0.73 *0.63,0.72*	1 *1,1*
MFA	-0.63 *-0.60,-0.53*	-0.42 *-0.32,-0.28*	-0.57 *-0.55,-0.39*	-0.31 *-0.59,-0.29*	0.23 ***0.04**,0.40*	-0.23 *-0.27,**-0.14***	0.57 *0.53,0.30*	-0.45 *-0.38,-0.18*	-0.29 *-0.16,-0.18*	-0.33 ***-0.14**,-0.27*	0.15 *0.37,**-0.13***	-0.38 *-0.25,-0.18*	-0.50 *-0.40,-0.30*	1 *1,1*
	MOE	**FS**	**COMP S**	**AGE**	**RW**	**EWP**	**TWP**	**LWP**	**BULK DEN**	**SS DENS**	**EW DEN**	**TW DEN**	**LW DEN**	**MFA**

Abbreviations

All correlations derived from means for small clear specimens

MOE Modulus of elasticity

FS Flexural strength

COMP S Compressive strength

AGE Cambial age

RW Ring width

EWP Earlywood proportion

TWP Transition-wood proportion

LWP Latewood proportion

BULK DEN Bulk density

SS DEN SilviScan-3 whole ring density

EW DEN Earlywood density

TW DEN Transition-wood density

LW DEN Latewood density

MFA Whole ring microfibril angle

Note: Correlation coefficients in italics display separate results for juvenile wood (L) and mature wood (R) results displayed in bold were not statistically significant

7.2.2 Correlations with density

In the determination of correlation coefficients, relationships with two whole specimen density parameters were assessed, as shown in Table 7-1. Bulk density was determined utilising dimensions and masses recorded on each specimen directly prior to conducing mechanical testing. The SilviScan-3 density was determined by the matching of small clear specimens with the equivalent SilviScan-3 analysis results. The results presented in Table 7-1 show that a strong relationship was found between the densities determined by means of the two methods ($r = 0.87$), with similar coefficients for the two methods also returned when the variables were correlated against other anatomical and mechanical characteristics. Table 7-2 shows the differences between the recorded values obtained using the two methods, with SilviScan-3 derived mean specimen density lower than that determined through direct measurements. The comparable coefficients of variation for both methods indicate a similar dispersion about the mean. The lower mean density within the SilviScan-3 results is most likely due to the fact that these specimens had been subjected to Soxhlet extraction prior to testing, resulting in the removal of extractives from the cell lumens and consequently some mass. Differences between the results may also be attributed to inaccuracies in the matching of small clear specimens to SilviScan-3 data, differences in the moisture content of specimens at the time of determining density, with values of 8.5 and 12 % for SilviScan-3 and bulk calculations respectively and due to the fact that variations which may have occurred along the length of the small clear specimens were not reflected in the smaller specimens used to obtain the SilviScan-3 data. In light of the fact that a strong relationship was found between the two methods, and due to a number of other parameters being assessed utilising the SilviScan-3 results, all references to density in the following discussions refer to that obtained through use of the SilviScan-3 system, unless noted otherwise.

Table 7-2: Small clear specimen density derived by direct measurement and SilviScan-3

	Bulk density	**SilviScan-3 density**
Mean (kg/m^3)	510	480
Coefficient variation (%)	14	15

At the whole tree level, density was found to have the strongest overall correlation with mechanical properties of all anatomical characteristics evaluated. Relationships were moderate to strong and positive for all three mechanical properties, with correlation coefficients of the order of $r = 0.7$, indicating that an increase in density was associated with an increase in

stiffness and strengths. For the modulus of elasticity, correlations were found to be weaker in the juvenile wood, while strength characteristics showed no large differences between juvenile or mature growth rings for either methodology of density measurement. Explanations for the variations in the strengths of correlations observed with age are presented in Section 7.3. The findings observed were in good agreement with those shown for Douglas-fir mature wood modulus of elasticity and flexural strength determined on small clear specimens by Lachenbruch et al. (2010), where bulk density correlations were in the range of r = 0.6 to 0.7 and also by Vikram et al. (2011) using structural sized sections with an average age of nine years to determine modulus of elasticity (r = 0.67). These results are also in agreement with behaviour observed in Black spruce (Alteyrac et al., 2006), Norway spruce (Gindl and Teischinger, 2002), Radiata pine (Ivkovi et al., 2009) and Red pine (Deresse et al., 2003).

It was found that when evaluating the correlations between individual density components at the whole tree level, earlywood density was less strongly associated with increases in the magnitude of mechanical properties than was that of either transition or latewood. It was also noted that weak correlations existed between the earlywood density and all three mechanical properties within juvenile wood growth rings. Differences between the correlations of transition and latewood density with mechanical properties in juvenile and mature wood were generally smaller and less consistent than those seen for earlywood. The three density components were found to be similarly related with whole specimen mean density at the whole tree level, although correlation coefficients were weaker within juvenile growth rings for both early and latewood. The causes of the patterns of correlations observed among density components is assessed in Section 7.3.4

7.2.3 Correlations with microfibril angle

At the whole tree level the correlations displayed between specimen mean microfibril angle and mechanical properties ranged from r = -0.42 to r = -0.63, with the weakest relationship observed being that with flexural strength. The negative coefficients indicate that a decreasing microfibril angle was associated with increases in both stiffness and strength characteristics. Correlation coefficients were found to show a reduction in magnitude within the mature wood specimens. It was noted by Lachenbruch et al. (2010) in Douglas-fir that microfibril angle displayed weaker correlations with flexural strength than modulus of elasticity, in agreement with the findings presented here. The correlations with modulus of elasticity recorded by Lachenbruch et al. and also those found by Vikram et al. (2011) were both lower than those which are reported here (r = - 0.42 and -0.50) and those found in a number of other studies

noted below. This was postulated by Vikram et al. to potentially be as a result of the limited distribution of the microfibril angles of the specimens tested due to their limited age range. Correlation coefficients found in other softwood species have shown similar results to those recorded here for both modulus of elasticity and flexural strength, including Black spruce (Alteyrac et al., 2006), Radiata pine (Ivkovi et al., 2009) and Red pine (Deresse et al., 2003). No previous literature was found directly correlating microfibril angle to compressive strength. Due to the lack of detailed data regarding microfibril angle intra-ring variations, it was not possible to assess the impact of early, transition or latewood microfibril angles on the mechanical characteristics.

7.2.4 Correlations with proportions of wood types

At the whole tree level, the proportion of latewood within a specimen was found to show moderate to strong positive correlations with whole ring mean density ($r = 0.70$). Conversely, an increase in early and transition-wood proportions was negatively correlated with mean density, although the strength of the relationships was significantly weaker. These results were to be expected, given the higher densities observed within latewood in Section 4.6. It was noted that increases in earlywood proportion had a weaker association with decreasing density than did increases in the proportions of transition-wood. This is likely due to the relationships that exist between the proportions of wood types within a growth ring, where increases in earlywood proportion demonstrated stronger correlations with decreasing transition-wood proportions, than a decreasing latewood proportion ($r = -0.57$ and $r = -0.27$). An increase in latewood proportion was also associated with a decrease in the microfibril angle ($r = -0.45$), with the opposite true of a rise in the quantity of transition-wood present within a specimen. This is in agreement with the results regarding the magnitude of microfibril angle in different regions of the growth ring presented in Section 4.7, in which values in the transition-wood were found to be lower than those in latewood. The correlation coefficients also showed that an increase in the proportions of earlywood was associated with a decrease in the angle of cellulose microfibrils, although the relationship was weak ($r = -0.23$). This result was most likely due to the interactions between the changing proportions of tracheid types within a growth ring discussed previously.

An assessment of the associations between proportions and mechanical properties also returned some moderate to strong correlations, to be expected in light of the relationships with anatomical properties described above. All mechanical properties displayed an increase in magnitude as the proportion of latewood within a specimen rose, with whole tree correlation

coefficients ranging from r =0.50 to r = 0.61, with stronger relationships being observed within juvenile growth rings. Increases in transition-wood proportion produced an almost equal and opposite response, while the majority of the correlation coefficients returned for earlywood proportions were non-significant or very weak. The differences in the strengths of the correlations recorded between juvenile and mature wood can be attributed to the fact that the greatest range of variations in the proportions of tracheid types was found within the juvenile growth rings, as observed in Section 4.3. The weak relationships with earlywood proportion is likely due to the limited range of the values found in both juvenile and mature wood, combined with the relationships between earlywood proportion and anatomical properties described above.

7.2.5 Correlations with cambial age and ring width

As a result of the large degrees of variability of many anatomical and mechanical properties with age, and to a lesser extent growth rate, shown previously in Chapters 4, 5 and 6, a number of statistically significant correlations were achieved when assessing the relationships of specimen mean cambial age and ring width with other characteristics. Specimen mean cambial age displayed correlation coefficients of r = 0.56 and r = -0.31 for whole ring mean density and microfibril angle respectively, with markedly stronger correlations observed in the juvenile wood for microfibril angle. Correlations with ring width ranged from r = -0.44 for density to r = 0.23 for microfibril angle, again with variations in the strengths of correlations being found between juvenile and mature wood for microfibril angle. The strengths of correlations observed between anatomical properties and mean ring widths are largely in agreement with those presented in Section 5.2. Differences in the values attained in this section can be apportioned in part to the fact that the correlations reported also account for changes in ring widths observed in the natural process of stem maturation, not considered in Section 5.2, where correlations were evaluated at a ring by ring level.

All three mechanical properties showed moderate positive correlations with cambial age within the juvenile wood, ranging from r = 0.56 to r = 0.60, while in the mature wood all correlations were found to be weak and in the case of modulus of elasticity, statistically non-significant. Specimen mean ring width was also found to show weak to moderate correlations with all mechanical properties studied, with stronger correlations found in the mature growth rings.

The correlations between various combinations of independent and dependent variables presented in this section has allowed for the quantification of several relationships and trends presented in previous chapters. Many of the relationships reported are however not strictly causal, due to concurrent variations occurring in numerous properties. In the next section, path analysis is used to help gain a greater understanding of the links that exist between some of the relationships presented here. In Section 7.4 the results found are used to inform the development of statistical models for the prediction of mechanical properties based on specimen anatomical characteristics.

7.3 Causation from path analysis

7.3.1 Outline

In the previous section the correlations between several combinations of anatomical and mechanical properties were presented. While allowing for the quantification of the linear relationships that exist between variables, the analysis conducted did not allow for the determination of any cause and effect relationships, as several other properties not being evaluated may have also had an indirect influence on the dependent variable studied. In this section path analysis is used to better understand the direct and indirect associations between several combinations of independent and dependent variables, allowing the relationships presented previously to be better understood. Path analysis assesses the direct relationship that exists between an independent and dependent variable if no changes occur in the values of the other independent variables present within the model. A description of the methodology used and its implementation can be found in Section 3.10.7.

In conducting the path analysis, several models were used, each containing different combinations of independent and dependent variables. All models evaluated relationships at the whole tree level and also separately for juvenile and mature wood. A summary of the variables included within each of the models is given in Table 7-3. As was shown in Table 7-1, interactions between independent variables are extensive. The variables included in the models presented in the following sections were selected on the basis of those that would allow new insights into the interactions between anatomical and mechanical properties to be gained. The list of variables included in the models is however not exhaustive, and it is likely the case that interactions with independent variables not included in the models will also influence the magnitude of the dependent variables. All variables were the mean values for small clear specimens, calculated as described in the previous section. Density refers to that determined

through SilviScan-3 analysis. A complete set of standardised regression coefficients for each model can be found in Appendix D, as noted at the start of each sub-section. Path diagrams showing the correlation between independent variables (r) and standardised regression coefficients between independent and dependent variables (β) at the whole tree level can be found in the following sub-sections.

Table 7-3: Path analysis model variable summary

	Independent variables	**Dependent variables**
Model 1	Whole ring density Whole ring microfibril angle	Modulus of elasticity Flexural strength Compressive strength
Model 2	Whole ring density Whole ring microfibril angle Cambial age Ring width	Modulus of elasticity Flexural strength Compressive strength
Model 3	Earlywood density Transition-wood density Latewood density Whole ring microfibril angle	Modulus of elasticity Flexural strength Compressive strength

7.3.2 Model 1

7.3.2.1 Modulus of elasticity path coefficients

The path diagram in Figure 7-1 shows the relationships between specimen mean whole ring density, whole ring microfibril angle and modulus of elasticity at the whole tree level. Path coefficients for juvenile and mature wood are shown in Table D-1.

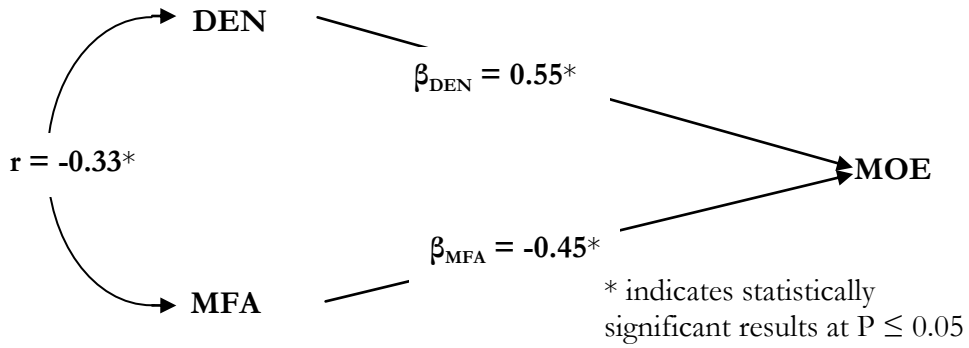

Figure 7-1: Model 1 modulus of elasticity path diagram for whole tree path coefficients with direct effects displayed by straight arrows and indirect effects curved arrows

In Section 7.2 both mean density and microfibril angle displayed moderate to strong correlations with modulus of elasticity at the whole tree level. When evaluated with the use of path analysis, most of these correlations were found to lie on the direct paths (r_{DEN} = 0.70 β_{DEN} = 0.55, r_{MFA} = -0.63 β_{MFA} = -0.45), with the remainder due to the indirect relationship between density and microfibril angle, which takes account of the fact that in general as microfibril angle declines density rises, as observed in Chapter 4. The relationships found within specimens containing either juvenile or mature growth rings were different to those observed at the whole tree level. Within the juvenile wood, path analysis demonstrated that most correlations were derived from direct relationships. The magnitude of the results indicated that a decreasing microfibril angle was more strongly related with increasing modulus of elasticity than was a rise in density ($r_{DEN\text{-}JUVENILE}$ = 0.54 $\beta_{DEN\text{-}JUVENILE}$ = 0.44, $r_{MFA\text{-}JUVENILE}$ = -0.60 $\beta_{MFA\text{-}JUVENILE}$ = -0.55). Within mature growth rings, direct relationships still accounted for the large majority of the correlations observed between density and modulus of elasticity in Table 7-1, however compared to the juvenile wood, a greater proportion of the relationships between microfibril angle and modulus of elasticity were through the indirect relationship with density. The magnitude of the results was also reversed to those seen within the juvenile wood, with higher standardised regression coefficients between density and modulus of elasticity than microfibril angle (r_{DEN} = 0.69 β_{DEN} = 0.59, r_{MFA} = -0.53 β_{MFA} = -0.26).

7.3.2.2 Flexural strength path coefficients

The path diagram in Figure 7-2 shows the relationships between specimen mean whole ring density, whole ring microfibril angle and flexural strength at the whole tree level. Path coefficients for juvenile and mature wood are shown in Table D-2.

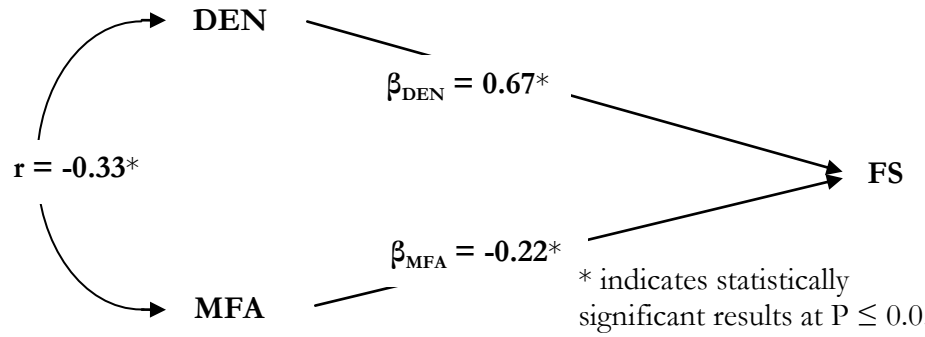

Figure 7-2: Model 1 flexural strength path diagram for whole tree path coefficients with direct effects displayed by straight arrows and indirect effects curved arrows

At the whole tree level, the majority of the correlations observed in Table 7-1 between density and flexural strength were found to lie on direct paths (r_{DEN} = 0.76 β_{DEN} = 0.67), indicating a moderate to strong relationship between the two properties. For microfibril angle however the indirect relationship with density also played an important role. As such the difference between the correlations observed in Table 7-1 and the standardised regression coefficient was greater than that found for density (r_{MFA} = -0.42 β_{MFA} = -0.22), the standardised regression coefficient was also significantly lower for microfibril angle, indicating a weak relationship with flexural strength. The path analysis also showed that in both the juvenile and mature wood, virtually all correlations with density lie on direct paths, exhibiting moderate to strong relationships ($\beta_{DEN\text{-}JUVENILE}$ = 0.64, $\beta_{DEN\text{-}MATURE}$= -0.65). For microfibril angle, the weak relationship observed at the whole tree level was also found within the juvenile and mature wood, with standardised regression coefficient within the mature wood found to be statistically non-significant ($\beta_{MFA\text{-}JUVENILE}$ = -0.23, $\beta_{MFA\text{-}MATURE}$= -0.11).

7.3.2.3 Compressive strength path coefficients

The path diagram in Figure 7-3 shows the relationships between specimen mean whole ring density, whole ring microfibril angle and compressive strength at the whole tree level. Path coefficients for juvenile and mature wood are shown in Table D-3.

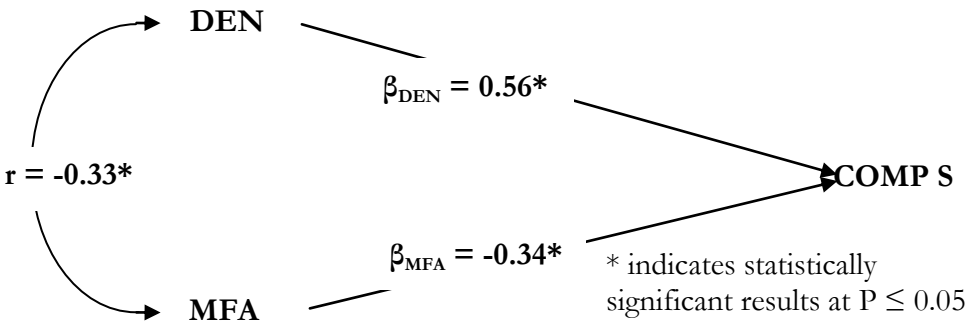

Figure 7-3: Model 1 compressive strength path diagram for whole tree path coefficients with direct effects displayed by straight arrows and indirect effects curved arrows

As reported previously for flexural strength, the majority of the correlations observed in Table 7-1 between density and compressive strength were found to lie on direct paths (r_{DEN} = 0.70 β_{DEN} = 0.56), with the values indicating a moderate to strong relationship between the two properties. For microfibril angle a greater degree of the relationship with compressive strength was due to indirect associations with density (r_{MFA} = -0.57 β_{MFA} = -0.34), however the magnitude of the standardised regression coefficients do show that a weak relationship between compressive strength and microfibril angle does exist at the whole tree level. Both density and microfibril angle displayed weak to moderate standardised regression coefficients with compressive strength within the juvenile wood ($\beta_{DEN\text{-}JUVENILE}$ = 0.52, $\beta_{MFA\text{-}JUVENILE}$= -0.40), however in mature wood the relationship with microfibril angle was observed to be weaker ($\beta_{DEN\text{-}MATURE}$ = 0.49, $\beta_{MFA\text{-}MATURE}$= -0.24). Within both juvenile and mature wood the proportion of the relationship with compressive strength found to lie on direct paths was similar to that observed at the whole tree level for both independent variables.

7.3.2.4 Discussion of model 1 results

In the findings presented for mature Douglas-fir by Lachenbruch (2010), density was found to have a greater influence on both modulus of elasticity and flexural strength, with path coefficients similar to those reported for mature specimens here. Vikram et al. (2011) also identified similar relationships with modulus of elasticity utilising path analysis in sections with a mean age of nine years. In the case of both studies, the need to identify relationships in Douglas-fir specimens with a greater age range, encompassing both juvenile and mature wood variations, was identified by the authors. It was noted in the juvenile wood of Longleaf pine (Via et al., 2009) and Radiata pine (Baltunis et al., 2007, Ivkovi et al., 2009) that microfibril angle was more important in determining the modulus of elasticity than density. It was also noted by Ivkovi et al. that the direct effect of density on flexural strength was greater than that

of microfibril angle, in agreement with the results presented here. As with past studies demonstrating results in both juvenile and mature wood, those detailing relationships with compressive strength were limited.

One common factor observed in the strengths of all previous relationships of mechanical properties with density and microfibril angle, was that the magnitude of the standardised regression coefficients for microfibril angle decreased on moving from juvenile to mature wood, while those for density increased or remained at a similar value. Many of the variations due to individual relationships with mechanical properties, to be discussed in the following pages, can be better understood if the differences in the developmental profiles of the two characteristics are highlighted. Although the transitional age from juvenile to mature wood varied widely between the sample trees, as shown in Section 5.3, by selecting a representative age of 20 years at breast height it can be seen that the increase in density from the minimum values in each region was marginally higher in the juvenile wood than mature, at 20 % and 15 % respectively. Conversely, microfibril angle displayed large decreases within the juvenile wood, much greater than those seen in mature specimens, with declines in values of 50 % and 15 % respectively.

In the past density was often regarded as the best predictor of wood modulus of elasticity, due to its ease of measurement and the good correlations between the two characteristics (e.g. Rozenberg et al., 1999), as was shown in Table 7-1. However, with the advent of measurement techniques enabling the easier collection of microfibril angle data, it is now accepted that, as shown in the results presented in Section 7.3.2.1, modulus of elasticity is under the control of both microfibril angle and density (Cave and Walker, 1994). The development of a micromechanical model detailing the relationship between the angle of cellulose microfibrils and density within the fibrilar and layered structure of tracheid cell walls, and the resultant impact on the modulus of elasticity within juvenile and mature wood is presented in Chapter 8.

The roles and interrelationships of density and microfibril angle leading to failure in axial compression are not as well documented as for other mechanical properties. In the results presented here, it was shown that within mature specimens, microfibril angle had only a weak direct relationship with compressive strength, while standardised regression coefficients of moderate strength were identified for density in both juvenile and mature wood. The prediction of wood compressive strengths by means of methods such as the critical buckling

load for axial loading in cellular structures proposed by Gibson and Ashby (1997), or that proposed by Grossman and Wold (1971) regarding compression failure following the delamination of the double cell wall, were shown by Gindl and Teischinger (2002) to be inaccurate. This is largely due to the fact that axial compressive failure is thought to primarily occur as a result of localised buckling due to the deviation of tracheids in the region of rays (Dinwoodie, 2000). The implications of these deviations in tracheids can be better understood with reference to Equation 7-1, presented in Gindl and Teischinger (2002).

$$\sigma_c = \frac{\tau_y}{\theta} \qquad 7\text{-}1$$

Where: σ_c compressive failure initiation stress

τ_y shear yield strength of cell wall

θ microfibril angle

From the equation it can be seen that an increase in shear yield strength or decrease in the microfibril angle can be attributed to an increase in the stress sustained prior to the initiation of compressive failure. Assuming that the properties of the cell wall constituents remain constant with age, increasing shear yield strength can be attributed to an increase in cell wall thickness which is related to density. Assuming loading parallel to the grain, in regions where tracheids deviate around rays, the S_2 layer microfibril angle in one of the tangential cell walls with respect to the direction of loading increases, due to microfibrils on opposite cell walls being orientated in opposing directions. As a result, the load at which compressive failure is initiated is reduced. It can therefore be seen that as microfibril angle declines and density increases with cambial age, as shown in Chapter 4, compressive strength also rises. The limited range of microfibril angles within the mature wood is therefore a likely contributor to the weak relationship with compressive strength observed within this region. Correlations between density, microfibril angle and chemical constituents not studied here may also play a role in influencing compressive strengths. It was postulated by Via (2009) that lignin exhibits greater plastic deformation when loaded at large angles to the microfibril orientation. Via discovered that high lignin contents occurred in juvenile wood, where cellulose microfibril angle is also high.

The flexural strength of specimens was found to be largely under the control of density, with a weak association with microfibril angle in the juvenile wood. The mechanism leading to the failure of specimens in flexure is a result of a combination of factors, summarised below.

Specimens subject to flexure experience compression above the neutral axis and tension below. As shown in Dinwoodie (2000) and to be discussed in Section 8.2.1, the limit of proportionality, above which plastic deformations occur, is reached first in timber subject to compression. As a result of this, the mechanisms dictating the ultimate stress that can be sustained in tracheids above the neutral axis will be similar to those discussed previously for compressive specimens, in which both density and microfibril angle were identified to have an influence on the mechanical behaviour within the juvenile wood. The point at which failure occurs in the compressed tracheids has an important influence on a specimens behaviour, as the reduced effective cross section results in the neutral axis moving downward within the section imposing increased stresses on the tracheids subjected to tension.

Failure of wood in tension typically is initiated at the microscopic level when the stress over the S_1-S_2-S_3 laminate wall structure becomes sufficiently great to initiate separation at the S_1-S_2 interface, with the transfer of stresses to the S_2-S_3 layers. Ultimate failure typically occurs in the S_2 layer, with the occurrence of first inter-polymer then intra-polymer separation through the breaking of covalent bonds, during which time large irrecoverable deformations occur in the wood molecular structure (Rowell, 2005). It can therefore be seen that an increase in density, and hence the available area over which imposed forces can be carried, will result in a rise in the ultimate stress that can be sustained prior to failure, explaining the strong direct relationships observed in the previous path analysis shown in Section 7.3.2.2. It is unlikely however, even in the defect free specimens used here, that this is the sole mechanism responsible for section flexural strength. The presence of resin canals, internal checking and small areas of compression wood not easily identifiable can act as stress raisers, which initiate crack propagation leading to failure, and are factors which complicate the prediction of specimen ultimate failure load (Lachenbruch et al., 2010).

7.3.3 Model 2

7.3.3.1 Path coefficients

In the correlations displayed in Section 7.2, specimen mean age and ring width were both shown to be moderately correlated with changes in the magnitudes of the three mechanical properties at the whole tree level, and also in the majority of juvenile and mature wood regions. In the model presented in this section, the direct and indirect relationships of these parameters with mechanical properties, alongside those of specimen mean whole ring density and whole ring microfibril angle, are evaluated. Path diagrams displaying the path coefficients

between all dependent and independent variables at the whole tree level are shown in Figure 7-4. Path coefficients for juvenile and mature wood for each mechanical property are shown in Tables D-4 to D-6.

At the whole tree level, the standardised regression coefficients between density, microfibril angle and mechanical properties were found to be marginally reduced compared to those presented in model 1. This was to be expected, given the inclusion of additional parameters within the model. The standardised regression coefficients for age at the whole tree level were very weak for all three mechanical properties (β = 0.1 to 0.16), with those between age and compressive strength statistically non-significant. When compared with the correlation coefficients between age and mechanical properties shown in Table 7-1 (r = 0.51 to 0.59), it can be seen that the large majority of these correlations are due to indirect relationships between age and both density and microfibril angle. Similar results were observed for specimen mean ring width, with the standardized regression coefficients at the whole tree level very weak (β =-0.07 to -0.22) with those between ring width and compressive strength statistically non-significant. Compared with the correlation coefficients observed in Table 7-1 (r = -0.37 to -0.53), the majority of the relationships were again due to those which lie on the indirect paths.

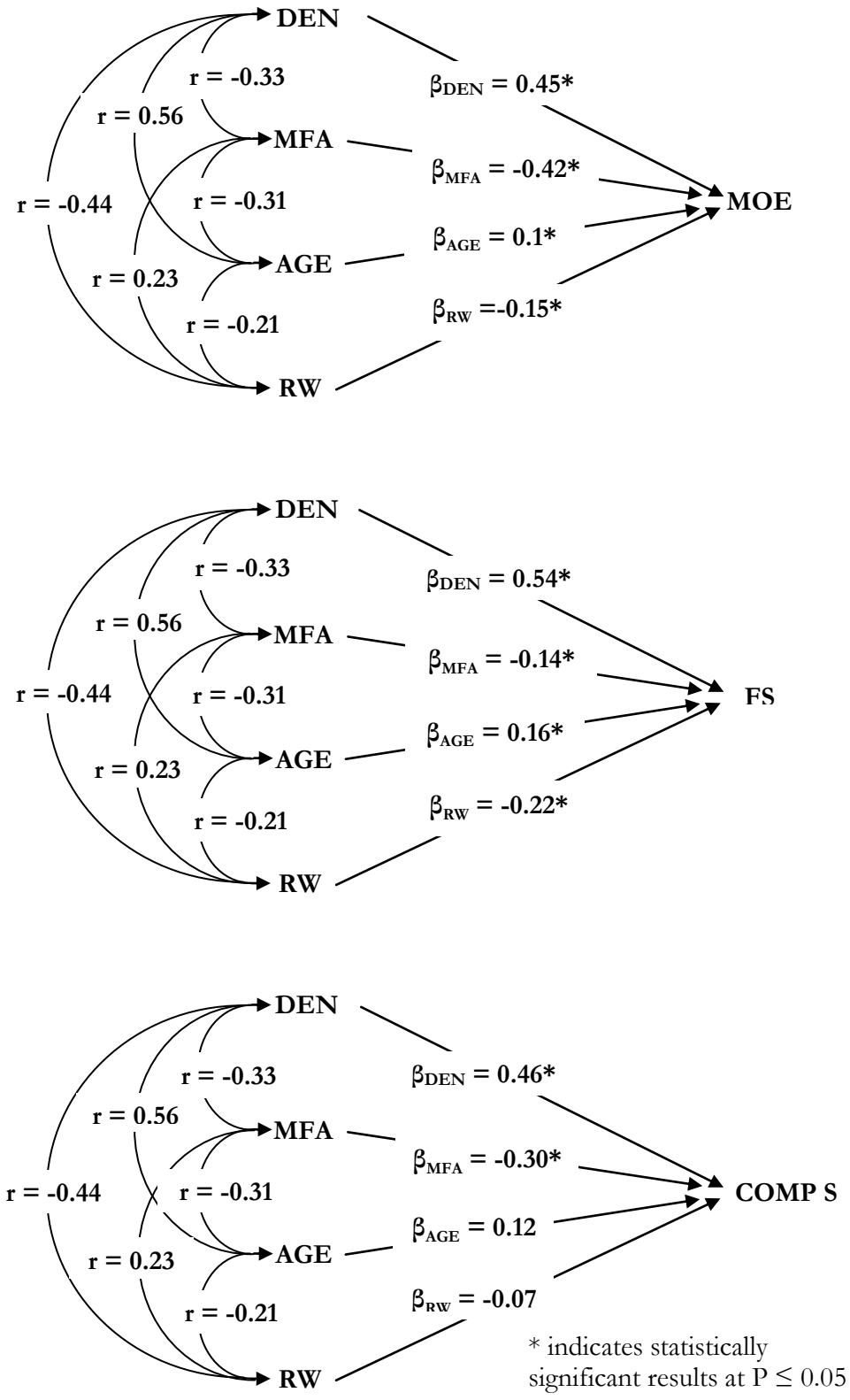

Figure 7-4: Model 2 path diagrams for whole tree path coefficients with direct effects displayed by straight arrows and indirect effects curved arrows

Within trees, the standardised regression coefficients between specimen age and mechanical properties were found to be marginally stronger in the juvenile growth rings than mature, with statistically non-significant results being returned in the mature wood in the case of all three mechanical properties. Again the large majority of the relationships observed in the correlations shown in Table 7-1 within juvenile and mature wood were found to be due to indirect interactions. The reverse was true of mean ring width, with stronger standardised regression coefficients being found within mature growth rings, ranging from β = -0.25 to -0.30 for modulus of elasticity and flexural strength respectively, with a greater degree of the interactions observed in Table 7-1 being due to direct effects than was seen for age. Standardised regression coefficients between ring width and compressive strength were found to be non-significant in both juvenile and mature wood.

7.3.3.2 Discussion of model 2 results

In Chapter 4 all anatomical properties studied exhibited a degree of variation with age over at least part of the time period for which they were assessed. The same was true in most instances for the response to increasing growth rates displayed in Chapter 5. As such, the results presented here in which specimen mean age and ring widths were, for the most part, found to be indirectly related to mechanical properties through relationships with density and microfibril angle were to be expected. In some cases, although typically weak, both age and ring width were found to display statistically significant standardised regression coefficients with mechanical properties, indicating that indirect relationships with the anatomical characteristics included in the model do not account fully for the changes in the mechanical properties of the specimens assessed. The most likely cause of this is the lack of complete fit of the results from small clear specimens to SilviScan-3 data, as discussed in Section 7.2, and the fact that the interactions between proportions of wood types with age and ring width are not considered in the model. The proportions of wood types have been shown in Chapters 4, 5 and Section 7.2 to be related to age and growth rate. Whilst the impact of changing proportions on density and microfibril angle should be negated while these parameters are held constant, there are likely other effects of increasing proportions of latewood on mechanical properties, such as chemical constituent variations (e.g. Via et al., 2009), not accounted for by changes in density or microfibril angle, which may explain the existence of weak direct interactions.

The differential observed in the strengths of the correlations of modulus of elasticity and compressive strength with age between juvenile and mature wood in the results presented in

Table 7-1, can be seen here to be in part accounted for by reductions in the strengths of indirect correlations between age and the microfibril angle ($r_{MFA - AGE\ JUVENILE}$ = -0.59 $r_{MFA - AGE\ MATURE}$ = -0.28). This can be explained with reference to the radial development profiles displayed in Section 4.7, in which it was observed that the large majority of the variation in the fibril angle occurred within the juvenile region. Although not assessed here, it is likely that due to the large majority of changes in the proportions of tracheid types also occurring within the juvenile zone, that this was also a contributing factor. Density was found to show similar relationships with age between juvenile and mature wood, despite the slight reduction in the range of density values observed within mature wood. The most likely explanation for this is the initial decline in whole ring mean density observed upon moving away from the pith in Figure 4-23. This region of non-linearity within the juvenile wood region will have resulted in a reduction in the strengths of the correlations between age and density.

The correlations of specimen mean ring width with modulus of elasticity and compressive strength also displayed a marked difference between the juvenile and mature regions in the results shown in Table 7-1. On inspection of the indirect path coefficients, this appears to be largely due to the increased strength of the relationship between mean ring width and microfibril angle within the mature wood ($r_{MFA - RW\ JUVENILE}$ = 0.04 $r_{MFA - RW\ MATURE}$ = 0.40), with microfibril angle shown in model 1 to be an important determinant of both modulus of elasticity and compressive strength. The interactions between flexural strength and mean ring width were observed to display less of a change in the correlation coefficients presented in Table 7-1 on moving from juvenile and mature wood, due to the limited change in the strength of relationships shown in the indirect path correlations with mean density ($r_{DEN - RW\ JUVENILE}$ = -0.43 $r_{DEN - RW\ MATURE}$ = -0.38), shown in model 1 to be a key determinant of flexural strength.

7.3.4 Model 3

In Section 7.2 it was shown, in either juvenile and/or mature wood, that early, transition and latewood density had moderate to strong correlations with mechanical properties. In the path analysis model presented here, the direct and indirect coefficients for the specimen means of the three constituent density components and whole ring mean microfibril angle with the three assessed mechanical properties are evaluated. Path diagrams displaying the path coefficients between all dependent and independent variables at the whole tree level are shown in Figure 7-5. Path coefficients for juvenile and mature wood for each mechanical property are shown in Tables D-7 to D-9.

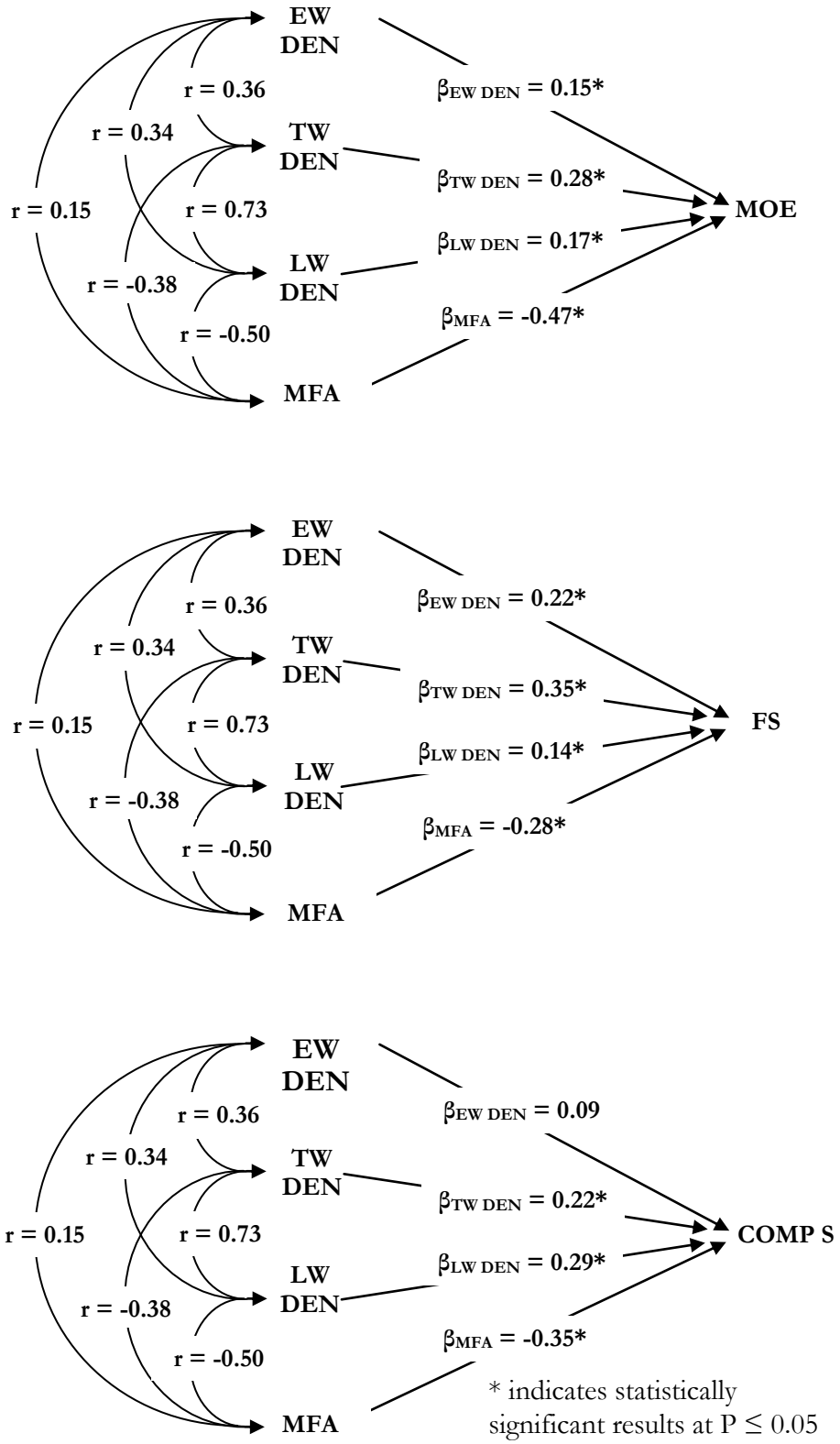

Figure 7-5: Model 3 path diagrams for whole tree path coefficients with direct effects displayed by straight arrows and indirect effects curved arrows

At the whole tree level and within both juvenile and mature wood, the standardised regression coefficients observed between microfibril angle and the three mechanical properties displayed similar values to those obtained in model 1. This finding was expected, given that within both models the fundamental properties assessed were the same. Within juvenile specimens, both early and latewood density were found to have statistically non-significant standardised regression coefficients with all three mechanical properties. The density of transition-wood was therefore the only density component that was significantly correlated with mechanical properties through direct relationships within this region, with coefficients ranging from $\beta = 0.30$ to $\beta = 0.43$. A greater proportion of the correlations between transition-wood density and flexural strength given within the juvenile wood in Table 7-1, were due to direct relationships than for either modulus of elasticity or compressive strength. Given the findings presented in model 1, regarding the extent to which the assessed mechanical properties are under the control of different anatomical characteristics, this result was expected. Indirect path coefficients showed that a combination of relationships of transition-wood density with rising early and latewood density and a falling microfibril angle accounted for a large majority of the remainder of the variations. The moderately strong correlations displayed between latewood density and mechanical properties within juvenile growth rings in Table 7-1, are therefore mainly due to indirect associations with transition-wood density and microfibril angle.

Within mature specimens, earlywood density was observed to have the strongest standardised regression coefficients with mechanical properties of the three density components. Coefficients were found to range from $\beta = 0.3$ to $\beta = 0.45$ with modulus of elasticity and flexural strength respectively. Compressive strength coefficients were found to lie between these values. The standardised regression coefficients between mechanical properties and the densities of transition and latewood were statistically significant in all cases; however the strengths were typically weak, particularly for transition-wood. Consequently, a large proportion of the correlations observed between the mechanical properties and densities of transition and latewood in Table 7-1 can be apportioned to indirect relationships with increases in other density components, particularly that of earlywood, and declines in microfibril angle. This is also true in the case of earlywood density, although to a lesser extent due to more of the relationships being found to lie on direct paths.

An investigation of potential explanations for the relationships between density components and modulus of elasticity is given in Chapter 8 with the use of a micromechanical composite

model. However, in consulting the profiles of proportions of wood types shown in Section 4.3 and the density profiles displayed in Section 4.6, additional factors which explain the observed relationship with all three mechanical properties can be proposed. Within juvenile growth rings, increases in transition-wood density were shown to be most strongly correlated with a rise in the values of mechanical proprieties of all density components. In the comparison of Figures 4-6 to 4-8, it can be seen that within the early juvenile growth rings, the largest proportion of tracheids were of the transitional type. As such, increases in transition-wood density would have the greatest impact on increasing specimen mean density in this region. At the 8 m sampling location, earlywood quickly rises with age to gain the greatest proportion within a growth ring, however a combination of falling density within the earlywood during the same period and the slower rise in proportion at breast height accounts for the non-significant standardised regression coefficients observed. The proportion of latewood was also low in the juvenile wood, as a result increases in latewood density will have resulted in only limited gains in specimen mean density. On moving to mature tracheids, changes in earlywood density were found to be more closely associated with increasing mechanical properties. This can be explained by the fact that within mature growth rings, earlywood tracheids make up by far the greatest proportion of the growth ring, while transition and latewood occupy similar proportions, accounting for the similarity in the standardised regression coefficients calculated.

7.4 Multiple regression models for the prediction of mechanical properties from wood component traits

7.4.1 Outline

Within this section multiple regression modelling is used for the prediction of specimen modulus of elasticity, flexural and compressive strength within the 40 - 50 year old sample trees. The micro and macroscopic anatomical properties shown in previous sections to be either directly or indirectly related to mechanical properties are used as input parameters for these models. A description of multiple regression analysis for the prediction of a dependent variable based on a combination of independent variables is given in Section 3.10.3.

Dependent on the size of section and the tools available for its examination, a different combination of anatomical properties will be known. For example, it is possible to measure age, ring width and latewood proportion with relative ease on whole log sections arriving at a saw mill, whereas within a laboratory environment age may not be known but it may be possible to measure density or microfibril angle. Due to this, in the following sub-sections results from a range of different models are presented, first for microscopic anatomical characteristics, followed by macroscopic properties and finally combinations of each. The density values used are those determined through the SilviScan-3 system. The complete results including coefficients from each regression analysis are included in Appendix D, as indicated at the start of each sub-section. Each of the models is presented at the whole tree level, again reflecting the fact that the height from which a section was obtained and the age of demarcation from juvenile to mature wood may not always be known, or easily determined.

7.4.2 Modulus of elasticity multiple regression models

In this section, statistical predictive models for modulus of elasticity are derived. The results shown in Table 7-4 give a summary of the variations accounted for by models with various combinations of independent variables. A complete set of coefficients for each multiple regression equation are given in Table D-10.

Table 7-4: Summary of multiple regression model results for the prediction of modulus of elasticity

	Coefficients	**Adjusted R^2**	**Coefficients**	**Adjusted R^2**
Microscopic properties models				
	DEN, MFA	0.65*		
Macroscopic properties models				
	AGE, RW	0.46*	LWP, RW	0.45*
	AGE, LWP	0.49*	AGE,RW,LWP	0.53*
Combination models				
	AGE, LWP, DENS	0.62*	AGE, LWP, DENS, MFA	0.68*
	AGE, LWP, MFA	0.54*	AGE, LWP, RW, DENS, MFA	0.70*

* indicates statistically significant results at $P \leq 0.05$

In Section 7.3, it was demonstrated with the use of path analysis that at the whole tree level modulus of elasticity is under the control of both density and microfibril angle. As such, the relatively high proportion of variation accounted for, at 65 %, by the multiple regression equation including these two variables was to be expected. It was also observed by Lachenbruch et al. (2010) in Douglas-fir that the inclusion of both density and microfibril angle within a regression model accounted for a greater degree of variation than when considering either characteristic individually. The model produced by Lachenbruch et al. accounted for 51 % of the variation observed. When knots were also included in a model alongside microfibril angle and density by Vikram et al. (2011), 59 % of the variation in modulus of elasticity observed in structural sized Douglas-fir sections was accounted for.

The correlations found in Section 7.2 highlighted the moderate to strong relationship between the proportion of latewood contained within the growth rings present in a specimen and its modulus of elasticity, an occurrence arising due to the high densities and low microfibril angles associated with latewood. As such, it was found that a regression model combining latewood proportion with age, which was also shown to be moderately correlated with modulus of elasticity due to indirect relationships, accounted for almost half of the variations observed. Due to the strong interrelationships between the macroscopic characteristics used, models combining ring width with either age or latewood proportion also accounted for a

moderate proportion of the variation observed, with a combination of the three returning an adjusted R^2 of 0.53.

It was found that the inclusion of either density or microfibril angle alongside the two macroscopic property variables that gave the strongest results when combined, age and latewood proportion, that a slight improvement in the adjusted R^2 values was returned. The addition of both microscopic characteristics alongside these two variables provided only small improvements in predictions over those found when the microscopic properties were considered by themselves. This result was to be expected, given that the large majority of the relationships assessed between age and modulus of elasticity in Section 7.3.3 were found to lie on indirect paths, with the majority of the associations with latewood proportions also likely due to indirect relationships. Similar results were observed for the other combinations of two macroscopic property variables. The inclusion of all parameters in the regression model gave an adjusted R^2 value of 0.70, with a residual standard error of 1100 N/mm^2 for modulus of elasticity. The graph in Figure 7-6 displays the relationship between observed modulus of elasticity values and those predicted by the combination regression model encompassing all parameters.

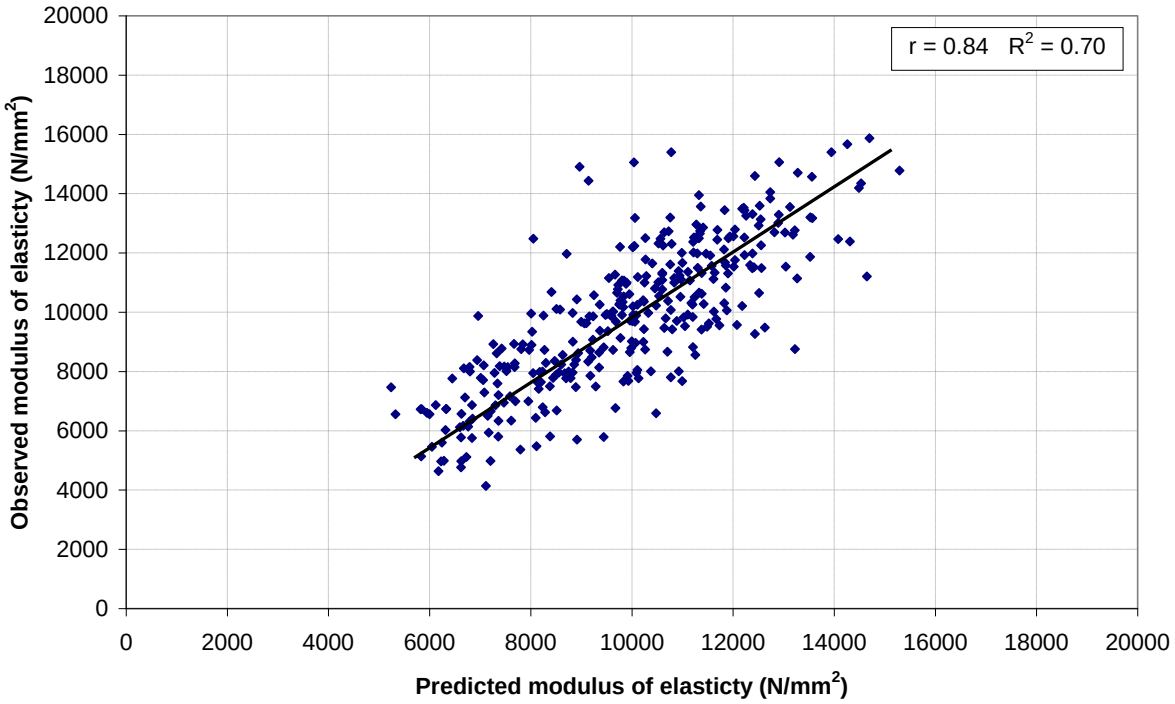

Figure 7-6: Observed modulus of elasticity values against combined regression model predicted values

7.4.3 Flexural strength multiple regression models

In this section, statistical predictive models for flexural strength are derived. The results shown in Table 7-5 give a summary of the variations accounted for by models with various combinations of independent variables. A complete set of coefficients for each multiple regression equation are given in Table D-11.

Table 7-5: Summary of multiple regression model results for the prediction of flexural strength

	Coefficients	**Adjusted R^2**	**Coefficients**	**Adjusted R^2**
Microscopic properties model				
	DEN, MFA	0.61*		
Macroscopic properties models				
	AGE, RW	0.51*	LWP, RW	0.51*
	AGE, LWP	0.53*	AGE,RW,LWP	0.56*
Combination models				
	AGE, LWP, DENS	0.66*	AGE, LWP, DENS, MFA	0.66*
	AGE, LWP, MFA	0.54*	AGE, LWP, RW, DENS, MFA	0.68*

* indicates statistically significant results at $P \leq 0.05$

It was shown in Section 7.3.2.2 that the flexural strength of small clear specimens was most strongly associated with variations in density, with little direct relationship existing with microfibril angle. The result found when both density and microfibril angle were included in the microscopic properties regression model reflects this association, with the adjusted R^2 value of 0.61 returned by the model being little improvement over the R^2 of 0.58 that was achieved when density alone was used to predict flexural strength. A similar result was observed in the prediction of flexural strength in Douglas-fir mature wood by Lachenbruch et al. (2010), although the variation accounted for by the model presented here is greater than the 39 % achieved in that study.

The models of macroscopic wood features were, as with the modulus of elasticity results, also found to account for a moderate proportion of the variations observed in flexural strength. All combinations of two of the three macroscopic properties returned adjusted R^2 values of

approximately 0.5. When all three macroscopic variables were considered in combination the adjusted R^2 value of 0.56 achieved was almost equivalent to that found for microscopic properties. The inclusion of density alongside age and latewood proportion, the two macroscopic property variables that accounted for the greatest degree of variability, resulted in an increase of the adjusted R^2 value to 0.63 being observed. The inclusion of microfibril angle in the model provided no increase in the accuracy of the predicted results. Similar results were observed for the other combinations of two macroscopic property variables. Given the strong relationship between density and flexural strength discussed previously this finding was to be expected. The inclusion of all parameters in the regression model gave an adjusted R^2 value of 0.68 with a residual standard error of 7 N/mm^2. The graph in Figure 7-7 displays the relationship between observed flexural strength values and those predicted by the combination regression model including all parameters.

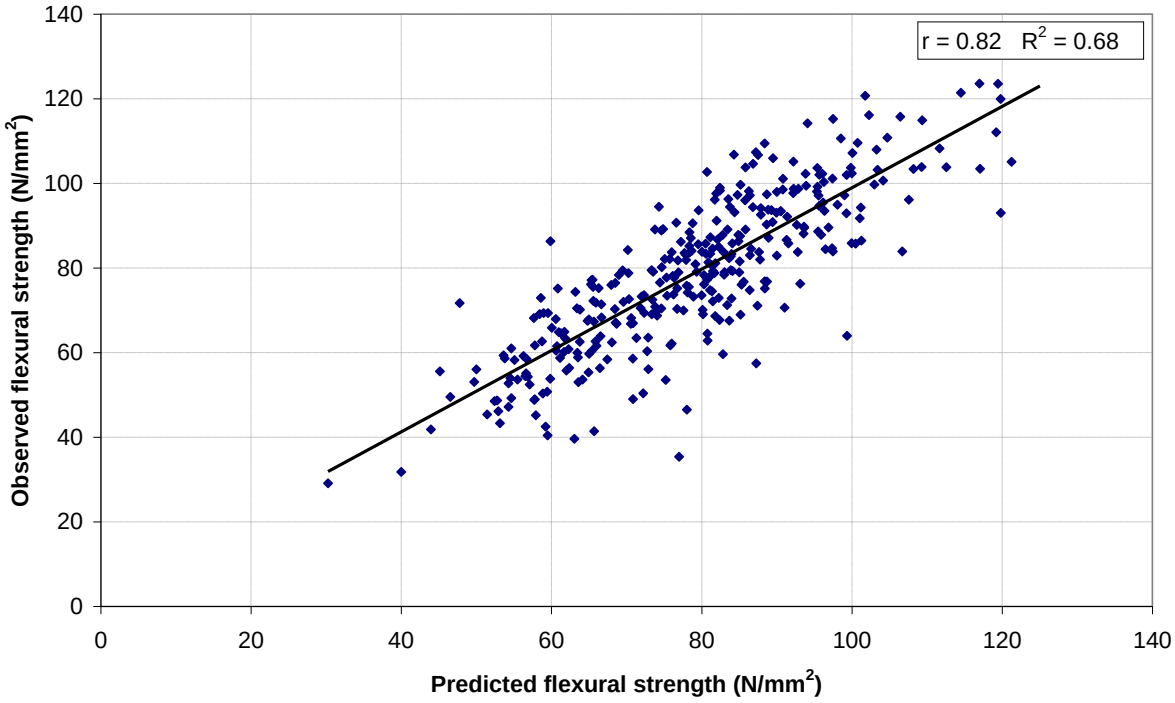

Figure 7-7: Observed flexural strength values against combined regression model predicted values

7.4.4 Compressive strength multiple regression models

In this section, statistical predictive models for compressive strength are derived. The results shown in Table 7-6 give a summary of the variations accounted for by models with various combinations of independent variables. A complete set of coefficients for each multiple regression equation are given in Table D-12.

Table 7-6: Summary of multiple regression model results for the prediction of compressive strength

	Coefficients	**Adjusted R^2**	**Coefficients**	**Adjusted R^2**
Microscopic properties models				
	DEN, MFA	0.56*		
Macroscopic properties models				
	AGE, RW	0.44*	LWP, RW	0.40*
	AGE, LWP	0.46*	AGE,RW,LWP	0.48*
Combination models				
	AGE, LWP, DENS	0.54*	AGE, LWP, DENS, MFA	0.59*
	AGE, LWP, MFA	0.48*	AGE, LWP, RW, DENS, MFA	0.59*

* indicates statistically significant results at $P \leq 0.05$

In the prediction of compressive strength, the use of both density and microfibril angle accounted for a moderate proportion of the variations observed at 56 %, a value which was in line with those observed previously for modulus of elasticity and flexural strength. Models combining two of the three macroscopic properties also returned similar results. In combining either density or microfibril angle with the macroscopic model which retuned the highest adjusted R^2 values, that of age and latewood proportion, an increase in the variations accounted for was observed. The increase with the inclusion of density, shown in Section 7.3.2.3 to have the strongest direct relationship with compressive strength of the two microscopic properties, was greater than when microfibril angle was added to the model. In combining both microscopic properties, the R^2 values were found to rise further still to 0.59. The addition of ring widths to the model, such that all parameters were included, gave no improvement in the variability accounted for, as a result of the statistically non-significant direct relationship observed between ring width and compressive strength in Section 7.3.3.

The graph in Figure 7-8 displays the relationship between observed compressive strength values and those predicted by the combination regression model including all parameters, which had a residual standard error of 5 N/mm^2.

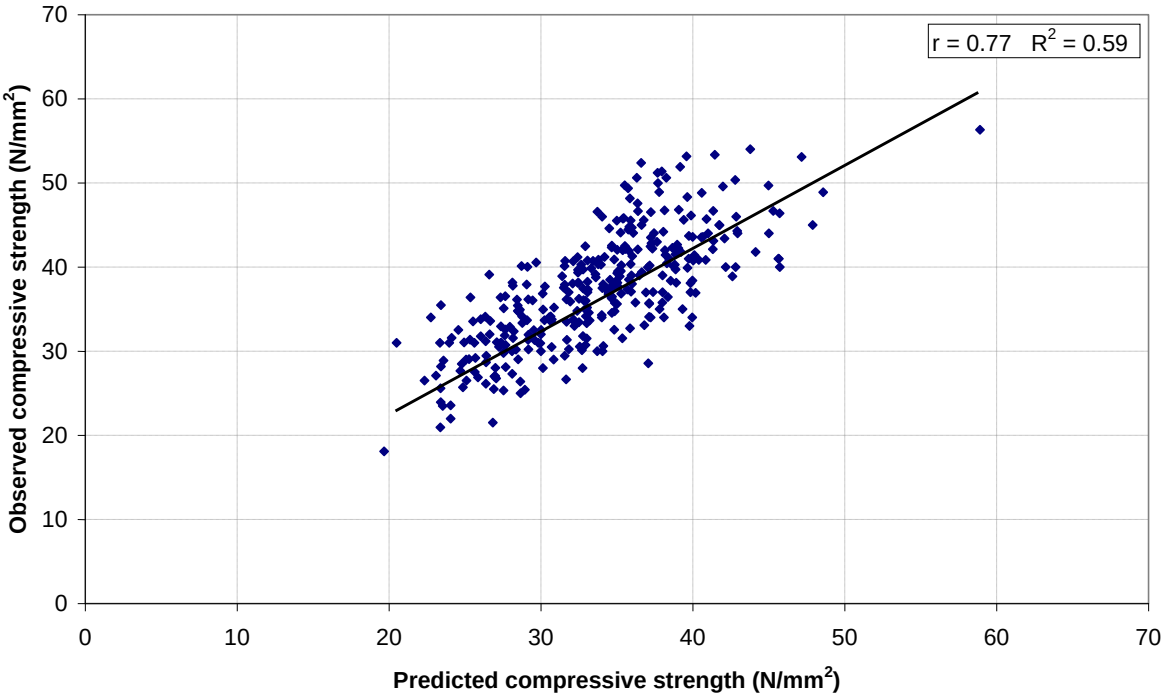

Figure 7-8: Observed compressive strength values against combined regression model predicted values

7.4.5 Potential utilisation of regression modelling results

While it is not possible for statistical models to accurately predict the exact behaviour of wood cut from a particular tree, they do provide a powerful tool in the demonstration of the key trends present within a sample dataset, as shown in the models presented previously. The extent to which the variations in the results were accounted for by the models was found to be dependent upon the nature of the parameters included, with those formed from macroscopic property measurements generally accounting for the lowest degree of variation, while combination models provided the best fit. Within all models however a proportion of the variation remained unaccounted for. The most obvious sources of this unaccounted variation, aside from experimental error, are inaccuracies in the end matching of small clear specimens to the equivalent SilviScan-3 data, a factor which has been discussed previously. Further inaccuracies may have arisen from the averaging of specimen cambial ages and ring widths, SilviScan-3 density measurements that were unrepresentative of those along the length of the small clears and the presence of other anomalies within the small clear specimens that may have resulted in inconsistencies between tests. Changes in the chemical make up and

quantities of cellulose, hemicellulose and lignin with age (e.g. Via et al., 2009), which may not be fully accounted for through indirect relationships, may have also contributed to the unaccounted variation in results.

While statistical models allow for a greater understanding of relationships between properties, their use in practice lies in being able to predict parameters, utilising characteristics that are easier to assess than the property which is to be determined. As such, the results presented here in which it was shown that it is possible to gain a relatively accurate estimation of mechanical properties from visually identifiable wood features are of significance. In all cases, specimen mean cambial age and latewood proportion were the two macroscopic features that allowed for the most accurate prediction of mechanical properties, although latewood proportions and mean ring width also returned similar results. It is perhaps this latter relationship which is of the greatest importance in terms of being able to identify the mechanical properties of any piece of timber, regardless of being able to identify its position within a tree. The determination of anatomical properties with the use of the SilviScan-3 system is perhaps less efficient than the direct determination of mechanical properties. However, the use of the relatively easily obtainable directly derived bulk density combined with visually identified characteristics is likely to provide a good predictive tool, given the strong correlations with SilviScan-3 density shown in Section 7.2.2.

The findings presented here suggest that it may be possible to improve the efficiency of the methods currently used to visually grade timber. At present the method outlined in BS 4978:2007 (BSI, 2007) prescribes mean ring widths for a timber section not to be exceeded for classification as either GS or SS grades. As has been shown, mean ring width alone accounts for relatively little of the variation observed in clear wood specimen mean properties, with R-squared values ranging from 0.14 to 0.27, a factor likely to remain true for full sized structural members. As has been demonstrated in this chapter, the inclusion of latewood proportion, a characteristic that can also be visually assessed, alongside ring width allows for a greater proportion of the variability observed in mechanical properties to be accounted for. While the existence of other factors prescribed within BS 4978:2007, such as knots and a sloping grain, will remain key factors in determining the properties of full sized sections, it has been demonstrated here that potential exists for the development of more efficient visual grading methods.

7.5 Concluding remarks

In this chapter, statistical methods were used to study the relationships between wood micro and macroscopic anatomical characteristics and mechanical properties. Models for the prediction of these mechanical properties utilising a range of input variables were also developed. It was found that both density and microfibril angle had moderate to strong linear correlations with the modulus of elasticity, flexural and compressive strength of a specimen. Macroscopic features such as ring width and cambial age were also found to show moderately strong linear correlations with the three assessed mechanical properties. These were however identified through the use of path analysis to be largely a result of interrelationships with density and microfibril angle.

It was also found through the use of path analysis that within the juvenile wood microfibril angle was more strongly associated with increases in the magnitude of modulus of elasticity than density, while in mature wood this relationship was reversed. Flexural and compressive strength were found to be more strongly associated with changes in density than microfibril angle in both juvenile and mature wood. Finally, multiple regression models were developed to predict all mechanical properties to a good degree of accuracy. It was found through the use of these models that the inclusion of latewood proportion as a measure in visual grading methods may improve accuracy compared with the use of ring width alone.

Chapter 8 - Micromechanical composite modelling

8.1 Introduction

In previous chapters, variations in the anatomical and mechanical properties of wood specimens with position in the Douglas-fir sample trees were evaluated. The relationships between them were then assessed with the use of statistical methods, with a view of developing predictive models for mechanical properties based on relatively easily obtainable characteristics. The use of path analysis also allowed basic conclusions to be drawn regarding the influence of characteristics such as density and microfibril angle on mechanical properties at different stages in the development of the sample trees, and hence the impact on wood quality.

In this chapter, a multi-scale micromechanical composite model of wood is developed. Such a model serves a different purpose to the statistical models generated previously. While the level of data resolution required does not make them amenable to wide scale practical applications (Evans, 2006), micromechanical models have an important role in improving the understanding of the behaviour of wood at a fundamental level, particularly as the quantity and quality of the available input parameters increases. The wood cell wall model developed here was constructed from a) experimental data obtained with the use of the SilviScan-3 system, b) the results of previously published work on the properties of cellulose, hemicellulose and lignin and c) previously published work on cell wall structures.

With the use of outputs from the composite model, it was hoped to improve the understanding of the interactions between anatomical and mechanical properties at a number of levels within the sample trees, in order to explain relationships observed in previous

chapters. A further objective was the verification of the model through the prediction of the mechanical behaviour of small clear specimens, utilising their anatomical characteristics as input parameters. The methodologies and theories employed in the model development are described in Section 8.2. This is followed by the presentation and discussion of the results obtained in Section 8.3, and potential improvements that may be applied to the model to improve its accuracy in Section 8.4.

8.2 Micromechanical composite model development

8.2.1 Outline

The mechanisms associated with the failure of timber specimens in both flexure and compression, and therefore those responsible for determining section strength, were discussed in Section 7.3.2. Due to the failure modes postulated, the prediction of behaviour and the resultant ultimate stress capable of being carried by a specimen was not possible from the data obtained using the SilviScan-3 system. As such, in the development of the micromechanical model the focus was on the prediction of the flexural modulus of elasticity of test specimens.

In sections subject to pure bending which are symmetric about their neutral axis, elastic bending theory shows that the stresses within the section vary linearly with the distance from the neutral axis up to the limit of proportionality, as shown in Figure 8-1. Tracheids above the neutral axis are subject to compressive stresses, while those below experience tension. The three point bending method used for the testing of small clear specimens in this study did not allow for the presence of a true pure bending situation, a fact that is discussed in Section 9.3.4. However, as the specimen span to depth ratio was sufficiently large, such that displacements due to shear and the likelihood of shear failure were minimal, the existence of a stress distribution as represented in Figure 8-1 is assumed.

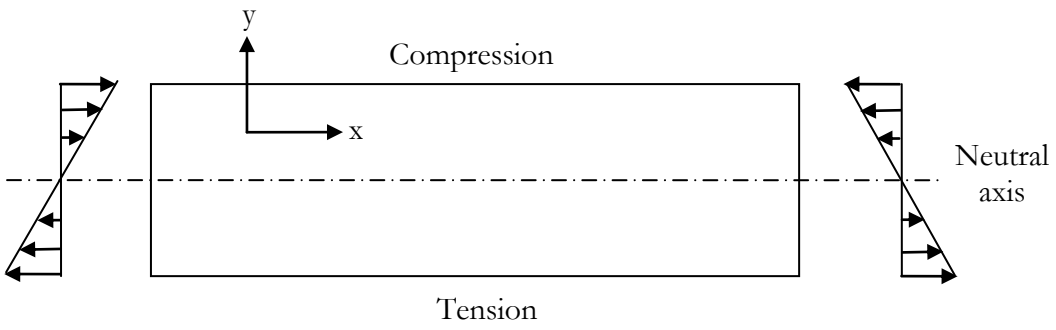

Figure 8-1: Specimen stress variation due to pure bending up to limit of proportionality

For timber subject to compression and tension parallel to the grain, the load deflection plots are as shown in Figure 8-2. From the plots it can be observed that the limit of proportionality, below which behaviour is elastic, is lower for timber subjected to compression than tension. Below the limit of proportionality for compression however, the longitudinal elastic modulus can be taken to be equal for both compression and tension (Dinwoodie, 2000).

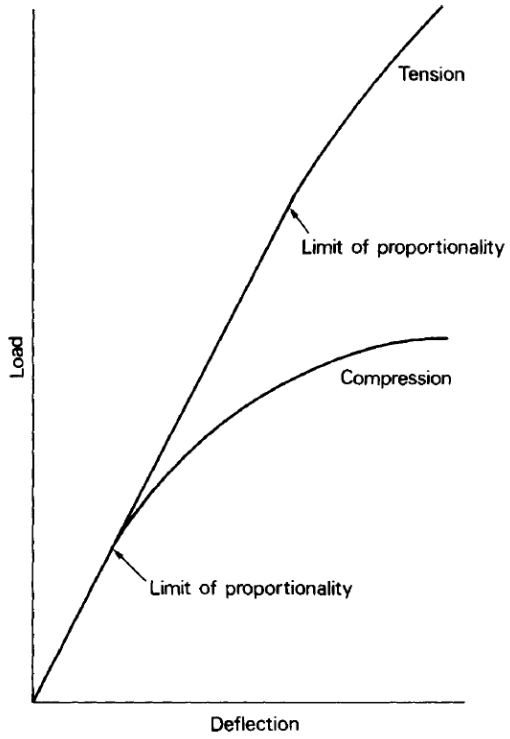

Figure 8-2: Load deflection plot for timber stressed in compression and tension parallel to the grain from Dinwoodie (2000)

Given this equivalence of the elastic modulus and assuming that the tracheids within the small clear specimens tested in this study are aligned such that they lie longitudinally in the x-x plane as indicated in Figure 8-1, then it is theoretically possible to calculate the flexural modulus of elasticity of the small clear specimens utilising longitudinal modulus of elasticity values for tracheids. Although the stress at which the limit of proportionality is reached is largely determined by the characteristics of the tracheids on the upper surface during testing, where compression forces are greatest, the way in which specimens were orientated during testing, discussed in Section 3.6.3, means that the variation in properties across the growth rings present within a specimen can be accounted for.

In the review of literature given in Section 2.3, the multi-level composite nature of woody material was described, with cellulose microfibrils embedded in a matrix of hemicellulose and lignin forming the cell wall material, which itself is part of a multilayer laminate at the cellular and growth ring levels. In light of this, the approach adopted for the development of the micromechanical model to predict the longitudinal modulus of elasticity of tracheids was similar to that taken by Persson (2000). In the model, wood properties were determined at a number of levels, reflecting the hierarchical composite nature, before being combined. Five distinct stages were used, as summarised in the flow chart shown in Figure 8-3. In the sub-sections that follow, the methodologies, assumptions and simplifications employed in the development of the composite model at each stage are detailed.

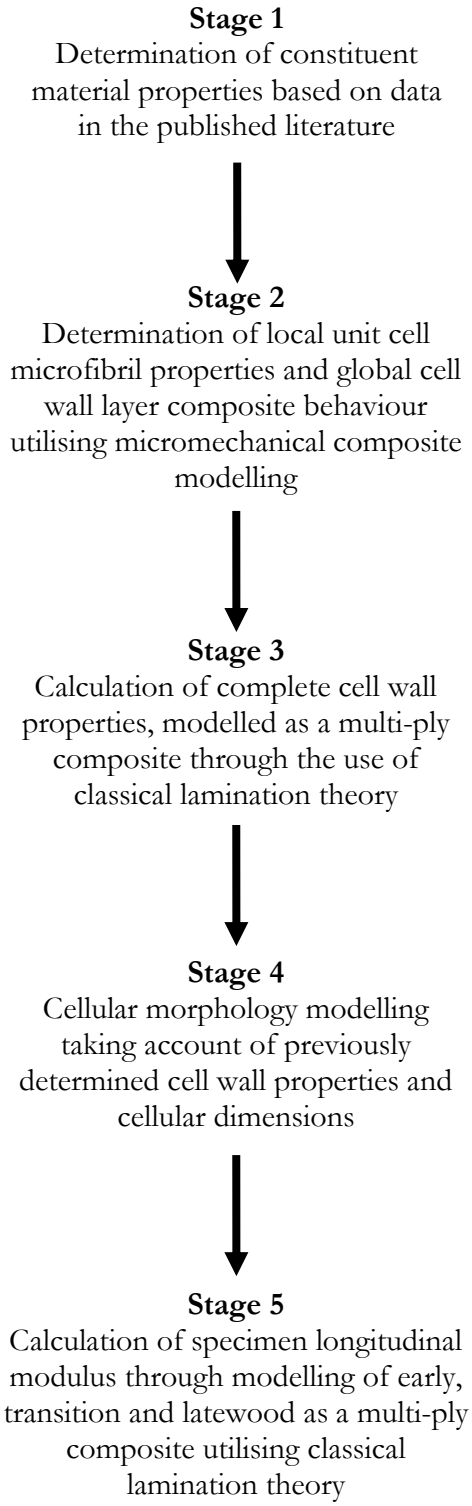

Figure 8-3: Key stages in composite micromechanical model development

8.2.2 Stage 1 - Determination of constituent material properties

8.2.2.1 Outline

The three primary chemical constituents of wood based materials are cellulose, hemicellulose and lignin (Dinwoodie, 2000). The first stage therefore in the building of a micromechanical model to predict longitudinal modulus of elasticity was the quantification of the mechanical properties of these component parts. All quoted values were obtained from the literature, as discussed in Section 2.3.

8.2.2.2 Cellulose

Due to its role as a reinforcing material and therefore importance in determining the properties of the cell wall, a large quantity of literature was found relating to the mechanical properties of cellulose. Within the cell walls, cellulose is present in monoclinic and triclinic crystalline forms, which require between 14 and 21 parameters to describe their elastic behaviour (Harrington et al., 1998). For the purpose of this work, cellulose was treated as a transversely isotropic material, significantly reducing the number of input parameters required within the model. This is a commonly used assumption (e.g. Persson, 2000) and reasonable, given the lack of evidence to suggest that there is any preferred crystalline orientation, other than in the longitudinal direction (Harrington et al., 1998). While the properties of crystalline cellulose regions are independent of changes in moisture content (Salmén, 2004), amorphous areas are known to absorb water. As a further simplifying assumption, the impact of water absorption in these regions was disregarded within the model, a similar approach was adopted by Persson (2000).

In the review of the mechanical properties of cellulose given in Section 2.3.2.2, a relatively large range of values were reported, as shown in Table 2-1. Given the varied theoretical and experimental methodologies used for their determination this was to be expected. In the absence of definitive values, three distinct levels were used in modelling behaviour, namely the lower, middle and upper bounds. The properties for each were selected so as to capture the range of values observed within the literature, with the values used for each category presented in Table 8-1.

Table 8-1: Cellulose mechanical properties used for model calculations

	Lower bound	**Middle bound**	**Upper bound**
E_x (N/mm^2)	130000	150000	170000
E_y (N/mm^2)	15000	22500	30000
G_{xy} (N/mm^2)	3000	4000	5000
ν_{xy}	0.1	0.1	0.1

where: E_x longitudinal modulus of elasticity

E_y transverse modulus of elasticity

G_{xy} shear modulus

ν_{xy} Poisson's ratio

8.2.2.3 Hemicellulose

In comparison to cellulose, mechanical properties data for hemicellulose is relatively scarce, this is largely as a result of the difficulties associated with obtaining representative values for the material once it has been isolated, with the occurrence of post isolation crystallisation common (Salmén, 2004). As with cellulose, it is possible for hemicellulose to be treated as a transversely isotropic material, with it being shown that hemicellulose shares a similar orientation with cellulose chains within the cell wall (Åkerholm and Salmén, 2001). Unlike crystalline cellulose, hemicellulose is hygroscopic, with the magnitude of the elastic modulus decreasing as the moisture content increases, as demonstrated by Cousins (1978). Where properties known to be moisture dependent were required as an input to the model, the values of the parameters at 12 % moisture content were used where possible. This moisture content was selected so as to correspond with the equilibrium moisture content of the small clear specimens during testing.

Even when comparable moisture contents were considered, a large variation in the mechanical properties of hemicellulose was still observed between studies, due to difficulties in the measurement of properties and uncertainty regarding the orthotropic ratio of longitudinal to transverse elastic constants (Bergander and Salmén, 2002), these are shown in Table 2-1. Hence, the same system of lower, middle and upper bound values as used for cellulose was adopted. The range of the parameters selected for use in the model is shown in Table 8-2.

Table 8-2: Hemicellulose mechanical properties used for model calculations

	Lower bound	Middle bound	Upper bound
E_x (N/mm^2)	2000	4000	8000
E_y (N/mm^2)	800	1500	3500
G_{xy} (N/mm^2)	1000	1500	2000
ν_{xy}	0.2	0.2	0.2

8.2.2.4 Lignin

Lignin is typically regarded as an isotropic amorphous material (e.g. Cousins, 1976), this assumption was therefore used in the development of the micromechanical model and results in a reduction in the number of elastic constants required for modelling. Although to a lesser extent than hemicellulose, lignin is also hygroscopic and as such a range of values were stated in the literature for material tested at varying moisture contents, as well as variation in results due to alternative extraction methods. As lignin was to be treated as an isotropic material, the standard method shown in Equation 8-1 was used in order to calculate the shear modulus based on the values of modulus of elasticity and poisons ratio. This returned a range of results in line with those found in the literature shown in Table 2-1.

$$G = \frac{E}{2(1+\nu)} \qquad 8\text{-}1$$

The three categories of model parameters for lignin are displayed in Table 8-3.

Table 8-3: Lignin mechanical properties used for model calculations

	Lower bound	Middle bound	Upper bound
E (N/mm^2)	2000	2750	3500
G (N/mm^2)	800	1050	1350
ν	0.3	0.3	0.3

8.2.3 Stage 2 - Cell wall composite modelling

8.2.3.1 Outline

Having identified the mechanical properties of the constituent components to be used in the wood micromechanical model, the next developmental stage was the determination of the mechanical properties of the cell wall layers. Within the model, each double cell wall was considered as a layered laminate comprising of seven layers, with the middle lamella and primary cell walls combined into a layer termed the compound middle lamella (CML), due to the difficulty associated with differentiating them (Jyske, 2008). A depiction of the layered

laminate system is given in Figure 8-4. The presence of helical thickening on the inner surfaces of the S_3 layer was not taken into account in the model. Further details regarding the modelling of this layered laminate system can be found within Section 8.2.4.

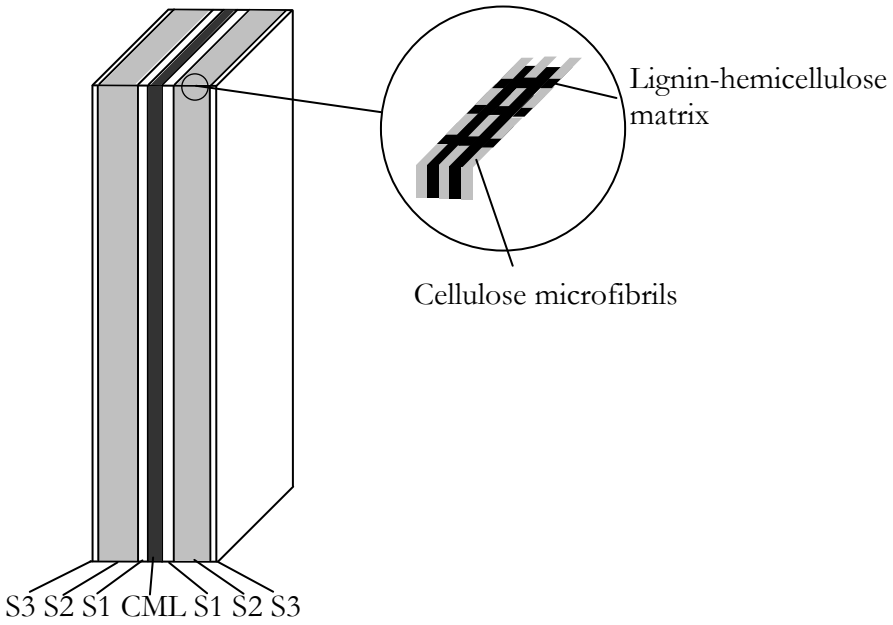

Figure 8-4: Layered laminate structure of the double cell wall and embedment of cellulose microfibrils modified from Bergander and Salmén (2002)

Each of the distinct cell wall layers was itself considered to be a composite material, with the cellulose fibrils embedded in a matrix of hemicellulose and lignin, also shown in Figure 8-4. In the modelling of this system it was first necessary to identify the proportion of constituents within each layer, discussed in Section 8.2.3.2, before the rule of mixtures method and transformation equations were used in order to determine the mechanical characteristics of each individual layer at both local and global scales, as detailed in Section 8.2.3.3.

8.2.3.2 Cell wall constituent component volume fractions

As previously discussed in the review of the literature given in Section 2.3.3, the volume fractions of the constituent wood components cellulose, hemicellulose and lignin are not constant within the different layers of the cell wall. As such, in the development of the composite model it was necessary to define the proportions of each of the components to be included within the separate lamina. One simplifying assumption made in the model development was that the volume fractions within each lamina remained constant throughout the processes of maturation. It has been shown that this is unlikely to be the case (e.g. Via et

al., 2009), however in the absence of detailed quantifications of the variations in the proportions of the constituent components with increasing cambial age, it was taken to be a reasonable simplifying assumption.

The fact that not all cell wall constituents possess the same affinity for water has been discussed previously. In line with the practice utilised for other properties, the proportions of each constituent component at a moisture content of 12 % were utilised. The values used were obtained from those presented in previous studies detailed in Section 2.3.3 and are displayed as percentages in Table 8-4.

Table 8-4: Cell wall lamina constituent property proportions

	Cellulose (%)	Hemicellulose (%)	Lignin (%)
CML	5	40	55
S_1	30	30	40
S_2	50	30	20
S_3	50	35	15

8.2.3.3 Determination of cell wall mechanical properties

In the modelling of each of the cell wall layers as a unidirectional fibre reinforced composite to determine the required elastic properties, a two dimensional unit cell system was utilised. In this unit cell, cellulose microfibrils were centrally located in a volumetrically proportionally representative mixture of the two matrix components, hemicellulose and lignin, the formation of which is detailed further below. It was assumed that due to the ratio of length to cross sectional size, the cellulose microfibrils were infinitely long in the longitudinal direction. In the absence of a complete understanding of the relationships between the organisations of lignin, hemicellulose and cellulose within the cell wall this is a commonly used approach to modelling, adopted by Salmén (2004) and Qing and Mishnaevsky Jr (2009).

In order to calculate the elastic properties of the unit cell system a two stage homogenisation process was used, depicted in Figure 8-5. In the first stage of the process the outer two layers forming the matrix of the composite were combined. Elastic properties in this stage were calculated from those presented in Section 8.2.2 for hemicellulose and lignin according to the volume fraction proportions of each material present within the cell wall layer concerned. As a result, the elastic properties of the matrix varied between different cell wall layers. The ordering of the two matrix components shown in Figure 8-5 is for representative purposes only and was of no relevance in the homogenisation process.

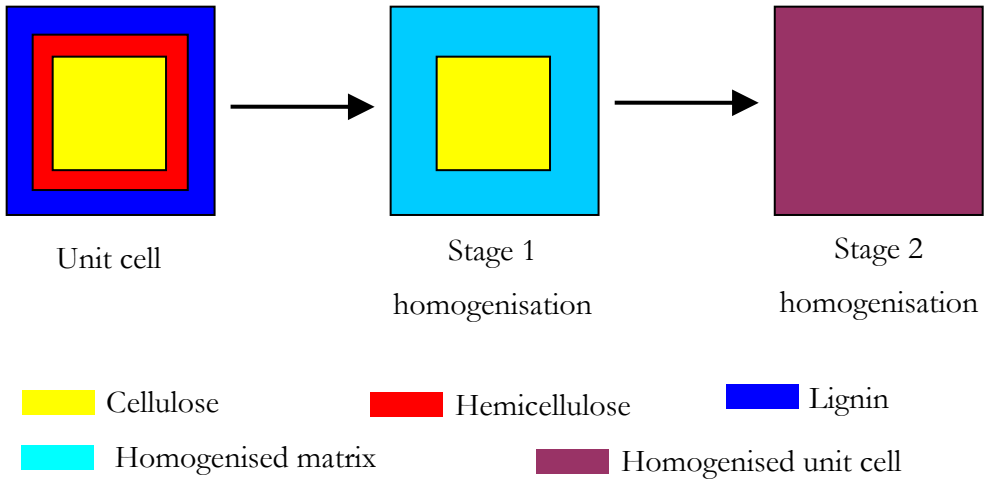

Figure 8-5: Homogenisation procedure for the unit cell system modified from Qing and Mishnaevsky Jr (2009)

Following the first stage and the defining of the matrix properties, the mechanical characteristics of the complete unit cell were calculated, such that stage 2 in Figure 8-5 was attained. Two coordinate systems were used for this purpose, as depicted in Figure 8-6. The global 1-2 coordinate system was aligned with the longitudinal and transverse cell wall orientations, while the local x-y system was aligned with the longitudinal and transverse orientations of the cellulose microfibrils within the cell wall. The angle between the longitudinal orientation of the global system, 1, and the longitudinal microfibril orientation, x, termed θ, was equivalent to the microfibril angle for the given cell wall layer.

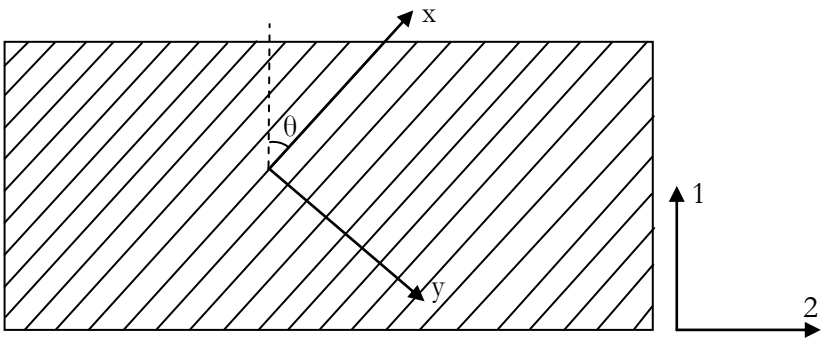

Figure 8-6: Global (1-2) and local (x-y) coordinate systems for cell wall layer micromechanical model

The first step in calculating the properties of each cell wall layer was the determination of those in the local x-y orientation, equivalent to the longitudinal and transverse properties of the global system if the microfibril angle were to be zero. This was done utilising the rule of mixtures methodology, in which the properties of a composite are taken as the combination of those of the fibre and matrix, related by the volume fraction of the constituent materials. In the use of the rule of mixtures method several key assumptions are made, namely that fibres are uniformly distributed throughout the matrix, perfect bonding exists between the fibre and matrix material and that all materials behave in a linear elastic manner. These assumptions were reasonable for an idealised wood structure, given the descriptions of organisation and behaviour given by Dinwoodie (2000) and Barnett and Jeronimidis (2003). A further assumption made when using the rule of mixtures method is that there are no voids present within the matrix, and as such the presence of pits between adjacent tracheids was ignored. The equations used in the determination of the composite behaviour of the unit cell system are given in Equations 8-2 to 8-5 below.

$$E_x = V_f E_f + V_m E_m \qquad 8\text{-}2$$

$$E_y = \frac{E_f E_m}{E_m V_f + E_f V_m} \qquad 8\text{-}3$$

$$G_{xy} = V_f G_f + V_m G_m \qquad 8\text{-}4$$

$$v_{xy} = V_f v_f + V_m v_m \qquad 8\text{-}5$$

where: E_x and E_y longitudinal and transverse composite elastic modulus

E_f and E_m fibre and matrix elastic modulus

V_f and V_m fibre and matrix volume fractions

G_{xy}, G_f, G_m composite, fibre and matrix shear modulus

v_{xy}, v_f, v_m composite, fibre and matrix Poisson's ratio

Having calculated the on-axis mechanical properties of the composite system using the rule of mixtures, the results obtained were then used to calculate the longitudinal modulus of elasticity of the cell wall when the unidirectional ply was rotated into an off-axis orientation, representing the effects of an increasing microfibril angle. This was done utilising Equation 8-6, derived from the transformation matrices given by Bank (2006).

$$\frac{1}{E_1} = \frac{\cos^4\theta}{E_x} + \frac{\sin^4\theta}{E_y} + \left(\frac{1}{G_{xy}} - \frac{2\nu_{xy}}{E_x}\right)\sin^2\theta\cos^2\theta \qquad 8\text{-}6$$

where: E_1 Global longitudinal elastic modulus

θ Microfibril angle

The modelling of each of the cell wall layers was undertaken utilising the microfibril angles given in Table 8-5, with the exception of angles in the S_2 layer, these were obtained from a review of the literature presented in Section 2.3.3. While these values were not obtained for Douglas-fir, in the absence of directly determined data it is assumed that they are representative of those which are present within the sample trees used here. The microfibril angles used for the S_2 layer were the mean values derived utilising the Silviscan-3 system reported in Section 4.7. The mean values were categorised separately for early, transition and latewood, as detailed in Section 8.3.4. For the compound middle lamella, S_1 and S_3 layers the microfibril angle was modelled as though the microfibrils were evenly distributed across the range of values present. Within the S_2 layer the microfibril angle was assumed to remain constant across the thickness of the layer.

Table 8-5: Cell wall layer microfibril angles

	Microfibril angle (Deg)
CML	0 to 90
S_1	-45 to 70
S_2	Variable
S_3	± 50

8.2.4 Stage 3 - Cell wall layered laminate modelling

8.2.4.1 Outline

Having determined the longitudinal modulus of elasticity for each of the constituent cell wall layers individually, the next stage in the development of the micromechanical model was the calculation of the elastic properties of the cell wall system with all layers acting in combination. This was done utilising classical lamination theory, as described in Section 8.2.4.3. Prior to this, the constituent make up of the complete wall system with regards to the proportions of each layer present was determined, as detailed in the following sub-section.

8.2.4.2 Cell wall layer volume fractions

In a similar manner to the changing proportions of the chemical constituents detailed in Section 8.2.3.2, the proportions of each of the cell wall layers making up the complete cellular structure is also known to change in the transition from early to latewood. In order to take account of this change within the micromechanical model, three distinct sets of parameters for the proportions of each cell wall layer, one for each of the early, transition and latewood, were identified. The proportions of each layer were calculated based on the thicknesses identified in previous studies reviewed in Section 2.3.3. In the review of literature, no data for the thickness of the cell wall layers within the transition-wood zone was found, so it was assumed that the transition-wood had properties equivalent to the mid-point between those reported for early and latewood. A further simplifying assumption made was that as with the chemical constituents, no variation in properties existed as the wood matured with increasing cambial age. The ultra structural parameters for the proportions of each cell wall layer used in modelling are shown in Table 8-6.

Table 8-6: Cell wall layer proportions within different wood types

	Earlywood (%)	**Transition-wood (%)**	**Latewood (%)**
CML	18	11	7
S_1	10	7	7
S_2	70	81	85
S_3	2	1	1

8.2.4.3 Determination of elastic properties

In order to determine the longitudinal modulus of elasticity of the complete cell wall structure including all layers, the classical lamination method for multi-directional flat plate laminates was used. A detailed description of the underlying theory of the method can be found in Bank (2006). Prior to conducting the analysis several simplifying assumptions were made, principal among which was that the double cell wall structure, S_3, S_2, S_1, CML, S_1, S_2, S_3, could be modelled as a symmetric system. Within a symmetric laminate layup it is assumed that for every material type and thickness of ply on one side of the mid-plane, there exists a ply of identical properties on the opposite side at an equivalent distance. Although a gradual transition in cellular properties has been shown to occur with radial distance from the pith, the difference between adjacent cells is likely to be sufficiently small such that this simplification is justified. It was also assumed that each cell wall was subject to a uniform temperature and the same average moisture content. The impact of these simplifications on the use of the classical lamination theory was to remove the need to consider bending - extension coupling when

determining the longitudinal modulus. As a result, only the stiffness coefficient terms from the stiffness matrix A_{ij}, used to define the extensional response of the laminate system, were required for the determination of the longitudinal modulus of elasticity. The $[A]$ sub-matrices of the stiffness matrix are shown in Equation 8-7.

$$\begin{Bmatrix} N_1 \\ N_2 \\ N_6 \end{Bmatrix} = \begin{bmatrix} A_{11} & A_{12} & A_{16} \\ A_{21} & A_{22} & A_{26} \\ A_{61} & A_{62} & A_{66} \end{bmatrix} \begin{Bmatrix} \varepsilon_1^0 \\ \varepsilon_2^0 \\ \varepsilon_6^0 \end{Bmatrix} \qquad 8\text{-}7$$

where: N_i extensional stress resultant

A_{ij} stiffness coefficient

ε_i^0 mid-plane strain

In the determination of the longitudinal modulus of elasticity, it was necessary to calculate the value of the A_{11} stiffness coefficient shown in Equation 8-7. This was done through the summation of the longitudinal modulus of elasticity of the individual cell wall layers utilising Equation 8-8.

$$A_{11} = \sum_{k=1}^{n} E_{11}^{k} h_k \qquad 8\text{-}8$$

where: A_{11} longitudinal modulus of elasticity of cell wall system

E_{11}^{k} longitudinal modulus of elasticity of k^{th} cell wall layer

h_k cell wall layer volume proportion

Following this, the $[A]$ sub-matrices was then inverted to give the extensional compliance matrix [*a*], which for the calculation of longitudinal modulus of elasticity can be written simply as shown in Equation 8-9.

$$a_{11} = A_{11}^{-1} \qquad 8\text{-}9$$

where: a_{11} longitudinal component of extensional compliance matrix

The longitudinal in plane elastic modulus was then defined for the laminate system by defining an average in plane stress in the laminate, as shown in Equation 8-10.

$$\bar{\sigma}_1 = \frac{N_1}{h} \qquad 8\text{-}10$$

where: $\bar{\sigma}_1$ average in-plane laminate stress

h total composite thickness

Under the methodology employed in the analysis, whereby proportions rather than thicknesses of laminates within the composite were used, the total thickness of the double cell wall representation was set as one. Hence, the longitudinal modulus of elasticity of the system was calculated utilising the expression shown in Equation 8-11.

$$E_{CW} = \frac{\bar{\sigma}_1}{\varepsilon_1^0} = \frac{1}{a_{11}} \qquad 8\text{-}11$$

where: E_{CW} longitudinal cell wall modulus of elasticity

An analysis of the results from this stage of the model development, demonstrating the impact of a change in the S_2 layer microfibril angle on the longitudinal modulus of elasticity of the complete cell wall composite system, is presented and discussed in Section 8.3.2.

8.2.5 Stage 4 - Cellular morphological modelling

Having identified the longitudinal elastic properties of the unified cell wall system, the next stage in the modelling process was the calculation of properties taking into account the cellular structure of the wood material. As discussed in Section 2.9, several representations of cellular structures have been used in previous studies. However, given the arrangement of Douglas-fir tracheids shown in Figure 8-7, the development of a representative model of the cell organisation that captures the largely random order of cellular shapes could not be done with ease through the adoption of one particular system. As such, the first simplifying assumption made in the production of the cellular model was that the cellular structure could be represented as a series of rectangular elements. Such a representative model was successfully utilised by Guitard and Gachet (2004) and allows for the direct use of the radial and tangential cellular dimensions derived by the SilviScan-3 system in this study. A further simplifying assumption made was that cell wall thickness is uniform around the circumference of the cell, again enabling the direct use of radial wall thickness measurements obtained utilising SilviScan-3.

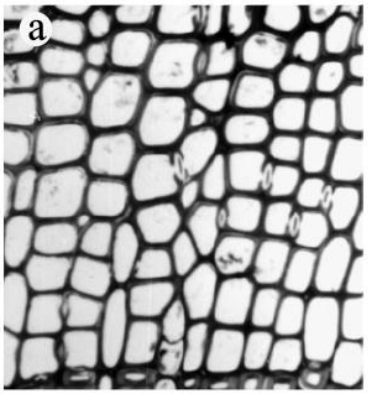

Figure 8-7: Tracheid cell arrangement in Douglas-fir from Bower et al. (2002)

The representation of the layered cell wall structure shown in Figure 8-4 for which elastic properties were calculated in Section 8.2.4, provided longitudinal modulus of elasticity values for a unit area, assuming that properties remained consistent at all locations incorporating equivalent cell wall layers. A similar unit modelling philosophy was adopted when determining cellular properties. The representation of the cellular structure used is shown in Figure 8-8, with the dimensional values used in the calculation of cell wall area determined by the use of SilviScan-3 also indicated.

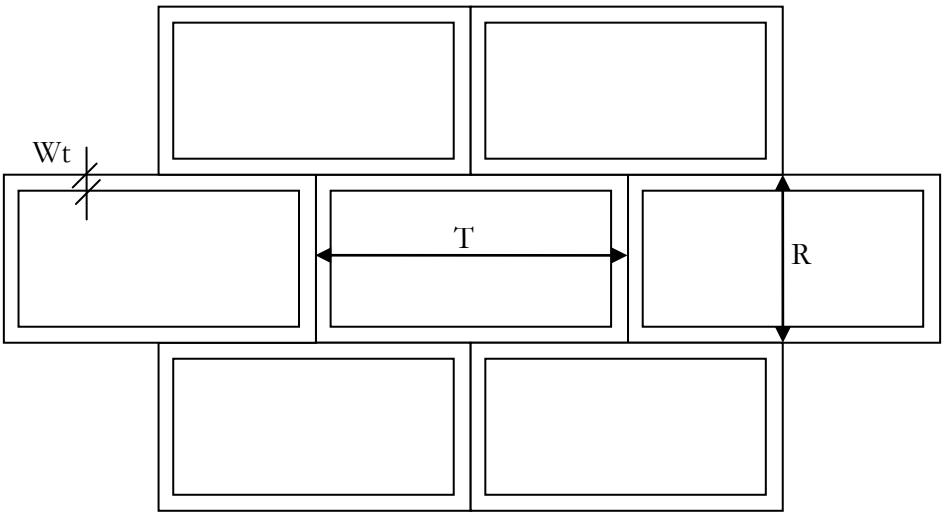

Figure 8-8: Cellular structure model and SilviScan-3 derived dimensions

where: Wt tracheid wall thickness
T tracheid radial diameter
R tracheid radial diameter

The unit for which the longitudinal modulus of elasticity was calculated was the individual tracheid cell, assumed to be composed of half the cell wall structure shown in Figure 8-4. Despite only incorporating half of the double cell wall thickness within the cellular model, the modulus values calculated in Section 8.2.4 still apply, as the proportions of each cell wall lamina are equivalent. The longitudinal modulus of elasticity of the individual cells was determined utilising Equation 8-12, which calculates the proportion of cell wall material within the area occupied by the represented cell, multiplied by the calculated cell wall longitudinal modulus of elasticity.

$$E_{cell} = \frac{RT - (R - 2W_t)(T - 2W_t)}{(RT)} E_{CW} \qquad 8\text{-}12$$

where: E_{Cell} tracheid cell longitudinal modulus of elasticity

The cellular dimensions used within Equation 8-12 were taken as the average values for distinct bands of early, transition and latewood when predicting the properties of the small clear specimens, to be discussed in Section 8.2.6. As such, a further simplifying assumption made was that the cellular dimensions used were representative of each wood type band. As

wood density is a function of the quantity of material within a given volume, the results calculated in this section are used in Section 8.3.3 to assess the impact of increasing density on longitudinal modulus of elasticity.

8.2.6 Stage 5 - Specimen growth ring modelling

The final stage in the development of the micromechanical composite model was in representing the influence of varying proportions of early, transition and latewood on the longitudinal modulus of elasticity of the small clear specimens. As was detailed in stages 3 and 4, the microfibril angles and cellular dimensions used in the generation of results were grouped as mean values for each of the three constituent wood types within a specimen. As a result, varying proportions of wood types may have a large influence on the modulus values calculated. As is shown in the small clear specimen representation in Figure 8-9, the different wood types present within a growth ring can be modelled as a multi-layered laminate utilising classical lamination theory, as was done in section 8.2.4.3. While in stage 3 modelling it was possible to reasonably assume that the double cell wall system could be represented as a symmetrical laminate, this was not the case when modelling growth ring layers about the vertical mid-plane, as shown in Figure 8-9. However, given the large degree of variability between the laminate layup of individual small clear specimens, the simplifying assumption that the arrangement could be modelled as symmetrical within each specimen was made. This simplification was reasonable, given the fact that a large majority of the specimens tested contained in excess of four growth rings, and therefore 12 laminates. As a result of this, the overall influence of bending - extensional coupling effects on the final calculated results due to differences in laminate layup about the vertical mid-plane would likely be limited. The nature of the organisation of early, transition and latewood within specimens resulting from this modelling approach is shown in Figure 8-9. The ordering of the laminates indicated is for representative purposes only.

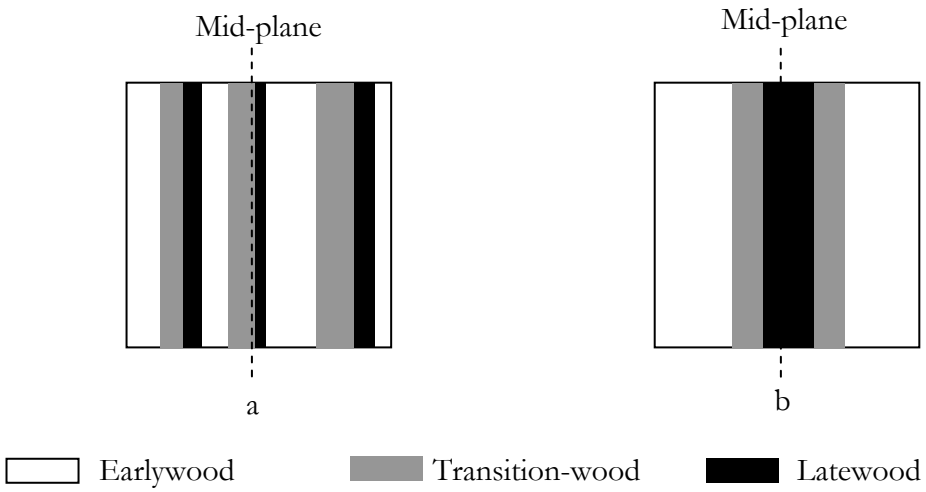

Figure 8-9: Small clear specimen growth ring laminate models a.) actual representation b) simplified symmetrical representation (view of end face cross-section)

In the determination of the elastic properties of the complete specimen the equations used were as described in section 8.2.4.3. As with layers within the cell walls, proportions of each growth ring wood type present within a specimen were used in calculations, rather than the actual laminate dimensions. The longitudinal modulus values for each laminate were taken from those calculated in Section 8.2.5, with the assumption that all tracheids were aligned such that the longitudinal orientation was parallel to the x-x plane shown in Figure 8-1, representing no slope of grain, and that the boundaries between adjacent wood types were straight and parallel.

8.2.7 Computation of results

Having completed the development of the model, results were calculated utilising Microsoft Excel. A series of macros were used to input the required specimen parameters and output results.

8.3 Micromechanical composite model results

8.3.1 Outline

As well as providing an estimate of the flexural modulus of elasticity for each small clear specimen, the micromechanical composite model developed also allowed for several additional datasets to be obtained at different scales. These aided in gaining a greater understanding of the relationships between anatomical properties and the modulus of elasticity of specimens derived from the Douglas-fir sample trees. In the following sub-sections the results obtained during the modelling process are presented and discussed.

8.3.2 Cell wall longitudinal modulus of elasticity

In the determination of the longitudinal modulus of elasticity of the cell wall material, up to and including stage 3 in the model development described in Section 8.2, several variable parameters were included within the model. Figures 8-10 to 8-12 display the theoretical variation in longitudinal modulus of the cell wall for early, transition and latewood as the S_2 layer microfibril angle varies from 0° to 45°.

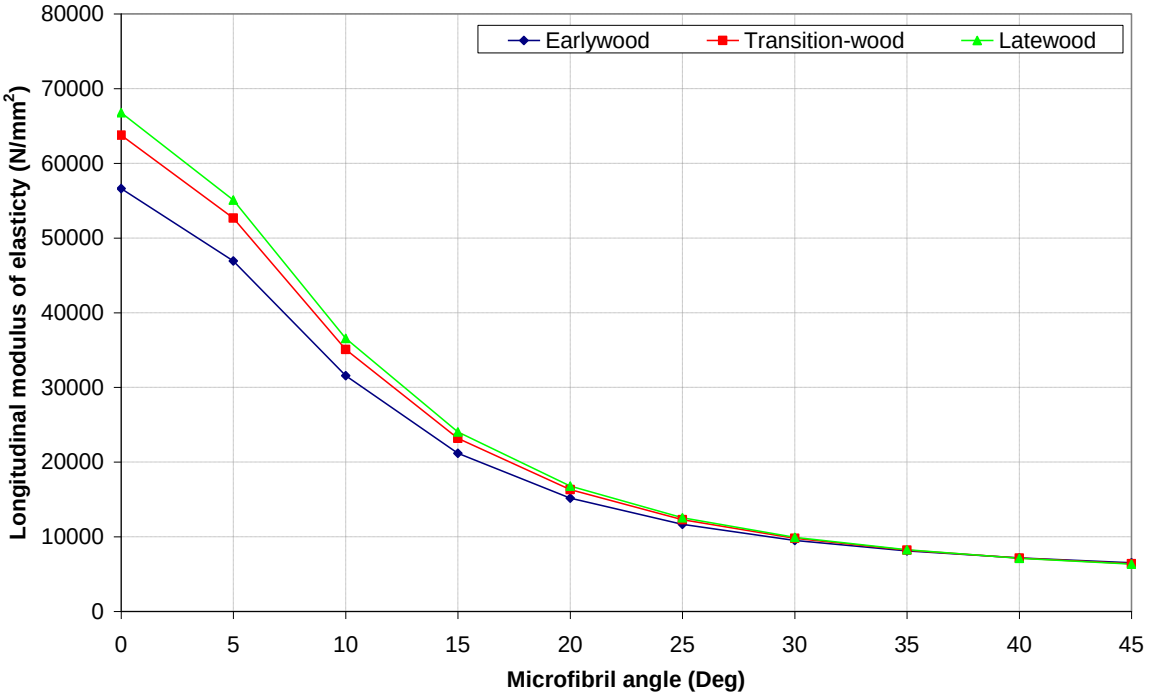

Figure 8-10: Lower bound cell wall longitudinal modulus of elasticity variation with S_2 microfibril angle and tracheid type

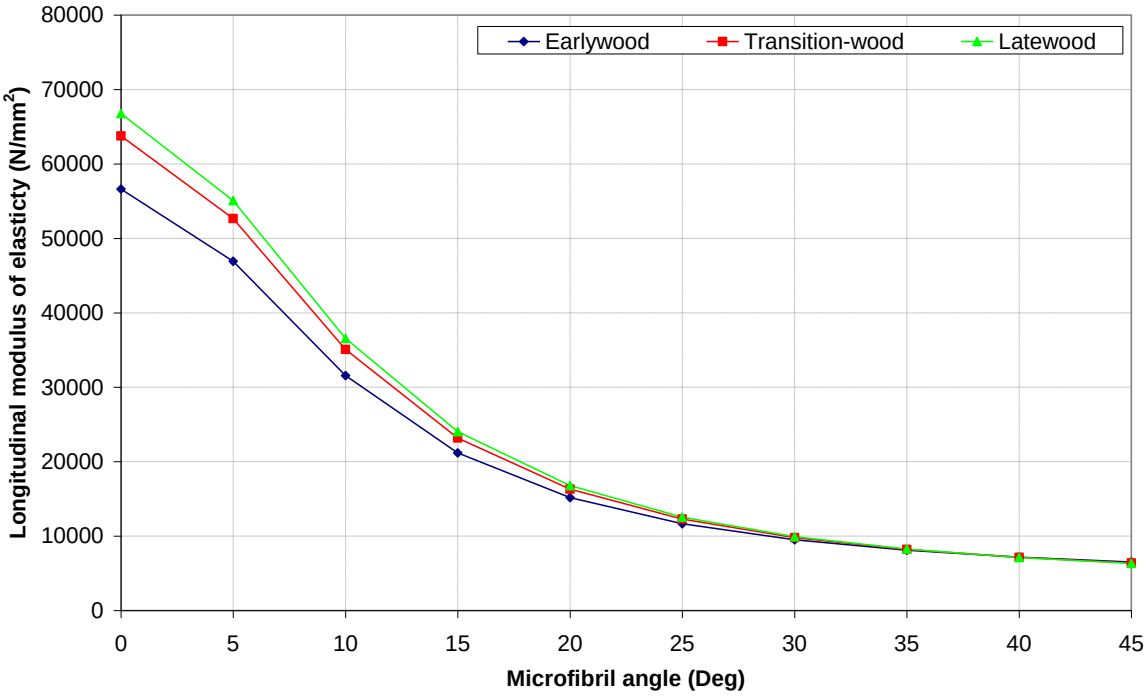

Figure 8-11: Middle bound cell wall longitudinal modulus of elasticity variation with S_2 microfibril angle and tracheid type

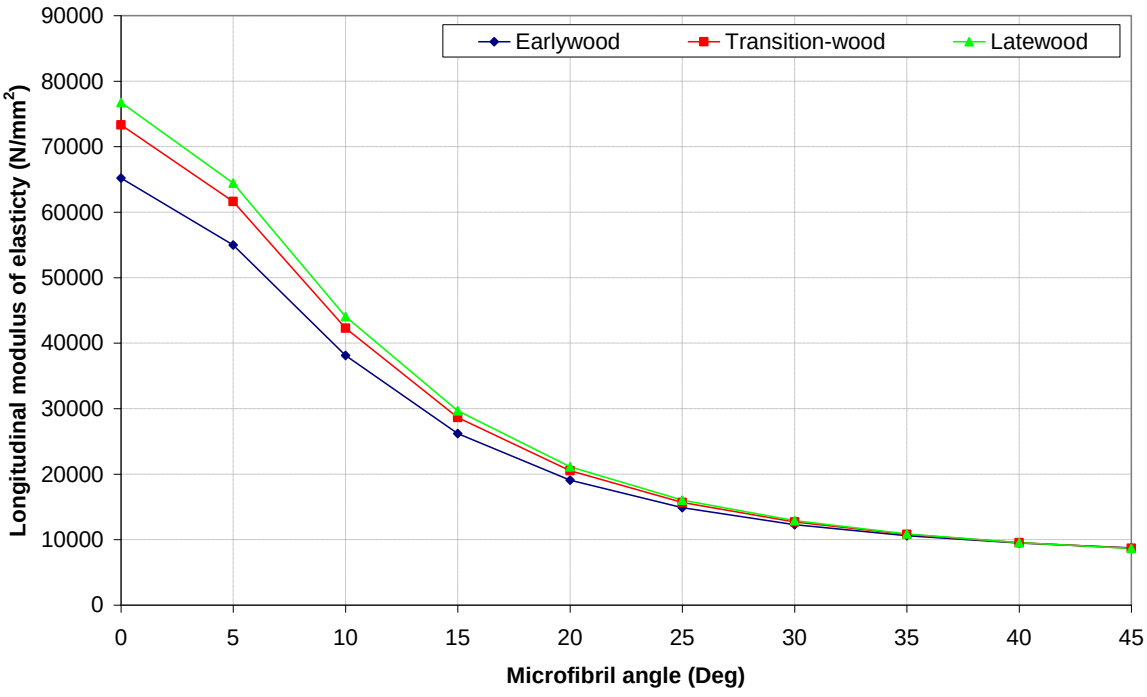

Figure 8-12: Upper bound cell wall longitudinal modulus of elasticity variation with S_2 microfibril angle and tracheid type

On inspection of the results obtained through cell wall modelling, it is apparent that all variable input parameters influenced the longitudinal modulus predicted. Within each of the constituent property bounds modelled, the angle of the cellulose microfibrils within the S_2 wall layer can clearly be seen to be the primary determinant of longitudinal modulus of elasticity for the complete cell wall system. In Section 4.7, it was reported that the mean whole ring microfibril angle for all test specimens varied from approximately 30° to between 15° and 10° depending on stem height during the maturation process. This corresponds to an increase of three to four times in the longitudinal modulus of elasticity of the cell wall. This large increase in the magnitude of the modulus with a decreasing angle is due to the significant differential that exists between the longitudinal and transverse properties of the cellulose and hemicellulose, identified in Section 8.2.2.

It can also be observed in Figures 8-10 to 8-12 that a difference exists between the longitudinal modulus of the cell wall for early, transition and latewood. At high fibril angles, greater than 25°, the differences between the tracheid types are negligible, due to the overall low stiffnesses at these angles. However, as the fibril angle decreases past 15°, the difference between the early and latewood becomes evident, with an increase in cell wall modulus of elasticity of between 5000 and 10000 N/mm^2. This difference between tracheid types can be attributed to an increase in the relative proportion of the S_2 layer present within the latewood cell walls, with its preferentially orientated microfibrils and marginally increased cellulose content compared to either the S_1 or S_3 layers. The values recorded for transition-wood were found to be more closely matched to latewood values, as a result of similar proportions of cell wall layers compared to the earlywood.

The profiles of cell wall longitudinal modulus of elasticity variation with S_2 layer microfibril angle displayed here correspond well to the results obtained from theoretical models developed by Yamamoto and Kojima (2002) and Salmén (2004). However, when comparing the values achieved by the theoretical models, the lack of a complete understanding of the mechanical properties of the component parts of the composite system, and the resultant use of differing values between studies, means that the longitudinal modulus predictions for the tracheid cell wall are not directly comparable. The range of results recorded in this work did however encompass the range of values found in the two aforementioned studies, which were between 10000 - 70000 N/mm^2. Experimentally derived variations in longitudinal modulus of elasticity with S_2 layer microfibril angle, determined from thin Radiata pine specimens by Cave (1968) and Sugi specimens by Sobue and Asano (1976), also show similar profiles to

those found here, with the reported results of approximately 10000 - 55000 N/mm^2 encompassed within the range of values formed by the three bounds calculated here. More recent studies using nano-indentation on just the S_2 layer (e.g. Tze et al., 2007) have also shown similar results.

8.3.3 Cellular longitudinal modulus of elasticity

Previously, the impact of a changing microfibril angle within the S_2 layer on the cell wall longitudinal modulus was evaluated. In this sub-section the calculated properties of the complete cellular system are presented, considering variations in both cell dimensions and microfibril angle and relating the results found to those observed in the development of statistical models in Chapter 7.

In stage 4 of the micromechanical composite model development, Equation 8-12 was used to allow the impact of changing cellular dimensions on the longitudinal cellular properties to be accounted for. Changes in cellular dimensions are directly related to density, due to an increase or decrease in the quantity of wall material for a given volume. Knowing that the density of oven-dry cell wall material, ρ_{Wall} , is approximately 1500 kg/m^3 (Weatherwax and Tarkow, 1968), it is possible to quantify changes in cellular dimensions from the perspective of density by simply replacing E_{CW} with ρ_{Wall} in Equation 8-12. Figure 8-13 shows the result of using this method to predict small clear specimen density based on using mean cellular dimensions as input parameters, obtained by end matching small clear specimen and SilviScan-3 data, as described in Section 3.9, plotted against the mean SilviScan-3 derived whole ring density of the specimen, again obtained through end matching.

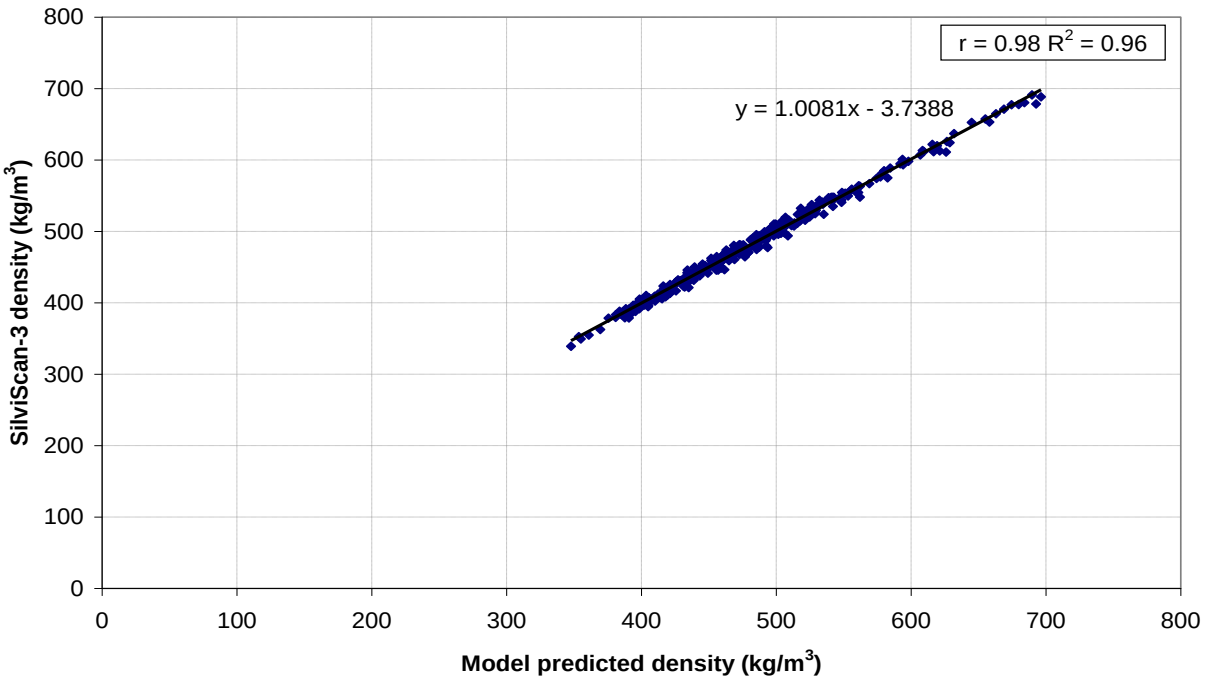

Figure 8-13: Model predicted specimen density against SilviScan-3 derived specimen density for 40 - 50 year old sample trees

The results show that a very strong correlation exists between the density values found using the two methods, with a correlation coefficient of r = 0.98 returned. This high degree of correlation between the results was to be expected, given the partial auto-correlation between them arising from the fact that the SilviScan-3 x-ray densitometry output and optically derived cellular dimensions were used for the derivation of wall thickness data as well as density, as described in Section 3.5.3.2.

Figure 8-14 shows the model predicted density values for small clear specimens utilising the same value of ρ_{Wall} and cellular dimensions as used previously, plotted against the bulk density values calculated for each small clear specimen, utilising directly measured dimensions obtained prior to flexural testing.

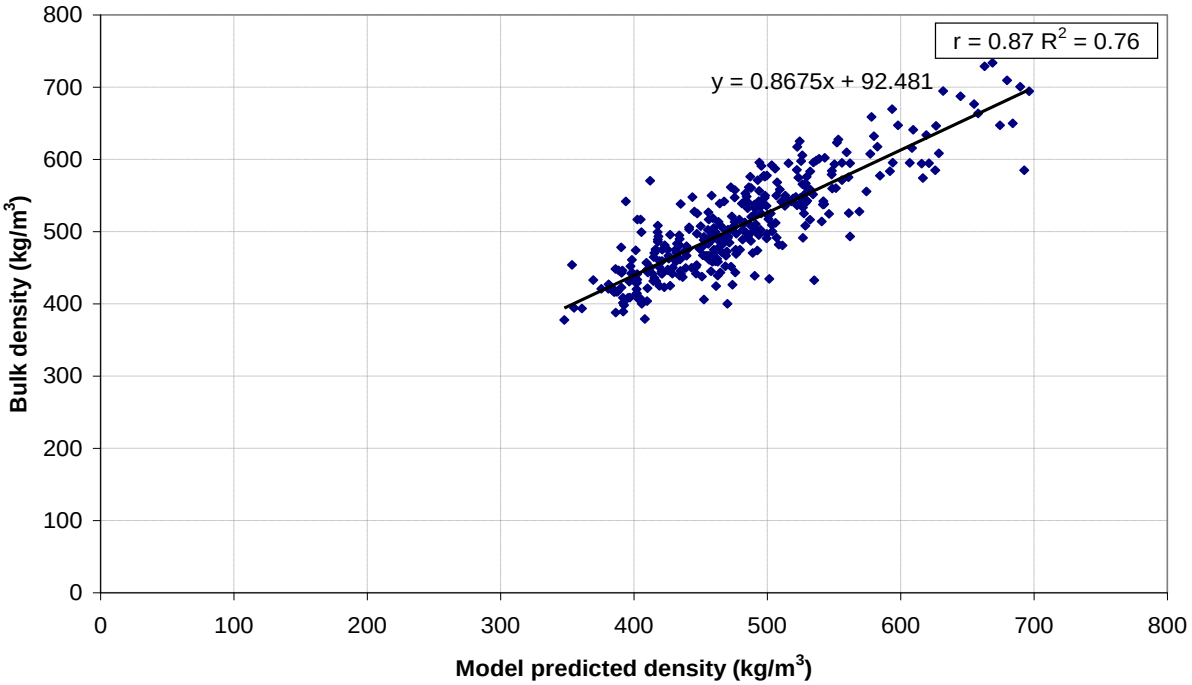

Figure 8-14: Model predicted specimen density against bulk specimen density for 40 - 50 year old sample trees

Given the strong correlation with SilviScan-3 results seen in Figure 8-13, it is not unexpected that the correlation between the density values predicted by the model and those calculated based on directly measured values returned a correlation coefficient the same as that observed between bulk and SilviScan-3 density in Table 7-1, of r = 0.87. The density values recorded directly from specimens were found to be higher than those predicted by the model. The potential reasons for this are as discussed in Section 7.2.2, with the additional factor that the cell wall density value used in the calculation may not accurately represent the actual values in all cases, due to chemical and moisture content differences.

It was demonstrated in Section 7.3.2.1 with the use of path analysis that, within the juvenile wood, cellulose microfibril angle was more strongly associated with increases in specimen modulus of elasticity than density, while in the mature wood this relationship was reversed. It was also noted in Section 7.3.4 that the correlations between the early, transition and latewood components of density experienced different strengths with modulus of elasticity with respect to each other between the juvenile and mature wood. Utilising the previously shown strong correlations between ρ_{Wall} and specimen bulk density, a series of profiles for early, transition and latewood were produced showing the variations in cellular longitudinal modulus of elasticity that can be attributed to changes in density and S_2 layer microfibril angle. These are shown in Figures 8-15 to 8-17.

Each profile was produced based on the middle bound constituent properties for the respective tracheid type; the overall trends shown would be the same for the lower and upper bounds. The changes in density were modelled by varying the proportion of cell wall material present, assuming that cell wall density remained constant with increasing cambial age. On each of the three graphs, the changes in the longitudinal modulus of elasticity associated with variations in density and the microfibril angle of the S_2 layer are shown separately for juvenile and mature wood. The change in density and microfibril angle values reported are those which occurred between the first and last growth rings within either juvenile or mature wood, based on means reported at breast height for 40 - 50 year old trees in Chapter 4. Trends at the 8 m sampling location are expected to be similar, due to similarities in the developmental profiles. The microfibril angle values used are based upon the sub-sample of high resolution SilviScan-3 results. For simplification a juvenile mature wood boundary of 19 years was selected, an age that was shown in Section 5.3 to encompass the mean demarcation age for both density and microfibril angle at breast height.

Taking Figure 8-15 which depicts changes in earlywood cellular longitudinal modulus as an example, juvenile wood microfibril angle decreased by 10° and density decreased by 125 kg/m^3 between the first and last growth rings. The approximate changes in cellular longitudinal modulus associated with these variations were determined from the graphs. In the case of juvenile wood in Figure 8-15, this was done by recording the rise in modulus of elasticity as the microfibril angle reduced from 30° to 20°, approximately 1750 N/mm^2, followed by the changes due to a fall in density from 400 kg/m^3 to 275 kg/m^3, approximately -1750 N/mm^2. Within the mature wood, no change was observed in microfibril angle values; as such no change in modulus of elasticity is associated with the microfibril angle. Density exhibited an increase of 25 kg/m^3 between the first and last growth rings within the mature wood. From the graph it is observed that this results in an increase in cellular longitudinal modulus of approximately 500 N/mm^2.

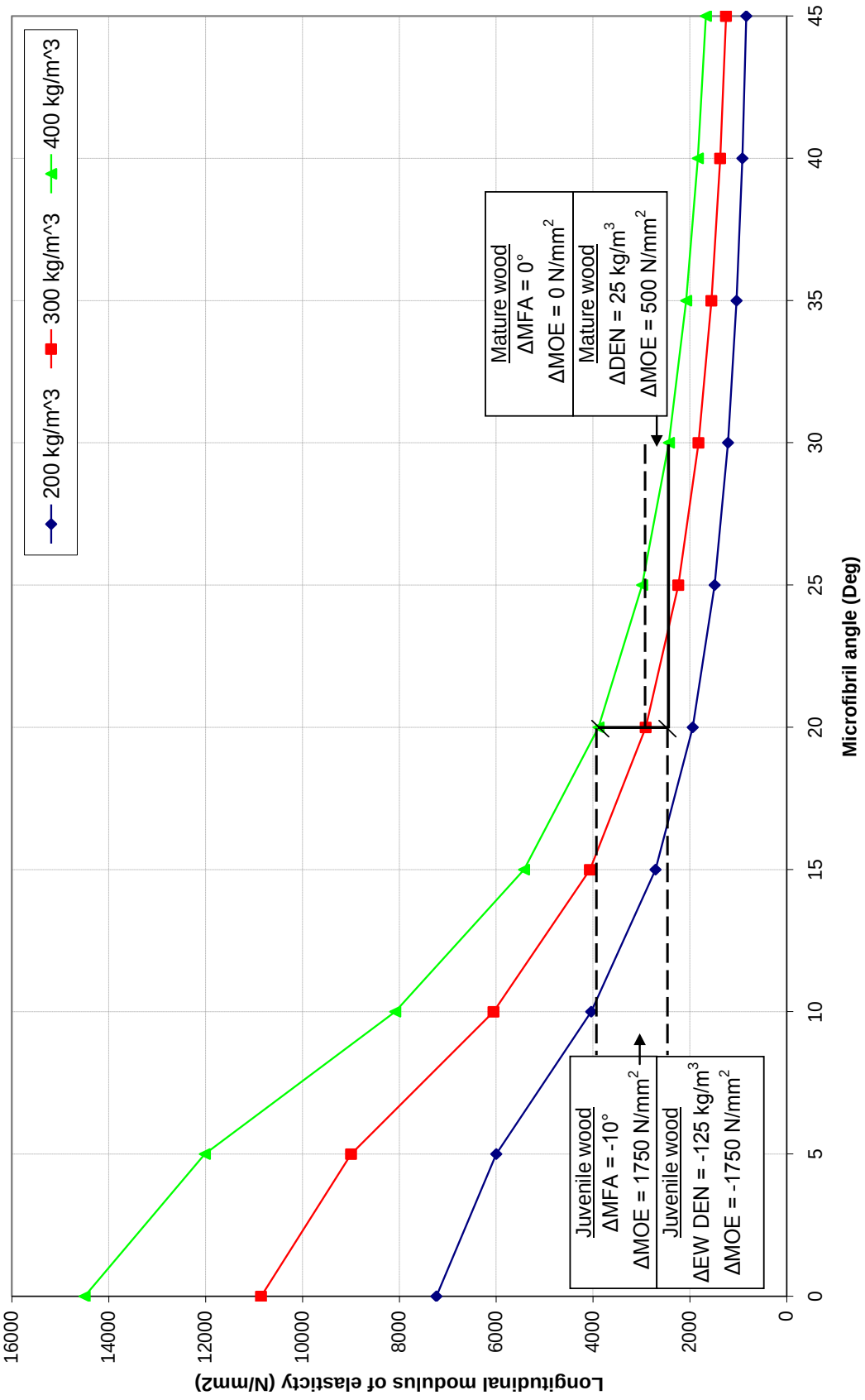

Figure 8-15: Earlywood cellular longitudinal modulus of elasticity variation with S_2 microfibril angle and density

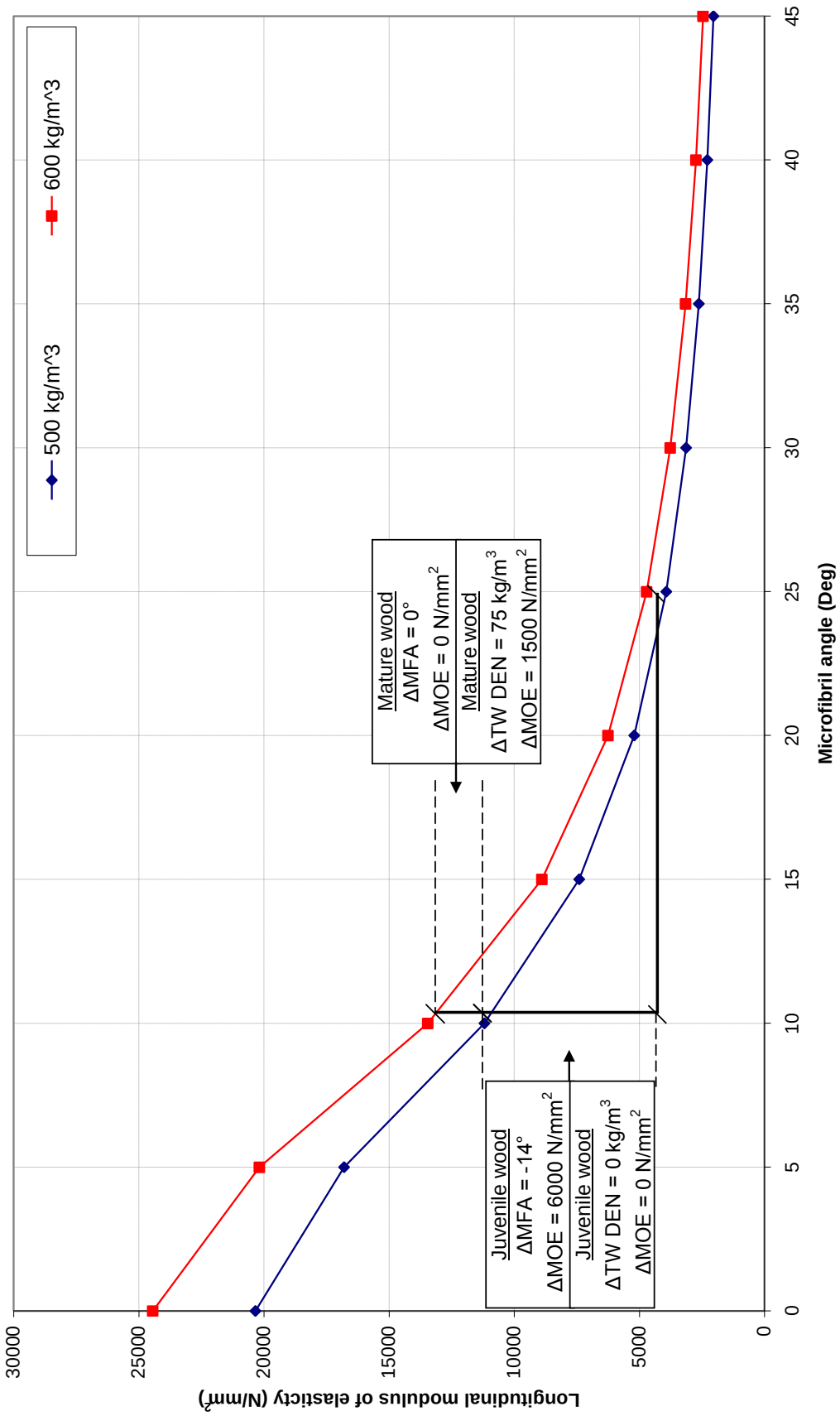

Figure 8-16: Transition-wood cellular longitudinal modulus of elasticity variation with S_2 microfibril angle and density

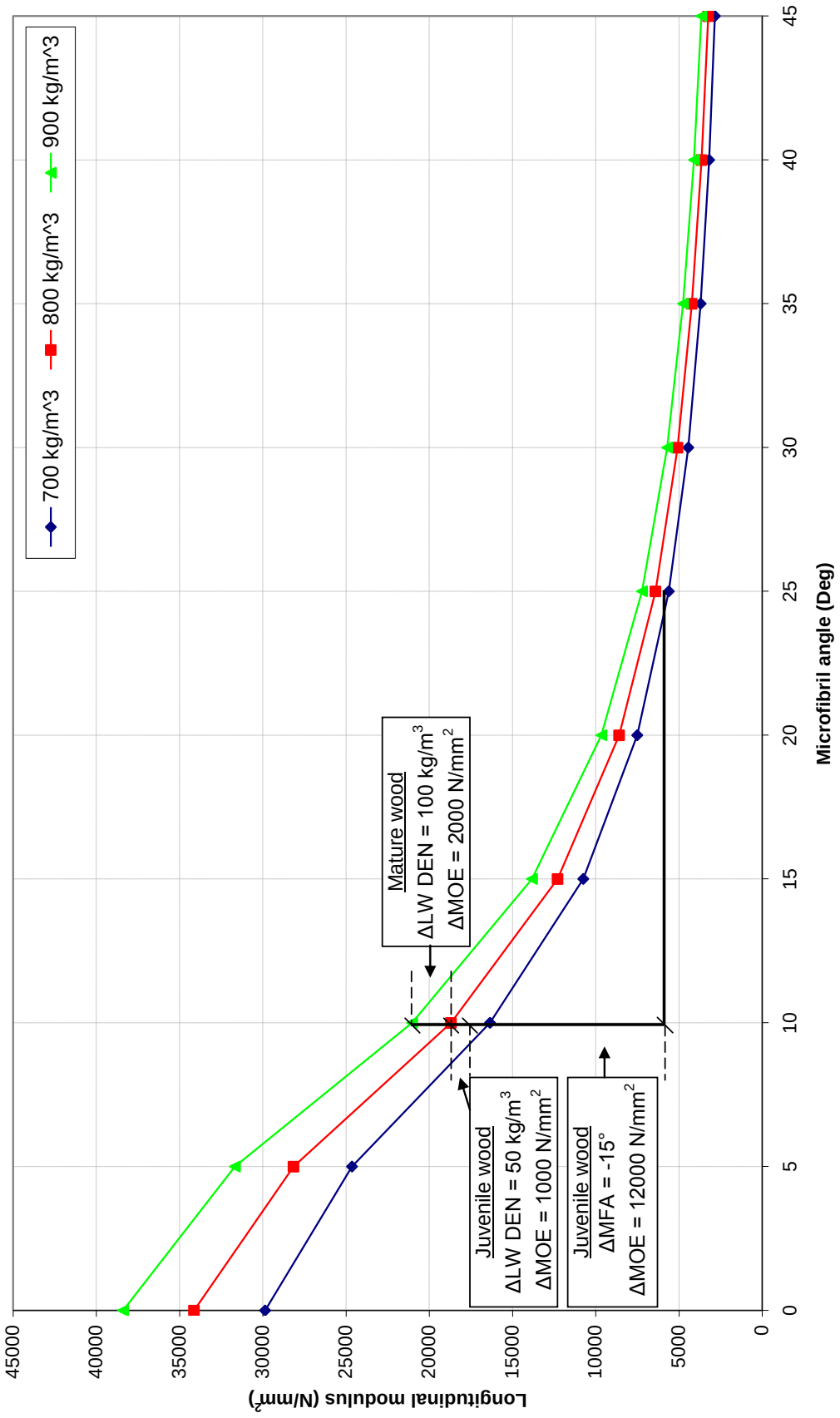

Figure 8-17: Latewood cellular longitudinal modulus of elasticity variation with S_2 microfibril angle and density

In the results displayed in Figures 8-15 to 8-17, a differential between the influence of microfibril angle and density on the longitudinal modulus of elasticity within juvenile and mature wood can clearly be seen. Within the juvenile wood for early, transition and latewood, increases in the longitudinal modulus of elasticity due to changes in microfibril angle were found to be significantly greater than changes arising due to density, which in the case of the earlywood were negative. This was due to a combination of factors, including the large decreases in microfibril angle compared to only modest changes in density, and the mechanistic relationship between cellulose microfibril angle and longitudinal modulus. Within mature wood, changes associated with density were still comparatively small, however negligible decreases in microfibril angle resulted in density being responsible for the increases seen in the longitudinal modulus of elasticity. These observations account for the change in the strength of the standardised regression coefficients at the whole tree level for density and microfibril angle between juvenile and mature wood, shown in Table D-1 and discussed in Section 7.3.2.1. They also explain the greater impact of density than microfibril angle on flexural modulus in the results reported by Lachenbruch et al. (2010) conducted on mature Douglas-fir specimens.

Differences in behaviour between early, transition and latewood were also observed in Figures 8-15 to 8-17. In Section 7.3.4 it was postulated that the varying proportions of the three tracheid types within a growth ring were, in part, responsible for the variations in the magnitude of the standardised regression coefficients observed between the three density components and flexural modulus of elasticity on moving from juvenile to mature wood. On inspection of the results presented here, differing mechanistic behaviour of the tracheids can also be attributed to being partially responsible for variations in the strength of the coefficients. Within the earlywood (Figure 8-15), the comparatively low proportions of the S_2 layer within the cell wall, the low overall density and high microfibril angle result in the influence that changes in either density or microfibril angle can have on longitudinal modulus of elasticity being limited. Within the juvenile wood this factor, the low proportions of earlywood discussed in Section 7.3.4 and the large decrease in earlywood density, followed by a gentle rise on moving away from the pith, account for the statistically non-significant standardised regression coefficients between earlywood density and flexural modulus of elasticity observed in Table D-7. While similar small changes were observed within the mature wood, the greater proportion of earlywood within this region accounts for the increased strength of the standardised regression coefficients recorded compared to the other density components.

In comparing the influence of transition-wood (Figure 8-16) and latewood (Figure 8-17) density on longitudinal modulus, it is observed that increases in the density of latewood within the juvenile region would result in a greater increase in the longitudinal stiffness of tracheids than an equivalent rise in transition-wood density. This is due to the increased S_2 layer thickness within the latewood. However, as with earlywood, the limited proportions of latewood, within the juvenile region, are likely to have resulted in the statistically non-significant standardised regression coefficients observed between latewood density and flexural modulus of elasticity in Table D-7, while the reverse is true for transition-wood. On moving to the mature region, the strength of relationships was observed to be similar within both earlywood and latewood, despite their typically being a lower proportion of latewood within growth rings. This can be seen to be due to the significantly greater increases in longitudinal modulus associated with a rise in latewood than earlywood density. The strength of the standardised regression coefficient between transition-wood density and flexural modulus was found to be lower than that for latewood despite similar proportions. This can be attributed to smaller increases in modulus of elasticity associated with a rise in transition-wood density.

8.3.4 Small clear specimen modulus of elasticity predictions

In order to verify the accuracy of the micromechanical composite model developed, anatomical properties determined through the use of the SilviScan-3 system were used as input parameters for the prediction of flexural modulus of elasticity. This was done firstly by generating modulus of elasticity profiles as a function of cambial age, followed by the prediction of values for individual small clear flexural specimens.

Within Chapters 4 and 6, radial development profiles were obtained for the mean values of cellular and mechanical properties over equivalent cambial ages. In Figures 8-18 and 8-19, predicted flexural modulus of elasticity profiles as a function of cambial age, determined through the use of the mean values of anatomical properties in early, transition and latewood are shown. Results for lower, middle and upper bounds are plotted against the flexural modulus of elasticity profiles depicted in Figure 6-5 separately for the two assessed stem heights in 40 - 50 year old sample trees. As has been discussed previously, it was not possible to determine the intra-ring variations of microfibril angle at a sufficiently high resolution such that early, transition and latewood mean values could be obtained for all specimens. Therefore, adjustment factors were calculated at each cambial age and height to be applied to the mean microfibril angle values determined for all specimens in order to obtain values

within the three intra-ring zones. These were determined based on the differences seen between mean values and early, transition and latewood microfibril angle for each cambial age within the higher resolution results. While not fully representing the actual values, it was felt that given the similarities between the mean profiles of the low and high resolution datasets, that this represented a good compromise in improving the accuracy of the model.

At both 1.3 m and 8 m, predicted results were found to show a good overall fit to those obtained through mechanical testing at cambial ages of 10 years or greater. Below this age, predicted values were found to be lower than those observed, with results in the growth rings immediately adjacent to the pith, particularly at the lower sampling height, exceeding even those for upper bound predictions. Inconsistencies in the actual and predicted values within relatively young tracheids are likely accounted for by the occurrence of compression wood within this region of the stem (Kennedy, 1995 in McLean 2008), leading to differences in cell morphology and constituent properties to those within normal wood (e.g. Donaldson et al., 2004), which are difficult to model. Beyond 10 years of age at 1.3 m, the mean flexural test results were found to lie between the middle and upper bound predicted results. The reduction in the rate of change in the increase of modulus of elasticity seen on moving into mature wood was clearly evident in the predicted results. This was found to also be the case for the model output at 8 m, however the results obtained through testing were found to lie between lower and middle bound predictions.

The close agreement between the profiles of the actual and predicted results, outside of the early juvenile wood, appears to confirm that the mechanistic relationships identified in Section 8.3.3 provide a good account of the actual relationships that exist between the various properties. While differences were observed between the modulus of elasticity values recorded at the two stem heights through mechanical testing, they weren't of the same magnitude as those predicted by the micromechanical model. Data regarding the within stem longitudinal variation of chemical constituent proportions is scarce. That which does exist has shown differences with height, although with no statistically significant patterns (e.g. Sykes et al., 2008). As such, differences in chemical constituent proportions may explain the limited variations observed with height compared to those predicted, alongside potential differences in the properties of the constituents.

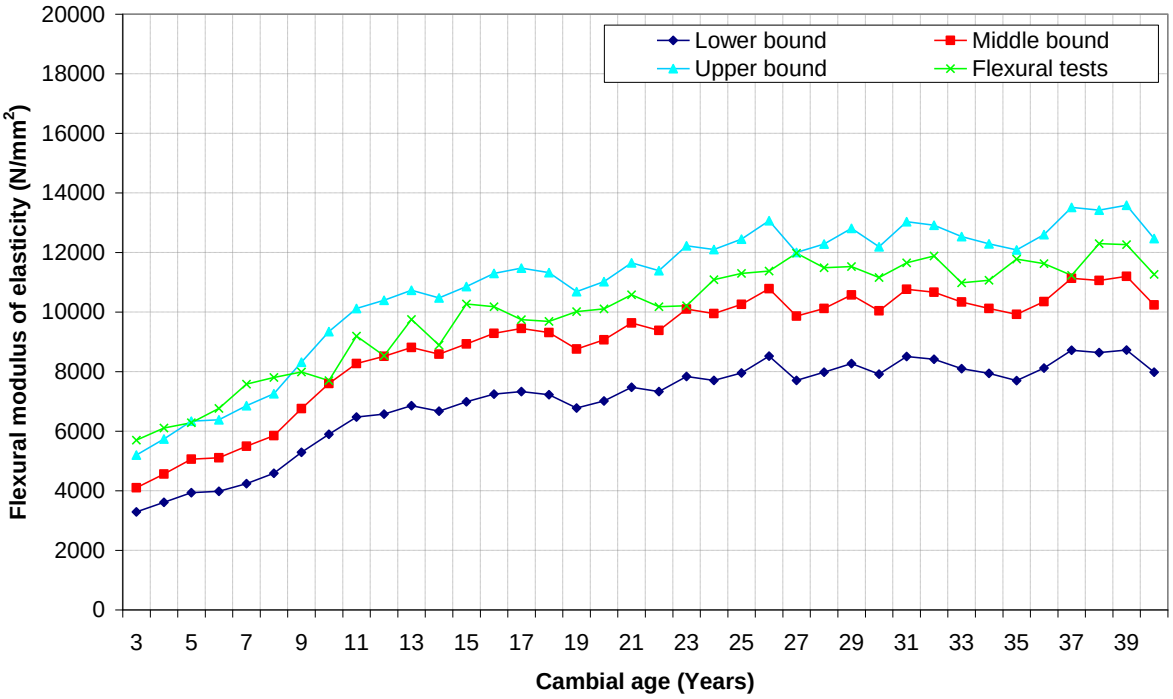

Figure 8-18: Predicted flexural modulus of elasticity against observed results for three constituent bounds at 1.3 m fro 40 - 50 year old sample trees

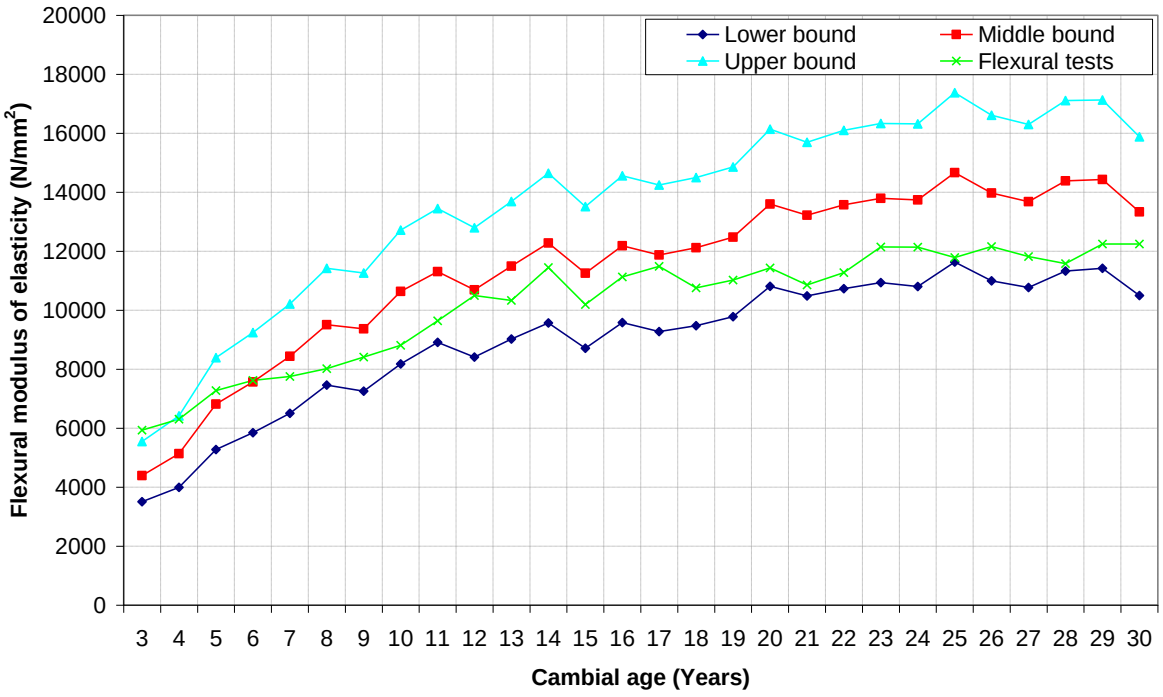

Figure 8-19: Predicted flexural modulus of elasticity against observed results for three constituent bounds at 8 m fro 40 - 50 year old sample trees

In utilising the methodology of matching small clear specimens to the equivalent radial position on the corresponding SilviScan-3 specimen, described in Section 3.9, it was possible for the mean anatomical characteristics of each small clear specimen to be obtained. Utilising this data as input parameters for the micromechanical model, individual predictions for the flexural modulus of elasticity of each small clear specimen were obtained. The potential inaccuracies associated with the use of the end matching method were discussed in Section 7.2.2. In specimens where detailed intra-ring microfibril angle data for early, transition and latewood were not available, the method detailed earlier in this section, whereby a modification factor from mean values based on results obtained from high resolution analysis, was utilised. Results from predictions based on lower, middle and upper bound constituent property parameters, including linear correlation coefficients and coefficients of determination determined according to the methodologies given in Section 3.10.3, are shown in Figures 8-20 to 8-22.

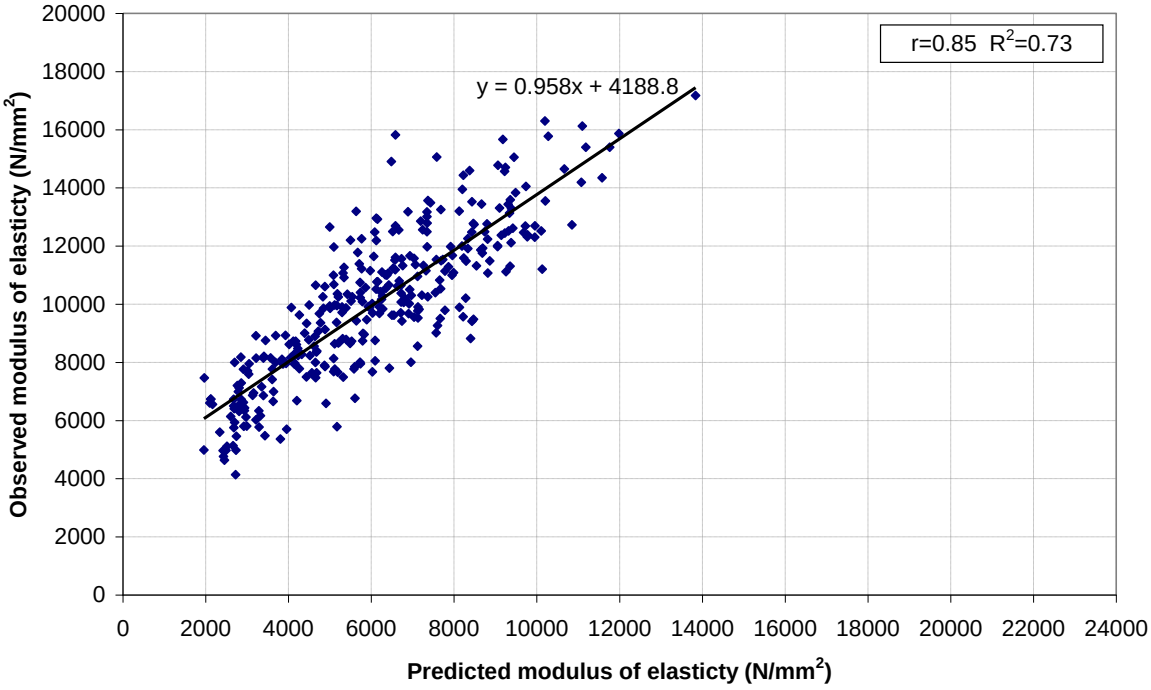

Figure 8-20: Small clear specimen predicted against observed flexural modulus of elasticity lower bound prediction for 40 - 50 year old trees

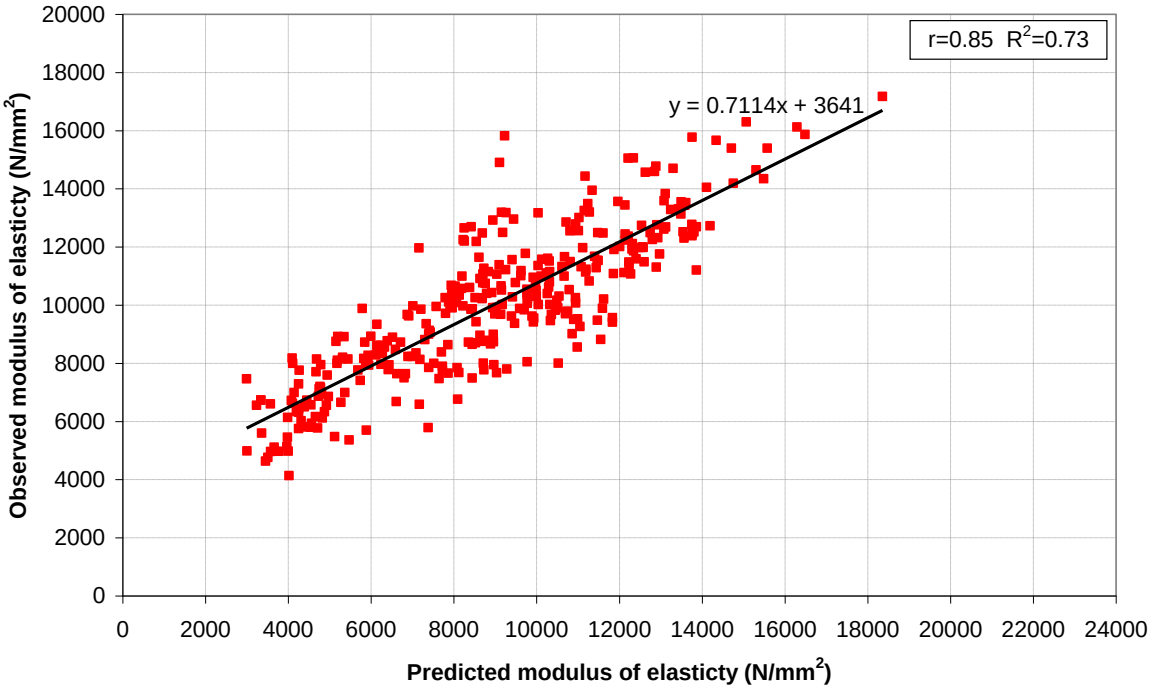

Figure 8-21: Small clear specimen predicted against observed flexural modulus of elasticity middle bound prediction for 40 - 50 year old trees

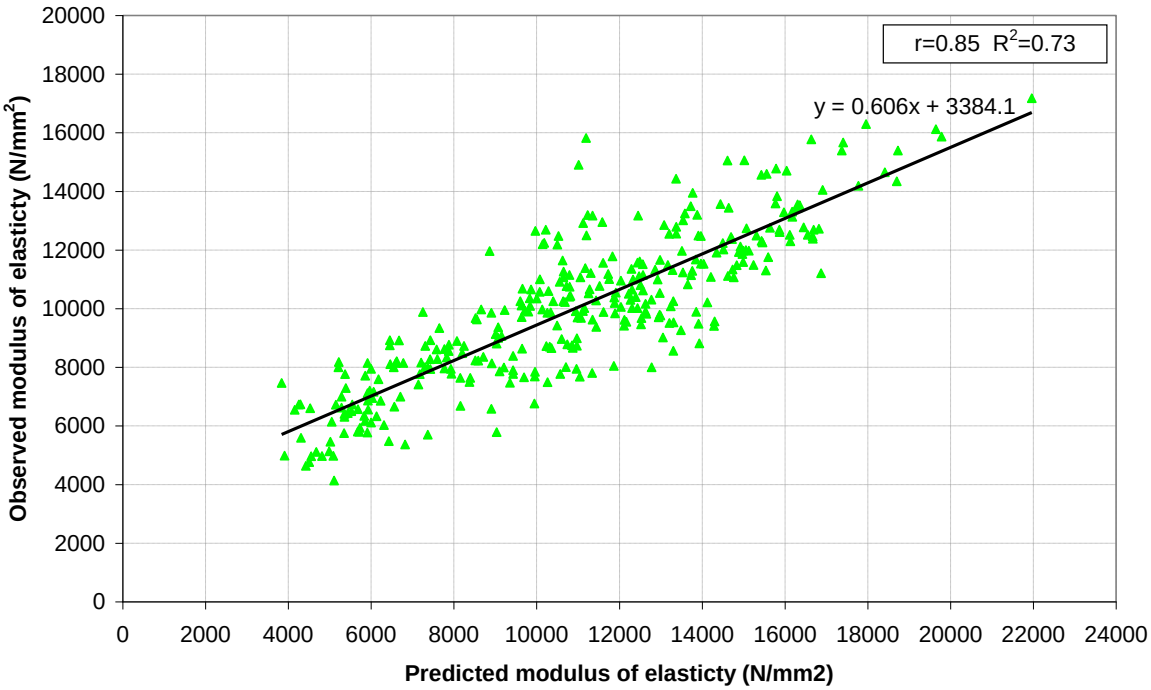

Figure 8-22: Small clear specimen predicted against observed flexural modulus of elasticity upper bound prediction for 40 - 50 year old trees

For lower, middle and upper bound predictions, a strong linear correlation with results obtained through mechanical testing was found, with a correlation coefficient of r = 0.85 and the resultant linear regression equations accounting for 73 % of the variation observed. On inspection of the regression equations plotted on each of the graphs, it can be seen that for specimens with lower observed values of modulus of elasticity, the predicted results for all three bounds were generally underestimated. This finding is in agreement with observations made for the development profile displayed in Figures 8-18 and 8-19, in which it was postulated that the presence of compression wood at younger cambial ages, where modulus of elasticity is low, was a potential cause of the poor fit. Beyond observed modulus of elasticity values of between 6000 - 8000 N/mm^2, the accuracy of the predicted results was found to improve, with observed values generally better fitted to upper bound predictions at lower moduli, and middle bound predictions as the values of the modulus of elasticity increased. This is again in agreement with the results shown in the previous profiles, if the averaging of results from the two sampling heights is accounted for. The lower bound predictions were found in general to underestimate the observed values. Potential improvements that may increase the accuracy of the results predicted by the micromechanical model are given in the following section.

8.4 Potential improvements to micromechanical model

While the results returned by the micromechanical composite model were found to account for a good degree of the variations exhibited in those determined through mechanical testing, several assumptions were made in the developmental stages which represent potential areas for improvement. The properties of the chemical constituents of wood are perhaps the area where the greatest improvements in model accuracy could be made. The range of values for chemical constituents used here enabled a large proportion of the mechanical test results to be encompassed. It was the case however that the range of predictions between lower and upper bounds was large. In order to improve the accuracy of the predictions, a detailed understanding of the properties of the chemical constituents and their changing proportion within the Douglas-fir cell wall with position, both radially and longitudinally, within the stem is required.

The arrangement of the chemical constituents with respect each other in the cell wall represents a further area where the potential for improved accuracy exists. The arrangement used here, whereby cellulose fibrils were embedded in a lignin-hemicellulose matrix, has been widely adopted. However other arrangements have been suggested, such as that employed by

Bergander and Salmén (2002), in which cellulose fibrils were embedded within a matrix of hemicellulose with layers of lignin placed between. While the differences in the longitudinal modulus results returned utilising the two methods were small when compared by Bergander and Salmén, it does represent a further source of potential variation. It is also the case that in the model used here that the angles of the cellulose microfibrils within the S_2 wall layer within the early, transition and latewood were not fully representative of the actual properties of each specimen. A further improvement would therefore be the utilisation of high resolution microfibril angle data derived utilising SilviScan-3 for all specimens.

In the model developed by Persson (2000), images of wood micrographs were used in order to replicate the cell structure of wood, in contrast to the regular cellular structure that was modelled here. Adopting a more representative cellular arrangement represents a further improvement which may have allowed for more accurate results to be gained, particularly in the early juvenile wood where such micrographs may allow for the more accurate modelling of any compression wood tracheids that may be present. However, the quantity of data that it would be necessary to collect in order to construct a fully representative cellular arrangement model for each specimen is large and it is unknown if a sub-sample of equivalent data would produce any increase in model accuracy.

A final factor which is likely to have contributed to differences between the actual and predicted results is the presence of anomalies and defects within the physical test specimens themselves. The use of micro bending specimens with their reduced section sizes, such as those prepared by Bendtsen and Senft (1986), would have reduced the probability of the presence of variations along the specimen length and hence improve the model accuracy. Within the constraints of the work conducted here it was however not possible to prepare and test such specimens.

8.5 Concluding remarks

In this chapter a micromechanical composite model of the Douglas-fir cellular structure was developed. Utilising published data and that obtained through experimental work conducted in this study, the model was used to investigate the interactions between wood anatomical properties and its modulus of elasticity. Utilising the results obtained it was then possible to explain and predict the changes in the mechanical behaviour of small clear test specimens observed with changing location within the sample trees.

Through the model it was shown that differences in the density of the cellular structure, and to a lesser extent the changing proportions of cell wall layers, results in significant increases in the maximum theoretical stiffnesses attainable on moving from early to latewood. It was also demonstrated that increases in wood density and decreases in microfibril angle can result in significant increases in the magnitude of the flexural modulus. However, given the range of values for S_2 layer microfibril angle and density observed in the sample trees within the early, transition and latewood, decreases in microfibril angle accounted for a significantly greater increase in the flexural modulus of elasticity than increases in specimen density. Due to the nature of the developmental profiles for microfibril angle, virtually all increases in modulus of elasticity due to decreases in microfibril angle were found to occur within the juvenile wood of sample trees.

Overall, a good agreement was found between the flexural modulus of elasticity results obtained during the mechanical testing of small clear specimens and those predicted through the use of the micromechanical composite model. However it was noted that for more accurate predictions to be made, a greater understanding of the properties and behaviour of the chemical constituent components is required.

Chapter 9 - Discussion of methodologies and results

9.1 Introduction

In this chapter, the suitability of the methodologies used and the extent to which the range of results obtained fulfilled the objectives of the project is discussed. The potential wider implications and relevance of the results is also discussed, and recommendations made for future work within the subject area.

9.2 Fulfilment of research objectives

In Section 1.5 a series of objectives to be fulfilled by the work undertaken in this study were set out. All objectives were met by the work presented in this thesis, as detailed in the following summary:

- The design of a sampling and testing programme to allow for the within stem assessment of variations in both anatomical and mechanical properties of a representative sample of Douglas-fir trees obtained from the South West region of England.

In total 27 Douglas-fir trees were sampled from sites across the South West of England from a mix of private and public ownership. Trees with ages of 40 - 50 years, representing the current peak in the age distribution of the resource within the South West, formed the core of the sample material, with a number of older trees with ages > 50 years also sampled to allow for the continuation of any trends observed in younger trees to be verified. The use of small clear specimens for mechanical testing allowed for detailed profiles of intra-tree variations in mechanical properties to be gained, while the implementation of the SilviScan-3 system

allowed for the generation of within tree profiles of anatomical properties at a resolution not previously recorded in Douglas-fir. A discussion of experimental methodologies used, their limitations and potential improvements is given in Section 9.3.

- The measurement of wood anatomical properties at micro and macroscopic scales and a quantification of variability with age, longitudinal position in the stem and rate of growth.

The utilisation of the SilviScan-3 system for the measurement of anatomical properties allowed for a previously unseen level of understanding of the variations with increasing cambial age and longitudinal position in the stem of density, S_2 layer microfibril angle and cellular dimensions within the Douglas-fir sample trees. The results presented in Chapter 4 showed a change in the magnitude of all anatomical properties with increasing cambial age, particularly so in the earliest formed growth rings in most cases. The use of the SilviScan-3 system also allowed for the quantification of the proportions of transition-wood tracheids within a growth ring, in addition to the typical practice of quantifying earlywood and latewood proportions. Such results have not been widely quantified for any softwood species, and aided in the explanation of the variations in anatomical properties observed as trees matured. Small differences in many anatomical properties were observed between trees quantified as slower and faster growing in the results reported in Section 5.2, with the distinct classification of transition-wood aiding in the interpretation of results relating to differences in growth rate.

- The measurement of mechanical properties relevant for uses in structural applications and a quantification of variability with age, longitudinal position in the stem and rate of growth.

Through the use of small clear flexural and compressive specimens, a detailed understanding of the variations in the flexural modulus of elasticity, flexural and compressive strength with increasing cambial age and longitudinal position within the sample trees was attained. Within Chapter 6, cambial age was identified as the primary cause of variability in mechanical properties, with large increases observed at younger ages in particular. An increased rate of growth was found to have a negative impact on properties, although changes in values were less substantial than those recorded with increasing cambial age. Within Section 6.7 these results were interpreted with reference to the timber grades for structural applications set out in BS EN 338 (BSI, 2003), the implications of the findings presented are discussed in Section 9.4.

- The quantification of the ages of demarcation from juvenile to mature wood production, and an assessment of the influence of rate of growth on demarcation age.

Through the detailed inter-ring variations for microfibril angle and density that were obtained from the SilviScan-3 system, it was possible to implement a segmented regression method to determine the age of demarcation from juvenile to mature wood production for both variables. The difficulty associated with obtaining detailed microfibril angle data means that quantifications for demarcation ages for this property are rare, with no previous literature found specifically relating to Douglas-fir. The results presented in Section 5.3 led to the conclusions that for both density and microfibril angle, lower transitional ages were observed higher in the sample trees, with microfibril angle profiles also exhibiting mature behaviour earlier than those for density. The influence of rate of growth of sample trees on demarcation age was also studied, with it observed that in faster growing trees the mean demarcation ages were greater than those observed in slower grown trees. Results were interpreted with reference to stand dynamics and tree development. The potential implications of these findings with regard to the implementation of silvicultural practices are discussed in Section 9.4.2.

- The development of statistical and micromechanical composite models to enable a better understanding to be gained of the ways in which wood anatomical properties determine the mechanical characteristics of the timber derived from it.

A range of statistical techniques were employed in Chapter 7 to aid in the development of a greater understanding of the relationships between anatomical and mechanical properties. The results showed that at the whole tree level, flexural modulus of elasticity was more strongly associated with variations in microfibril angle than density, while both flexural and compressive strengths were more strongly associated with density variations. Differences were observed in the strength of the relationships between juvenile and mature wood, the potential reasons for this with respect to flexural and compressive strengths were discussed in Section 7.3.2. The micromechanical composite model developed in Chapter 8 allowed for a detailed insight to be gained into the relationships between microfibril angle, density and its intra-ring components with modulus of elasticity within both juvenile and mature wood. Studies demonstrating the relationships between anatomical and mechanical properties within both juvenile and mature wood utilising directly determined values are limited, and as such the results presented here are a valuable contribution to the knowledge of the interaction of properties within softwoods, and Douglas-fir in particular.

- The use of the models developed for the prediction of the assessed mechanical properties based on the values of the assessed anatomical properties, from which suggestions will be made regarding the best visually identifiable features to be used in the determination of wood quality for structural applications.

Through the use of multiple regression modelling in Chapter 7 and micromechanical composite modelling in Chapter 8, predictions of the mechanical properties of small clear specimens based on their anatomical characteristics were made. Both the statistical and composite models enabled a large proportion of the variability in the modulus of elasticity of small clear specimens to be accounted for, with the predictions obtained utilising the micromechanical model accounting for a slightly greater proportion of variations than the statistically derived models. This was to be expected, given that the input parameters of anatomical properties for the statistical model were simply whole ring values for density and microfibril angle, while the micromechanical model utilised separate values for early, transition and latewood. An advantage of the statistical model over the micromechanical model was however its ability to give a tool for the prediction of flexural and compressive strength.

Through the use of the statistical model it was also possible to demonstrate that a reasonable level of variation in mechanical properties could be accounted for utilising visually identifiable features such as cambial age, ring width and latewood proportion. The potential implications of these results for visual grading methods are discussed in Section 9.4.3.

9.3 Discussion of experimental methodologies

9.3.1 Outline

In total 27 Douglas-fir trees were obtained from the South West region of England for the collection of the results presented in this thesis. In the following sub-sections the sampling and experimental methodologies used to achieve the required objectives, their limitations and potential improvements that could be made are discussed.

9.3.2 Site and tree sampling methods

The implementation of the sampling methodology described in Section 3.2 enabled a good understanding of the range of properties that could be expected to be found within the sample sites to be identified, once trees with obvious anomalies such as excessively swept lower stems or storm damage were removed. An intention of the sampling methodology develop for the

selection of trees within a site was for it to be random It is acknowledged that the removal of trees from the sample population displaying particular growth characteristics does not represent a fully random design, with the final sample population from which test trees were selected representing the upper bound of quality within a site. It is however the case that for the production of structural timber sections, trees with excessively swept stems would not typically be used, due to the inability to extract the required lengths of timber from them. Given this, the selective-random sampling design used in this thesis is relevant to the intended end use assessed. It is also acknowledged that as all sites selected in the 40 - 50 year age range were from managed, publicly owned estates, it is unlikely that trees sampled are fully representative of the complete profile of sites of a similar age containing Douglas-fir within the South West of England. However, the data that is presented gives a good indication of the potential quality of timber that is available. The removal of the sampling site in the region of Dartmoor National park resulted in a slightly uneven regional distribution in those that were selected. Sample trees were still however obtained from a wide geographic range, with the 40 - 50 years old sites representing areas where there are large numbers of Douglas-fir plantations. While the three trees with ages > 50 years that were sampled allowed for an understanding of developmental trends with increasing age to be gained, it would have been preferential to obtain a greater number of trees from different sites within this age range, however a number of logistical constraints prevented this.

9.3.3 SilviScan-3 anatomical property evaluation method

With the exception of some slight damage caused to two specimens during the preparation stages detailed in Section 3.5.3, the analysis of the 54 specimens utilising the SilviScan-3 method was implemented successfully. The analysis process allowed for the collection of quantities of data that would not have been possible within the same time frame utilising manual optical and gravimetric methods. The SilviScan-3 system does however have some limitations, perhaps the most significant of which is the time intensive nature of analysing x-ray diffraction patterns, which was a restriction in obtaining high resolution profiles of inter and intra-ring variations of S_2 layer microfibril angle. This resulted in developmental profiles for early, transition and latewood microfibril angle displayed in Section 4.7 being available for only a sub-sample of trees. As a result, it was not possible to conduct statistical path analysis utilising intra-ring microfibril angles in Chapter 7, and assumptions regarding the magnitude of the microfibril angle at intra-ring locations had to be made when inputting parameters into the micromechanical model, detailed in Section 8.3.4. The accuracy of the x-ray diffraction method is also known to fall when the angle of the cellulose microfibrils is very high, such as

in early juvenile growth rings, due to weaker diffraction signals and in the event of excessive fibre tilt (Donaldson, 2008, Verrill et al., 2011). It is also the case that while values for σ_{add} within Equation 3-5 were determined empirically utilising several thousand diffraction profiles (Evans, 1999), the potential for variations in values between species and specimens exists, potentially influencing the accuracy of the results returned.

The method used for the calculation of tracheid wall thickness described in Section 3.5.3.2 was a further limitation that resulted in it only being possible to obtain radial values, with the assumption that thicknesses are isotropic on radial and tangential walls. Previous research has shown that this is unlikely to be the case (e.g. Rathgeber et al., 2006). Aside from not being able to present results showing variations in tangential wall thickness, the greatest potential impact of this was on the accuracy of the cellular morphological modelling in the development of the micromechanical composite models, detailed in Section 8.2.5.

9.3.4 Small clear specimen mechanical testing methods

The small clear specimen preparation methods described in Section 3.6 were successfully implemented, with only nine flexural specimens removed from the sample set prior to testing due to the presence of defects and no compressive specimens removed. A disadvantage of both the flexural and compressive methodologies employed is that the mechanical properties determined were a result of characteristics averaged over several individual growth rings, and as such the opportunity for the precise determination of properties for individual growth rings, and therefore at specific cambial ages, did not exist. A potential alterative method to overcome this would have been the use of micro flexural and compression specimens, between 30 - 55 mm in length and one growth ring wide, such as those used by Bendtsen and Senft (1986) and Lacrosse (2010). While the use of such specimens would have allowed the mechanical properties of individual growth rings to be calculated, the quantity of specimens that this method would require would have significantly increased the preparation and testing time needed. The small nature of the specimens would also increase the potential of variations in results due to inaccuracies in specimen preparation.

While the three point bending methodology implemented allowed for relatively fast acquisition of data, it is noted that it does have its limitations. The first of these is due to the fact that the deflection at mid-span was inferred from the displacement of the loading head. During the course of testing, it was noted that in some cases localised embedment of the loading head occurred. While the embedment was minimal, with values lower than 1 mm, it

would have had a negative impact on the values of modulus of elasticity calculated due to overestimations of specimen deflection. It is also the case that the presence of shear forces at the mid-span results in the displacements observed not being solely related to pure bending, and as such the modulus of elasticity values calculated by the beam formula are underestimated. However, the specimen span to depth ratio was sufficiently large, such that displacements due to shear and the likelihood of shear failure were minimal.

9.4 Relevance and implications of results

9.4.1 Utilisation of South West grown Douglas-fir

The results presented within Chapter 6 demonstrated that based on the findings of mechanical testing of small clear specimens, the properties of Douglas-fir grown within the South West of England are comparable to those found in similar tests conducted on Douglas-fir grown at other locations internationally. In Chapter 1, the contribution of a lack of understanding of timber quality to the under utilisation of the timber resource within the South West of England was discussed, given this, the finding stated above is of particular significance in its own right. Based on the findings from all test specimens obtained from 40 - 50 year old trees presented in Section 6.7, timber properties equivalent to the criteria required for the C20 grade specified in BS EN 338 were attained, which is suitable for use in a wide range of structural applications. The age of timber was identified as being of far greater significance than rate of growth in determining mechanical properties. As a result of this, the mechanical properties of timber obtained from the mature wood of 40 - 50 year old sample trees exceeded those required for the C24 structural grade. While these results show that the potential for the production of good quality Douglas-fir for end uses in structural applications does exist within the region, further consideration needs to be given to structural sized sections containing defects, and which silvicultural management practices are best suited to the production of timber with the fewest defects that allows its full potential to be harnessed, whilst remaining economically viable.

9.4.2 Silvicultural practices

While the work conducted in this study was intended to investigate variations occurring within trees, many of the results found may, with confirmation from further research, aid in informing silvicultural practices to ensure that trees are grown in the most efficient and economically viable manner for the given end use.

While the rate of growth of trees did have an influence on most anatomical and mechanical properties, as identified in Sections 5.2 and 6.5, this was generally small when compared to the changes in the magnitude of properties that were observed with increasing cambial age. The magnitude of many of the assessed properties was found to stabilise within the mature wood, a result that was confirmed in the assessment of older sample trees. This highlights the improved yields of high quality timber that may be gained by increasing the age at which trees are felled. It was identified in Section 5.3 that within slower growing trees, the demarcation from juvenile to mature wood production occurred at a younger age. Combined with the superior mechanical properties identified in these trees, the promotion of slower growth appears to be a preferential practice in order to maximise the quality of the material produced. However, given the results shown in Section 5.3.5, in which it was demonstrated that the quantity of mature wood produced in the slower growing trees was limited compared to those which were faster growing, and also considering the modest increase in the grade criteria satisfied in the mature wood of slower and faster growing trees shown in Table 6-4, the continual production of slower growth over the whole life time does not appear to be a viable economic practice. However, the minimisation of the juvenile core volume within even aged stands, by promoting initial slow growth by practices such as a high stocking density, followed by the promotion of increased growth rates by practices such as thinning, following crown closure and recession, and therefore the commencement of mature wood production, appears to be a viable option. The promotion of faster growth following crown recession and lower branch mortality also offers the advantage of knot free mature wood in the valuable lower region of the stem. The development of continuous cover silvicultural practices within a stand, in which a range of ages are present and where younger trees experience slower growth initially due to their subsidiary position within the stand, with faster growth occurring in later years as the availability of light and nutrients increases as a result of a more dominant position within the canopy, and the removal of some older surrounding trees, will also provide similar results.

9.4.3 Visual timber grading

A significant result that was identified with the development of multiple regression models for the prediction of mechanical properties in Chapter 7, was that ring width alone accounted for relatively little of the variations observed in the mechanical properties, while the inclusion of further parameters, such as latewood proportion, allowed for a greater degree of the variability to be accounted for. This indicates, as discussed in Section 7.4.5, that the potential exists to improve the efficiency of the criteria for visually grading timber currently specified in

BS 4978:2007 (BSI, 2007). Further potential improvements that may be made to improve the efficiency with which visually graded Douglas-fir may be used were identified in Section 6.7. At present, BS EN 1912:2004 'Structural timber - Strength classes - Assignment of visual grades and species' (BSI, 2004) specifies that visually graded Douglas-fir grown in the United Kingdom graded as GS or SS is equivalent to C14 or C18 grades specified within BS EN 338 respectively. Douglas-fir grown within the USA or Canada graded as either GS or SS for use in the United Kingdom is equivalent to C16 and C24 grades respectively. Given that within Section 6.3, the mechanical properties of the small clear specimens obtained from mature wood were assessed as being comparable to results that were returned within other Douglas-fir studies conducted internationally, potential exists for a reassessment of the structural grades that may be achieved by visually graded Douglas-fir grown within the United Kingdom. This is supported by the findings shown in Section 6.7, in which the estimations of the mechanical properties of structural sized sections containing defects equivalent to those specified for either GS or SS visual grades, demonstrated that the mechanical properties estimated for the SS grade far exceeded those that were required.

9.5 Recommendations for continuing research

9.5.1 Outline

The results presented in this thesis have allowed for a new understanding of the quality of Douglas-fir grown within the South West of England, the factors influencing its variability and the interrelationships between the studied anatomical and mechanical properties to be gained. While providing valuable information that will enable better informed decisions to be made regarding the most efficient and economical management practices and end uses for material growing in the region, the analysis and interpretation of the results has also identified several areas where continuing research may allow for further knowledge to be gained into how to make the best use of the available material. These are discussed in the sub-sections below.

9.5.2 Regional timber quality variations

It was noted within the review of literature conducted in Section 2.8 that several factors may induce variability in the properties of wood produced between different growing sites, given this it recommended that two further studies are conducted. Firstly, a study of the influence of varying silvicultural practices such as initial stocking density, thinning, pruning, rotation length and at a broader scale the use of continuous cover forestry systems on the quality of the material produced, production yields gained and economic viability. Secondly, a study of the

extent to which factors such as climatic variations within the region and microclimatic effects at a particular site, site topography, soil conditions and the genetics of the seed material used influence the productivity and quality characteristics of the Douglas-fir that is produced.

In combining the information obtained from conducting this additional research with that which has been presented in this study, the development of models able to predict the properties of Douglas-fir grown within the region based on input parameters such as site location, age and mean ring width, and ultimately the production of wood quality maps, may be achievable. While important to South West forestry, Douglas-fir accounts for only 25 % of the coniferous growing stock found within the region. As such, the extension of this work to other softwoods, and the abundant hardwood resource found within the region, may potentially allow for significant improvements to be made in both the efficiency with which material is used, and the economic viability of the forest products industry within the region.

9.5.3 Improved efficiency of visual grading methods

Within Section 9.4.3, the potential improvements that may be made to the criteria currently prescribed in BS 4978:2007 for the establishment of visual timber grades, such that the characteristics which are assessed allow for the properties of the section to be more accurately accounted for were discussed. As such, it is recommended that further research is conducted utilising full sized structural sections containing a range of defects to determine the added benefit, if any, of improving the efficiency of visual grading methods by the inclusion of latewood proportion as a measured parameter. It was also discussed within Section 9.4.3 that the grades currently assigned to Douglas-fir classified as either GS or SS sections through visual grading may not allow for the full potential of the material to be harnessed. As such, a further recommendation is that additional research needs to be conducted utilising structural sized sections of Douglas-fir containing a range of defects to assess if changes can be made to BS EN 1912:2004. This may allow Douglas-fir grown within the United Kingdom achieving either GS or SS grades to have its specified characteristic modulus of elasticity and strength values increased, in order to bring the grade classification closer to that specified for imported Douglas-fir sections.

9.5.4 Use of mechanical properties for the determination of demarcation age from juvenile to mature wood production

Within Chapter 5 density and microfibril angle were used as parameters to establish the demarcation age from the production of juvenile to mature wood. Given that the concept of juvenile and mature wood was largely developed for practical rather than biological usage, it is likely that in the context of the results reported here, in which the suitability of the material for end uses in structural applications is a key consideration, that value will also be gained in establishing the demarcation age from the perspective of mechanical properties. It is therefore recommend that further research into the use of mechanical properties to determine juvenile to mature wood demarcation age is conducted, and the relationship with the results obtained utilising anatomical properties explored.

Chapter 10 - Conclusions

Within this thesis, research undertaken with an aim of improving understanding of the quality of the abundant Douglas-fir resource found within the South West of England, from the perspective of uses in structural applications, has been presented. The results and relationships reported offer new insights into both the variability of within tree timber quality and the factors influencing it, while also demonstrating the potential of Douglas-fir grown within the region.

Experimental work was conducted on 27 Douglas-fir trees obtained from across the South West of England. A sampling methodology was developed that allowed the influence of increasing cambial age, longitudinal position in the stem and rate of growth on anatomical and mechanical properties to be quantified. Anatomical properties including density, S_2 cell wall layer microfibril angle, tracheid dimensions and the proportions of early, transition and latewood were assessed with the use of the SilviScan-3 system. Flexural modulus of elasticity, flexural and compressive strength were assessed with the use of small clear test specimens.

All anatomical properties showed variations in their magnitude with increasing cambial age over at least part of the time periods for which they were assessed. For ring width, the proportions of early, transition and latewood within a growth ring, radial and tangential tracheid diameters, microfibril angle and its intra-ring components, these were largest in the growth rings immediately adjacent to the pith, with rates of change decreasing significantly in later years of growth. The whole ring mean radial wall thickness of tracheids and wood density continued to exhibit increasing values across the whole assessment period. Results showing variations in the proportions and properties of transition-wood within a growth ring, alongside detailed profiles of intra-ring microfibril angle, have not previously been widely reported for Douglas-fir.

Although typically small compared with differences in the values of anatomical properties observed with cambial age, an increase in the rate of growth of sample trees did produce statistically significant differences in properties when compared to those that were slower grown in a number of cases. Faster growth induced a lower latewood proportion, identified to be associated with increases in the proportions of transition-wood. An increased rate of growth also resulted in an increase in tracheid diameters, thinner cell walls, and due to a combination of these two factors, a decrease in wood density. The influence of growth rate on microfibril angle was inconclusive. Analysis also showed that for most properties studied, there was no statistically significant relationship with ring width at younger cambial ages.

A segmented regression model was used for the determination of demarcation ages from juvenile to mature wood production for both density and microfibril angle. A large range of results was observed across the sample trees for both properties, in part due to the difficulty in defining the exact transition point. It was also observed that microfibril angle developmental profiles exhibited mature behaviour earlier than those for density. Higher densities and lower microfibril angles characterised the mature wood of all trees. Trees that were faster grown exhibited demarcation ages that were greater than those observed in slower grown trees, differences were largely statistically significant and varied dependent upon the property and sampling height assessed. These differences were found to correspond well with tree live crown ratio, with faster growing trees having an increased mean stem live crown ratio.

Results obtained from testing defect free small clear specimens showed that large increases in flexural modulus of elasticity, flexural and compressive strength occurred with increasing cambial age in the early years of growth. The rates of change in mechanical properties reduced significantly beyond cambial ages of 10 to 15 years. An increased rate of growth was found to have a negative impact on the magnitude of mechanical properties; however the change in values were less substantial than those recorded with increasing cambial age.

In later growth rings, results showed that the mechanical properties of South West grown Douglas-fir compare favourably with documented results for material obtained from different locations globally. The potential implications of the mechanical properties results for utilisation in structural applications were assessed by means of a comparison with characteristic values for timber structural grades specified in BS EN 338:2003. Findings demonstrated that the characteristic values for various combinations of age and growth rate, obtained utilising specimens devoid of defects, satisfied the requirements for the widely used

C16 grade, with mature wood material satisfying the requirement of the C24 grade, indicting the potential for the production high quality sections. From these findings it can be concluded that with the implementation of silvicultural practices leading to a low incidence of defects such as knots and minimisation of variable quality juvenile wood, the potential exists for the production of high quality structural timber sections from South West grown Douglas-fir.

The collection and matching of pith to bark profiles of variations in anatomical and mechanical properties enabled a new level of understanding of the relationships between density, microfibril angle and mechanical properties to be gained. Through statistical path analysis, it was shown that juvenile wood microfibril angle was more strongly associated with increases in the magnitude of modulus of elasticity than density, while in mature wood this relationship was reversed. Flexural and compressive strength were found to be more strongly associated with changes in density than microfibril angle in both juvenile and mature wood, a confirmation of results reported elsewhere. Through the development of multiple regression models, it was shown that it is possible to predict mechanical properties to a good degree of accuracy utilising various combinations of micro and macroscopic properties as input parameters. A finding of particular significance through statistical modelling was that the inclusion of latewood proportion as a measure in the visual grading methods alongside ring width, prescribed in BS 4978:2007, may improve the accuracy of the method in the prediction of mechanical properties over the current practice of using ring width alone.

The development of a micromechanical composite model, built utilising previously published data on the cellular constituent properties of wood and those obtained through the SilviScan-3 system as input parameters, allowed accurate predictions for the trends recorded in the flexural modulus of elasticity of small clear specimens to be made. The model also aided in the interpretation of results obtained by statistical modelling.

The new understanding of the properties and their interrelationships of Douglas-fir grown within the South West of England that have been gained through this work presents opportunities for the improved utilisation of the material. The results have shed new light on visual grading practices and provided recommendations for further investigative work to improve their accuracy. The results have also indicated improvements in material quality that may be gained through the adoption of enhanced silvicultural management practices that minimise juvenile wood production, such as continuous cover forestry, and recommendations made for further research.

References

ABDEL-GADIR, A. Y. 1991. *Intra-ring variations in mature Douglas-fir trees from provenance plantations.* PhD thesis, Oregon State University.

ABDEL-GADIR, A. Y. & KRAHMER, R. 1993. Genetic variation in the age of demarcation between juvenile and mature wood in Douglas-fir. *Wood and Fiber Science,* 25**,** 384-394.

ABDEL-GADIR, A. Y., KRAHMER, R. & MCKIMMY, M. 1993. Relationships between intra-ring variables in mature Douglas-fir trees from provenance plantations. *Wood and Fiber Science,* 25**,** 182-191.

ABE, H. & FUNADA, R. 2005. Review-The orientation of cellulose microfibrils in the cell walls of tracheids in conifers. A model based on observations by field emission-scanning electron microscopy. *IAWA J,* 26**,** 161-174.

ABE, H., FUNADA, R., OHTANI, J. & FUKAZAWA, K. 1995. Changes in the arrangement of microtubules and microfibrils in differentiating conifer tracheids during the expansion of cells. *Annals of Botany,* 75**,** 305.

ABE, H., OHTANI, J. & FUKAZAWA, K. 1991. FE-SEM observations on the microfibrillar orientation in the secondary wall of tracheids. *IAWA Bull. ns,* 12**,** 431-438.

ÅKERHOLM, M. & SALMÉN, L. 2001. Interactions between wood polymers studied by dynamic FT-IR spectroscopy. *Polymer,* 42**,** 963-969.

ALTEYRAC, J., CLOUTIER, A., UNG, C. & ZHANG, S. 2006. Mechanical properties in relation to selected wood characteristics of black spruce. *Wood and Fiber Science,* 38**,** 229-237.

ANDERSSON, S., SERIMAA, R., TORKKELI, M., PAAKKARI, T., SARANPÄÄ, P. & PESONEN, E. 2000. Microfibril angle of Norway spruce [Picea abies (L.) Karst.] compression wood: comparison of measuring techniques. *Journal of Wood Science,* 46**,** 343-349.

ARMSTRONG, J., SKAAR, C. & DEZEEUW, C. 1984. The effect of specific gravity on several mechanical properties of some world woods. *Wood Science and Technology,* 18**,** 137-146.

ASTLEY, R., STOL, K. & HARRINGTON, J. 1998. Modelling the elastic properties of softwood. *European Journal of Wood and Wood Products,* 56**,** 43-50.

ASTM 2000. ASTM D245 Standard practice for establishing structural grades and related allowable properteis for visually graded lumber. West Consohocken: American Society for Testing and Materials.

ASTM 2007. ASTM D143-94 Standard test methods for small clear specimens of timber. West Consohocken: American Society for Testing and Materials.

AUTY, D. & ACHIM, A. 2008. The relationship between standing tree acoustic assessment and timber quality in Scots pine and the practical implications for assessing timber quality from naturally regenerated stands. *Forestry,* 81**,** 475.

BAILEY, I. & KERR, T. 1935. The visible structure of the secondary wall and its significance in physical and chemical investigations of tracheary cells and fibers. *Journal of the Arnold Arboretum,* 16**,** 273-300.

BAILEY, I. & VESTAL, M. R. 1937. The orientation of cellulose in the secondary wall of tracheary cells. *Journal of the Arnold Arboretum,* 18**,** 185-195.

BALTUNIS, B. S. B. B. S., WU, H. X. W. H. X. & POWELL, M. B. P. M. B. 2007. Inheritance of density, microfibril angle, and modulus of elasticity in juvenile wood of Pinus radiata at two locations in Australia. *Canadian Journal of Forest Research,* 37**,** 2164-2174.

BANK, L. C. 2006. *Composites for construction: structural design with FRP materials*, Wiley.

BAO, F., JIANG, Z., JIANG, X., LU, X., LUO, X. & ZHANG, S. 2001. Differences in wood properties between juvenile wood and mature wood in 10 species grown in China. *Wood Science and Technology,* 35**,** 363-375.

BARBER, N. & MEYLAN, B. 1964. The anisotropic shrinkage of wood. A theoretical model. *Holzforschung-International Journal of the Biology, Chemistry, Physics and Technology of Wood,* 18**,** 146-156.

BARBOUR, R., BERGQVIST, G., AMUNDSON, C., LARSSON, B. & JOHNSON, J. 1997. New methods for evaluating intra-ring X-ray densitometry data: maximum derivative methods as compared to Mork's index. *In:* AL., Z. E., ed. CTIA/IUFRO International Wood Quality Workshop Proceedings, Québec City. 1161-67.

BARBOUR, R. & KELLOGG, R. M. 1990. Forest management and end-product quality: a Canadian perspective. *Canadian Journal of Forest Research,* 20**,** 405-414.

BARNETT, J. 2004. Xylem physiology. *In:* BURLEY, J., EVANS, J. & YOUNGQUIST, J. A. (eds.) *Encyclopedia of Forest Sciences.* Oxford, San Diego: Elsevier Academic Press.

BARNETT, J. & BONHAM, V. 2004. Cellulose microfibril angle in the cell wall of wood fibres. *Biological reviews,* 79**,** 461-472.

BARNETT, J. & JERONIMIDIS, G. 2003. *Wood quality and its biological basis*, CRC Pr I Llc.

BARRETT, J. & KELLOGG, R. M. 1991. Bending strength and stiffness of second-growth Douglas-fir dimension lumber. *Forest products journal,* 41**,** 35-43.

BEERY, W. H., IFJU, G. & MCLAIN, T. E. 1983. Quantitative wood anatomy-relating anatomy to transverse tensile strength. *Wood Fiber Sci,* 15**,** 395-407.

BENDTSEN, B. & SENFT, J. 1986. Mechanical and anatomical properties in individual growth rings of plantation-grown Eastern cottonwood and Loblolly pine. *Wood and Fiber Science,* 18**,** 23-38.

BENHAM, C., HOLLAND, C. & ENJILY, V. 2003. Guide to machine strength grading of timber, BRE digest 476. London: Building Research Establishment.

BERGANDER, A. & SALMÉN, L. 2002. Cell wall properties and their effects on the mechanical properties of fibers. *Journal of Materials Science,* 37**,** 151-156.

BERGSTEN, U., LINDEBERG, J., RINDBY, A. & EVANS, R. 2001. Batch measurements of wood density on intact or prepared drill cores using x-ray microdensitometry. *Wood Science and Technology,* 35**,** 435-452.

BIBLIS, E. J. 1971. Flexural properties of southern yellow pine small beams loaded on true radial and tangential surfaces. *Wood science and technology,* 5**,** 95-100.

BOATRIGHT, S. & GARRETT, G. 1983. The effect of microstructure and stress state on the fracture behaviour of wood. *Journal of Materials Science,* 18**,** 2181-2199.

BODIG, J. & JAYNE, B. 1982. *Mechanics of wood and wood composites*, Van Nostrand Reinhold New York.

BOOKER, R. 1993. The importance of the S3 cell wall layer in collapse prevention and wood hardness. *In:* 24th Forest Products Research Conference, Victoria Australia. 1-13.

BOOKER, R. & SELL, J. 1998. The nanostructure of the cell wall of softwoods and its functions in a living tree. *European Journal of Wood and Wood Products,* 56**,** 1-8.

BOWYER, J., SHMULSKY, R. & HAYGREEN, J. 2002. *Forest products and wood science: an introduction*, Iowa State Pr.

BOWYER, J., SHMULSKY, R. & HAYGREEN, J. G. 2007. *Forest products and wood science: an introduction*, Wiley-Blackwell.

BRANDSTROM, J. 2001. Micro- and ultrastructural aspects of Norway spruce tracheids: a review. *IAWA Journal,* 22**,** 333-354.

BRAZIER, J., HANDS, R. & SEAL, D. 1985. Structural wood yields from Sitka spruce: the effect of planting spacing. *Forestry and British Timber,* 14**,** 34-35.

BRE 2003. Gudie to machine strength grading of timber.

BRE 2006. *Building sustainably with timber,* London, Building Research Establishment.

BRIGGS, D., INGARAMO, L. & TURNBLOM, E. 2007. Number and diameter of breast-height region branches in a Douglas-fir spacing trial and linkage to log quality. *Forest Products Journal,* 57**,** 28.

BRIGGS, D. & SMITH, W. 1986. Effects of silvicultural practices on wood properties of conifers: A review. *In:* HANLEY, D. P. & JOHNSON, J. J., eds. Douglas-fir: Stand management for the future, 1986 Institute of Forest Resources, University of Washington, Seattle. 108-117.

BRIX, H. & MITCHELL, A. 1980. Effects of thinning and nitrogen fertilization on xylem development in Douglas-fir. *Canadian Journal of Forest Research,* 10**,** 121-128.

BSI 1957. BS 373:1957 Method of testing small clear specimens of timber. London: British Standards Institution.

BSI 1971. CP 112:1971 The structural use of timber. London: British Standards Institution.

BSI 1973. BS 4978:1973 Specification for timber grades for structural use. London: British Standards Institution.

BSI 2003. BS EN 338:2003 Structural timber. Strength classes. London: British Standards Institution.

BSI 2004. BS EN 1912:2004 Structural timber - Strength classes - Assignment of visual grades and species. London: British Standards Institution.

BSI 2007. BS4978:2007 Visual strength grading of softwood. Specification. London: British Standards Institution.

BSI 2010a. BS EN 384:2010 Structural timber - Determination of characteristic values of mechanical properties and density. London: British Standards Institution.

BSI 2010b. BS EN 408:2010 Timber structures - Structural timber and glued laminated timber - Determination of some physical and mechanical properties London: British Standards Institution.

BURDON, R., BRITTON, R. & WALFORD, G. 2001. Wood stiffness and bending strength in relation to density in four native provenances of *Pinus radiata*. *New Zealand Journal of Forestry Science,* 31**,** 130-146.

BURDON, R., KIBBLEWHITE, R. P., WALKER, J. C. F., MEGRAW, R. A., EVANS, R. & COWN, D. J. 2004. Juvenile versus mature wood: a new concept, orthogonal to corewood versus outerwood, with special reference to *Pinus radiata* and *P. taeda*. *Forest Science,* 50**,** 399-415.

CAMERON, A., LEE, S., LIVINGSTON, A. & PETTY, J. 2005. Influence of selective breeding on the development of juvenile wood in Sitka spruce. *Canadian Journal of Forest Research,* 35**,** 2951-2960.

CAVE, I. 1966. X-ray measurement of microfibril angle. *Forest Products Journal,* 16**,** 37-42.

CAVE, I. 1968. The anisotropic elasticity of the plant cell wall. *Wood Science and Technology,* 2**,** 268-278.

CAVE, I. 1976. Modelling the structure of the softwood cell wall for computation of mechanical properties. *Wood Science and Technology,* 10**,** 19-28.

CAVE, I. 1978. Modelling moisture-related mechanical properties of wood Part I: Properties of the wood constituents. *Wood Science and Technology,* 12**,** 75-86.

CAVE, I. & WALKER, J. C. F. 1994. Stiffness of wood in fast-grown plantation softwoods: the influence of microfibril angle. *Forest Products Journal,* 44**,** 43-48.

CHALK, L. 1953. Variation of density in stems of Douglas-fir. *Forestry,* 26**,** 33.

CHERRY, M. L. C. M. L., VIKRAM, V. V. V., BRIGGS, D. B. D., CRESS, D. W. C. D. W. & HOWE, G. T. H. G. T. 2008. Genetic variation in direct and indirect measures of wood stiffness in coastal Douglas-fir. *Canadian Journal of Forest Research,* 38**,** 2476-2486.

CLARK, A., DANIELS, R. & JORDAN, L. 2006. Juvenile/mature wood transition in Loblolly pine as defined by annual ring specific gravity, proportion of latewood, and microfibril angle. *Wood and Fiber Science,* 38**,** 292-299.

COCKRELL, R. A. 1974. A comparison of latewood pits, fibril orientation, and shrinkage of normal and compression wood of giant sequoia. *Wood Science and Technology,* 8**,** 197-206.

COED CYMRU 2007. Woodland owners handbook. Coed Cymru.

CORONA, P., SCOTTI, R. & TARCHIANI, N. 1998. Relationship between environmental factors and site index in Douglas-fir plantations in central Italy. *Forest Ecology and Management,* 110**,** 195-207.

COUSINS, W. 1976. Elastic modulus of lignin as related to moisture content. *Wood Science and Technology,* 10**,** 9-17.

COUSINS, W. 1978. Young's modulus of hemicellulose as related to moisture content. *Wood Science and Technology,* 12**,** 161-167.

COWN, D. 1992. *New Zealand Radiata pine and Douglas-fir: suitability for processing,* Rotorua, Forest Research.

COWN, D. & CLEMENT, B. 1983. A wood densitometer using direct scanning with x-rays. *Wood Science and Technology,* 17**,** 91-99.

COWN, D., HEBERT, J. & BALL, R. 1999. Modelling *Pinus radiata* lumber characteristics. Part 1: Mechanical properties of small clears. *New Zealand Journal of Forestry Science,* 29**,** 203-213.

DECOUX, V., VARCIN, É. & LEBAN, J. M. 2004. Relationships between the intra-ring wood density assessed by x-ray densitometry and optical anatomical measurements in conifers. Consequences for the cell wall apparent density determination. *Annals of Forest Science,* 61**,** 251-262.

DENNE, M. 1973. Tracheid dimensions in relation to shoot vigour in Picea. *Forestry,* 46**,** 117.

DERESSE, T., SHEPARD, R. & SHALER, S. 2003. Microfibril angle variation in red pine (*Pines resinosa Ait.*) and its relation to the strength and stiffness of early juvenile wood. *Forest Products Journal,* 53**,** 34-40.

DESCH, H. & DINWOODIE, J. 1981. *Timber, its structure, properties, and utilisation,* London, The Macmillan Press Ltd.

DHUBHAIN, A., EVERTSEN, J. & GARDINER, J. 1988. The influence of compression wood on the strength properties of Sitka spruce. *Forest Products Journal,* 38**,** 67-69.

DI LUCCA, C. M. 1987. *Juvenile-mature wood transition in second-growth coastal Douglas-fir.* PhD thesis, The University of British Columbia.

DI LUCCA, C. M. 1989. Juvenile-mature wood transition. *In:* KELLOGG, R. M. (ed.) *Second growth Douglas-fir: its management and conversion for value: a report of the Douglas-fir task force.* Vancouver: Forintek Canada Corp.

DINWOODIE, J. M. 1961. Tracheid and fibre length in timber: a review of literature. *Forestry,* 34**,** 125-44.

DINWOODIE, J. M. 1981. *Timber, its nature and behaviour*, Van Nostrand Reinhold Company.

DINWOODIE, J. M. 2000. *Timber, its nature and behaviour*, Taylor & Francis.

DIXON, J. R. 1971. An attempt at site assessment for Douglas-fir in Perthshire. *Scot. For,* 25**,** 26-33.

DODD, R. S. & FOX, P. 1990. Kinetics of tracheid differentiation in Douglas-fir. *Annals of Botany,* 65**,** 649.

DOMEC, J. C. & GARTNER, B. L. 2002. How do water transport and water storage differ in coniferous earlywood and latewood? *Journal of Experimental Botany,* 53**,** 2369.

DONALDSON, L. 1991. The use of pit apertures as windows to measure microfibril angle in chemical pulp fibers. *Wood and Fiber Science,* 23**,** 290-295.

DONALDSON, L. 1992. Within- and between-tree variation in microfibril angle in Pinus radiata. *New Zealand Journal of Forestry Science,* 22**,** 77-86.

DONALDSON, L. 1996. Effect of physiological age and site on microfibril angle in *Pinus radiata*. *Iawa Journal,* 17**,** 421-429.

DONALDSON, L. 2008. Microfibril angle: measurement, variation and relationships: a review. *IAWA Journal,* 29**,** 345-386.

DONALDSON, L. & FRANKLAND, A. 2004. Ultrastructure of iodine treated wood. *Holzforschung,* 58**,** 219-225.

DONALDSON, L., GRACE, J. & DOWNES, G. 2004. Within-tree variation in anatomical properties of compression wood in Radiata pine. *IAWA Journal,* 25**,** 253-272.

DONALDSON, L. & XU, P. 2005. Microfibril orientation across the secondary cell wall of Radiata pine tracheids. *Trees-Structure and Function,* 19**,** 644-653.

DOWNES, G. M., NYAKUENGAMA, J. G., EVANS, R., NORTHWAY, R., BLAKEMORE, P., DICKSON, R. L. & LAUSBERG, M. 2002. Relationship between wood density, microfibril angle and stiffness in thinned and fertilized Pinus radiata. *IAWA Journal,* 23**,** 253-266.

DROW, J. T. 1957. Relationship of locality and rate of growth to density and strength of Douglas-fir. University of Wisconsin: US Forest Service, Forest Products Laboratory Report 2078.

DUNBAR, A., DHUBHAIN, A. N. & BULFIN, M. 2002. The productivity of Douglas-fir in Ireland. *Forestry,* 75**,** 537.

EKOGEN 2009. South West England Woodland & Forestry Strategic Economic Study.

ELIAS, T. S. 1980. *The complete trees of North America. Field guide and natural history*, Van Nostrand Reinhold, New York, New York, USA.

ERICKSON, H. & ARIMA, T. 1974. Douglas-fir wood quality studies part II: Effects of age and stimulated growth on fibril angle and chemical constituents. *Wood Science and Technology,* 8**,** 255-265.

ERICKSON, H. & HARRISON, A. T. 1974. Douglas-fir wood quality studies part I: Effects of age and stimulated growth on wood density and anatomy. *Wood Science and Technology,* 8**,** 207-226.

ERIKSSON, D., LINDBERG, H. & BERGSTEN, U. 2006. Influence of silvicultural regime on wood structure characteristics and mechanical properties of clear wood in *Pinus sylvestris*. *Silva Fennica,* 40**,** 743-762.

EVANS, R. 1994. Rapid measurement of the transverse dimensions of tracheids in radial wood sections from *Pinus radiata*. *Holzforschung,* 48**,** 168-172.

EVANS, R. 1999. A variance approach to the x-ray diffractometric estimation of microfibril angle in wood. *Appita Journal,* 52**,** 283-289.

EVANS, R. 2006. Wood Stiffness by X Ray Diffractometry. *In:* STOKKE, D. D. & GROOM, L. H. (eds.) *Characterisation of the Cellulosic Cell Wall.* Blackwell Publishing.

EVANS, R. & ILIC, J. 2001. Rapid prediction of wood stiffness from microfibril angle and density. *Forest Products Journal,* 51**,** 53-57.

EVANS, R., ILIC, J. & MATHESON, C. 2000. Rapid estimation of solid wood stiffness using SilviScan. *In:* SCHIMLECK, L. & BLAKEMORE, P., eds. Proceedings of the 26th forest products research conference, Clayton. CSIRO Forestry and Forest Products, 49-50.

FABRIS, S. 2000. *Influence of cambial ageing, initial spacing, stem taper and growth rate on wood quality of three coastal conifers*. PhD thesis, The University of British Columbia.

FENGEL, D. & STOLL, M. 1973. On the variation of the cell cross area, the thickness of the cell wall and of the wall layers of sprucewood tracheids within an annual ring. *Holzforschung,* 27**,** 1-7.

FLETCHER, A. M. & SAMUEL, C. J. A. 2010. Choice of Douglas-fir Seed Origins for Use in British Forests. Bulletin 129. Edinburgh: Forestry Commission.

FONTES, L. 2002. *The performance, constraints and potential of Douglas-fir [Pseudotsuga menziesii (Mirb.) Franco] in Portugal.* PhD thesis, University of Oxford.

FOREST RESEARCH 2009. Assessing the Current Growing Conifer Resource in the South West of England.

FORESTRY COMMISSION 2002. National Inventory of Woodland and Trees - South West Regional Report. Edinburgh: Forestry Commission.

FORESTRY COMMISSION 2007. Forestry Statistics 2007. Edinburgh.

FORESTRY COMMISSION 2010. Forestry Facts and Figures 2010. Edinburgh: Forestry Commission.

FPL 1999. *Wood handbook: wood as an engineering material,* Madison, USDA Forest Service, Forest Products Laboratroy.

GARDINER, B., LEBAN, J. M., AUTY, D. & SIMPSON, H. 2011. Models for predicting wood density of British-grown Sitka spruce. *Forestry,* 84**,** 119.

GARTNER, B., NORTH, E., JOHNSON, G. & SINGLETON, R. 2002. Effects of live crown on vertical patterns of wood density and growth in Douglas-fir. *Canadian Journal of Forest Research,* 32**,** 439-447.

GARTNER, B., ROBBINS, J. M. & NEWTON, M. 2005. Effects of pruning on wood density and tracheid length in young Douglas-fir. *Wood and Fiber Science,* 37**,** 304-313.

GIBSON, L. J. & ASHBY, M. F. 1997. *Cellular solids structure and properties*, Cambridge Univerity Press.

GINDL, W. & TEISCHINGER, A. 2002. Axial compression strength of Norway spruce related to structural variability and lignin content. *Composites Part A: Applied Science and Manufacturing,* 33**,** 1623-1628.

GROSSMAN, P. & WOLD, M. 1971. Compression fracture of wood parallel to the grain. *Wood Science and Technology,* 5**,** 147-156.

GROTTA, A. T., LEICHTI, R. J., GARTNER, B. L. & JOHNSON, G. R. 2005. Effect of growth ring orientation and placement of earlywood and latewood on MOE and MOR of very small clear Douglas-fir beams. *Wood and Fiber Science,* 37**,** 207-212.

GUITARD, D. & GACHET, C. 2004. Paramètres structuraux et/ou ultrastructuraux facteurs de la variabilité intra-arbre de l'anisotropie élastique du bois. *annals of Forest Science,* 61**,** 129-139.

HARADA, H. & CÔTÉ JR, W. 1985. Structure of wood. *In:* HIGUCHI, T. (ed.) *Biosynthesis and Biodegradation of Wood Components.* New York: Academic Press.

HARADA, H., MIYAZAKI, Y. & WAKASHIMA, T. 1958. Electron microscopic investigation on the cell wall structure of wood. *Bulletin of the Government Forestry Experiment Station,* 104**,** 1-115.

HARRINGTON, J., ASTLEY, R. & BOOKER, R. 1998. Modelling the elastic properties of softwood. *European Journal of Wood and Wood Products,* 56**,** 37-41.

HEIN, S., WEISKITTEL, A. R. & KOHNLE, U. 2008. Effect of wide spacing on tree growth, branch and sapwood properties of young Douglas-fir [*Pseudotsuga menziesii (Mirb.) Franco*] in South Western Germany. *European Journal of Forest Research,* 127**,** 481-493.

HERMAN, M., DUTILLEUL, P. & AVELLA SHAW, T. 1999. Growth rate effects on intra-ring and inter-ring trajectories of microfibril angle in Norway spruce (*Picea abies*). *IAWA Journal,* 20**,** 3-21.

HERMANN, R. 1982. The genus Pseudotsuga: historical records and nomenclature. Corvallis: Forest Research Laboratory, School of Forestry, Oregon State University.

HERMANN, R. & LAVENDER, D. P. 1999. Douglas-fir planted forests. *New Forests,* 17**,** 53-70.

HILLIS, W. 1987. *Heartwood and tree exudates*, Springer-Verlag Berlin, Heidelberg, New York, London, Paris, Tokyo.

HUANG, C. 1995. Revealing fibril angle in wood sections by ultrasonic treatment. *Wood and Fiber Science,* 27**,** 49-54.

HUANG, C., KUTSCHA, N., LEAF, G. & MEGRAW, R. 1998. Comparison of microfibril angle measurement techniques. *In:* BUTTERFIELD, B., ed. Microfibril angle in wood, University of Canterbury. 177-205.

HUANG, C., LINDSTRÖM, H., NAKADA, R. & RALSTON, J. 2003. Cell wall structure and wood properties determined by acoustics - a selective review. *European Journal of Wood and Wood Products,* 61**,** 321-335.

IFJU, G. & KENNEDY, R. 1962. Some variables affecting microtensile strength of Douglas-fir. *Forest Products Journal,* 12**,** 213-217.

IVKOVI, M., GAPARE, W. J., ABARQUEZ, A., ILIC, J., POWELL, M. B. & WU, H. X. 2009. Prediction of wood stiffness, strength, and shrinkage in juvenile wood of Radiata pine. *Wood Science and Technology,* 43**,** 237-257.

JACOBSEN, A. L., EWERS, F. W., PRATT, R. B., PADDOCK, W. A. & DAVIS, S. D. 2005. Do xylem fibers affect vessel cavitation resistance? *Plant physiology,* 139**,** 546.

JAMES, N. D. G. 1990. *A history of English forestry,* Oxford, Basil Blackwell.

JOHANSSON, K. 1993. Influence of initial spacing and tree class on the basic density of *Picea abies*. *Scandinavian Journal of Forest Research,* 8**,** 18-27.

JOHNSON, G. & GARTNER, B. L. 2006. Genetic variation in basic density and modulus of elasticity of coastal Douglas-fir. *Tree Genetics & Genomes,* 3**,** 25-33.

JORDAN, L., DANIELS, R. F., CLARK III, A. & HE, R. 2005. Multilevel nonlinear mixed-effects models for the modeling of earlywood and latewood microfibril angle. *Forest Science,* 51**,** 357-371.

JOZSA, L. 1995. An overview of forest pruning and wood quality in British Columbia. *In:* HANLEY, D., OLIVER, C., MAGUIRE, D., BRIGGS, D. & FIGHT, R. (eds.) *Forest pruning and wood quality.* Seattle: College of Forest Resources, University of Washington.

JOZSA, L. & BRIX, H. 1989. The effects of fertilization and thinning on wood quality of a 24-year-old Douglas-fir stand. *Canadian Journal of Forest Research,* 19**,** 1137-1145.

JOZSA, L. & MIDDLETON, G. R. 1994. A discussion of wood quality attributes and their practical implications, Special Publication SP-34. Vancouver: Forintek Canada Corp.

JOZSA, L. & OLIVEIRA, L. 1992. The structure of wood in relation to drying. Vancouver: Forintek Canada Corp.

JUTE, S. & LEVY, J. 1973. Helical thickenings in the tracheids of *Taxus* and *Pseudotsuga* as revealed by the scanning reflection electron microscope. *Acta Botanica Neerlandica,* 22**,** 100-105.

JYSKE, T. 2008. *The effects of thinning and fertilisaton on wood and tracheid properties of Norway spruce (Picea abies) - the results of long-term experiments.* Dissertationes Forestales 55.

JYSKE, T., MÄKINEN, H. & SARANPÄÄ, P. 2008. Wood density within Norway spruce stems. *Silva Fennica,* 42**,** 439-455.

KENNEDY, R. 1995. Coniferous wood quality in the future: concerns and strategies. *Wood Science and Technology,* 29**,** 321-338.

KING, J., YEH, F., HEAMAN, J. & DANCIK, B. 1988. Selection of wood density and diameter in controlled crosses of coastal Douglas-fir. *Silvae Genet,* 37**,** 152-157.

KLIGER, I., PERSTORPER, M. & JOHANSSON, G. 1998. Bending properties of Norway spruce timber. Comparasion between fast-and slow-grown stands and influence of radial position of sawn timber. *Annals of Forest Science,* 55**,** 349-358.

KLIGER, I., PERSTORPER, M., JOHANSSON, G. & PELLICANE, P. 1995. Quality of timber products from Norway spruce. *Wood Science and Technology,* 29**,** 397-410.

KOGA, S. & ZHANG, S. Y. 2004. Inter-tree and intra-tree variations in ring width and wood density components in Balsam-fir (*Abies balsamea*). *Wood Science and Technology,* 38**,** 149-162.

KOUBAA, A., ISABEL, N., ZHANG, S. Y., BEAULIEU, J. & BOUSQUET, J. 2005. Transition from juvenile to mature wood in Black spruce (*Picea mariana (Mill.) BSP*). *Wood and Fiber Science,* 37**,** 445-455.

KOUBAA, A., TONY ZHANG, S. & MAKNI, S. 2002. Defining the transition from earlywood to latewood in Black spruce based on intra-ring wood density profiles from x-ray densitometry. *Annals of Forest Science,* 59**,** 511-518.

KWON, M., BEDGAR, D., PIASTUCH, W., DAVIN, L. & LEWIS, N. 2001. Induced compression wood formation in Douglas-fir (*Pseudotsuga menziesii*) in microgravity. *Phytochemistry,* 57**,** 847-857.

LACHENBRUCH, B., JOHNSON, G., DOWNES, G. & EVANS, R. 2010. Relationships of density, microfibril angle, and sound velocity with stiffness and strength in mature wood of Douglas-fir. *Canadian Journal of Forest Research,* 40**,** 55-64.

LACROSSE, V. 2010. *Microfibril angle and the mechanical properties of Douglas-fir wood.* University of Bath.

LARSON, P. 1960. A physiological consideration of the springwood summerwood transition in Red pine Pinus resinosa. *Forest Science,* 6**,** 110-122.

LARSON, P. 1962. Auxin gradients and the regulation of cambial activity. *In:* KOZLOWSKI, T. T. (ed.) *Tree growth.* New York: Ronald Press.

LARSON, P. 1964. Some indirect effects of environment on wood formation. *In:* ZIMMERMANN, M. H. (ed.) *The formation of wood in forest trees.* New York: Academic Press.

LARSON, P. 1969. Wood formation and the concept of wood quality. *Yale University School Forestry, Bulletin 74***,** 1-54.

LARSON, P. 1973. The physiological basis for wood specific gravity in conifers. *IUFRO Division,* 5**,** 672-680.

LARSON, P. 1994. *The vascular cambium: development and structure,* Berlin, Springer-verlag.

LARSON, S. P. 2001. Formation and properties of juvenile wood in Southern pines: a synopsis. *General Technical Report FPL-GTR-129.* Madison: USDA, Forest Service, Forest Products laboratory.

LAVERS, G. M. 1983. *The strength properties of timber. Building Research Establishment*, HMSO: London.

LEBOURGEOIS, F. 2000. Climatic signals in earlywood, latewood and total ring width of Corsican pine from Western France. *Annals of Forest Science,* 57**,** 155-164.

LENEY, L. 1981. A technique for measuring fibril angle using polarized light. *Wood and Fiber Science,* 13**,** 13-16.

LICHTENEGGER, H., REITERER, A., STANZL-TSCHEGG, S. & FRATZL, P. 1999. Variation of cellulose microfibril angles in softwoods and hardwoods - A possible strategy of mechanical optimization. *Journal of Structural Biology,* 128**,** 257-269.

LICHTENEGGER, H., REITERER, A., TSCHEGG, S. & FRATZL, P. 1998. Determination of spiral angles of elementary fibrils in the wood cell wall: comparison of small-angle X-ray scattering and wide-angle X-ray diffraction. *In:* BUTTERFIELD, B., ed. Microfibril Angle in Wood: Proceedings of the IAWA/IUFRO International Workshop on the Significance of Microfibril Angle to Wood Quality, Wesport, New Zealand. University of Canterbury Press, 140-156.

LIVINGSTON, A., CAMERON, A., PETTY, J. & LEE, S. 2004. Effect of growth rate on wood properties of genetically improved Sitka spruce. *Forestry,* 77**,** 325.

LONG, J. M., CONN, A. B., BATCHELOR, W. J. & EVANS, R. 2000. Comparison of methods to measure fibril angle in wood fibres. *Appita Journal,* 53**,** 206-209.

LOO-DINKINS, J., YING, C. & HAMM, E. 1991. Stem volume and wood relative density of a non-local Douglas-fir provenance in British Columbia. *Silvae Genet,* 40**,** 29-35.

LOTFY, M., EL-OSTA, M., KELLOGG, R., FOSCHI, R. & BUTTERS, R. 1973. A direct x-ray technique for measuring microfibril angle. *Wood and Fiber Science,* 5**,** 118-128.

LUNDGREN, C. 2004. Cell wall thickness and tangential and radial cell diameter of fertilized and irrigated Norway spruce. *Silva Fennica,* 38**,** 95-106.

MACDONALD, E., GARDINER, B. & MASON, W. 2010. The effects of transformation of even-aged stands to continuous cover forestry on conifer log quality and wood properties in the UK. *Forestry,* 83**,** 22.

MACDONALD, E. & HUBERT, J. 2002. A review of the effects of silviculture on timber quality of Sitka spruce. *Forestry,* 75**,** 107.

MACHADO, J. S. & CRUZ, H. P. 2005. Within stem variation of Maritime pine timber mechanical properties. *European Journal of Wood and Wood Products,* 63**,** 154-159.

MAGEL, E., JAY-ALLEMAND, C. & ZIEGLER, H. 1994. Formation of heartwood substances in the stemwood of Robinia pseudoacacia L. II. Distribution of nonstructural carbohydrates and wood extractives across the trunk. *Trees-Structure and Function,* 8**,** 165-171.

MAGUIRE, D. A., KERSHAW, J. A. & HANN, D. W. 1991. Predicting the effects of silvicultural regime on branch size and crown wood core in Douglas-fir. *Forest Science,* 37**,** 1409-1428.

MÄKINEN, H., SARANPÄÄ, P. & LINDER, S. 2002. Effect of growth rate on fibre characteristics in Norway spruce (*Picea abies (L.) Karst.*). *Holzforschung,* 56**,** 449-460.

MANSFIELD, S. D., PARISH, R., DI LUCCA, C. M., GOUDIE, J., KANG, K. Y. & OTT, P. 2009. Revisiting the transition between juvenile and mature wood: a comparison of fibre length, microfibril angle and relative wood density in Lodgepole pine. *Holzforschung,* 63**,** 449-456.

MARK, H. 1980. Fifty years of cellulose research. *Cellul. Chem. Technol,* 14**,** 569-581.

MARK, R. 1967. *Cell wall mechanics of tracheids*, Yale University Press New Haven.

MATSUO, M., SAWATARI, C., IWAI, Y. & OZAKI, F. 1990. Effect of orientation distribution and crystallinity on the measurement by X-ray diffraction of the crystal lattice moduli of cellulose I and II. *Macromolecules,* 23**,** 3266-3275.

MCLEAN, J. 2008. *Wood properties of four genotypes of Sitka spruce.* Phd Thesis, University of Glasgow.

MEGRAW, R. Year. Douglas-fir wood properties. *In:* OLIVER, C. D., HINLEY, D. P. & JOHNSON, J. A., eds. Symposium on Douglas-fir Stand Management for the Future, 1986 University of Washington. 81-95.

MEYLAN, B. 1967. Measurement of microfibril angle by X-ray diffraction. *Forest Poducts Journal,* 17**,** 51-58.

MEYLAN, B. & BUTTERFIELD, B. 1972. *Three-dimensional structure of wood. A scanning electron microscope study,* London, Chapman & Hall Ltd.

MITCHELL, A. F. 1972. *Conifers in the British Isles. A descriptive handbook,* London, H.M.S.O.

MITCHELL, H. L. 1961. A concept of intrinsic wood quality, and nondestructive methods for determining quality in standing timber. Report No 2233. Madison: Forest Products Laboratory.

MOLTEBERG, D. & HØIBØ, O. 2006. Development and variation of wood density, kraft pulp yield and fibre dimensions in young Norway spruce (*Picea abies*). *Wood Science and Technology,* 40**,** 173-189.

MOORE, N. 2006. Improved timber utilisation statistics. Timbertrends.

MORK, E. 1928. Die Qualität des Fichtenholzes unter besonderer Rücksichtnahme auf Schleif-und Papierholz. *Der Papier-Fabrikant,* 26**,** 741-747.

NISHINO, T., TAKANO, K. & NAKAMAE, K. 1995. Elastic modulus of the crystalline regions of cellulose polymorphs. *Journal of Polymer Science Part B: Polymer Physics,* 33**,** 1647-1651.

O'HARA, K. L. 1991. A biological justification for pruning in coastal Douglas-fir stands. *Western Journal of Applied Forestry,* 6**,** 59-63.

OLESEN, P. 1978. On cyclophysis and topophysis. *Silvae Genetica,* 27**,** 173-178.

OLESEN, P. 1982. The effect of cyclophysis on tracheid width and basic density in Norway spruce. *Forest Tree Improvement: Kobenhavn***,** 80.

OLESEN, P. & ROULUND, H. 1971. The water displacement method: a fast and accurate method of determining the green volume of wood samples. *Forest Tree Improvement,* 3**,** 3-23.

OLIVER, C., LARSON, B. & BALL, J. 1997. Forest Stand Dynamics. Update Edition. *Journal of Natural Resources and Life Sciences Education,* 26**,** 81.

OLLINMAA, P. 1961. Reaktiopuututkimuksia. [Study on reaction wood.]. *Acta Forestalia Fennica,* 72**,** 1-54.

OLSSON, L. 2010. *Information regarding accuracy of SilviScan-3 system* [e-mail]

OPRIMAN, G. & TARANU, N. 2004. Strengthening of the timber members using fibre reinforced polymer composites. *The Bulletin of the Polytechnic Institute of Jassy, Construction. Architecture Section***,** 67-76.

PAGE, D. 1969. A method for determining the fibrillar angle in wood tracheids. *Journal of Microscopy,* 90**,** 137-143.

PANSHIN, A. J. & ZEEUW, C. 1980. *Textbook of wood technology,* New York, McGraw-Hill Book Co.

PARK, Y., BRAIS, S. & MAZEROLLE, M. 2009. Effects of cambial age and stem height on wood density and growth of Jack pine grown in boreal stands. *Wood and Fiber Science,* 41**,** 346-358.

PARKER, M. 1976. Improving tree-ring dating in Northern Canada by X-ray densitometry. *Syesis,* 9**,** 163-172.

PARKER, M., BRUCE, R. & JOZSA, L. 1980. X-ray densitometry of wood at the WFPL Technical Report No. 10. . Vancouver: Forintek Canada Corp.

PÉREZ, J., MUNOZ-DORADO, J., DE LA RUBIA, T. & MARTINEZ, J. 2002. Biodegradation and biological treatments of cellulose, hemicellulose and lignin: an overview. *International Microbiology,* 5**,** 53-63.

PERSSON, K. 2000. *Micromechanical modelling of wood and fibre properties.* PhD thesis, Lund Institute of Technology.

PHILLIPS, E. 1960. The beta-ray method of determining the density of wood and the proportion of summer wood. *Journal of the Institute of Wood Science,* 5**,** 16-28.

PIRIE, I. 2009. Home grown timber and the supply chain. *Carbon benefits of timber in construction.* Edinburgh Napier University.

PLOMION, C., LEPROVOST, G. & STOKES, A. 2001. Wood formation in trees. *Plant physiology,* 127**,** 1513.

POLGE, H. 1963. Une nouvelle méthodede détermination de la texture du bois-L'analyse densitométrique de clichés radiographiques. *Annals of Forest Science,* 20**,** 533-580.

POLGE, H. 1978. Fifteen years of wood radiation densitometry. *Wood Science and Technology,* 12**,** 187-196.

POPE, D., MARCROFT, J. & WHALE, L. 2005. The effect of global slope of grain on the bending strength of scaffold boards. *European Journal of Wood and Wood Products,* 63**,** 321-326.

PRESTON, R. 1934. The organization of the cell wall of the conifer tracheid. *Philosophical Transactions of the Royal Society of London. Series B, Biological Sciences,* 224**,** 131-174.

PRICE, A. 1929. A mathematical discussion on the structure of wood in relation to its elastic properties. *Philosophical Transactions of the Royal Society of London. Series A, Containing Papers of a Mathematical or Physical Character,* 228**,** 1-62.

QING, H. & MISHNAEVSKY JR, L. 2009. 3D hierarchical computational model of wood as a cellular material with fibril reinforced, heterogeneous multiple layers. *Mechanics of Materials,* 41**,** 1034-1049.

QUIRK, J. T. 1984. Shrinkage and related properties of Douglas-fir cell walls. *Wood and Fiber Science,* 16**,** 115-133.

RATHGEBER, C. B. K., DECOUX, V. & LEBAN, J. M. 2006. Linking intra-tree-ring wood density variations and tracheid anatomical characteristics in Douglas fir (*Pseudotsuga menziesii* (*Mirb.*) *Franco*). *Annals of Forest Science,* 63**,** 699-706.

RENNINGER, H. J., GARTNER, B. L. & GROTTA, A. T. 2006. Effects of release from suppression on wood functional characteristics in young Douglas-fir and western hemlock. *Canadian Journal of Forest Research,* 36**,** 2038-2046.

RIDLEY-ELLIS, D., MOORE, J., LYON, A., SEARLES, G. & GARDINER, B. A. 2009. Strategic Integrated Research in Timber: Getting the most out of the UK's timber resource. *In:* WALKER, P., GHAVAMI, K., PAINE, K., HEATH, A., LAWRENCE, M. & FODDE, E., eds. 11th International Conference on Non-conventional Materials and Technologies, University of Bath.

ROMBERGER, J., HEJNOWICZ, Z. & HILL, J. 1993. *Plant structure: Function and development,* Berlin, Springer-Verlag.

ROWELL, R. M. 2005. *Handbook of wood chemistry and wood composites,* University of Wisconsin, Madison, CRC Press.

ROZENBERG, P., FRANC, A., MAMDY, C., LAUNAY, J., SCHERMANN, N. & BASTIEN, J. C. 1999. Genetic control of stiffness of standing Douglas-fir; from the standing stem to the standardised wood sample, relationships between modulus of elasticity and wood density parameters. Part II. *Annals of Forest Science,* 56**,** 145-154.

SAKURADA, I., NUKUSHINA, Y. & ITO, T. 1962. Experimental determination of the elastic modulus of crystalline regions in oriented polymers. *Journal of Polymer Science,* 57**,** 651-660.

SALMÉN, L. 2004. Micromechanical understanding of the cell-wall structure. *Comptes Rendus Biologies,* 327**,** 873-880.

SALMÉN, L. & DE RUVO, A. 1985. A model for the prediction of fiber elasticity. *Wood and Fiber Science,* 17**,** 336-350.

SAMUELS, A., KANEDA, M. & RENSING, K. 2006. The cell biology of wood formation: from cambial divisions to mature secondary xylem. *Botany,* 84**,** 631-639.

SAREN, M. P., SERIMAA, R., ANDERSSON, S., SARANPÄÄ, P., KECKES, J. & FRATZL, P. 2004. Effect of growth rate on mean microfibril angle and cross-sectional shape of tracheids of Norway spruce. *Trees-Structure and Function,* 18**,** 354-362.

SARKANEN, K. V. & LUDWIG, C. H. 1971. *Lignins: occurrence, formation, structure and reactions,* New York, Wiley Intersci.

SAUTER, U. H., MUTZ, R. & MUNRO, B. D. 1999. Determining juvenile-mature wood transition in Scots pine using latewood density. *Wood and Fiber Science,* 31**,** 416-425.

SCHNIEWIND, A. P. 1966. Über Unterschiede in der Zugfestigkeit von Früh= und Spätholztracheiden. *European Journal of Wood and Wood Products,* 24**,** 502-506.

SCHWEINGRUBER, F. H., BÖRNER, A. & SCHULZE, E. D. 2006. *Atlas of woody plant stems: evolution, structure, and environmental modifications,* Berlin, Springer Verlag.

SENFT, J. F. & BENDTSEN, B. A. 1985. Measuring microfibrillar angles using light microscopy. *Wood and Fiber Science,* 17**,** 564-567.

SENFT, J. F., QUANCI, M. J. & BENDTSEN, B. A. Year. Property profile of 60-year-old Douglas-fir. *In:* A technical workshop: Juvenile wood - what does it mean to forest management and forest products, 1986 Madison, Forest Products Research Society. 17-28.

SHULER, C. E., MARKSTROM, D. D. & RYAN, M. G. 1989. Fibril angle in young-growth Ponderosa pine as related to site index, DBH, and location in tree. US Forest Service.

SIAU, J. 1984. *Transport processes in wood*, Springer-Verlag.

SIMPSON, W. T. 1993. Specific gravity, moisture content, and density relationship for wood. US Forest Service, Forest Products Laboratory.

SMITH, D. M. 1956. Effect of growth zone on specific gravity and percentage of summerwood in wide-ringed Douglas-fir. University of Wisconsin: USDA, Forest Service, Forest Products Laboratory.

SMITH, D. M. 1967. MICROSCOPIC METHODS FOR DETERMINING CROSS-SECTIONAL CELL DIMENSIONS. DTIC Document.

SMITH, S. & GILBERT, J. 2003. National Inventory of Woodland and Trees, Great Britain. Edinburgh: Forestry Commission.

SOBUE, N. & ASANO, I. 1976. Studies on the fine structure and mechanical properties of wood: On the longitudinal Young's modulus and shear modulus of rigidity of cell wall. *Journal of the Japan Wood Research Society*.

SPICER, R. & GARTNER, B. 2001. The effects of cambial age and position within the stem on specific conductivity in Douglas-fir (*Pseudotsuga menziesii*) sapwood. *Trees - Structure and Function,* 15**,** 222-229.

SPICER, R., GARTNER, B. & DARBYSHIRE, R. 2000. Sinuous stem growth in a Douglas-fir (*Pseudotsuga menziesii*) plantation: growth patterns and wood-quality effects. *Canadian Journal of Forest Research,* 30**,** 761-768.

STEIGER, R. & ARNOLD, M. 2009. Strength grading of Norway spruce structural timber: revisiting property relationships used in EN 338 classification system. *Wood Science and Technology,* 43**,** 259-278.

STIRLING-MAXWELL, J. 1931. Sitka spruce on poor soils and at high elevations. *Forestry,* 5**,** 96-99.

SYKES, R., KODRZYCKI, B., TUSKAN, G., FOUTZ, K. & DAVIS, M. 2008. Within tree variability of lignin composition in Populus. *Wood Science and Technology,* 42**,** 649-661.

TAIZ, L. 1984. Plant cell expansion: regulation of cell wall mechanical properties. *Annual Review of Plant Physiology,* 35**,** 585-657.

TANG, R. C. 1973. The microfibrillar orientation in cell-wall layers of Virginia pine tracheids. *Wood Science,* 5**,** 181-186.

TASHIRO, K. & KOBAYASHI, M. 1991. Theoretical evaluation of three-dimensional elastic constants of native and regenerated celluloses: role of hydrogen bonds. *Polymer,* 32**,** 1516-1526.

TAYLOR, A., BROOKS, J., LACHENBRUCH, B. & MORRELL, J. 2007. Radial patterns of carbon isotopes in the xylem extractives and cellulose of Douglas-fir. *Tree physiology,* 27**,** 921.

TIMBER TRADE FEDERATION 2011. Statistical Review 2011: Industry Facts and Figures for the year 2010. London: Timber Trade Federation.

TIMELL, T. 1986. Compression wood in gymnosperms. Vol. 1-3. *Springer-Verlag, Berlin,* 2150**,** 3-540.

TOWNEND, J. 2002. *Practical statistics for environmental and biological scientists*, John Wiley & Sons.

TSEHAYE, A., BUCHANAN, A. & WALKER, J. 2000. Selecting trees for structural timber. *European Journal of Wood and Wood Products,* 58**,** 162-167.

TYLER, A. L., MACMILLAN, D. C. & DUTCH, J. 1995. Predicting the yield of Douglas-fir from site factors on better quality sites in Scotland. *Annals of Forest Science,* 52**,** 619-634.

TZE, W., WANG, S., RIALS, T., PHARR, G. & KELLEY, S. 2007. Nanoindentation of wood cell walls: continuous stiffness and hardness measurements. *Composites Part A: Applied Science and Manufacturing,* 38**,** 945-953.

UGGLA, C., MAGEL, E., MORITZ, T. & SUNDBERG, B. 2001. Function and dynamics of auxin and carbohydrates during earlywood/latewood transition in Scots pine. *Plant physiology,* 125**,** 2029.

VARGAS-HERNANDEZ, J. & ADAMS, W. 1991. Genetic variation of wood density components in young coastal Douglas-fir: implications for tree breeding. *Canadian Journal of Forest Research,* 21**,** 1801-1807.

VERRILL, S. P., KRETSCHMANN, D. E., HERIAN, V. L., WIEMANN, M. C. & ALDEN, H. A. 2011. Concerns about a variance approach to X-ray diffractometric estimation of microfibril angle in wood. *Wood and Fiber Science,* 43**,** 153-168.

VIA, B., SO, C., SHUPE, T., GROOM, L. & WIKAIRA, J. 2009. Mechanical response of Longleaf pine to variation in microfibril angle, chemistry associated wavelengths, density, and radial position. *Composites Part A: Applied Science and Manufacturing,* 40**,** 60-66.

VIKRAM, V. 2008. *Stiffness of Douglas-fir lumber: effects of wood properties and genetics.* Masters thesis, Oregon State University.

VIKRAM, V., CHERRY, M. L., BRIGGS, D., CRESS, D. W., EVANS, R. & HOWE, G. T. 2011. Stiffness of Douglas-fir lumber: effects of wood properties and genetics. *Canadian Journal of Forest Research,* 41**,** 1160-1173.

WALKER, J. 1993. *Primary wood processing: Principles and practice,* London, Chapman and Hall.

WALKER, J. 2006. *Primary Wood Processing: Principles and Practice,* London, Chapman & Hall.

WANG, H., DRUMMOND, J., REATH, S., HUNT, K. & WATSON, P. 2001. An improved fibril angle measurement method for wood fibres. *Wood Science and Technology,* 34**,** 493-503.

WANG, X., CARTER, P., ROSS, R. J. & BRASHAW, B. K. 2007. Acoustic assessment of wood quality of raw materials - a path to increased profitability. *Forest Products Journal,* 57**,** 6-15.

WARDROP, A. B. 1952. The low-angle scattering of X-rays by conifer tracheids. *Textile Research Journal,* 22**,** 288.

WARDROP, A. B. 1954. The fine structure of the conifer tracheid. *Holzforschung-International Journal of the Biology, Chemistry, Physics and Technology of Wood,* 8**,** 12-29.

WARDROP, A. B. 1957. The organization and properties of the outer layer of the secondary wall in conifer tracheids. *Holzforschung,* 11**,** 102-110.

WARDROP, A. B. 1958. The organization of the primary wall in differentiating conifer tracheids. *Australian Journal of Botany,* 6**,** 299-305.

WARDROP, A. B. 1964. The structure and formation of the cell wall in xylem. *In:* ZIMMERMAN, M. (ed.) *The formation of wood in forest trees.* New York: Academic Press.

WARDROP, A. B. & HARADA, H. 1965. The formation and structure of the cell wall in fibres and tracheids. *Journal of Experimental Botany,* 16**,** 356.

WEATHERWAX, R. & TARKOW, H. 1968. Density of wood substance. Importance of penetration and adsorption compression of the displacement fluid. *Forest Poducts Journal,* 18**,** 44-46.

WELLWOOD, R., SASTRY, C., MICKO, M. & PASZNER, L. 1974. On some possible specific gravity, holo-and alpha-cellulose, tracheid weight/length and cellulose crystallinity relationships in a 500-year-old Douglas-fir tree. *Holzforschung-International Journal of the Biology, Chemistry, Physics and Technology of Wood,* 28**,** 91-94.

WELLWOOD, R. & SMITH, J. G. H. 1962. Variation in some important qualities of wood from young Douglas-fir and Hemlock trees. *Research report number 50.* University of British Colombia, Faculty of Forestry.

XU, P. & WALKER, J. 2004. Stiffness gradients in Radiata pine trees. *Wood Science and Technology,* 38**,** 1-9.

YAMAMOTO, H. & KOJIMA, Y. 2002. Properties of cell wall constituents in relation to longitudinal elasticity of wood. *Wood Science and Technology,* 36**,** 55-74.

YANG, K. & HAZENBERG, G. 1994. Impact of spacing on tracheid length, relative density, and growth rate of juvenile wood and mature wood in *Picea mariana*. *Canadian Journal of Forest Research,* 24**,** 996-1007.

YANG, S. 2006. Ecological wood adaptation and horizontal variations of vessel element and fibre length of Calligonum mongolicum. *Electronic Journal of Biology,* 2**,** 19-23.

ZHANG, S. 1995. Effect of growth rate on wood specific gravity and selected mechanical properties in individual species from distinct wood categories. *Wood Science and Technology,* 29**,** 451-465.

ZIMMERMANN, M. H. & BROWN, C. L. 1971. *Trees. structure and function,* Berlin, Springer Verlag.

ZOBEL, B. & JETT, J. B. 1995. *Genetics of wood production,* New York, Springer-Verlag.

ZOBEL, B. & SPRAGUE, J. R. 1998. *Juvenile wood in forest trees,* Berlin, Springer.

ZOBEL, B. & VAN BUIJTENEN, J. 1989. *Wood variation-its causes and control,* Berlin, Springer Verlag.

Appendix A - Chapter 4 supplementary results

Table A-1: Whole ring width descriptive statistics for 40 - 50 year old trees

Growth period (Years)	All		2 - 10		11 - 20		21 - 30		31 - 40
Stem height (m)	**1.3**	**8**	**1.3**	**8**	**1.3**	**8**	**1.3**	**8**	**1.3**
Mean (mm)	4.4	5.2	5.1	6.4	4.1	4.7	4.3	3.9	4.2
CV (%)	42	38	33	25	42	36	42	43	46
Min (mm)	0.4	0.4	0.6	2.3	0.6	1.2	0.7	0.4	0.4
Max (mm)	11.2	9.9	9.9	9.9	9.7	9.1	9.4	7.7	11.2

Table A-2: Whole ring width repeated measures univariate analysis of variance and t-test results for 40 - 50 year old trees

Growth period (Years)	2 - 10		11 - 20		21 - 30		31 - 40
Stem height (m)	**1.3**	**8**	**1.3**	**8**	**1.3**	**8**	**1.3**
F value	4.31*	14.0*	2.10*	4.78*	0.88	6.54*	2.26*
t value	-7.94*		-4.83*		2.57*		N/A
Variance component							
Site (%)	4	21	5	3	4	4	6
Tree within site (%)	16	30	31	35	69	54	49
Error (%)	80	65	64	62	27	42	55

* indicates statistically significant results at $P \leq 0.05$

Table A-3: Earlywood width descriptive statistics for 40 - 50 year old trees

Growth period (Years)	All		2 - 10		11 - 20		21 - 30		31 - 40
Stem height (m)	**1.3**	**8**	**1.3**	**8**	**1.3**	**8**	**1.3**	**8**	**1.3**
Mean (mm)	1.9	2.4	2.0	3.0	1.8	2.4	1.9	1.8	1.7
CV (%)	46	41	48	33	46	36	42	43	47
Min (mm)	0.1	0.3	0.2	0.5	0.3	0.6	0.3	0.3	0.1
Max (mm)	5.6	5.5	5.6	5.5	4.9	5	4.8	3.9	4.9

Table A-4: Earlywood width repeated measures univariate analysis of variance and t-test results for 40 - 50 year old trees

Growth period (Years)	2 - 10		11 - 20		21 - 30		31 - 40
Stem height (m)	**1.3**	**8**	**1.3**	**8**	**1.3**	**8**	**1.3**
F value	2.78*	9.28*	2.27*	5.73*	0.63	8.33*	3.17*
t value	-9.87*		-7.65*		2.53*		
Variance component							
Site (%)	3	3	4	2	4	2	4
Tree within site (%)	18	21	33	40	54	36	51
Error (%)	79	76	63	58	42	62	45

* indicates statistically significant results at $P \leq 0.05$

Table A-5: Transition-wood width descriptive statistics for 40 - 50 year old trees

Growth period (Years)	All		2 - 10		11 - 20		21 - 30		31 - 40
Stem height (m)	**1.3**	**8**	**1.3**	**8**	**1.3**	**8**	**1.3**	**8**	**1.3**
Mean (mm)	1.5	1.6	2.2	2.6	1.3	1.3	1.2	1.0	1.2
CV (%)	72	70	54	47	76	54	67	68	72
Min (mm)	0.1	0.1	0.1	0.5	0.1	0.2	0.1	0.2	0.1
Max (mm)	6.0	7.7	5.6	7.7	4.5	3.3	4.1	3.2	6.0

Table A-6: Transition-wood width repeated measures univariate analysis of variance and t-test results for 40 - 50 year old trees

Growth period (Years)	**2 - 10**		**11 - 20**		**21 - 30**		**31 - 40**
Stem height (m)	**1.3**	**8**	**1.3**	**8**	**1.3**	**8**	**1.3**
F value	7.84*	7.44*	2.54*	4.42*	0.82	5.83*	1.86
t value	-3.54*		-1.47		3.18*		
Variance component							
Site (%)	1	2	2	4	1	2	2
Tree within site (%)	8	21	15	32	58	50	52
Error (%)	90	77	83	64	41	48	46

* indicates statistically significant results at $P \leq 0.05$

Table A-7: Latewood width descriptive statistics for 40 - 50 year old trees

Growth period (Years)	**All**		**2 - 10**		**11 - 20**		**21 - 30**		**31 - 40**
Stem height (m)	**1.3**	**8**	**1.3**	**8**	**1.3**	**8**	**1.3**	**8**	**1.3**
Mean (mm)	1.0	1.0	0.8	0.8	1.0	1.1	1.1	1.0	1.1
CV (%)	54	57	79	70	61	47	61	55	56
Min (mm)	0.1	0.1	0.1	0.1	0.1	0.2	0.17	0.1	0.1
Max (mm)	5.9	4.5	4.2	4.5	4.3	2.8	5.9	3.4	3.7

Table A-8: Latewood width repeated measures univariate analysis of variance and t-test results for 40 - 50 year old trees

Growth period (Years)	**2 - 10**		**11 - 20**		**21 - 30**		**31 - 40**
Stem height (m)	**1.3**	**8**	**1.3**	**8**	**1.3**	**8**	**1.3**
F value	15.7*	17.2*`	1.80	1.85	1.89	0.95	0.65
t value	-1.95		-1.47		1.89		
Variance component							
Site (%)	2	2	2	2	2	3	3
Tree within site (%)	10	24	33	40	43	37	41
Error (%)	88	74	65	58	55	60	56

* indicates statistically significant results at $P \leq 0.05$

Table A-9: Whole ring width descriptive statistics for all growth periods in 40 - 50 year old trees by site

Site	1		2		3		4	
Stem height (m)	**1.3**	**8**	**1.3**	**8**	**1.3**	**8**	**1.3**	**8**
Mean (mm)	4.2	4.5	4.2	4.8	4.6	5.4	4.6	5.1
CV (%)	43	33	44	43	41	37	40	37
Min (mm)	0.6	0.7	0.4	0.4	0.6	1.1	0.4	0.7
Max (mm)	9.0	7.5	11.2	9.3	9.7	9.9	9.9	8.9

Note: Site numbers correspond to those given in Table 3-1

Table A-10: Earlywood proportion descriptive statistics for 40 - 50 year old trees

Growth period (Years)	All		2 - 10		11 - 20		21 - 30		31 - 40
Stem height (m)	**1.3**	**8**	**1.3**	**8**	**1.3**	**8**	**1.3**	**8**	**1.3**
Mean (%)	45	49	40	48	45	50	46	49	46
CV (%)	25	22	36	28	24	18	18	19	21
Min (%)	8	7	8	11	17	17	10	7	9
Max (%)	78	96	78	88	73	73	64	96	69

Table A-11: Earlywood proportion repeated measures univariate analysis of variance and t-test results for 40 - 50 year old trees

Growth period (Years)	2 - 10		11 - 20		21 - 30		31 - 40
Stem height (m)	**1.3**	**8**	**1.3**	**8**	**1.3**	**8**	**1.3**
F value	1.33	4.74*	4.04*	1.99*	0.59	1.26	1.31
t value	-5.59*		-6.21*		-2.60*		N/A
Variance component							
Site (%)	5	5	7	7	9	8	7
Tree within site (%)	30	34	31	44	69	58	57
Error (%)	65	61	62	49	22	34	36

* indicates statistically significant results at $P \leq 0.05$

Table A-12: Transition-wood proportion descriptive statistics for 40 - 50 year old trees

Growth period (Years)	All		2 - 10		11 - 20		21 - 30		31 - 40
Stem height (m)	**1.3**	**8**	**1.3**	**8**	**1.3**	**8**	**1.3**	**8**	**1.3**
Mean (%)	31	29	43	39	28	26	26	23	27
CV (%)	49	43	59	54	52	35	39	41	41
Min (%)	6	5	7	9	6	6	6	5	6
Max (%)	83	77	83	77	78	59	56	55	57

Table A-13: Transition-wood proportion repeated measures univariate analysis of variance and t-test results for 40 - 50 year old trees

Growth period (Years)	2 - 10		11 - 20		21 - 30		31 - 40
Stem height (m)	**1.3**	**8**	**1.3**	**8**	**1.3**	**8**	**1.3**
F value	9.23*	5.64*	2.27*	2.07*	1.24	2.46*	1.53
t value	2.90*		2.78*		2.93*		N/A
Variance component							
Site (%)	4	3	4	4	4	4	4
Tree within site (%)	5	12	8	12	34	27	38
Error (%)	91	85	88	84	62	69	58

* indicates statistically significant results at $P \leq 0.05$

Table A-14: Latewood proportion descriptive statistics for 40 - 50 year old trees

Growth period (Years)	All		2 - 10		11 - 20		21 - 30		31 - 40
Stem height (m)	**1.3**	**8**	**1.3**	**8**	**1.3**	**8**	**1.3**	**8**	**1.3**
Mean (%)	25	21	17	13	27	23	27	27	27
CV (%)	54	52	77	62	51	42	40	37	46
Min (%)	1	2	1	2	2	3	5	3	6
Max (%)	80	57	69	56	70	50	71	57	80

Table A-15: Latewood proportion repeated measures univariate analysis of variance and t-test results for 40 - 50 year old trees

Growth period (Years)	**2 - 10**		**11 - 20**		**21 - 30**		**31 - 40**
Stem height (m)	**1.3**	**8**	**1.3**	**8**	**1.3**	**8**	**1.3**
F value	17.5*	9.94*	1.91	4.68*	1.86	2.94*	1.36
t value	2.00*		2.11*		-0.374		N/A
Variance component							
Site (%)	5	4	7	4	7	5	7
Tree within site (%)	20	15	49	26	51	41	45
Error (%)	75	81	44	70	42	54	48

* indicates statistically significant results at $P \leq 0.05$

Table A-16: Earlywood proportion descriptive statistics for all growth periods in 40 - 50 year old trees by site

Site	**1**		**2**		**3**		**4**	
Stem height (m)	**1.3**	**8**	**1.3**	**8**	**1.3**	**8**	**1.3**	**8**
Mean (mm)	46	51	46	52	44	48	42	47
CV (%)	21	22	24	21	24	22	28	20
Min (mm)	10	7	10	28	15	12	8	19
Max (mm)	68	89	76	97	79	82	78	76

Note: Site numbers correspond to those given in Table 3-1

Table A-17: Transition-wood proportion descriptive statistics for all growth periods in 40 - 50 year old trees by site

Site	**1**		**2**		**3**		**4**	
Stem height (m)	**1.3**	**8**	**1.3**	**8**	**1.3**	**8**	**1.3**	**8**
Mean (mm)	31	29	28	27	30	30	34	31
CV (%)	44	45	53	42	50	47	45	45
Min (mm)	6	5	6	6	7	6	6	6
Max (mm)	74	68	80	62	78	77	83	76

Note: Site numbers correspond to those given in Table 3 - 1

Table A-18: Latewood proportion descriptive statistics for all growth periods in 40 - 50 year old trees by site

Site	1		2		3		4	
Stem height (m)	**1.3**	**8**	**1.3**	**8**	**1.3**	**8**	**1.3**	**8**
Mean (mm)	23	22	25	21	26	21	25	20
CV (%)	44	50	54	50	53	55	60	54
Min (mm)	2	2	2	3	3	2	1	2
Max (mm)	56	57	80	52	71	56	7	53

Note: Site numbers correspond to those given in Table 3-1

Table A-19: Whole ring radial tracheid diameter descriptive statistics for 40 - 50 year old trees

Growth period (Years)	All		2 - 10		11 - 20		21 - 30		31 - 40
Stem height (m)	**1.3**	**8**	**1.3**	**8**	**1.3**	**8**	**1.3**	**8**	**1.3**
Mean (μm)	30.5	32.6	29.0	31.5	30.4	33.1	31.4	33.2	31.2
CV (%)	8	8	9	10	9	6	7	6	8
Min (μm)	19.4	23.8	23.1	23.8	23.7	25.0	24.1	25.3	19.4
Max (μm)	37.2	38.6	36.1	37.2	35.2	37.9	37.2	38.6	37.0

Table A-20: Whole ring radial tracheid diameter repeated measures univariate analysis of variance and t-test results for 40 - 50 year old trees

Growth period (Years)	2 - 10		11 - 20		21 - 30		31 - 40
Stem height (m)	**1.3**	**8**	**1.3**	**8**	**1.3**	**8**	**1.3**
F value	20.4*	98.5*	6.28*	1.58	1.18	1.78	1.87
t value	-8.64*		-12.5*		-8.74*		N/A
Variance component							
Site (%)	2	3	3	4	4	4	4
Tree within site (%)	21	29	55	68	69	60	66
Error (%)	76	68	42	28	27	36	30

* indicates statistically significant results at $P \leq 0.05$

Table A-21: Earlywood radial tracheid diameter descriptive statistics for 40 - 50 year old trees

Growth period (Years)	All		2 - 10		11 - 20		21 - 30		31 - 40
Stem height (m)	**1.3**	**8**	**1.3**	**8**	**1.3**	**8**	**1.3**	**8**	**1.3**
Mean (µm)	35.7	37.1	32.2	34.5	35.3	37.9	37.3	38.7	37.6
CV (%)	9	9	10	11	7	6	6	6	7
Min (µm)	20.4	24.1	24.0	24.1	26.5	28.5	30.2	29.7	20.4
Max (µm)	42.6	44.1	40.3	41.1	39.9	43.2	42.6	44.1	42.6

Table A-22: Earlywood radial tracheid diameter repeated measures univariate analysis of variance and t-test results for 40 - 50 year old trees

Growth period (Years)	2 - 10		11 - 20		21 - 30		31 - 40
Stem height (m)	**1.3**	**8**	**1.3**	**8**	**1.3**	**8**	**1.3**
F value	42.3*	165*	8.87*	6.03*	4.77*	1.11	1.50
t value	-6.49*		-12.4*		-6.71*		N/A
Variance component							
Site (%)	9	2	9	3	8	4	5
Tree within site (%)	14	31	44	58	67	69	64
Error (%)	77	67	47	39	25	27	31

* indicates statistically significant results at $P \leq 0.05$

Table A-23: Transition-wood radial tracheid diameter descriptive statistics for 40 - 50 year old trees

Growth period (Years)	All		2 - 10		11 - 20		21 - 30		31 - 40
Stem height (m)	**1.3**	**8**	**1.3**	**8**	**1.3**	**8**	**1.3**	**8**	**1.3**
Mean (µm)	29.3	31.6	28.3	30.3	29.8	31.8	29.9	32.4	29.1
CV (%)	11	11	10	11	11	10	12	12	12
Min (µm)	18.6	23.0	21.6	23.0	20.6	23.3	21.9	23.4	18.6
Max (µm)	42.8	42.0	37.7	39.5	39.1	42.0	42.8	40.9	40.5

Table A-24: Transition-wood radial tracheid diameter repeated measures univariate analysis of variance and t-test results for 40 - 50 year old trees

Growth period (Years)	**2 - 10**		**11 - 20**		**21 - 30**		**31 - 40**
Stem height (m)	**1.3**	**8**	**1.3**	**8**	**1.3**	**8**	**1.3**
F value	11.5*	34.9*	2.30*	3.67*	2.13	0.74	1.07
t value	-6.77*		-7.18*		-9.15*		N/A
Variance component							
Site (%)	5	5	5	2	6	3	8
Tree within site (%)	25	37	48	48	59	59	54
Error (%)	70	58	47	50	35	38	38

* indicates statistically significant results at $P \leq 0.05$

Table A-25: Latewood radial tracheid diameter descriptive statistics for 40 - 50 year old trees

Growth period (Years)	**All**		**2 - 10**		**11 - 20**		**21 - 30**		**31 - 40**
Stem height (m)	**1.3**	**8**	**1.3**	**8**	**1.3**	**8**	**1.3**	**8**	**1.3**
Mean (μm)	22.5	23.2	22.3	22.6	22.7	23.4	22.5	23.8	22.4
CV (%)	9	9	10	10	9	10	9	9	9
Min (μm)	16.7	16.8	16.7	16.9	18.5	16.8	17.4	18.8	18.3
Max (μm)	32.7	34.6	31.5	29.8	31.3	30.8	32.7	34.6	28.9

Table A-26: Latewood radial tracheid diameter repeated measures univariate analysis of variance and t-test results for 40 - 50 year old trees

Growth period (Years)	**2 - 10**		**11 - 20**		**21 - 30**		**31 - 40**
Stem height (m)	**1.3**	**8**	**1.3**	**8**	**1.3**	**8**	**1.3**
F value	1.99	8.33*	1.29	2.23*	1.89	0.48	0.57
t value	-1.03		-3.33*		-6.93*		N/A
Variance component							
Site (%)	4	3	3	1	4	3	4
Tree within site (%)	21	36	33	38	54	65	57
Error (%)	75	61	64	61	42	32	39

* indicates statistically significant results at $P \leq 0.05$

Table A-27: Whole ring radial tracheid diameter descriptive statistics for all growth periods in 40 - 50 year old trees by site

Site	1		2		3		4	
Stem height (m)	**1.3**	**8**	**1.3**	**8**	**1.3**	**8**	**1.3**	**8**
Mean (mm)	30.9	32.5	30.4	33.1	29.9	32.1	30.9	32.8
CV (%)	7	8	9	7	9	9	8	7
Min (mm)	23.1	23.9	19.4	24.2	23.1	23.8	23.4	24.1
Max (mm)	36.1	36.7	37.0	38.6	35.6	38.3	37.2	37.9

Note: Site numbers correspond to those given in Table 3-1

Table A-28: Whole ring tangential tracheid diameter descriptive statistics for 40 - 50 year old trees

Growth period (Years)	All		2 - 10		11 - 20		21 - 30		31 - 40
Stem height (m)	**1.3**	**8**	**1.3**	**8**	**1.3**	**8**	**1.3**	**8**	**1.3**
Mean (μm)	29.1	31.4	26.8	28.8	29.1	32.1	30.0	33.0	30.1
CV (%)	8	10	7	10	7	7	7	7	7
Min (μm)	23.2	23.1	23.2	23.1	24.1	27.2	24.8	27.7	25.3
Max (μm)	36.1	42.0	32.8	36.9	36.1	39.1	35.6	42.0	35.6

Table A-29: Whole ring tangential tracheid diameter repeated measures univariate analysis of variance and t-test results for 40 - 50 year old trees

Growth period (Years)	2 - 10		11 - 20		21 - 30		31 - 40
Stem height (m)	**1.3**	**8**	**1.3**	**8**	**1.3**	**8**	**1.3**
F value	22.6*	108*	11.2*	5.74*	1.95*	1.04	0.78
t value	-8.36*		-15.2*		-14.7*		N/A
Variance component							
Site (%)	3	3	4	5	6	7	5
Tree within site (%)	41	46	56	58	65	55	69
Error (%)	56	51	40	37	29	38	26

* indicates statistically significant results at $P \leq 0.05$

Table A-30: Earlywood tangential tracheid diameter descriptive statistics for 40 - 50 year old trees

Growth period (Years)	All		2 - 10		11 - 20		21 - 30		31 - 40
Stem height (m)	**1.3**	**8**	**1.3**	**8**	**1.3**	**8**	**1.3**	**8**	**1.3**
Mean (μm)	31.6	33.6	26.8	30.6	29.1	34.5	30.0	35.4	30.1
CV (%)	9	10	7	11	7	7	7	7	7
Min (μm)	23.6	24.0	23.2	24.0	24.1	29.2	24.8	29.3	25.3
Max (μm)	40.0	42.5	37.2	39.1	38.7	41.6	40.0	42.5	39.4

Table A-31: Earlywood tangential tracheid diameter repeated measures univariate analysis of variance and t-test results for 40 - 50 year old trees

Growth period (Years)	2 - 10		11 - 20		21 - 30		31 - 40
Stem height (m)	**1.3**	**8**	**1.3**	**8**	**1.3**	**8**	**1.3**
F value	23.9*	123*	7.16*	5.94*	2.85*	0.84	0.77
t value	18.7*		12.4*		-12.1*		N/A
Variance component							
Site (%)	3	7	6	5	10	6	10
Tree within site (%)	29	35	49	60	60	42	59
Error (%)	68	58	45	35	30	52	31

* indicates statistically significant results at $P \leq 0.05$

Table A-32: Transition-wood tangential tracheid diameter descriptive statistics for 40 - 50 year old trees

Growth period (Years)	All		2 - 10		11 - 20		21 - 30		31 - 40
Stem height (m)	**1.3**	**8**	**1.3**	**8**	**1.3**	**8**	**1.3**	**8**	**1.3**
Mean (μm)	28.0	30.2	25.9	27.6	28.2	30.8	28.9	31.8	28.8
CV (%)	9	11	8	10	8	8	9	10	9
Min (μm)	22.6	22.0	22.6	22.0	23.4	23.5	23.6	23.6	23.1
Max (μm)	38.9	40.1	32.0	35.5	35.8	38.8	37.4	40.1	38.9

Table A-33: Transition-wood tangential tracheid diameter repeated measures univariate analysis of variance and t-test results for 40 - 50 year old trees

Growth period (Years)	**2 - 10**		**11 - 20**		**21 - 30**		**31 - 40**
Stem height (m)	**1.3**	**8**	**1.3**	**8**	**1.3**	**8**	**1.3**
F value	17.4*	58.5*	6.41*	6.74*	1.26	1.34	0.81
t value	-7.45*		-11.8*		-13.4*		N/A
Variance component							
Site (%)	1	1	2	4	5	4	6
Tree within site (%)	41	49	51	57	55	58	58
Error (%)	58	50	47	39	40	48	36

* indicates statistically significant results at $P \leq 0.05$

Table A-34: Latewood tangential tracheid diameter descriptive statistics for 40 - 50 year old trees

Growth period (Years)	**All**		**2 - 10**		**11 - 20**		**21 - 30**		**31 - 40**
Stem height (m)	**1.3**	**8**	**1.3**	**8**	**1.3**	**8**	**1.3**	**8**	**1.3**
Mean (μm)	26.1	27.9	24.8	25.7	25.9	28.3	26.6	29.4	26.9
CV (%)	8	10	7	8	7	8	7	8	8
Min (μm)	20.4	20.8	20.4	20.8	21.6	24.0	23.0	24.7	23.1
Max (μm)	33.1	44.8	30.6	33.2	32.3	35.4	32.6	44.8	33.1

Table A-35: Latewood tangential tracheid diameter repeated measures univariate analysis of variance and t-test results for 40 - 50 year old trees

Growth period (Years)	**2 - 10**		**11 - 20**		**21 - 30**		**31 - 40**
Stem height (m)	**1.3**	**8**	**1.3**	**8**	**1.3**	**8**	**1.3**
F value	3.48*	13.8*	3.21*	4.10*	2.54*	2.61*	0.82
t value	-13.9*		-12.9*		-4.3*		N/A
Variance component							
Site (%)	1	2	3	4	6	4	7
Tree within site (%)	28	31	51	57	56	52	61
Error (%)	71	67	46	39	38	44	32

* indicates statistically significant results at $P \leq 0.05$

Table A-36: Whole ring tangential tracheid diameter descriptive statistics for all growth periods in 40 - 50 year old trees by site

Site	1		2		3		4	
Stem height (m)	**1.3**	**8**	**1.3**	**8**	**1.3**	**8**	**1.3**	**8**
Mean (mm)	29.5	30.9	29.1	31.8	29.0	31.8	28.6	31.1
CV (%)	9	9	8	9	7	9	10	11
Min (mm)	23.2	23.1	23.7	23.8	24.2	23.9	23.3	23.5
Max (mm)	36.1	37.1	35.6	42.0	35.4	39.4	35.6	39.1

Note: Site numbers correspond to those given in Table 3-1

Table A-37: Whole ring radial tracheid wall thickness descriptive statistics for 40 - 50 year old trees

Growth period (Years)	All		2 - 10		11 - 20		21 - 30		31 - 40
Stem height (m)	**1.3**	**8**	**1.3**	**8**	**1.3**	**8**	**1.3**	**8**	**1.3**
Mean (μm)	2.6	2.7	2.2	2.3	2.4	2.7	2.7	3.0	2.9
CV (%)	16	16	11	11	11	12	13	12	13
Min (μm)	1.7	1.8	1.7	1.8	1.7	2.0	1.9	2.1	1.9
Max (μm)	4.5	4.1	3.1	3.2	3.1	3.7	4.1	4.1	4.5

Table A-38: Whole ring radial tracheid wall thickness repeated measures univariate analysis of variance and t-test results for 40 - 50 year old trees

Growth period (Years)	2 - 10		11 - 20		21 - 30		31 - 40
Stem height (m)	**1.3**	**8**	**1.3**	**8**	**1.3**	**8**	**1.3**
F value	1.81	6.25*	2.69*	5.82*	7.45*	6.88*	4.93*
t value	-3.87*		-9.38*		-10.1*		N/A
Variance component							
Site (%)	5	10	4	6	4	5	3
Tree within site (%)	55	48	47	36	38	42	44
Error (%)	40	42	49	58	58	53	53

* indicates statistically significant results at $P \leq 0.05$

Table A-39: Earlywood radial tracheid wall thickness descriptive statistics for 40 - 50 year old trees

Growth period (Years)	All		2 - 10		11 - 20		21 - 30		31 - 40
Stem height (m)	**1.3**	**8**	**1.3**	**8**	**1.3**	**8**	**1.3**	**8**	**1.3**
Mean (μm)	1.6	1.7	1.5	1.6	1.5	1.7	1.7	1.8	1.8
CV (%)	15	13	16	13	12	11	12	14	13
Min (μm)	1.0	1.3	1.0	1.3	1.2	1.3	1.3	1.4	1.3
Max (μm)	1.6	4.2	2.4	2.5	2.1	2.5	2.4	4.2	2.6

Table A-40: Earlywood radial tracheid wall thickness repeated measures univariate analysis of variance and t-test results for 40 - 50 year old trees

Growth period (Years)	2 - 10		11 - 20		21 - 30		31 - 40
Stem height (m)	**1.3**	**8**	**1.3**	**8**	**1.3**	**8**	**1.3**
F value	20.8*	12.1*	8.57*	4.29*	3.52*	1.68	1.78
t value	-6.14*		-10.9*		-4.64*		N/A
Variance component							
Site (%)	7	7	5	9	7	4	4
Tree within site (%)	36	37	40	49	52	58	62
Error (%)	57	56	55	42	41	36	34

* indicates statistically significant results at $P \leq 0.05$

Table A-41: Transition-wood radial tracheid wall thickness descriptive statistics for 40 - 50 year old trees

Growth period (Years)	All		2 - 10		11 - 20		21 - 30		31 - 40
Stem height (m)	**1.3**	**8**	**1.3**	**8**	**1.3**	**8**	**1.3**	**8**	**1.3**
Mean (μm)	2.8	3.1	2.4	2.6	2.8	3.1	3.0	3.4	3.2
CV (%)	17	17	13	13	15	11	13	14	12
Min (μm)	1.5	1.6	1.5	1.9	1.6	2.3	1.7	1.6	2.1
Max (μm)	4.9	4.8	3.3	3.7	3.7	4.1	4.3	4.8	4.9

Table A-42: Transition-wood radial tracheid wall thickness repeated measures univariate analysis of variance and t-test results for 40 - 50 year old trees

Growth period (Years)	**2 - 10**		**11 - 20**		**21 - 30**		**31 - 40**
Stem height (m)	**1.3**	**8**	**1.3**	**8**	**1.3**	**8**	**1.3**
F value	0.83	19.2*	3.13*	3.82*	3.20*	2.69*	2.68*
t value	-6.47*		-11.0*		-11.9*		N/A
Variance component							
Site (%)	11	7	14	5	5	4	4
Tree within site (%)	59	33	31	45	30	47	36
Error (%)	30	60	55	50	65	49	60

* indicates statistically significant results at $P \leq 0.05$

Table A-43: Latewood radial tracheid wall thickness descriptive statistics for 40 - 50 year old trees

Growth period (Years)	**All**		**2 - 10**		**11 - 20**		**21 - 30**		**31 - 40**
Stem height (m)	**1.3**	**8**	**1.3**	**8**	**1.3**	**8**	**1.3**	**8**	**1.3**
Mean (μm)	3.9	4.3	3.3	3.7	3.7	4.3	4.1	4.7	4.3
CV (%)	17	16	15	13	14	12	13	13	12
Min (μm)	2.3	2.2	2.3	2.6	2.5	3.0	2.7	2.2	2.7
Max (μm)	5.7	6.3	5.1	5.4	4.8	6.1	5.6	6.3	5.7

Table A-44: Latewood radial tracheid wall thickness repeated measures univariate analysis of variance and t-test results for 40 - 50 year old trees

Growth period (Years)	**2 - 10**		**11 - 20**		**21 - 30**		**31 - 40**
Stem height (m)	**1.3**	**8**	**1.3**	**8**	**1.3**	**8**	**1.3**
F value	2.01	22.5*	7.19*	5.53*	5.69*	5.45*	4.24*
t value	-9.11*		-15.0*		-12.0*		N/A
Variance component							
Site (%)	16	3	15	6	11	2	6
Tree within site (%)	40	43	32	42	41	41	42
Error (%)	44	54	53	52	48	57	52

* indicates statistically significant results at $P \leq 0.05$

Table A-45: Whole ring radial tracheid wall thickness descriptive statistics for all growth periods in 40 - 50 year old trees by site

Site	1		2		3		4	
Stem height (m)	**1.3**	**8**	**1.3**	**8**	**1.3**	**8**	**1.3**	**8**
Mean (μm)	2.6	2.7	2.6	2.6	2.6	2.7	2.5	2.6
CV (%)	12	16	18	19	17	16	14	15
Min (μm)	1.9	1.8	1.8	1.8	1.7	1.9	1.7	1.8
Max (μm)	3.6	4.0	4.5	4.1	4.0	3.9	3.5	3.5

Note: Site numbers correspond to those given in Table 3-1

Table A-46: Whole ring density descriptive statistics for 40 - 50 year old trees

Growth period (Years)	All		2 - 10		11 - 20		21 - 30		31 - 40
Stem height (m)	**1.3**	**8**	**1.3**	**8**	**1.3**	**8**	**1.3**	**8**	**1.3**
Mean (kg/m³)	490	478	444	433	474	477	505	519	536
CV (%)	15	14	13	12	11	12	13	12	14
Min (kg/m³)	337	342	337	342	343	351	359	356	386
Max (kg/m³)	870	700	672	605	650	665	787	700	870

Table A-47: Whole ring density repeated measures univariate analysis of variance and t-test results for 40 - 50 year old trees

Growth period (Years)	2 - 10		11 - 20		21 - 30		31 - 40
Stem height (m)	**1.3**	**8**	**1.3**	**8**	**1.3**	**8**	**1.3**
F value	5.08*	7.41*	5.60*	8.12*	5.35*	5.75*	4.37*
t value	2.25*		-0.56		-2.47*		N/A
Variance component							
Site (%)	4	8	5	6	5	6	3
Tree within site (%)	32	41	39	41	40	46	44
Error (%)	64	51	56	53	55	48	53

* indicates statistically significant results at $P \leq 0.05$

Table A-48: Earlywood density descriptive statistics for 40 - 50 year old trees

Growth period (Years)	All		2 - 10		11 - 20		21 - 30		31 - 40
Stem height (m)	**1.3**	**8**	**1.3**	**8**	**1.3**	**8**	**1.3**	**8**	**1.3**
Mean (kg/m³)	282	281	289	293	263	272	283	280	293
CV (%)	15	15	21	19	10	11	12	13	14
Min (kg/m³)	190	208	190	208	206	213	215	216	214
Max (kg/m³)	488	588	488	524	376	381	416	588	484

Table A-49: Earlywood density repeated measures univariate analysis of variance and t-test results for 40 - 50 year old trees

Growth period (Years)	2 - 10		11 - 20		21 - 30		31 - 40
Stem height (m)	**1.3**	**8**	**1.3**	**8**	**1.3**	**8**	**1.3**
F value	47.5*	89.0*	1.56	3.19*	1.86	2.75*	1.20
t value	-1.01		-1.47		0.96		N/A
Variance component							
Site (%)	4	10	6	5	4	3	3
Tree within site (%)	33	28	70	49	66	48	61
Error (%)	63	62	24	46	30	59	36

* indicates statistically significant results at $P \leq 0.05$

Table A-50: Transition-wood density descriptive statistics for 40 - 50 year old trees

Growth period (Years)	All		2 - 10		11 - 20		21 - 30		31 - 40
Stem height (m)	**1.3**	**8**	**1.3**	**8**	**1.3**	**8**	**1.3**	**8**	**1.3**
Mean (kg/m³)	543	544	490	497	523	550	559	579	595
CV (%)	16	15	14	12	16	13	15	16	14
Min (kg/m³)	278	340	298	340	278	354	297	350	375
Max (kg/m³)	925	808	682	652	701	710	830	808	925

Table A-51: Transition-wood density repeated measures univariate analysis of variance and t-test results for 40 - 50 year old trees

Growth period (Years)	2 - 10		11 - 20		21 - 30		31 - 40
Stem height (m)	1.3	8	1.3	8	1.3	8	1.3
F value	3.25*	2.88*	1.22	1.41	2.16*	1.25	2.84*
t value	-1.28		-4.05*		-2.83*		N/A
Variance component							
Site (%)	3	8	13	5	3	5	5
Tree within site (%)	39	31	44	59	44	39	41
Error (%)	58	61	43	41	53	56	54

* indicates statistically significant results at $P \leq 0.05$

Table A-52: Latewood density descriptive statistics for 40 - 50 year old trees

Growth period (Years)	All		2 - 10		11 - 20		21 - 30		31 - 40
Stem height (m)	1.3	8	1.3	8	1.3	8	1.3	8	1.3
Mean (kg/m³)	806	844	726	786	773	852	840	888	878
CV (%)	14	12	14	10	12	11	12	11	10
Min (kg/m³)	454	315	454	582	458	622	555	315	639
Max (kg/m³)	1070	1070	972	990	990	1062	1066	1070	1070

Table A-53: Latewood density repeated measures univariate analysis of variance and t-test results for 40 - 50 year old trees

Growth period (Years)	2 - 10		11 - 20		21 - 30		31 - 40
Stem height (m)	1.3	8	1.3	8	1.3	8	1.3
F value	3.57*	4.13*	6.56*	2.15*	3.78*	3.16*	3.61*
t value	-7.26*		-9.30*		-5.18*		N/A
Variance component							
Site (%)	10	5	10	3	11	3	6
Tree within site (%)	32	37	35	44	40	39	41
Error (%)	58	58	55	53	49	58	53

* indicates statistically significant results at $P \leq 0.05$

Table A-54: Whole ring density descriptive statistics for all growth periods in 40 - 50 year old trees by site

Site	1		2		3		4	
Stem height (m)	**1.3**	**8**	**1.3**	**8**	**1.3**	**8**	**1.3**	**8**
Mean (kg/m³)	492	486	494	466	500	489	480	470
CV (%)	10	12	16	16	16	15	14	13
Min (kg/m³)	385	356	358	342	347	369	337	342
Max (kg/m³)	668	643	870	700	786	690	670	631

Note: Site numbers correspond to those given in Table 3-1

Table A-55: Whole ring microfibril angle descriptive statistics for 40 - 50 year old trees

Growth period (Years)	All		2 - 10		11 - 20		21 - 30		31 - 40
Stem height (m)	**1.3**	**8**	**1.3**	**8**	**1.3**	**8**	**1.3**	**8**	**1.3**
Mean (Deg)	17	14	23	19	16	12	14	11	14
CV (%)	31	42	28	35	20	30	17	31	21
Min (Deg)	7	3	11	8	7	6	8	3	8
Max (Deg)	36	34	36	34	25	25	20	24	22

Table A-56: Whole ring microfibril angle repeated measures univariate analysis of variance and t-test results for 40 - 50 year old trees

Growth period (Years)	2 - 10		11 - 20		21 - 30		31 - 40
Stem height (m)	**1.3**	**8**	**1.3**	**8**	**1.3**	**8**	**1.3**
F value	42.5*	100.43*	10.3*	4.56*	1.28	2.78*	3.35*
t value	5.34*		6.38*		4.76*		N/A
Variance component							
Site (%)	6	5	4	7	8	3	4
Tree within site (%)	26	30	51	49	62	62	58
Error (%)	68	65	45	44	30	35	38

* indicates statistically significant results at $P \leq 0.05$

Table A-57: Earlywood microfibril angle descriptive statistics for sub-sample of 40 - 50 year old trees

Growth period (Years)	All		2 - 10		11 - 20		21 - 30		31 - 40
Stem height (m)	**1.3**	**8**	**1.3**	**8**	**1.3**	**8**	**1.3**	**8**	**1.3**
Mean (Deg)	21	18	25	22	20	17	20	16	20
CV (%)	22	34	22	31	18	28	19	24	18
Min (Deg)	11	6	14	10	11	9	12	6	11
Max (Deg)	47	37	47	37	28	30	27	31	31

Table A-58: Transition-wood microfibril angle descriptive statistics for sub-sample of 40 - 50 year old trees

Growth period (Years)	All		2 - 10		11 - 20		21 - 30		31 - 40
Stem height (m)	**1.3**	**8**	**1.3**	**8**	**1.3**	**8**	**1.3**	**8**	**1.3**
Mean (Deg)	13	9	19	22	12	17	11	16	10
CV (%)	47	64	38	51	35	31	37	34	18
Min (Deg)	4	1	7	5	5	1	5	1	4
Max (Deg)	35	35	35	35	24	29	24	27	21

Table A-59: Latewood microfibril angle descriptive statistics for sub-sample of 40 - 50 year old trees

Growth period (Years)	All		2 - 10		11 - 20		21 - 30		31 - 40
Stem height (m)	**1.3**	**8**	**1.3**	**8**	**1.3**	**8**	**1.3**	**8**	**1.3**
Mean (Deg)	11	9	18	15	11	10	10	8	9
CV (%)	51	67	39	66	43	50	44	48	37
Min (Deg)	2	1	6	5	4	1	4	1	2
Max (Deg)	30	28	30	28	24	26	19	24	18

Table A-60: Whole ring microfibril angle descriptive statistics for all growth periods in 40 - 50 year old trees by site

Site	**1**		**2**		**3**		**4**	
Stem height (m)	**1.3**	**8**	**1.3**	**8**	**1.3**	**8**	**1.3**	**8**
Mean (kg/m³)	16	13	16	13	16	14	17	14
CV (%)	30	40	33	44	30	42	31	41
Min (kg/m³)	7	3	8	8	9	7	9	8
Max (kg/m³)	36	34	35	32	32	34	32	31

Note: Site numbers correspond to those given in Table 3-1

Appendix B - Chapter 5 supplementary results

Table B-1: Correlation coefficients for earlywood width against whole ring width for individual growth rings in 40 - 50 year old trees

Cambial age (Years)	r		Cambial age (Years)	r		Cambial age (Years)	r	
	1.3 m	8 m		1.3 m	8 m		1.3m	8 m
2	0.50*	0.36	**15**	0.82*	0.88*	**28**	0.91*	0.68*
3	0.27	0.40	**16**	0.79*	0.90*	**29**	0.89*	0.92*
4	0.52*	0.26	**17**	0.93*	0.81*	**30**	0.80*	0.91*
5	0.65*	0.04	**18**	0.86*	0.89*	**31**	0.90*	-
6	0.53*	0.59*	**19**	0.93*	0.84*	**32**	0.95*	-
7	0.63*	0.44*	**20**	0.96*	0.81*	**33**	0.88*	-
8	0.72*	0.37	**21**	0.89*	0.87*	**34**	0.95*	-
9	0.65*	0.82*	**22**	0.80*	0.89*	**35**	0.93*	-
10	0.91*	0.91*	**23**	0.93*	0.96*	**36**	0.88*	-
11	0.90*	0.87*	**24**	0.93*	0.91*	**37**	0.93*	-
12	0.81*	0.86*	**25**	0.91*	0.91*	**38**	0.80*	-
13	0.86*	0.91*	**26**	0.92*	0.93*	**39**	0.88*	-
14	0.79*	0.83*	**27**	0.88*	0.92*	**40**	0.90*	-

* indicates statistically significant results at $P \leq 0.05$

Table B-2: Correlation coefficients for transition-wood width against whole ring width for individual growth rings in 40 - 50 year old trees

Cambial age (Years)	r		Cambial age (Years)	r		Cambial age (Years)	r	
	1.3 m	8 m		1.3 m	8 m		1.3m	8 m
2	0.74*	0.76*	**15**	0.75*	0.80*	**28**	0.78*	0.86*
3	0.77*	0.80*	**16**	0.86*	0.80*	**29**	0.79*	0.85*
4	0.69*	0.67*	**17**	0.84*	0.72*	**30**	0.75*	0.63*
5	0.77*	0.77*	**18**	0.77*	0.80*	**31**	0.76*	-
6	0.63*	0.71*	**19**	0.79*	0.78*	**32**	0.70*	-
7	0.82*	0.74*	**20**	0.92*	0.78*	**33**	0.68*	-
8	0.76*	0.61*	**21**	0.91*	0.67*	**34**	0.91*	-
9	0.69*	0.81*	**22**	0.87*	0.83*	**35**	0.81*	-
10	0.85*	0.81*	**23**	0.89*	0.82*	**36**	0.89*	-
11	0.71*	0.84*	**24**	0.87*	0.88*	**37**	0.87*	-
12	0.86*	0.85*	**25**	0.86*	0.90*	**38**	0.92*	-
13	0.70*	0.85*	**26**	0.76*	0.84*	**39**	0.94*	-
14	0.85*	0.76*	**27**	0.72*	0.84*	**40**	0.90*	-

* indicates statistically significant results at $P \leq 0.05$

Table B-3: Correlation coefficients for latewood width against whole ring width for individual growth rings in 40 - 50 year old trees

Cambial age (Years)	r		Cambial age (Years)	r		Cambial age (Years)	r	
	1.3 m	8 m		1.3 m	8 m		1.3m	8 m
2	0.38	0.37	**15**	0.67*	0.58*	**28**	0.80*	0.63*
3	0.22	0.14	**16**	0.47*	0.55*	**29**	0.61*	0.64*
4	0.53*	0.05	**17**	0.34	0.66*	**30**	0.62*	0.69*
5	0.21	0.57*	**18**	0.69*	0.59*	**31**	0.69*	-
6	0.39	0.65*	**19**	0.39	0.62*	**32**	0.67*	-
7	0.41	0.67*	**20**	0.48*	0.43*	**33**	0.65*	-
8	0.48*	0.47*	**21**	0.52*	0.47*	**34**	0.71*	-
9	0.53*	0.35	**22**	0.65*	0.76*	**35**	0.71*	-
10	0.37	0.38	**23**	0.79*	0.76*	**36**	0.65*	-
11	0.32	0.35	**24**	0.77*	0.85*	**37**	0.49*	-
12	0.20	0.40	**25**	0.66*	0.82*	**38**	0.84*	-
13	0.35	0.59*	**26**	0.64*	0.72*	**39**	0.74*	-
14	0.34	0.48*	**27**	0.87*	0.71*	**40**	0.70*	-

* indicates statistically significant results at $P \leq 0.05$

Table B-4: Comparisons of mean whole ring width values between slower and faster grown trees in the 40 - 50 year old sample group

	Whole ring			Earlywood			Transition-wood			Latewood		
	C	**S**	**F**	**C**	**S**	**F**	**C**	**S**	**F**	**C**	**S**	**F**
Mean (mm)	4.7	3.9	5.4	2.1	1.8	2.5	1.5	1.2	1.8	1.0	0.9	1.1
CV (%)	40	51	77	45	51	36	70	77	61	62	62	56
Min (mm)	0.4	0.4	0.6	0.4	0.1	0.4	0.1	0.1	0.1	0.1	0.1	0.1
Max (mm)	11.2	9.0	11.2	5.6	5.6	5.4	7.7	5.2	7.7	1.1	4.5	5.9
t value	-16.86*			-15.24*			-13.02*			-8.24*		

Note: C = Combined mean of slower and faster grown trees S = Slower grown F = Faster grown, * indicates statistically significant results at $P \leq 0.05$

Table B-5: t-test results comparing mean ring widths in slower and faster growing trees within 40 - 50 year old sampling sites

Site	**1**	**2**	**3**	**4**
Whole ring	-11.11*	-6.32*	-5.16*	-12.37*
Earlywood	-12.90*	-4.50*	-4.77*	-11.12*
Transition-wood	-6.30*	-5.08*	-2.80*	-6.33*
Latewood	-4.54*	-3.12*	-3.70*	-4.79*

Note: Site numbers correspond to those given in Table 3-1, * indicates statistically significant results at $P \leq 0.05$

Table B-6: Correlation coefficients for earlywood proportion against whole ring width for individual growth rings in 40 - 50 year old trees

Cambial age (Years)	r		Cambial age (Years)	r		Cambial age (Years)	r	
	1.3 m	8 m		1.3 m	8 m		1.3m	8 m
2	-0.01	-0.17	**15**	-0.34	-0.13	**28**	0.03	-0.26
3	-0.36	-0.14	**16**	-0.33	-0.05	**29**	0.00	-0.18
4	-0.02	-0.15	**17**	-0.13	-0.13	**30**	-0.30	-0.36
5	-0.04	-0.28	**18**	-0.36	-0.05	**31**	-0.29	-
6	0.00	-0.33	**19**	-0.02	-0.13	**32**	0.06	-
7	-0.11	-0.21	**20**	-0.32	-0.25	**33**	-0.38	-
8	-0.06	-0.34	**21**	-0.39*	0.03	**34**	-0.37	-
9	-0.23	-0.35	**22**	-0.37	-0.30	**35**	0.33	-
10	0.06	-0.12	**23**	-0.29	-0.39	**36**	-0.01	-
11	0.22	-0.09	**24**	-0.36	-0.26	**37**	0.15	-
12	-0.04	-0.09	**25**	-0.05	-0.39	**38**	-0.24	-
13	0.08	-0.02	**26**	-0.13	-0.29	**39**	-0.29	-
14	-0.26	-0.21	**27**	-0.31	-0.29	**40**	-0.36	-

* indicates statistically significant results at $P \leq 0.05$

Table B-7: Correlation coefficients for transition-wood proportion against whole ring width for individual growth rings in 40 - 50 year old trees

Cambial age (Years)	r		Cambial age (Years)	r		Cambial age (Years)	r	
	1.3 m	8 m		1.3 m	8 m		1.3m	8 m
2	0.10	0.41*	**15**	0.65*	0.73*	**28**	0.71*	0.79*
3	0.48*	0.55*	**16**	0.86*	0.66*	**29**	0.84*	0.69*
4	0.09	0.49*	**17**	0.75*	0.52*	**30**	0.66*	0.65*
5	0.21	0.62*	**18**	0.74*	0.57*	**31**	0.74*	-
6	0.61*	0.52*	**19**	0.76*	0.64*	**32**	0.63*	-
7	0.47*	0.63*	**20**	0.90*	0.74*	**33**	0.72*	-
8	0.54*	0.62*	**21**	0.71*	0.53*	**34**	0.75*	-
9	0.44*	0.80*	**22**	0.64*	0.71*	**35**	0.71*	-
10	0.64*	0.76*	**23**	0.80*	0.63*	**36**	0.65*	-
11	0.53*	0.75*	**24**	0.76*	0.57*	**37**	0.69*	-
12	0.82*	0.85*	**25**	0.72*	0.88*	**38**	0.83*	-
13	0.43*	0.63*	**26**	0.65*	0.70*	**39**	0.71*	-
14	0.75*	0.66*	**27**	0.70*	0.82*	**40**	0.75*	-

* indicates statistically significant results at $P \leq 0.05$

Table B-8: Correlation coefficients for latewood proportion against whole ring width for individual growth rings in 40 - 50 year old trees

Cambial age (Years)	r		Cambial age (Years)	r		Cambial age (Years)	r	
	1.3 m	8 m		1.3 m	8 m		1.3m	8 m
2	-0.20	-0.44*	**15**	-0.62*	-0.62*	**28**	-0.28	-0.52*
3	-0.02	-0.24	**16**	-0.59*	-0.44*	**29**	-0.54*	-0.63*
4	-0.04	-0.41	**17**	-0.45*	-0.68*	**30**	-0.40*	-0.52*
5	-0.20	-0.40*	**18**	-0.17	-0.57*	**31**	-0.54*	-
6	-0.19	-0.41*	**19**	-0.55*	-0.64*	**32**	-0.42*	-
7	-0.39*	-0.53*	**20**	-0.58*	-0.52*	**33**	-0.35	-
8	-0.40*	-0.63*	**21**	-0.38	-0.52*	**34**	-0.61*	-
9	-0.31	-0.75*	**22**	-0.55*	-0.55*	**35**	-0.63*	-
10	-0.42*	-0.65*	**23**	-0.58*	-0.53*	**36**	-0.36	-
11	-0.49*	-0.67*	**24**	-0.51*	-0.62*	**37**	-0.50*	-
12	-0.44*	-0.53*	**25**	-0.53*	-0.51*	**38**	-0.48*	-
13	-0.52*	-0.46*	**26**	-0.40*	-0.51*	**39**	-0.48*	-
14	-0.62*	-0.52*	**27**	-0.52*	-0.52*	**40**	-0.68*	-

* indicates statistically significant results at $P \leq 0.05$

Table B-9: Comparisons of wood type proportions within a growth ring between slower and faster grown trees in the 40 - 50 year old sample group

	Earlywood			Transition-wood			Latewood		
	C	**S**	**F**	**C**	**S**	**F**	**C**	**S**	**F**
Mean (%)	47	47	47	30	29	31	23	24	22
CV (%)	24	26	23	47	50	43	53	54	52
Min (%)	7	8	7	5	5	7	1	2	1
Max (%)	96	96	82	83	83	80	80	80	69
t value	0.41			-3.83*			3.93*		

Note: C = Combined mean of slower and faster grown trees S = Slower grown F = Faster grown, * indicates statistically significant results at $P \leq 0.05$

Table B-10: t-test results comparing mean proportions in slower and faster growing trees within 40 - 50 year old sampling sites

Site	1	2	3	4
Earlywood	-0.19	0.50	-0.06	-0.17
Transition-wood	-2.48*	-2.39*	-1.92	-3.60*
Latewood	2.93*	2.45*	2.16*	3.45*

Note: Site numbers correspond to those given in Table 3-1, * indicates statistically significant results at $P \leq 0.05$

Table B-11: Correlation coefficients for whole ring radial tracheid diameter against whole ring width for individual growth rings in 40 - 50 year old trees

Cambial	r		Cambial	r		Cambial	r	
age (Years)	1.3 m	8 m	age (Years)	1.3 m	8 m	age (Years)	1.3m	8 m
2	0.21	0.03	**15**	0.34	0.27	**28**	0.33	0.28
3	0.03	0.12	**16**	0.34	0.26	**29**	0.35	0.39*
4	0.08	0.27	**17**	0.18	0.41*	**30**	0.32	0.41*
5	0.22	0.10	**18**	0.26	0.34	**31**	0.34	-
6	0.09	0.41*	**19**	0.31	0.34	**32**	0.22	-
7	0.21	0.32	**20**	0.32	0.23	**33**	0.26	-
8	0.25	0.39	**21**	0.27	0.48*	**34**	0.23	-
9	0.34	0.34	**22**	0.38	0.16	**35**	0.36	-
10	0.26	0.35	**23**	0.32	0.41*	**36**	0.39*	-
11	0.45*	0.27	**24**	0.38	0.41*	**37**	0.42*	-
12	0.29	0.21	**25**	0.28	0.32	**38**	0.38	-
13	0.37	0.40*	**26**	0.39*	0.06	**39**	0.19	-
14	0.32	0.33	**27**	0.46*	0.30	**40**	0.31	-

* indicates statistically significant results at $P \leq 0.05$

Table B-12: Correlation coefficients for earlywood radial tracheid diameter against whole ring width for individual growth rings in 40 - 50 year old trees

Cambial age (Years)	r		Cambial age (Years)	r		Cambial age (Years)	r	
	1.3 m	8 m		1.3 m	8 m		1.3m	8 m
2	0.05	0.03	**15**	0.28	0.32	**28**	0.37	-0.24
3	0.21	-0.14	**16**	-0.27	0.21	**29**	0.30	-0.10
4	0.34	-0.12	**17**	0.31	0.24	**30**	0.24	0.20
5	0.29	0.26	**18**	-0.23	0.43*	**31**	-0.27	-
6	0.36	0.34	**19**	-0.22	0.34	**32**	0.21	-
7	0.16	-0.11	**20**	0.44*	-0.26	**33**	0.43*	-
8	-0.12	0.20	**21**	0.26	0.24	**34**	0.39*	-
9	0.27	0.53*	**22**	-0.05	-0.25	**35**	-0.31	-
10	-0.35	0.34	**23**	0.34	0.14	**36**	0.36	-
11	0.16	0.42*	**24**	-0.24	0.24	**37**	0.21	-
12	0.38	0.33	**25**	0.18	0.40*	**38**	-0.24	-
13	-0.04	0.22	**26**	0.37	0.10	**39**	0.31	-
14	0.35	-0.31	**27**	0.41*	-0.27*	**40**	0.22	-

* indicates statistically significant results at $P \leq 0.05$

Table B-13: Correlation coefficients for transition-wood radial tracheid diameter against whole ring width for individual growth rings in 40 - 50 year old trees

Cambial age (Years)	r		Cambial age (Years)	r		Cambial age (Years)	r	
	1.3 m	8 m		1.3 m	8 m		1.3m	8 m
2	0.13	0.08	**15**	0.57*	0.26	**28**	0.33	0.31
3	0.27	0.03	**16**	0.33	0.33	**29**	0.27	0.47*
4	0.16	0.15	**17**	0.23	0.38	**30**	0.49*	0.51*
5	0.22	0.29	**18**	0.22	0.38	**31**	0.26	-
6	0.35	0.33	**19**	0.21	0.36	**32**	0.39	-
7	0.54*	0.36	**20**	0.30	0.30	**33**	0.35	-
8	0.11	0.25	**21**	0.29	0.42*	**34**	0.43*	-
9	0.31	0.44*	**22**	0.30	0.26	**35**	0.41*	-
10	0.21	0.31	**23**	0.37	0.45*	**36**	0.35	-
11	0.40*	0.27	**24**	0.47*	0.19	**37**	0.34	-
12	0.33	0.38	**25**	0.35	0.16	**38**	0.17	-
13	0.29	0.38	**26**	0.34	0.28	**39**	0.22	-
14	0.35	0.29	**27**	0.41*	0.39*	**40**	0.35	-

* indicates statistically significant results at $P \leq 0.05$

Table B-14: Correlation coefficients for latewood radial tracheid diameter against whole ring width for individual growth rings in 40 - 50 year old trees

Cambial age (Years)	r		Cambial age (Years)	r		Cambial age (Years)	r	
	1.3 m	8 m		1.3 m	8 m		1.3m	8 m
2	0.02	0.07	**15**	0.42*	0.38	**28**	0.35	0.32
3	0.23	0.15	**16**	0.17	0.43*	**29**	0.36	0.24
4	0.10	0.03	**17**	0.14	0.33	**30**	0.27	0.48*
5	0.16	0.31	**18**	0.44	0.42*	**31**	0.45*	-
6	0.15	0.46*	**19**	0.32	0.31	**32**	0.23	-
7	0.14	0.35	**20**	0.11	0.30	**33**	0.26	-
8	0.36	0.20	**21**	0.45*	0.23	**34**	0.39*	-
9	0.25	0.32	**22**	0.47*	0.18	**35**	0.25	-
10	0.22	0.28	**23**	0.23	0.20	**36**	0.16	-
11	0.31	0.19	**24**	0.37	0.30	**37**	0.45*	-
12	0.27	0.31	**25**	0.31	0.43*	**38**	0.45*	-
13	0.11	0.21	**26**	0.21	0.38	**39**	0.18	-
14	0.19	0.33	**27**	0.30	0.47*	**40**	0.29	-

* indicates statistically significant results at $P \leq 0.05$

Table B-15: Correlation coefficients for whole ring tangential tracheid diameter against whole ring width for individual growth rings in 40 - 50 year old trees

Cambial age (Years)	r		Cambial age (Years)	r		Cambial age (Years)	r	
	1.3 m	8 m		1.3 m	8 m		1.3m	8 m
2	0.04	0.05	**15**	0.29	0.33	**28**	0.35	0.42*
3	0.13	0.02	**16**	0.40*	0.44*	**29**	0.42*	0.35
4	0.13	0.13	**17**	0.28	0.37	**30**	0.41*	0.41*
5	0.14	0.25	**18**	0.43*	0.36	**31**	0.49*	-
6	0.26	0.35	**19**	0.42*	0.43*	**32**	0.42*	-
7	0.30	0.41*	**20**	0.35	0.28	**33**	0.35	-
8	0.49*	0.46	**21**	0.17	0.35	**34**	0.41*	-
9	0.43*	0.29	**22**	0.42*	0.40*	**35**	0.47*	-
10	0.36	0.31	**23**	0.35	0.34	**36**	0.42*	-
11	0.36	0.27	**24**	0.28	0.35	**37**	0.36	-
12	0.45*	0.34	**25**	0.41*	0.41*	**38**	0.41*	-
13	0.36	0.33	**26**	0.36	0.48*	**39**	0.33	-
14	0.42*	0.45*	**27**	0.41*	0.41*	**40**	0.34	-

* indicates statistically significant results at $P \leq 0.05$

Table B-16: Correlation coefficients for earlywood tangential tracheid diameter against whole ring width for individual growth rings in 40 - 50 year old trees

Cambial age (Years)	r		Cambial age (Years)	r		Cambial age (Years)	r	
	1.3 m	8 m		1.3 m	8 m		1.3m	8 m
2	0.04	0.08	**15**	0.23	0.39*	**28**	0.33	0.42*
3	0.11	0.04	**16**	0.22	0.46*	**29**	0.43*	0.32
4	0.19	0.19	**17**	0.50*	0.25	**30**	0.61*	0.42*
5	0.25	0.29	**18**	0.54*	0.35	**31**	0.44*	-
6	0.35	0.33	**19**	0.43*	0.44*	**32**	0.43*	-
7	0.45*	0.41*	**20**	0.33	0.22	**33**	0.33	-
8	0.43*	0.49*	**21**	0.35	0.32	**34**	0.31	-
9	0.44*	0.33	**22**	0.43*	0.30	**35**	0.47*	-
10	0.33	0.36	**23**	0.33	0.52*	**36**	0.32	-
11	0.34	0.40*	**25**	0.42*	0.62*	**37**	0.33	-
12	0.58*	0.31	**25**	0.32	0.52*	**38**	0.42*	-
13	0.34	0.30	**26**	0.54	0.71	**39**	0.30	-
14	0.44*	0.47*	**27**	0.61	0.62	**40**	0.31	-

* indicates statistically significant results at $P \leq 0.05$

Table B-17: Correlation coefficients for transition-wood tangential tracheid diameter against whole ring width for individual growth rings in 40 - 50 year old trees

Cambial age (Years)	r		Cambial age (Years)	r		Cambial age (Years)	r	
	1.3 m	8 m		1.3 m	8 m		1.3m	8 m
2	0.05	0.07	**15**	0.18	0.28	**28**	0.31	0.30
3	0.19	0.11	**16**	0.34	0.43*	**29**	0.32	0.35
4	0.10	0.16	**17**	0.23	0.50*	**30**	0.31	0.38
5	0.22	0.27	**18**	0.44*	0.37	**31**	0.39*	-
6	0.27	0.21	**19**	0.36	0.40*	**32**	0.31	-
7	0.25	0.32	**20**	0.21	0.04	**33**	0.31	-
8	0.44*	0.40*	**21**	0.14	0.37	**34**	0.37	-
9	0.37	0.20	**22**	0.32	0.33	**35**	0.34	-
10	0.40*	0.31	**23**	0.31	0.39*	**36**	0.31	-
11	0.35	0.26	**24**	0.23	0.07	**37**	0.17	-
12	0.42*	0.42*	**25**	0.34	0.31	**38**	0.40*	-
13	0.32	0.66	**26**	0.32	0.40*	**39**	0.23	-
14	0.45*	0.47	**27**	0.35	0.31	**40**	0.30	-

* indicates statistically significant results at $P \leq 0.05$

Table B-18: Correlation coefficients for latewood tangential tracheid diameter against whole ring width for individual growth rings in 40 - 50 year old trees

Cambial age (Years)	r		Cambial age (Years)	r		Cambial age (Years)	r	
	1.3 m	8 m		1.3 m	8 m		1.3m	8 m
2	0.05	0.09	**15**	0.19	0.23	**28**	0.29	0.29
3	0.12	0.11	**16**	0.32	0.41*	**29**	0.25	0.26
4	0.10	0.15	**17**	0.25	0.12	**30**	0.29	0.41*
5	0.32	0.22	**18**	0.40*	0.32	**31**	0.36	-
6	0.23	0.23	**19**	0.27	0.39*	**32**	0.19	-
7	0.21	0.34	**20**	0.29	0.15	**33**	0.14	-
8	0.36	0.45*	**21**	0.35	0.20	**34**	0.39*	-
9	0.34	0.21	**22**	0.45*	0.45*	**35**	0.38	-
10	0.28	0.32	**23**	0.36	0.31	**36**	0.37	-
11	0.30	0.46*	**24**	0.27	0.17	**37**	0.27	-
12	0.34	0.20	**25**	0.17	0.47*	**38**	0.34	-
13	0.41*	0.45*	**26**	0.41*	0.29	**39**	0.45*	-
14	0.23	0.19	**27**	0.23	0.21	**40**	0.41*	-

* indicates statistically significant results at $P \leq 0.05$

Table B-19: Comparisons of radial tracheid diameter between slower and faster grown trees in the 40 - 50 year old sample group

	Whole ring			Earlywood			Transition-wood			Latewood		
	C	**S**	**F**	**C**	**S**	**F**	**C**	**S**	**F**	**C**	**S**	**F**
Mean (µm)	31.4	31.2	31.6	36.3	36.3	36.2	30.3	30.0	30.6	22.8	22.8	22.9
CV (%)	9	9	8	9	10	9	12	12	12	10	9	10
Min (µm)	19.4	19.4	23.1	20.4	20.4	24.0	18.6	18.6	21.6	16.7	16.7	16.8
Max (µm)	38.6	38.6	38.3	44.1	44.1	44.1	42.8	40.5	42.8	34.6	34.6	32.7
t value	-2.99*			0.61			-3.43*			-1.18		

Note: C = Combined mean of slower and faster grown trees S = Slower grown F = Faster grown, * indicates statistically significant results at $P \leq 0.05$

Table B-20: Comparisons of tangential tracheid diameter between slower and faster grown trees in the 40 - 50 year old sample group

	Whole ring			Earlywood			Transition-wood			Latewood		
	C	**S**	**F**	**C**	**S**	**F**	**C**	**S**	**F**	**C**	**S**	**F**
Mean (μm)	30.1	29.5	30.6	32.5	31.9	33.1	28.9	28.5	29.3	26.9	26.5	27.2
CV (%)	10	9	10	10	10	10	11	11	11	9	9	10
Min (μm)	23.2	23.1	23.2	23.6	23.9	23.6	22.0	22.0	22.7	20.4	20.8	20.4
Max (μm)	42.0	42.0	39.4	42.5	41.9	42.5	40.1	37.6	40.1	44.8	44.8	36.9
t value	-7.46*			-7.55*			-5.11*			-5.96*		

Note: C = Combined mean of slower and faster grown trees S = Slower grown F = Faster grown, * indicates statistically significant results at $P \leq 0.05$

Table B-21: t-test results comparing mean radial tracheid diameters in slower and faster growing trees within 40 - 50 year old sampling sites

Site	**1**	**2**	**3**	**4**
Whole ring	-2.53*	-1.89	-3.60*	-3.15*
Earlywood	1.81	1.54	-0.38	-0.77
Transition-wood	-4.36*	-2.27*	-2.35*	-3.74*
Latewood	-1.64	-0.17	-2.95*	-1.05

Note: Site numbers correspond to those given in Table 3-1, * indicates statistically significant results at $P \leq 0.05$

Table B-22: t-test results comparing mean tangential tracheid diameters in slower and faster growing trees within 40 - 50 year old sampling sites

Site	**1**	**2**	**3**	**4**
Whole ring	-5.31*	-1.99*	-3.07*	-11.3*
Earlywood	-4.31*	-1.92*	-1.16	-9.51*
Transition-wood	-3.74*	-2.40*	-4.10*	-8.99*
Latewood	-5.26*	-2.82*	-5.49*	-9.83*

Note: Site numbers correspond to those given in Table 3-1, * indicates statistically significant results at $P \leq 0.05$

Table B-23: Correlation coefficients for whole ring tracheid radial wall thickness against whole ring width for individual growth rings in 40 - 50 year old trees

Cambial age (Years)	r		Cambial age (Years)	r		Cambial age (Years)	r	
	1.3 m	8 m		1.3 m	8 m		1.3m	8 m
2	-0.07	-0.02	**15**	-0.24	-0.31	**28**	-0.22	-0.10
3	-0.07	-0.12	**16**	-0.31	-0.34	**29**	-0.35	-0.41*
4	-0.18	-0.20	**17**	-0.27	-0.37	**30**	-0.22	-0.31
5	-0.24	-0.28	**18**	-0.30	-0.26	**31**	-0.35	-
6	-0.20	-0.31	**19**	-0.37	-0.33	**32**	-0.22	-
7	-0.24	-0.31	**20**	-0.27	-0.31	**33**	-0.34	-
8	-0.20	-0.33	**21**	-0.35	-0.40*	**34**	-0.39	-
9	-0.34	-0.21	**22**	-0.27	-0.38	**35**	-0.38	-
10	-0.35	-0.28	**23**	-0.23	-0.16	**36**	-0.37	-
11	-0.31	-0.34	**24**	-0.15	-0.30	**37**	-0.22	-
12	-0.42*	-0.21	**25**	-0.24	-0.21	**38**	-0.37	-
13	-0.03	-0.35	**26**	-0.31	-0.31	**39**	-0.31	-
14	-0.21	-0.20	**27**	-0.39	-0.31	**40**	-0.22	-

* indicates statistically significant results at $P \leq 0.05$

Table B-24: Correlation coefficients for earlywood tracheid radial wall thickness against whole ring width for individual growth rings in 40 - 50 year old trees

Cambial age (Years)	r		Cambial age (Years)	r		Cambial age (Years)	r	
	1.3 m	8 m		1.3 m	8 m		1.3m	8 m
2	-0.03	-0.05	**15**	-0.06	-0.14	**28**	0.10	-0.19
3	-0.08	-0.01	**16**	-0.25	-0.31	**29**	-0.10	-0.43*
4	-0.16	-0.20	**17**	-0.39	-0.33	**30**	-0.24	-0.30
5	-0.25	-0.24	**18**	-0.20	-0.28	**31**	-0.18	-
6	-0.13	-0.32	**19**	-0.34	-0.17	**32**	-0.10	-
7	-0.22	-0.38	**20**	-0.45*	-0.24	**33**	-0.20	-
8	-0.31	-0.23	**21**	-0.36	-0.39	**34**	-0.19	-
9	-0.26	-0.28	**22**	-0.33	-0.29	**35**	-0.28	-
10	-0.28	-0.22	**23**	-0.04	-0.01	**36**	-0.36	-
11	-0.30	-0.35	**24**	-0.22	-0.11	**37**	-0.31	-
12	-0.35	-0.27	**25**	0.03	-0.27	**38**	-0.36	-
13	-0.01	-0.44*	**26**	-0.32	-0.25	**39**	-0.18	-
14	-0.24	-0.18	**27**	-0.27	-0.21	**40**	-0.04	-

* indicates statistically significant results at $P \leq 0.05$

Table B-25: Correlation coefficients for transition-wood tracheid radial wall thickness against whole ring width for individual growth rings in 40 - 50 year old trees

Cambial age (Years)	r		Cambial age (Years)	r		Cambial age (Years)	r	
	1.3 m	8 m		1.3 m	8 m		1.3m	8 m
2	-0.01	-0.09	**15**	-0.07	-0.04	**28**	-0.06	-0.13
3	-0.03	-0.08	**16**	-0.08	-0.27	**29**	-0.19	-0.49*
4	-0.03	-0.04	**17**	-0.10	-0.30	**30**	-0.05	-0.35
5	-0.22	-0.22	**18**	-0.24	-0.43*	**31**	-0.22	-
6	-0.01	-0.17	**19**	-0.06	-0.11	**32**	-0.11	-
7	-0.16	-0.36	**20**	-0.21	-0.31	**33**	-0.04	-
8	-0.17	-0.23	**21**	-0.35	-0.11	**34**	-0.14	-
9	-0.17	-0.07	**22**	-0.45*	-0.28	**35**	-0.01	-
10	-0.04	-0.34	**23**	-0.21	-0.02	**36**	-0.13	-
11	-0.33	-0.14	**24**	-0.31	-0.13	**37**	-0.19	-
12	-0.45*	-0.07	**25**	-0.11	-0.37	**38**	-0.16	-
13	-0.06	-0.29	**26**	-0.14	-0.27	**39**	-0.45*	-
14	-0.12	-0.01	**27**	-0.56*	-0.17	**40**	-0.11	-

* indicates statistically significant results at $P \leq 0.05$

Table B-26: Correlation coefficients for latewood tracheid radial wall thickness against whole ring width for individual growth rings in 40 - 50 year old trees

Cambial age (Years)	r		Cambial age (Years)	r		Cambial age (Years)	r	
	1.3 m	8 m		1.3 m	8 m		1.3m	8 m
2	-0.02	-0.04	**15**	-0.15	-0.10	**28**	-0.11	-0.08
3	-0.03	-0.01	**16**	-0.24	-0.23	**29**	-0.15	-0.14
4	-0.16	-0.04	**17**	-0.10	-0.30	**30**	-0.14	-0.26
5	-0.25	-0.04	**18**	-0.14	-0.31	**31**	-0.27	-
6	-0.19	-0.36	**19**	-0.11	-0.22	**32**	-0.04	-
7	-0.09	-0.44*	**20**	-0.22	-0.23	**33**	-0.12	-
8	-0.08	-0.03	**21**	-0.30	-0.45*	**34**	-0.22	-
9	-0.35	-0.02	**22**	-0.47*	0.10	**35**	-0.10	-
10	-0.05	-0.21	**23**	-0.12	0.03	**36**	-0.27	-
11	-0.32	-0.18	**24**	-0.17	-0.12	**37**	-0.10	-
12	-0.42*	0.00	**25**	-0.16	-0.09	**38**	-0.37	-
13	-0.31	-0.27	**26**	-0.30	-0.29	**39**	-0.19	-
14	-0.08	-0.11	**27**	-0.34	-0.17	**40**	-0.09	-

* indicates statistically significant results at $P \leq 0.05$

Table B-27: Comparisons of tracheid radial wall thickness between slower and faster grown trees in the 40 - 50 year old sample group

	Whole ring			Earlywood			Transition-wood			Latewood		
	C	**S**	**F**	**C**	**S**	**F**	**C**	**S**	**F**	**C**	**S**	**F**
Mean (μm)	2.6	2.6	2.6	1.7	1.7	1.7	2.9	3.0	2.9	4.0	4.1	4.0
CV (%)	16	16	16	14	14	15	17	17	18	17	16	18
Min (μm)	1.7	1.8	1.7	1.0	1.2	1.0	1.5	1.5	1.6	2.2	2.2	2.3
Max (μm)	4.5	4.5	4.0	4.2	4.2	2.5	4.9	4.9	4.7	6.3	6.1	6.3
t value	4.12*			3.75*			2.09*			2.20*		

Note: C = Combined mean of slower and faster grown trees S = Slower grown F = Faster grown, * indicates statistically significant results at $P \leq 0.05$

Table B-28: t-test results comparing mean tracheid radial wall thicknesses in slower and faster growing trees within 40 - 50 year old sampling sites

Site	**1**	**2**	**3**	**4**
Whole ring	3.29*	3.02*	3.54*	2.08*
Earlywood	2.74*	3.97*	3.33*	0.45
Transition-wood	0.12	5.66*	2.05*	2.70*
Latewood	2.15*	7.68*	3.65*	2.13*

Note: Site numbers correspond to those given in Table 3-1, * indicates statistically significant results at $P \leq 0.05$

Table B-29: Correlation coefficients for whole ring density against whole ring width for individual growth rings in 40 - 50 year old trees

Cambial age (Years)	r		Cambial age (Years)	r		Cambial age (Years)	r	
	1.3 m	8 m		1.3 m	8 m		1.3m	8 m
2	-0.04	0.02	**15**	-0.51*	-0.28	**28**	-0.38	-0.63*
3	0.03	-0.05	**16**	-0.51*	-0.52*	**29**	-0.40*	-0.51*
4	-0.22	-0.03	**17**	-0.40*	-0.41*	**30**	-0.42*	-0.40*
5	-0.35	-0.12	**18**	-0.33	-0.58*	**31**	-0.43*	-
6	-0.51*	-0.40*	**19**	-0.50*	-0.45*	**32**	-0.38	-
7	-0.61*	-0.40*	**20**	-0.48*	-0.42*	**33**	-0.48*	-
8	-0.53*	-0.25	**21**	-0.53*	-0.52*	**34**	-0.51*	-
9	-0.44*	-0.41*	**22**	-0.55*	-0.53*	**35**	-0.44*	-
10	-0.57*	-0.54*	**23**	-0.44*	-0.51*	**36**	-0.40*	-
11	-0.53*	-0.64*	**24**	-0.55*	-0.42*	**37**	-0.61*	-
12	-0.53*	-0.42*	**25**	-0.30	-0.56*	**38**	-0.49*	-
13	-0.63*	-0.45*	**26**	-0.49*	-0.55*	**39**	-0.55*	-
14	-0.41*	-0.58*	**27**	-0.60*	-0.46*	**40**	-0.43*	-

* indicates statistically significant results at $P \leq 0.05$

Table B-30: Correlation coefficients for earlywood density against whole ring width for individual growth rings in 40 - 50 year old trees

Cambial age (Years)	r		Cambial age (Years)	r		Cambial age (Years)	r	
	1.3 m	8 m		1.3 m	8 m		1.3m	8 m
2	-0.09	-0.05	**15**	-0.36	-0.15	**28**	-0.21	-0.37
3	-0.06	0.04	**16**	-0.34	-0.57*	**29**	-0.28	-0.37
4	-0.12	-0.13	**17**	-0.47*	-0.49*	**30**	0.23	-0.38
5	-0.23	-0.22	**18**	-0.44*	-0.50*	**31**	-0.40*	-
6	-0.15	-0.24	**19**	-0.51*	-0.41*	**32**	-0.38	-
7	-0.37	-0.26	**20**	-0.47*	-0.25	**33**	-0.46*	-
8	-0.40*	-0.45*	**21**	-0.61*	-0.15	**34**	-0.03	-
9	-0.40*	-0.37	**22**	-0.57*	0.25	**35**	-0.44*	-
10	-0.44*	-0.39*	**23**	-0.30	-0.21	**36**	-0.44*	-
11	-0.31	-0.21	**24**	-0.30	-0.30	**37**	-0.38	-
12	-0.30	-0.41*	**25**	-0.21	-0.44*	**38**	-0.40*	-
13	-0.18	-0.43*	**26**	-0.41*	-0.34	**39**	-0.27	-
14	-0.40*	0.21	**27**	-0.38	-0.37	**40**	-0.29	-

* indicates statistically significant results at $P \leq 0.05$

Table B-31: Correlation coefficients for transition-wood density against whole ring width for individual growth rings in 40 - 50 year old trees

Cambial age (Years)	r		Cambial age (Years)	r		Cambial age (Years)	r	
	1.3 m	8 m		1.3 m	8 m		1.3m	8 m
2	-0.06	0.05	**15**	-0.27	-0.37	**28**	-0.30	-0.14
3	-0.11	-0.15	**16**	-0.35	-0.21	**29**	-0.37	-0.49*
4	-0.24	-0.03	**17**	-0.39*	-0.47*	**30**	-0.52*	-0.48*
5	-0.32	-0.27	**18**	-0.33	-0.56*	**31**	-0.32	-
6	-0.42*	-0.36	**19**	-0.12	-0.28	**32**	-0.27	-
7	-0.12	-0.55*	**20**	-0.35	-0.39*	**33**	-0.34	-
8	0.04	-0.23	**21**	-0.47*	-0.38	**34**	-0.33	-
9	-0.35	-0.38	**22**	-0.50*	-0.43*	**35**	-0.40*	-
10	-0.43*	-0.41*	**23**	-0.23	-0.30	**36**	-0.26	-
11	0.39*	-0.35	**24**	-0.52*	-0.28	**37**	-0.35	-
12	0.32	-0.42*	**25**	-0.24	-0.38	**38**	-0.44*	-
13	0.32	-0.51*	**26**	-0.39*	-0.42*	**39**	-0.36	-
14	0.41*	-0.25	**27**	-0.52*	0.29	**40**	-0.27	-

* indicates statistically significant results at $P \leq 0.05$

Table B-32: Correlation coefficients for latewood density against whole ring width for individual growth rings in 40 - 50 year old trees

Cambial age (Years)	r		Cambial age (Years)	r		Cambial age (Years)	r	
	1.3 m	8 m		1.3 m	8 m		1.3m	8 m
2	-0.09	-0.05	**15**	-0.38	-0.31	**28**	-0.34	-0.28
3	-0.10	-0.06	**16**	-0.28	-0.46*	**29**	-0.34	0.15
4	--0.23	-0.02	**17**	-0.21	-0.52*	**30**	-0.21	0.47*
5	-0.28	-0.28	**18**	-0.32	-0.45*	**31**	-0.28	-
6	-0.35	-0.49*	**19**	-0.36	-0.40*	**32**	-0.24	-
7	-0.40*	-0.47*	**20**	-0.28	-0.31	**33**	-0.28	-
8	-0.22	-0.32	**21**	-0.43*	0.34	**34**	0.40*	-
9	-0.34	-0.25	**22**	-0.45*	-0.24	**35**	0.22	-
10	-0.29	-0.19	**23**	-0.20	-0.38	**36**	-0.40*	-
11	-0.28	-0.39*	**24**	-0.31	-0.29	**37**	-0.26	-
12	-0.39*	-0.25	**25**	-0.27	-0.31	**38**	-0.44*	-
13	-0.36	-0.43*	**26**	-0.42*	-0.28	**39**	0.31	-
14	-0.46*	-0.21	**27**	-0.50*	-0.28	**40**	-0.43*	-

* indicates statistically significant results at $P \leq 0.05$

Table B-33: Comparisons of density between slower and faster grown trees in the 40 - 50 year old sample group

	Whole ring			Earlywood			Transition-wood			Latewood		
	C	**S**	**F**	**C**	**S**	**F**	**C**	**S**	**F**	**C**	**S**	**F**
Mean (kg/m³)	485	498	472	282	288	275	543	551	535	822	830	814
CV (%)	14	14	14	15	15	15	16	15	16	13	11	14
Min (kg/m³)	337	342	337	190	208	190	278	342	278	315	315	454
Max (kg/m³)	870	870	754	588	588	487	925	925	830	1070	1063	1070
t value	7.58*			6.05*			4.26*			4.41*		

Note: C = Combined mean of slower and faster grown trees S = Slower grown F = Faster grown, * indicates statistically significant results at $P \leq 0.05$

Table B-34: t-test results comparing density in slower and faster growing trees within 40 - 50 year old sampling sites

Site	**1**	**2**	**3**	**4**
Whole ring	4.5*	6.15*	2.3*	5.37*
Earlywood	3.0*	3.97*	3.2*	3.81*
Transition-wood	2.68*	5.47*	2.5*	1.12
Latewood	7.8*	7.49*	1.7	2.20*

Note: Site numbers correspond to those given in Table 3-1, * indicates statistically significant results at $P \leq 0.05$

Table B-35: Correlation coefficients for whole ring microfibril angle against whole ring width for individual growth rings in 40 - 50 year old trees

Cambial age (Years)	r		Cambial age (Years)	r		Cambial age (Years)	r	
	1.3 m	8 m		1.3 m	8 m		1.3m	8 m
2	-0.23	-0.16	**15**	0.01	0.28	**28**	0.34	0.35
3	0.14	0.13	**16**	0.22	0.16	**29**	0.45*	-0.11
4	0.15	0.09	**17**	0.23	0.36	**30**	0.43*	-0.11
5	-0.07	0.06	**18**	0.29	0.23	**31**	0.31	-
6	-0.39*	0.08	**19**	0.37	0.26	**32**	0.39	-
7	-0.40*	0.20	**20**	0.54*	0.35	**33**	0.30	-
8	0.04	0.15	**21**	0.53*	0.19	**34**	0.39*	-
9	0.18	0.09	**22**	0.53*	0.30	**35**	0.44*	-
10	0.46*	0.41*	**23**	0.50*	0.15	**36**	0.33	-
11	-0.50*	0.23	**24**	0.37*	0.20	**37**	0.54*	-
12	-0.33*	0.25	**25**	0.18	0.23	**38**	0.31	-
13	0.35*	-0.19	**26**	-0.07	0.37	**39**	0.34	-
14	0.00	-0.02	**27**	0.18	0.23	**40**	0.48*	-

* indicates statistically significant results at $P \leq 0.05$

Table B-36: Comparisons of low resolution microfibril angle between slower and faster grown trees in the 40 - 50 year old sample group

	Whole ring		
	C	**S**	**F**
Mean (Deg)	15	15	16
CV (%)	36	38	33
Min (Deg)	7	8	7
Max (Deg)	35	34	35
t value	-1.85		

Note: C = Combined mean of slower and faster grown trees S = Slower grown F = Faster grown, * indicates statistically significant results at $P \leq 0.05$

Table B-37: Comparisons of high resolution microfibril angle between slower and faster grown trees in the 40 - 50 year old sample group

	Whole ring			Earlywood			Transition-wood			Latewood		
	C	**S**	**F**	**C**	**S**	**F**	**C**	**S**	**F**	**C**	**S**	**F**
Mean (Deg)	15	15	14	19	20	19	10	11	10	10	11	9
CV (%)	38	37	40	30	29	31	61	60	63	66	62	72
Min (Deg)	3	3	5	6	6	9	1	1	1	1	1	1
Max (Deg)	36	33	36	37	35	37	35	32	35	30	30	30
t value	2.48*			1.97*			1.40			2.50*		

Note: C = Combined mean of slower and faster grown trees S = Slower grown F = Faster grown, * indicates statistically significant results at $P \leq 0.05$

Table B-38: t-test results comparing low resolution microfibril angle results in slower and faster growing trees within 40 - 50 year old sampling sites

Site	**1**	**2**	**3**
Whole ring	0.53	-0.48	-1.32

Note: Site numbers correspond to those given in Table 3-1, * indicates statistically significant results at $P \leq 0.05$

Table B-39: Comparisons of live crown ratio between slower and faster grown trees in the 40 - 50 year old sample group

	Live crown ratio		
	C	**S**	**F**
Mean	0.42	0.37	0.46
CV (%)	22	18	26
Min	0.29	0.29	0.38
Max	0.52	0.43	0.52

Note: C = Combined mean of slower and faster grown trees S = Slower grown F = Faster grown

Table B-40: Comparisons of live crown ratio between slower and faster grown trees in the 40 - 50 year old sampling sites

Site	1			2			3			4		
	C	**S**	**F**	**C**	**S**	**F**	**C**	**S**	**F**	**C**	**S**	**F**
Mean	0.40	0.35	0.45	0.41	0.37	0.45	0.42	0.36	0.47	0.43	0.38	0.47
Min	0.29	0.29	0.38	0.30	0.30	0.40	0.29	0.29	0.41	0.31	0.31	0.44
Max	0.50	0.41	0.50	0.49	0.43	0.49	0.52	0.40	0.52	0.50	0.43	0.50

Note: C = Combined mean of slower and faster grown trees S = Slower grown F = Faster grown, site numbers correspond to those given in Table 3-1

Table B-41: Descriptive statistics for the demarcation age from juvenile to mature wood production in 40 - 50 year old sample trees

	Density		**Microfibril angle**	
Height (m)	**1.3**	**8**	**1.3**	**8**
Mean (Years)	19	14	16	12
CV (%)	30	41	26	34
Min (Years)	9	6	11	6
Max (Years)	30	29	25	21
Confidence interval mean ± (Years)	4	4	3	2
Confidence interval min ± (Years)	2	2	1	4
Confidence interval min ± (Years)	8	8	1	4

Table B-42: t-test results comparing mean demarcation ages between sampling heights in 40 - 50 year old trees

	Density	**Microfibril angle**
t value	2.98*	3.71*

* indicates statistically significant results at $P \leq 0.05$

Table B-43: t-test results comparing mean demarcation ages between density and microfibril angle in 40 - 50 year old trees

	1.3 m	**8 m**
t value	2.37*	2.47*

* indicates statistically significant results at $P \leq 0.05$

Table B-44: Descriptive statistics for density demarcation age from juvenile to mature wood between slower and faster grown trees in 40 - 50 year old sample group

	1.3 m		8 m	
	S	**F**	**S**	**F**
Mean (Years)	17	21	14	16
CV (%)	34	26	38	44
Min (Years)	9	13	6	8
Max (Years)	26	30	25	29

Note S = Slower grown F = Faster grown

Table B-45: t-test results comparing mean density demarcation ages with slower and faster growth in 40 - 50 year old trees

	1.3 m	8 m
t value	-2.09*	-1.46

* indicates statistically significant results at $P \leq 0.05$

Table B-46: Descriptive statistics for microfibril angle demarcation age from juvenile to mature wood between slower and faster grown trees in 40 - 50 year old sample group

	1.3 m		8 m	
	S	**F**	**S**	**F**
Mean (Years)	15	18	10	13
CV (%)	26	24	32	32
Min (Years)	11	13	6	7
Max (Years)	21	25	18	21

Note S = Slower grown F = Faster grown

Table B-47: t-test results comparing mean microfibril angle demarcation ages with slower and faster growth in 40 - 50 year old trees

	1.3 m	8 m
t value	2.01*	2.34*

* indicates statistically significant results at $P \leq 0.05$

Appendix C - Chapter 6 supplementary results

Table C-1: Modulus of elasticity descriptive statistics for 40 - 50 year old trees

Growth period (Years)	All		2 - 10		11 - 20		21 - 30		31 - 40
Stem height (m)	**1.3**	**8**	**1.3**	**8**	**1.3**	**8**	**1.3**	**8**	**1.3**
Mean (N/mm²)	9900	10000	7000	7500	9600	10700	11100	11800	11600
CV (%)	25	22	25	21	21	16	18	15	16
Min (N/mm²)	3700	4700	3700	4700	4900	6900	4600	8000	7800
Max (N/mm²)	17200	16300	13000	14000	15900	15000	17200	16300	16000

Table C-2: Modulus of elasticity repeated measures univariate analysis of variance and t-test results for 40 - 50 year old trees

Growth period (Years)	2 - 10		11 - 20		21 - 30		31 - 40
Stem height (m)	**1.3**	**8**	**1.3**	**8**	**1.3**	**8**	**1.3**
F value	5.15*	9.29*	3.90*	4.31*	2.10*	2.84*	1.87
t value	-4.00*		-3.96*		-3.08*		N/A
Variance component							
Site (%)	9	8	8	10	5	8	6
Tree within site (%)	40	37	46	43	51	57	68
Error (%)	51	55	52	47	44	35	26

* indicates statistically significant results at $P \leq 0.05$

Table C-3: Modulus of elasticity descriptive statistics for all growth periods in 40 - 50 year old trees by site

Site	1		2		3		4	
Stem height (m)	**1.3**	**8**	**1.3**	**8**	**1.3**	**8**	**1.3**	**8**
Mean (N/mm²)	10200	10300	9600	9700	9400	9600	10000	10000
CV (%)	16	18	26	23	28	22	24	21
Min (N/mm²)	7500	6900	4900	4700	3700	5100	4100	5000
Max (N/mm²)	17200	16300	14500	14500	16000	15900	15000	14400

Note: Site numbers correspond to those given in Table 3-1

Table C-4: Flexural strength descriptive statistics for 40 - 50 year old trees

Growth period (Years)	All		2 - 10		11 - 20		21 - 30		31 - 40
Stem height (m)	**1.3**	**8**	**1.3**	**8**	**1.3**	**8**	**1.3**	**8**	**1.3**
Mean (N/mm²)	83	77	57	57	82	80	93	95	100
CV (%)	19	18	17	18	21	20	16	14	15
Min (N/mm²)	28	24	28	24	35	32	38	62	60
Max (N/mm²)	140	124	110	107	126	124	140	116	123

Table C-5: Flexural strength repeated measures univariate analysis of variance and t-test results for 40 - 50 year old trees

Growth period (Years)	2 - 10		11 - 20		21 - 30		31 - 40
Stem height (m)	**1.3**	**8**	**1.3**	**8**	**1.3**	**8**	**1.3**
F value	1.86	1.79	6.22*	5.00*	3.27*	`1.48	2.43*
t value	0.46		0.91		-1.94		N/A
Variance component							
Site (%)	10	6	7	12	6	8	7
Tree within site (%)	60	56	39	31	45	49	51
Error (%)	30	38	54	57	49	43	42

* indicates statistically significant results at $P \leq 0.05$

Table C-6: Flexural strength descriptive statistics for all growth periods in 40 - 50 year old trees by site

Site	1		2		3		4	
Stem height (m)	**1.3**	**8**	**1.3**	**8**	**1.3**	**8**	**1.3**	**8**
Mean (N/mm²)	89	81	82	76	80	75	84	77
CV (%)	19	20	22	24	22	19	23	20
Min (N/mm²)	43	38	35	24	37	39	28	31
Max (N/mm²)	140	124	122	103	121	113	124	111

Note: Site numbers correspond to those given in Table 3-1

Table C-7: Compressive strength descriptive statistics for 40 - 50 year old trees

Growth period (Years)	All		2 - 10		11 - 20		21 - 30		31 - 40
Stem height (m)	**1.3**	**8**	**1.3**	**8**	**1.3**	**8**	**1.3**	**8**	**1.3**
Mean (N/mm²)	38	38	31	33	38	39	41	41	42
CV (%)	20	21	18	18	17	18	15	16	13
Min (N/mm²)	25	18	25	18	25	28	26	31	30
Max (N/mm²)	56	55	45	48	51	54	56	54	55

Table C-8: Compressive strength repeated measures univariate analysis of variance and t-test results for 40 - 50 year old trees

Growth period (Years)	2 - 10		11 - 20		21 - 30		31 - 40
Stem height (m)	**1.3**	**8**	**1.3**	**8**	**1.3**	**8**	**1.3**
t value	-0.69		-0.34		0.26		N/A

* indicates statistically significant results at $P \leq 0.05$

Table C-9: Compressive strength descriptive statistics for all growth periods in 40 - 50 year old trees by site

Site	1		2		3		4	
Stem height (m)	**1.3**	**8**	**1.3**	**8**	**1.3**	**8**	**1.3**	**8**
Mean (N/mm²)	41	42	37	36	35	34	39	38
CV (%)	11	13	20	20	20	18	19	17
Min (N/mm²)	35	35	26	18	25	18	25	25
Max (N/mm²)	55	55	55	54	56	53	48	48

Note: Site numbers correspond to those given in Table 3-1

Table C-10: Modulus of elasticity descriptive statistics by position in the stem for all growth periods in 40 - 50 year old trees

Direction	North		East		South		West	
Stem height (m)	**1.3**	**8**	**1.3**	**8**	**1.3**	**8**	**1.3**	**8**
Mean (N/mm²)	9800	10200	10100	9900	9600	10000	10000	10300
CV (%)	24	20	19	21	24	18	23	20
Min (N/mm²)	4100	5700	5000	4700	3700	6200	5600	6300
Max (N/mm²)	15700	16000	14200	16300	14500	14100	17200	15400

Table C-11: Modulus of elasticity univariate analysis of variance results comparing mean values by position in the stem for all growth periods in 40 - 50 year old trees

Stem height	1.3 m	8 m
F value	1.32	1.24

* indicates statistically significant results at $P \leq 0.05$

Table C-12: Modulus of elasticity univariate analysis of variance results comparing mean values by position in the stem for all growth periods in 40 - 50 year old trees by site

Site	1		2		3		4	
Stem height (m)	**1.3**	**8**	**1.3**	**8**	**1.3**	**8**	**1.3**	**8**
F value	0.91	0.94	1.28	1.01	1.44	0.98	1.05	1.37

* indicates statistically significant results at $P \leq 0.05$

Table C-13: Flexural strength descriptive statistics by position in the stem for all growth periods in 40 - 50 year old trees

Direction	North		East		South		West	
Stem height (m)	**1.3**	**8**	**1.3**	**8**	**1.3**	**8**	**1.3**	**8**
Mean (N/mm²)	82	79	86	78	82	79	83	80
CV (%)	22	22	15	20	19	18	22	20
Min (N/mm²)	28	32	47	37	37	48	32	24
Max (N/mm²)	124	124	117	116	119	111	140	116

Table C-14: Flexural strength univariate analysis of variance results comparing mean values by position in the stem for all growth periods in 40 - 50 year old trees

Stem height	1.3 m	8 m
F value	2.02	1.14

* indicates statistically significant results at $P \leq 0.05$

Table C-15: Flexural strength univariate analysis of variance results comparing mean values by position in the stem for all growth periods in 40 - 50 year old trees by site

Site	1		2		3		4	
Stem height (m)	**1.3**	**8**	**1.3**	**8**	**1.3**	**8**	**1.3**	**8**
F value	2.02	1.98	1.32	1.02	1.91	1.32	1.01	1.28

* indicates statistically significant results at $P \leq 0.05$

Table C-16: Comparisons of mean modulus of elasticity between slower and faster grown trees in the 40 - 50 year old sample group

	C	S	F
Mean (N/mm²)	9900	10300	9600
CV (%)	21	24	23
Min (N/mm²)	3700	4600	3700
Max (N/mm²)	17200	16300	17200
t value	7.60*		

Note: C = Combined mean of slower and faster grown trees S = Slower grown F = Faster grown, * indicates statistically significant results at $P \leq 0.05$

Table C-17: t-test results comparing mean modulus of elasticity in slower and faster growing trees within 40 - 50 year old sampling sites

Site	**1**	**2**	**3**	**4**
t value	4.38*	1.94	3.98*	2.46*

Note: Site numbers correspond to those given in Table 3-1, * indicates statistically significant results at $P \leq 0.05$

Table C-18: Comparisons of mean flexural strength between slower and faster grown trees in the 40 - 50 year old sample group

	C	**S**	**F**
Mean (N/mm²)	80	83	77
CV (%)	18	21	22
Min (N/mm²)	24	28	24
Max (N/mm²)	140	124	140
t value	7.50*		

Note: C = Combined mean of slower and faster grown trees S = Slower grown F = Faster grown, * indicates statistically significant results at $P \leq 0.05$

Table C-19: t-test results comparing mean flexural strength in slower and faster growing trees within 40 - 50 year old sampling sites

Site	**1**	**2**	**3**	**4**
t value	3.96*	1.28	3.12*	3.94*

Note: Site numbers correspond to those given in Table 3-1, * indicates statistically significant results at $P \leq 0.05$

Table C-20: Comparisons of mean compressive strength between slower and faster grown trees in the 40 - 50 year old sample group

	C	**S**	**F**
Mean (N/mm²)	38	39	37
CV (%)	20	17	21
Min (N/mm²)	18	25	18
Max (N/mm²)	56	54	56
t value	5.28*		

Note: C = Combined mean of slower and faster grown trees S = Slower grown F = Faster grown, * indicates statistically significant results at $P \leq 0.05$

Table C-21: t-test results comparing mean compressive strength in slower and faster growing trees within 40 - 50 year old sampling sites

Site	**1**	**2**	**3**	**4**
t value	4.93*	2.31*	1.98	2.48*

Note: Site numbers correspond to those given in Table 3-1, * indicates statistically significant results at $P \leq 0.05$

Appendix D - Chapter 7 supplementary results

Table D-1: Model 1 juvenile and mature wood path coefficients for modulus of elasticity

	Juvenile	Mature
β_{DEN}	0.44*	0.59*
β_{MFA}	-0.55*	-0.26*
$r_{DEN - MFA}$	-0.14*	-0.27*

* indicates statistically significant results at $P \leq 0.05$

Table D-2: Model 1 juvenile and mature wood path coefficients for flexural strength

	Juvenile	Mature
β_{DEN}	0.64*	0.65*
β_{MFA}	-0.23*	-0.11
$r_{DEN - MFA}$	-0.14*	-0.27*

* indicates statistically significant results at $P \leq 0.05$

Table D-3: Model 1 juvenile and mature wood path coefficients for compressive strength

	Juvenile	Mature
β_{DEN}	0.53*	0.49*
β_{MFA}	-0.40*	-0.22*
$r_{DEN - MFA}$	-0.14*	-0.27*

* indicates statistically significant results at $P \leq 0.05$

Table D-4: Model 2 juvenile and mature wood path coefficients for modulus of elasticity

	Juvenile	**Mature**
β_{DEN}	0.41*	0.52*
β_{MFA}	-0.48*	-0.30*
β_{AGE}	0.14*	0.02
β_{RW}	-0.13*	-0.25*
$r_{DEN - MFA}$	-0.14*	-0.27*
$r_{DEN - AGE}$	0.33*	0.34*
$r_{DEN - RW}$	-0.43*	-0.38*
$r_{MFA - AGE}$	-0.59*	-0.28*
$r_{MFA - RW}$	0.04	0.40*
$r_{AGE- RW}$	-0.31*	0.04

* indicates statistically significant results at $P \leq 0.05$

Table D-5: Model 2 juvenile and mature wood path coefficients for flexural strength

	Juvenile	**Mature**
β_{DEN}	0.54*	0.59*
β_{MFA}	-0.12*	-0.02
β_{AGE}	0.18*	0.02
β_{RW}	-0.20*	-0.30*
$r_{DEN - MFA}$	-0.14*	-0.27*
$r_{DEN - AGE}$	0.33*	0.34*
$r_{DEN - RW}$	-0.43*	-0.38*
$r_{MFA - AGE}$	-0.59*	-0.28*
$r_{MFA - RW}$	0.04	0.40*
$r_{AGE- RW}$	-0.31*	0.04

* indicates statistically significant results at $P \leq 0.05$

Table D-6: Model 2 juvenile and mature wood path coefficients for compressive strength

	Juvenile	**Mature**
β_{DEN}	0.40*	0.57*
β_{MFA}	-0.26	-0.05
β_{AGE}	0.18*	-0.06
β_{RW}	-0.04	0.14
$r_{DEN - MFA}$	-0.14*	-0.27*
$r_{DEN - AGE}$	0.33*	0.34*
$r_{DEN - RW}$	-0.43*	-0.38*
$r_{MFA - AGE}$	-0.59*	-0.28*
$r_{MFA - RW}$	0.04	0.40*
$r_{AGE- RW}$	-0.31*	0.04

* indicates statistically significant results at $P \leq 0.05$

Table D-7: Model 3 juvenile and mature wood path coefficients for modulus of elasticity

	Juvenile	**Mature**
$\beta_{EW\ DEN}$	0.10	0.30*
$\beta_{TW\ DEN}$	0.31*	0.20*
$\beta_{LW\ DEN}$	0.10	0.27*
β_{MFA}	-0.52*	-0.26*
$r_{EW\ DEN - TW\ DEN}$	0.28*	0.45*
$r_{EW\ DEN - LW\ DEN}$	0.19*	0.56*
$r_{EW\ DEN - MFA}$	0.37*	-0.13
$r_{TW\ DEN - LW\ DEN}$	0.63*	0.72*
$r_{TW\ DEN - MFA}$	-0.25*	-0.18*
$r_{LW\ DEN - MFA}$	-0.40*	-0.30*

* indicates statistically significant results at $P \leq 0.05$

Table D-8: Model 3 juvenile and mature wood path coefficients for flexural strength

	Juvenile	Mature
$\beta_{EW\ DEN}$	0.13	0.45*
$\beta_{TW\ DEN}$	0.43*	0.20*
$\beta_{LW\ DEN}$	0.08	0.19*
β_{MFA}	-0.23*	-0.04
$r_{EW\ DEN\ -\ TW\ DEN}$	0.28*	0.45*
$r_{EW\ DEN\ -\ LW\ DEN}$	0.19*	0.56*
$r_{EW\ DEN\ -\ MFA}$	0.37*	-0.13
$r_{TW\ DEN\ -\ LW\ DEN}$	0.63*	0.72*
$r_{TW\ DEN\ -\ MFA}$	-0.25*	-0.18*
$r_{LW\ DEN\ -\ MFA}$	-0.40*	-0.30*

* indicates statistically significant results at $P \leq 0.05$

Table D-9: Model 3 juvenile and mature wood path coefficients for compressive strength

	Juvenile	Mature
$\beta_{EW\ DEN}$	0.01	0.35*
$\beta_{TW\ DEN}$	0.30*	0.19*
$\beta_{LW\ DEN}$	0.14	0.25*
β_{MFA}	-0.34*	-0.11
$r_{EW\ DEN\ -\ TW\ DEN}$	0.28*	0.45*
$r_{EW\ DEN\ -\ LW\ DEN}$	0.19*	0.56*
$r_{EW\ DEN\ -\ MFA}$	0.37*	-0.13
$r_{TW\ DEN\ -\ LW\ DEN}$	0.63*	0.72*
$r_{TW\ DEN\ -\ MFA}$	-0.25*	-0.18*
$r_{LW\ DEN\ -\ MFA}$	-0.40*	-0.30*

* indicates statistically significant results at $P \leq 0.05$

Table D-10: Regression equation coefficients for the prediction of modulus of elasticity within 40 - 50 year old sample trees

Microscopic property models		**R^2/Adj R^2**
DEN	-99331 + 29712 Log(DEN)	0.49*
MFA	32839 - 10544Log(MFA)	0.40*
DEN, MFA	-61413 + 23876Log(DEN) - 7559Log(MFA)	0.65*
Macroscopic property models		
AGE	487 + 4337Log(AGE)	0.26*
RW	21185 - 6740Log(RW)	0.21*
LWP	-9074 + 7375Log(LWP)	0.36*
AGE, RW	9952 + 3898Log(AGE) - 5056Log(RW)	0.46*
AGE, LWP	-7324 + 3390Log(AGE) + 3886Log(LWP)	0.49*
LWP, RW	213 + 6442Log(LWP) - 4081Log(RW)	0.45*
AGE, RW, LWP	2185 +3263Log(AGE) - 3818Log(RW) + 2784Log(LWP)	0.53*
Combination models		
AGE, RW, DEN	-65519 +2172Log(AGE) - 2439Log(RW) + 20350Log(DEN)	0.56*
AGE, RW, MFA	28649 + 2169Log(AGE) - 4493Log(RW) - 7342Log(MFA)	0.53*
AGE, RW, DEN, MFA	-39113 + 1005Log(AGE) - 2458Log(RW) + 17738Log(DEN) - 6544Log(MFA)	0.67*
AGE, LWP, DEN	-78710 + 2116Log(AGE) + 1811Log(LWP) + 21622Log(DEN)	0.62*
AGE, LWP, MFA	9597 + 2383Log(AGE) + 2841Log(LWP) - 5565Log(MFA)	0.54*
AGE, LWP, DEN, MFA	-61365 + 1177Log(Age) + 850Log(LWP) + 21256Log(DEN) - 5307Log(MFA)	0.68*
LWP, RW, DEN	-76662 + 3435Log(LWP) - 1583Log(RW) + 21882Log(DEN)	0.58*
LWP, RW, MFA	25570 + 3073Log(LWP) - 4328Log(RW) - 7511Log(MFA)	0.52*
LWP, RW, DEN, MFA	-46464 + 1130Log(LWP) - 2260Log(RW) +19358Log(DEN) - 6383Log(MFA)	0.67*
AGE, LWP, RW, DEN, MFA	-49698 + 1187Log(AGE) + 362Log(LWP) - 2309Log(RW) + 18724Log(DEN) - 5656Log(MFA)	0.70*

* indicates statistically significant results at $P \leq 0.05$

Table D-11: Regression equation coefficients for the prediction of flexural strength within 40 - 50 year old sample trees

Microscopic property models		**R^2/Adj R^2**
DEN	-801 + 239Log(DEN)	0.58*
MFA	196 - 54Log(MFA)	0.18*
DEN, MFA	-709 + 227Log(DEN) - 21Log(MFA)	0.61*
Macroscopic property models		
AGE	9 + 33Log(AGE)	0.31*
RW	176 - 58Log(RW)	0.27*
LWP	-53 + 51Log(LWP)	0.37*
AGE, RW	95 + 28Log(AGE) - 45Log(RW)	0.51*
AGE, LWP	-38 + 25Log(AGE) + 25Log(LWP)	0.53*
LWP, RW	44 + 40Log(LWP) - 41Log(RW)	0.51*
AGE, RW, LWP	2185 +3263Log(AGE) - 3818Log(RW) + 2784Log(LWP)	0.56*
Combination models		
AGE, RW, DEN	-527 +14Log(AGE) - 23Log(RW) + 167Log(DEN)	0.63*
AGE, RW, MFA	142 + 23Log(AGE) - 41Log(RW) - 20Log(MFA)	0.52*
AGE, RW, DEN, MFA	-478 + 12Log(AGE) - 23Log(RW) + 162Log(DEN) - 12Log(MFA)	0.65*
AGE, LWP, DEN	-686 + 13Log(AGE) + 6Log(LWP) + 196Log(DEN)	0.66*
AGE, LWP, MFA	-30 + 24Log(AGE) + 25Log(LWP) - 3Log(MFA)	0.54*
AGE, LWP, DEN, MFA	-684 + 13Log(AGE) + 6Log(LWP) + 196Log(DEN) - 1Log(MFA)	0.66*
LWP, RW, DEN	-622 + 15Log(LWP) - 19Log(RW) + 189Log(DEN)	0.63*
LWP, RW, MFA	129 + 29Log(LWP) - 40Log(RW) - 26Log(MFA)	0.46*
LWP, RW, DEN, MFA	-554 + 10Log(LWP) - 21Log(RW) +183Log(DEN) - 14Log(MFA)	0.65*
AGE, LWP, RW, DEN, MFA	-544 + 13Log(AGE) + 2Log(LWP) - 21Log(RW) + 173Log(DEN) - 4Log(MFA)	0.68*

* indicates statistically significant results at $P \leq 0.05$

Table D-12: Regression equation coefficients for the prediction of compressive strength within 40 - 50 year old sample trees

Microscopic property models		**R^2/Adj R^2**
DEN	-237 + 75Log(DEN)	0.49*
MFA	88 - 23Log(MFA)	0.32*
DEN, MFA	-192 + 71Log(DEN) - 14Log(MFA)	0.56*
Macroscopic property models		
AGE	12 + 12Log(AGE)	0.35*
RW	65 - 16Log(RW)	0.14*
LWP	-7 + 17Log(LWP)	0.25*
AGE, RW	27 + 12Log(AGE) - 9Log(RW)	0.44*
AGE, LWP	-3 + 10Log(AGE) + 8Log(LWP)	0.46*
LWP, RW	10 + 16Log(LWP) - 8Log(RW)	0.40*
AGE, RW, LWP	13 +10Log(AGE) - 7Log(RW) + 6Log(LWP)	0.48*
Combination models		
AGE, RW, DEN	-140 +7Log(AGE) - 5Log(RW) + 46Log(DEN)	0.52*
AGE, RW, MFA	61 + 8Log(AGE) - 9Log(RW) - 12Log(MFA)	0.47*
AGE, RW, DEN, MFA	-102 + 5Log(AGE) - 5Log(RW) + 43Log(DEN) - 9Log(MFA)	0.57*
AGE, LWP, DEN	-192 + 7Log(AGE) + 3Log(LWP) + 57Log(DEN)	0.54*
AGE, LWP, MFA	-27 + 8Log(AGE) + 6Log(LWP) - 10Log(MFA)	0.48*
AGE, LWP, DEN, MFA	-160 + 5Log(AGE) + Log(LWP) + 55Log(DEN) - 9Log(MFA)	0.59*
LWP, RW, DEN	-183 + 8Log(LWP) - 3Log(RW) + 56Log(DEN)	0.50*
LWP, RW, MFA	62 + 9Log(LWP) - 9Log(RW) - 15Log(MFA)	0.42*
LWP, RW, DEN, MFA	-125 + 4Log(LWP) - 4Log(RW) +50Log(DEN) - 12Log(MFA)	0.57*
AGE, LWP, RW, DEN, MFA	-142 + 5Log(AGE) + Log(LWP) - 3Log(RW) + 52Log(DEN) - 9Log(MFA)	0.59*

* indicates statistically significant results at $P \leq 0.05$